

Cyclometallated N[^]C and N[^]C[^]N Complexes of Pyridines and Pyridones: Synthesis and Reactivity

Thesis submitted for the degree of

Doctor of Philosophy

at the University of Leicester

By

Meshari M. Aljohani, MSc

Department of Chemistry

University of Leicester

November 2018

Cyclometallated N[^]C and N[^]C[^]N Complexes of Pyridines and Pyridones: Synthesis and Reactivity

Meshari M. Aljohani

Abstract:

In order to develop the applications of transition-metal complexes in the coordination chemistry and catalysis, the synthesis of cyclometallated N[^]C and N[^]C[^]N complexes of pyridines and pyridones are described.

Chapter one presents an overview of C-H activation: its importance and mechanisms, ligand types, and multifunctional ligands and their role in catalysis. **Chapter two** describes the synthesis and characterisation of cyclopalladated complexes with a variety of 6-aryl-2-methoxypyridine ligands (aryl = H **2.5**, 4-MePh **2.6**, 4-CF₃Ph **2.7**, 4-FPh **2.8** and 2-MePh **2.9**). Further reaction chemistry of these complexes, including disassembly, ligand exchange and stoichiometric reactions are discussed as well. The dimeric Pd^{II} complexes are shown to be efficient catalysts for the aerobic oxidation of benzyl alcohol. The reactivity of **2.6** towards two different Au^{III} sources, H[AuCl₄] and K[AuCl₄], are described in this chapter. **Chapter three** shows divergent behaviour in the reactivity of 6-aryl-2-pyridones from those in Chapter 2. Cyclopalladation of the 6-aryl-2-pyridones proceeds smoothly forming the acetate-bridged complexes; however, on standing in solution the dimeric complexes undergo slow pyridinol-pyridonate conversion to the tetrameric species with loss of acetic acid. Different behaviours are also observed in all the subsequent reactions. The electronic effect of different substituents (in particular H vs Me vs CF₃) in reactivity is investigated. The role of the *ortho*-hydroxy group in the stability, reactivity and hydrolysis of PF₆ and BF₄ is demonstrated as remarkable differences have been shown between the two types, pyridine- and pyridone-based complexes. **Chapter four** describes the synthesis of novel symmetrical N[^]C[^]N pyridine- and pyridone-based ligands and investigates their reactivities and selectivity towards several transition metals, such as Pd^{II}, Pt^{II}, Hg^{II} and Ag^{III}. A new microwave method is developed to afford cyclometallated N[^]C[^]N complexes of pyridones. All the experimental work and full characterisation data of the ligands and complexes described in this thesis are detailed in **Chapter 5**.

Acknowledgment

I am truly blessed to receive so much help and support from so many people during my studies.

First of all, I would like to express my gratitude to my supervisor, Prof Eric G. Hope, for his endless support. Thanks for your patience and guidance you have provided me throughout my PhD studies. I will never forget your encouragement when you always say “this is your thesis” which motivated me to do my best and accomplish my set targets. I have really enjoyed working with you, so many thanks for being my supervisor. I would also like to thank Dr Gregory A. Solan, for his dedicated supervision on my research, without your assistance it would have been challenging and difficult to finish my PhD.

I would like to thank all the people who have been involved in this project, Dr Gerry Griffith for NMR spectral analysis, Mr Kuldip Singh for the X-ray structure determinations and Mr Mick Lee for mass spectra. To members of the Department of Chemistry, thank you for your respectfulness and friendship. Also, the lab technicians deserve my gratitude for their help supplying most of the chemicals and equipment that were used.

Many thanks go to the lab group: Dr Gemma Geary, Dr Amin Ajlouni, Dr Rena Simayi, Ahmad, Rusul, Martyna, Will, Alice, Jinting, Emad, Simran, Amina and Mona for being really helpful and friendly to me throughout the course of my studies. I would also like to acknowledge Dr Amandeep Singh and William Dale who started the study of the cyclopalladated 6-aryl-2-pyridones.

I must of course thank my mother (حصه), my parents-in-law and all my brothers & sisters, for their continuous love and support. I only wish my father (محمد) could have been here with us to see me completing my PhD.

Most importantly, I would like to deeply express my gratitude to my *lovely wife Abeer* for her support and enthusiasm along my study period. I could not have done it without you as you have always made me feel that I can do it. To my children Rahaf, Mohammed, Ghassan and Mona: I LOVE YOU.

Finally, I would like to thank the University of Tabuk in Saudi Arabia for their funding and supporting my study throughout the study period.

This thesis is dedicated

To

My Lovely Family

Statement

This thesis is based on work conducted by the author in the Department of Chemistry at the University of Leicester, during the period between January 2015 and December 2017. The work has not been submitted, and is not presently being submitted, for any other degree at this or any other university. All experimental work described in this thesis is original unless otherwise acknowledged in the text or by references.

Signed:

Date: / /

Meshari M. Aljohani

Table of Contents

	Page
Abstract	ii
Acknowledgements	iii
Table of Contents	vi
Abbreviations	ix
Chapter 1: Introduction	1
1.1 Introduction	2
1.2 C-H Activation	2
1.2.1 The Importance of C-H Activation	2
1.2.2 Types and Mechanisms of C-H Activation by Metal Complexes	3
1.2.3 Selectivity of C-H Activation	10
1.3 Ligand Types	13
1.3.1 Monodentate Ligands	13
1.3.2 Bidentate Ligands	17
1.3.3 Tridentate Ligands	20
1.4 Multifunctional Ligands	23
1.4.1 OH-Functionalised Ligand	25
1.4.2 Pyridone-Pyridinol Tautomerism and their Binding Modes	28
1.5 Overall Conclusions to Chapter 1	33
1.6 Research Aims	33
References for Chapter 1	35
Chapter 2: Synthesis of Cyclometallated N[^]C-Pyridine Complexes and their Reactivity as Catalysts for Aerobic Alcohol Oxidation	40
2.1 Introduction	41
2.1.1 Cyclometallated Complexes	41
2.1.1.1 N-Cyclometallated Ligands	42
2.1.1.2 Applications of Pd-Catalysed C-H Activation in Catalysis	44
2.2 Aims and Objectives of Chapter 2	45
2.3 Results and Discussion	47
2.3.1 Synthesis of OMe-N [^] C Ligands	47
2.3.2 Complexation of OMe-N [^] C Ligands to Palladium(II)	50
2.3.3 Synthesis of Mononuclear Pd ^{II} Complexes	54

2.3.4	Synthesis of $[\text{Pd}(\kappa^2\text{-N}^{\wedge}\text{C})(\text{PPh}_3)\text{Cl}]$	59
2.3.5	Stoichiometric Reactions with Silver Salts	60
2.3.6	Reactions of 2.6 with Gold(III) Salts	62
2.3.6.1	Attempts at Achieving C-H Activation with Au^{III}	67
2.3.7	Aerobic Oxidation of Benzyl Alcohol Catalysed by Dinuclear Palladium(II) Complexes	69
2.4	Conclusions and Future Work	73
	References for Chapter 2	75
	Chapter 3: Cyclopalladated $\text{N}^{\wedge}\text{C}$-Pyridone Complexes with Hydrogen Bonding Interactions	78
3.1	Introduction	79
3.1.1	OH-Substituted Bidentate Ligands	79
3.2	Aims and Objectives of Chapter 3	86
3.3	Results and Discussion	88
3.3.1	Synthesis of 6-aryl-2-pyridones	88
3.3.2	Complexation of 6-aryl-2-pyridones to Palladium(II)	90
3.3.3	Synthesis of Tetrameric Complexes, $[\text{Pd}(\mu\text{:}\kappa^2\text{-6-aryl-2-pyridonate})]_4$	93
3.3.4	Reactivity of 6-Aryl-2-pyridones towards Dimeric Complexes	96
3.6-3.9		
3.3.5	Reactions of Dimeric Complexes 3.6-3.9 with 3,5-lutidine	98
3.3.6	Reactions of Dimeric Complexes 3.6-3.9 with PPh_3	104
3.3.7	Subsequent Ligand Exchange Reactions with NaCl	108
3.3.8	Reactions of Cl-Containing Complexes with Different Silver Salts	117
3.3.9	Hydrolysis of PF_6 and BF_4	130
3.4	Conclusions and Future Work	133
	References for Chapter 3	136
	Chapter 4: Symmetrical, Monoanionic $\text{N}^{\wedge}\text{C}^{\wedge}\text{N}$ Pincer Ligands for Palladium, Platinum and Gold	139
4.1	Introduction	140
4.1.1	Amine-based Pincer Ligands	140
4.1.2	Pyridine- and Pyridone-based Pincer Ligands	141
4.2	Aims and Objectives of Chapter 4	146

4.3 Results and Discussion	148
4.3.1 Synthesis of N ^C N Pyridine Ligands	148
4.3.2 Synthesis of N ^C N Pyridone Ligands	152
4.3.3 Complexation of Tridentate N ^C N Ligands to Palladium (Pd ^{II})	155
4.3.4 Transmetallation Reactions	164
4.3.5 Direct Synthesis of Palladium Pyridine and Pyridone complexes (4.13-4.16)	170
4.3.6 Stoichiometric Reactions with AgPF ₆	174
4.3.7 Complexation of Tridentate N ^C N Ligands to Platinum (Pt ^{II})	176
4.3.8 Complexation of Tridentate N ^C N Ligands to Gold (Au ^{III})	179
4.4 Conclusions and Future Work	186
References for Chapter 4	188
Chapter 5: Experimental	191
5.1 General Experimental	192
5.1.1 Reagents	192
5.1.2 Solvents	192
5.1.3 Physical Measurements	193
5.1.3.1 Elemental Analysis	193
5.1.3.2 Infrared Spectroscopy	193
5.1.3.3 Mass Spectrometry	193
5.1.3.4 Nuclear Magnetic Resonance (NMR) Spectroscopy	193
5.1.3.5 X-ray Crystallography	193
5.2 Experimental Procedures for Chapter 2	194
5.3 Experimental Procedures for Chapter 3	211
5.4 Experimental Procedures for Chapter 4	244
References for Chapter 5	260
Appendix	261

Abbreviations

OAc	acetate
MeCN	acetonitrile
acac	acetylacetone
α	alfa
AMLA	ambiphilic metal-ligand activation
<i>et al.</i>	and others
Å	angstroms
Ar	aryl
ASAP	atmospheric solids analysis probe
Bn	benzyl group
bpy	bipyridine
BQ	benzoquinone
br s	broad singlet
Bu	'Normal' butyl
β	beta
br	broad peak
cat	catalyst
<i>ca.</i>	circa (around/about)
CHCl ₃	chloroform
cod	1,5-cyclooctadiene
<i>J</i>	coupling constant
COSY	correlation spectroscopy
°	degrees
°C	degrees centigrade
δ	delta (NMR chemical shift)
DCM	dichloromethane
DMSO	dimethylsulfoxide
Et ₂ O	diethyl ether
dipp	2,6-diisopropylphenyl
d	doublet
dd	doublet of doublets
dt	doublet of triplets

ES	electrophilic substitution
ES	electrospray
eqn.	equation
eq.	equivalents
η	eta
EtOH	ethanol
<i>fac</i> -	facial arrangement
FAB	fast atom bombardment
Fig.	figure
g	gram
Hz	hertz
h	hours
HMBC	heteronuclear multiple bond correlation
HMQC	heteronuclear multiple quantum correlation
HSQC	heteronuclear single quantum coherence
OH	hydroxy
i.e.	Id est (that is)
IR	infra-red
ⁱ Pr	isopropyl
κ	kappa
L	ligand
<i>m/z</i>	mass/charge ratio
Mp	melting point
MS	mass spectrometry
<i>mer</i> -	meridional arrangement
M	metal
MeOH	methanol
Me	methyl
Mg	milligrams
mL	millilitres
mol	moles
μ	mu
m	multiplet

NOESY	nuclear overhauser effect spectroscopy
NMR	nuclear magnetic resonance
OA	oxidative addition
OTf	triflate
ppm	parts per million
Cp^*	pentamethylcyclopentadienyl anion
Ph	phenyl
Pc	phthalocyanine
π	pyridonate
py	pyridinol
pyO	pi
pyOH	pyridine
q	quartet
r.t.	room temperature
σ	sigma
SBM	sigma-bond metathesis
s	singlet
sept	septet
TOFMS	time-of-flight mass spectrometry
THF	tetrahydrofuran
NEt ₃	triethylamine
TFA	trifluoroacetic acid
OTf	trifluoromethanesulfonate
PMe ₃	trimethylphosphine
PPh ₃	triphenylphosphine
Tp	trispyrazolylborate
tpy	terpyridine
^t Bu	<i>tert</i> -butyl
t	triplet
td	triplet of doublets

Chapter 1

Introduction

1.1 Introduction

This thesis is focused on the development of pyridine and pyridone ligands for applications in the coordination chemistry of transition metals and catalysis. The synthesis of transition-metal complexes of pyridines and pyridones that proceeds with C-H activation is considered to be a class of transformations that have the potential to provide opportunities for building new organometallic complexes, and have affected the field of organic synthesis when they are used as catalysts. This chapter will begin with an overview of C-H activation: its importance and mechanisms, ligand types, and will finish by considering multifunctional ligands and their role in catalysis.

1.2 C-H Activation

Carbon-hydrogen bonds are generally viewed as a non-functional group due to their high stability and kinetic inertness.¹ However, when a carbon-hydrogen bond is catalytically activated, it can be easily broken and then replaced with a carbon-X bond (where X is usually carbon, oxygen or nitrogen). This process (**eqn. 1.1**) is generally known as C-H activation (*or* C-H functionalisation). The term often refers to metallation reactions in which metal complexes oxidise an unreactive C-H bond to form a reactive C-M bond which can undergo further transmetallations under milder conditions. Over the last few years, extensive progress and improvements have been made in this field.²⁻⁴ In this section (**1.2**), the main area that will be considered is the C-H activation that can be achieved *via* transition metal complexes.



1.2.1 The Importance of C-H Activation

The field of C-H activation is of both commercial and academic interest. Methanol, for instance, plays a significant role in many important industrial processes, such as the syntheses of plastics and paints. Therefore, chemists are now able to produce methanol from methane to make it a viable and transportable energy source. This conversion is usually performed using a C-H activation reaction which is catalysed by soluble metal salts.⁵

Carbon-carbon bond formation *via* the direct activation of C-H bonds has attracted increasing attention in the medical field.⁶ Drug discovery and production can be readily

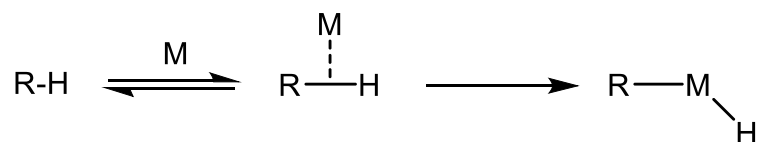
accelerated without the need to prepare starting materials containing a C-X (X = Cl, Br or I) bond. This is actually a useful process for making multi-step synthesis (which is widely used in medicinal chemistry) shorter and reducing the cost and waste in drug production.

Although the field of C-H activation is continuing to grow, experts in organometallic chemistry believe that its progress is particularly slow and they are still far from the ultimate aim.⁷ Many mechanistic problems in this field still need to be solved and developed; for example, targeting a specific C-H bond for functionalisation in a chemical system containing various reactive C-H bonds is extremely difficult. Therefore, C-H activation reactions could truly revolutionise the synthesis of natural, organic and pharmaceutical products if the ability to activate selected C-H bonds was well developed.

1.2.2 Types and Mechanisms of C-H Activation by Metal Complexes

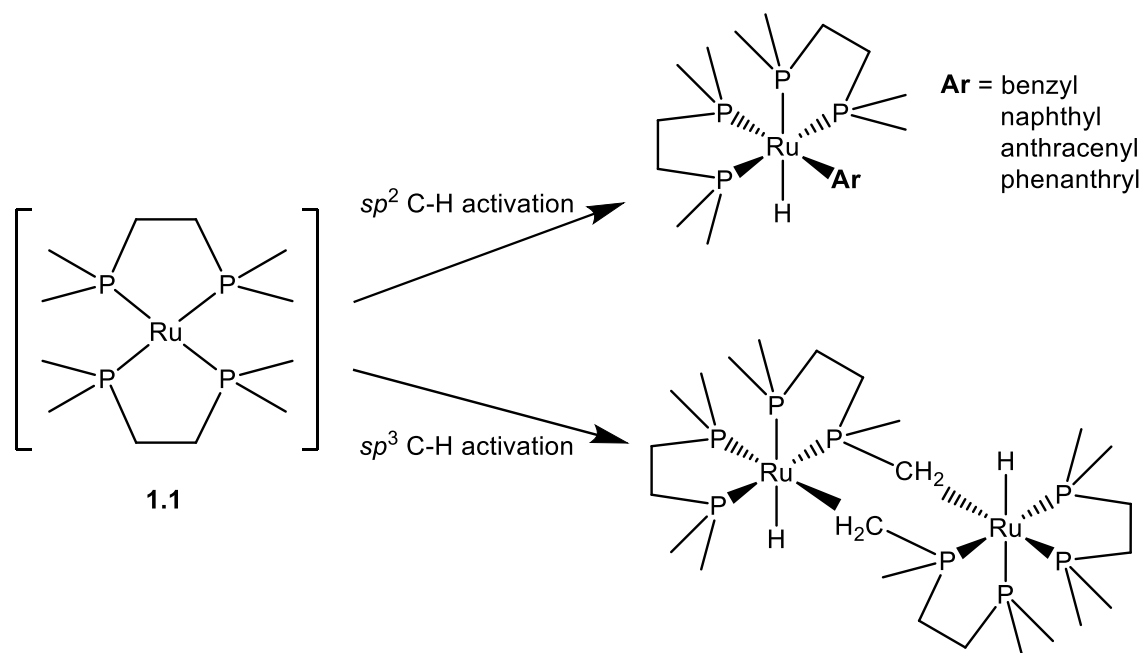
C-H activation mechanisms have been extensively studied in order to gain a better understanding of how these reactions work. Four main mechanisms have been identified for C-H activation processes prior to 2000,⁸ including oxidative addition (OA), sigma-bond metathesis (SBM), electrophilic substitution/activation (ES/EA) and radical mechanisms. These mechanisms were then followed by 1,2-addition⁹⁻¹² and ambiphilic metal-ligand activation (AMLA)^{13,14} which is also known as concerted metallation-deprotonation (CMD).¹⁵ Each mechanism will be briefly discussed, except for the radical mechanism which will not be considered further in this work as it is not a related synthetic pathway.

Synthetic chemists have been interested in mechanisms of C-H activation for several decades, and have exerted considerable effort to develop this field during this time,^{8,16} in particular those researchers who have focused on the activation of C-H bonds using organometallic routes (i.e. reactions involving the formation of a bond between carbon and a central metal). In one of these routes, C-H activation can be achieved with the assistance of a metal from a soluble metal salt or complex. This reaction is commonly known as an oxidative addition reaction, during which the C-H bond is weakly bound to the metal centre in the first step, followed by C-H bond breaking and formation of the M-C bond to give an intermediate containing both a carbon-metal and a metal-hydrogen bond (**Scheme 1.1**).⁵



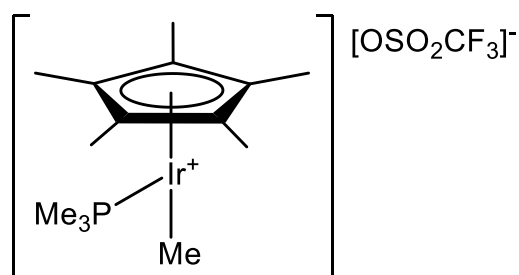
Scheme 1.1: C-H activation by oxidative addition

The first oxidative addition of a C-H bond was reported by Chatt and Davidson in 1965.¹⁷ The authors showed that a C-H bond of arenes (sp^2) or an alkyl side-chain of the 1,2-bis(dimethylphosphino)ethane (dmpe) ligand (sp^3) can be activated by the Ru^0 complex, $[\text{Ru}(\text{dmpe})_2]$ (**1.1**) to give a new series of hydrido-aryl complexes of ruthenium(II) and $[\text{Ru}^{\text{II}}\text{H}(\text{CH}_2\text{-PMe-CH}_2\text{-CH}_2\text{-PMe}_2)(\text{dmpe})]$, respectively (**Scheme 1.2**).



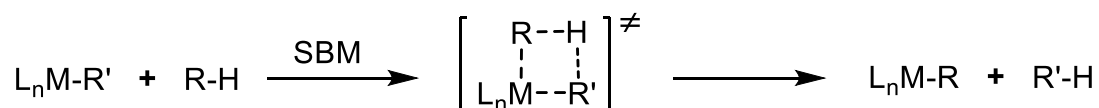
Scheme 1.2: First example of oxidative addition reaction¹⁷

C-H activation by oxidative addition typically gives rise to an increase in both the oxidation state and coordination number of a metal centre. Highly electron-rich metal centres were thought to be necessary for oxidative addition to occur until 1993, when Bergman *et al.*¹⁸ published evidence of a new cationic Ir^{III} complex, $[\text{Cp}^*\text{IrMe}(\text{PMe}_3)](\text{OTf})$ (**1.2**) that was able to activate the C-H bond of an alkane.

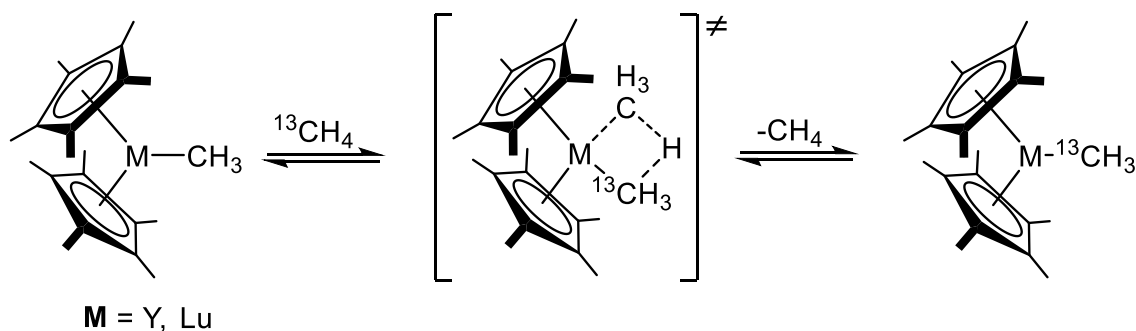


1.2

Sigma-bond metathesis is one of the more common mechanisms that have also been used to replace alkane hydrogens with other atoms or chemical groups, forming a new σ -bond (**Scheme 1.3**). This approach is usually suitable for early transition metals in their highest oxidation states (d^0), and also lanthanide complexes (d^{0f^n}). For this reason, it is not possible for this mechanism type to react *via* oxidative addition, as d -electrons are required for OA to be involved in redox reactions.

**Scheme 1.3:** C-H activation by σ -bond metathesis

In the early 1980s, Watson¹⁹ reported the first well-characterised lanthanide complexes obtained by σ -bond metathesis. They found that the C-H bond in methane ($^{13}\text{CH}_4$) was activated by an organometallic complex, $[(\text{Cp}^*)_2\text{M}(\text{CH}_3)]$ ($\text{M} = \text{Y}$ or Lu) to form a four-membered transition state which then coordinated to the metal centre, replacing the original methyl group (**Scheme 1.4**).

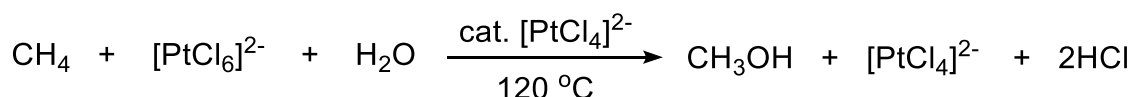
**Scheme 1.4:** First example of σ -bond metathesis

The third mechanistic type of C-H activation is electrophilic C-H activation. This occurs when a C-H bond is activated by an electrophilic metal compound, which is then able to eliminate a proton and create a complex bearing a metal-carbon bond (**Scheme 1.5**).



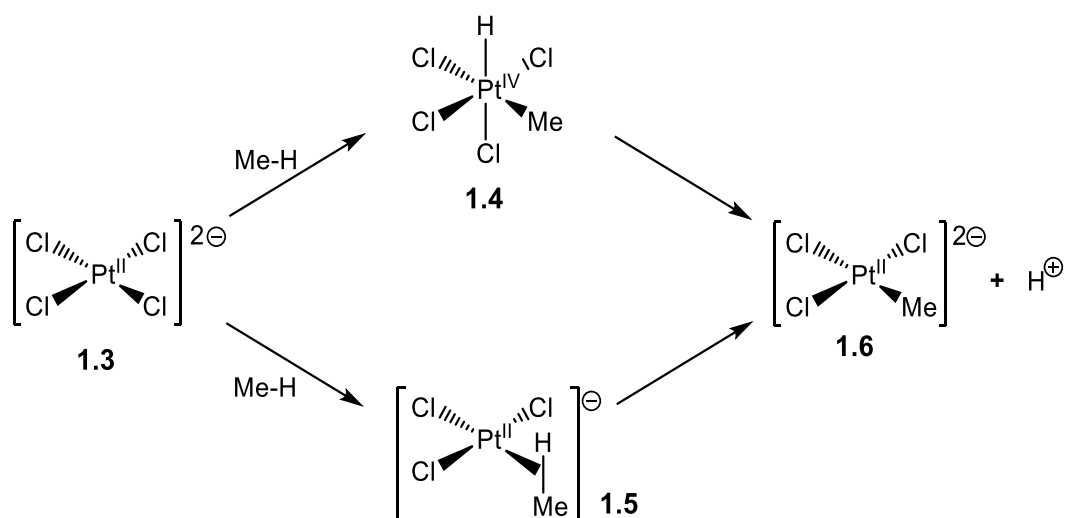
Scheme 1.5: C-H activation by electrophilic activation

Early examples of electrophilic C-H activation reactions were initially reported in 1969 by Shilov *et al.*²⁰ The authors indicated that a mixture of $Na_2[Pt^{II}Cl_4]$ and $H_2[Pt^{IV}Cl_6]$ in aqueous solution activates a C-H bond of methane to obtain the Pt-CH₃ species as an intermediate, followed by production of methanol and other products (**Scheme 1.6**). This significant activation process was ignored for more than a decade²¹ until subsequent studies²² discovered a selective oxidation reaction of methane that later became known as Shilov chemistry.



Scheme 1.6: Shilov chemistry used for methane C-H bond activation

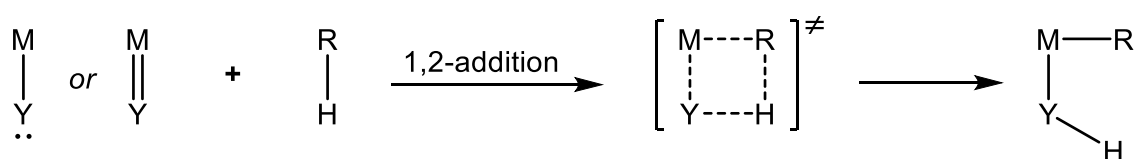
Although the mechanism behind the methane oxidative reaction using platinum salts is still not fully understood,⁵ it is generally thought to proceed *via* an electrophilic C-H activation.²³ Two potential mechanisms for the Shilov reaction have been reported in the literature (**Scheme 1.7**).²⁴⁻²⁶



Scheme 1.7: Proposed mechanisms for methane C-H activation by Pt^{II} salts²⁷

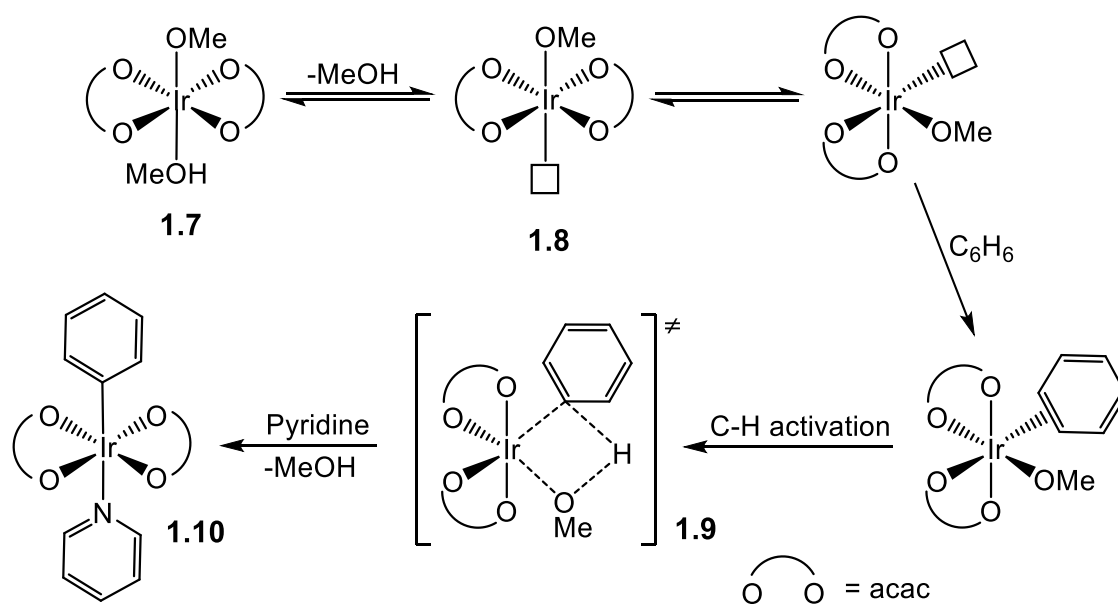
One involves oxidative addition of a methane C-H bond at Pt^{II} (**1.3**), giving a Pt^{IV}-methylhydride intermediate (**1.4**), followed by deprotonation to yield **1.6**. The second involves direct deprotonation of Pt^{II}(σ -Me-H) (**1.5**) which acts as a Lewis acid.

1,2-Addition of a C-H bond across an M-Y bond (where Y is an anionic N- or O-based ligand) is another type of C-H activation mechanism. This type is quite similar to the σ -bond metathesis reaction, where both mechanisms proceed *via* a four-membered ring transition state. However, 1,2-addition was distinguished due to this type of reaction in fact proceeds with the assistance of a lone pair (M-Y:) or π -bonding orbital (M=Y) found in the starting complex (**Scheme 1.8**).²⁸



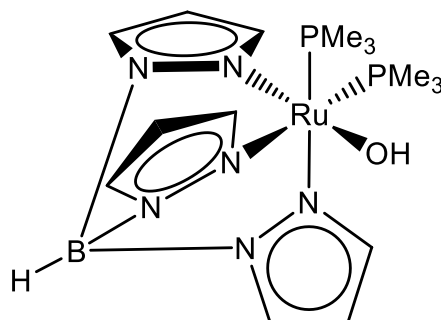
Scheme 1.8: C-H activation by 1,2-addition across metal–ligand bonds

The 1,2-addition to (M-Y:) usually occurs with a late transition metal-N/O single bond, which has at least one lone pair to facilitate the hydrogen transfer in the reaction. The first experimental results of this type were independently presented by two different groups around the same time (2005).^{9,10} Periana *et al.*⁹ demonstrated that one of the C-H bonds of benzene can be activated by an Ir^{III} alkoxo complex (**1.7**) to create the corresponding phenyl complex (**1.10**) in high yield (**Scheme 1.9**).

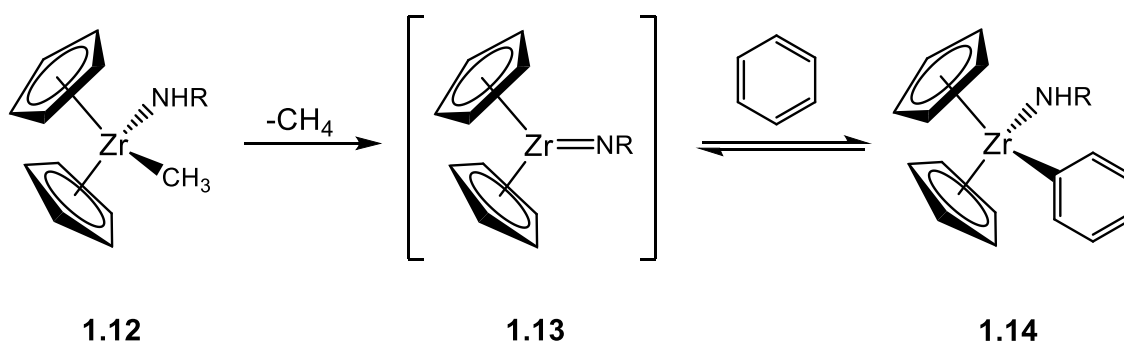


Scheme 1.9: Proposed mechanism for 1,2-addition to (M-Y:)

They proposed a mechanism in which MeOH dissociates from **1.7** to form **1.8**, with a vacant coordination site, before benzene association. C-H activation *via* a four-membered transition state (**1.9**) is then able to take place.⁹ Gunnoe *et al.*¹⁰ later reported a similar result with a monomeric Ru^{II}-hydroxide complex. The authors performed kinetic studies and suggested that [TpRu(PMe₃)₂OH] (**1.11**) can activate one of the C-H bonds of benzene to proceed *via* a 1,2-addition mechanism.

**1.11**

The second pathway for the 1,2-CH-addition reaction, however, seems to take place with a reactive early/middle transition metal-ligand multiple bond (M=Y). This was demonstrated by Bergman and co-workers¹¹ in 1988 when they were able to activate a C-H bond in benzene using imidozirconocene (Cp₂Zr=NR) complexes, where R = *t*Bu, Ph, *t*Bu or *m*-xylene (**Scheme 1.10**). In this reaction, methane is apparently eliminated from **1.12** to generate **1.13**, which subsequently promotes C-H bond cleavage in benzene to afford the phenyl-substituted complex **1.14**. Later, a computational study on similar chemistry found that benzene C-H activation by Zr^{IV} complexes does indeed proceed *via* the 1,2-addition mechanism through the involvement of π -bonding orbitals.^{29,30}

**Scheme 1.10:** C-H activation by 1,2-addition using an imidozirconocene complex¹¹

“Ambiphilic Metal-Ligand Activation” (AMLA) has recently been identified as a form of C-H activation mechanisms and will be briefly discussed here. This mechanism was identified and termed AMLA by Davies and Macgregor⁸ in 2009, while Fagnou *et al.*¹⁵ selected “Concerted Metallation-Deprotonation” (CMD) as the name for a similar process. The mechanism is a bifunctional system in which a C-H bond is activated by an electrophilic metal working together with the assistance of an intramolecular base, such as NaOAc. There are two possible transition states that may be generated during the AMLA C-H activation.²⁷ One is called an AMLA-4 process, in which a four-membered transition state is formed with an oxygen atom of a monodentate acetate group (**Fig. 1.1a**). The other proceeds *via* the formation of a six-membered transition state which is thus known as an AMLA-6 process and involves both oxygen atoms of the [bidentate] acetate ligand (**Fig. 1.1b**).

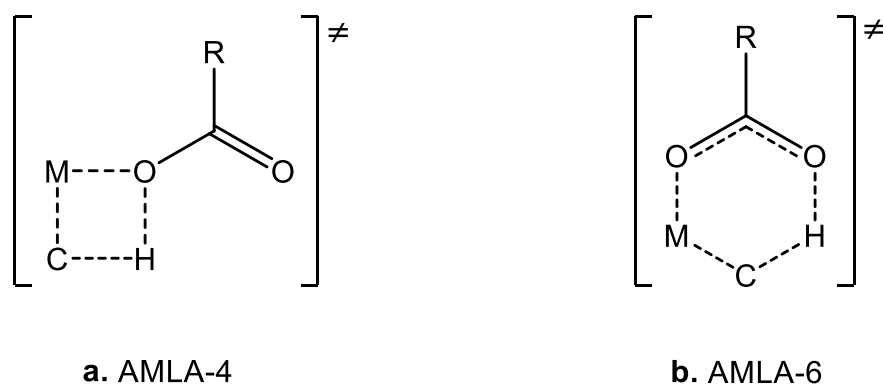
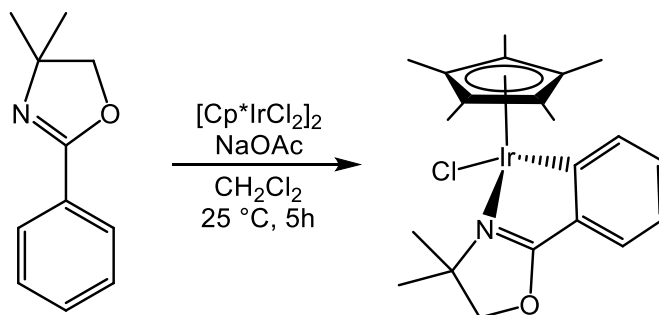


Figure 1.1: The two proposed transition states formed during AMLA C-H activation

The role of the acetate in the AMLA mechanism was synthetically noticed by Davies *et al.*³¹ when one of the C-H bonds in amine-, imine- and oxazoline-base bidentate ligands was activated by a dimeric Ir^{III} complex at room temperature (**Scheme 1.11**).



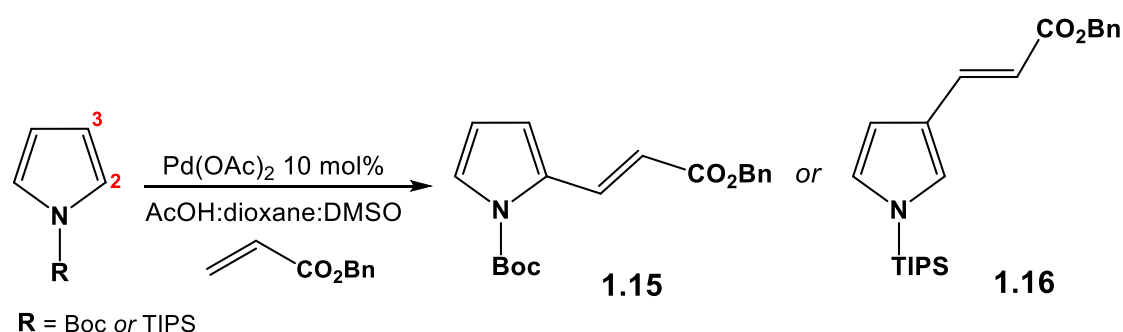
Scheme 1.11: C-H activation of an oxazoline at room temperature

Attempts to carry out the reactions without a base or with NEt_3 instead of NaOAc were unsuccessful. This suggested that the acetate may play an important role in breaking the dimer, exchanging a chloride and generating a cyclic transition state. In order to better understand, and gain further insight into, the AMLA reaction mechanism, various directing groups have been employed by Khamker.²⁷

1.2.3 Selectivity of C-H Activation

As mentioned above (**Section 1.2.1**), the main issue found in the C-H activation field is how to control the selectivity. In order to overcome this problem, numerous research groups³² have carried out kinetic and thermodynamic studies of C-H bonds in various systems. Electronic effects are one of the factors by which a specific C-H bond can be selected. Fagnou *et al.*^{33,34} reported an experimental study on direct intermolecular arylation reactions using $\text{Pd}(\text{OAc})_2$; the results were not in agreement with the selectivity observed in traditional aromatic electrophilic substitution reactions. They found that methoxybenzene, bearing an electron-donating group, leads to a *meta*-selective C-H arylation while fluorobenzene, containing an electron-withdrawing group, directs the new substituent to the *ortho* position. The authors concluded that product selectivity tends to be much more dependent on C-H acidity than arene nucleophilicity.

Another important factor in controlling the selectivity of C-H activation reactions is that of steric effects. The catalytic aerobic pyrrole C-H bond olefination reaction has been developed by Gaunt and co-workers³⁵ to give **1.15** or **1.16** by activating either the C2 or C3 position, respectively (**Scheme 1.12**).

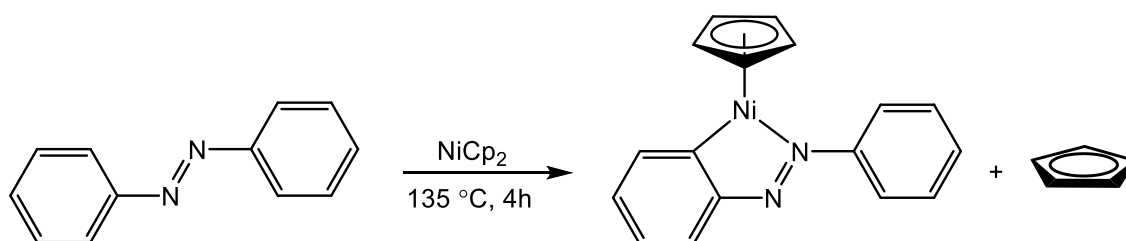


Scheme 1.12: Steric effect on pyrrole C-H olefination

The authors found when an N-protecting group such as tert-butyloxycarbonyl (Boc) was used, the reaction is directed to occur solely at the C2 position to form **1.15**, but when a bulky group such as triisopropylsilyl (TIPS) was employed as a protecting group, the

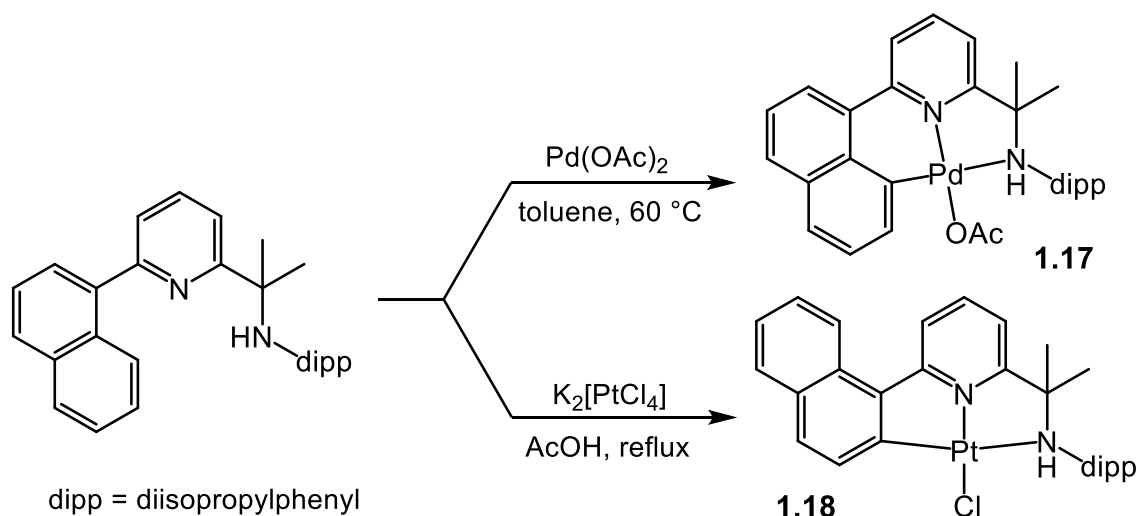
reaction selectivity goes on the C3 position to generate **1.16**. In the latter case, the large TIPS group appeared to prevent C-H activation at the C2 position.

The third factor used for controlled site-selective C-H activation is the use of a directing group. In this process, the reactions are often initiated by the binding of an electrophilic metal centre to an organic chelating ligand through the donor group, such as N, O or P, followed by C-H activation which usually occurs at the *ortho* position to eventually form a cyclometallated complex. Kleiman *et al.*³⁶ first reported the selectivity of C-H activation *via* a directing group in 1963. They carried out the cyclometallation of azobenzene with NiCp₂ and showed that the azo group can direct the metal centre to activate the *ortho* C-H bond (**Scheme 1.13**).



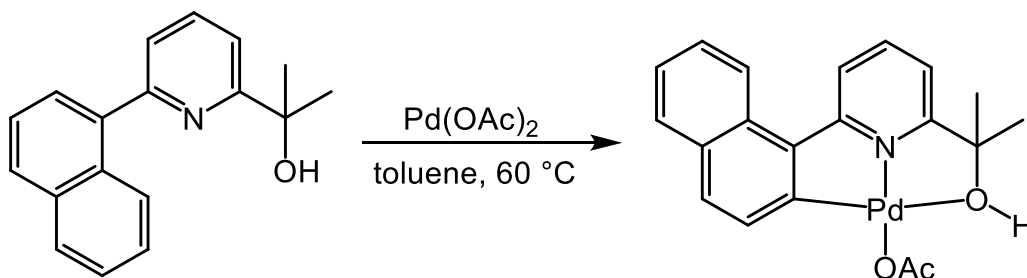
Scheme 1.13: Selective C-H activation through the use of a directing group

Our research group has recently reported the palladium/platinum chemistry of naphthyl-armed *NNC* and *ONC* pyridine-based pincer ligands.^{37,38} The reaction of *NNC*_{nap} with Pd(OAc)₂ gave the *peri*-activated product (**1.17**), while with K₂[PtCl₄] the *ortho*-activated platinum(II) pincer complex (**1.18**) was obtained exclusively (**Scheme 1.14**).



Scheme 1.14: C-H activations with naphthyl-armed *NNC* ligand

They also investigated the influences of varied donor atoms on C-H activation by using alcohol-armed analogue, ONC_{nap} ligand. The reaction of this pincer ligand with $Pd(OAc)_2$ showed *ortho*-C-H activation on the naphthyl moiety to afford *ortho*- $[(ONC_{nap})Pd(OAc)]$ (**Scheme 1.15**).^{37,38}



Scheme 1.15: C-H activation of ONC_{nap} with $Pd(OAc)_2$

1.3 Ligand Types

In coordination chemistry, a ligand is an ionic or neutral molecule which is able to bind to a metal centre to form a metal-ligand complex. Most ligands have one or more lone pairs of electrons, allowing them to act as electron donors (Lewis bases) toward the acceptor metal centres (Lewis acids) leading to the formation of a covalent bond. Ligands can be classified in different ways, however, the main means of classification is by the number of the donor sites (the denticity), that includes monodentate (κ^1), bidentate (κ^2), tridentate (κ^3), and so on.

1.3.1 Monodentate Ligands

Ligands with only one potential donor atom are known as monodentate, such as halides, water, phosphines and nitrogen-based ligands. A brief discussion here will focus on these four types of monodentate ligands.

a. Halide Ligands

Monodentate halide ligands that fall into this category include F, Cl, Br and I. In addition to being good σ -donors, the halides also act as good π -donors. These ligands usually bind to a central metal in a terminal manner (though sometimes in a bridging manner, albeit far less frequently) to give a metal halide salt. There are numerous examples in the literature of metal halide salts such as AlF_3 , K_2PtCl_4 , $[\text{NEt}_4]_2[\text{Pd}_2\text{Br}_6]$ and NiI_2 . The structure of K_2PtCl_4 tends to adopt a square planar geometry where all four chloride ligands are terminally connected to the metal centre with all atoms lying in the same plane (**Fig. 1.2a**). In contrast, the bromo-bridged complex (**Fig. 1.2b**) is preferentially formed, in which each bridging (μ) bromide forms a coordinate (dative covalent) bond with a different Pd centre.³⁹

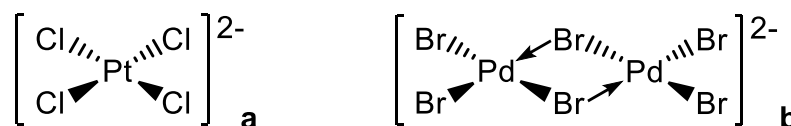


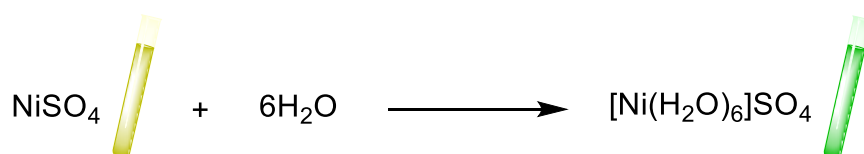
Figure 1.2: Tetrachloroplatinate(II) anion (**a**) and dimeric tribromopalladate(II) anion (**b**)

b. Aqua Ligands

Metals coordinated with one or more water molecules as ligands are known as metal aqua complexes, including homoleptic and heteroleptic hydrate complexes. In the

homoleptic case, water is the only ligand bonded to the metal centre. These are mostly reported as examples with the general formula $[M(H_2O)_6]^{2+}$ and $[M(H_2O)_6]^{3+}$, though metal aqua complexes with lower coordination numbers are also possible, such as square-planar hydrate palladium(II) and platinum(II) complexes with the general formula $[M(H_2O)_4]^{2+}$.⁴⁰ There have been extensive studies made with the preparation, isolation,^{41,42} structural analysis and ligand substitution mechanism⁴³ of both homoleptic aqua Pd^{II} and Pt^{II} complexes. However, to the best of my knowledge, solid-state X-ray crystal structure determination of both complexes has not been reported to date; this might be attributed to their stability in the solid state.⁴⁰

When transition metal salts undergo the hydration process, a colour change reaction usually occurs affording the hydrated complexes. For instance, a solution of anhydrous NiSO₄ gradually changes in colour from yellow to green, indicating that water molecules have coordinated to the metal centre to give hexahydrate nickel(II) sulphate, $[Ni(H_2O)_6][SO_4]$ (**Scheme 1.16**). The starting material and product will have different structural, geometric, and physical properties.



Scheme 1.16: Colour change on adding water to the anhydrous Ni^{II} salt

Heteroleptic *octahedral* hydrate complexes, for example, tend to adopt the general formula $[ML_n(H_2O)_{6-n}]^{\pm}$, where the central metal is coordinated by a mix of aqua and other different ligands. There are many examples in the literature of this type of complex, but the most well-known class is the hydrated metal halide derivatives, such as *trans*- $[FeBr_2(H_2O)_4]$, *trans*- $[CoCl_4(H_2O)_2]$ and *cis*- $[NiCl_2(H_2O)_4]$.

c. Phosphine Ligands

Monophosphines, which have the general formula PR₃ (where R = alkyl, aryl, H, halide, etc.), are one of the most widely used monodentate ligand systems for coordination chemistry. Some typical monodentate phosphine ligands are shown in **Figure 1.3**.

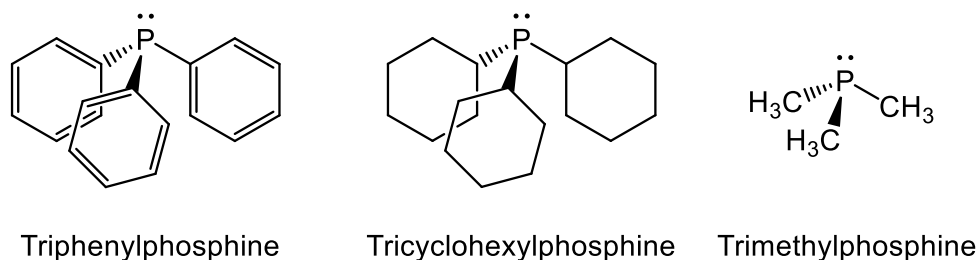


Figure 1.3: Monodentate phosphine ligands

Various elements, including transition metals, have a high coordination affinity for a variety of phosphine ligands. This phenomenon appears to be due to the ability of phosphines to act as both σ -donors *and* π -acceptors with the central metal, affording metal phosphine complexes (**Fig. 1.4**). Specifically, σ -donation occurs from the lone pair of the phosphorus atom to empty metal orbitals, whilst the π -acidity involves electron density acceptance from the filled metal orbitals to empty orbitals of the phosphorus ligand (strong π -backbonding). This feature can be easily tuned by varying the steric and/or electronic nature of the R groups on the phosphorus atom (PR_3),⁴⁴ which may lead to large changes in activity, basicity, selectivity, solubility and the stability of many catalytic processes these ligands are involved in.⁴⁵⁻⁴⁷

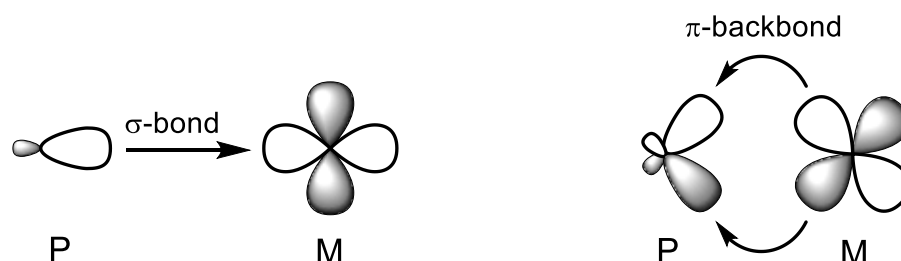


Figure 1.4: Bonding in phosphine complexes

The most common organophosphorus compound used in the synthesis of organometallic complexes is triphenylphosphine (PPh_3), which can be easily oxidised by air to give triphenylphosphine oxide (OPPh_3), with a strong $\text{P}=\text{O}$ bond. Metal- PPh_3 complexes are widely used as catalysts in many catalytic reactions, including hydrogenation,⁴⁸ cyclisation⁴⁹ and cross-coupling reactions.⁵⁰ Several transition metal complexes incorporating PPh_3 as a ligand form these types of highly effective catalysts, such as first-generation Grubbs' catalysts, Wilkinson's catalyst $[\text{Rh}(\text{PPh}_3)_3\text{Cl}]$ and tetrakis(triphenylphosphine)palladium(0) $[\text{Pd}(\text{PPh}_3)_4]$.

d. Nitrogen-based Ligands

N-donor ligands normally act as good σ -donors and are able to bind easily to a central metal forming a metal-nitrogen (M-N) bond. A wide variety of complexes containing monodentate nitrogen donor ligands with different metals have been reported in the literature.⁵¹ These can be grouped into classes according to the type of nitrogen coordinated to the metal centre. Elsevier *et al.*⁵¹ have been able to synthesise and isolate unusual room temperature stable $[\text{Pd}^0(\kappa^1\text{-L})_2(\eta^2\text{-ma})]$ complexes, where L = ammonia (1.19), aniline (1.20), diethylamine (1.21) or pyridine (1.22); and ma is maleic anhydride (Fig. 1.5).

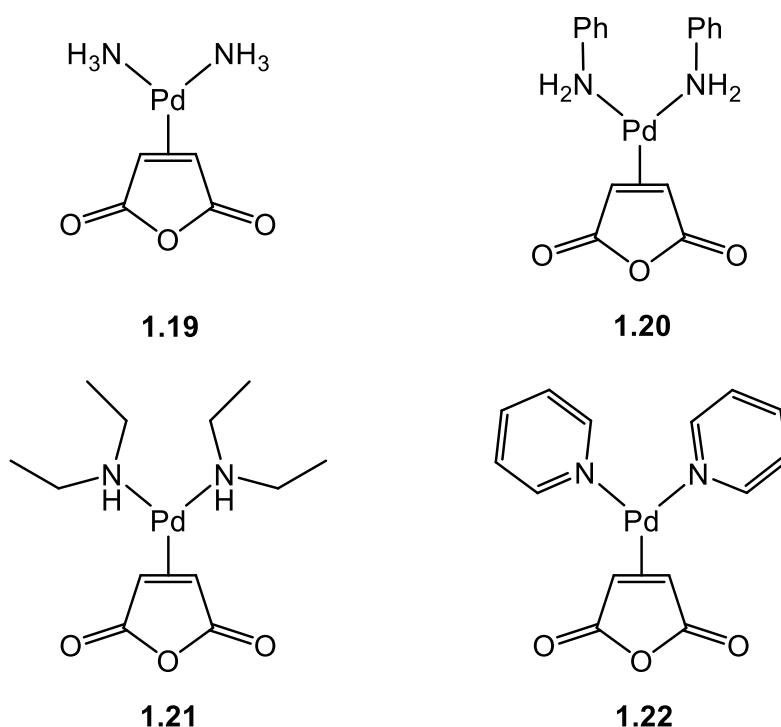
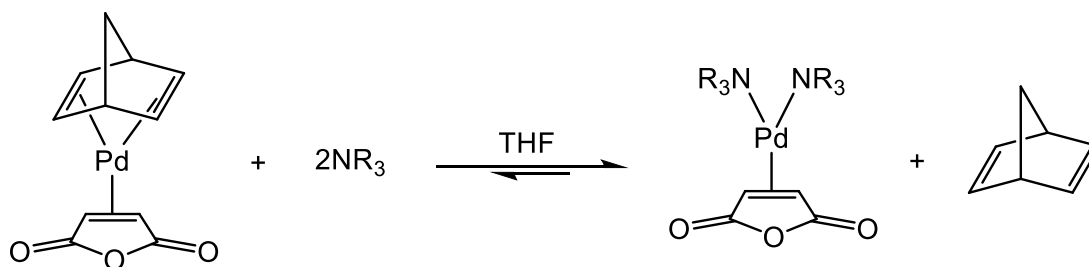


Figure 1.5: Structure of $[\text{Pd}^0(\kappa^1\text{-L})_2(\eta^2\text{-ma})]$ complexes

These Pd^0 complexes containing simple monodentate N ligands were prepared using the precursor complex, $[\text{Pd}(\eta^2, \eta^2\text{-norbornadiene})(\eta^2\text{-ma})]$, which undergoes a ligand exchange reaction with an excess of the N ligand in THF (**Scheme 1.17**). The isolated products were then characterised using a variety of techniques including FT-IR, and ^1H and ^{13}C NMR spectroscopies. They were also able to obtain crystals of X-ray quality for $[\text{Pd}^0(\kappa^1\text{-py})_2(\eta^2\text{-ma})]$ using a solvent diffusion technique with pyridine/THF/diethyl ether. X-ray crystallographic studies of the compound revealed a slightly distorted trigonal planar structure with the palladium atom bonded to two pyridines, and to the C=C bond of the maleic anhydride.⁵¹



Scheme 1.17: Synthesis of $[\text{Pd}^0(\kappa^1\text{-L})_2(\eta^2\text{-ma})]$ complexes

1.3.2 Bidentate Ligands

The term “bidentate” refers to the ligand binding to the metal centre through two atoms. A variety of binding modes are possible for bidentate ligands in general. These include terminal, chelating and bridging binding modes^{52,53} (**Fig. 1.6**).

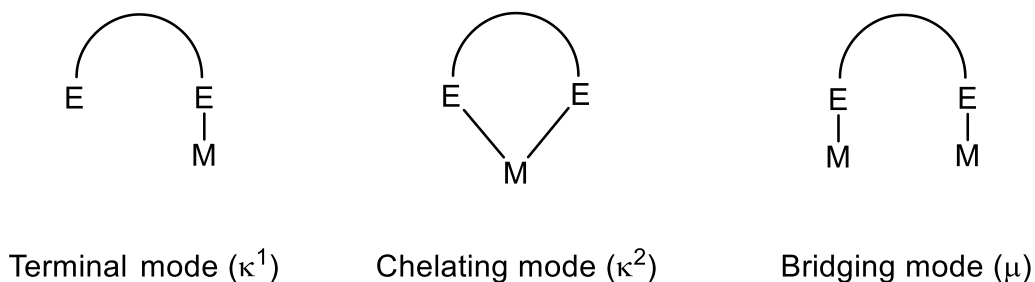


Figure 1.6: Bidentate binding modes (E = donating group)

Terminal binding (κ^1) involves the binding of one donor atom of the ligand to one metal centre with the second donor atom left “dangling”. The chelating binding mode (κ^2) involves binding between both donor atoms and only one metal centre, forming a metalated ring, while the bridging binding mode (μ) involves the binding of both donor atoms, but each to a separate metal centre.

In the coordination chemistry of transition metals, bidentate ligands can be classified, based on their charges, into two different categories: neutral and anionic.

a. Neutral Bidentate Ligands

A neutral bidentate ligand normally has no charge and acts as a Lewis base (electron donor) to bind to a transition metal centre, forming a dative covalent bond (i.e., no charge will be given to the metal centre from the ligand). Symmetrical and unsymmetrical bidentate ligands are both widely used in coordination chemistry.

However, symmetrical ligands are often more preferable in organometallic synthesis due to their ease of coordination and characterisation. Among the many neutral and symmetrical bidentate ligands that have been used with transition metals, N^N and P^P bidentate ligands are amongst the most common (**Fig. 1.7**).

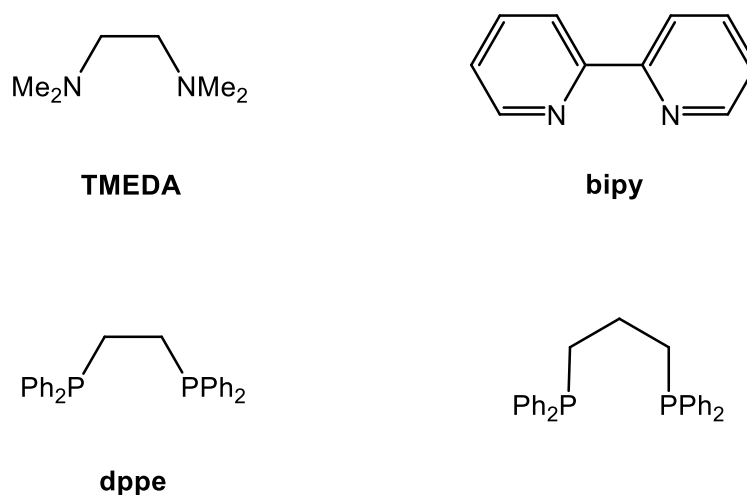


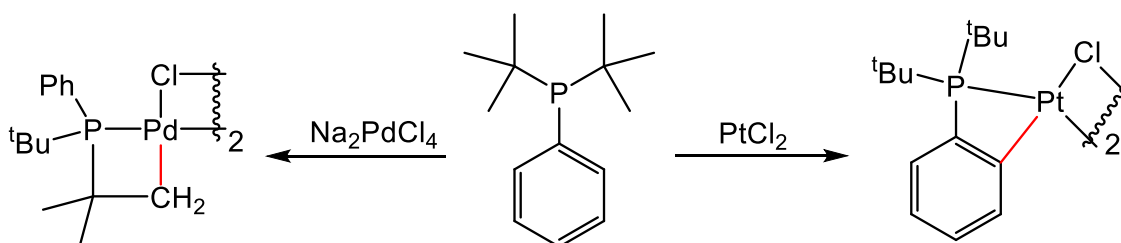
Figure 1.7: Common neutral and symmetrical bidentate ligands (where **TMEDA** = *N, N', N'*-tetramethylethylenediamine, **bipy** = 2,2'-bipyridine, **dppe** = 1,2-bis(diphenylphosphino)ethane, **dppp** = 1,3-bis(diphenylphosphino)propane)

Ligands with two donor atoms may stabilise metal centres more than two monodentate ligands due to the chelate effect. One of the favoured P^P ligands that can bind tightly to transition metals is Ph₂P-X-PPh₂ (where X = a spacer group). They are very important because the steric properties of the phenyl substituents on the phosphorus atoms of such ligands plays a dominant role in determining the coordination geometry present in metal complexes. Also, the steric and electronic properties of the phenyl diphosphine ligands can be altered in a periodic and systematic fashion by varying the nature of the ligand backbone.⁵⁴ Diphenylphosphine ligands are used to give a complex where the ligand, in most cases, coordinates to a single metal centre (chelating mode). It is well known that the P^P chelates possess a rigid P-M-P angle, often called the “bite angle”.⁵⁵ The use of chelating ligands in coordination and organometallic compounds generally involves a slow attack by one arm of the ligand on the metal followed by rapid ring closure by the second arm.⁵⁶ There are a great number of mono-metal complexes with chelating P^P ligands reported in the literature.

b. Anionic Bidentate Ligands

Monoanionic bidentate ligands have the ability to occupy two coordination sites, with only one valence electron to form a covalent bond with metal centres (M-X where X = C, O, N etc.). The most convenient type of monoanionic bidentate ligands is N⁺C⁻-bidentate ligands. They have commonly been employed in organometallic chemistry, normally to afford cyclometallated complexes through C-H activation.

Metallacycles, initially synthesised by Kleiman and Dubeck in 1963,³⁶ have recently attracted considerable interest because their reactions could provide for the spontaneous cleavage of strong, unreactive C-H bonds in suitable positions after the formation of an E-M bond. Moreover, the cyclometallation leads to the formation of organometallic compounds with remarkable stability. A number of transition metals have been shown to form a variety of cyclometallated complexes. The vast majority of these organometallic compounds involve the platinum group metals: Ru, Os, Rh, Ir, Pd and Pt.⁵⁷ Notably, the nature of the transition metal used in cyclometallation plays a significant role in the selectivity. The C_{aryl}-H bond in PPh^tBu₂ prefers to be activated to form a four-membered C⁺P-cyclometallated complex when platinum(II) chloride is used.⁵⁸ However, Na₂PdCl₄ favourably activates a C(sp³)-H bond rather than an aromatic C-H bond (**Scheme 1.18**).⁵⁹



Scheme 1.18: Selectivity in cyclometallation

There are various types of chelating ligands that have been used in cyclometallation reactions. P-substituted ligands and their reactivity with many transition metals have been extensively investigated, while fewer studies have been performed regarding the use of N-substituents in cyclometallation reactions.⁵⁷ In general, Lewis bases can be classified based on their affinity toward transition metals into hard and soft donor groups. Therefore, cyclometallation with early transition metals appears to be the most convenient when the ligand contains hard donor bases, such as amines. Late transition metals are found to react

smoothly with soft phosphine and sulphide bases to yield metallacycles. However, there are numerous examples in the literature of complexes that show a mismatch between hard/soft Lewis-acidic metal centres and their hard/soft Lewis-basic counterparts. Palladium(II) salts, for example, have been successfully used in cyclometallation reactions with hard amine donors.⁶⁰ The metal-nitrogen bond (M-N) in late transition metal complexes is considered to be weaker, and hence less stable, than the bond with a phosphorus atom (M-P). This could actually explain why the syntheses of organometallic compounds containing N-cyclometallated ligands are much fewer in number than those with P-substituents.

1.3.3 Tridentate Ligands

Tridentate ligands have three donor atoms by which they are able to coordinate a metal centre at three positions. Such ligands can be found as either symmetrical or unsymmetrical and either neutral or anionic. Highly stable metal complexes can be achieved when these tridentate ligands act as chelating ligands with a metal centre, forming two four-, five-, six- or seven-membered rings. Pincer metallacycles are a well-studied area of organometallic complexes with applications in synthesis and catalysis.⁵⁷ Therefore, a variety of complexes containing tridentate ligands have been reported; however, only those bearing carbon-based pincer ligands will be discussed in this section. Examples of symmetric and unsymmetric pincer ligands are shown in **Figure 1.8**.

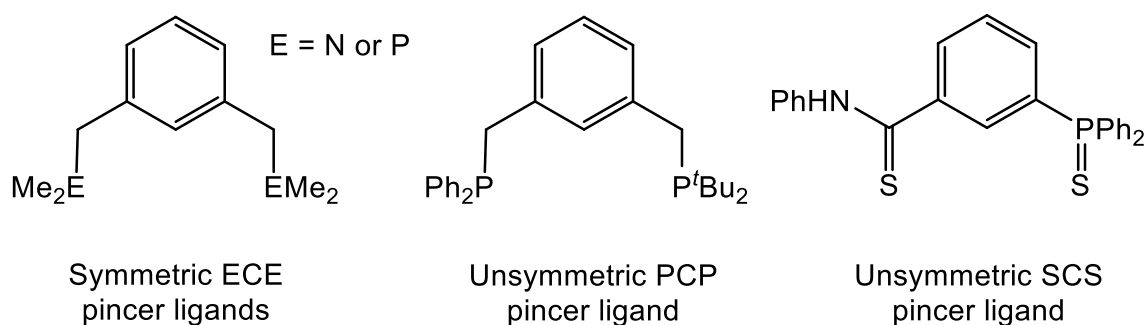


Figure 1.8: Examples of symmetric and unsymmetric pincer ligands

Pincer ligands, also called “monoanionic” tridentate ligands, have received considerable attention from academic and industrial researchers since their discovery in the late 1970s.⁶¹ In cyclometallation, a pincer ligand usually binds to a metal centre *via* a central anionic carbon (C₂) and two pendant donor groups. Such complexes have been extensively employed in various applications, such as asymmetric allylic alkylation,⁶²

asymmetric aldol condensation,⁶³ Heck reactions⁶⁴ and aliphatic dehydrogenation⁶⁵ reactions in which C-H bonds in substrates are activated. They have also been used in bio-organometallic applications as they show interesting photochemical and photophysical properties.⁵⁷

The most widely used type of ligands with transition metals is an E^κC^κE-pincer (where E = P, S or N). The P^κC^κP- and S^κC^κS-pincer ligands with a central aromatic ring have shown tridentate binding as a dominant mode, while a variety of binding modes involving a C₂-M bond are possible for N^κC^κN-ligands. These include monodentate C-, bidentate C^κN-, tridentate N^κC^κN- and three centre-two electron bridge-bonding modes (**Fig. 1.9**).⁶⁶ C- and C^κN-bonded N^κC^κN-pincer complexes are typically obtained when one or both of N-substituents cannot bind to the central metal. The formation of such complexes was noted in the case of the presence of other stronger donor ligands in the system. *mer*- and *fac*-N^κC^κN-tridentate binding modes are possible when the three atoms bind to the metal centre at the same time.⁶⁷ The last mode, [κ^3 -(N^κ(μ -C₂)^κN)], involves the binding of the C₂ to a separate metal centre, and each N-arm ligand is coordinated to one of the bridged metal centres.

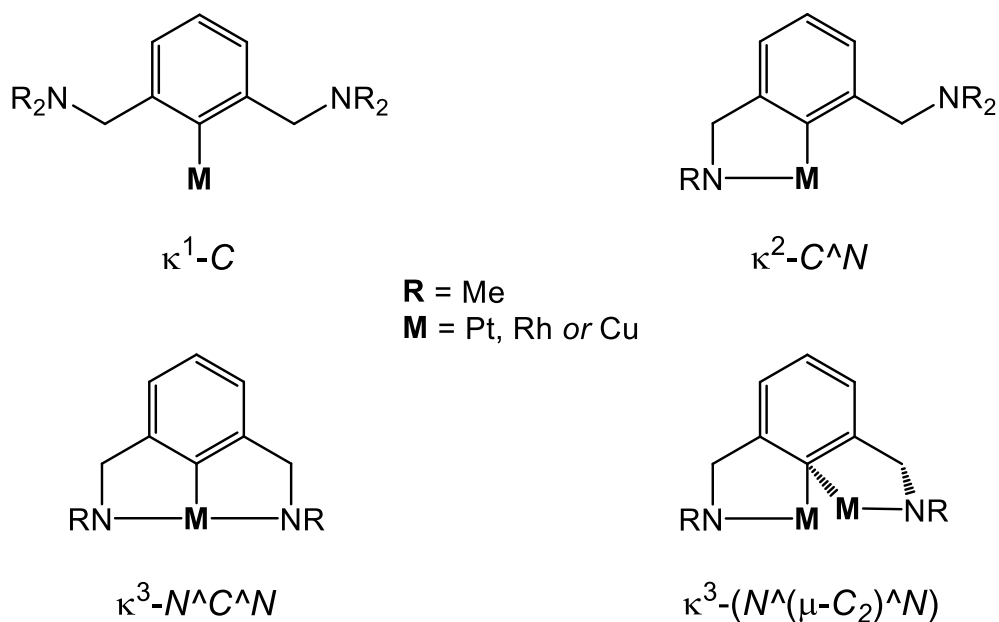
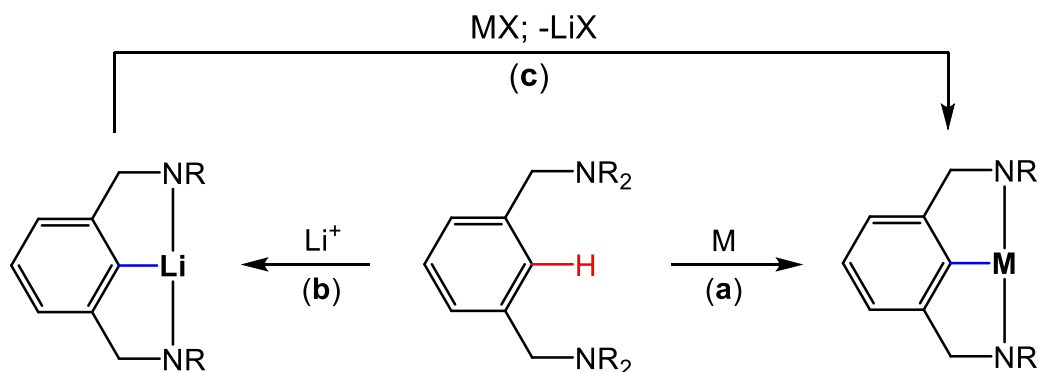


Figure 1.9: N^κC^κN-pincer ligand binding modes

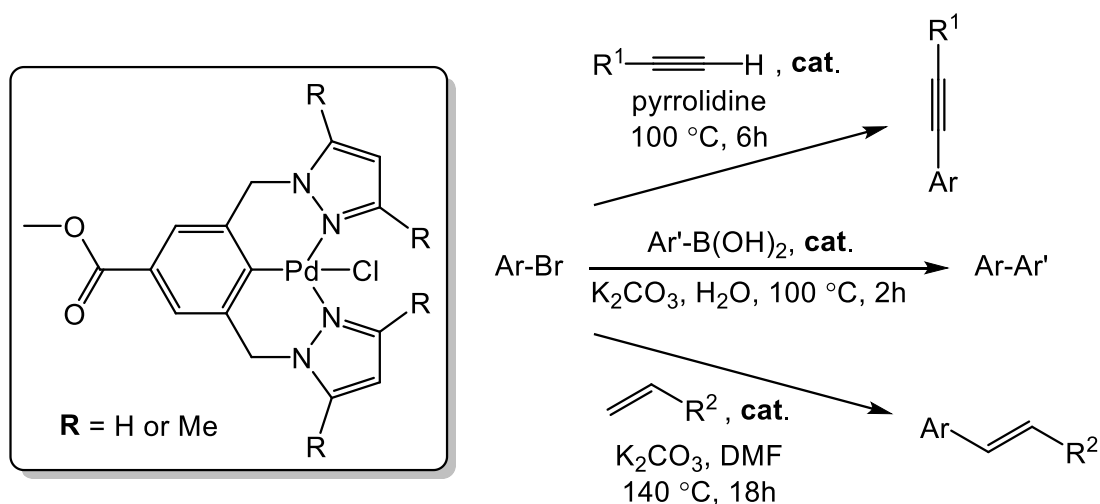
The application of pincer ligands in the coordination chemistry of a number of transition metals, such as Ti, Ta, Fe, Co, Rh, Ir, Ru, Ni, Pd and Pt, has been reported.⁶⁶

$N^{\wedge}C^{\wedge}N$ -pincer transition metal complexes are usually prepared by either direct biscyclometallation (a) or a two-step reaction (b,c) in which the C_2 atom is treated with a reagent, such as lithium, before reacting the ligand with an appropriate metal (transmetallation);⁴⁴ **Scheme 1.19** shows how these two synthetic methods may work.



Scheme 1.19: Synthesis of $N^{\wedge}C^{\wedge}N$ -pincer metal complexes

In aryl-based pincer metal complexes, the C-M sigma bond, supported by two E-M bonds, enables these complexes to increase their stabilities towards heat, air and moisture.⁶⁸ As a result, these types of pincer metal complexes have found applications in organic synthesis as catalysts, even under high temperature conditions. Some useful applications of $N^{\wedge}C^{\wedge}N$ pincer palladium complexes are illustrated below in **Scheme 1.20**.⁶⁹



Scheme 1.20: Coupling reactions of aryl bromide catalysed by pincer Pd^{II} complexes

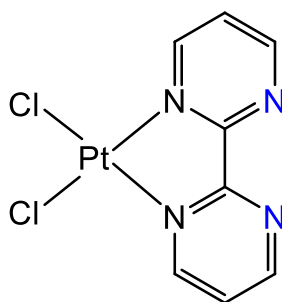
1.4 Multifunctional Ligands

Functionalisation of ligands has been the focus of intense research among the variety of techniques used in coordination chemistry in order to develop the applications of transition metal complexes. It is believed that adding new functional groups on a ligand coordinated to the transition metal may enhance their ability to impart different properties to the metal complex.⁷⁰ The role of functionalised ligands is more than just that of binding to a metal centre; there are many useful additional functions that may help complexes to play other roles, in particular in organic synthesis. These functions⁷⁰ include:

1. Proton-responsive ligands; able to accept or donate one or more protons.
2. H-bonding ligands; indicating partial proton transfer between two partners.
3. Electron-responsive ligands; able to gain or lose one or more electrons.
4. Photo-responsive ligands; able to undergo useful changes upon irradiation.
5. Hemilabile ligands; able to provide a vacant coordination site on a central metal complex.
6. Ligands that have molecular recognition.
7. Polymer- and biopolymer-based ligands

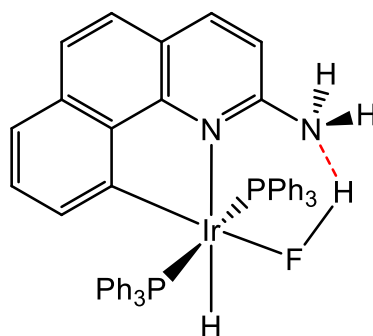
Considering the above-mentioned functions, extensive research has been conducted in the synthesis and modification of ligands to optimise and improve the catalytic chemical processes.⁷¹ This section will give a brief discussion of the first four functions (1-4).

In catalytic transformations, proton-responsive ligands have the ability to transfer protons to or from the substrate and hence act as greater or lesser donors, respectively. Periana *et al.*^{72,73} have provided an excellent illustration of the role of proton-responsive ligands in the catalytic conversion of alkanes to oxygenates, *through* C-H activation followed by functionalisation of the M-C intermediates. The authors found that using (bpym)PtCl₂ (**1.23**), where bpym is 2,2'-bipyrimidine, in strong acidic media can generate methanol from methane through ligand protonation. The free nitrogen lone pairs of the coordinated bpym (shown in blue in **1.23**) are able to accept two protons from the strongly acid solvent. The protonation therefore leads to the enhancement of the π -donor power of the ligand and hence coordination of the ligand to the metal centre would be stronger and more stable, even in the harsh acid environment. The ligand protonation would therefore facilitate C-H activation by increasing the electrophilicity of the catalyst (in particular at the metal centre).



1.23

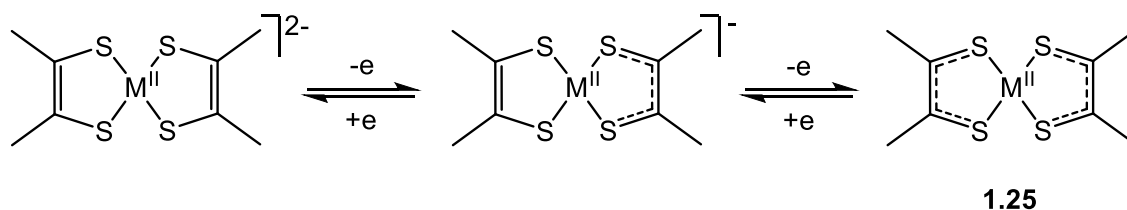
Hydrogen bonding is a type of molecular recognition in which a non-covalent bond can be formed between two or more molecules. Hydrogen-bonding ligands are quite similar to proton-responsive ligands, as the hydrogen bond is actually an “incomplete” proton transfer. It has been found that coordinated H-bonding ligands may help a metal centre to bind a substrate through a hydrogen bonding group such as OH, NH₂ or HF. The Ir-(FH) complex (**1.24**) represents an example of complexes stabilised by a hydrogen bond that is provided by the pendant amino group attached directly to the ligand. The ¹H NMR spectrum showed a high value for the H-F coupling (¹J_{H-F} = 440 Hz) which is characteristic of a hydrogen-bonded N···H-F structure, rather than a hydrogen-bonded N-H···F system (where ¹J_{H···F} is normally much lower, ~52 Hz).⁷⁴



1.24

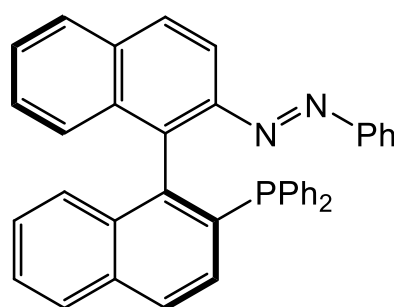
Electron-responsive ligands are not only able to exhibit different properties by gaining or losing electrons but to take part in multi-electron processes in which the metal and ligand can combine their redox powers. Gray *et al.*⁷⁵ studied the molecular and electronic structures of metal bis-dithiolene complexes [ML₂]^Z (M = Ni, Pd or Pt; and z = 2-, 1- or 0) and described **1.25** as a neutral M^{II} species in which each ligand possesses

a radical anion character. Other more recent examples of this type of ligand can be found in the literature.⁷⁶



M = Ni, Pd or Pt

Photo-responsive ligands are another important function that have been used extensively in molecular switches and other applications.⁷⁰ Azo compounds are excellent examples of molecular switches since they can transform between two isomeric forms, *cis* (*Z*) and *trans* (*E*), through irradiation. Kudo and co-workers⁷⁷ reported the first chiral azo-phosphine (**1.26**) which was found to display a *trans*-to-*cis* photoisomerisation upon exposure to UV light (354 nm), and back-isomerise (*cis* to *trans*) upon heating. The authors demonstrated the activity and enantioselectivity of this ligand in Pd-catalysed asymmetric allylic alkylation. Performance of the reaction of *rac*-1,3-diphenyl-2-propenyl acetate with dimethyl malonate as a nucleophile afforded the alkylated product in high yield and with up to 90% enantiomeric excess.



1.26

1.4.1 OH-Functionalised Ligands

In recent years, functionalised ligands have received great attention due to their ability to influence the properties of metal complexes.⁷⁰ Various studies have been conducted in this field in order to improve catalytic systems proceeding with transition metals.⁷¹ The hydroxyl (OH) group is one of the most important functional groups that

has attracted great attention. Ligands with an OH group are usually able to form a hydrogen bond between two partners. H-bonds play a significant role in stabilising a chemical structure and increasing water solubility. These features, and indeed others, have led many researchers to attempt to introduce H-bonds in their synthesis. Shvo's^{78,79} and Knolker's⁸⁰ (**Fig. 1.10**) catalysts, in which a hydroxyl group is coordinated to the cyclopentadienyl ligand, are the best examples of this type of system. These catalysts are known as bifunctional catalysts and have been used in transfer hydrogenation⁸¹ and regioselective oxidation⁸² reactions.

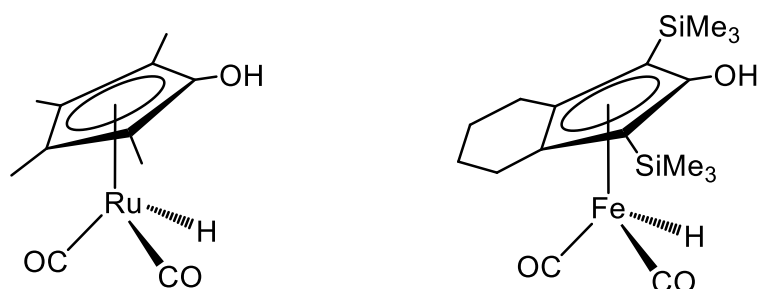
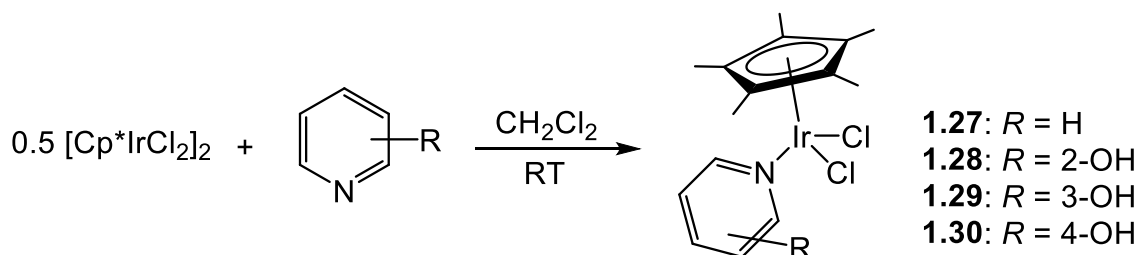


Figure 1.10: Shvo's (left) and Knolker's (right) catalysts

Recently, Fujita *et al.*⁸³ have designed novel Cp*Ir^{III} hydroxypyridine complexes and found them to be efficient catalysts for the dehydrogenative oxidation of alcohols. The catalysts **1.27**, **1.28**, **1.29** and **1.30** were synthesised by the reaction of [Cp*IrCl₂]₂ with pyridine and various hydroxypyridine ligands in DCM at room temperature (**Scheme 1.21**). Solid-state X-ray diffraction analysis of the last three complexes showed that N-bonded Cp*Ir^{III} hydroxypyridine complexes were obtained.

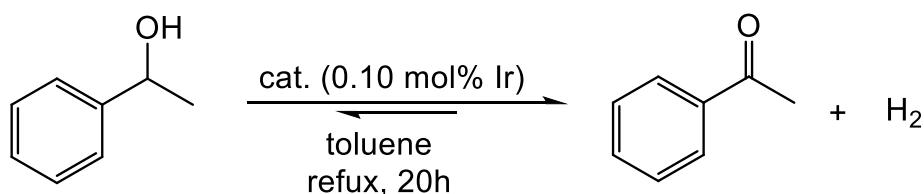


Scheme 1.21: Synthesis of **1.27** and Cp*Ir^{III} hydroxypyridine complexes

As mentioned above, Fujita and co-workers observed a new catalytic system for dehydrogenative oxidation of secondary alcohols to ketones using Cp*Ir^{III} hydroxypyridine complexes in toluene under reflux (**Table 1.1**). When the

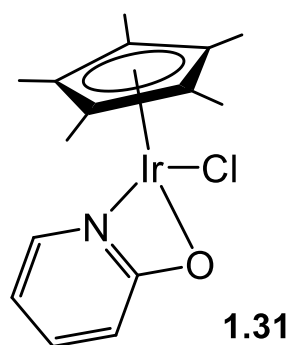
dehydrogenation reaction of 1-phenylethanol was performed in the presence of **1.27** ($R = H$), acetophenone was given in only a 9% yield (entry 1). However, the catalyst with a 2-hydroxypyridine ligand (**1.28**) showed a higher activity and the yield of the product increased up to 70% with a turnover number (700) (entry 2). The reactions using catalysts **1.29** and **1.30** gave the corresponding ketone as well, but only in 10% (entry 3) and 13% (entry 4) yields, respectively.⁸³

Table 1.1: Dehydrogenation of 1-phenylethanol catalysed by various Cp^*Ir^{III} complexes



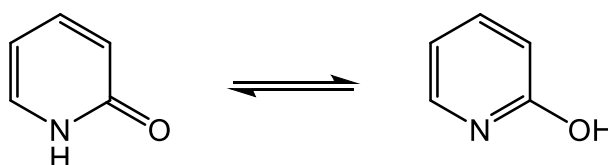
Entry	Catalyst	Conversion (%)	Yield (%)	TON
1	1.27	10	9	90
2	1.28	70	70	700
3	1.29	10	10	100
4	1.30	13	13	130

These results reported in **Table 1.1** led the authors to conclude that the Ir^{III} -catalysed oxidation of alcohols was promoted by the hydroxyl substituent at the 2-position of the pyridine ligand. They proposed a mechanism in which a 2-hydroxypyridonate-chelated intermediate (**1.31**) may act as an active catalytic species in this reaction type. This was supported by synthesising and using **1.31** as a catalyst for alcohol oxidation; **1.31** has a greater activity than **1.28**, giving a high yield of acetophenone.⁸³



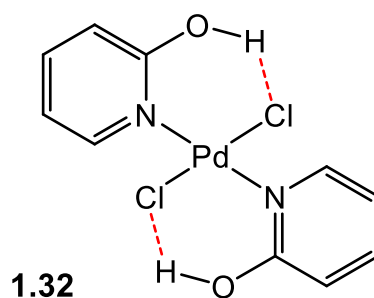
1.4.2 Pyridone-Pyridinol Tautomerism and their Binding Modes

2-Pyridone (2-hydroxypyridine) is a typical example of an organic N-heterocyclic ligand that can undergo lactam-lactim tautomerisation (**Scheme 1.22**). In this case, the hydrogen coordinated to the nitrogen atom in 2-pyridone (lactam form) can also migrate to the oxygen to form 2-hydroxypyridine (lactim form). The lactam tautomer is greatly favoured when the compound exists in the solid state, as determined by high-resolution X-ray and IR data, but the lactim form usually occurs in solution.⁸⁴ Thus, the lactam-lactim tautomeric interconversion of 2-pyridone may coexist in equilibrium as two different tautomers, but a preference for one form may be observed under particular conditions.

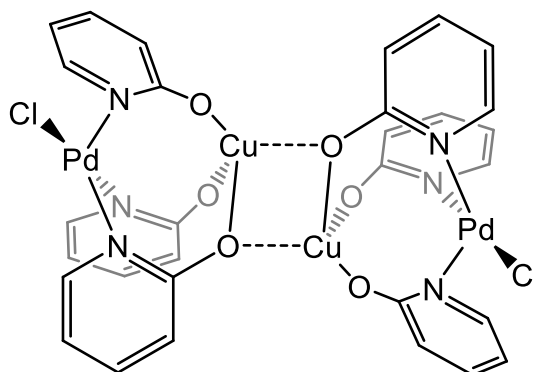


Scheme 1.22: Lactam-lactim tautomerism between 2-hydroxypyridine and 2-pyridone

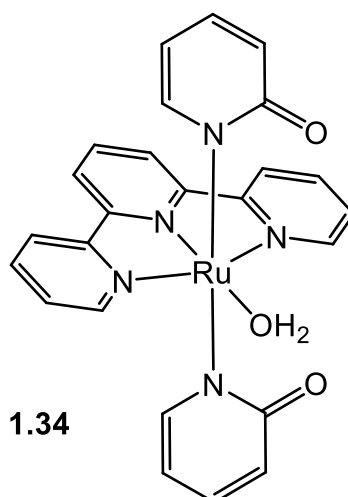
Lactam-lactim tautomeric isomers have attracted considerable attention from various research groups due to their ability to show a variety of coordination modes.⁸⁵ Experimental studies have led to a greater understanding of the reactivity of, in particular, 2-hydroxypyridine as a ligand towards different transition metals. Kong and Rochon reported a range of platinum complexes bearing hydroxypyridine/pyridone derivatives that showed significant anti-tumour activities, in particular the *cis*-isomeric form.⁸⁶ Later, the authors reported similar *cis*- and *trans*-palladium complexes derived from the same ligands.⁸⁷ One of these Pd^{II} complexes is complex **1.32**, which was synthesised by adding 2-hydroxypyridine to Na₂PdCl₄ in water. The infrared spectrum of **1.32** displayed a number of characteristic peaks, indicating that the ligand is in the 2-hydroxypyridine form and coordinates to the Pd^{II} centre through the N-atom. Elemental analysis also confirmed the empirical formula of **1.32**.



In 2004, complex **1.32** was used by Djakovitch *et al.*⁸⁸ as a precursor for the synthesis of a new efficient bimetallic $[\text{PdCl}(\mu\text{-pyridonate})_3\text{Cu}]_2$ catalyst (**1.33**) in indole synthesis *via* the Sonogashira cross-coupling reaction. In this case, the ligand adopts an N[^]O-bridging mode between metal centres. The catalyst **1.33** was obtained by treating **1.32** with CuCl_2 in EtOH and one equivalent of 2-hydroxypyridine.

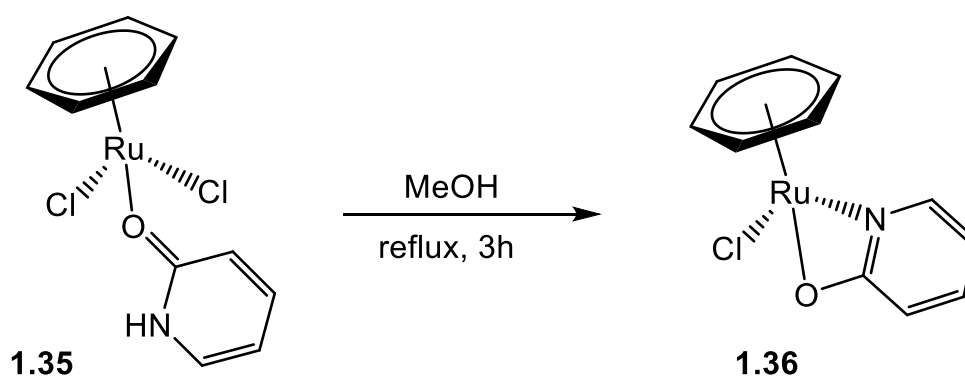
**1.33**

A monodentate N-bound 2-pyridonate ligand is another coordination mode in which the ligand acts as an anionic ligand and coordinates to the metal centre purely through the N-atom. There are only a limited number of examples reported in the literature of transition metal complexes bearing the N-bound 2-pyridonate ligand, including platinum, osmium, ruthenium and cobalt complexes. *trans*- $[(\text{tpy})\text{Ru}(\kappa^1\text{-N-(2-pyridonate)})_2(\text{H}_2\text{O})]$ (**1.34**) was reported as the first example of a ruthenium(II) complex having the 2-pyridonate ligand as a monodentate N-bound lactam ligand.⁸⁵ Complex **1.34** was prepared by reacting $(\text{tpy})\text{RuCl}_3$ with an excess of 2-hydroxypyridine in the presence of NaOH in a mixture of EtOH and water (2:1) under reflux. Using **1.34** as a catalyst for the transfer hydrogenation of ketones led to a high yield (up to 99%) of the corresponding products.⁸⁵

**1.34**

A 2-pyridone (2-hydroxypyridine) ligand acting as an *O*-terminal or as an $N^{\wedge}O$ chelate on a single metal centre is relatively rare.⁸⁹ Tocher and co-workers⁹⁰ found that the reaction of $[\text{Ru}(\eta^6\text{-C}_6\text{H}_6)\text{Cl}_2]_2$ with 2-pyridone in MeOH at ambient temperature gave $[\text{Ru}(\eta^6\text{-C}_6\text{H}_6)\text{Cl}_2(\kappa^1\text{-2-pyridone})]$ (**1.35**) in a 38% yield as an orange solid. The results of ^1H NMR spectroscopy, mass spectrometry and elemental analysis of the product confirmed that benzene, chlorides and 2-pyridone (1:2:1) are coordinated to the ruthenium(II) centre. In addition, the infrared spectrum of **1.35** exhibited stretching bands at 1618 and 3439 cm^{-1} representing vibrations of the C=O and N-H bonds, respectively. The presence of these bands may indicate that the ligand is coordinated to the Ru^{II} centre in a monodentate lactam form *via* the pyridone oxygen atom.

When a methanol solution of **1.35** was heated to reflux for only 3 hours, $[\text{Ru}(\eta^6\text{-C}_6\text{H}_6)\text{Cl}(\kappa^2\text{-pyridonate})]$ **1.36** was obtained as a light brown solid. The same complex (**1.36**) was also generated in even higher yield (66%) by reacting the precursor $[\text{Ru}(\eta^6\text{-C}_6\text{H}_6)\text{Cl}(\text{O}_2\text{CCF}_3)]$ with the 2-pyridone ligand in MeOH under reflux. The results from FT-IR and NMR spectroscopies, elemental analysis, and mass spectrometry are consistent with the $N^{\wedge}O$ chelate Ru^{II} complex (**1.36**). The structure of the complex was further confirmed by a single crystal X-ray determination. The X-ray crystallographic structure for **1.36** revealed that the complex has a distorted tetrahedral molecular geometry with one chelating ($\kappa^2\text{-N}^{\wedge}\text{O}$) pyridonate ligand having a bite angle (O-Ru-N) of approximately 62.5° .⁹⁰



The most important feature of 2-pyridone is the amide group through which dimerisation of two molecules can spontaneously occur through molecular self-assembly or, specifically, by hydrogen bond interactions. There are three possible interactions for making dimeric compounds between the lactam-lactim tautomeric isomers of 2-pyridone,

depending on the form that is involved (**Fig. 1.11**). These include (2-hydroxypyridine)₂, (2-pyridone)₂ and mixed 2-pyridone/2-hydroxypyridine dimerisation modes.⁹¹ However, the last one may require a donating group at the 6-position to show this binding mode.⁹²

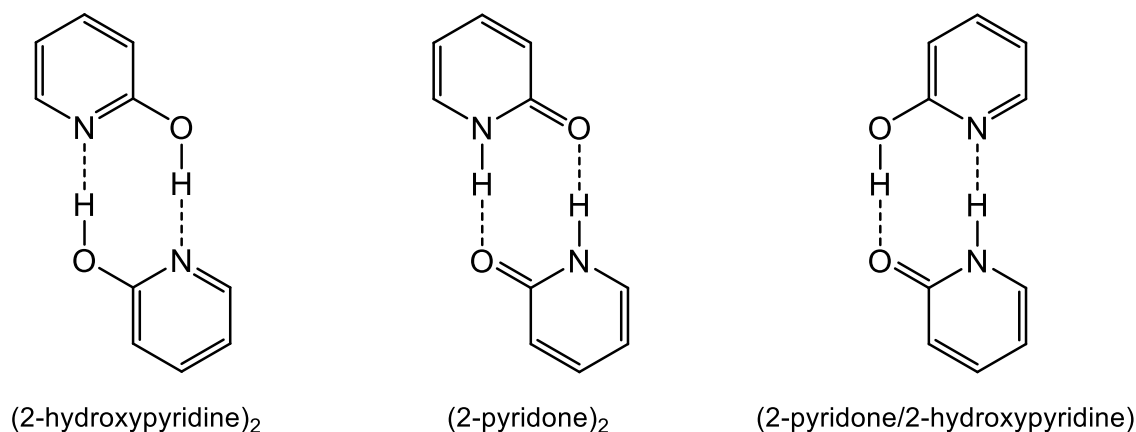
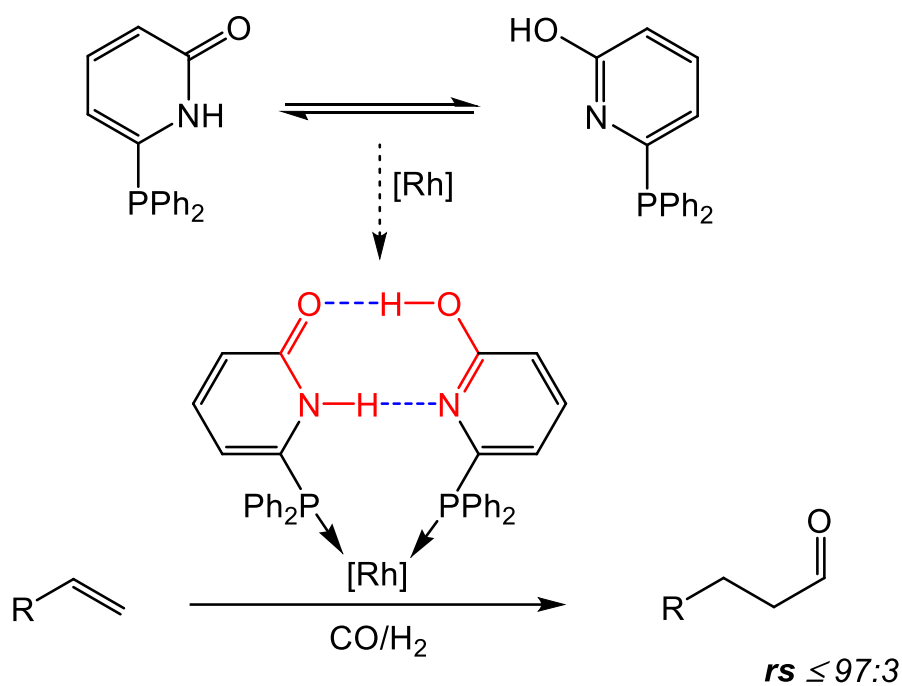


Figure 1.11: Potential hydrogen-bonded assemblies of the two tautomers of 2-pyridone

In this context, in 2003 Breit *et al.*⁹² reported a new concept for building self-assembling bidentate ligands through hydrogen bonding of monodentate ligands. They found that 6-diphenylphosphanyl-2-pyridone (6-DPPon) is able to undergo monodentate-to-bidentate ligand self-assembly by hydrogen bonding and behave as a chelating ligand in the presence of a late transition metal centre such as platinum(II) or rhodium(I). The reaction of two equivalents of 6-DPPon with dichloro(1,5-cyclooctadiene)platinum(II) gave a quantitative yield of *cis*-[PtCl₂(6-DPPon)₂]. X-ray crystallographic studies of the compound revealed a distorted square planar structure with the platinum atom bonded to two chlorines in the *cis*-position, and also to two phosphorus atoms from two 6-DPPon ligands coordinating in a chelating mode. In both solution and crystal state, the hydrogen-bonding network between the two tautomeric molecules in the *cis*-Pt^{II} complex remains stable as a result of the chelate effect. However, high temperatures (≥ 110 °C) or solvents bearing a protic functional group, such as methanol and DMSO, may disrupt the H-bonding intermediate, resulting in the decomposition of the complex.

A rhodium(I) complex derived from the same ligand (6-DPPon) using [Rh(CO)₂(acac)] has also been obtained, by the same group (Breit *et al.*).⁹² The authors examined the potential of this complex as a catalyst for alkene hydroformylation in toluene and found it to be a highly effective and highly regioselective catalyst, showing the linear aldehyde to be favoured over the branched isomer (**Scheme 1.23**).



Scheme 1.23: Rh-catalysed hydroformylation of terminal alkenes using 6-DPPon⁹²

1.5 Overall Conclusions to Chapter 1

C-H activation is an ongoing field of research that plays a significant role in generating numerous products that are used in medicinal chemistry. Various types of C-H activation and their mechanisms have been illustrated. In this field, three factors (electronic and steric effects and the use of a directing group) considered for solving the selectivity issue have also been briefly discussed.

The structural characteristics of different ligand types and their coordination modes with metal centres have been described. N[^]C and N[^]C[^]N ligands are the most convenient type that are able to undergo C-H activation to afford cyclometallated complexes.

New, additional functional groups on ligands enhance their ability to act as more than just traditional binding to a metal centre. The hydroxyl (OH) group is one of these most important functional groups. Different ligand properties in binding and catalytic systems have been shown when the hydroxyl (OH) group was introduced to ligands.

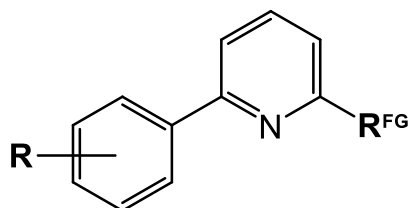
1.6 Research Aims

This thesis is concerned with the development of pyridine- and pyridone-based, monoanionic N[^]C bidentate and N[^]C[^]N pincer ligands and their applications in the coordination chemistry of transition metals and catalysis.

The overall aims of this project are to: **1)** synthesise novel cyclometallated complexes with OH-functionalised N[^]C and N[^]C[^]N ligands using a variety of metal salts including Pd^{II}, Pt^{II}, Hg^{II} and Au^{III} and characterise them using various spectroscopic techniques, including elemental analysis, FT-IR, NMR spectroscopies, mass spectrometry and X-ray crystallography; and **2)** determine whether these complexes have similar behaviours and structural, geometric and physical property relationships to the corresponding cyclometallated complexes which do not incorporate OH as a functional group. These complexes may also serve as starting materials for further chemical studies.

Varying the ligands should aid in the understanding of how the ligand properties influence the C-H activation step and other issues, such as binding modes and catalytic reactions. Therefore, a range of 6-aryl-2-pyridine- and pyridone-based bidentate ligands have been targeted with the general structure [2-FG-(6-aryl)pyridine] (FG = OMe *or* OH; aryl = Ph, 4-MePh, 4-CF₃Ph, 4-FPh *or* 2-MePh) as well as phenyl pyridine- and pyridone-

based pincer ligands with the general formula [1,3-bis(2-(6-FG-pyridyl)-4,6-X-phenyl)] (FG = OMe or OH; X = H or Me), as shown in **Figures 1.12** and **1.13**



2.5 $R^{FG} = \text{OMe}$ and $R = \text{H}$

2.6 $R^{FG} = \text{OMe}$ and $R = 4\text{-Me}$

2.7 $R^{FG} = \text{OMe}$ and $R = 4\text{-CF}_3$

2.8 $R^{FG} = \text{OMe}$ and $R = 4\text{-F}$

2.9 $R^{FG} = \text{OMe}$ and $R = 2\text{-Me}$

3.1 $R^{FG} = \text{OH}$ and $R = \text{H}$

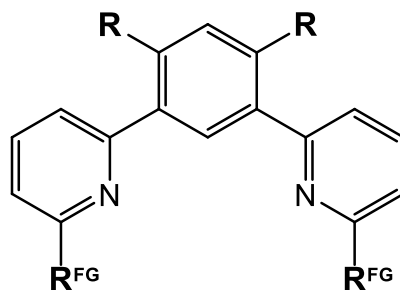
3.2 $R^{FG} = \text{OH}$ and $R = 4\text{-Me}$

3.3 $R^{FG} = \text{OH}$ and $R = 4\text{-CF}_3$

3.4 $R^{FG} = \text{OH}$ and $R = 4\text{-F}$

3.5 $R^{FG} = \text{OH}$ and $R = 2\text{-Me}$

Figure 1.12: Bidentate ligands targeted in this thesis



4.3 $R^{FG} = \text{OMe}$ and $R = \text{H}$

4.4 $R^{FG} = \text{OMe}$ and $R = \text{Me}$

4.5 $R^{FG} = \text{OH}$ and $R = \text{H}$

4.6 $R^{FG} = \text{OH}$ and $R = \text{Me}$

Figure 1.13: Pincer ligands targeted in this thesis

References

1. A. Sen, *Acc. Chem. Res.*, 1998, **31**, 550.
2. D. Alberico, M. E. Scott and M. Lautens, *Chem. Rev.*, 2007, **107**, 174.
3. T. Satoh and M. Miura, *Chem. Lett.*, 2006, **36**, 200.
4. D. R. Stuart and K. Fagnou, *Science*, 2007, **316**, 1172.
5. R. G. Bergman, *Nature*, 2007, **446**, 391.
6. D. Leow, G. Li, T. S. Mei and J. Q. Yu, *Nature*, 2012, **486**, 518.
7. R. H. Crabtree, *J. Chem. Soc. Dalton Trans.*, 2001, 2437.
8. Y. Boutadla, D. L. Davies, S. A. Macgregor and A. I. Poblador-Bahamonde, *Dalton Trans.*, 2009, 5820.
9. W. J. Tenn, K. J. Young, G. Bhalla, J. Oxgaard, W. A. Goddard and R. A. Periana, *J. Am. Chem. Soc.*, 2005, **127**, 14172.
10. Y. Feng, M. Lail, K. A. Barakat, T. R. Cundari, T. B. Gunnoe and J. L. Petersen, *J. Am. Chem. Soc.*, 2005, **127**, 14174.
11. P. J. Walsh, F. J. Hollander and R. G. Bergman, *J. Am. Chem. Soc.*, 1988, **110**, 8729.
12. C. C. Cummins, S. M. Baxter and P. T. Wolczanski, *J. Am. Chem. Soc.*, 1988, **110**, 8731.
13. D. L. Davies, S. M. Donald and S. A. Macgregor, *J. Am. Chem. Soc.*, 2005, **127**, 13754.
14. D. L. Davies, S. M. Donald, O. Al-Duaij, J. Fawcett, C. Little and S. A. Macgregor, *Organometallics*, 2006, **25**, 5976.
15. S. I. Gorelsky, D. Lapointe and K. Fagnou, *J. Am. Chem. Soc.*, 2008, **130**, 10848.
16. H. M. Davies and R. E. Beckwith, *Chem. Rev.*, 2003, **103**, 2861.
17. J. Chatt and J. Davidson, *J. Chem. Soc.*, 1965, 843.
18. P. Burger and R. G. Bergman, *J. Am. Chem. Soc.*, 1993, **115**, 10462.
19. P. L. Watson, *J. Am. Chem. Soc.*, 1983, **105**, 6491.
20. N. Goldshleger, M. Tyabin, A. Shilov and A. Shteinman, *Russ. J. Phys. Chem.*, 1969, **43**, 1222.

21. D. Astruc, *Organometallic Chemistry and Catalysis*, Wiley-VCH: Heidelberg, Germany, 2007.
22. N. Goldshleger, A. Shteinman, A. Shilov and V. Eskova, *Russ. J. Phys. Chem.*, 1972, **46**, 1353.
23. S. S. Stahl, J. A. Labinger and J. E. Bercaw, *Angew. Chem. Int. Ed.*, 1998, **37**, 2180.
24. L. Kushch, V. Lavrushko, Y. S. Misharin, A. Moravsky and A. Shilov, *Nouv. J. Chim.*, 1983, **7**, 729.
25. J. A. Labinger, A. M. Herring, D. K. Lyon, G. A. Luinstra, J. E. Bercaw, I. T. Horvath and K. Eller, *Organometallics*, 1993, **12**, 895.
26. P. E. Siegbahn and R. H. Crabtree, *J. Am. Chem. Soc.*, 1996, **118**, 4442.
27. Q. Khamker, *Ambiphilic CH Activation Routes to Heterocycles*, The University of Leicester, 2014.
28. J. R. Webb, S. A. Burgess, T. R. Cundari and T. B. Gunnoe, *Dalton Trans.*, 2013, **42**, 16646.
29. L. M. Slaughter, P. T. Wolczanski, T. R. Klinckman and T. R. Cundari, *J. Am. Chem. Soc.*, 2000, **122**, 7953.
30. T. R. Cundari, T. R. Klinckman and P. T. Wolczanski, *J. Am. Chem. Soc.*, 2002, **124**, 1481.
31. D. L. Davies, O. Al-Duaij, J. Fawcett, M. Giardiello, S. T. Hilton and D. R. Russell, *Dalton Trans.*, 2003, 4132.
32. B. Meunier, *Biomimetic Oxidations Catalyzed by Transition Metal Complexes*, Imperial College Press: London, 2000.
33. M. Lafrance and K. Fagnou, *J. Am. Chem. Soc.*, 2006, **128**, 16496.
34. M. Lafrance, C. N. Rowley, T. K. Woo and K. Fagnou, *J. Am. Chem. Soc.*, 2006, **128**, 8754.
35. E. M. Beck, N. P. Grimster, R. Hatley and M. J. Gaunt, *J. Am. Chem. Soc.*, 2006, **128**, 2528.
36. J. P. Kleiman and M. Dubeck, *J. Am. Chem. Soc.*, 1963, **85**, 1544.
37. R. Simayi, *Synthesis and Reaction Chemistry of Various N,N,C- and O,N,C-Palladium Pincer Complexes*, The University of Leicester, 2017.
38. W. B. Cross, E. G. Hope, Y. Lin, S. A. Macgregor, K. Singh, G. A. Solan and N. Yahya, *Chem. Commun.*, 2013, **49**, 1918.

39. C. Harris, S. Livingstone and N. Stephenson, *J. Chem. Soc.*, 1958, 3697.
40. R. Ayala, E. S. Marcos, S. Díaz-Moreno, V. A. Solé and A. Muñoz-Páez, *J. Phys. Chem. B*, 2001, **105**, 7588.
41. L. I. Elding, *Inorg. Chim. Acta*, 1976, **20**, 65.
42. L. I. Elding, *Acta Chem. Scand.*, 1970, **24**, 1331.
43. L. I. Elding and L. F. Olsson, *J. Phys. Chem.*, 1978, **82**, 69.
44. J. M. Brown, *Chem. Soc. Rev.*, 1993, **22**, 25.
45. J. K. Whitesell, *Chem. Rev.*, 1989, **89**, 1581.
46. M. Sunjuk, M. Al-Noaimi, Y. Al-Degs, T. Al-Qirem, E. Lindner and A. S. Abu-Surrah, *J. Polym. Sci. A: Polym. Chem.*, 2009, **47**, 6715.
47. M. Sunjuk, M. Al-Noaimi, G. A. Sheikha, E. Lindner, B. El-Eswed and K. Sweidan, *Polyhedron*, 2009, **28**, 1393.
48. J. A. Osborn, F. Jardine, J. F. Young and G. Wilkinson, *J. Chem. Soc. A: Inorg. Phys. Theor.*, 1966, 1711.
49. A. W. Freeman, M. Urvoy and M. E. Criswell, *J. Org. Chem.*, 2005, **70**, 5014.
50. F. Bellina, A. Carpita and R. Rossi, *Synthesis*, 2004, **2004**, 2419.
51. A. M. Kluwer, C. J. Elsevier, M. Bühl, M. Lutz and A. L. Spek, *Angew. Chem. Int. Ed.*, 2003, **42**, 3501.
52. R. Ball, G. Domazetis, D. Dolphin, B. James and J. Trotter, *Inorg. Chem.*, 1981, **20**, 1556.
53. M. M. Olmstead, C. L. Lee and A. L. Balch, *Inorg. Chem.*, 1982, **21**, 2712.
54. Z. Zhang and H. Cheng, *Coord. Chem. Rev.*, 1996, **147**, 1.
55. T. Mayer, E. Parsa and H. Böttcher, *J. Organomet. Chem.*, 2011, **696**, 3415.
56. J. Albert, R. Bosque, L. D'Andrea, J. Granell, M. Font-Bardia and T. Calvet, *Eur. J. Inorg. Chem.*, 2011, **2011**, 3617.
57. M. Albrecht, *Chem. Rev.*, 2009, **110**, 576.
58. A. Cheney, B. Mann, B. Shaw and R. Slade, *J. Chem. Soc. A: Inorg. Phys. Theor.*, 1971, 3833.
59. B. Mann, B. Shaw and R. Slade, *J. Chem. Soc. A: Inorg. Phys. Theor.*, 1971, 2976.

60. A. C. Cope and E. C. Friedrich, *J. Am. Chem. Soc.*, 1968, **90**, 909.
61. G. van Koten, J. T. Jastrzebski, J. G. Noltes, A. L. Spek and J. C. Schoone, *J. Organomet. Chem.*, 1978, **148**, 233.
62. J. M. Longmire and X. Zhang, *Tetrahedron Lett.*, 1997, **38**, 1725.
63. J. M. Longmire, X. Zhang and M. Shang, *Organometallics*, 1998, **17**, 4374.
64. M. Ohff, A. Ohff, van der Boom, Milko E and D. Milstein, *J. Am. Chem. Soc.*, 1997, **119**, 11687.
65. C. Jensen, *Chem. Comm.*, 1999, 2443.
66. G. Van Koten, *Organometallic Pincer Chemistry*, Springer-Verlag, Berlin, 2013.
67. J. Sutter, S. L. James, P. Steenwinkel, T. Karlen, D. M. Grove, N. Veldman, W. J. Smeets, A. L. Spek and G. van Koten, *Organometallics*, 1996, **15**, 941.
68. J. Niu, X. Hao, J. Gong and M. Song, *Dalton Trans.*, 2011, **40**, 5135.
69. F. Churrua, R. SanMartin, I. Tellitu and E. Domínguez, *Synlett*, 2005, **20**, 3116.
70. R. H. Crabtree, *New J. Chem.*, 2011, **35**, 18.
71. A. M. Allgeier and C. A. Mirkin, *Angew. Chem. Int. Ed.*, 1998, **37**, 894.
72. R. A. Periana, D. J. Taube, S. Gamble, H. Taube, T. Satoh and H. Fujii, *Science*, 1998, **280**, 560.
73. B. G. Hashiguchi, K. J. Young, M. Yousufuddin, W. A. Goddard III and R. A. Periana, *J. Am. Chem. Soc.*, 2010, **132**, 12542.
74. D. Lee, H. J. Kwon, B. P. Patel, L. M. Liable-Sands, A. L. Rheingold and R. H. Crabtree, *Organometallics*, 1999, **18**, 1615.
75. E. Billig, R. Williams, I. Bernal, J. H. Waters and H. B. Gray, *Inorg. Chem.*, 1964, **3**, 663.
76. M. D. Ward and J. A. McCleverty, *J. Chem. Soc. Dalton Trans.*, 2002, 275.
77. M. Kawamura, R. Kiyotake and K. Kudo, *Chirality*, 2002, **14**, 724.
78. Y. Blum and Y. Shvo, *J. Organomet. Chem.*, 1985, **282**, C7.
79. Y. Shvo, D. Czarkie, Y. Rahamim and D. F. Chodosh, *J. Am. Chem. Soc.*, 1986, **108**, 7400.
80. H. Knölker, E. Baum, H. Goesmann and R. Klauss, *Angew. Chem. Int. Ed.*, 1999, **38**, 2064.

81. B. L. Conley, M. K. Pennington-Boggio, E. Boz and T. J. Williams, *Chem. Rev.*, 2010, **110**, 2294.
82. Y. Yuki, K. Takahashi, Y. Tanaka and K. Nozaki, *J. Am. Chem. Soc.*, 2013, **135**, 17393.
83. K. Fujita, N. Tanino and R. Yamaguchi, *Org. Lett.*, 2007, **9**, 109.
84. H. Yang and B. Craven, *Acta Crystallogr. Sect. B: Struct. Sci.*, 1998, **54**, 912.
85. E. P. Kelson and P. P. Phengsy, *J. Chem. Soc. Dalton Trans.*, 2000, 4023.
86. P. Kong and F. Rochon, *Can. J. Chem.*, 1979, **57**, 526.
87. P. Kong and F. Rochon, *Can. J. Chem.*, 1981, **59**, 3293.
88. S. Chouzier, M. Gruber and L. Djakovitch, *J. Mol. Catal. A: Chem.*, 2004, **212**, 43.
89. T. C. Flood, J. K. Lim and M. A. Deming, *Organometallics*, 2000, **19**, 2310.
90. E. Morrison, C. Palmer and D. Tocher, *J. Organomet. Chem.*, 1988, **349**, 405.
91. B. Breit, *Angew. Chem. Int. Ed.*, 2005, **44**, 6816.
92. B. Breit and W. Seiche, *J. Am. Chem. Soc.*, 2003, **125**, 6608.

Chapter 2

*Synthesis of Cyclometallated Pyridine-based
Complexes and their role in Catalytic Aerobic
Alcohol Oxidation*

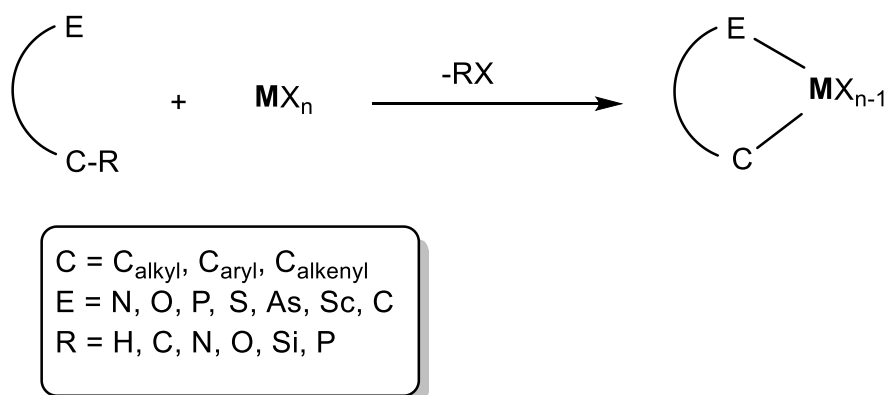
2.1 Introduction

Cyclometallation reactions, in which an organic compound is coordinated to a metal centre to generate a metal complex (usually *via* C-H activation) are common for both transition metals, such as Au^{III}, Ir^{III}, Pd^{II}, Pt^{II}/Pt^{IV} and Rh^{III}, and non-transition metals, such as Hg^{II}, Tl^{III} and Pb^{IV}.¹ Using transition metal complexes in organic synthesis to activate C-H bonds represents the more desirable route and has attracted considerable attention due to their high reactivity and selectivity. In addition, the metal complexes display a particular stability, which plays a significant role in allowing the complexes to act as recyclable reagents in catalytic systems. These favourable characteristics appear to be restricted to complexes containing late transition metals, mainly those located in the second and third rows of the periodic table. One of the more common of these transition metals to be used in organic synthesis is palladium.²

Complexes of palladium have brought a huge change to the field of organic synthesis over the last four decades.³ Although Pd-catalysed C-H activation has been a very important area of research for this time, the field remains an ongoing and developing area, particularly regarding the need to overcome difficulties concerning selectivity and other issues. Experimental studies have led to a greater understanding of the Pd-catalysed C-H activation mechanisms of, specifically, arenes.

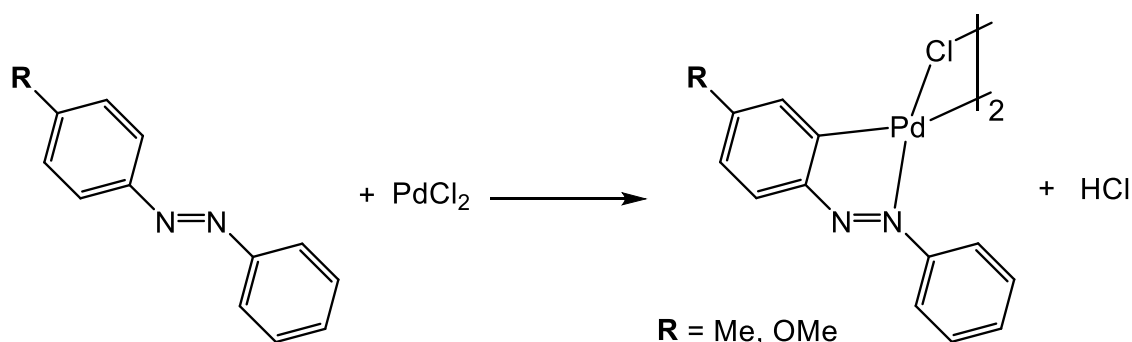
2.1.1 Cyclometallated Complexes

As mentioned above, reactions in which an organic chelating ligand coordinates to a central metal to form a ring containing an M-C sigma bond are known as cyclometallation reactions (**Scheme 2.1**).⁴



Scheme 2.1: General pathway of the cyclometallation reaction

was also found to preferentially form Pd-C sigma bonds with benzene rings containing electron-donating groups (**Scheme 2.3**).⁹



Scheme 2.3: Cyclopalladation of asymmetric azobenzenes

$C_{\text{aryl}}\text{-H}$ bond activation reactions, with the help of pyridine donors, have also been achieved. In this process, $N^{\wedge}C$ ligands are able to undergo cyclometallation in a bidentate binding mode (κ^2). 1-Naphthoquinoline (**2.c**),¹⁰ 2-phenylpyridine (**2.d**)¹¹ and 2-(2-thienyl)pyridine (**2.e**)¹² are the most widely used chelating ligands for cyclometallation (**Fig. 2.1**).

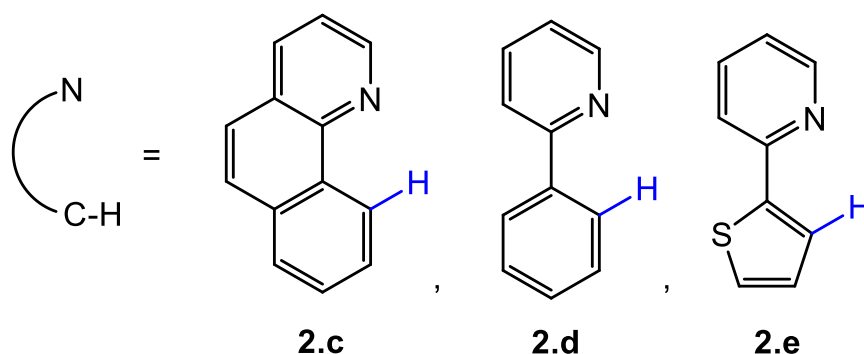
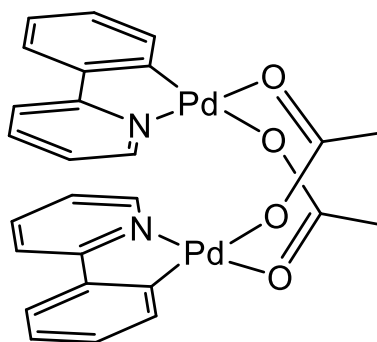


Figure 2.1: Common examples of $N^{\wedge}C$ -chelating ligands

The most common salt for cyclopalladation is $\text{Pd}(\text{OAc})_2$ due to its unique characteristics.⁴ With $N^{\wedge}C$ ligands, acetate ligands play a significant role in the formation of cyclometallated products. The two bridging acetate ligands usually hold two palladium atoms and, therefore, allow two $N^{\wedge}C$ -chelating ligands to undergo cyclopalladation in which the nitrogen and carbon atoms of the ligands are *trans* to two different oxygen atoms. The simplest example that would represent a $C_{\text{aryl}}\text{-Pd}^{\text{II}}\text{-N}_{\text{py}}$ system is [(2-phenylpyridine) $\text{Pd}(\mu\text{-OAc})_2$] (**2.f**). The dimer was first synthesised in 1979 by Davis and co-workers; however, they did not give any spectral or analytical data to support their

claim.¹³ A year later, Gutierrez *et al.* were able to re-synthesise the complex and characterise it using elemental analysis and ¹H NMR spectroscopic techniques. They found that chloroform proved to be a better choice of solvent for the reaction and obtained a 52% yield.¹⁴



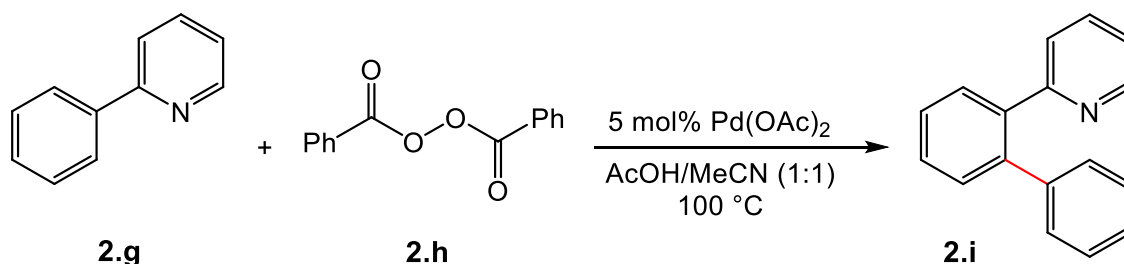
2.f

The most fascinating feature in these dimers is the relative proximity of the two metals, which is of interest in both inorganic and organometallic chemistry. Few electrochemical studies of Pd dimers have been reported in contrast to the well-investigated Rh, Ir and Pt dimers. Bercaw *et al.*¹⁵ have found that there are attractive d^8 - d^8 interactions in Pd^{II} dimers of the type [(2-phenylpyridine)Pd(μ -X)]₂ (X = OAc or TFA). However, the Pd-Pd interaction was found to be relatively weak in comparison to those in analogous Rh, Ir and Pt dimers.¹⁵ These, and related, species have recently been of interest as they were successfully used to prepare Pd^{III}-Pd^{III} or Pd^{II}-Pd^{IV} dimers that have been found to be active catalysts for C-C bond-forming reactions, such as C-H arylation.¹⁶

2.1.1.2 Applications of Pd-Catalysed C-H Activation in Catalysis

Over the past decade, various studies have been carried out on homogeneous catalysis using palladacycles as catalysts.¹⁷ For example, Moberga *et al.*¹⁸ demonstrated that the cyclopalladated complex [(2-phenylpyridine)Pd(μ -OAc)]₂ (**2.f**) can be used as an efficient catalyst in the presence of pyridine for the aerobic oxidation of primary and secondary alcohols to their corresponding products in high yields. The authors found that the reaction worked better with **2.f** than palladium(II) acetate.^{17,18} Experimental and computational studies led to a better understanding of the mechanisms of alcohol oxidation;¹⁹ this mechanism will be discussed in more detail in **Section 2.3.7**.

Palladium-catalysed C-H activation reactions have also received considerable attention due to their ability to undergo transformation and form many different types of bonds such as C-C, C-N, C-O, C-S and C-halogen without using pre-functionalised substrates. This is a highly useful strategy in organic synthesis for generating a variety of pharmaceuticals, polymers, agrochemicals, natural products, and other different chemicals.²⁰ In 2009, Yu *et al.*²¹ reported a new strategy to synthesise various unsymmetrical biaryl compounds by a Pd^{II}-catalysed arene-phenyl radical coupling reaction *via* C-H activation. The formation of 2-(biphenyl-2-yl)-pyridine (**2.i**) obtained from the reaction between 2-phenylpyridine (**2.g**) and a phenyl radical derived from benzoyl peroxide (**2.h**) is an example of this process (**Scheme 2.4**). The reaction is mechanistically initiated by cyclometallation of 2-phenylpyridine (**2.g**) to form the cyclopalladated compound (**2.f**), which would subsequently react with the phenyl radical generated by high-temperature decomposition of benzoyl peroxide (**2.h**) to produce 2-(biphenyl-2-yl)-pyridine (**2.i**).



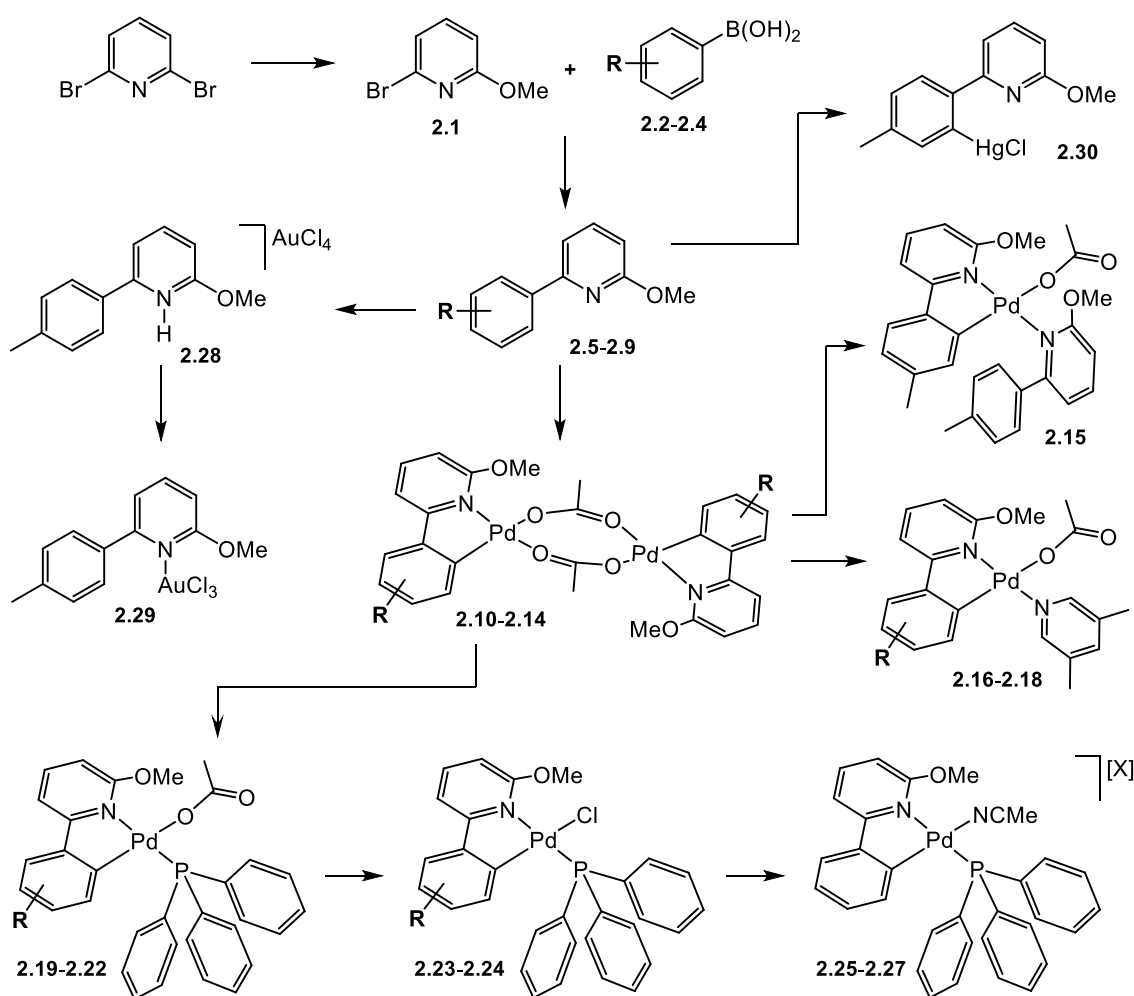
Scheme 2.4: Unsymmetrical biaryl formation

2.2 Aims and Objectives of Chapter 2

The aim of the work in this chapter is to prepare various aryl-pyridine ligands with the general formula [6-aryl-2-methoxypyridine], where aryl = Ph **2.5**, 4-MePh **2.6**, 4-CF₃Ph **2.7**, 4-FPh **2.8** or 2-MePh **2.9**, and investigate and compare their reactivities towards palladium(II). The resultant complexes, of the form [Pd(κ^2 -N[^]C)(μ -OAc)]₂ (**2.10-2.14**), will undergo a disassembly process with simple monodentate ligands, 3,5-lutidine and triphenylphosphine, and the same ligand used for complexation in order to have monomeric complexes adopting the general formula [Pd(N[^]C)(OAc)L] (**2.15-2.22**). Monopalladated complexes of the type [Pd(N[^]C)(PPh₃)Cl] (**2.23** and **2.24**) will be also obtained in order to test their reactivity with various silver salts in acetonitrile to afford complexes with the general structure [Pd(N[^]C)(PPh₃)(MeCN)][X] (X = PF₆, BF₄ or OTf) (**2.25-2.27**). This will allow a comparison to be made between pyridine (**Chapter 2**) and

pyridone (**Chapter 3**) ligands for applications in the coordination chemistry of palladium(II) acetate and catalysis. The cyclometallated complexes (**2.10-2.13**) will be tested as catalysts in the aerobic oxidation of benzyl alcohol into benzaldehyde in the presence of a ligand. 6-(4-methylphenyl)-2-methoxypyridine (**2.6**) will be also used as an example to investigate its activity towards $\text{H}[\text{AuCl}_4]$ and $\text{K}[\text{AuCl}_4]$.

All organic compounds and complexes shown in **Scheme 2.5** are fully characterised using suitable spectrometric (ESMS, HRMS) and spectroscopic (^1H , $^{13}\text{C}\{^1\text{H}\}$, ^{31}P and ^{19}F NMR and IR) techniques as well as by single crystal X-ray diffraction.



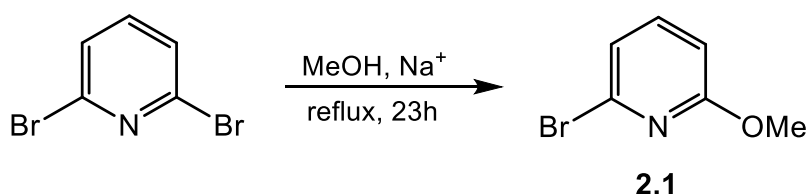
Scheme 2.5: Compounds described in **Chapter 2**

2.3 Results and Discussion

2.3.1 Synthesis of OMe-N[^]C Ligands

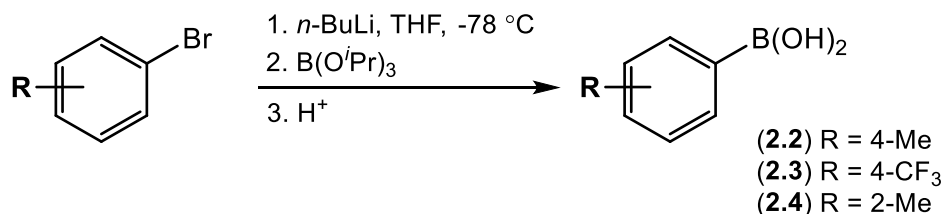
For the purposes of this section, the 6-aryl-2-methoxypyridine ligands (**2.5-2.9**) were prepared and then reacted with Pd(OAc)₂ so as to undergo cyclopalladation. The resulting products were then thoroughly characterised.

The preparation of 6-aryl-2-methoxypyridine ligands (**2.5-2.9**) began with the synthesis of 6-bromo-2-methoxypyridine (**2.1**) (**Scheme 2.6**) using a synthetic route established by Nguyen *et al.*²² A mixture of 2,6-dibromopyridine and sodium methoxide (CH₃ONa), which was prepared *in-situ* by reaction with sodium metal, was heated to reflux under nitrogen. The reaction had to be heated to reflux for no more than 23 h in order to prevent the 6-bromo-2-methoxypyridine (**2.1**) from being converted to dimethoxypyridine. The reaction gave an approximately 79% yield of the desired product with a small impurity (4%) of dimethoxypyridine, as seen in the ¹H NMR spectrum. No peaks associated with the starting material were observed. The ¹H NMR data of the product were consistent with those reported in the literature.²² The product was then used without further purification.



Scheme 2.6: Synthesis of 6-bromo-2-methoxypyridine (**2.1**)

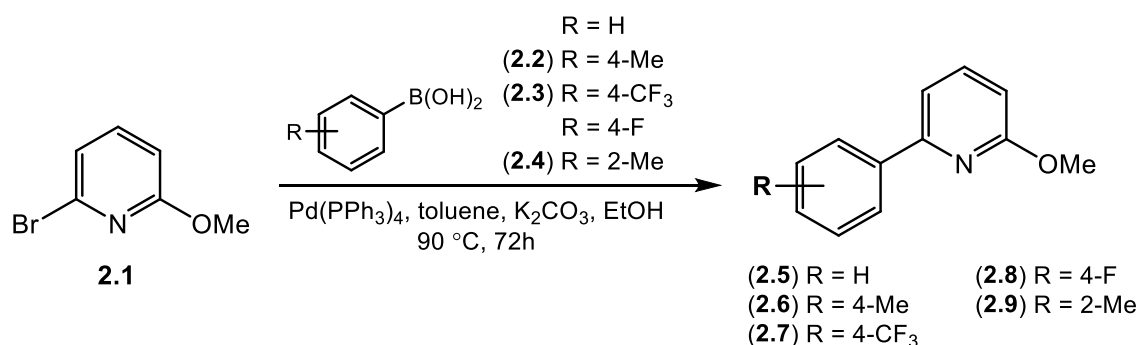
The most useful synthetic method in organic chemistry for making a C-C bond between two partners is the Suzuki cross-coupling reaction. In order to carry out the Suzuki coupling reaction with 6-bromo-2-methoxypyridine (**2.1**) for N[^]C ligand synthesis, a suitable boronic acid was required. Phenylboronic and 4-fluorophenylboronic acids were purchased at high purity from Aldrich, while 4-methylphenylboronic acid (**2.2**), (4-trifluoromethyl) phenylboronic acid (**2.3**) and 2-methylphenylboronic acid (**2.4**) were typically prepared by treating their corresponding brominated precursors with *n*-butyllithium solution at low temperature followed by the addition of triisopropylborate to afford a white precipitate (**Scheme 2.7**).²³



Scheme 2.7: Synthesis of aryl-B(OH)₂ compounds (2.2-2.4)

It was noted that the reaction with 4-bromobenzotrifluoride (**2.3**) produced the product at a slightly slower rate than the reactions with 4- and 2-bromotoluene, (**2.2**) and (**2.4**), respectively. However, all reactions were allowed to stir overnight to maximise the yields. It was also found that replacing THF with Et₂O in the preparation of 4-methylphenylboronic acid (**2.2**) was unsuccessful. The three aryl-boronic acids were all characterised by ¹H, ¹⁹F (for **2.3**) and ¹³C{¹H} NMR spectroscopy and by mass spectrometry to confirm their formation. All data obtained were consistent with those reported in the literature.^{24,25} The materials were used in the subsequent Suzuki coupling reaction without any further purification.

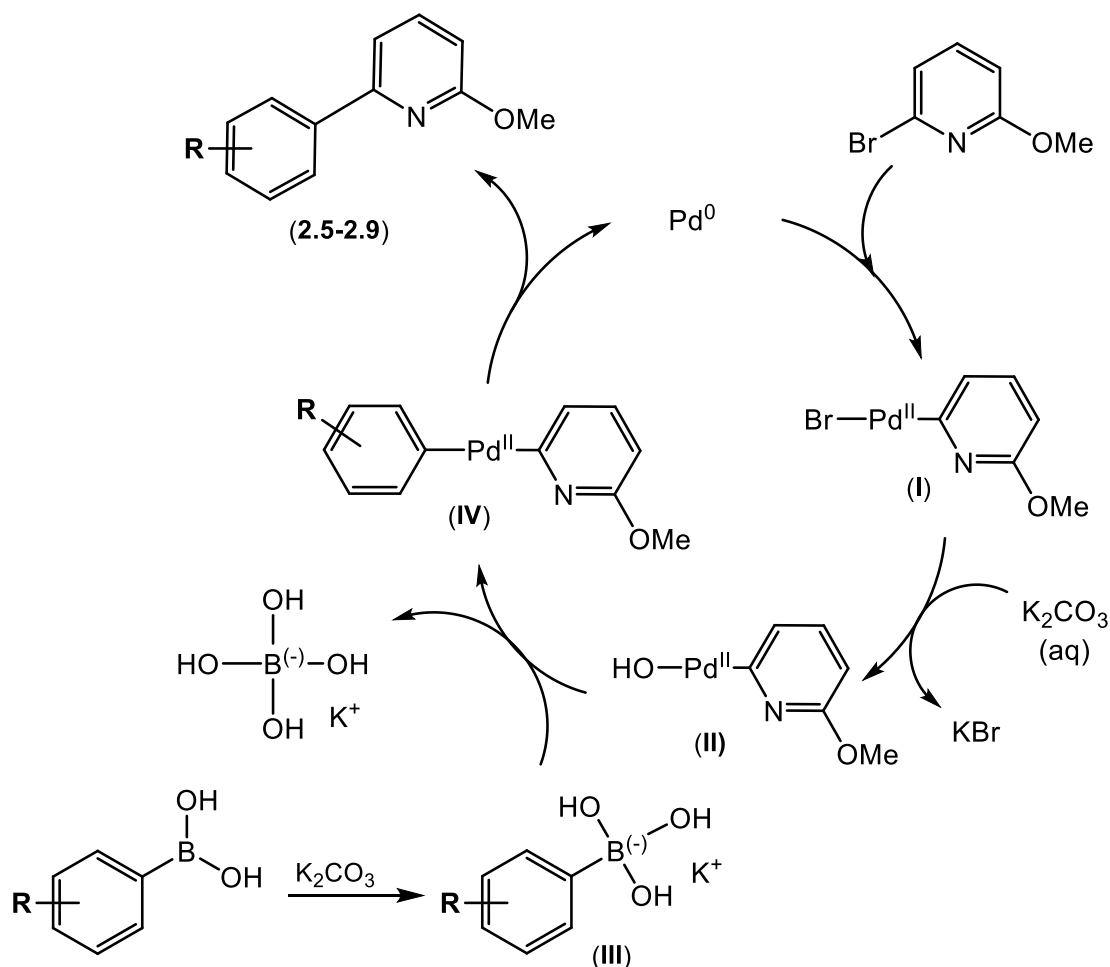
Treatment of 6-bromo-2-methoxypyridine (**2.1**) with the range of aromatic boronic acids mentioned above using typical Suzuki coupling conditions (**Scheme 2.8**) afforded the desired 6-aryl-2-methoxypyridine ligands (**2.5-2.9**) in good yields.



Scheme 2.8: Synthesis of N[^]C ligands (2.5-2.9)

The catalytic cycle would involve a sequence of steps in which the palladium was introduced to the 6-bromo-2-methoxypyridine (**2.1**) *via* oxidative addition to give the organopalladium compound (**I**), which is treated with a base to generate an intermediate containing a Pd^{II}-OH bond (**II**). With the boronate compound (**III**), the intermediate

undergoes transmetalation to give the organopalladium species (IV). The desired ligands (2.5-2.9) and Pd⁰ were then obtained *via* a reductive elimination process (Scheme 2.9).²⁶



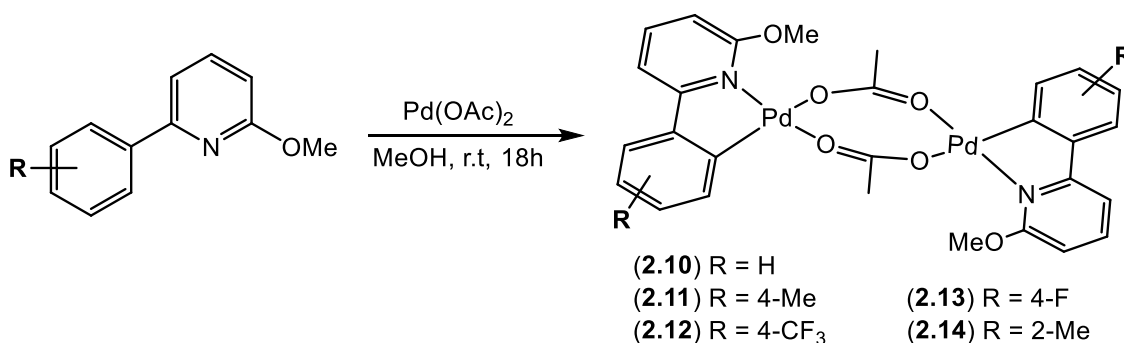
Scheme 2.9: The catalytic cycle for the synthesis of N^{^C} ligands

All crude products obtained were purified using the same procedure, whereby a short (10 cm) silica column was eluted with a dichloromethane:petroleum ether:diethyl ether (80:20:1) solution. This approach allows the catalyst residues to be separated from the products. The ¹H NMR spectrum of the material obtained from the preparation of **2.6** showed that about 40% of the crude product was unreacted bromo-starting material. Therefore, a poor pure isolated yield (29%) was obtained after a second column. On the second attempt, it was found that increasing both the equivalent amount of the boronic acid from 1.1 to 1.5 and the reaction time gave a remarkably high yield (97%). The ¹H and ¹³C{¹H} NMR data for all five N^{^C} ligands synthesised (**2.5-2.9**) were recorded to compare with those previously reported.²⁷⁻³¹ The ¹H NMR spectra recorded for all ligands exhibited a singlet between 3.95 and 4.03 ppm corresponding to the methoxy protons. A

singlet was also observed at 2.44 and 2.31 ppm, representing the methyl protons in **2.6** and **2.9**, respectively. In general, the peaks in the aromatic region were observed between 6.5 and 8.13 ppm. These peaks represented the pyridyl and aryl rings. All data for the five ligands are found to be consistent with those given in the literature.²⁷⁻³¹

2.3.2 Complexation of OMe-N[^]C Ligands to Palladium(II)

The five pyridine N[^]C ligands (**2.10-2.14**) were reacted with Pd(OAc)₂ to examine their ability to undergo cyclopalladation. The reactions were carried out by stirring in MeOH at room temperature for 18 hours, with the acetate-bridged cyclopalladated complexes being formed in 14-87% yield (**Scheme 2.10**). These complexes are [Pd(κ²-6-phenyl-2-methoxypyridine)(μ-OAc)]₂ (**2.10**), [Pd(κ²-6-(4-methylphenyl)-2-methoxypyridine)(μ-OAc)]₂ (**2.11**), [Pd(κ²-6-(4-trifluoromethylphenyl)-2-methoxypyridine)(μ-OAc)]₂ (**2.12**), [Pd(κ²-6-(4-fluorophenyl)-2-methoxypyridine)(μ-OAc)]₂ (**2.13**) and [Pd(κ²-6-(2-methylphenyl)-2-methoxypyridine)(μ-OAc)]₂ (**2.14**).



Scheme 2.10: Synthesis of [Pd(κ²-N[^]C)(μ-OAc)]₂ (**2.10-2.14**)

During the course of the reactions, **2.10**, **2.11** and **2.13** were found to precipitate as yellow solids and thus were directly isolated from their reaction solutions, while the reactions with **2.12** and **2.14** gave dark yellow solutions for which precipitation processes were required. Low yields were obtained for **2.12** (22%) and **2.14** (14%). The low yield of the former could be attributed to the presence of the trifluoromethyl group (-CF₃), as this substituent is considered to be a deactivating group which would lead to a decrease in the rate of the reaction. For complex **2.14**, the *o*-methyl group present in the 6-(2-methylphenyl)-2-methoxypyridine ligand (**2.9**) could allow the 2-methylphenyl and pyridyl rings to be fixed in a non-planar geometry. If this is the case, the possibility of the *o*-C_{aryl}-H activation process might be much lower due to the relatively larger distance between the H attached to the *o*-C_{aryl} and the central metal (Pd).

Infrared spectroscopy was used to identify the structure of the acetate-bridged complexes (**2.10-2.14**). All sample spectra were run as solids and scanned over the range of 600-4000 cm^{-1} . These complexes were expected to demonstrate bands consistent with acetate-bridged binding (μ). According to work previously reported by Nakamoto,³² the asymmetric and symmetric carboxylate stretching bands should show a characteristic separation ($\Delta\nu$) of 40 cm^{-1} or more when bound in the bridging or monodentate arrangements; in this work, all IR spectra obtained were consistent with this observation (**Table 2.1**). The asymmetric stretching bands fall in the range of 1563-1571 cm^{-1} and the symmetric stretching bands between 1392 and 1404 cm^{-1} .

Table 2.1: Asymmetric and symmetric acetate (CO_2) IR bands of **2.10-2.14**

Complex	$\nu_{\text{asym}} (\text{C-O})$ (cm^{-1})	$\nu_{\text{sym}} (\text{C-O})$ (cm^{-1})	$\Delta\nu (\nu_{\text{asym}} - \nu_{\text{sym}})$ (cm^{-1})
2.10	1571	1399	172
2.11	1570	1404	166
2.12	1575	1404	171
2.13	1563	1396	167
2.14	1570	1392	178

NMR spectroscopy was also used in the analysis of these five complexes. In particular, ^1H and $^{13}\text{C}\{^1\text{H}\}$ NMR spectra were recorded for all the complexes and ^{19}F NMR spectra for **2.12** and **2.13**. The ^1H NMR spectrum provides valuable structural information about the products. Common to all five complexes is the presence of two singlets representing the methoxy (OMe) and acetate methyl protons. An extra singlet was also observed at 2.34 and 2.17 ppm in the ^1H NMR spectra of both **2.11** and **2.14** corresponding to the *para*- and *ortho*-methyl protons, respectively. Each cyclopalladated complex contains an *o*- $\text{C}_{\text{aryl}}\text{-Pd}$ bond, which forms as a result of the C-H activation. The presence of this bond could be confirmed by either the absence of the proton on the *o*- C_{aryl} from the ^1H NMR spectra or by the presence of a quaternary carbon in the $^{13}\text{C}\{^1\text{H}\}$ NMR spectra. Further evidence that may help confirm this finding is a singlet peak in the aromatic region of complexes **2.11**, **2.12** and **2.13**, where each contains a substituent group at their *para* positions. These singlets, in the ^1H NMR spectra of **2.11**, **2.12** and **2.13**, were observed at 6.84, 7.30 and 6.71 ppm, respectively. The $^{13}\text{C}\{^1\text{H}\}$ and DEPT

135 NMR spectra of each complex demonstrated an additional quaternary carbon, which is representative of the carbon bound to the palladium centre. The mass (ES/ASAP) spectra of **2.10**, **2.11**, **2.12**, **2.13** and **2.14** showed a peak as the highest fragment corresponding to $[M-OAc]^+$ at m/z 640.9784, 669.0058, 777.9493, 676.9556 and 669.0058, respectively. Peaks that may represent the molecular ion $[M]^+$ were only observed for **2.10** and **2.13** at m/z 698.9662 and 734.9364, respectively.

Single crystal X-ray diffraction is a very important technique in the determination of solid-state structures. This technique provides extensive structural data including bond lengths, bond angles and information about the unit cell. X-ray structures were obtained of single crystals of the novel complexes (**2.10-2.14**). The complexes **2.10**, **2.11**, **2.13** and **2.14** were recrystallised from their original solvents (MeOH) while X-ray quality crystals of **2.12** were obtained by the slow evaporation of chloroform solution containing the complex. The benefit of using methanol for the recrystallisation process is that it was also used in the synthesis and, therefore, a new solvent would not be introduced to the sample, thus minimising the potential of having a variety of molecules of solvation. All crystal structures obtained supported the spectral analysis previously discussed.

Structural diagrams of each complex are given in **Figures 2.2-2.6** with selected bond lengths and bond angles of these structures reported in **Table 2.2**. The structural parameters of the dimeric complexes (**2.10-2.14**) are given in **Table A1** in the **Appendix**.

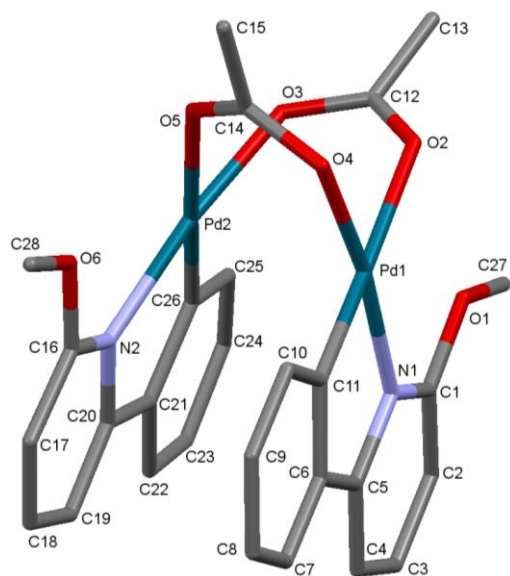


Figure 2.2: Structure of **2.10** with hydrogens and H₂O omitted for clarity

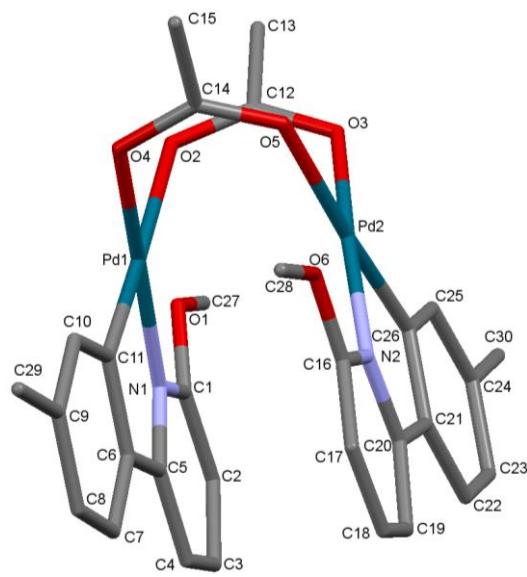


Figure 2.3: Structure of **2.11** with hydrogens omitted for clarity

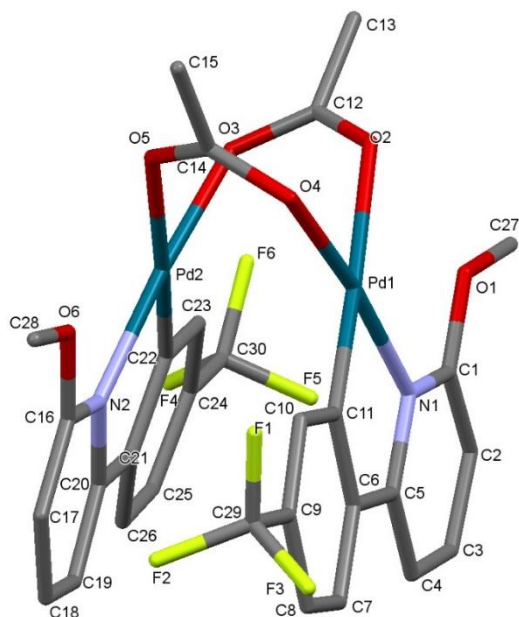


Figure 2.4: Structure of **2.12** with hydrogens, H₂O and CHCl₃ omitted for clarity

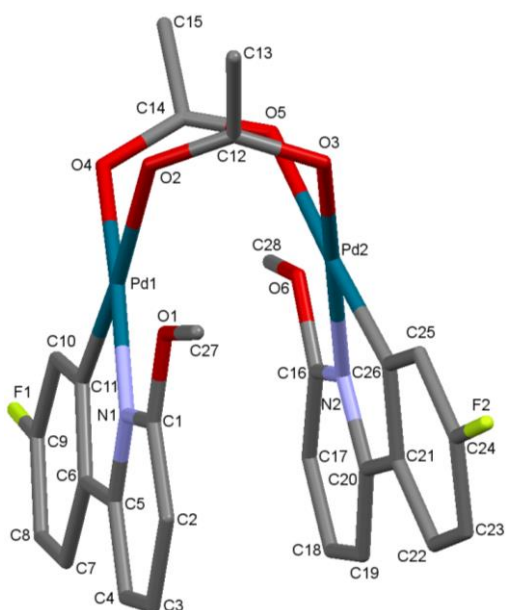


Figure 2.5: Structure of **2.13** with hydrogens omitted for clarity

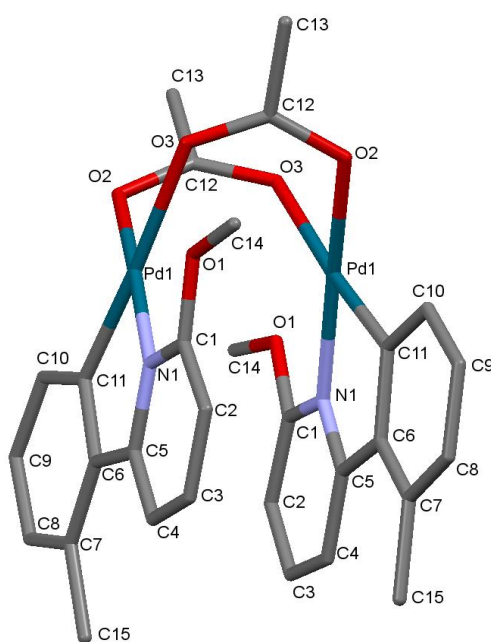


Figure 2.6: Structure of **2.14** with hydrogens omitted for clarity

All complexes have a square-planar geometry with one chelating (κ^2) N^C ligand per Pd with each metal centre linked by two bridging acetate ligands, forming a dimeric complex. Their structures are commonly referred to as “open-book” or “cleft” complexes due to their geometries.³³ As can be seen in **Table 2.2**, the bite-angle of the N^C ligands

(C-Pd-N) was approximately 80.5° for all five compounds (**2.10-2.14**). These angles are found to be within the range of bite angles previously observed for similar N[^]C-ligand complexes.²⁰ The X-ray data demonstrated that the electronic nature of the N[^]C ligands did not affect the overall structure of the products.

Table 2.2: Selected Pd-X bond lengths and bite angles of complexes **2.10 – 2.14**

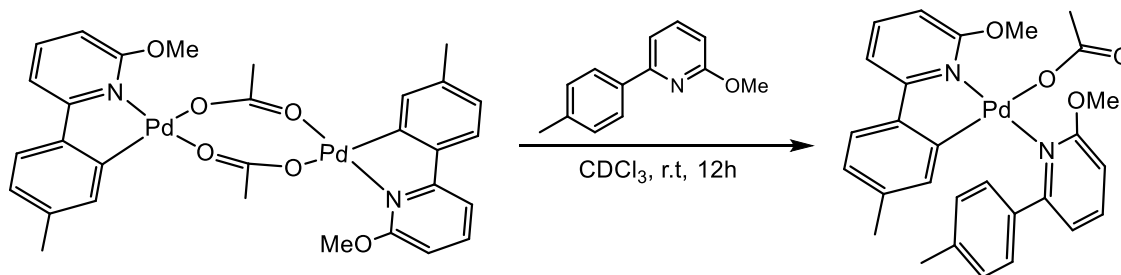
Complex	Bond lengths (Å)					Bond angles (°)
	Pd---Pd	Pd-O (<i>trans</i> to C)	Pd-O (<i>trans</i> to N)	Pd-N	Pd-C	C-Pd-N
2.10	2.8519(15)	2.126(8)	2.032(8)	2.060(10)	1.912(14)	81.2(5)
2.11	2.8187(11)	2.160(4)	2.037(4)	2.061(5)	1.937(7)	81.5(3)
2.12	2.8602(16)	2.146(4)	2.051(4)	2.069(5)	1.947(5)	81.2(2)
2.13	2.8423(11)	2.143(6)	2.037(6)	2.048(8)	1.945(9)	81.0(4)
2.14	2.8462(6)	2.187(2)	2.045(2)	2.044(2)	1.950(3)	80.16(10)

The data reported in **Table 2.2** illustrates a significant *trans* influence present in the complexes' structures. There are two basic types of palladium-oxygen bonds in complexes (**2.10-2.14**); those that are *trans* to a carbon atom and those that are *trans* to a nitrogen atom. From the table, it can be seen that the bonds between palladium and oxygen that are *trans* to carbon are longer than those *trans* to nitrogen. The lengths of the former range between 2.118 and 2.189 Å, while those that are *trans* to nitrogen range between 2.024 and 2.055 Å. This difference could be attributed to the stronger *trans* influence of the aryl group versus the N-donor ligand.³⁴ The Pd---Pd distances are found to fall within the range of 2.8198–2.8618 Å, which are within the range observed for related dipalladated complexes (2.55 to 3.05 Å) and shorter than their van der Waals radii (3.26 Å).¹⁵ The Pd-C and Pd-N bond lengths (~1.940 and ~2.050 Å, respectively) are similar to those previously reported.^{33,34}

2.3.3 Synthesis of Mononuclear Pd^{II} Complexes

The dimer **2.11** was reacted with 6-(4-methylphenyl)-2-methoxypyridine (**2.6**) (2 eq.) in CDCl₃ to form monomeric **2.15** (**Scheme 2.11**). This reaction was monitored by ¹H NMR spectroscopy at room temperature, which showed that the reaction went to completion after 12 hours. The product (**2.15**) could not be isolated; evaporation of the

solvent or precipitation of the product by hexane led to decomposition of the product affording the starting materials, the dimeric complex (**2.11**) and free ligand (**2.6**).



Scheme 2.11: Synthesis of $[\text{Pd}(\kappa^2\text{-2.6})(\text{OAc})(\kappa^1\text{-2.6})]$ (**2.15**)

Therefore, the monomeric complex (**2.15**) had to be characterised in solution. The ^1H NMR spectrum displayed eleven non-equivalent aromatic resonances between 5.80 and 7.95 ppm, two of which represented two protons for each peak, as seen at 7.25 and 7.94 ppm. A single resonance for the monodentate acetate ligand was observed at 2.20 ppm. Downfield proton chemical shifts for the methyl and methoxy protons (2.40 and 4.03 ppm, respectively) were clearly seen for the monodentate ligand, as compared to the free ligand (2.31 and 3.95 ppm for the methyl and methoxy protons, respectively). Complex **2.15** showed a molecular peak at m/z 503 in its mass spectrum (ES) corresponding to the product with a loss of the acetate ligand $[\text{M}-\text{OAc}]^+$.

This type of reaction could generate either two, or one of two, isomers, where the ligand can be in either the *trans* or *cis* position to the pyridyl nitrogen atom of the chelating ligand, as demonstrated in **Figure 2.7**.

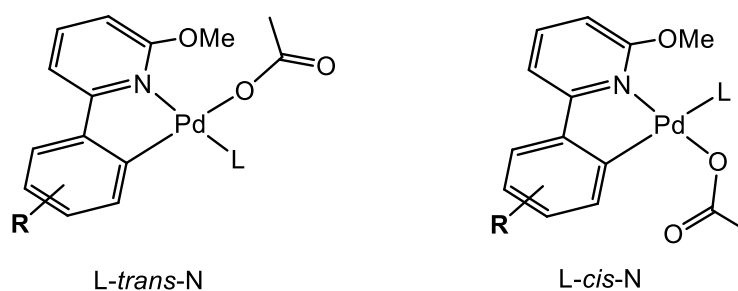
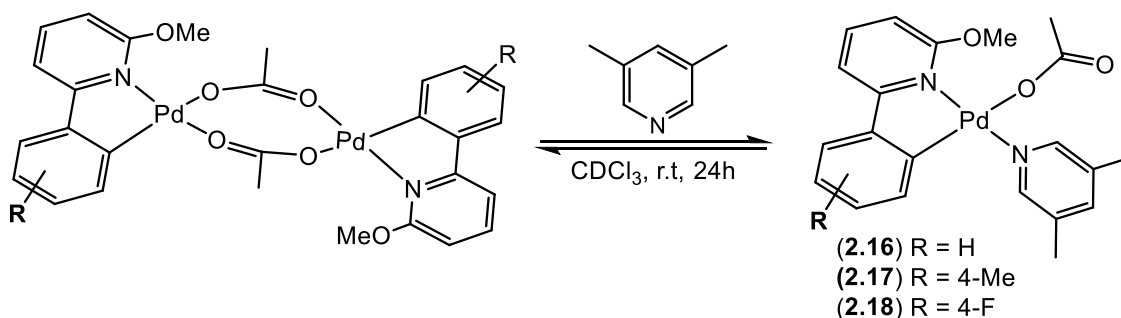


Figure 2.7: Possible structures of mononuclear Pd^{II} complexes

However, only one isomer was generated from this reaction, as confirmed by the ^1H and $^{13}\text{C}\{^1\text{H}\}$ NMR spectra of the mononuclear complex. In addition, the NOESY NMR

spectrum of the product showed a proton-proton correlation from the methyl group of the acetate to the signal assigned to the methoxy protons of the chelating ligand, suggesting that the *L-trans-N* species may have been formed. This is in agreement with data collected on other derivatives in the literature.^{16,35,36}

The dimers **2.10**, **2.11** and **2.13** were also all converted into mononuclear species by reactions with another simple ligand, namely 3,5-lutidine (**Scheme 2.12**). These mononuclear Pd^{II} complexes are [Pd(κ^2 -6-phenyl-2-methoxypyridine)(OAc)(3,5-lutidine)] (**2.16**), [Pd(κ^2 -6-(4-methylphenyl)-2-methoxypyridine)(OAc)(3,5-lutidine)] (**2.17**) and [Pd(κ^2 -6-(4-fluorophenyl)-2-methoxypyridine)(OAc)(3,5-lutidine)] (**2.18**). The reactions were carried out at room temperature in CDCl₃ to monitor the progress of the reactions. It was found that, after 24 hours, none of the reactions had gone to completion when 1:2 (dimer:ligand) equivalents were used (leaving about 20-30% of unreacted starting materials). Further stirring for 48 hours did not help improve the associated yields. Adding further 3,5-lutidine ligand (~1 eq.) to the reaction mixtures pushed the equilibrium to the product side and hence 96, 98 and 94% conversions were obtained for the reactions of **2.10**, **2.11** and **2.13**, respectively, in solution. However, attempts to isolate these products, including evaporation, precipitation and recrystallisation, were unsuccessful.

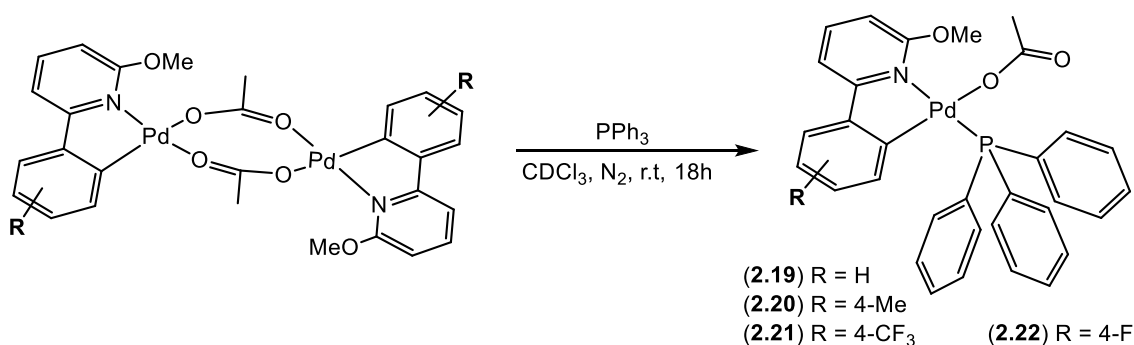


Scheme 2.12: Synthesis of mononuclear Pd^{II} complexes containing 3,5-lutidine

The mononuclear Pd^{II} complexes obtained were all characterised by solution spectroscopic techniques in the presence of the 3,5-lutidine ligand. The ¹H NMR spectra showed the formation of 1:1:1 (N[^]C-ligand/OAc/3,5-lutidine)-Pd complexes. Singlets corresponding to the methoxy protons were found to be shifted downfield by approximately 0.23-0.37 ppm upon addition of 3,5-lutidine. The mass (ES) spectra of **2.16**, **2.17** and **2.18** demonstrated a peak representing [M-OAc]⁺ at *m/z* 397, 411 and 415,

respectively. Two, or one of two, isomers are possible for these reactions; however, the *N-trans-N* form (as drawn above) was found to be more likely to occur, as confirmed for complex **2.15** and by related complexes in the literature.³⁶

Introducing the triphenylphosphine ligand (PPh₃) to the cyclometallated dimers (**2.10-2.13**) resulted in the formation of mononuclear compounds, [Pd(κ^2 -**2.5**)(OAc)(PPh₃)] (**2.19**), [Pd(κ^2 -**2.6**)(OAc)(PPh₃)] (**2.20**), [Pd(κ^2 -**2.7**)(OAc)(PPh₃)] (**2.21**) and [Pd(κ^2 -**2.8**)(OAc)(PPh₃)] (**2.22**) in good yields (71, 69, 75 and 74%, respectively). In these reactions (**Scheme 2.13**), the PPh₃ could displace one acetate-bridged ligand and bind to the Pd^{II} core in a monodentate fashion. Initially, the reaction of dimer **2.10** with PPh₃ (1:2) was performed on a small scale (0.028 mmol of **2.10**) under ambient conditions. The progress of the reaction was monitored in CDCl₃. After 24 hours of stirring, the ¹H NMR spectrum of the reaction mixture showed that the desired product had been generated along with some unreacted Pd^{II} dimer. Consumption of the PPh₃ ligand was established from the ³¹P NMR spectrum, which displayed two peaks at 45.6 and 29.2 ppm. These peaks correspond to the coordinated PPh₃ and triphenylphosphine oxide (OPPh₃), respectively. No sign of the free ligand (PPh₃) was observed in the ³¹P NMR spectrum. A second reaction was attempted under an inert atmosphere in order to prevent oxidation of the ligand using the same equivalents of the reactants. After 24 hours reaction time, the target compound (**2.19**) was obtained and isolated as a light grey powder in excellent purity and then characterised by several analytical methods.



Scheme 2.13: Synthesis of mononuclear Pd^{II} complexes containing PPh₃

The ¹H NMR spectra of the products **2.19** to **2.22** in CDCl₃ exhibited singlets between 1.27 and 1.38 ppm corresponding to the acetate methyl protons and singlets between 3.84 and 3.91 ppm which represented the methoxy protons. The former had an approximately 0.9 ppm lower chemical shift than those of the dimeric complexes, where

the latter was found to be deshielded by approximately 0.3 ppm. A singlet was also observed for complex **2.20** at 1.62 ppm which is assigned to the aryl methyl protons while being found at 2.23 ppm in the starting dimeric complex **2.11**. Other signals in the aromatic regions are assigned to be the protons on the pyridyl and aryl rings of the four complexes (**2.19-2.22**).

Only one peak at around 45 ppm was observed in the ^{31}P NMR spectra for all monopalladated complexes, representing the presence of PPh_3 as a monodentate ligand. In the ^{19}F NMR spectra of **2.21** and **2.22**, a singlet was observed, for each, at -63.3 and -111.5 ppm corresponding to CF_3 and F, respectively. The TOFMS (ASAP) spectra of the mononuclear complexes **2.19**, **2.20**, **2.21** and **2.22** displayed a peak representing the fragment $[\text{M-OAc}]^+$ for each complex at 552.0792, 566.0877, 620.0579 and 570.0626, respectively. The infrared spectra of these complexes showed characteristic COO_{asym} and COO_{sym} absorption peaks at approximately 1570 and 1433 cm^{-1} , respectively. The high characteristic separation ($\Delta\nu$) of ~ 137 cm^{-1} may be indicative of a monodentate acetate ligand bound to the Pd^{II} centre.

All complexes containing PPh_3 proved unstable in CDCl_3 solution and decomposed into their starting dimeric complexes and OPPh_3 . However, crystals suitable for a single crystal X-ray diffraction could be obtained for **2.22** from a DCM solution of the product layered with hexane. The X-ray structure of **2.22** is shown in **Figure 2.8**; selected bond distances and the C-Pd-N bond angle are reported in **Table 2.3**.

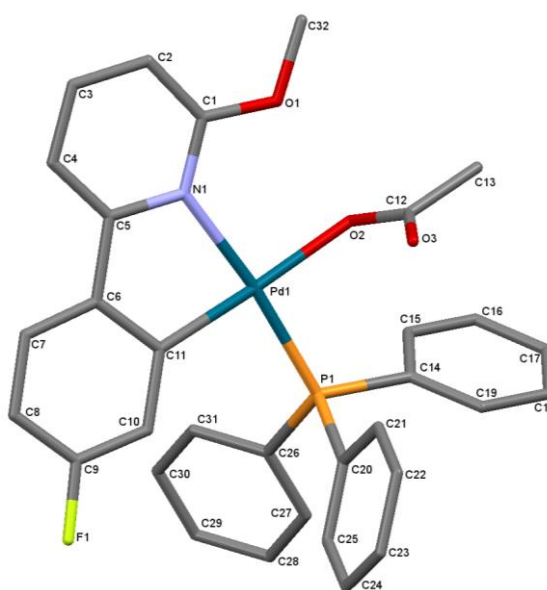


Figure 2.8: X-ray structure of **2.22** with hydrogens omitted for clarity

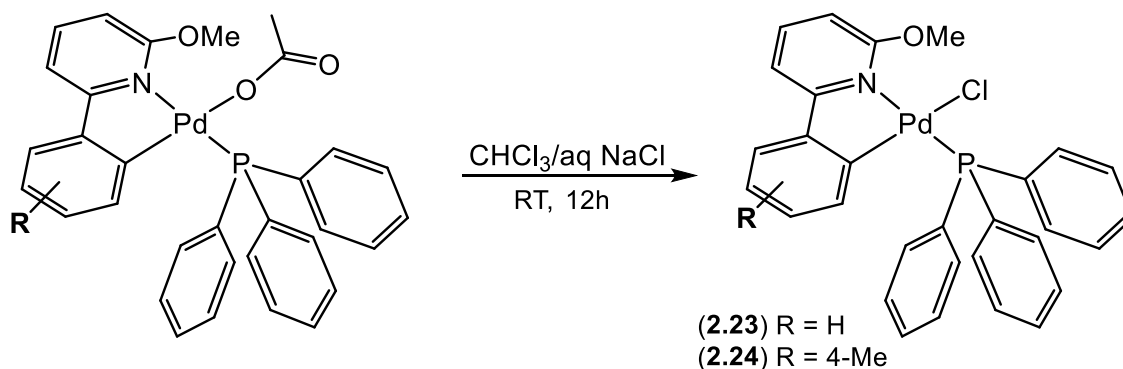
Table 2.3: Selected Pd-X bond lengths and the bite angle of **2.22**

Complex	Bond lengths (Å)				Bond angles (°)
	Pd-N	Pd-C	Pd-O	Pd-P	C-Pd-N
2.22	2.140(2)	2.002(3)	2.1028(19)	2.2366(10)	80.77(10)

The data revealed a Pd^{II} complex in a distorted square planar geometry supported by a monoanionic bidentate ligand. The Pd-N, Pd-C, Pd-O and Pd-P bond lengths are consistent with similar Pd-X bond lengths reported in the literature.³⁷ The bite angle of the chelating ligand (80.8°) is somewhat similar to that observed for the starting dimeric complex (**2.13**) (81.0°).

2.3.4 Synthesis of [Pd(κ^2 -N[^]C)(PPh₃)Cl]

Following the cleavage of the acetate bridge in **2.10** and **2.11** with PPh₃, the exchange of the acetate ligand with chloride (Cl) was achieved by reacting the monometallic acetate complexes **2.19** and **2.20** with an aqueous solution of sodium chloride. The reactions were carried out at room temperature and gave [Pd(κ^2 -6-phenyl-2-methoxypyridine)(PPh₃)Cl] (**2.23**) and [Pd(κ^2 -6-(4-methylphenyl)-2-methoxypyridine)(PPh₃)Cl] (**2.24**) in quantitative yields (**Scheme 2.14**).

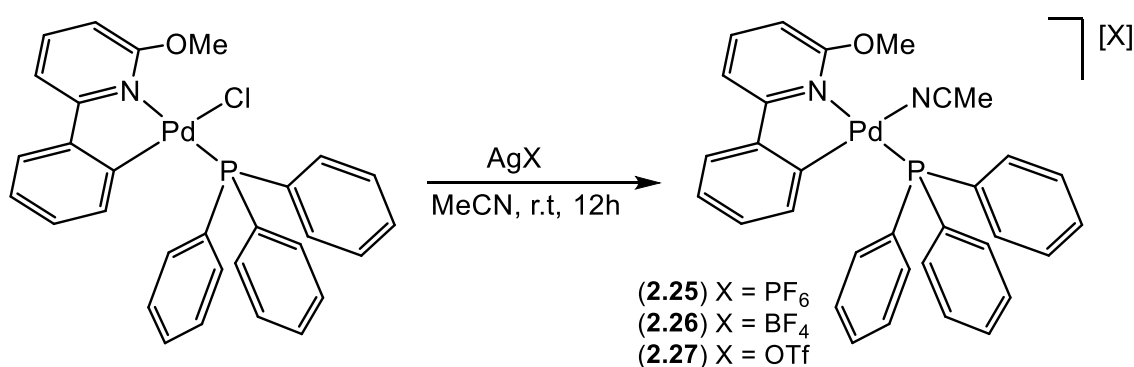
**Scheme 2.14:** Synthesis of [Pd(κ^2 -L_R)(PPh₃)Cl]

The complexes were characterised by spectroscopic (¹H, ³¹P NMR, IR) and mass spectrometric techniques. ¹³C{¹H} NMR data could not be obtained for these two palladium complexes due to their poor solubility in organic solvents. In the ¹H NMR spectra of complexes **2.23** and **2.24**, the 3H singlet (at 1.38 and 1.29 ppm, respectively) representing the methyl group of the acetate ligand in both complexes (**2.19** and **2.20**) had

apparently disappeared. The methoxy protons for the two complexes were shifted downfield by approximately 0.15 ppm as a result of the exchange reactions. In addition, analysis of **2.23** and **2.24** by ^{31}P NMR spectroscopy revealed a singlet at 45.1 and 44.1 ppm, respectively. Upon analysis of **2.23** and **2.24** by electrospray mass spectrometry, it was possible to view a strong fragmentation peak ($[\text{M}-\text{Cl}]^+$) at m/z 552.0719 and 566.0880, respectively. Recrystallisation of the two complexes to give crystals suitable for a single crystal X-ray diffraction was not successful due to their extreme insolubility.

2.3.5 Stoichiometric Reactions with Silver Salts

Complexes of the form $[\text{Pd}(\kappa^2\text{-6-phenyl-2-methoxypyridine})(\text{PPh}_3)(\text{MeCN})][\text{X}]$, where $\text{X} = \text{PF}_6$ (**2.25**), BF_4 (**2.26**) and OTf (**2.27**), have been synthesised by silver-mediated chloride abstraction from **2.23** with AgPF_6 , AgBF_4 and $\text{AgOSO}_2\text{CF}_3$ in the presence of acetonitrile, as driven by the elimination of AgCl (**Scheme 2.15**). The chloride ligand is considered to be relatively labile; therefore, replacing the chloride with acetonitrile was anticipated. The reactions showed a large increase in solubility on adding silver salts to the mixture of the starting material and acetonitrile. The products **2.25**, **2.26** and **2.27** were isolated by cannula filtration and subsequent removal of solvent *in vacuo*, in 93, 78, and 97% yields, respectively.



Scheme 2.15: Chloride abstraction of **2.23** using Ag salts in the presence of acetonitrile

Analysis of **2.25**, **2.26** and **2.27** by ^1H NMR spectroscopy revealed a 3H singlet peak at 1.90, 1.91 and 1.88 ppm, respectively. These peaks are representative of the coordinated MeCN protons. Similar methoxy peaks were seen at 3.98 ppm in the proton NMR spectra of the complexes, and the ^1H NMR pattern of peaks in the aromatic region were found to not vary between all three compounds (**2.25-2.27**). The product **2.25** contains two phosphorus centres due to the presence of a monodentate PPh_3 ligand and the counterion, PF_6^- . The latter is centred at approximately -144 ppm as a septet with a

coupling constant of 705 Hz, where the phosphorus atom is coupling with six equivalent fluorine atoms. The ^{31}P singlet peak at 44.7 ppm integrates in a 1:1 ratio with the PF_6^- peak in the ^{31}P NMR spectrum of **2.25**. For complexes **2.26** and **2.27**, a singlet was also observed at around 45 ppm corresponding to the coordinated PPh_3 ligand. Additionally, the ^{19}F NMR spectrum of **2.25** showed a doublet at -73 ppm with a coupling constant of 711 Hz representing the anion, PF_6^- , while a singlet for both **2.26** and **2.27** was detected in the associated ^{19}F NMR spectra at -153 (BF_4) and -78 (OSO_2CF_3) ppm, respectively. Upon analysis by TOFMS (ES), the presence of a strong fragmentation peak at m/z 522.0723 was found to be common to all three complexes, as ascribed to $[\text{M-MeCN}]^+$. The mass spectra of **2.25**, **2.26** and **2.27** also demonstrated a peak corresponding to the counterion species at m/z 145 (PF_6), 87 (BF_4) and 149 (OTf), respectively.

Suitable crystals of **2.25** and **2.27** for single crystal X-ray diffraction analysis could be grown by slow diffusion of hexane into a solution of the product in dichloromethane/MeCN (95/5 v/v). The same trend was observed for the two complexes as the X-ray structure confirmed the cationic and anionic species, as shown in **Figures 2.9** and **2.10**.

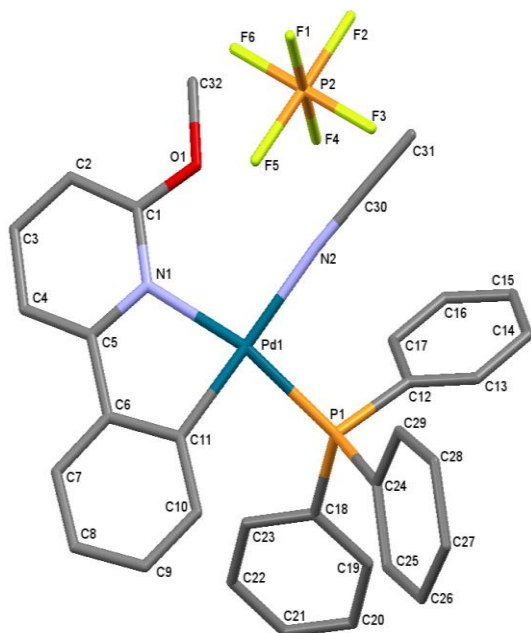


Figure 2.9: X-ray structure of **2.25** with hydrogens omitted for clarity

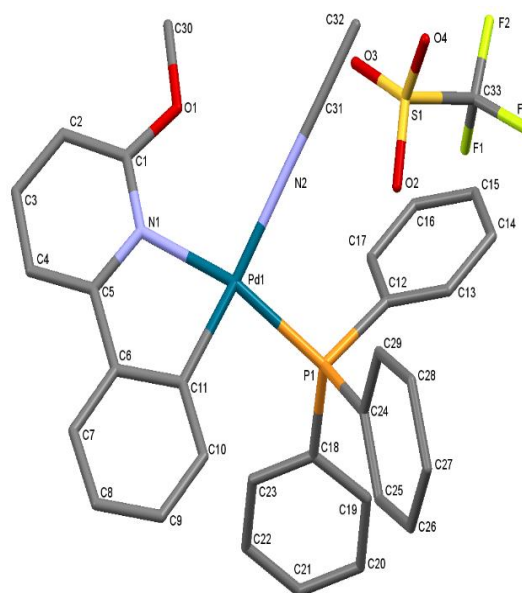


Figure 2.10: X-ray structure of **2.27** with hydrogens omitted for clarity

Table 2.4: Selected Pd-X bond lengths and angles for complexes **2.25** and **2.27**

Complex	Bond lengths (Å)				Bond angles (°)	
	Pd-N1	Pd-C	Pd-N2	Pd-P	P-Pd-N1	C-Pd-N1
2.25	2.133(3)	2.003(4)	2.113(4)	2.2685(13)	158.91(10)	80.49(16)
2.27	2.132(2)	1.986(3)	2.105(2)	2.2687(9)	158.55(7)	80.55(10)

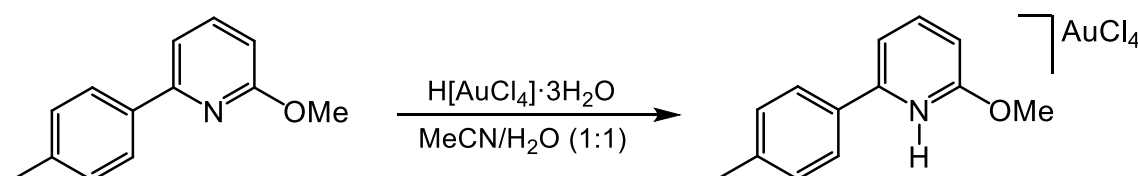
The crystal structure analysis essentially revealed a tetracoordinate and distorted square planar environment about a Pd^{II} centre with a P-Pd-N1 angle of 158.91° and 158.55° for **2.25** and **2.27**, respectively. In both complexes, the bond lengths to the central metal of the pyridine and acetonitrile nitrogen atoms (Pd-N) are almost identical (~2.12 Å) and significantly shorter than the Pd-P bond distance (~2.27 Å) and longer than the Pd-C bond length (~2.00 Å), as reported in **Table 2.4**. The C-Pd-N1 bite angles of the five-membered chelate rings in both complexes are similar to those previously seen in **2.10-2.14** and **2.22**.

All three complexes, **2.25-2.27** were found to be stable in their NMR solutions. The stable formation of these complexes on standing in solution at room temperature was evidenced by the associated ¹H, ¹³C{¹H}, ¹⁹F, (and ³¹P for **2.25**) NMR spectroscopy and mass spectrometry. The presence of a singlet coordinated MeCN resonance in the ¹H NMR spectra and a [counterion]⁻ peak in MS (ES) spectra provided strong corroboration that all three complexes remained intact in solution and had not undergone any form of transformation over time.

2.3.6 Reactions of **2.6** with Gold(III) Salts

A series of cyclometallated gold(III) complexes have been reported and investigated for their biological properties and their ability to act as catalysts in organic synthesis.³⁸ Therefore, synthesis of cycloaurated complexes containing bidentate N^C ligands was the main aim of this section. Unfortunately, however, attempts at cyclometallation of 6-(4-methylphenyl)-2-methoxypyridine (**2.6**) at a gold(III) centre “through C-H activation” were ultimately unsuccessful. In the course of these cycloauration reactions, it was realised that achievement of C-H activation in this type of ligand *via* Au^{III} salts is not an easy task and is usually performed under harsh experimental conditions, albeit in moderate yields.³⁹

Tetrachloroauric acid, $\text{H}[\text{AuCl}_4]$, initially was chosen as the gold(III) starting material. In this instance, it was observed that direct reaction of $\text{H}[\text{AuCl}_4] \cdot 3\text{H}_2\text{O}$ with **2.6** in a mixture of acetonitrile and water (1:1) at room temperature afforded a mono-protonated salt, $[(\mathbf{2.6})(\kappa^1\text{-H})][\text{AuCl}_4]$ (**2.28**), as a yellow precipitate in almost quantitative yield (98%) (**Scheme 2.16**). The salt of the mono-protonated ligand was characterised, *inter alia*, by single crystal X-ray diffraction studies.



Scheme 2.16: Synthesis of $[(\mathbf{2.6})(\kappa^1\text{-H})][\text{AuCl}_4]$ (**2.28**)

The ^1H NMR spectrum showed a complex set of resonances with one significant difference with respect to the free ligand (**2.6**), which was for the methyl and methoxy protons which were shifted *ca.* 0.17 and 0.41 ppm downfield, respectively. The downfield position of these signals can be attributed to removal of electron density caused by coordinated hydrogen. The presence of five aromatic proton resonances between 7.20 and 8.38 ppm in the ^1H NMR spectrum confirmed the formation of the non-C-H activated product $[(\mathbf{2.6})(\kappa^1\text{-H})]\text{AuCl}_4$ (**2.28**). The NH peak was not observed in the ^1H NMR spectrum when the sample was dissolved and the spectrum recorded in CDCl_3 . However, when it was recorded in CD_3CN at room temperature, a resonance representing the newly introduced proton on the pyridyl ring (NH) was seen as a broad peak at 12.57 ppm. The downfield position of the proton in the NH group can be attributed to hydrogen bonding interactions with neighbouring molecules (H_2O or AuCl_4). In addition, the $^{13}\text{C}\{^1\text{H}\}$ NMR spectrum of **2.28** revealed unique carbon environments for the four quaternary aromatic carbon peaks which are in agreement with the predicted structure.

It should be noted that numerous gold complexes with pyridine-based bidentate ligands have been reported in the literature,^{40,41} but it was not until 2017 that the generation of pyridyl salts from the reaction with the gold acid, $\text{H}[\text{AuCl}_4]$, was described. Therefore, it was thought that protonation (not complexation) of **2.6** occurred due to the presence of the methoxy group. However, Stoccoro *et al.*³⁹ mentioned that they could prepare the $[\text{AuCl}_4]^-$ salt of the protonated 2-phenylpyridine, but they did not provide any spectral or analytical data to support their claim (unpublished results). In 2018, structural

and spectroscopic studies performed by Pazderski *et al.*⁴² showed the first reported example of the N[^]C-bidentate ligand protonated by H[AuCl₄]. The bis(7,8-benzoquinolinium) tetrachloroaurate(III) chloride, [(bqnH⁺)₂(AuCl₄⁻)Cl], was obtained from the reaction of H[AuCl₄] with two equivalents of 7,8-benzoquinoline in a mixture of HCl (0.1 M) and ethanol. Whilst the reason for this protonation is unclear, the authors indicated that this is not an unusual coordination.

A broad ν(NH) absorption band centred at *ca.* 3200 cm⁻¹ in the IR spectrum of the product (**2.28**) is consistent with the protonated ligand. Upon analysis of **2.28** by mass spectrometry, a protonated molecular ion peak at *m/z* 200.1080 (Calcd: *m/z* 200.1075) was observed. Further confirmation of the structure of **2.28** was obtained by X-ray diffraction analysis (**Figure 2.11**). Single crystals suitable for analysis were grown by layering the dichloromethane solution of the product with hexane. Selected bond lengths and angles are reported in **Table 2.5**.

The X-ray structure of **2.28** consists of the packing of [HN[^]C] cations and [AuCl₄]⁻ anions in a 1:1 molar ratio in the monoclinic space group P2₁/n. All bond lengths and angles in the cationic ligand and the tetrachloroaurate(III) counterion are as normal. The solid-state of **2.28** showed that the organic cation was protonated at the pyridyl nitrogen. From **Table 2.5**, the solid-state structure of **2.28** showed that the [AuCl₄]⁻ tends to adopt a slightly distorted square planar geometry with the Au-Cl bond distances of 2.281 ± 0.005 Å. The torsion angle between the pyridine and phenyl ring is -30.0(8)°.

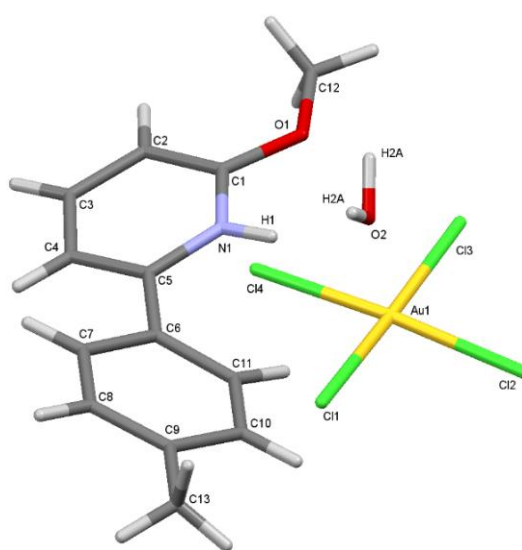
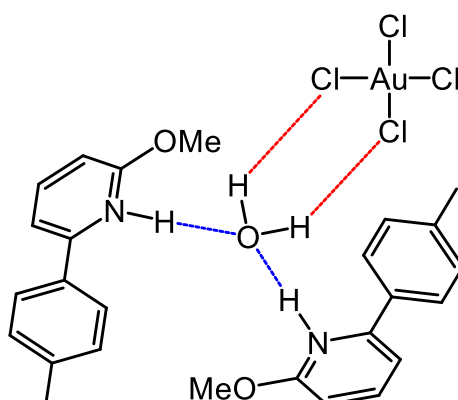


Figure 2.11: X-ray structure of **2.28** with water molecule

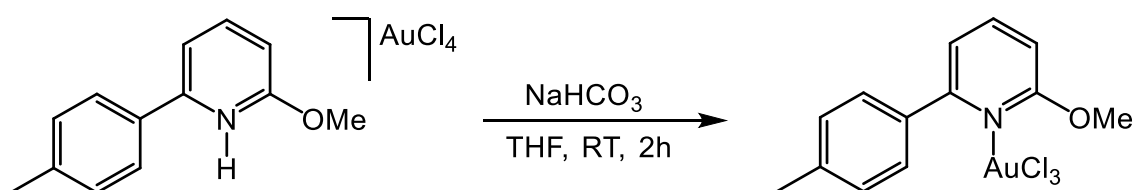
Table 2.5: Selected bond lengths and angles for complex **2.28**

Complex	Bond lengths (Å)		Bond angles (°)	Torsion angles (°)
	C1-O1	Au-Cl	C1-N1-C5	N(1)-C(5)-C(6)-C(11)
2.28	1.331(7)	~2.282(4)	123.7(5)	-30.0(8)

Each two neighbouring cations in the crystal structure are found to be linked by N-H···O···H-N hydrogen bonds (2.05 Å), where the O atom derives from water molecules of solvation that remained in the final product. Moreover, each anion is obviously linked with the H₂O hydrogens through OH···Cl hydrogen bonding interactions (~2.60 Å), in which each hydrogen is hydrogen bonded to a neighbouring chloride. **Figure 2.12** demonstrates all these hydrogen-bonding interactions between the three different molecules, namely two neighbouring pyridyl cations, water and the AuCl₄⁻ anion.

**Figure 2.12:** Intermolecular hydrogen bonding interactions in **2.28**

Treatment of [2.6(κ^1 -H)][AuCl₄] (**2.28**) with a stoichiometric amount of NaHCO₃ in THF at room temperature resulted in deprotonation and thus formation of the N-bonded gold Au^{III} complex, [Au(κ^1 -2.6)Cl₃] (**2.29**) in a 50% yield (**Scheme 2.17**). Further stirring for up to 24 hours did not improve the yield of the product, as the ¹H NMR spectrum of the reaction showed a mixture of the desired product and the free ligand.

**Scheme 2.17:** Synthesis of [Au(κ^1 -2.6)Cl₃] (**2.29**)

Complex **2.29** could be also obtained directly in a similar yield from the reaction of **2.6** with $\text{K}[\text{AuCl}_4]$ in a mixture of acetonitrile and water (1:1) at room temperature. The complex was found to be highly soluble in organic solvents but was not stable in solution, which slowly resulted in product decomposition. The ^1H NMR spectrum of **2.29** revealed five resonances in the aromatic region, indicating that the ligand did not undergo C-H activation with the gold salt. Instead, a monodentate ligand coordinated to the AuCl_3 *via* the nitrogen atom was observed. The methyl and methoxy proton peaks were both shifted to lower frequency with respect to the protonated ligands (**2.28**); this is due to addition of electron density into the ligand system. Furthermore, analysis of **2.29** by $^{13}\text{C}\{^1\text{H}\}$ NMR spectroscopy displayed eleven carbon peaks with five aromatic CH carbons and four quaternary carbon environments. The TOFMS (ES) spectrum obtained from an MeCN solution showed peaks at m/z 523.9623 and 1026.9327, corresponding to the fragments $[\text{M}+\text{Na}^+]^+$ and $[2\text{M}+\text{Na}^+]^+$, respectively.

The solid-state structure of **2.29** was also determined by X-ray diffraction analysis. The single crystals were grown by slow diffusion of hexanes into a DCM solution of the product. The X-ray structure of **2.29** showed to have the AuCl_3 core supported by an N-monodentate ligand (**Figure 2.13**). The product has an almost perfectly square-planar geometry, with the gold atom bound to three chloride ions as well as the nitrogen atom of the pyridine-based ligand, wherein the AuCl_3 unit is nearly perpendicular to the plane of the pyridyl ring, as evidenced by the $\text{Cl}(2)\text{-Au}(1)\text{-N}(1)\text{-C}(1)$ torsion angle of $-89.6(10)^\circ$.

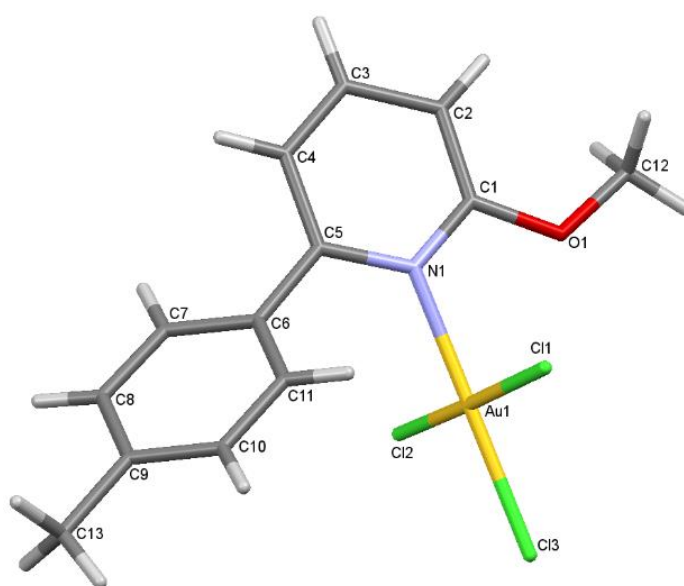


Figure 2.13: X-ray structure of **2.29**

The data reported in **Table 2.6** illustrated that the Au–N(1) bond length of 2.046(10) Å was similar to those previously reported for Au^{III} complexes containing a pyridine ligand.⁴³⁻⁴⁶ The bond length between the Au^{III} centre and Cl(3) is 2.252(4) Å, which is slightly shorter than those of 2.291(4) and 2.273(4) Å for Au–Cl(1) and Au–Cl(2), respectively. The same difference has been observed by other researchers⁴⁶ and can be attributed to the mutual *trans* effect of Cl atoms that are opposite to each other.⁴⁷ The Au–N1 and Au–Cl bond lengths are within the typical range of values and consistent with those for related gold(III) complexes.⁴³⁻⁴⁶

Table 2.6: Selected bond lengths and the bite angle for complex **2.29**

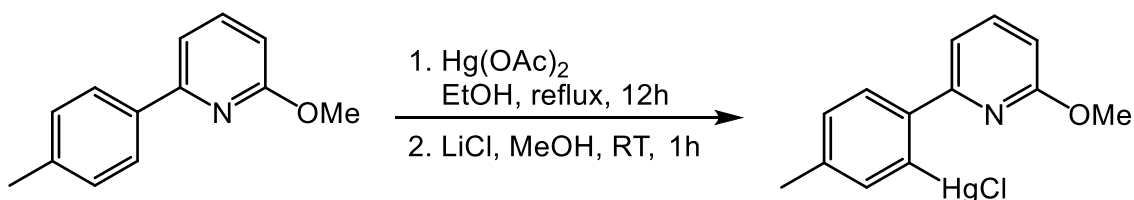
Complex	Bond lengths (Å)				Bond angles (°)	
	Au-N1	Au-Cl3	Au-Cl1	Au-Cl2	N1-Au-Cl1	Cl2-Au-Cl3
2.29	2.046(10)	2.252(4)	2.291(4)	2.273(4)	89.6(3)	90.33(14)

2.3.6.1 Attempts at Achieving C-H Activation with Au^{III}

As mentioned earlier, attempts to synthesise a cyclometallated gold(III) complex using **2.29** as a starting material did not succeed. It is worth noting that cyclometallated complexes of gold(III) are significantly more difficult to obtain compared to those of palladium(II) and platinum(II).³⁸ However, many researchers were able to successfully overcome this challenging problem by using extremely harsh reaction conditions or undesirable transmetallation reactions from organomercury compounds to gold.³⁸ When **2.29** was dissolved in a mixture of acetonitrile and water (1:1) or (5:1) and then heated at reflux to see if the compound underwent direct cyclometallation, it did not. The reaction was also attempted using different solvents, such as acetic acid and chloroform, but it did not yield any cyclometallated product. In addition, microwave radiation, which was used to heat the reaction mixture to high temperature, also proved unsuccessful and indeed showed product decomposition to the free ligand and metallic gold. The N[^]C-cycloaurated complexes are usually reported as light yellow solids, but this was not observed during these reactions.

In order to investigate the second synthetic method (transmetallation) for making a cyclometallated complex of gold(III), it was necessary to synthesise the *ortho*-mercurated compound [Hg(**2.6**)Cl] (**2.30**) for use as a precursor. The organomercury(II) intermediate

(**2.30**) was obtained in a very low yield (19%) from the reaction between 6-(4-methylphenyl)-2-methoxypyridine (**2.6**) and mercury(II) acetate in EtOH, followed by adding one equivalent of LiCl to replace the acetate ligand by chloride (**Scheme 2.18**). A similar low yield has been noted previously by other researchers and attributed to the formation of undesirable products including the *bis*-mercurated compound $[\text{Hg}(\mathbf{2.6})_2]$.⁴⁸ Therefore, the product was slightly impure (ca. 7%) according to ^1H NMR spectroscopy.



Scheme 2.18: Synthesis of $[\text{Hg}(\mathbf{2.6})\text{Cl}]$ (**2.30**)

Analysis of the compound **2.30** by ^1H NMR spectroscopy revealed the presence of a singlet at 7.25 ppm which is accompanied by satellites due to coupling to ^{199}Hg ($^3J_{\text{H-Hg}} = 202$ Hz), indicating that the C-Hg bond had formed. The methyl and methoxy proton singlet peaks were observed at 2.30 and 4.04 ppm. The latter was found to be shifted slightly downfield compared to that of the free ligand (**2.6**). Although the organomercury complex **2.30** is only slightly soluble in organic NMR solvents, its HMQC 2D-NMR spectrum showed six inequivalent CH systems which correspond to all carbon-H atoms in the aromatic region. Fragmentation peaks at m/z 400.0627 and 436.0384 corresponding to the loss of a chlorine ($[\text{M}-\text{Cl}]^+$) and the product ($[\text{M}+\text{H}]^+$), respectively, were observed by TOFMS (ASAP).

Transmetalation from the corresponding organomercury compound (**2.30**) was first attempted with $\text{H}[\text{AuCl}_4]$ in ethanol in the presence of NaHCO_3 . After 15 hours stirring at room temperature and work-up, the ^1H NMR spectrum of the crude product displayed only unreacted starting material (**2.30**). In a second attempt, a dichloromethane solution of **2.30** was added to a solution of $\text{K}[\text{AuCl}_4]$ in acetonitrile. The reaction mixture was then left to stir at room temperature for 12 hours to give a light yellow precipitate which was filtered and washed with EtOH and Et_2O . The ^1H NMR spectrum of the crude product showed that the cycloaurated complex of **2.6** (with some impurities, ca. 15%) might have been obtained as a clear singlet in the aromatic region can be seen in the ^1H NMR spectrum (**Figure 2.14**).

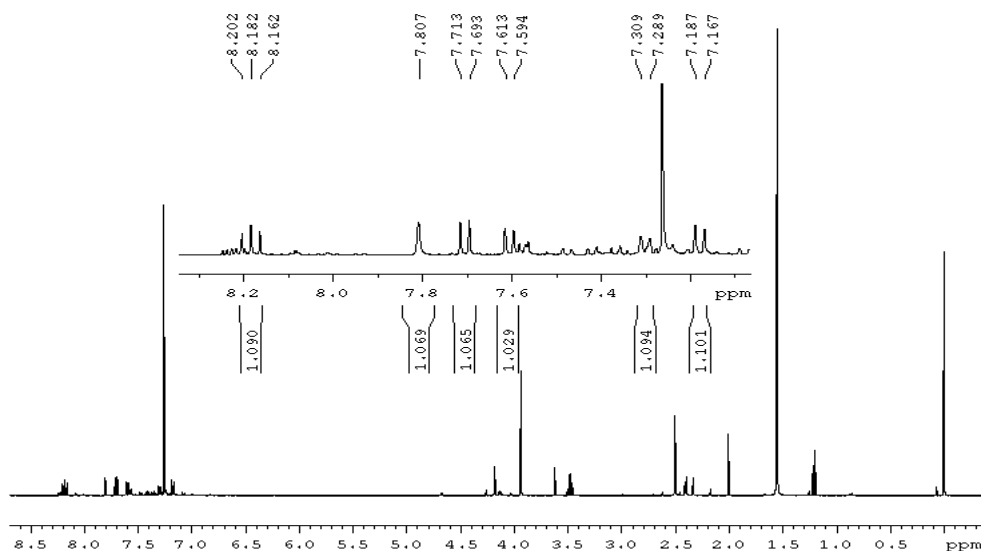


Figure 2.14: ^1H NMR spectrum of the crude product obtained from the gold-mercury exchange reaction

Further evidence as to the presence of the cyclometallated gold(III) complex could not be provided due to its poor solubility in CDCl_3 and other NMR solvents. It was also found that on standing in solution at room temperature, the product underwent slow decomposition, as was subsequently confirmed by ^1H NMR spectroscopy. Attempts to purify the product by crystallisation were unsuccessful.

It should be noted that there was another procedure,^{41,49} which was attempted in order to obtain the cyclometallated complex of gold(III) rather than transmetallation and traditional heating under reflux reactions. The method involves a direct heating of the corresponding N-bonded Au^{III} complex $[\text{Au}(\mathbf{2.6})\text{Cl}_3]$ (**2.29**), in a ceramic dish in an oven at high temperature ($170\text{ }^\circ\text{C}$) for 6 hours, in order to activate the C-H bond. However, this experiment was found to lead to decomposition of the starting material (**2.29**) instead of formation of the chelating complex.

2.3.7 Aerobic Oxidation of Benzyl Alcohol Catalysed by Dinuclear Palladium(II) Complexes

As an application of the complexes synthesised in this work, the oxidation of benzyl alcohol to benzaldehyde, as catalysed by cyclopalladated complexes in the presence of a base, has been examined (**Figure 2.15**).

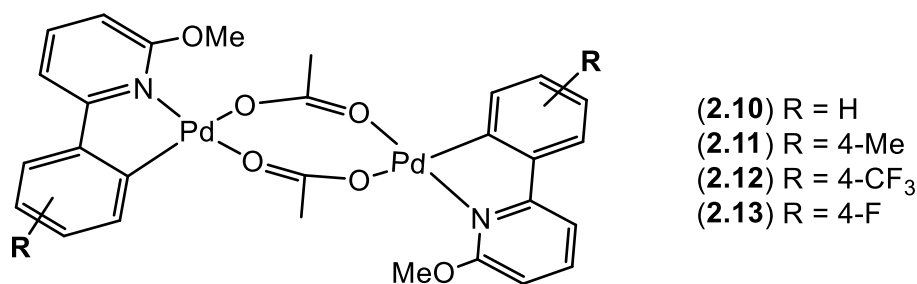
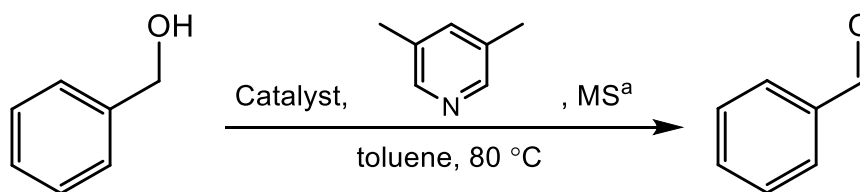


Figure 2.15: Dimeric Pd^{II} complexes used as catalysts for the oxidation of benzyl alcohol

The palladacycles **2.10**, **2.11**, **2.12** and **2.13** were found to be highly efficient catalysts for aerobic alcohol oxidation in the presence of a base, such as 3,5-lutidine or triphenylphosphine, using oxygen in the air as an oxidising agent. Typically, the catalytic reactions were carried out in dry toluene (3 mL) at 80 °C using a palladium catalyst (5 mol% Pd), a base (20 mol%) and a solution of benzyl alcohol (1 mmol) in dry toluene (4 mL) to give the product in excellent conversion, as determined by ¹H NMR spectroscopic analysis of the reaction mixture based on the benzyl alcohol starting material (**Table 2.7**).

Table 2.7: Oxidation of benzyl alcohol catalysed by palladacycles



Entry	Cat. (mol% Pd)	Base (20 mol%)	Solv.	Temp. (°C)	Conversion (%) ^b after:			
					4h	8h	12h	24h
1	Pd(OAc) ₂ (5)	3,5-lutidine	toluene	80	83	100	-	-
2	2.10 (5)	3,5-lutidine	toluene	80	67	89	>99	100
3	2.11 (5)	3,5-lutidine	toluene	80	72	94	100	-
4	2.12 (5)	3,5-lutidine	toluene	80	86	96	98	100
5	2.13 (5)	3,5-lutidine	toluene	80	69	88	96	100
6	No Catalyst	3,5-lutidine	toluene	80	0	0	0	0
7	2.11 (2.5)	3,5-lutidine	toluene	80	57	72	81	90
8	2.11 (5)	No Base	toluene	80	2	5	10	27
9	2.11 (5)	PPh ₃	toluene	80	14	23	33	50
10	2.11 (5)	3,5-lutidine	toluene	100	87	94	96	100
11	2.11 (5)	3,5-lutidine	MeCN	80	4	8	11	14

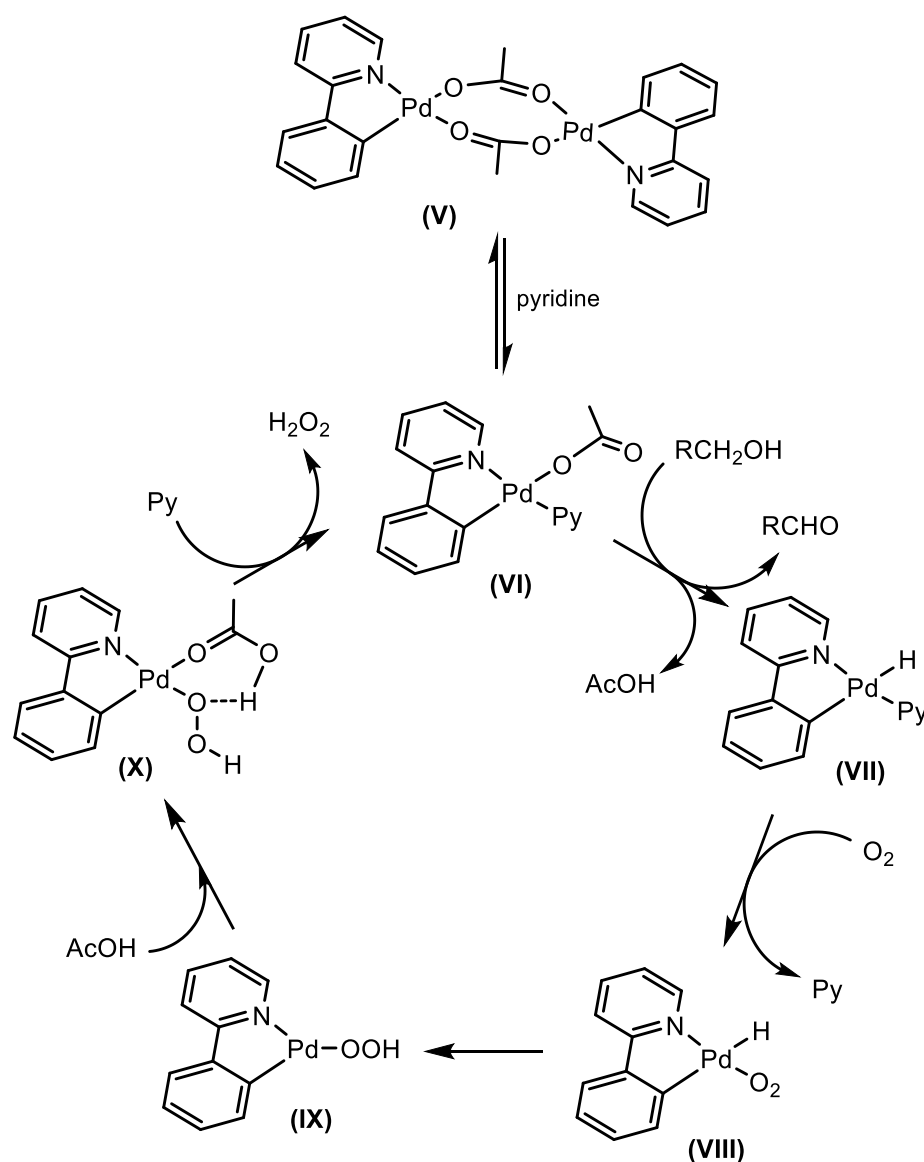
^a molecular sieves; ^b Conversion was determined with ¹H NMR analysis

First of all, the catalytic activity was examined under the basic condition (Entry 1) with the most common Pd^{II} catalyst used for these type of reactions, palladium(II) acetate. This catalytic reaction would help investigate the role of the coordinated bidentate ligands in the stability of those dimeric complexes used as catalysts (**2.10-2.13**). It was found that Pd(OAc)₂ gave complete conversion after only 8 hours (Entry 1). The performance of four dimeric palladium complexes (**2.10-2.13**) as catalysts for the oxidation of benzyl alcohol were then examined (Entries 2-5). The initial reaction conditions were selected according to the catalytic studies reported by Moberg and co-workers.^{17,18} Though the data reported in **Table 2.7** shows that all complexes displayed excellent catalytic activity for aerobic alcohol oxidation under basic conditions, formation of benzaldehyde was somewhat faster towards the beginning of the reaction with **2.12** (Entry 4). However, product formation was then found to slow down after a few hours, while the catalytic reaction with **2.11** (Entry 3) went to completion within the same time (12 hours). The initial reaction rates for complexes **2.10** and **2.13** were generally found to be lower than those for **2.11** and **2.12** (Entries 2-5). It may also be noticed from **Table 2.7** (Entry 6) that there was no reaction at all in the absence of a palladium catalyst, while decreasing the catalyst loading by half (2.5 mol%), reduced product formation to 81% in 12 hours, and furthermore the reaction did not go to completion even after 24 hours (Entry 7). Due to the product conversion after 12 hours being the highest when complex **2.11** (Entry 3) was employed as a catalyst, it was consequently selected as a catalyst for the reaction optimisation.

To examine the role of the base, the catalytic oxidation of benzyl alcohol in the presence of **2.11** was carried out without using a base. The reaction displayed a very slow conversion to the product (27% within 24 hours), as shown in **Table 2.7** (Entry 8). This finding demonstrates that the aerobic alcohol oxidation is a base-dependent reaction in which the base plays a significant role in producing an active catalyst state. When PPh₃ was used as a base for the oxidation of alcohol, the reaction was affected and did not lead to complete conversion of the substrate, even after 24 hours (50%), as seen in Entry 9. This indicates that the use of 3,5-lutidine for this type of reaction in toluene at 80 °C is better than using PPh₃. It is worth noting that the experimental studies carried out by Moberg *et al.*¹⁸ suggested that pyridine was the best choice among a variety of bases employed for alcohol oxidation and can act not only as a base but also as a ligand in the catalytic cycle, as will be shown later.

The activity of the catalyst (**2.11**) within the first four hours increased when the reaction temperature was raised to 100 °C (Entry 10). However, after 12 hours the catalytic oxidation reaction resulted in a 96% conversion of the product versus a complete conversion at 80 °C. As shown in **Table 2.7** (Entry 11), reduced conversion was observed when acetonitrile was used as a solvent. The lower catalytic activity in acetonitrile is consistent with other studies on aerobic alcohol oxidation catalysed by Pd^{II} complexes¹⁹ and could be attributed to the instability of the solvent during the reaction process, as acetonitrile can compete with 3,5-lutidine to act as a ligand.

In 2005, Moberg *et al.*¹⁸ performed a computational study on aerobic alcohol oxidation with a related palladium catalyst. The results of this study support the mechanism shown in **Scheme 2.19**.



Scheme 2.19: Mechanism for aerobic alcohol oxidation proposed by Moberg *et al.*¹⁸

The proposed mechanism of the Pd^{II}/pyridine/O₂ system was suggested to proceed through the formation of a Pd alkoxide intermediate followed by β -hydride elimination as the rate-determining step. This reaction is first initiated by the ligand (pyridine) by which the dimeric palladium complex (**V**) is cleaved into two moles of [Pd(N[^]C)(Py)(OAc)] (**VI**). The substrate (alcohol compound) would then be able to displace the terminal acetate ligand from **VI** and bind to the Pd^{II} centre in a monodentate fashion through the O atom, followed by the release of the product and formation of a Pd-H species (**VII**). The insertion of molecular oxygen into the palladium-hydride (**VII**) yields **VIII**, in which the Pd-O₂ bond is formed in the *cis*-position to the Pd-H bond, allowing an interaction between the two atoms (H and O) so as to form a hydroperoxide species (**IX**). This is subsequently protonated by AcOH to release hydrogen peroxide (H₂O₂) from the intermediate **X** in the presence of pyridine.

2.4 Conclusions and Future Work

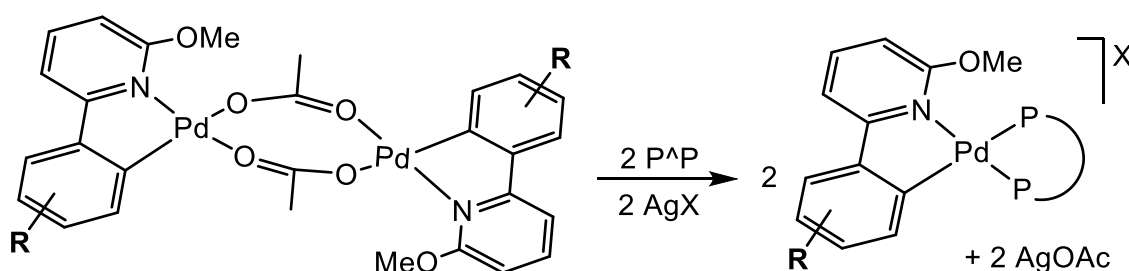
A variety of OMe-bidentate ligands with different aryl groups (**2.5-2.9**) have been successfully synthesised *via* a series of steps, followed by the synthesis of novel dimeric palladium(II) complexes of the general formula [Pd(κ^2 -N[^]C)(μ -OAc)]₂ (**2.10-2.14**). The solid-state structures of these complexes tend to adopt an open-book geometry with two chelating N[^]C ligands bridged by two acetate groups. A series of novel mononuclear Pd^{II} complexes have been obtained *via* a disassembly reaction from the dimeric Pd^{II} complexes using 3,5-lutidine (with **2.10-2.12**), PPh₃ (with **2.10-2.13**) and **2.6** (with only **2.11**). Complexes converted into mononuclear species using 3,5-lutidine were only obtained in solution and found to be in equilibrium, while those with PPh₃ could be isolated as solids. The stability of these complexes may be explained by a relatively strong Pd-P bond, as phosphines act as both good σ -donors and good π -acids. The X-ray structure of **2.22** revealed a Pd^{II} complex in a distorted square planar geometry supported by a monoanionic bidentate ligand, where the carbon atom is *trans* to the acetate ligand and the pyridyl nitrogen is *trans* to the PPh₃ ligand. The palladium(II) complexes (**2.10-2.13**) showed significant catalytic activity for the aerobic oxidation of benzyl alcohol by giving the corresponding aldehyde in excellent conversions.

Following the cleavage of the dimeric complexes in **2.10** and **2.11** with PPh₃, the replacement of the acetate ligand with chloride (Cl) was achieved by reacting the monometallic acetate complexes **2.19** and **2.20** with an aqueous solution of sodium chloride to give the corresponding Pd-Cl complexes (**2.23-2.24**). The potential of the Pd-

Cl complex (**2.23**) to act as a precursor to cation-anion pairs has been explored using a halide abstraction reaction in acetonitrile with different silver salts including AgPF₆, AgBF₄ or AgOTf. All three complexes, **2.25-2.27**, were found to be stable in solution, as confirmed by ¹H, ¹³C{¹H}, ¹⁹F, (³¹P for **2.25**) NMR spectroscopy and mass spectrometry.

All attempts, including traditional activation, transmetallation and direct heating, at the cyclometallation of 6-(4-methylphenyl)-2-methoxypyridine (**2.6**) at a gold(III) centre “through C-H activation” were unsuccessful. However, reactions of **2.6** with H[AuCl₄] and K[AuCl₄] gave [(**2.6**)(κ¹-H)][AuCl₄] (**2.28**) and [Au(κ¹-**2.6**)Cl₃] (**2.29**), respectively. Complex **2.29** could be also obtained by treating **2.28** with a stoichiometric amount of NaHCO₃ in THF at room temperature.

In order to further investigate the interactions in these dimeric systems synthesised in this chapter, it may be of interest in the future to carry out the disassembly reactions with symmetrical bidentate ligands (such as a P[^]P system) to produce monopalladated complexes with the general formula [Pd(κ²-N[^]C)(κ²-P[^]P)][X] upon addition of an appropriate silver salt (**Scheme 2.20**).



Scheme 2.20: Reactions of dimeric Pd^{II} complexes with diphosphine ligands

References

1. A. E. Shilov and G. B. Shul'pin, *Chem. Rev.*, 1997, **97**, 2879.
2. J. A. Labinger and J. E. Bercaw, *Nature*, 2002, **417**, 507.
3. E. Negishi, *Handbook of Organopalladium Chemistry for Organic Synthesis*, Wiley Interscience, New York, 2002.
4. M. Albrecht, *Chem. Rev.*, 2009, **110**, 576.
5. Y. Boutadla, D. L. Davies, S. A. Macgregor and A. I. Poblador-Bahamonde, *Dalton Trans.*, 2009, 5820.
6. A. D. Ryabov, *Chem. Rev.*, 1990, **90**, 403.
7. D. Aguilar, R. Bielsa, M. Contel, A. Lledós, R. Navarro, T. Soler and E. P. Urriolabeitia, *Organometallics*, 2008, **27**, 2929.
8. A. C. Cope and R. W. Siekman, *J. Am. Chem. Soc.*, 1965, **87**, 3272.
9. H. Takahashi and J. Tsuji, *J. Organomet. Chem.*, 1967, **10**, 511.
10. P. Spellane, R. J. Watts and A. Vogler, *Inorg. Chem.*, 1993, **32**, 5633.
11. F. W. Vanhelfmont, G. F. Strouse, H. U. Güdel, A. C. Stückl and H. W. Schmalte, *J. Phys. Chem. A*, 1997, **101**, 2946.
12. F. W. Vanhelfmont and H. U. Güdel, *Inorg. Chem.*, 1997, **36**, 5512.
13. R. C. Davis, T. J. Grinter, D. Leaver and R. M. O'Neil, *Tetrahedron Lett.*, 1979, **20**, 3339.
14. M. A. Gutierrez, G. R. Newkome and J. Selbin, *J. Organomet. Chem.*, 1980, **202**, 341.
15. J. E. Bercaw, A. C. Durrell, H. B. Gray, J. C. Green, N. Hazari, J. A. Labinger and J. R. Winkler, *Inorg. Chem.*, 2010, **49**, 1801.
16. N. R. Deprez and M. S. Sanford, *J. Am. Chem. Soc.*, 2009, **131**, 11234.
17. K. Hallman and C. Moberg, *Adv. Synth. Catal.*, 2001, **343**, 260.
18. S. Paavola, K. Zetterberg, T. Privalov, I. Csöregy and C. Moberg, *Adv. Synth. Catal.*, 2004, **346**, 237.
19. T. Privalov, C. Linde, K. Zetterberg and C. Moberg, *Organometallics*, 2005, **24**, 885.
20. Y. B. Dudkina, D. Y. Mikhaylov, T. V. Gryaznova, A. I. Tufatullin, O. N. Kataeva, D. A. Vicic and Y. H. Budnikova, *Organometallics*, 2013, **32**, 4785.

21. W. Yu, W. N. Sit, Z. Zhou and A. S. Chan, *Org. Lett.*, 2009, **11**, 3174.
22. T. Nguyen, M. A. Wicki and V. Snieckus, *J. Org. Chem.*, 2004, **69**, 7816.
23. R. Pathak, K. Vandayar, W. A. van Otterlo, J. P. Michael, M. A. Fernandes and C. B. de Koning, *Org. Biomol. Chem.*, 2004, **2**, 3504.
24. S. Bruns, V. Sinnwell and J. Voss, *Magn. Reson. Chem.*, 2003, **41**, 269.
25. C. Zhao, D. Xue, Z. Jia, C. Wang and J. Xiao, *Synlett*, 2014, **25**, 1577.
26. K. Matos and J. A. Soderquist, *J. Org. Chem.*, 1998, **63**, 461.
27. G. Kerric, E. Le Grogneq, F. Zammattio, M. Paris and J. Quintard, *J. Organomet. Chem.*, 2010, **695**, 103.
28. L. Ackermann, H. K. Potukuchi, A. R. Kapdi and C. Schulzke, *Chem. A Eur. J.*, 2010, **16**, 3300.
29. D. X. Yang, S. L. Colletti, K. Wu, M. Song, G. Y. Li and H. C. Shen, *Org. Lett.*, 2008, **11**, 381.
30. N. Liu and Z. Wang, *J. Org. Chem.*, 2011, **76**, 10031.
31. C. L. Smith, C. Hirschhäuser, G. K. Malcolm, D. J. Nasrallah and T. Gallagher, *Synlett*, 2014, **25**, 1904.
32. K. Nakamoto, *Infrared and Raman spectra of inorganic and coordination compounds*, Wiley Interscience, New York, 1986.
33. D. J. Cárdenas, A. M. Echavarren and M. C. Ramírez de Arellano, *Organometallics*, 1999, **18**, 3337.
34. R. F. Carina, A. F. Williams and G. Bernardinelli, *J. Organomet. Chem.*, 1997, **548**, 45.
35. A. D. Ryabov, *Inorg. Chem.*, 1987, **26**, 1252.
36. D. Niedzielska, T. Pawlak, A. Wojtczak, L. Pazderski and E. Szlyk, *Polyhedron*, 2015, **92**, 41.
37. L. Piche, J. Daigle, R. Poli and J. P. Claverie, *Eur. J. Inorg. Chem.*, 2010, **2010**, 4595.
38. W. Henderson, *Adv. Organomet. Chem.*, 2006, **54**, 207.
39. S. Stoccoro, G. Alesso, M. A. Cinellu, G. Minghetti, A. Zucca, M. Manassero and C. Manassero, *Dalton Trans.*, 2009, 3467.
40. E. C. Constable and T. A. Leese, *J. Organomet. Chem.*, 1989, **363**, 419.

41. M. Ivanov and M. Puzyk, *Russ. J. Gen. Chem.*, 2001, **71**, 1660.
42. D. Niedzielska, L. Pazderski, A. Wojtczak, M. Kurzawa, J. Ścianowski and E. Szłyk, *Polyhedron*, 2018, **139**, 155.
43. V. Ferretti, P. Gilli, V. Bertolasi, G. Marangoni, B. Pitteri and G. Chessa, *Acta Crystallogr. Sect. C: Cryst. Struct. Commun.*, 1992, **48**, 814.
44. K. Ortner and U. Abram, *Inorg. Chem. Comm.*, 1998, **1**, 251.
45. V. Bertolasi, G. Annibale, G. Marangoni, G. Paolucci and B. Pitteri, *J. Coord. Chem.*, 2003, **56**, 397.
46. T. V. Segapelo, I. A. Guzei, L. C. Spencer, W. E. Van Zyl and J. Darkwa, *Inorg. Chim. Acta*, 2009, **362**, 3314.
47. A. G. Orpen and M. J. Quayle, *J. Chem. Soc. Dalton Trans.*, 2001, 1601.
48. R. Parish, J. P. Wright and R. G. Pritchard, *J. Organomet. Chem.*, 2000, **596**, 165.
49. D. E. Janzen, S. R. Doherty, D. G. VanDerveer, L. M. Hinkle, D. A. Benefield, H. M. Vashi and G. J. Grant, *J. Organomet. Chem.*, 2014, **755**, 47.

Chapter 3

*Cyclopalladated 6-Aryl-2-Pyridones: Synthesis
and Intra-/Inter-molecular Reactivity*

3.1 Introduction

2-pyridone-based compounds have recently attracted much attention due to their wide range of applications in different fields including biological systems,¹⁻³ natural product synthesis,⁴ organic dyes⁵ and fluorescence.⁶ The key physical characteristic that leads to these compounds being of particular interest is the attached hydroxyl group, which can play various roles in organic catalysis, such as a coordination partner, H-bonding donor/accepter as well as being a proton source. The hydroxyl group has been extensively exploited in the design of complexes that can be used as multifunctional catalysts in organometallic chemistry. The OH group also has the ability to increase water solubility, to allow easy introduction as a ligand and to allow the ligand to undergo acid-base reactions to provide pH-switchability to a metal complex. Moreover, a variety of binding modes are possible for 2-pyridone and substituted derivatives in general, as discussed earlier in section 1.4.2. These features and others have encouraged inorganic chemists to look for new developments in the synthesis of complexes containing 2-pyridone (2-hydroxypyridine) or its derivatives in the last few years.

Although there has been extensive work on 2-pyridone and its derivatives in the field of coordination chemistry,⁷ this area is still in its early and active stages of development.⁸ This introduction will deal with 2-pyridone-based bidentate ligands, in particular those substituted at the 6-position of the heterocyclic ring. Therefore, an overview of the properties and coordination capabilities of the functionalised bidentate ligands will be given followed by selected examples of coordination complexes including a discussion of their catalytic activities.

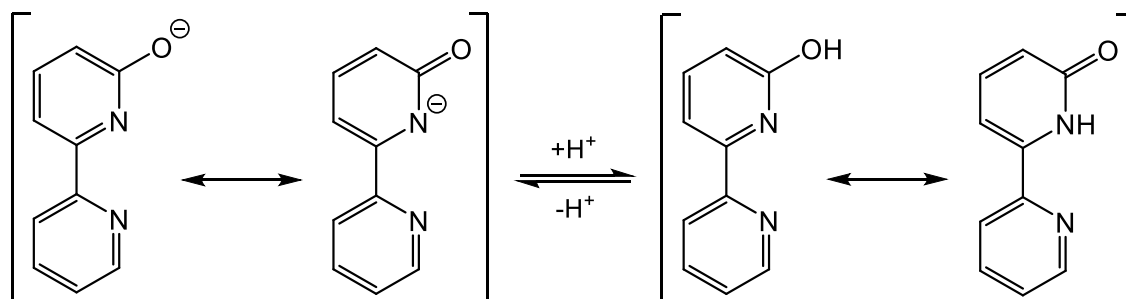
3.1.1 OH-Substituted Bidentate Ligands

In the coordination chemistry of transition metals, OH-functionalised bidentate ligands can be classified into a variety of categories according to their donor atoms (N, P, C, S, O etc...). However, only two related types will be discussed here, namely OH-functionalised N^N- and N^C-chelated bidentate N-heterocycles.

a. OH-Functionalised N^N-Chelate Ligands

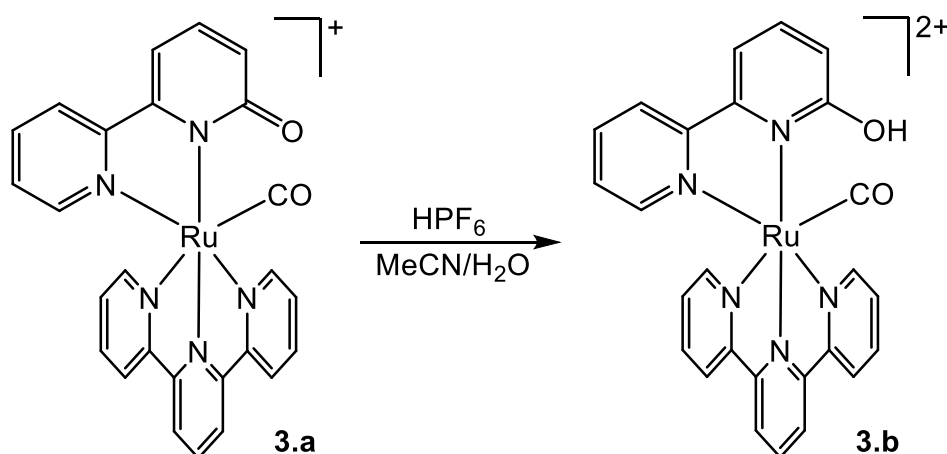
As mentioned earlier, the presence of a hydroxy group allows for an acid-base equilibrium between the protonated pyridinol and deprotonated pyridonate ligands to be formed, leading to remarkable changes in both electronic properties and polarity. This is attributed to the difference between the hydroxy (pyridinol) and oxyanion (pyridonate)

forms (**Scheme 3.1**).⁹ Specifically, the pyridinol form is expected to have relatively moderate electron donating ability and polarity, while the pyridonate form is able to show strong electron donating ability and polarity.



Scheme 3.1: Acid-base equilibrium between pyridonate (left) and pyridinol (right)

Only a few metal complexes with OH-functional N^N-chelate ligands have been reported to date. Tanaka *et al.*,¹⁰ who first discussed the acid-base equilibrium of complexes containing hydroxy-substituted bidentate ligands, were able to synthesise a Ru^{II} carbonyl complex (**3.a**) based on the 2,2'-bipyridin-6(1*H*)-one (bpyO) ligand. The authors found that treatment of **3.a** with an aqueous HPF₆ solution (1.5 equivalents) afforded the corresponding Ru^{II} carbonyl complex (**3.b**) bearing the ligand in its pyridinol form (bpyOH), as shown in **Scheme 3.2**.



Scheme 3.2: Synthesis of **3.b** from **3.a**

This interconversion plays an important role in controlling the electronic properties and polarity of this type of complex when they are used as catalysts purely through changing the pH.⁹ Recently, photophysical studies carried out by Xiang *et al.*¹¹ demonstrated that

emission properties of similar ruthenium(II) complexes, $[\text{Ru}^{\text{II}}(\text{bpy})_2(\text{bpyO})][\text{BF}_4]$ and $[\text{Ru}^{\text{II}}(\text{bpy})_2(\text{bpyOH})][(\text{BF}_4)_2]$, can also be varied significantly, depending on whether the complex exists in its protonated or deprotonated form.

In 2012, Fujita *et al.*¹² developed a new catalytic system for dehydrogenative oxidation of alcohols performed in water using a water-soluble Cp^*Ir catalyst, $[\text{Cp}^*\text{Ir}(\text{bpyOH})(\text{H}_2\text{O})][(\text{OTf})_2]$ (**3.c**), containing an OH-functional bipyridine ligand at the *ortho*-position. In order to demonstrate the role of the *ortho*-hydroxy group in the catalytic performance, the complex $[\text{Cp}^*\text{Ir}(\text{bpy})(\text{H}_2\text{O})][(\text{OTf})_2]$ (**3.d**) was also prepared (**Figure 3.1**). The authors found that there were remarkable differences in the catalytic activity for dehydrogenative oxidation of benzyl alcohol between the two complexes. Reaction with **3.d** gave the corresponding product in only a 25% yield, while the other catalyst (**3.c**) improved the yield to 51%. The results indicated that improved catalytic performance can be obtained by introducing a hydroxy substituent at the *ortho*-position of the bipyridine ligand.

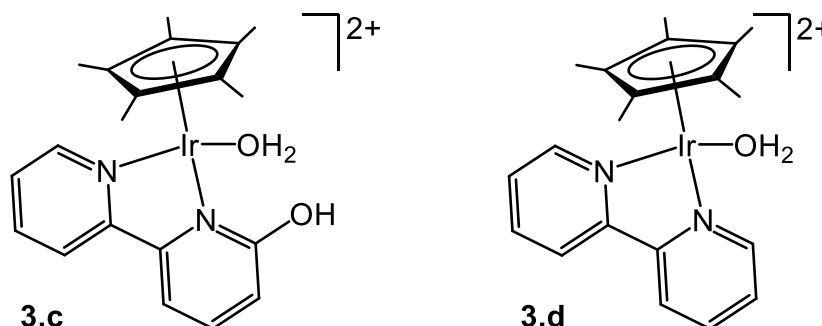
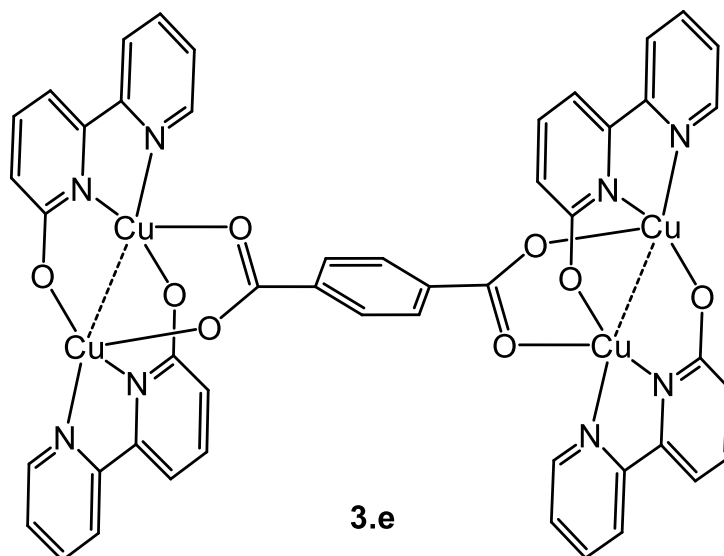


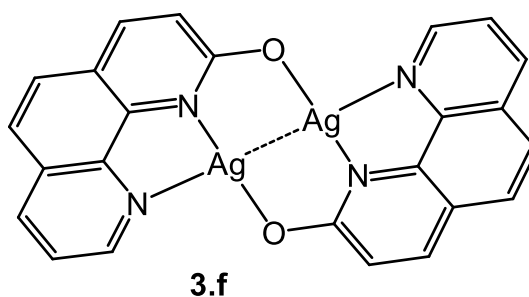
Figure 3.1: Water-soluble Cp^*Ir catalysts

In coordination chemistry, an interesting feature of *ortho*-hydroxylated bipyridine ligand and its derivatives is their ability to act with a variety of bonding modes on a metal centre, as seen for the 2-hydroxypyridine. An example of this is the mixed-valent dicopper complex which was synthesised by Chen *et al.*^{13,14} as a novel tetrameric complex, $[\text{Cu}_4(\text{bpyO})_4(\text{tp})]$ (**3.e**), where tp is terephthalate. The synthesis of the Cu_2^{III} mixed-valent complex was performed under hydrothermal conditions in which the bpy ligand was hydroxylated into the bpyO ligand during the reaction. Other ligands, such as 1,10-phenanthroline (phen/phenO), show similar behaviour. The X-ray structure of **3.e** revealed a pair of $[\text{Cu}_2(\text{bpyO})_2]$ moieties bridged by a terephthalate ligand. In addition to

the traditional binding to a metal centre in an N^N-chelate fashion, the bpyO ligand was also able to bridge two copper centres *via* the N and O atoms. The tetrameric complex (**3.e**) has an overall charge of 0, and therefore no counterion was required. The bond order of the Cu-Cu bond in the mixed-valent species is 1.5. Since the odd electron is delocalised between the two copper centres, the complex is more accurately formulated as valent-averaged Cu₂ (I^{1/2},I^{1/2}).



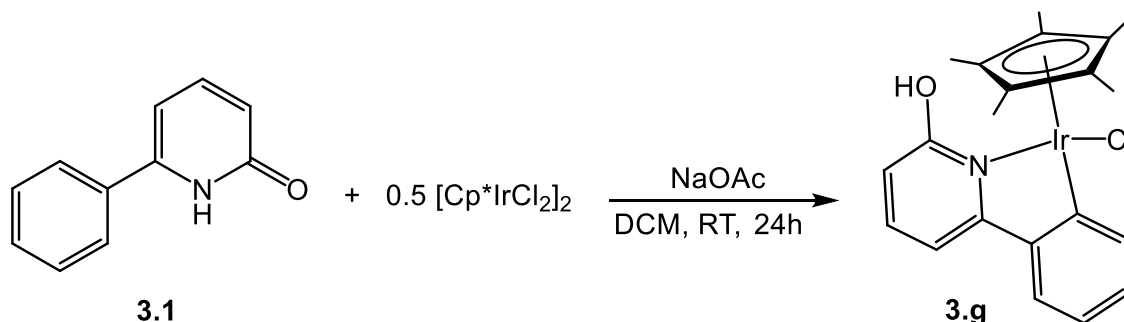
The same group, later synthesised a novel dimeric organosilver(I) complex, [Ag₂(phenO)₂] (**3.f**), using an OH-functional ligand as a starting material. The complex was prepared by the reaction of AgNO₃ (in MeCN) with phenO (in DCM) at room temperature using the liquid diffusion method. The authors were able to obtain single crystals suitable for analysis by X-ray diffraction. The structure showed that each metal centre is coordinated by two nitrogen atoms from a phenO ligand and one oxygen from another phenO ligand. The dinuclear silver(I) complex has a relatively short Ag...Ag distance which may indicate a strong metal...metal bonding interaction.¹⁵



b. OH-Functionalised N[^]C-Chelate Ligands

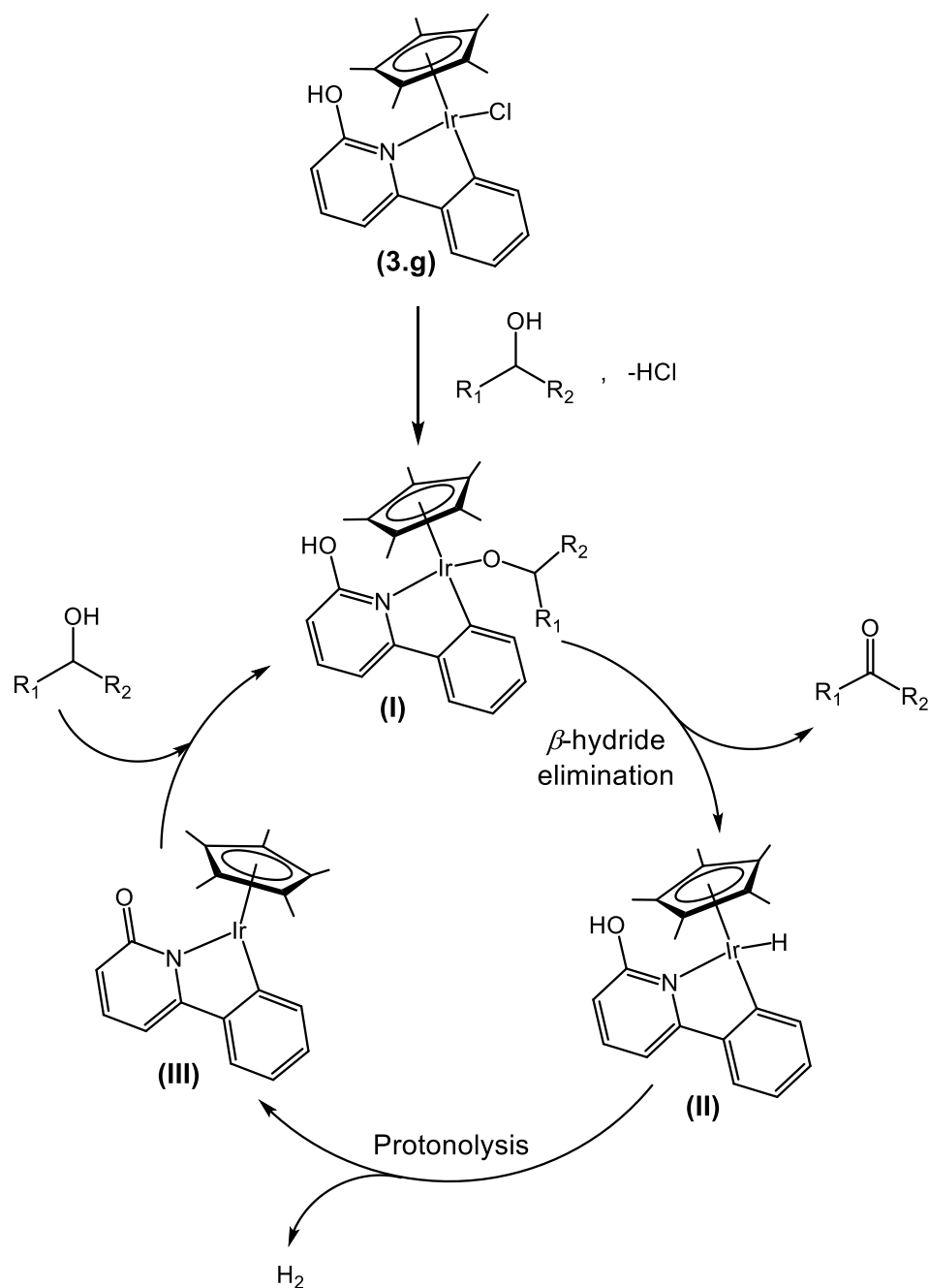
Functionalised N[^]C-chelate ligands with a hydroxy group at the 2-position of the pyridyl ring may be expected to have similar properties to those observed for the 2-hydroxy-substituted N[^]N-bidentate ligands. In addition to those properties, N[^]C ligands are also able to undergo C-H activation of the aryl group located at the 6-position of the pyridyl ring.

Surprisingly, only a few examples of the pyridone-based bidentate complexes involving C-H activation have been reported in the literature.¹⁶ The 6-phenyl-2-pyridone (**3.1**) is a typical member of the 2-pyridone family that show C-H activation of the phenyl group at the *ortho* position. In 2011, Yamaguchi *et al.*¹⁷ reported a new Cp*Ir complex bearing **3.1** as a functional ligand. The Cp*Ir complex (**3.g**) was obtained in 62% yield by reacting [Cp*IrCl₂]₂ with **3.1** in the presence of NaOAc in dichloromethane at room temperature (**Scheme 3.3**). The crystallographic data showed that the ligand coordinated to the metal centre *via* the pyridyl nitrogen and *ortho*-phenyl carbon atoms affording an N[^]C-cyclometallated Ir^{III} complex (**3.g**).



Scheme 3.3: Synthesis of the Cp*Ir complex containing 6-phenyl-2-pyridone

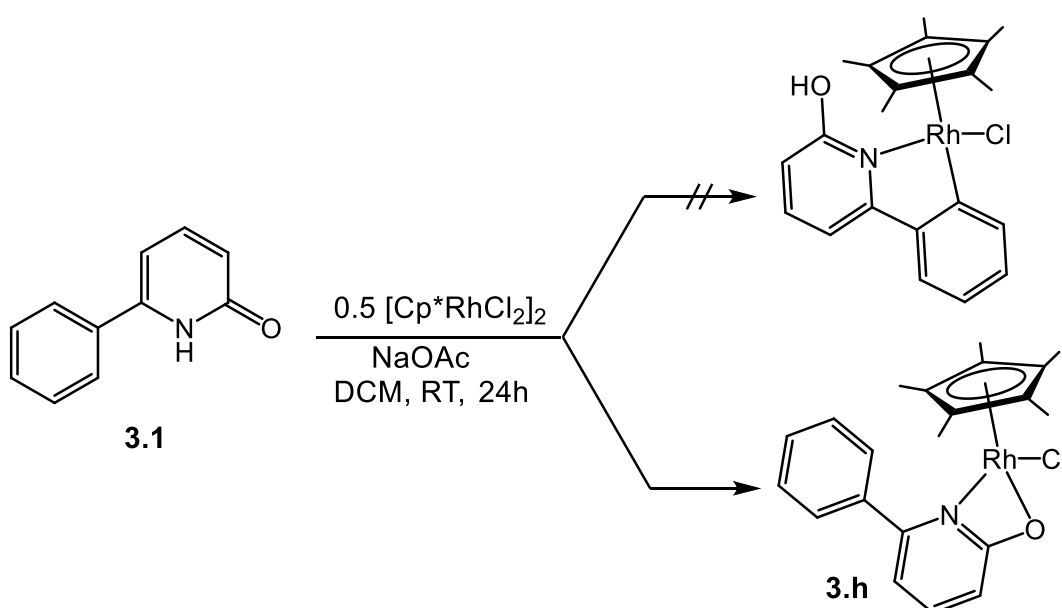
The iridium(III) complex (**3.g**) was found to be an efficient catalyst for the dehydrogenative oxidation of primary and secondary alcohols into their corresponding aldehydes and ketones, respectively. The authors proposed a mechanism (**Scheme 3.4**) in which the catalyst (**3.g**) reacts with an alcohol substrate to form an alkoxoiridium species (**I**) which would be able to undergo β -hydrogen elimination to generate the dehydrogenated product and a hydrido-Ir^{III} complex (**II**) as an active intermediate. The catalytically active hydrido-iridium complex (**II**) with the hydroxy proton of the chelating ligand undergoing protonolysis to release H₂ along with the formation of the unsaturated pyridonate-chelate complex (**III**).¹⁷



Scheme 3.4: Possible mechanism for the dehydrogenative oxidation of alcohols by **3.g**

In a more recent publication, Jones *et al.*¹⁸ attempted to synthesise a Cp*Rh^{III} complex bearing 6-phenyl-2-pyridone using the synthetic procedure reported for synthesis of the N[^]C-chelated Cp*Ir^{III} complex (**3.g**) in the presence of NaOAc.¹⁷ However, C-H activation using [Cp*RhCl₂]₂ could not be accomplished and the N[^]O-chelated Cp*Rh^{III} complex (**3.h**) was exclusively obtained (89% yield) instead of the desired N[^]C-chelated Rh^{III} product (**Scheme 3.5**). Using a stronger base, namely sodium benzoate, to promote C-H activation of the pyridone ligand (**3.1**) was also unsuccessful and gave the same product previously obtained with NaOAc. The authors believed that

the reason behind the unsuccessful formation of the N[^]C-chelated Rh^{III} complex is the electrophilicity of the rhodium(III) centre, which is less than that of the iridium(III) centre. They were able to grow single crystals of **3.h** suitable for analysis by X-ray diffraction by a diffusion process. The crystallographic data confirmed the proposed structure in which the ligand coordinated to the Rh^{III} centre in an N[^]O-chelating mode (pyridonate form) leaving the phenyl ring “dangling”. The N-Rh-O bite angle for the four-membered cyclometallated rhodium(III) complex (**3.h**) is 61.92°. It is interesting to note that the length of the carbon-oxygen bond is 1.295(3) Å, which is between that observed for C-O-type single and double bonds. This could be attributed to the associated electronic delocalisation, as seen in other related N[^]O-chelate complexes.¹⁸⁻²⁰



Scheme 3.5: Preference for N[^]O-chelate Rh^{III} complex formation over the formation of N[^]C-chelate Rh^{III} complex

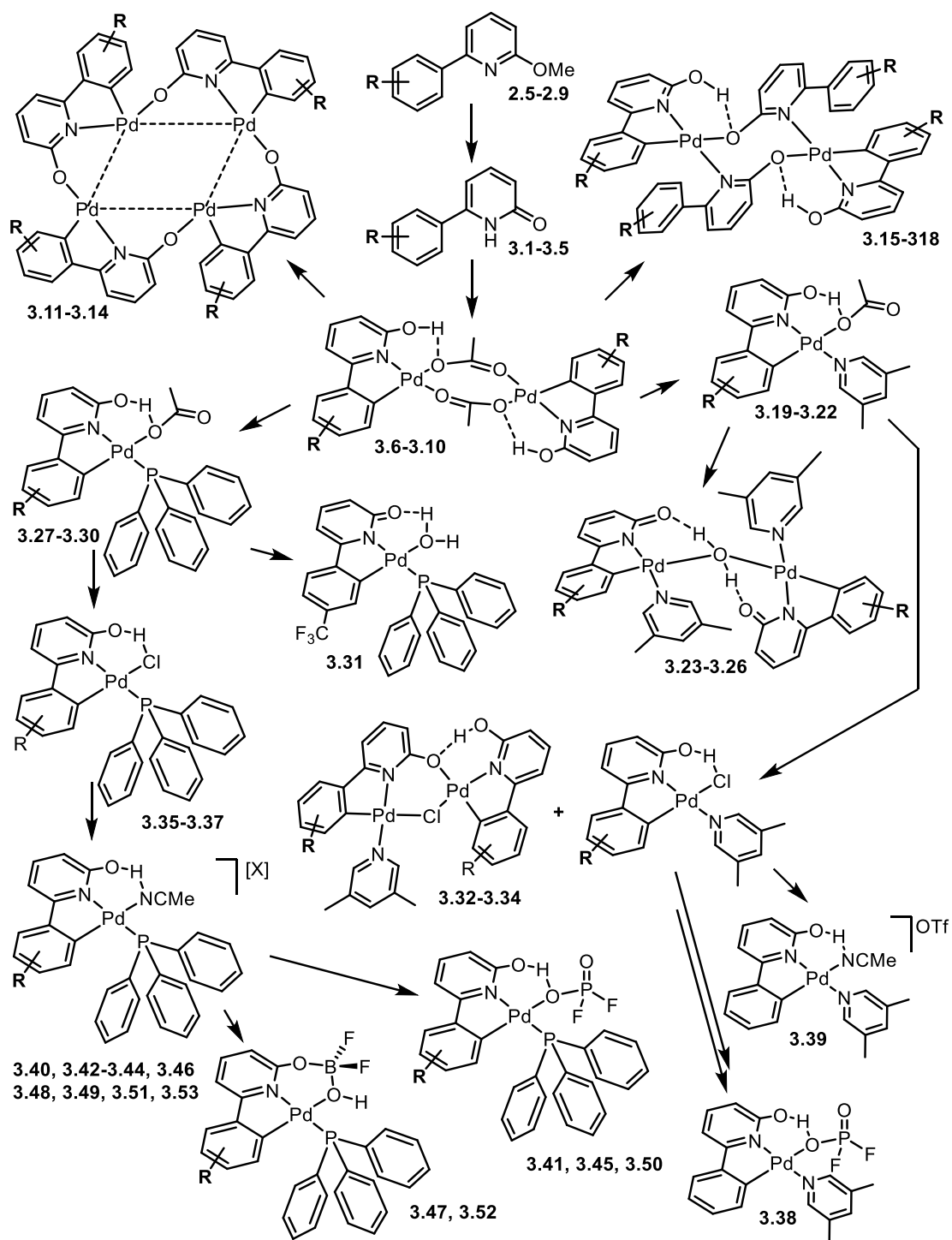
3.2 Aims and Objectives of Chapter 3

From this literature review it is apparent that the 2-pyridone unit has a variety of interesting features. In this chapter, synthesis of several pyridone-based N[^]C-bidentate ligands, with the general formula [6-aryl-2-pyridone] (aryl = Ph **3.1**, 4-MePh **3.2**, 4-CF₃Ph **3.3**, 4-FPh **3.4** or 2-MePh **3.5**), will be described and discussed. The reactivity of these ligands towards palladium(II) acetate will be investigated with different relative ratios of the ligands to the Pd^{II} centre. The dimeric Pd^{II} complexes bridged with acetate ligands will undergo a cleavage process in which simple monodentate ligands, such as 3,5-lutidine and triphenylphosphine, are able to break the dimers and act as monodentate

ligands. This will be followed by exchange of an acetate ligand by a chloride ion in order to examine their reactivity with various silver salts in acetonitrile. A comparison will be then made between pyridine-based (**Chapter 2**) and pyridone-based (**Chapter 3**) ligands for applications in the coordination chemistry of palladium(II) acetate and hydrolysis.

The hydroxy unit, in association with a suitable hydrogen bond acceptor, can facilitate the formation of linkages between neighbouring molecules. Therefore, the ability of hydroxylated bidentate ligands to undergo a self-assembly process through hydrogen bonding molecular interactions will be explored and developed for pyridone coordination chemistry.

All ligands and Pd^{II} complexes shown in **Scheme 3.6** have been fully characterised using several analytical methods including spectrometric (ESMS, HRMS) and spectroscopic (¹H, ¹³C, ³¹P and ¹⁹F NMR and IR) techniques as well as by single crystal X-ray diffraction.



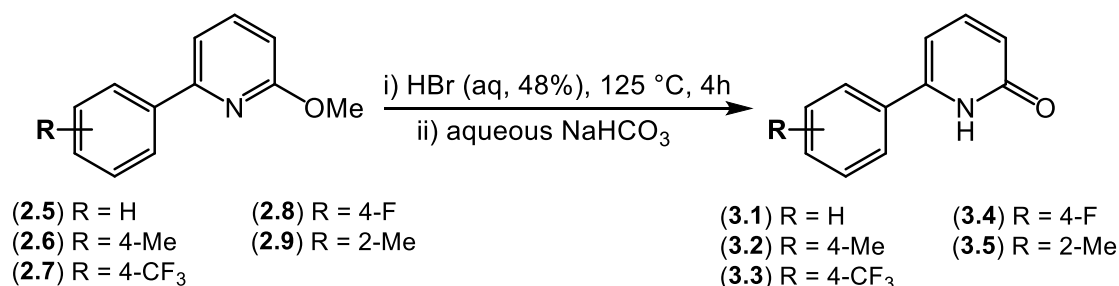
Scheme 3.6: Ligands and complexes described in **Chapter 3**

3.3 Results and Discussion

3.3.1 Synthesis of 6-aryl-2-pyridones

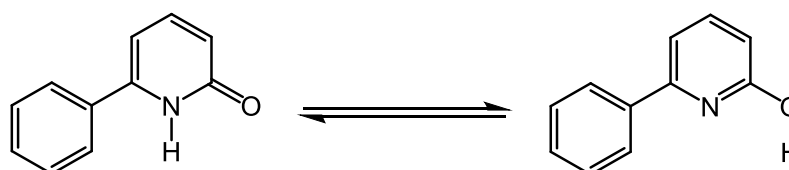
First of all, the work was directed towards the synthesis of 2-pyridone-based systems that had the potential to act as N[^]C-bidentate ligands (**3.1-3.5**), followed by the study of their reactivities towards palladium(II) acetate.

Demethylation reactions of the 6-aryl-2-methoxypyridine ligands (**2.5-2.9**) described in **Chapter 2** were carried out in order to prepare the corresponding 6-aryl-2-pyridone ligands (**3.1-3.5**). **Scheme 3.7** outlines the experimental conditions for the synthesis of the five pyridone ligands. In these reactions, each pyridine ligand was heated under reflux with an aqueous HBr solution (48%) for 4 hours to produce the desired products in moderate-to-good yields (64-90%).



Scheme 3.7: Synthesis of 6-aryl-2-pyridone ligands

Molecules containing an amide group usually exist as tautomers. Thus, this phenomenon is possible in these ligands as each has a 2-pyridone unit. In this case, the hydrogen coordinated to the nitrogen atom can also migrate to the oxygen to form a 2-hydroxypyridine product (**Scheme 3.8**).



Scheme 3.8: Lactam-lactim tautomerism of 6-phenyl-2-pyridone ligands

Upon analysis of the pyridone products by ¹H NMR spectroscopy, the methyl signal of the methoxy moieties in the starting materials had disappeared and a singlet peak at 12.15, 12.34, 13.13, 12.68 and 12.17 ppm, representing the NH groups in each of the spectra recorded for **3.1**, **3.2**, **3.3**, **3.4** and **3.5**, respectively, appeared instead. Furthermore, a carbon signal assigned to the carbonyl group was observed between 164.3 and 165.6

ppm in the $^{13}\text{C}\{^1\text{H}\}$ NMR spectra of the ligands. The MS (ES) spectra of all ligands illustrated a peak corresponding to the fragment $[\text{M}+\text{H}]^+$.

Infrared spectra of the five pyridone ligands displayed a very strong peak in the range $1637\text{-}1651\text{ cm}^{-1}$ which corresponded to vibrations of the $(\text{C}-\text{O})_{\text{ketone}}$ bonds. This may suggest that the pyridone tautomer is the dominant form of these ligands in their solid states. This was further confirmed by analysis of **3.3** by X-ray diffraction studies (**Fig. 3.2**). Selected bond distances and angles are reported in **Table 3.1**.

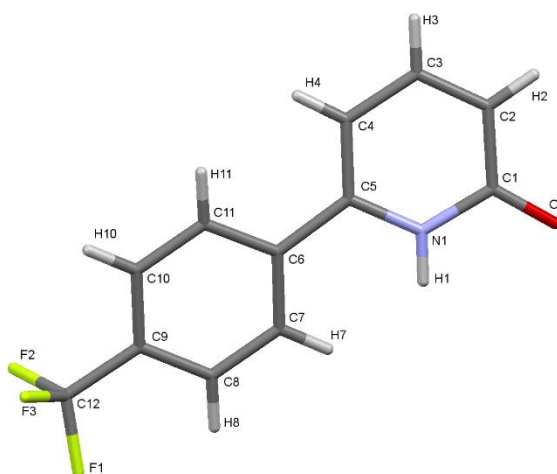


Figure 3.2: Molecular structure of **3.3** with full atom numbering

Table 3.1: Selected bond lengths and angles of complex **2.22**

Ligand	Bond lengths (Å)		Bond angles (°)	
	C-O	H...O	N-C1-O	O-C1-C2
3.3	1.245(3)	1.98	119.8(2)	124.5(2)

Single crystals of **3.3** were grown by slow evaporation of a methanol solution of the ligand. The crystal structure of **3.3** consists of a 2-pyridone coordinated with the 4-trifluoromethylphenyl ring at the 6-position. In the solid state, the X-ray structure showed that the ligand exists in the lactam (pyridone) form where the hydrogen atom is bound to the nitrogen atom rather than the oxygen atom. This was also supported by the carbon-oxygen bond length of $1.245(3)\text{ Å}$ which is consistent with double bond character; therefore, the ligand is protonated at the pyridyl nitrogen. Hydrogen bonding interactions between pairs of molecules were expected as shown in **Figure 3.3**. In this case, the

pyridone NH acts as a hydrogen-bonding donor while the O atom of the carbonyl group acts as a hydrogen bond acceptor.

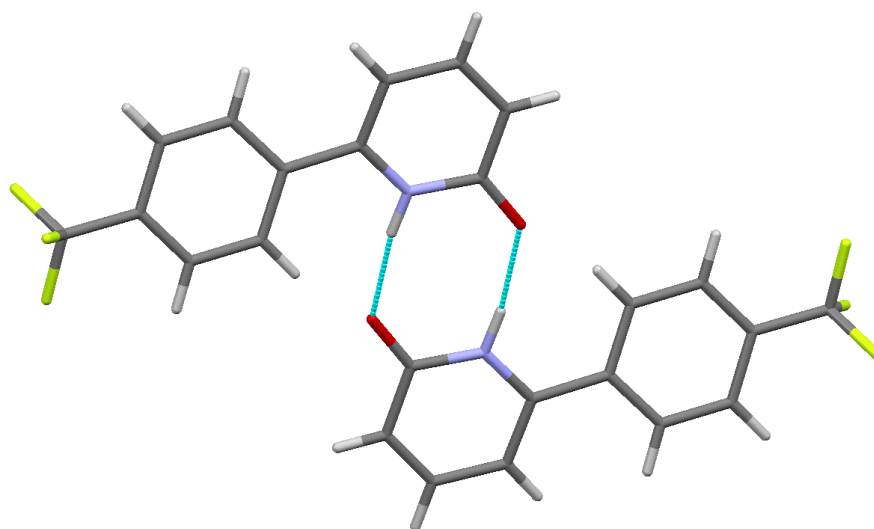
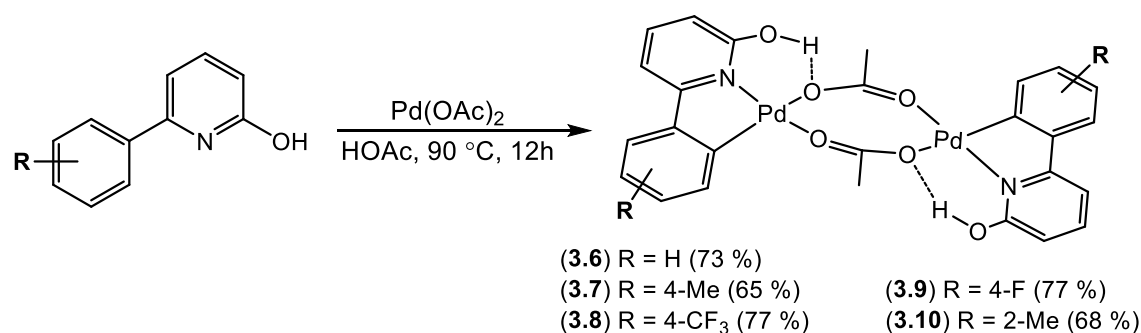


Figure 3.3: Hydrogen bonding between two neighbouring molecules of **3.3**

3.3.2 Complexation of 6-aryl-2-pyridones to Palladium(II)

To explore the reactivity of the 6-aryl-2-pyridones towards a Pd^{II} centre, reactions of these pre-ligands with one molar equivalent of Pd(OAc)₂ at 90 °C in acetic acid were carried out. All products precipitated out of solution after cooling to room temperature. The reactions gave the acetate-bridged dimers with a general formula [Pd(κ²-6-aryl-2-pyridinol)(μ-OAc)]₂ (**3.6-3.10**) in good yields (**Scheme 3.9**). These complexes are [Pd(κ²-6-phenyl-2-pyridinol)(μ-OAc)]₂ (**3.6**), [Pd(κ²-6-(4-methylphenyl)-2-pyridinol)(μ-OAc)]₂ (**3.7**), [Pd(κ²-6-(4-trifluoromethylphenyl)-2-pyridinol)(μ-OAc)]₂ (**3.8**), [Pd(κ²-6-(4-fluorophenyl)-2-pyridinol)(μ-OAc)]₂ (**3.9**) and [Pd(κ²-6-(2-methylphenyl)-2-pyridinol)(μ-OAc)]₂ (**3.9**).



Scheme 3.9: Synthesis of [Pd(κ²-6-aryl-2-pyridinol)(μ-OAc)]₂ (**3.6-3.10**)

All dimeric palladium(II) complexes **3.6**, **3.7**, **3.8**, **3.9** and **3.10** have been characterised by multinuclear NMR and IR spectroscopies, mass spectrometry and, for complexes **3.6**, **3.7** and **3.8**, by elemental analysis. Only complex **3.8** was structurally characterised by X-ray crystallography. It should be noted that the complex [Pd(κ^2 -6-phenyl-2-pyridinol)(μ -OAc)]₂ (**3.6**) has been previously synthesised and structurally characterised, *inter alia*, by single crystal X-ray crystallography for the first time by our group.²¹ The reaction had been performed in toluene and gave **3.6** with a slight reduction in yield (55% *versus* 73% in acetic acid). It is believed that the mechanism of these reactions usually begins with the coordination of the nitrogen atom in the pyridone ring followed by *ortho*-metallation at the aryl group.

Although the NMR spectra for complexes **3.7-3.10** are analogous to **3.6**, they still require the same analysis to accurately determine each signal. The achievement of C-H activation in the pyridone ligands by the Pd^{II} centres to form a C-M bond was evident upon analysis by ¹H and ¹³C NMR spectroscopy. This *ortho*-C_{aryl}-Pd bond in each cyclopalladated complex can be confirmed either by the absence of a peak in the aromatic regions in each of the associated ¹H NMR spectra or by the presence of one additional quaternary carbon environment in each of the ¹³C{¹H} NMR spectra of all five complexes. A singlet assigned to the hydroxy proton was observed between 9.53 and 9.77 ppm in the ¹H NMR spectra of all complexes, indicating that the ligands coordinated to the metal centre in the pyridinol form. This significant downfield shift of the OH proton was attributed to the hydrogen bonding interactions between the OH hydrogen and the adjacent oxygen of the bridging acetate. Common to all five complexes is the presence of a singlet at 2.27, 2.26, 2.30, 2.28 and 2.24 ppm representing the acetate methyl protons in complexes **3.6**, **3.7**, **3.8**, **3.9** and **3.10**, respectively. These peaks are shifted slightly downfield (~0.08 ppm) compared to those previously observed for the methoxy complexes in **Chapter 2**. A singlet peak seen in the aromatic region of complexes **3.7**, **3.8** and **3.9**, as each has a substituent group at their *para* positions, confirmed that these complexes had undergone a C-H activation process. There are no significant differences in the ¹⁹F NMR spectra between complexes **3.8** (CF₃) and **3.9** (F) and their free pro-ligands.

Elemental analysis of **3.6** has previously been carried out by our group²¹ while **3.7** and **3.8** were performed for the purpose of this thesis. The results of elemental analysis are in good accordance with the calculated elemental compositions. All complexes

dissolved in acetonitrile displayed molecular peaks in their mass spectra (ES) corresponding to $[\text{Pd}(\text{L})+\text{MeCN}]^+$, $[\text{Pd}(\text{L})+2\text{MeCN}]^+$ and $[\text{Pd}_2(\text{L})_2+2\text{MeCN}]^+$. These data may not give a realistic insight as to the structure of the dimeric complexes; however, they do confirm that the pyridone ligands have been successfully bound to Pd^{II} centres.

As expected, the infrared spectra of all five complexes showed characteristic $\text{COO}_{\text{asymm}}$ and COO_{symm} absorption peaks at approximately 1546 and 1409 cm^{-1} , respectively. The characteristic separation ($\Delta\nu$) of $\sim 137 \text{ cm}^{-1}$ is indicative of a bridging acetate ligand bound to two metal centres, as demonstrated by Nakamoto.²² However, this characteristic separation was found to be much less than those ($\sim 172 \text{ cm}^{-1}$) observed in **Chapter 2** for the pyridine-based dimeric complexes. This finding could be attributed to hydrogen bonding interactions ($\text{OH}\cdots\text{O}$) which allow the infrared stretching frequency of the carboxylate asymmetric stretching band to shift to a lower frequency.

All these complexes proved to have unstable structures in NMR solution that converted into tetrameric complexes (*vide infra*). However, crystals suitable for a single crystal X-ray diffraction were obtained for **3.8** from a dichloromethane solution of the product layered with hexane. The X-ray structure of **3.8** is shown in **Figure 3.4**; selected bond lengths and bond angles are given in **Table 3.2**.

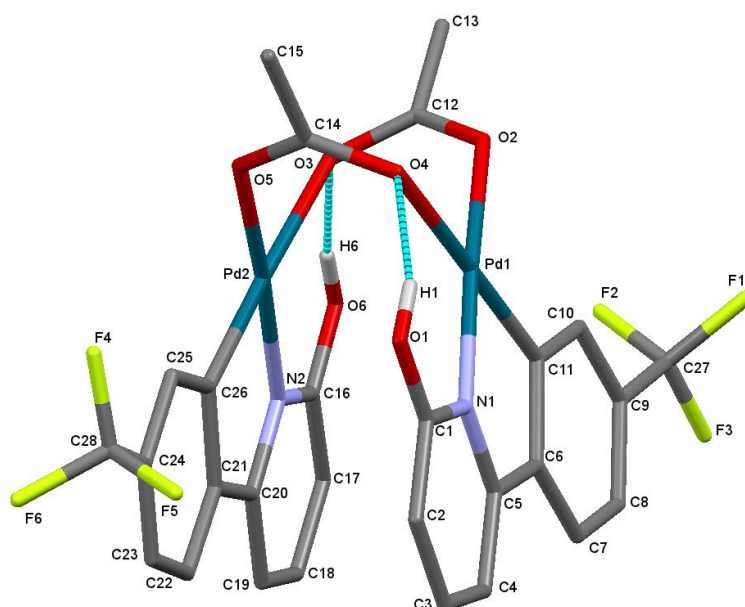


Figure 3.4: Structure of **3.8** with hydrogen atoms (except OH) omitted for clarity

Table 3.2: Selected Pd-X bond lengths and the bite angle of complex **3.8**

Complex	Bond lengths (Å)					Bond angles (°)
	Pd1-O4 (<i>trans</i> to C)	Pd1-O2 (<i>trans</i> to N)	Pd1-N1	Pd1-C11	C1-O1	C11-Pd1-N1
3.8	2.160(5)	2.050(5)	2.041(7)	1.948(8)	1.295(9)	81.5(3)

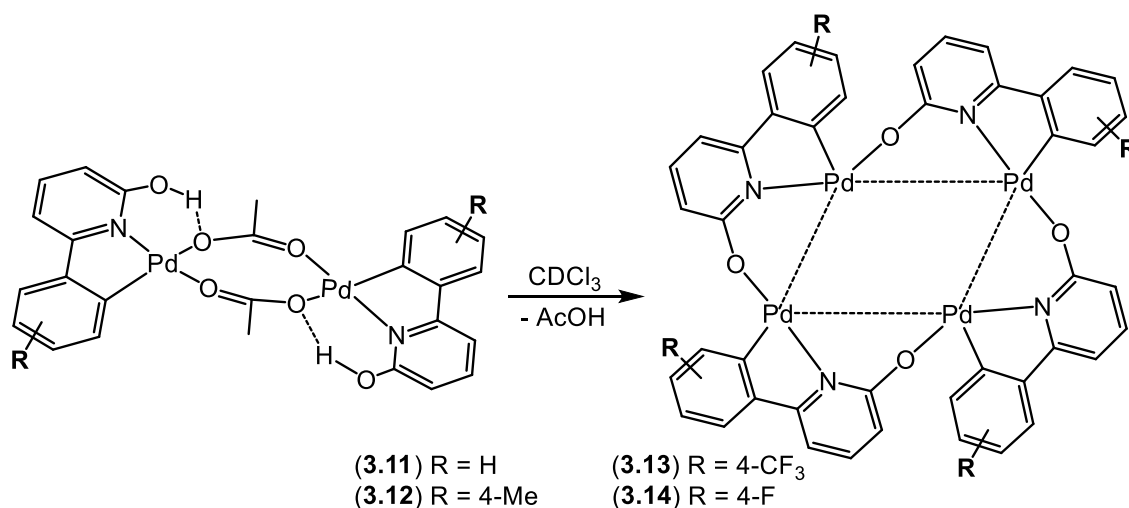
The X-ray structure of complex **3.8** showed a distorted square planar geometry supported by an N[^]C-chelating (κ^2) ligand connected to another Pd^{II} centre by two bridging acetate ligands, forming a dimeric complex. The molecular structure of this dimeric complex is commonly referred to as an “open-book” or “cleft” geometry.²³ The C-OH bond length in **3.8** was found to be 1.31 Å, which demonstrated that the complex is in the pyridinol form. In addition, each pyridinol OH hydrogen atom is able to form a hydrogen bond with a neighbouring acetate oxygen atom (OH \cdots H), with an associated bond length of 1.81 Å.

The electronic nature of the pyridone ligand (by comparison with those for the dimeric complexes of the methoxy pyridine ligands detailed in **Chapter 2**) does not seem to have a significant effect on the overall structure of the product. The C-Pd-N bite-angle of 81.5° was found to be within the range of other bite angles previously reported for related N[^]C-ligand Pd^{II} complexes.²⁴ The torsion angle between the 2-pyridinol and aryl rings was reduced from 9.0(3)° (in the free ligand) to 3.6(13)° (in **3.8**), as a result of the chelate effect. In the molecular structure of **3.8**, a significant *trans* influence was noticed (**Table 3.2**). The length of the bonds *trans* to the carbon atoms (2.160 Å) were longer than those *trans* to the nitrogen atoms (2.048 Å). This difference could be attributed to the stronger *trans* influence of the aryl group versus the N-donor ligand.²⁵ The Pd-C and Pd-N bond lengths (~1.95 and ~2.04 Å, respectively) are similar to those previously reported.^{23,25}

3.3.3 Synthesis of Tetrameric Complexes, [Pd(μ : κ^2 -6-aryl-2-pyridonate)]₄

Interestingly, on standing in a chloroform solution at room temperature, the dimeric pyridone complexes underwent slow pyridinol-pyridonate conversion to form the tetrameric species [Pd(μ : κ^2 -6-aryl-2-pyridonate)]₄ (aryl = Ph (**3.11**), 4-MePh (**3.12**), 4-CF₃Ph (**3.13**) and 4-FPh (**3.14**), as illustrated in **Scheme 3.10**. However, loss of acetic acid during the reaction stopped after few days before complete formation of the tetrameric complexes. In this case, removal of solvent and other volatiles under reduced

pressure, followed by the addition of chloroform, was required to drive the reaction to completion. Interestingly, the related transformation with the electron-withdrawing CF_3 group was found to need more forcing conditions such as heating. It should be noted that in the presence of acetic acid as a solvent conversion to tetrameric complexes did not occur. This may explain the significant increase in yield (73%) observed in the synthesis of **3.6** when acetic acid was used as a reaction solvent rather than toluene (55%).



Scheme 3.10: Synthesis of tetrameric complexes **3.11-3.14**

Complexes **3.11**, **3.12**, **3.13** and **3.14** have been characterised by NMR and IR spectroscopies, elemental analysis, mass spectrometry and X-ray crystallography. Analysis of these complexes by ^1H , ^{13}C and ^{19}F (for **3.13** and **3.14**) NMR spectroscopy revealed that the ligands coordinated to the metal centres are in equivalent environments, which confirmed the symmetry in the palladium tetramers. All ^1H NMR spectra showed no sign of a downfield-shifted NH/OH peak, which may indicate that the ligands had undergone a deprotonation process to eventually adopt a pyridonate form. The absence of acetate methyl protons, as well as a quaternary carbon signal in the ^1H and $^{13}\text{C}\{^1\text{H}\}$ NMR spectra, respectively, confirmed the loss of the bridging acetate ligands as acetic acid during the reaction. Neither C=O nor N-H stretches were observed in the solid-state IR spectra of the tetrameric complexes. The MS (ES) spectra of **3.11**, **3.12**, **3.13** and **3.14** each showed a peak corresponding to $[\text{M}]^+$ at m/z 1100, 1159, 1374 and 1174, respectively.

Crystals of complexes **3.12** and **3.13** suitable for the X-ray characterisation were grown by slow evaporation of a chloroform solution of the product. Structural diagrams

of each complex are given in **Figures 3.5** and **3.6** with selected bond lengths and angles of these structures reported in **Table 3.3**.

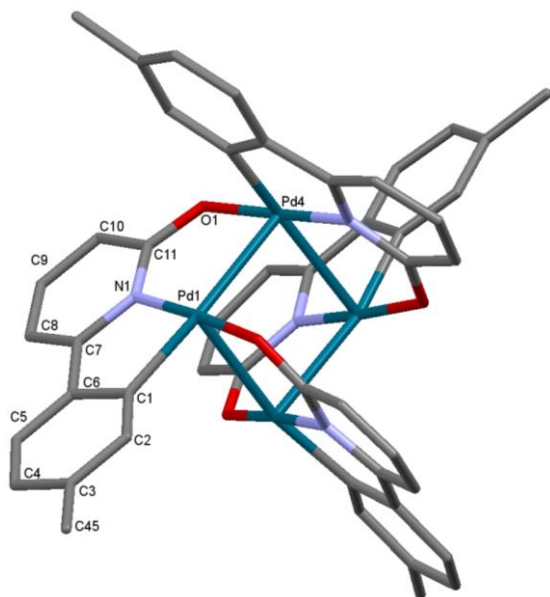


Figure 3.5: Structure of **3.12** with hydrogen atoms omitted for clarity

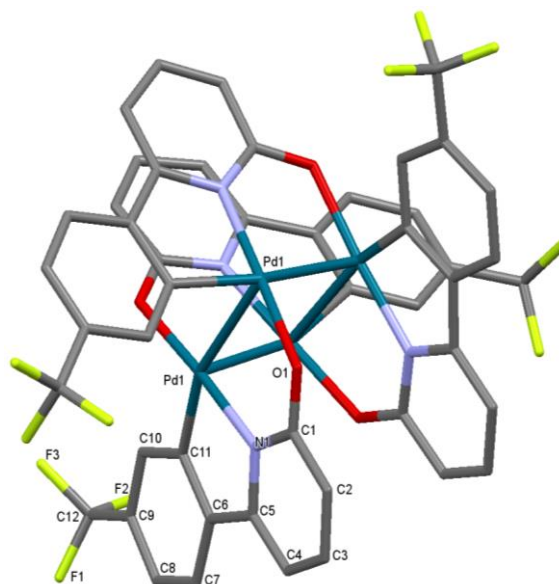


Figure 3.6: Structure of **3.13** with hydrogen atoms omitted for clarity

Table 3.3: Selected Pd-X bond lengths and bite angles for complexes **3.12** and **3.13**

Complex	Bond lengths (Å)					Bond angles (°)
	Pd-N	Pd-C	Pd-O	Pd---Pd	C-O	C-Pd-N
3.12	1.997(8)	1.970(8)	2.010(7)	~2.633(1)	1.275(9)	81.5(7)
3.13	2.004(3)	1.976(3)	2.003(2)	~2.642(1)	1.297(4)	82.28(14)

The molecular structures of both complexes (**3.12** and **3.13**) revealed a square Pd₄ framework of the tetramer (with almost 90° Pd-Pd-Pd angles) in which each palladium centre is supported by an N^C-chelate ligand and one oxygen atom from a deprotonated pyridyl hydroxy group of another pyridonate ligand, adopting a slightly distorted square planar geometry. Each pyridonate ligand in each complex was found to be arranged in axial or near axial coordination sites with respect to the tetrapalladium cluster plane (O(1)-Pd(4)-Pd(1) = 85.47(17)° and O(1)-Pd(1)-Pd(1)#1 = 84.76(7)° for complexes **3.12** and **3.13**, respectively), while one pair of ligands are almost perpendicular to the other pair (e.g., N(1)-Pd(1)-Pd(4)-N(4) = 178.5(3)° for complex **3.12**). The Pd···Pd distances

of approximately $\sim 2.633(1)$ and $\sim 2.642(1)$ Å (for **3.12** and **3.13**, respectively) are shorter than the sum of their van der Waals radii (3.26 Å) and are somewhat similar to those previously observed (2.6602(12) Å) by our group for complex **3.11**.²¹ These palladium-palladium distances are comparable to that found in the palladium carbonyl acetate cluster (2.663 Å), $[\text{Pd}(\mu\text{-O}_2\text{CCH}_3)(\mu\text{-CO})]_4$ (**Fig. 3.7**). The carbon-oxygen bond lengths of 1.275(9) and 1.297(4) Å (for complexes **3.12** and **3.13**, respectively) are considered to lie between those expected for single and double bonds, suggesting electronic delocalisation may occur over the bridging rings.¹⁸⁻²⁰ From **Table 3.3**, the Pd-C and Pd-N bond lengths in both complexes are similar to those previously reported in the literature.^{23,25}

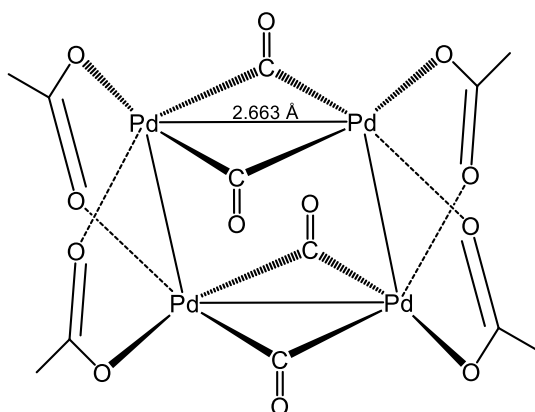
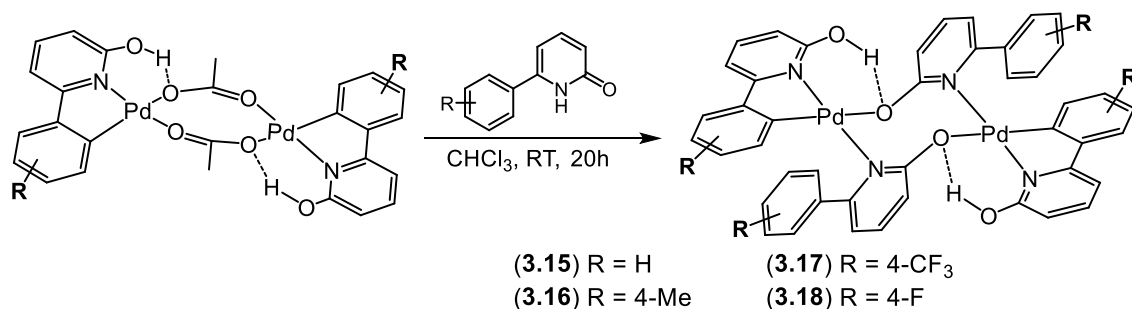


Figure 3.7: Molecular structure of $[\text{Pd}(\mu\text{-O}_2\text{CCH}_3)(\mu\text{-CO})]_4$

3.3.4 Reactivity of 6-aryl-2-pyridones towards Dimeric Complexes 3.6-3.9

The reactions of two equivalents of 6-aryl-2-pyridone with their corresponding dimeric complexes in chloroform at room temperature resulted in displacement of the bridging acetate ligands and formation of dimeric complexes bridged by two pyridonate ligands, with a general formula $[\text{Pd}(\mu\text{-6-aryl-2-pyridonate})(\kappa^2\text{-6-aryl-2-pyridinol})]_2$ (aryl = Ph **3.15**, 4-MePh **3.16**, 4-CF₃Ph **3.17** and 4-FPh **3.18**) (**Scheme 3.11**), in moderate-to-excellent yields (82, 58, 81 and 97%, respectively).



Scheme 3.11: Synthesis of $[\text{Pd}(\mu\text{-N}^{\text{O}}\text{-pyridonate})(\kappa^2\text{-N}^{\text{C}}\text{-pyridinol})]_2$ (**3.15-3.18**)

These dimers could be also formed by a direct reaction of Pd(OAc)₂ with two equivalents of 6-aryl-2-pyridones in toluene, as previously demonstrated by our group.²¹ The reaction of **3.13** (R = CF₃) was found to require a higher temperature (50 °C) to facilitate the formation of the dimeric complex **3.17**. It is possible that these reactions begin with cleavage of the dimer, in which the excess of the free ligands partially displaces the bridging carboxylate groups and bind to the Pd centres in a monodentate fashion through nitrogen, followed by subsequent elimination of acetic acid with the help of the pyridyl hydroxy protons to allow the coordinated ligands to act as an N[^]O-bridge.

Analysis of the dimeric complexes (**3.15-3.18**) by ¹H, ¹³C and ¹⁹F NMR spectroscopy revealed two sets of ligands in non-equivalent environments. Of the aryl protons, one contains no plane of symmetry as a result of C-H activation whilst the other appears with the symmetric aryl ring left “dangling”. The ¹H NMR spectra of complexes **3.15**, **3.16**, **3.17** and **3.18** also each showed a characteristic 1H singlet peak at 12.35, 12.27, 12.12 and 12.11 ppm, respectively, corresponding to the pyridinol OH environments. The downfield shift observed supports the presence of hydrogen bonding between the pyridinol proton and the oxygen of the pyridonate-bridged ligands. A very good agreement between the calculated and experimentally determined results of **3.15-3.17** were obtained upon elemental analysis. The C=O stretch was not observed in the solid-state IR spectra of the dimeric complexes as compared to the ν(C=O) peak observed at approximately 1643 cm⁻¹ for the corresponding free ligands. Further evidence for the formation of **3.15-3.18** was gleaned by the presence of a strong fragmentation peak corresponding to [M⁺] upon analysis by ASAP-MS spectrometry.

It was possible to grow single crystals of **3.16** and **3.17** suitable for analysis by X-ray diffraction. The X-ray structures of **3.16** and **3.17** are shown in **Figures 3.8** and **3.9**; selected bond lengths and angles are reported in **Table 3.4**. The molecular structures showed a distorted square planar palladium(II) dimer in which each Pd^{II} centre is supported by a bidentate ligand and bridged by two 6-aryl-2-pyridonate molecules. The pyridonate bridges are bound to one Pd^{II} centre by a neutral pyridine nitrogen and to the other centre by an anionic oxygen. The X-ray data showed that there is intramolecular hydrogen bonding between the hydroxy hydrogen and the oxygen atom from a deprotonated pyridyl hydroxy group coordinated to the palladium centre. The Pd···Pd bond lengths of 2.981(3) Å (in **3.16**) and 2.893(2) Å (in **3.17**) are slightly longer than that observed for related complex **3.15** (2.840 Å) obtained by our group.²¹ The bridging

pyridonate rings are nearly perpendicular to plane of the Pd-chelating ligand, as evidenced by the torsion angles C(11)-Pd(1)-N(2)-C(12) of $86.0(9)^\circ$ and C(11)-Pd(1)-N(2)-C(12) of $-90.2(9)^\circ$ for complexes **3.16** and **3.17**, respectively. All Pd-X (X = N, C and O) bond lengths are similar to those previously observed in complex **3.15**.²¹

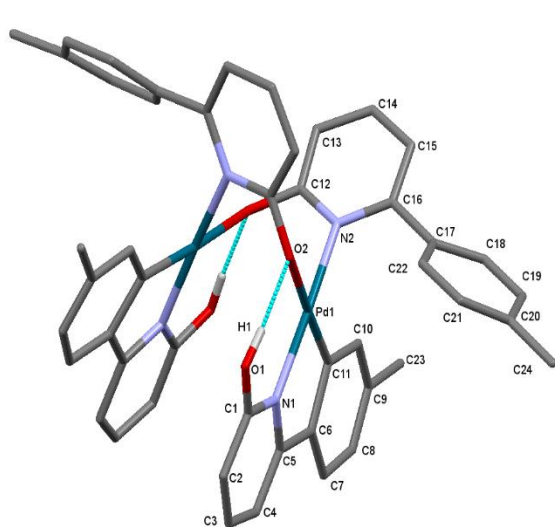


Figure 3.8: Structure of **3.16** with hydrogen atoms (except OH) omitted for clarity

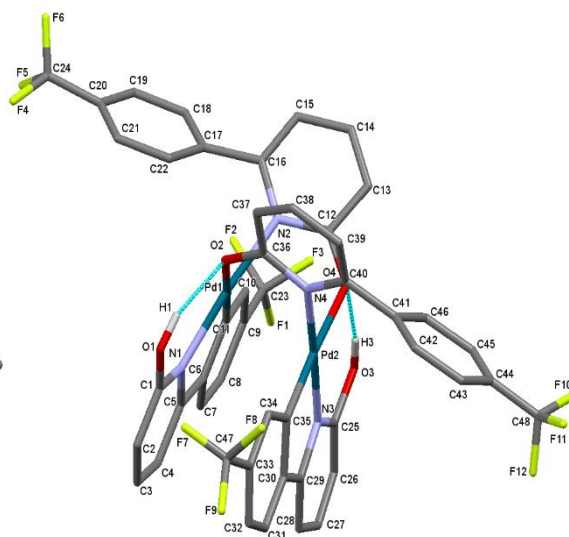


Figure 3.9: Structure of **3.17** with hydrogen atoms (except OH) omitted for clarity

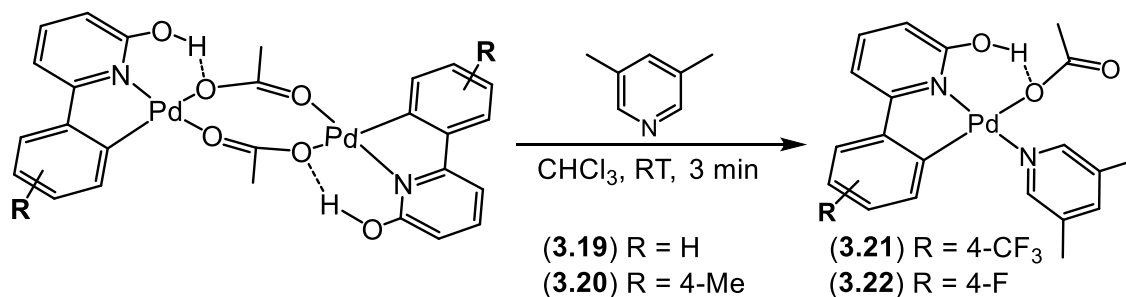
Table 3.4: Selected bond lengths and bite angles for complexes **3.16** and **3.17**

Complex	Bond lengths (Å)					Bond angles (°)
	Pd1-N1	Pd1-N2	Pd1-O2	Pd1-C11	Pd---Pd	C11-Pd1-N1
3.16	2.031(9)	2.045(9)	2.188(8)	1.963(11)	2.981(3)	83.7(5)
3.17	2.075(10)	2.053(9)	2.095(8)	1.920(12)	2.893(2)	83.2(5)

3.3.5 Reactions of Dimeric Complexes 3.6-3.9 with 3,5-lutidine

Dimers **3.6-3.9** were reacted with 2 equivalents of 3,5-lutidine in CHCl_3 to form their corresponding monomeric complexes **3.19-3.22** in excellent yields (**Scheme 3.12**). These disassembly reactions were monitored by ^1H NMR spectroscopy at room temperature and showed that the reactions went to completion immediately after adding 3,5-lutidine to the CDCl_3 solution of the dimer. The mononuclear Pd^{II} complexes containing 3,5-lutidine as a monodentate ligand are stable in solution and could be isolated as a solid by removing all volatiles under reduced pressure. With respect to the similar methoxy-containing complexes **2.16**, **2.17** and **2.18**, the additional stability of the

pyridinol complexes **3.19-3.22** could be attributed to the possible hydrogen bonding interactions between the OH hydrogen and coordinated acetate oxygen.

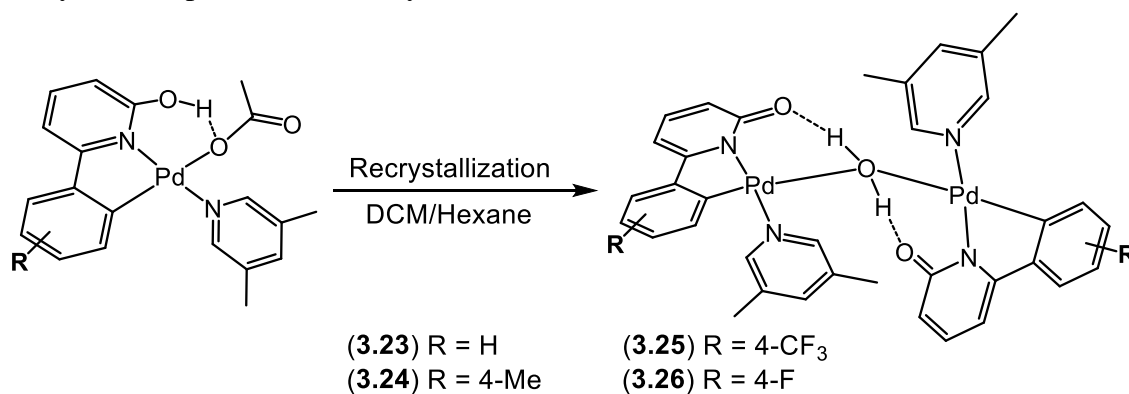


Scheme 3.12: Synthesis of [Pd(κ^2 -N^C-pyridinol)(κ^1 -OAc)(3,5-lutidine)] (**3.19-3.22**)

All four complexes **3.19-3.22** are stable to air and have been characterised using a combination of NMR (¹H, ¹³C and ¹⁹F) and IR spectroscopy, mass spectrometry and elemental analysis. The ¹H NMR spectra showed the formation of 1:1:1 (N^C-ligand/OAc/3,5-lutidine)-Pd complexes. Singlets corresponding to the acetate methyl protons were found to be shifted upfield by approximately 0.34 ppm upon addition of 3,5-lutidine. The hydroxy proton resonance of the pyridinol ligands was not observed in the ¹H NMR spectra for any of the complexes. As mentioned earlier, generation of two, or one of two, isomers is possible for this type of reaction (where 3,5-lutidine can be *trans* or *cis* to the pyridine nitrogen). ¹H and ¹³C{¹H} NMR spectra, however, showed only one isomer was generated from these reactions. In their IR spectra, a broad $\nu(\text{OH})$ absorption band centred at *ca.* 2920 cm⁻¹ is in agreement with the predicted structure of complexes **3.19-3.22**. Analysis by mass spectrometry (ES) revealed a strong fragmentation peak representing [M-OAc]⁺ at *m/z* 381, 397, 451 and 401 for complexes **3.19**, **3.20**, **3.21** and **3.22**, respectively. Further evidence for the proposed structures was obtained by elemental analysis, where experimentally the found results for **3.19-3.21** are in good accordance with the calculated elemental compositions.

On attempting to recrystallise **3.19**, **3.20**, **3.21** and **3.22** from CH₂Cl₂/hexane (1:3, v/v), hydrolysis of the acetate occurred to give the unusual aqua-bridged complexes [Pd(κ^2 -6-aryl-2-pyridonate)(3,5-lutidine)]₂(μ -OH₂) (aryl = Ph **3.23**, 4-MePh **3.24**, 4-CF₃Ph **3.25** and 4-FPh **3.26**) (**Scheme 3.13**). It was also possible to form monopalladated complexes with the general formula [Pd(κ^2 -6-aryl-2-pyridonate)(3,5-lutidine)(OH₂)] during recrystallisation (see later). All the complexes were obtained as yellow crystals in good yields, and were subsequently characterised by ¹H, ¹³C and ¹⁹F (for **3.25** and **3.26**)

NMR and IR spectroscopies, electrospray mass spectrometry (ESI-MS), elemental analysis (except **3.26**) and X-ray diffraction.



Scheme 3.13: Formation of [Pd(κ^2 -N[^]C-pyridonate)(3,5-lutidine)]₂(μ -OH₂) (**3.23-3.26**)

The ¹H NMR spectra of complexes **3.23**, **3.24**, **3.25** and **3.26** revealed the absence of the ancillary acetate ligand with the neighbouring pyridinol hydrogen; instead they showed the presence of a broad singlet peak representing the palladium-bridging water molecule at 13.39, 13.36, 14.28 and 14.18 ppm, respectively. The significant downfield shift observed for the H₂O protons could be due to the hydrogen-bonding interactions with the carbonyl oxygen atom of the pyridonate ligand. The absence of the acetate ligand was further confirmed by ¹³C{¹H} NMR spectroscopy. The ¹⁹F NMR spectra of **3.25** and **3.26** showed only a singlet for each at -62.6 and -112.2 ppm representing CF₃ and F, respectively. In their IR spectra, the $\nu(\text{C}=\text{O})_{\text{ketone}}$ absorption bands were all shifted by *ca.* 80 cm⁻¹ to lower wavenumber compared to those observed in the corresponding free ligands. In addition, analysis of **3.23**, **3.24**, **3.25** and **3.26** by FAB mass spectrometry showed a strong fragmentation peak ([M-OH₂]⁺) at *m/z* 767, 795, 903 and 803, respectively. Furthermore, the experimental results of the elemental analysis of **3.23-3.25** are consistent with the calculated elemental compositions.

The structures of **3.23**, **3.24**, **3.25** and **3.26** have been further confirmed by X-ray diffraction studies. The solid-state structural data of these complexes revealed a neutral dimeric unit consisting of two [Pd(L_{pyridonate})(3,5-lutidine)] moieties with a slightly distorted square-planar geometry, bridged by one water molecule through the oxygen atom (**Fig. 3.10-3.13**). The dimeric complexes are reinforced by intramolecular H-bonds between the hydrogen atoms of the bridging water molecule and the pyridonate O atom. The X-ray crystallographic data may provide valuable structural information about the coordination position of 3,5-lutidine ligand; this is *trans* to the pyridonate nitrogen atom,

which is in agreement with proposed structures of other palladium(II) complexes supported by the same bidentate ligands. The 3,5-lutidine was found to be inclined perpendicular to the plane of pyridonate ring in all complexes.

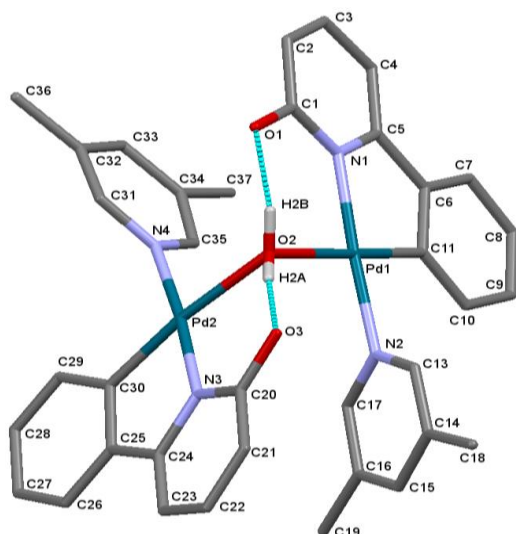


Figure 3.10: Structure of **3.23** with solvent H₂O molecule and hydrogen atoms (except H₂O) omitted for clarity

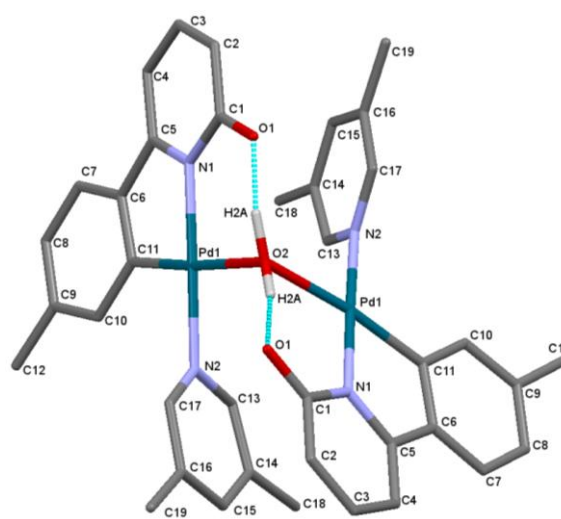


Figure 3.11: Structure of **3.24** with solvent CH₂Cl₂ molecule and hydrogen atoms (except H₂O) omitted for clarity

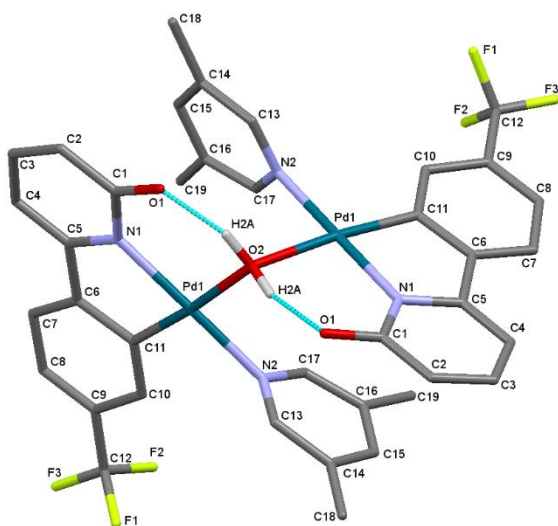


Figure 3.12: Structure of **3.25** with hydrogen atoms (except H₂O) omitted for clarity

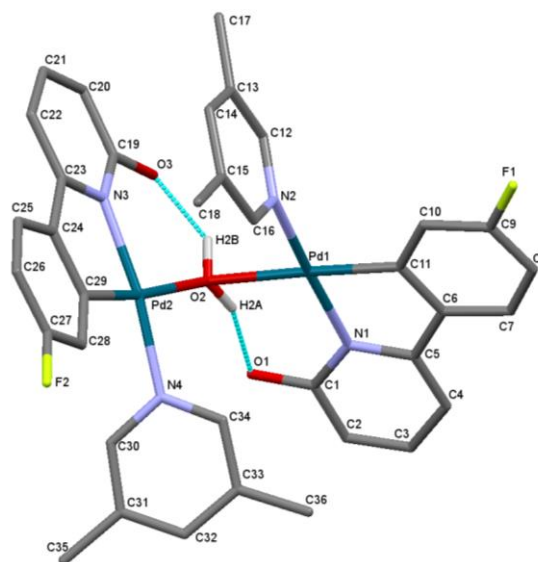


Figure 3.13: Structure of **3.26** with solvent CH₂Cl₂ molecule and hydrogen atoms (except H₂O) omitted for clarity

The data reported in **Table 3.5** illustrated that the Pd-C, Pd-N_{py} and Pd-N_{lut} bond lengths are consistent with similar Pd-X bond lengths reported in the literature.^{23,25} The basal positions of the two palladium centres are connected by the aqua bridge with average Pd-O (water) bond lengths of 2.155(25) Å. This is also comparable to those previously observed in complexes **3.16** and **3.17**. The pyridonate C=O bond distances fall between 1.279(4) and 1.303(11) Å and are consistent with a double bond character. Further evidence for this was supported by the bond lengths found in O_{water}-H···O_{pyridonate} (O_{water}-H = ~0.87 Å and H···O_{pyridonate} = ~1.65 Å) bonds. The bite angle of the chelating ligand (N_{py}-Pd-C) was approximately 82° for all four complexes (**3.23-3.26**). The Pd-O-Pd bond angle of 102.6(2)° in **3.25** is slightly larger than those in complexes **3.23** and **3.24** (100.5(2)° and 99.79(12)°, respectively) and significantly smaller than that of 112.4(3)° found in **3.26**. Several transition metals form these types of binuclear aqua-bridged complexes, such as Ni^{II}, Mn^{II}, Co^{II} and Cu^{II};²⁶⁻²⁹ however, other examples from the subject of this research (Pd^{II}) could not be found in the literature.

Table 3.5: Selected Pd-X bond lengths and angles of complexes **3.23-3.26**

Complex	Bond lengths (Å)				Bond angles (°)	
	Pd-N _{py}	Pd-N _{lut}	Pd-C	Pd-O	Pd-O-Pd	C-Pd-N _{py}
3.23	2.053(6)	2.058(6)	1.9361	2.142(5)	100.5(2)	82.60(19)
3.24	2.037(3)	2.036(3)	1.958(3)	2.142(1)	99.79(12)	82.43(12)
3.25	2.051(4)	2.038(5)	1.977(5)	2.129(3)	102.6(2)	83.5(2)
3.26	2.056(7)	2.067(7)	1.965(9)	2.183(5)	112.4(3)	81.8(4)

Although the ¹H, ¹³C and ¹⁹F (for **3.26** only) NMR spectra showed the presence of one product, the solid-state structural data of complexes **3.23** and **3.26** also revealed the terminal aqua complexes [Pd(κ²-6-phenyl-2-pyridonate)(3,5-lutidine)(OH₂)] (**3.23'**) and [Pd(κ²-6-(4-fluorophenyl)-2-pyridonate)(3,5-lutidine)(OH₂)] (**3.26'**) co-crystallised with **3.23** and **3.26**, respectively (**Fig. 3.14** and **3.15**). All Pd-X (X = N_{py}, N_{lut} and C) bond lengths and C-Pd-N_{py} bite angles in **3.23'** and **3.26'** are somewhat similar to those seen in their corresponding aqua-bridged Pd^{II} dimers **3.23** and **3.26**, respectively. As expected, however, the bond distance between the palladium centre and the oxygen atom of the terminal water molecule (Pd-O) in both complexes (**3.23'** and **3.26'**) is smaller (2.1032 and 2.125(6) Å, respectively) than those observed in complexes **3.23** and **3.26**. This is

likely to be due to the differences in the mode of water coordination (terminal *versus* bridging).

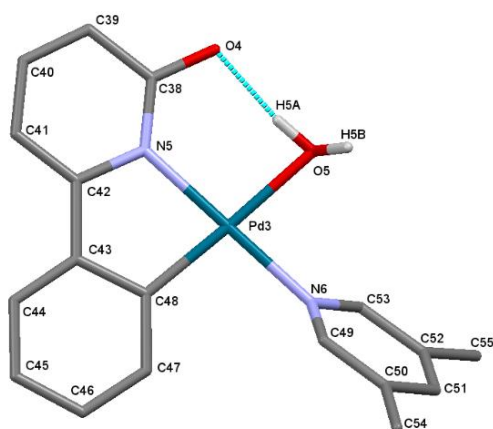


Figure 3.14: Structure of **3.23'** with solvent H₂O molecule and hydrogens (except H₂O) omitted for clarity

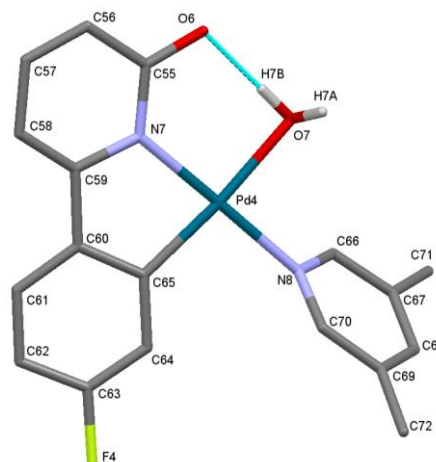


Figure 3.15: Structure of **3.24'** with solvent CH₂Cl₂ molecule and hydrogens (except H₂O) omitted for clarity

There are two hydrogen-bonding interactions in complex **3.23'**; one involves the terminal water proton (H5A) with the adjacent carbonyl oxygen (O4), and the other one is between the second water proton (H5B) and a molecule of solvate H₂O. In complex **3.24'**, however, two intermolecular hydrogen-bonding interactions are established for the terminal H₂O ligand alongside the intramolecular hydrogen bond to the carbonyl oxygen (**Fig. 3.16**). These include the hydrogen bond to the carbonyl oxygen in another molecule and that between the terminal H₂O oxygen and the terminal H₂O proton from another moiety.

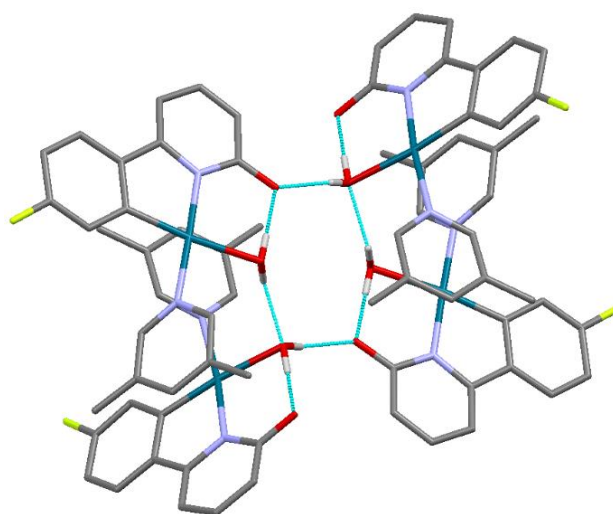
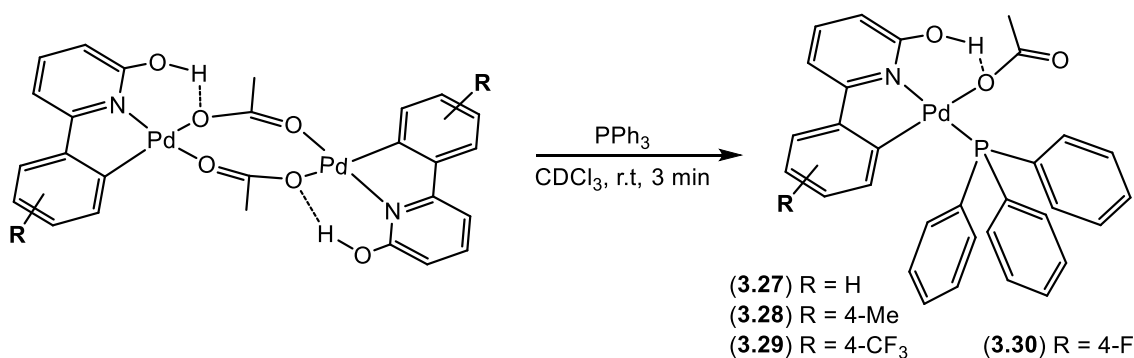


Figure 3.16: Intra- and intermolecular hydrogen bonding in **3.24'**

3.3.6 Reactions of Dimeric Complexes 3.6-3.9 with PPh₃

Upon reaction of the acetate-bridged dimers **3.6**, **3.7**, **3.8** and **3.9** with 2 equivalents of triphenylphosphine ligand (PPh₃), formation of mononuclear complexes with the general formula [Pd(κ^2 -6-aryl-2-pyridinol)(OAc)(PPh₃)] (aryl = Ph **3.27**, 4-MePh **3.28**, 4-CF₃Ph **3.29** and 4-FPh **3.30**) took place in moderate-to-excellent yields (96, 91, 73 and 91%, respectively) (Scheme 3.14).



Scheme 3.14: Synthesis of monopalladated complexes **3.27-3.30**

As mentioned earlier in section 2.3.3, the PPh₃ would be able to displace one arm of the acetate-bridged ligand and bind in a monodentate fashion to the Pd^{II} centre. The reaction reached completion after only 3 minutes of stirring, as confirmed by ¹H{³¹P} and ³¹P NMR spectroscopy. The ¹H{³¹P} NMR spectra of the products **3.27**, **3.28**, **3.29** and **3.30** in CDCl₃ displayed a singlet representing the acetate methyl protons at 1.29, 1.35, 1.40 and 1.39 ppm, respectively. These peaks were found to be significantly shifted upfield by approximately 0.9 ppm compared to their corresponding dimeric complexes. The OH proton in the monomeric complexes was found to have experienced a significant downfield shift from that observed in the acetate-bridged complexes, supporting the presence of relatively strong hydrogen bonding with the coordinated acetate oxygen. Analysis of **3.27-3.30** by ³¹P NMR spectroscopy revealed only a singlet peak (around 42 ppm) ascribed to be the PPh₃ phosphorus atom. ¹⁹F NMR spectroscopic data showed no significant differences between spectra recorded for these complexes and their dimeric starting materials.

The mass (ES) spectra of the mononuclear complexes **3.27**, **3.28**, **3.29** and **3.30** each displayed a strong peak corresponding to the fragment [M-OAc]⁺ at *m/z* 538, 552, 606 and 558, respectively. The infrared spectra of these complexes showed two peaks at approximately 1560 cm⁻¹ and 1435 cm⁻¹ which represent the asymmetric and symmetric

vibrations of the COO group of the acetate ligand, respectively. Although samples of **3.27-3.29** were dried *in vacuo* before submission, the elemental analysis showed larger results than the actual percentage of carbon. This could be attributed to the presence of coordinated solvents.

The structures of **3.29** and **3.30** have been further confirmed by X-ray diffraction studies (Figures 3.17 and 3.18). Single crystals of **3.29** and **3.30** were grown by slow diffusion of hexanes into a solution of the complexes in dichloromethane. Selected bond distances and the C-Pd-N bond angles are reported in Table 3.6.

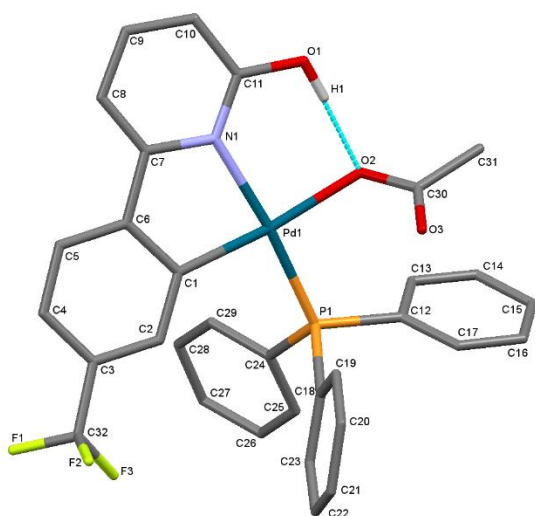


Figure 3.17: Structure of **3.29** with hydrogen atoms (except OH) omitted for clarity

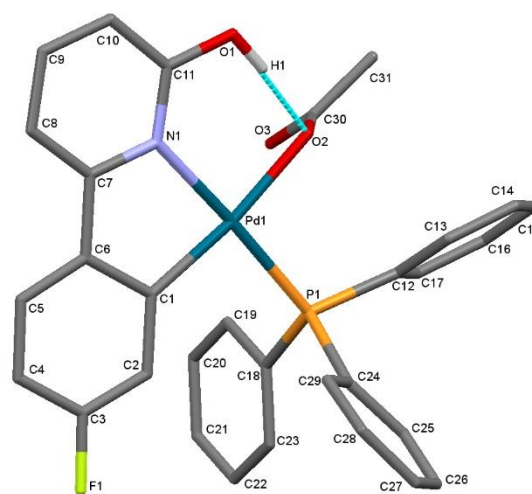


Figure 3.18: Structure of **3.30** with two solvent CH₂Cl₂ molecules and hydrogen atoms (except OH) omitted for clarity

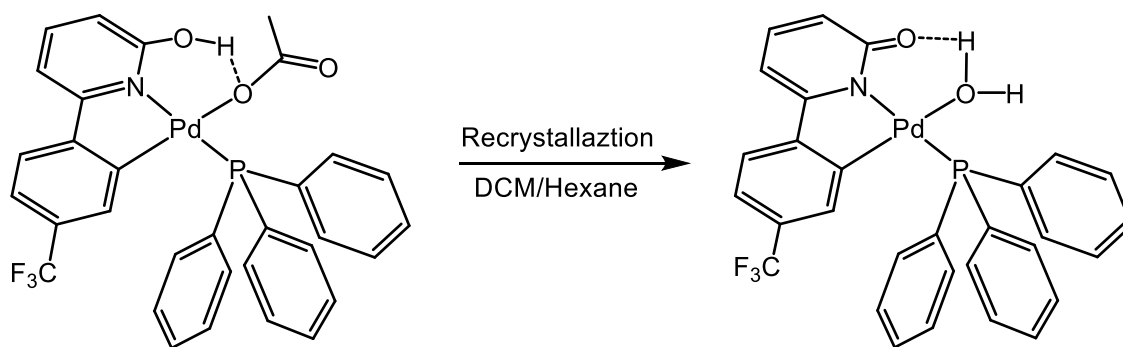
Table 3.6: Selected Pd-X bond lengths and angles of complexes **3.29** and **3.30**

Complex	Bond lengths (Å)					Bond angles (°)
	Pd1-N1	Pd1-C1	Pd1-O2	Pd1-P1	C11-O1	N1-Pd1-P1
3.29	2.118(3)	1.998(4)	2.107(2)	2.2507(11)	1.320(4)	81.94(13)
3.30	2.105(3)	1.983(4)	2.121(3)	2.2559(11)	1.319(6)	81.33(16)

For both complexes, the X-ray data revealed a Pd^{II} centre bound by a bidentate monoanionic ligand that forms a 5-membered chelating ring which, along with the acetate and PPh₃ ligands, completes a distorted square planar geometry with N-Pd-P angles of 171.08(8)° (**3.29**) and 175.91(10)° (**3.30**). The Pd-X (X = N, C, O and P) bond lengths

and bite angles are in agreement with similar Pd-X bond lengths and angles reported in the literature³⁰ and are identical to those observed in complex **2.22**, except for the N1-Pd1-O2 bond angles of 92.52(11)° in **3.29** and 92.35(13)° in **3.30** which were found to be significantly smaller than that of 98.16(8)° observed in **2.22**. This presumably reflects the constraints imposed on **3.29** and **3.30** by the hydrogen-bonding interactions between the hydroxy hydrogen and bound acetate oxygen.

Notably, upon recrystallisation from bench solvents (DCM/hexane), only the CF₃-containing complex (**3.29**) proved amenable to hydrolysis, forming the terminal aqua complex [Pd(κ^2 -N⁺C)(κ^1 -OH₂)(PPh₃)] (**3.31**) in a 45% yield (**Scheme 3.15**). Interestingly, repeated recrystallisation of the mixture in triplicate increased the amount of complex **3.31** up to 92% conversion. Further recrystallisation resulted in product decomposition.



Scheme 3.15: Synthesis of **3.31** from **3.29**

The $^1\text{H}\{^{31}\text{P}\}$ NMR spectrum of **3.31** in CDCl_3 showed the absence of the downfield-shifted OH peak and acetate ligand, indicating that the complex had undergone a deprotonation process with the loss of acetic acid, which allowed the ligand to adopt a pyridonate form. This finding is further confirmed by the absence of the acetate methyl carbon resonance at 22.8 ppm by both ^{13}C HMQC and DEPT 135 spectroscopies. The pyridonate environments had all shifted to significantly lower frequencies (0.95-1.16 ppm) with respect to the acetate complex (**3.29**), which is in agreement with deprotonation of the complex **3.31**. Substitution of the acetate group in **3.31** for a water molecule occurred as determined from the X-ray structure (*vide infra*). ^{31}P and ^{19}F NMR spectra of **3.31** displayed a singlet peak at 40.1 and -62.9 ppm, while for **3.29** these were found to be at 41.7 and -63.2 ppm, respectively. The C=O stretch appeared at 1640 cm^{-1} in the solid-state IR spectra of **3.31**. In addition, analysis of the complex by TOF mass

spectrometry showed strong fragmentation peaks at m/z 606 and 1213, corresponding to $[M-OH]^+$ and $[2M-2OH]^+$, respectively.

Further confirmation of the structure of **3.31** was obtained by single crystal X-ray diffraction studies. The molecular structure showed a palladium aqua-terminal complex supported by bidentate pyridonate and PPh_3 ligands (**Fig. 3.19**) to adopt a slightly distorted square planar geometry.

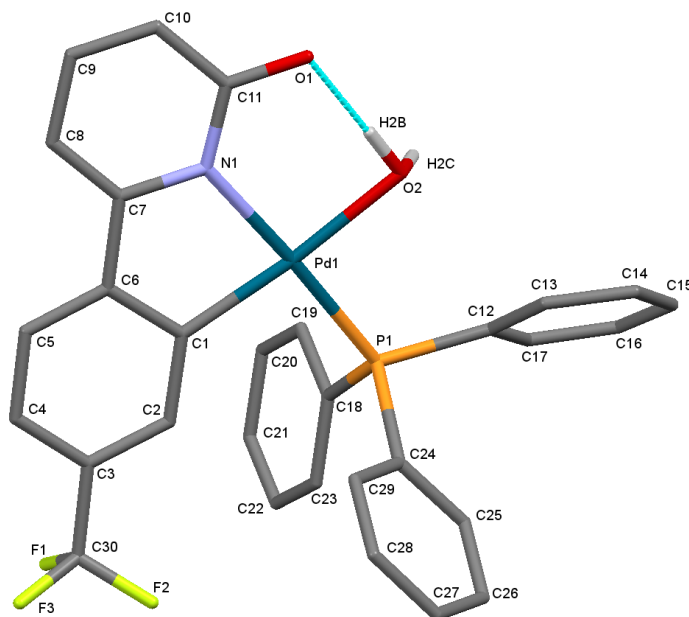


Figure 3.19: Structure of **3.31** with hydrogen atoms (except H_2O) omitted for clarity

Table 3.7: Selected Pd-X bond lengths and bite angle of complex **3.31**

Complex	Bond lengths (Å)					Bond angle (°)
	Pd1-N1	Pd1-C1	Pd1-O2	Pd1-P1	C11-O1	C1-Pd1-N1
3.31	2.101(3)	1.999(4)	2.114(3)	2.2637(18)	1.283(5)	81.23(15)

The X-ray data revealed that all Pd-X (X = N, C, O and P) bond distances are in agreement with those reported in the literature.³⁰ The C-O bond length of 1.283(5) Å is somewhat similar to that of 1.277(6) Å observed in the aqua-bridged complex (**3.25**) but it is much smaller than that of 1.320(4) Å found in the acetate one (**3.29**); this is consistent with double bond character. The deprotonation of the OH group resulted in the decrease of the mean C7-N1-C11 angle by *ca.* 2.4° compared to that for the coordinated pyridinol

ligand in complex **3.29**. The solid-state structural data unambiguously confirmed hydrolysis of the acetate to form the terminal aqua complex (**3.31**). As expected, the pendent aqua protons were involved in intra- and inter-molecular hydrogen-bonding interactions with the adjacent pyridonate oxygen (O1) and the pyridonate oxygen from another molecule, respectively, as demonstrated in **Figure 3.20**.

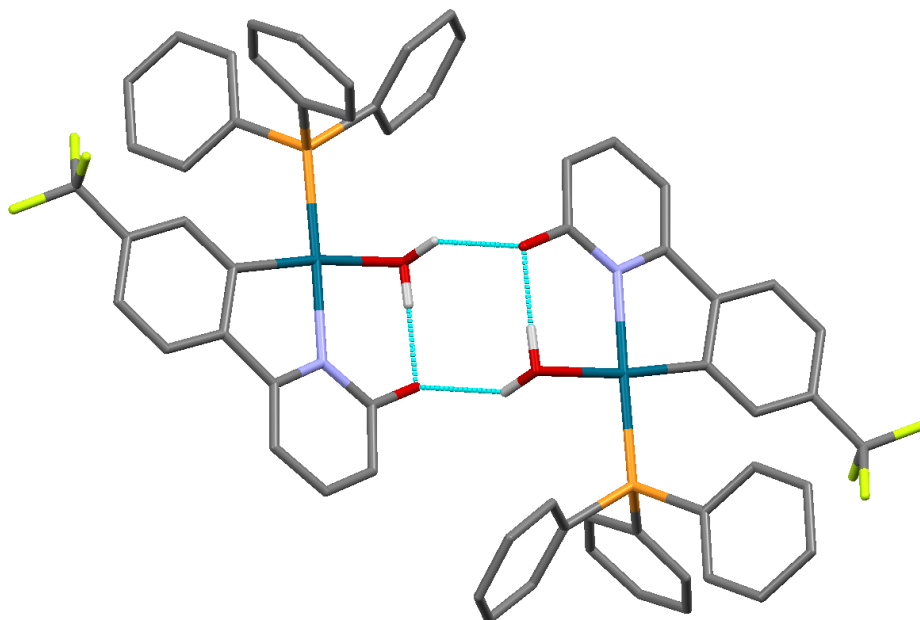
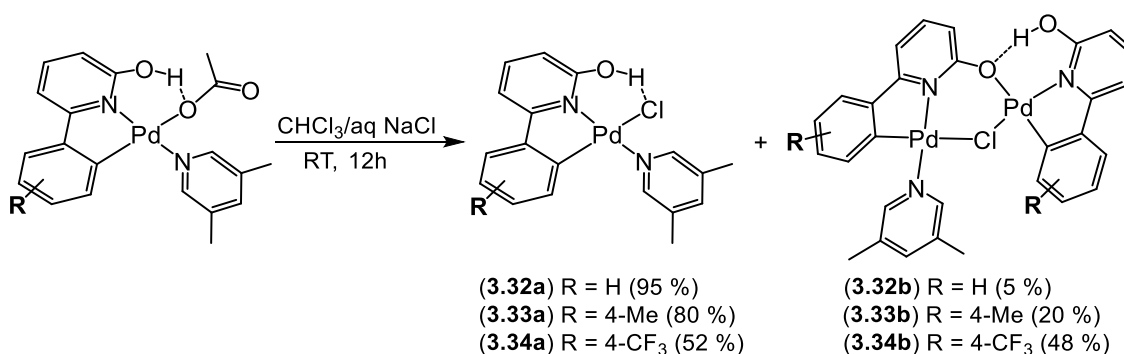


Figure 3.20: Inter- and intra-molecular hydrogen bonding interactions in **3.31**

3.3.7 Subsequent Ligand Exchange Reactions with aqueous NaCl

The reactions of **3.19-3.21** with aqueous solution of NaCl afforded a mixture of monomeric (**3.32a-3.34a**) and dimeric (**3.32b-3.34b**) complexes (**Scheme 3.16**).



Scheme 3.16: Reactions of acetate complexes **3.19-3.21** with aqueous NaCl

Upon analysis of **3.34a/3.34b** by ¹H NMR spectroscopy, decreasing or increasing the reaction time to 2 or 24 hours, respectively, gave the same percentage conversion. The

two distinct products could not be isolated; however, washing the mixtures with hexane partially helped to dissolve the monopalladated products from which ^1H and ^{19}F (for **3.34a**) NMR data could be obtained. All other techniques (^{13}C NMR spectroscopy, mass spectrometry and X-ray diffraction) were used to characterise the products together as a mixture, except IR spectroscopy which was not possible for a mixture of the products.

^1H NMR spectroscopy of the crude products showed the formation of the monomeric complexes **3.32a**, **3.33a** and **3.34a** with 95, 80 and 52% conversions, respectively. As mentioned above, these monopalladated products were isolated in small amounts and characterised by ^1H and ^{19}F (for **3.34a** only) NMR spectroscopy. Upon analysis by ^1H NMR spectroscopy, complexes **3.32a**, **3.33a** and **3.34a** revealed the absence of an ancillary acetate ligand, indicating that the exchange of the acetate ligand with chloride had been successful. This was further confirmed by analysis of the mixtures by $^{13}\text{C}\{^1\text{H}\}$ NMR spectroscopy wherein the acetate methyl signals at approximately 23.5 ppm for the starting material were also absent. Due to the hydrogen-bonding interaction with the chloride ligand, a downfield resonance assigned to the OH proton was observed at 11.98, 11.94 and 12.09 ppm in the respective ^1H NMR spectra of **3.32a**, **3.33a** and **3.34a**. A peak representing the CF_3 group in the ^{19}F NMR spectrum of **3.34a** was observed at -63.0 ppm which was at a similar chemical shift to that of 62.9 ppm seen for the starting material (**3.21**). In common with chloride complexes, a peak corresponding to the loss of the chloride ion ($[\text{M}-\text{Cl}]^+$) was observed at m/z 383, 397 and 451 in the mass spectra of **3.32a**, **3.33a** and **3.34a**, respectively.

It was possible to obtain single crystals of **3.33a** and **3.34a** suitable for X-ray diffraction studies. The structures of both complexes consist of one distorted square planar Pd^{II} centre supported by $\text{N}^{\wedge}\text{C}$ -pyridinol, 3,5-lutidine and chloride ligands (**Figures 3.21** and **3.22**). In both complexes, the solid-state X-ray diffraction analysis showed that the 3,5-lutidine was in a *trans* position, and almost perfectly perpendicular, to the plane of the pyridyl ring. This formation was confirmed by the torsion angles of $91.9(4)^\circ$ and $87.4(11)^\circ$ found for $\text{Cl}(1)\text{-Pd}(1)\text{-N}(2)\text{-C}(17)$ and $\text{Cl}(2)\text{-Pd}(3)\text{-N}(5)\text{-C}(43)$ in the solid-state structures of **3.33a** and **3.34a**, respectively. An intramolecular hydrogen-bonding interaction was found in **3.33a** (2.09 Å) and **3.34a** (2.19 Å) between the hydroxy protons and chloride ligands.

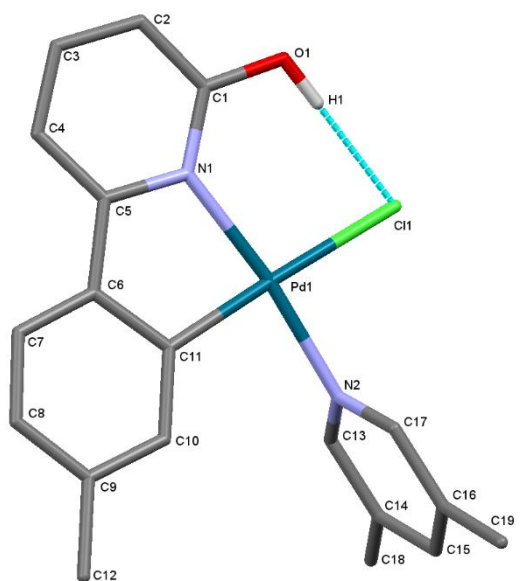


Figure 3.21: Structure of **3.33a** with hydrogen atoms (except OH) omitted for clarity

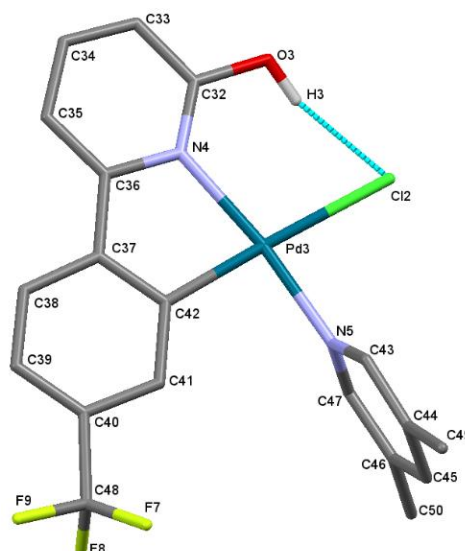


Figure 3.22: Structure of **3.34a** with hydrogen atoms (except OH) omitted for clarity

Table 3.8: Selected bond lengths and angles of complexes **3.33a** and **3.34a**

Complex	Bond lengths (Å)					Bond angles (°)
	Pd-N _{py}	Pd-N _{lut}	Pd-C	Pd-Cl	C-O	C-Pd-N _{py}
3.33a	2.073(5)	2.036(5)	1.976(6)	2.440(2)	1.320(7)	81.4(2)
3.34a	2.104(11)	2.025(11)	1.973(13)	2.442(4)	1.377(16)	80.4(5)

From **Table 3.8**, the bond distances of Pd-C and Pd-Cl and bite angles in both complexes are, in general, similar to those found in the literature for related complexes.³¹ The Pd-N_{py} bond lengths of 2.073(5) and 2.104(11) Å in **3.33a** and **3.34a** were found to be longer than those of 2.036(5) and 2.025(11) Å found for Pd-N_{lut} bonds, respectively. This reflects stronger Pd-N_{lut} bonds in comparison to the Pd-N_{py} bonds, which are not common for this type of complexes containing pyridine derivatives as a monodentate ligand, [Pd(ppy)(py)X] (where X is an anion).³¹⁻³⁴ The reason behind this is likely due to the presence of the methyl groups of the 3,5-lutidine ligand which is considered an electron donating group that can result in the bond length between the palladium and nitrogen (N_{lut}) being shorter. The C-O bond lengths are consistent with having single bond character.

As mentioned earlier, the ^1H , $^{13}\text{C}\{^1\text{H}\}$ and ^{19}F (for CF_3 -containing products) NMR spectra of the crude products obtained from the reactions of **3.19**, **3.20** and **3.21** with aqueous solutions of NaCl also showed the presence of dimeric complexes (**3.32b**, **3.33b** and **3.34b**) in which the two Pd^{II} centres are linked together by one chloride atom as well as by the NCO moiety of the pyridonate ligand. Analysis of **3.32b**, **3.33b** and **3.34b** by ^1H NMR spectroscopy demonstrated the asymmetry in the palladium dimers, as two sets of resonances for ligands in non-equivalent environments were observed. In addition to being coordinated to the Pd^{II} centre in a chelating mode, one $\text{N}^{\wedge}\text{C}$ -ligand also acts as an $\text{N}^{\wedge}\text{O}$ -bridge, while the other one remained in its pyridinol form with downfield OH peaks at 13.44, 13.36 and 13.35 ppm observed in the ^1H NMR spectra of **3.32b**, **3.33b** and **3.34b**, respectively. The presence of only one coordinated 3,5-lutidine was also confirmed by ^1H NMR spectroscopy. In addition, analysis of **3.34b** by ^{19}F NMR spectroscopy revealed two signals at -62.5 and -62.9 ppm corresponding to the CF_3 group present in each ligand. In the electrospray mass spectra of **3.33b** and **3.34b**, a peak assigned to loss of the chloride group was observed at m/z 688 and 795, respectively. A fragmentation peak corresponding to $[(\text{M}-\text{Cl})+\text{MeCN}]^+$ was also observed at m/z 699 by analysis of **3.32b** via mass spectrometry.

Crystals suitable for X-ray crystallography were obtained for **3.32b** (Fig. 3.23), **3.33b** (Fig. 3.24) and **3.34b** (Fig. 3.25). Complexes **3.32b** and **3.34b** were grown by slow diffusion of hexanes into a dichloromethane solution of the crude products while complex **3.33b** was obtained by slow evaporation of a solution of the product in methanol. Selected bond lengths and angles for all three complexes are reported in Tables 3.9 and 3.10, respectively. In the unit cell of **3.32b** and **3.33b**, there was only one unique dimeric complex molecule whereas **3.34b** was found to co-crystallise in a 1:1 ratio with the related monomeric complex (**3.34a**).

The X-ray structures of **3.32b**, **3.33b** and **3.34b** revealed unsymmetrical dimeric complexes bridged by chloride and an $\text{N}^{\wedge}\text{O}$ -pyridonate ligand, with a distorted square planar geometry at each Pd^{II} centre. One palladium(II) core consists of an $\text{N}^{\wedge}\text{C}$ -chelating pyridinol ligand in which the pyridyl nitrogen is *trans* to the bridged chloride atom. The other centre involves a monodentate 3,5-lutidine ligand along with an $\text{N}^{\wedge}\text{C}$ -chelating pyridonate ligand which is, as mentioned above, also able to act as a bridge between the two palladium centres through the pyridyl nitrogen and oxygen atoms. In this case, the aryl CH-activated carbon is *trans* to the bridged chloride atom.

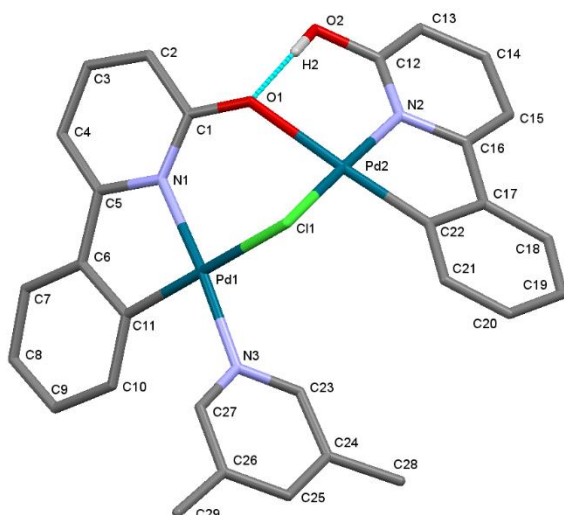


Figure 3.23: Structure of **3.32b** with hydrogen atoms (except OH) omitted for clarity

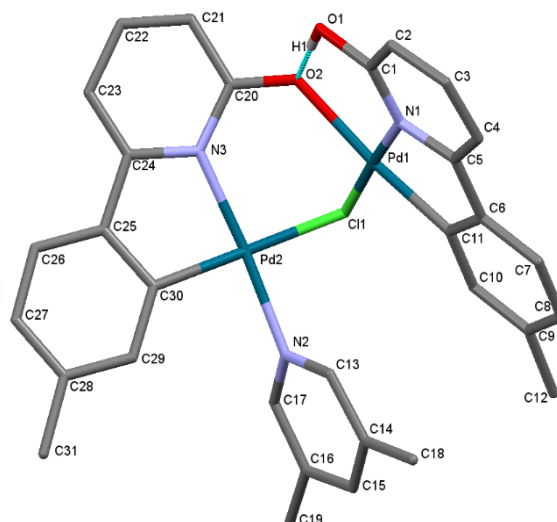


Figure 3.24: Structure of **3.33b** with hydrogen atoms (except OH) and a methanol molecule omitted for clarity

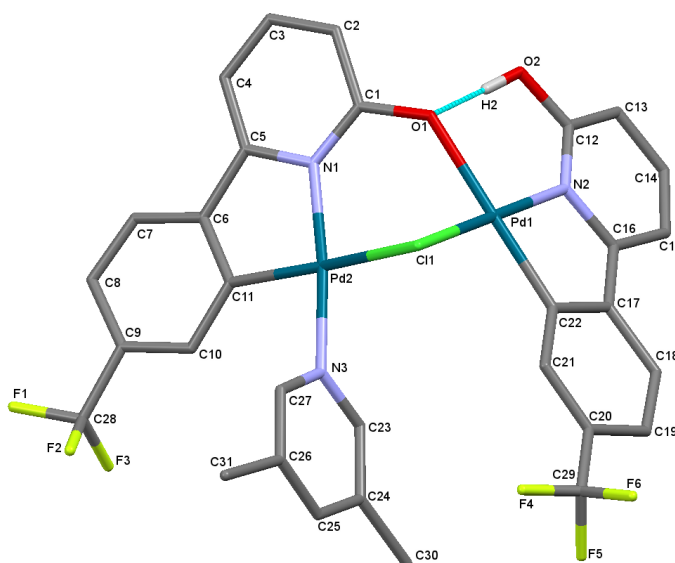


Figure 3.25: Structure of **3.34b** with hydrogen atoms (except OH) omitted for clarity

The solid-state X-ray data showed that the dimers preferred to adopt a V-shaped geometry instead of the planar geometry (D_{2h}) which is most common for Cl-bridged dimers.²⁴ This means that there could be a bonding interaction between the two Pd^{II} centres, particularly as the distance between them (3.0427(8) (**3.33b**) and 3.204(2) Å (**3.34b**)) is shorter than the sum of the van der Waals radii of palladium (3.26 Å). For all three complexes, there is a hydrogen-bonding interaction between the hydroxy proton and the coordinated

oxygen atom of the pyridonate ligand. This unambiguously explains why the OH proton was observed with a large low frequency shift (13.44, 13.36 and 13.35 ppm) in the ^1H NMR spectra of **3.32b**, **3.33b** and **3.34b**, respectively.

From **Table 3.9**, it can be seen that the length of the Pd- N_{py} bonds (whether the N_{py} atom is *trans* to N_{lut} or Cl) are longer than those for the Pd- N_{lut} bond lengths in general. This is in agreement with that observed in the related monomeric complexes **3.33a** and **3.34a** and is attributed to the presence of the methyl groups on the coordinated 3,5-lutidine ligand. The Pd-C bond lengths *trans* to the Cl atom were found to be somewhat similar to those *trans* to oxygen, suggesting that there was no differential *trans* effect between nitrogen and oxygen atoms. Interestingly, nitrogen and carbon atoms have had a different *trans* effect on the Pd-Cl bond lengths, wherein the Pd-Cl bonds *trans* to nitrogen are significantly shorter than those *trans* to oxygen. In all three complexes, the Pd-O bond lengths of approximately 2.145(12) Å are significantly longer than those previously observed for complexes **3.12**, **3.13**, **3.16** and **3.17** (2.010(7), 2.003(2), 2.188(8) and 2.095(8) Å, respectively). This is likely to be due to the steric effect related to the manner in which the oxygen coordinates to the Pd^{II} centre. The C-O bond lengths (in both types, pyridinol and pyridonate) are indicative of double bond character.

Table 3.9: Selected bond lengths of complexes **3.32b**, **3.33b** and **3.34b**

Complex	Bond lengths (Å)						
	Pd- N_{py} <i>trans</i> to N_{lut}	Pd- N_{py} <i>trans</i> to Cl	Pd- N_{lut}	Pd-C <i>trans</i> to Cl	Pd-C <i>trans</i> to O	Pd-Cl <i>trans</i> to N	Pd-Cl <i>trans</i> to C
3.32b	2.075(7)	2.064(8)	2.037(7)	1.985(9)	1.940(9)	2.287(2)	2.458(2)
3.33b	2.033(4)	2.055(5)	2.031(5)	1.975(5)	1.977(6)	2.318(2)	2.504(2)
3.34b	2.033(8)	2.038(9)	2.020(8)	1.989(9)	1.970(9)	2.320(4)	2.455(4)

As can be seen in **Table 3.10**, the bite angles of the chelating pyridonate and pyridinol ligands (C-Pd-N) were approximately 82° for all three complexes (**3.32b**-**3.34b**). This result is consistent with N[^]C-bidentate bite angles in other complexes previously described in this work. The solid-state X-ray structure clearly showed that the 3,5-lutidine is orientated perpendicular to the pyridyl plane, as confirmed by the torsion angles between them. The Pd-Cl-Pd bond angles are distorted from 90° to 87.98(8)°,

78.12(5)° and 84.24(14)° in **3.32b**, **3.33b** and **3.34b**, respectively.³⁵ This is most likely to be due to little strain in the 6-membered ring (Pd-Cl-Pd-O-C-N) caused by the coordination of the oxygen atom of the pyridonate ligand to the Pd^{II} centre. The Pd-O-C bond angles were found to be within the normal range for related complexes described in this work of approximately 124-133°.

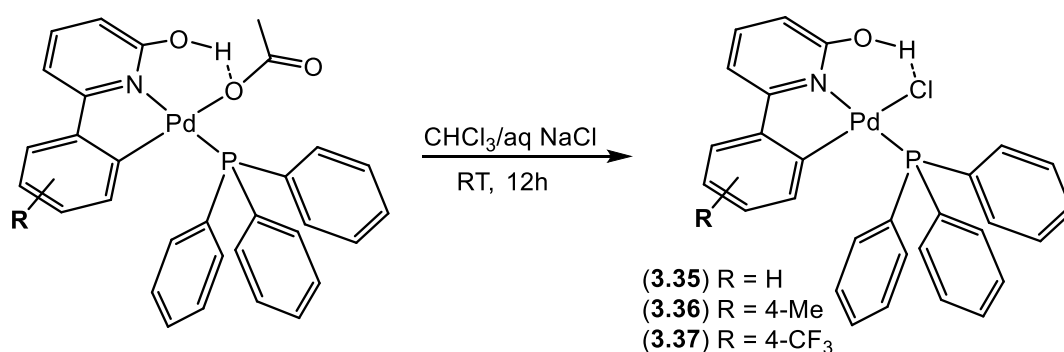
Table 3.10: Selected bond angles of complexes **3.32b**, **3.33b** and **3.34b**

Complex	Bond angles (°)			
	C-Pd-N _{pyridonate}	C-Pd-N _{pyridinol}	Pd-O-C	Pd-Cl-Pd
3.32b	81.7(4)	81.6(4)	129.5(7)	87.98(8)
3.33b	82.1(2)	81.6(2)	130.7(4)	78.12(5)
3.34b	81.6(6)	83.8(7)	129.4(8)	84.24(14)

As mentioned earlier in this section, in order to obtain only one product (either a monomer or dimer), attempts to control these reactions by time were unsuccessful. Heating a chloroform-*d* solution of a mixture of **3.34a** and **3.34b** to 45 °C for 6 hours did not improve the conversion. It should be noted that NaCl was used in excess and added as an aqueous solution either before or after adding a chloroform solution of the terminal-acetate complex (**3.21**) to the reaction flask. These different addition orders also did not favour any product over another. Although these attempts did not help in the determination of the mechanism behind the formation of the dimer (**3.34b**), it is possible, during the course of the reaction, that each of two molecules of **3.34a** had undergone complex self-dimerisation *via* hydrogen bonding to eventually form the dimer (**3.34b**). Structures comparable to these dimeric complexes could not be found in the literature.

From the outcome of these reactions, it is clear that the formation of the dimeric complexes can be affected by introducing either electron-donating or electron-withdrawing groups onto the phenyl ring. The CF₃-containing **3.34a** showed its greater ability to undergo self-dimerisation than others (**3.32a** and **3.33a**) while the complex **3.33a** with an electron-donating group (Me) displayed higher conversion (20%) to the dimeric complex (**3.33b**) than **3.32a** to **3.32b** (5%). Thus, the order of the reactivity is as follows: CF₃ > Me > H. This behaviour could also be seen in the rates of the reactions with silver salts in the next section (**3.3.8**).

Under similar conditions to those used for the reactions of the terminal-acetate complexes containing 3,5-lutidine with a saturated aqueous solution of sodium chloride, PPh₃-containing complexes **3.35**, **3.36** and **3.37** were obtained in 95, 92 and 79% yields, respectively. In these reactions, acetate-chloride exchange chemistry occurred; therefore, as expected, only one product was generated during the course of these reactions (**Scheme 3.17**). The identity of **3.35**, **3.36** and **3.37** were confirmed as monomeric complexes by ¹H{³¹P}, ¹³C and ¹⁹F (for **3.37**) NMR and IR spectroscopies as well as by mass spectrometry, elemental analysis (except **3.35**) and X-ray crystallography.



Scheme 3.17: Synthesis of Cl-containing complexes **3.35**, **3.36** and **3.37**

Analysis of **3.35**, **3.36** and **3.37** by ¹H{³¹P} NMR spectroscopy confirmed the absence of the 3H singlet corresponding to the acetate methyl group, i.e., the terminal acetate ligand had been successfully replaced by a chloride atom. Furthermore, no signals representing the acetate carbon atoms were observed in the ¹³C NMR spectra of these complexes. In the ¹H{³¹P} NMR spectra of these complexes, the OH proton was shifted upfield by approximately 1.00 ppm compared to those for the starting materials. The ³¹P and ¹⁹F NMR spectra of **3.35**, **3.36** and **3.37** showed only one signal as a singlet confirming the presence of only one product. In chloroform, these complexes were stable for up to 3 days. The IR spectra of all three complexes showed a broad peak between 2700 and 3000 cm⁻¹ which was assigned to $\nu(\text{OH})$ absorption band. Upon analysis by electrospray mass spectrometry, **3.35**, **3.36** and **3.37** displayed a peak representing the loss of the chloride ligand at m/z 538, 552 and 606, respectively. The empirical formulae of **3.36** and **3.37** were confirmed by elemental analysis. Further confirmation of the structures of **3.35**, **3.36** and **3.37** was obtained *via* X-ray diffraction studies (**Figures 3.26**, **3.27** and **3.28**, respectively). Single crystals suitable for analysis by X-ray diffraction

were grown by layering the DCM solution of the products with hexane. Selected bond lengths and angles are given in **Table 3.11**.

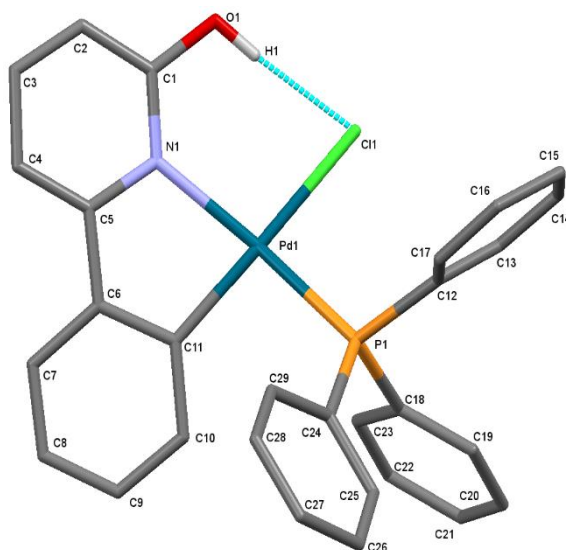


Figure 3.26: Structure of **3.35** with hydrogen atoms (except OH) omitted for clarity

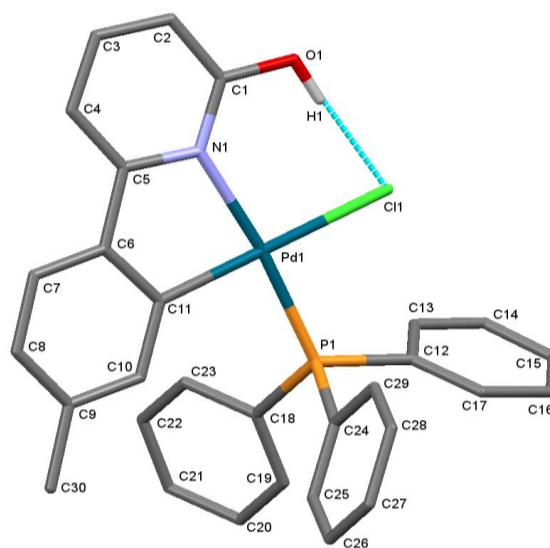


Figure 3.27: Structure of **3.36** with hydrogen atoms (except OH) omitted for clarity

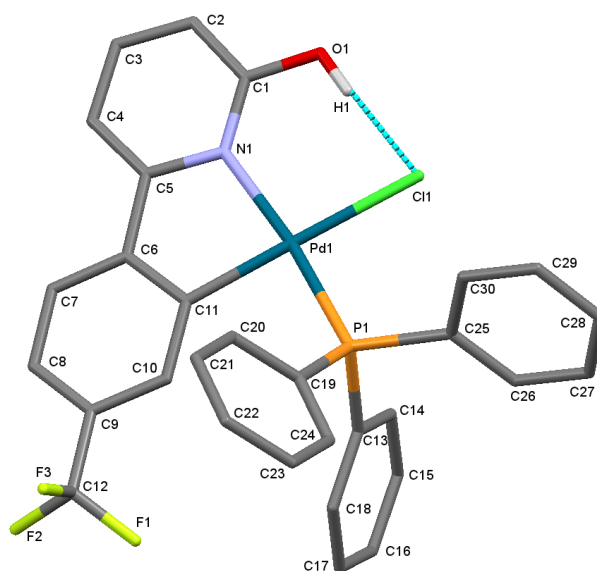


Figure 3.28: Structure of **3.37** with hydrogen atoms (except OH) omitted for clarity

Since the structures of **3.35**, **3.36** and **3.37** are very similar to each other, they will be described together here. All three complexes adopt the same distorted square planar geometry around the Pd^{II} centre with N-Pd-P angles of 168.1(2)^o (**3.35**), 173.80(5)^o (**3.36**)

and $173.61(7)^\circ$ (**3.37**). The solid-state X-ray diffraction analysis revealed a *trans* arrangement between the PPh₃ ligand and the pyridyl nitrogen atom. In all complexes, there is an intramolecular hydrogen bonding interaction between the OH proton and the chloride ligand. The data reported in **Table 3.11** illustrates that the Pd-X (X = N, C, Cl and P) bond lengths and bite angles are in agreement with similar Pd-X bond lengths and angles reported in the literature.³⁶ In addition, exchanging the chloride for acetate did not result in any significant differences from the related bond lengths and angles observed for the starting acetate complex (**3.29**) for complex **3.37**. Furthermore, the key bond lengths and angles in complexes **3.36** and **3.37** are also all reasonably similar to those in the related 3,5-lutidine-containing complexes **3.33a** and **3.34a** described in this work. The C-O bond lengths fall between 1.322(13) and 1.331(4) Å and are consistent with single bond character, indicating that the N⁺C-coordinated ligands are in a pyridinol form.

Table 3.11: Selected bond lengths and bite angles of complexes **3.35**, **3.36** and **3.37**

Complex	Bond lengths (Å)					Bond angles (°)
	Pd-N	Pd-C	Pd-P	Pd-Cl	C-O	C-Pd-N
3.35	2.145(8)	1.975(10)	2.259(3)	2.397(3)	1.322(13)	81.1(4)
3.36	2.142(2)	2.015(2)	2.2483(7)	2.4065(7)	1.321(3)	81.16(8)
3.37	2.138(2)	2.014(3)	2.2534(9)	2.400(1)	1.331(4)	80.86(11)

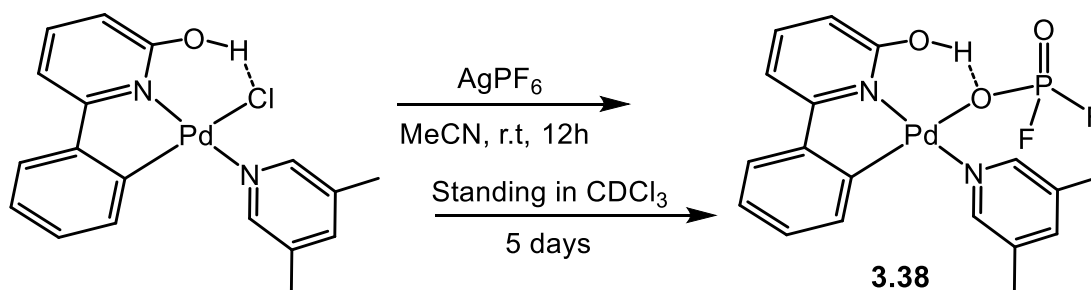
Since the acetate complexes containing 3,5-lutidine (**3.19**, **3.20** and **3.21**) reacted differently to an aqueous solution of NaCl than those containing PPh₃ (**3.27**, **3.28** and **3.29**), it can be concluded that the electronic and/or steric properties of the simple ligands (3,5-lutidine and PPh₃) play a significant role in altering the reactivity of the complexes during their substitution reactions. In comparison to 3,5-lutidine, PPh₃ should bind more tightly to metal centres, due to the Pd-P soft-soft interaction and hence it is better able to stabilise complex structures, as seen in **3.35**, **3.36** and **3.37**. The steric effects of the phenyl substituents on the phosphorus atom of such ligand are also dramatic, determining the coordination geometry present in palladium complexes.

3.3.8 Reactions of Cl-Containing Complexes with Different Silver Salts

Since the chloride ligand is relatively labile, replacing it with neutral, weakly-coordinating acetonitrile in the presence of a silver salt was the main aim of this section.

However, some interesting reactivity was observed during the course of these reactions. This took the project further into an investigation into the reactivity of different silver salts towards the Cl-containing complexes described in this chapter than was originally intended. The silver salts used include silver hexafluorophosphate (AgPF_6), silver tetrafluoroborate (AgBF_4) and silver trifluoromethanesulfonate (AgOTf). Varying the silver salts and complexes was intended to aid in the understanding of how their properties influence their reactivities.

Reaction of the desired monomeric **3.32a** (95%), as a mixture with the dimeric **3.32b** (5%), with AgPF_6 in acetonitrile resulted in the formation of a complex mixture of products along with the elimination of AgCl . On standing in a chloroform solution at room temperature for 5 days, the crude reaction mixture gave a yellow solution from which **3.38** was obtained as a result of partial hydrolysis³⁷ (*vide infra*) in an excellent purity with a yield of 73% (**Scheme 3.18**).



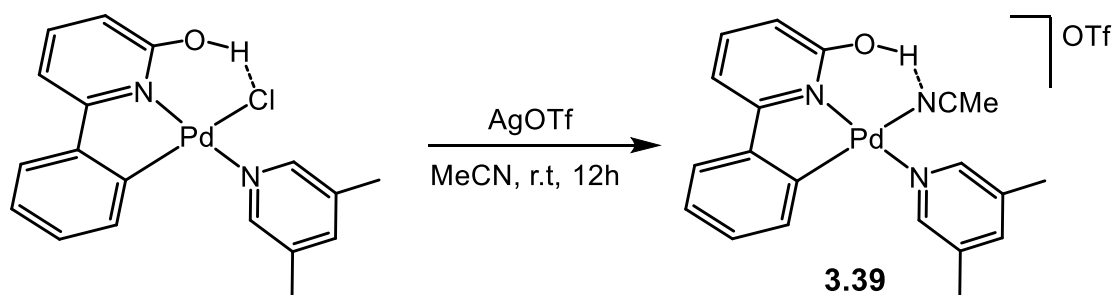
Scheme 3.18: Synthesis of $[\text{Pd}(\kappa^2\text{-6-phenyl-2-pyridinol})(3,5\text{-lutidine})(\text{PO}_2\text{F}_2)]$ (**3.38**)

The structure of the complex **3.38** was characterised by ^1H , $^{13}\text{C}\{^1\text{H}\}$, ^{31}P and ^{19}F NMR and IR spectroscopies in addition to electrospray mass spectrometry. In the ^1H NMR spectrum, a 6H singlet peak at 2.40 ppm corresponding to the lutidine-methyl proton environments was observed and confirmed the strong coordination of 3,5-lutidine over the reaction time. A downfield OH peak at 11.70 ppm indicated the OH proton was involved in a hydrogen-bonding interaction with a neighbouring H-acceptor (PO_2F_2^-). The $^{13}\text{C}\{^1\text{H}\}$ NMR spectrum of **3.38** showed 15 unique carbon resonances with the five quaternary aromatic carbon environments which are in agreement with the expected structure. The presence of the difluorophosphate (PO_2F_2^-) unit was evidenced by ^{31}P and ^{19}F NMR spectroscopy. Only a triplet peak centred at approximately -15.3 ppm with a $^1J_{\text{P-F}}$ coupling constant of 973 Hz was observed in the ^{31}P NMR spectrum, where the phosphorus atom shows coupling to two fluorine atoms. Analysis of **3.38** by ^{19}F NMR

spectroscopy revealed a doublet at -80.0 ppm with a $^1J_{\text{F-P}}$ coupling constant of 976 Hz representing the two fluorines from the PO_2F_2^- species. A strong P=O stretching band was observed at 1292 cm^{-1} in the IR spectrum which is in good agreement with the previous value found in the literature.³⁸ The electrospray mass spectrum of **3.38** displayed a fragmentation peak at m/z 383 corresponding to the proposed structure with the loss of a PO_2F_2^- group. Further peaks were also observed at m/z 767 and 101 corresponding to $[\text{2(M-PO}_2\text{F}_2)]^+$ and $[\text{PO}_2\text{F}_2]^-$, respectively.

AgBF_4 has also been employed with **3.32a** (95%) under similar conditions to that used for the synthesis of **3.38**. However, ^1H NMR spectroscopy revealed a complex mixture of products whilst the ^{19}F NMR spectrum showed only a singlet peak at -151.6 ppm, representative of the BF_4^- counterion used throughout. In addition, a peak corresponding to $[\text{BF}_4]^-$ was observed at m/z 87 upon analysis of the mixture by negative ion mass spectrometry. This may have suggested the presence of the acetonitrile-containing complex, $[\text{Pd}(\kappa^2\text{-6-phenyl-2-pyridinol})(3,5\text{-lutidine})(\text{MeCN})][\text{BF}_4]$, in the mixture. ^{19}F NMR and mass spectra proved that the counterion, BF_4^- , remained mostly intact in solution over time (10 days). However, there were other peaks observed in the ^{19}F NMR and mass spectra that may indicate that partial hydrolysis of BF_4 to OBF_2 occurred in a very small amount (3%). However, these peaks did not change over time (observed in the first minutes and after 10 days) and are thought to be due to the presence of an excess of AgBF_4 which may have somehow undergone hydrolysis in solution. In addition, nothing changed when the mixture in CDCl_3 was heated at higher temperature ($50\text{ }^\circ\text{C}$) for 12 hours.

When AgOTf was used in the same molar equivalence as the palladium chloride complex (**3.32a**, 95%), a stable MeCN-containing complex **3.39** was obtained, though with minor impurities, in a good yield (71%) (Scheme 3.19). The stability of **3.39** was examined by leaving it as a chloroform solution at room temperature for several weeks.



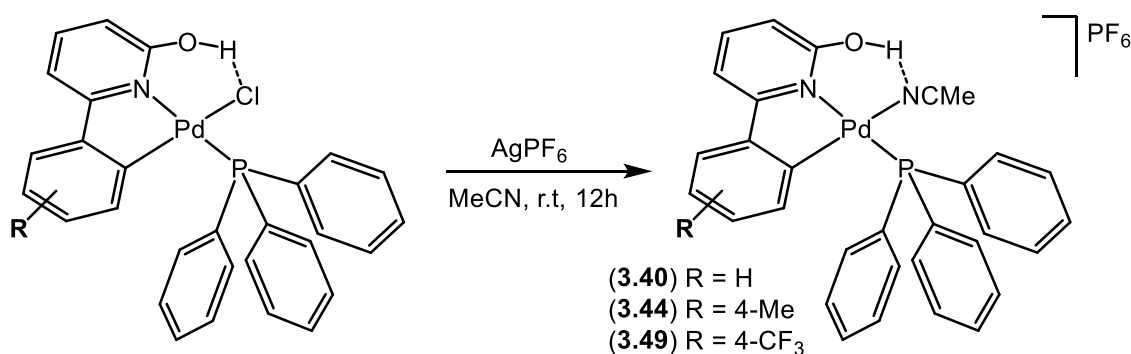
Scheme 3.19: Synthesis of the MeCN-containing complex (**3.39**)

Complex **3.39** was characterised by ^1H , 2D HMQC, ^{19}F NMR and IR spectroscopies, and also by electrospray mass spectrometry. The coordination of the acetonitrile ligand in **3.39** was evidenced by the observation of the 3H singlet at 2.02 ppm upon analysis by ^1H NMR spectroscopy. There was a broad singlet downfield at 10.39 ppm representing the OH proton involved in a hydrogen bonding interaction with the coordinated MeCN nitrogen. The 2D HMQC NMR spectrum showed nine aromatic CH carbon environments, consistent with the proposed structure. Only a single peak corresponding to the OSO_2CF_3 counterion (OTf) was observed at -78.1 ppm upon analysis of **3.39** by ^{19}F NMR spectroscopy. Furthermore, analysis of **3.39** by electrospray mass spectrometry revealed both cationic species with the loss of MeCN (m/z 383 $[\text{M}-\text{MeCN}]^+$) and anionic species (m/z 149 $[\text{OTf}]^-$).

Despite repeated attempts, it was not possible to grow single crystals of **3.38** and **3.39** suitable for X-ray diffraction. However, hydrolysis of PF_6^- and the stability of OTf were further demonstrated by the X-ray structures of related complexes containing PPh_3 instead of 3,5-lutidine (see below).

The unexpected finding of the hydrolysis of PF_6^- prompted an exploration of the reactivity of other Cl-containing Pd^{II} complexes (**3.35**, **3.36** and **3.37**) toward various silver salts. The choices of different complexes and silver salts were varied in order to investigate the effects of their properties on the rate of hydrolysis.

Firstly, the reactions of **3.35**, **3.36** and **3.37** with one equivalent of AgPF_6 in acetonitrile under nitrogen were examined. After 12 hours stirring at room temperature, the reaction solution was transferred by cannula filtration into another flask and then all volatiles were removed under reduced pressure to afford **3.40** (82%), **3.44** (93%) and **3.49** (98%) (Scheme 3.20).

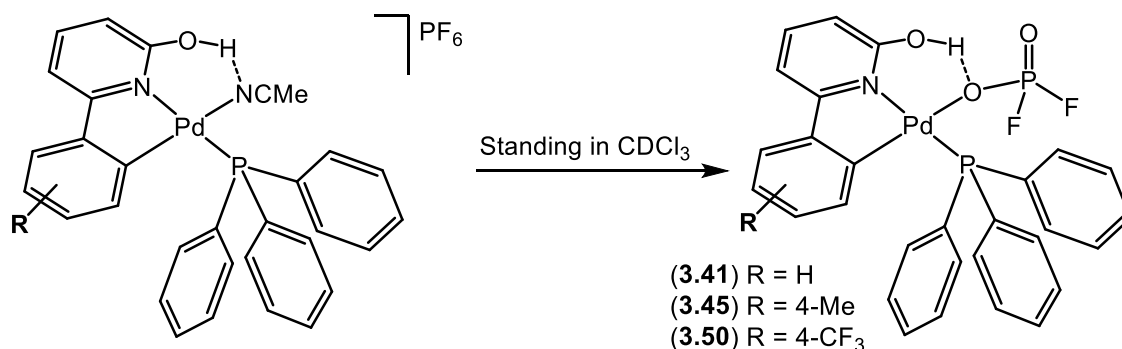


Scheme 3.20: Synthesis of the MeCN-containing complexes

Analysis of the complexes **3.40**, **3.44** and **3.49** by $^1\text{H}\{^{31}\text{P}\}$, ^{13}C , ^{31}P and ^{19}F NMR and IR spectroscopies, as well as by electrospray mass spectrometry, confirmed the proposed structures. A 3H singlet peak at 1.88, 1.83 and 1.77 ppm assigned to the coordinated MeCN protons was observed in each of the proton NMR spectra of **3.40**, **3.44** and **3.49**, respectively. Further confirmation of the coordinated MeCN was provided by ^{13}C NMR spectroscopy. As a result of the involvement of the hydroxy hydrogen in a hydrogen-bonding interaction with a coordinated acetonitrile nitrogen atom, all $^1\text{H}\{^{31}\text{P}\}$ NMR spectra showed a downfield chemical shift at 9.44, 9.11 and 9.74 ppm, representing the OH proton in **3.40**, **3.44** and **3.49**, respectively. In comparison to their starting materials (**3.35**, **3.36** and **3.37**), the OH peaks are significantly shifted to lower frequency by approximately 2.9 ppm, suggesting relatively weak hydrogen bonding interactions with the adjacent nitrogen of the coordinated acetonitrile. In their ^{31}P NMR spectra, as common to all three complexes synthesised, is the presence of a singlet and multiplet peaks representing the PPh_3 and counterion (PF_6^-), respectively. The peak positions of the PPh_3 phosphorus atom varied slightly between compounds while those for the PF_6^- counterion appeared to be centred at approximately -144 ppm for all three complexes. ^{19}F NMR spectra of all three complexes showed a doublet at about -73 ppm with a coupling constant of 711 Hz representing the anion, PF_6^- . Additionally, a singlet assigned to the CF_3 group was observed at -63.4 ppm upon analysis of **3.49** by ^{19}F NMR spectroscopy. In the electrospray mass spectra of **3.40**, **3.44** and **3.49**, a strong fragmentation peak ascribed to $[\text{M-MeCN}]^+$ was observed in each spectrum at m/z 538, 552 and 606, respectively. Common to all three complexes is the presence of a peak corresponding to the counterion species at m/z 145 $[\text{PF}_6]^-$.

On standing in the solutions at room temperature, hydrolysis of the counterion (PF_6^-) in **3.40**, **3.44** and **3.49** occurred to eventually give the hydrolysis products **3.41**, **3.45** and **3.50** in excellent yields of 97, 91 and 93%, respectively (**Scheme 3.21**). These conversions showed that the formation of **3.41** required at least 2 days to go to completion because the conversion slightly increased over the time, while the shortest reaction time (3 hours) was observed in the formation of **3.50**. In addition, the conversion to the methyl-containing complex (**3.45**) increased to 100% within 12 hours. These observations are found to be consistent with the reactivity order shown in the formation of the dimeric **3.32b**, **3.33b** and **3.34b** from their monomeric complexes (**3.32a**, **3.33a** and **3.34a**, respectively), suggested that the order of the conversion time rate is as follows: **3.50** (CF_3)

> **3.45** (Me) > **3.41** (H). Further confirmation of this order will also be found in the investigations into the hydrolysis of complexes containing BF_4^- (see later).



Scheme 3.21: Hydrolysis of silver hexafluorophosphate (PF_6) in solution

The identities of the hydrolysis products (**3.41**, **3.45** and **3.50**) were confirmed by a variety of techniques including $^1\text{H}\{^{31}\text{P}\}$, ^{13}C , ^{31}P and ^{19}F NMR and IR spectroscopies as well as by mass spectrometry and X-ray crystallography (for **3.45** and **3.50**). In the $^1\text{H}\{^{31}\text{P}\}$ NMR spectra of all three complexes, the absence of a singlet peak corresponding to the acetonitrile-methyl proton environment indicated that the acetonitrile ligands had been eliminated during the conversions. Further confirmation for the elimination of the acetonitrile ligands was obtained by $^{13}\text{C}\{^1\text{H}\}$ NMR spectroscopy, which demonstrated the absence of the acetonitrile-methyl carbon resonance. As expected, the OH proton underwent a downfield shift from 9.44, 9.11 and 9.74 ppm in **3.40**, **3.44** and **3.49** to 11.54, 11.51 and 11.63 ppm in **3.41**, **3.45** and **3.50**, respectively. These observations occurred as a result of the movement of the hydroxy proton from weak ($\text{OH}\cdots\text{N}$) to stronger ($\text{OH}\cdots\text{O}$) hydrogen-bonding environments. The presence of PO_2F_2^- species was confirmed by ^{31}P and ^{19}F NMR spectroscopy. The ^{31}P NMR spectra showed a singlet and triplet, with a $^1J_{\text{P-F}}$ coupling constant of approximately 975 Hz, assigned to the PPh_3 and the PO_2F_2^- ligands, respectively. Analysis of **3.41**, **3.45** and **3.50** by ^{19}F NMR spectroscopy revealed a doublet with a $^1J_{\text{F-P}}$ coupling constant of approximately 981 Hz which was ascribed to the two fluorine atoms of the PO_2F_2^- species. In addition, a singlet at -63.3 ppm was observed in the ^{19}F NMR spectrum of **3.50**, representing the CF_3 group. In the IR spectra of **3.41**, **3.45** and **3.50**, a strong $\text{P}=\text{O}$ stretch was detected at 1290, 1292 and 1306 cm^{-1} , respectively. Upon analysis by mass spectrometry, a fragmentation peak at m/z 101 corresponding to $[\text{PO}_2\text{F}_2]^-$ is common to all three complexes. ES mass spectra of **3.41**, **3.45** and **3.50** displayed a peak at m/z 538, 552 and 606, respectively. These peaks are representative of the proposed structures with the loss of a PO_2F_2^- ion.

Crystals suitable for X-ray crystallographic studies were grown by slow diffusion of hexane into a solution of **3.45** and **3.50** in DCM/MeCN (95/5 v/v). Structural diagrams of each complex are given in **Figures 3.29** and **3.30** with selected bond lengths and bond angles for these structures reported in **Table 3.12**.

In both complexes, the X-ray data showed a Pd^{II} complex supported by monodentate PPh₃ and PO₂F₂ ligands in addition to the pyridinol ligand, completing a distorted square planar geometry. The Pd-N, Pd-C, Pd-O and Pd-P bond lengths and bite angles were found to be within the normal range previously observed for related Pd complexes.³⁰ The presence of the pyridinol form was confirmed by the solid-state data as the carbon-oxygen bond length of 1.331(5) Å in **3.45** and 1.327(3) Å in **3.50** are consistent with a single-bond character. Therefore, there is a hydrogen-bonding interaction between the hydroxy proton and the bound oxygen atom from the PO₂F₂ ligand. The X-ray structures of **3.45** and **3.50** revealed the presence of PO₂F₂ species in a distorted tetrahedral geometry with the smallest F-P-F bond angles of 97.46(16)° and 99.34(13)° and with the largest O-P-O bond angles of 121.03(18)° and 121.36(13)°, respectively. All the bond lengths of the PO₂F₂ ion are in agreement with data previously reported for a comparable complex.³⁷

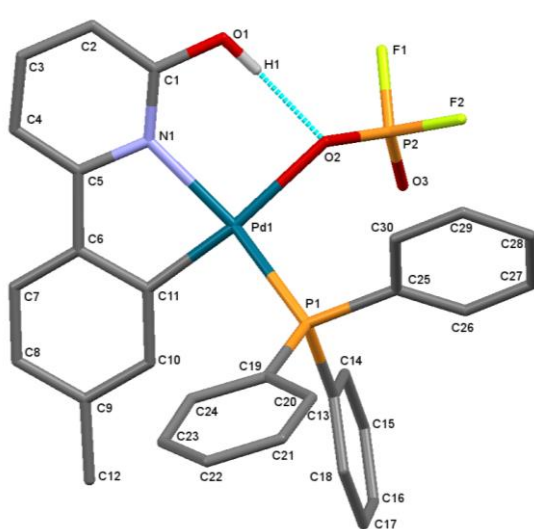


Figure 3.29: Structure of **3.45** with hydrogen atoms (except OH) omitted for clarity

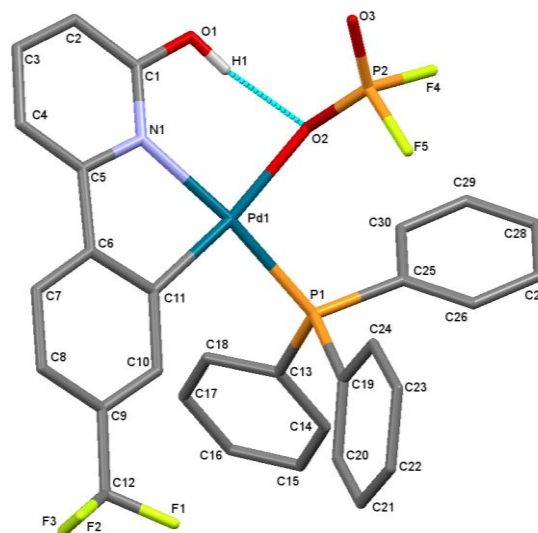
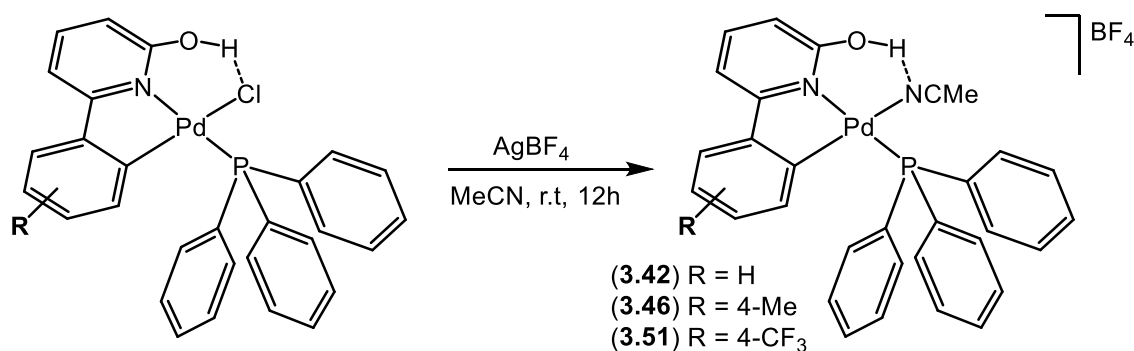


Figure 3.30: Structure of **3.50** with hydrogen atoms (except OH) omitted for clarity

Table 3.12: Selected bond lengths and bite angles of complexes **3.45** and **3.50**

Complex	Bond lengths (Å)					Bond angles (°)
	Pd-N	Pd-C	Pd-O	Pd-P	C-O	N-Pd-C
3.45	2.131(3)	1.985(4)	2.194(3)	2.269(1)	1.331(5)	81.25(13)
3.50	2.112(2)	1.993(3)	2.161(2)	2.279(1)	1.327(3)	81.47(10)
	Bond lengths (Å)					
	P-F	P-F	P-O	P=O		
3.45	1.544(3)	1.541(3)	1.489(3)	1.438(3)		
3.50	1.533(2)	1.539(2)	1.495(2)	1.449(2)		

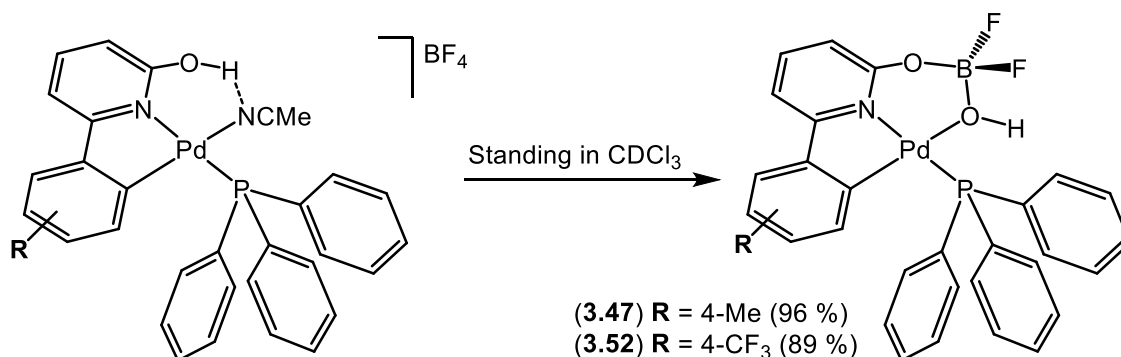
Under the same reaction conditions used to prepare the MeCN-containing complexes **3.40**, **3.44** and **3.49**, the reactions of **3.35**, **3.36** and **3.37** with one equivalent of AgBF_4 gave **3.42** (83%), **3.46** (93%) and **4.51** (97%) (**Scheme 3.22**). Analysis of these products by $^1\text{H}\{^{31}\text{P}\}$, ^{13}C , ^{31}P and ^{19}F NMR and IR spectroscopies in addition to electrospray mass spectrometry confirmed the proposed structures. These products had to be immediately characterised in solution as they underwent rapid hydrolysis in the presence of water (see later).

**Scheme 3.22:** Synthesis of the MeCN-containing complexes

The $^1\text{H}\{^{31}\text{P}\}$ NMR spectra of **3.42**, **3.46** and **3.51** displayed a 3H singlet peak at 1.82, 2.00 and 1.81 ppm, respectively, indicating the successful replacement of the chloride with acetonitrile ligands. Further confirmation for this was found upon analysis by ^{13}C NMR spectroscopy wherein a characteristic acetonitrile-methyl carbon peak was observed in their spectra. Interestingly, the downfield broad singlet corresponding to the OH proton was found to vary between the complexes according to their pyridinol ligands,

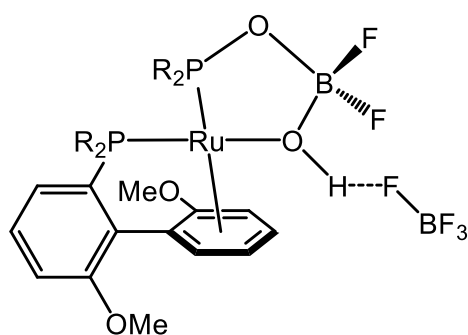
where they were observed at 12.31 ppm in **3.42**, 9.78 ppm in **3.46** and 15.30 ppm in **3.51**. The difference in the chemical shifts could be attributed to the different hydrogen bond lengths between the OH protons and the nitrogen atoms from the bound acetonitrile. A ^{31}P NMR singlet was observed at 44.6, 44.1 and 43.5 ppm for the complexes **3.42**, **3.46** and **3.51**, respectively. All ^{19}F NMR spectra showed a singlet at approximately -151.5 ppm representing the anion, BF_4^- , and an additional singlet was detected at -63.4 ppm (CF_3) in the associated ^{19}F NMR spectrum of **3.51**. The complexes **3.42**, **3.46** and **3.51** were also analysed by electrospray mass spectrometry and revealed a fragmentation peak corresponding to $[\text{M-MeCN}]^+$ at m/z 538, 552 and 606, respectively. The presence of a strong peak representing the counterion at m/z 87 $[\text{BF}_4]^-$ is common to all three complexes.

On standing in solution at room temperature, the complexes **3.46** and **3.51** proved amenable to BF_4 hydrolysis forming the corresponding products $[\text{Pd}(\kappa^2\text{-L}_R)(\text{PPh}_3)(\text{BF}_2\text{OH})]$ ($\text{R} = \text{Me}$ **3.47** and CF_3 **3.52**) (Scheme 3.23) while the H-containing complex (**3.42**) remained intact in solution and did not undergo any form of transformation over time (25 days). The conversion of the Me-containing complex (**3.46**) was complete in 2 days, whereas only 5 hours were required to obtain 100% conversion of **3.51**. Although the reactivity order of the BF_4 hydrolysis was found to be in agreement with those observed in the PF_6 hydrolysis ($\text{CF}_3 > \text{Me} > \text{H}$), the conversion time rate of BF_4 to form the BF_2OH species was relatively slow, in general. The structures of **3.47** and **3.52** were both characterised and confirmed by $^1\text{H}\{^{31}\text{P}\}$, ^{13}C , ^{31}P and ^{19}F NMR and IR spectroscopies as well as by electrospray mass spectrometry, elemental analysis (for **3.52**) and single crystal X-ray diffraction studies.

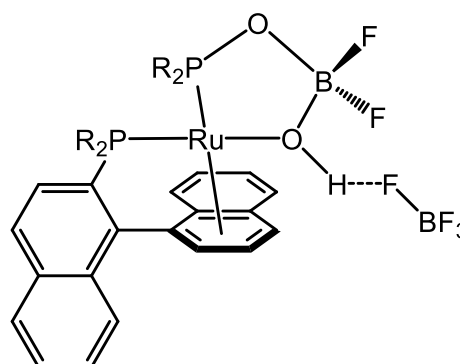


Scheme 3.23: Hydrolysis of silver tetrafluoroborate (BF_4) in solution

For both complexes, the absence of the bound acetonitrile was evident upon analysis by $^1\text{H}\{^{31}\text{P}\}$ and ^{13}C NMR spectroscopy. The characteristic downfield signal of the hydroxy proton was also not observed in the $^1\text{H}\{^{31}\text{P}\}$ NMR spectra of **3.47** and **3.52**. Instead, a broad singlet corresponding to the OH proton of BF_2OH species was detected at 3.48 and 3.54 ppm, respectively. These low chemical shifts may have suggested that the OH proton was not involved in an intramolecular hydrogen-bonding interaction. Analysis of **3.47** and **3.52** by ^{31}P NMR spectroscopy revealed only a singlet peak at 42.6 and 41.9 ppm, respectively, which are representative of the PPh_3 ligand. Interestingly, analysis by ^{19}F NMR spectroscopy revealed two sets of fluorine doublet peaks (δ -149.4 and -149.5 ppm in **3.47** and -149.5 and -149.6 ppm in **3.52**) each with $^2J_{\text{F-F}}$ coupling constants of 13.7 Hz. This indicated that the two fluorine atoms in BF_2OH species are in non-equivalent environments (axial and equatorial positions), and are thus coupled to each other through the boron atom. Analogous observations have been seen in related Ru^{II} complexes (e.g. **3.i** and **3.j**) previously synthesised by Pregosin *et al.*³⁹⁻⁴¹ In addition, a peak detected as a singlet at -62.9 ppm in the ^{19}F NMR spectrum of **3.52** was assigned to the CF_3 group. The electrospray mass spectra of **3.47** and **3.52** displayed a fragmentation peak (at m/z 552 and 605, respectively) assigned to the loss of BF_2OH from their molecular ion. In addition, a peak representing $[\text{BF}_2\text{OH}]^-$ at m/z 65 was also observed in their mass spectra. Elemental analysis of **3.52** confirmed the proposed structure.



(**3.i**) $\text{R} = \text{Ph}$
 $= 4\text{-tolyl}$
 $= 3,5\text{-di-}^t\text{Bu-phenyl}$



(**3.j**) $\text{R} = \text{Ph}$

In an attempt to characterise **3.47** and **3.52** by single crystal X-ray diffraction studies, a solution of each complex in dichloromethane/MeCN (95/5 v/v) was layered with hexane to form pale yellow crystals. The solid-state structures of **3.47** and **3.52**

revealed a neutral monomeric Pd^{II} unit which consists of an N[^]C-pyridonate ligand, PPh₃ and a BF₂OH ion as a bridging ligand between the Pd^{II} centre and the deprotonated pyridonate oxygen atom (**Figures 3.31** and **3.32**). Both complexes (**3.47** and **3.52**) adopt the same distorted square planar geometry around their Pd^{II} centres with C11-Pd-O1 angles of 168.7(2)° and 172.5(1)°, respectively. In the extended structures of **3.47** and **3.52**, the formation of dimers through intermolecular hydrogen-bonding interactions between the OH protons (H1) and deprotonated, coordinated oxygens (O2) from the other molecule were established.

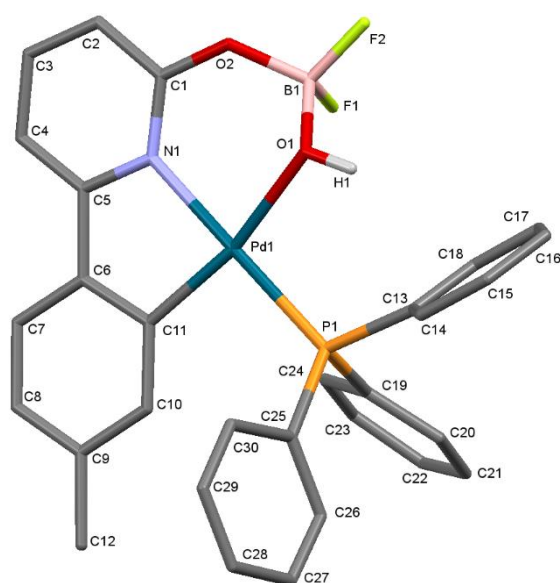


Figure 3.31: Structure of **3.47** with hydrogen atoms (except OH) omitted for clarity

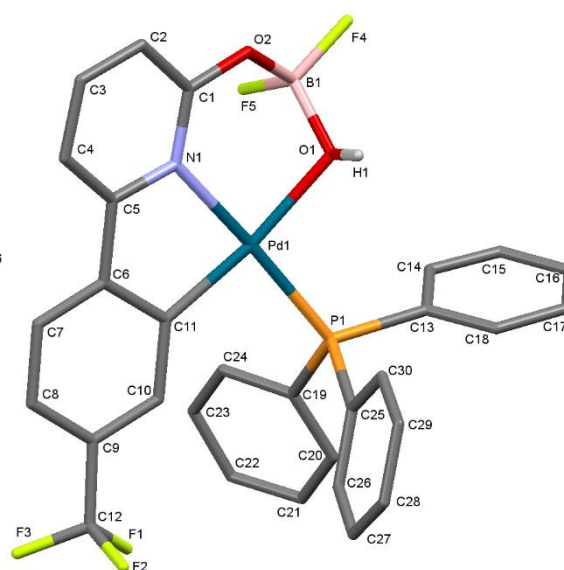


Figure 3.32: Structure of **3.52** with hydrogen atoms (except OH) omitted for clarity

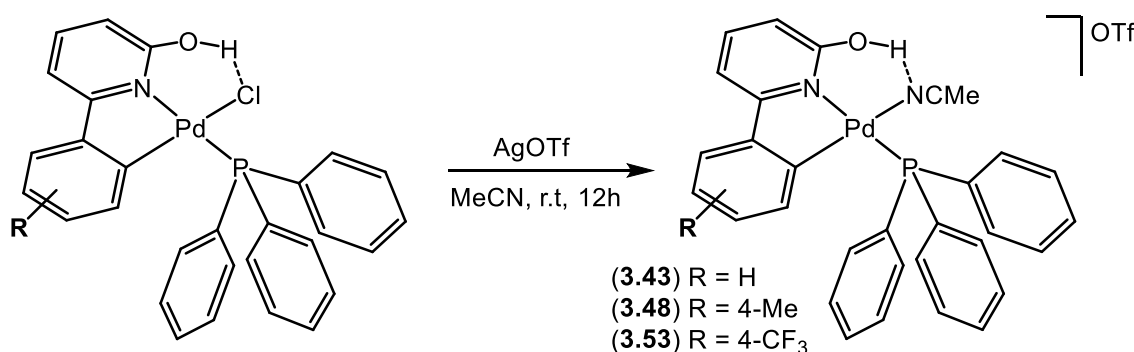
The Pd-X (X = N, C, O and P) bond lengths and bite angles reported in the **Table 3.13** were found to fall in their normal ranges³⁰ and are similar to those observed in the hydrolysis products (**3.45** and **3.50**) with a PO₂F₂ group. The solid-state data of both complexes showed that the C-O bond lengths have a single-bond character and the O atoms directly coordinated to the boron centre. The BF₂OH unit with the pyridonate oxygen was found to adopt a slightly distorted tetrahedral geometry with F-B-F and O-B-O bond angles in the range of 106-113°. The two B-F bond lengths in both complexes are almost identical, within experimental error, while significant differences were observed between the two B-O bond lengths in each complex. In addition, all the bond

lengths of the BF_2OH unit are consistent with the reported data obtained for related complexes.⁴¹

Table 3.13: Selected bond lengths and angles of complexes **3.47** and **3.52**

Complex	Bond lengths (Å)					Bond angles (°)	
	Pd-N1	Pd-C11	Pd-O1	Pd-P1	C1-O2	N-Pd-C	C-Pd-O
3.47	2.104(5)	1.993(6)	2.187(4)	2.254(2)	1.325(7)	81.8(2)	168.7(2)
3.52	2.090(3)	1.993(3)	2.113(2)	2.251(1)	1.321(4)	82.08(13)	172.5(1)
	Bond lengths (Å)					Bond angles (°)	
	B-F	B-F	B-O	B-OH	O-H	F-B-F	O-B-O
3.47	1.405(9)	1.371(9)	1.445(8)	1.508(8)	0.8511	110.5(6)	106.7(5)
3.52	1.390(5)	1.382(5)	1.498(5)	1.451(5)	0.8200	111.7(3)	112.7(3)

In order to better understand the reactivity of the Cl-containing complexes (**3.35**, **3.36** and **3.37**), silver trifluoromethanesulfonate (AgOTf) was also used as a source of counterion. In the presence of acetonitrile, these reactions proceeded rapidly at room temperature and gave the cationic solvent complexes **3.43**, **3.48** and **3.53** with yields of 84, 90 and 99%, respectively (**Scheme 3.24**). The cation-anion pairs showed a high stability in solution at different temperatures, as they remained intact in solution and had not undergone any new reactions over the time. This observation was confirmed by $^1\text{H}\{^{31}\text{P}\}$, ^{13}C , ^{31}P and ^{19}F NMR and IR spectroscopies and electrospray mass spectrometry in addition to elemental analysis and single crystal X-ray diffraction analysis for **3.53**.



Scheme 3.24: Synthesis of the MeCN-containing complexes

The $^1\text{H}\{^{31}\text{P}\}$ NMR spectra of **3.43**, **3.48** and **3.53** showed a singlet peak assigned to the acetonitrile-methyl protons at 1.81, 1.80 and 1.88 ppm, respectively. This indicated

that the chloride ligand had been successfully replaced by *N*-acetonitrile, forming a cationic species. The presence of acetonitrile as a monodentate ligand was also shown by a methyl carbon peak at 0.0, -1.9 and 0.0 ppm in the ^{13}C NMR spectra of **3.43**, **3.48** and **3.53**, respectively. Due to the hydrogen-bonding interaction with the acetonitrile nitrogen atom, a downfield resonance assigned to the OH proton was observed at 11.03, 10.61 and 11.19 ppm in the $^1\text{H}\{^{31}\text{P}\}$ NMR spectra of **3.43**, **3.48** and **3.53**, respectively. Analyses of these complexes by ^{31}P NMR spectroscopy displayed only a singlet peak (at approximately 44 ppm) ascribed to be the monodentate PPh_3 ligand. ^{19}F NMR spectroscopic data showed a singlet peak common to all the three complexes at -78 ppm which represents the counterion, OTf^- . In addition, the CF_3 group in **3.53** was seen as a singlet peak at -63.5 ppm. Further evidence for the formation of **3.43**, **3.48** and **3.53** was obtained by the presence of a strong fragmentation peak corresponding to $[\text{M-MeCN}]^+$ and $[\text{OTf}]^-$ upon analysis by electrospray mass spectrometry. The results of elemental analysis obtained for **3.53** was found to be in good agreement with the calculated elemental compositions.

It was only possible to grow single crystals suitable for analysis by X-ray diffraction of **3.53** by slow diffusion of hexane into a solution of the product in dichloromethane/MeCN (95/5 v/v). As expected, the X-ray data of the complex revealed a cationic and anionic species, as shown in **Figure 3.33**.

The cationic Pd^{II} centre, supported in a tetracoordinate environment, was found to adopt a distorted square planar geometry with a bite angle of the pyridinol ligand of $80.9(2)^\circ$. The bond lengths to the Pd^{II} centre show the same trend as those observed for the methoxy complex (**2.27**) in **Chapter 2**, where the Pd-N bond lengths (2.116(6) Å and 2.057(6) Å) are both longer than the Pd-C bond length of 1.983(6) Å and significantly shorter than the Pd-P bond length of 2.279(2) Å, as reported in **Table 3.14**. The solid-state structure confirmed the presence of an intramolecular hydrogen bonding interaction between the hydroxy proton and the bound acetonitrile through its nitrogen atom, explaining a significant low frequency shift observed in the $^1\text{H}\{^{31}\text{P}\}$ NMR spectrum. Other intermolecular hydrogen bonding interactions were also established between the cation-anion pairs and a water molecule of solvation that remained in the X-ray crystals.

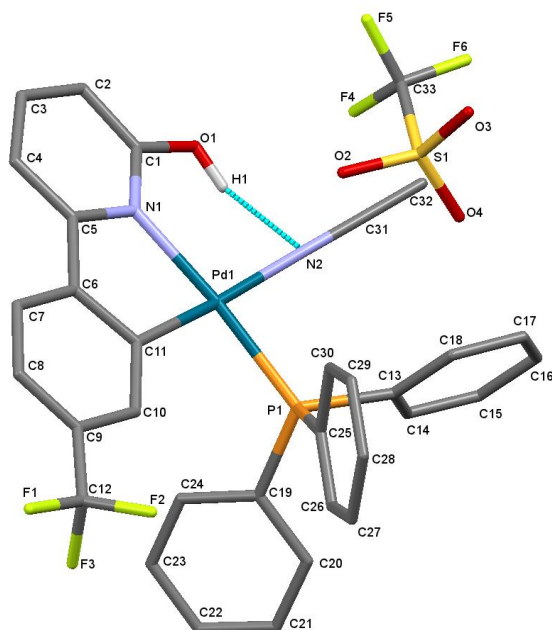


Figure 3.33: X-ray structure of **3.53** with hydrogen atoms (except OH) and water omitted for clarity

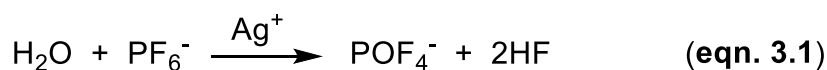
Table 3.14: Selected Pd-X bond lengths and the bite angle of complex **3.53**

Complex	Bond lengths (Å)					Bond angles (°)
	Pd1-N1	Pd1-C11	Pd1-N2	Pd1-P1	C1-O1	C11-Pd1-N1
3.53	2.116(6)	1.983(6)	2.057(6)	2.279(2)	1.336(8)	80.9(2)

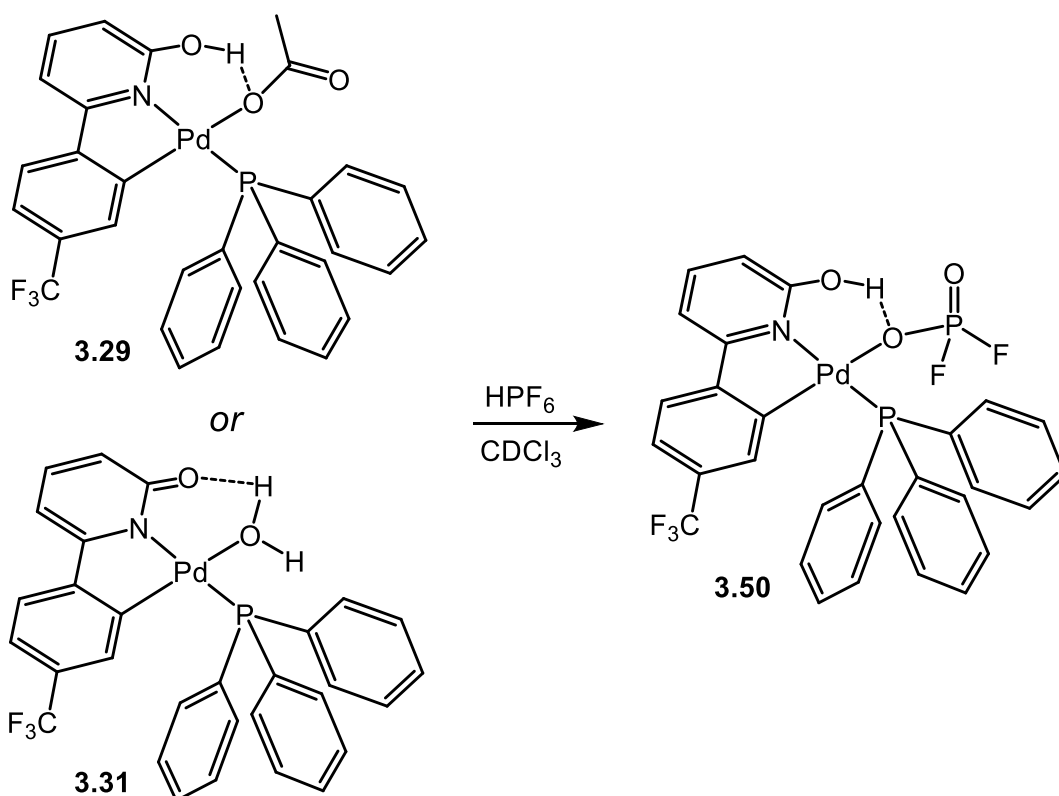
3.3.9 Hydrolysis of PF₆ and BF₄

As confirmed in **Section 3.3.8**, PF₆ and BF₄ had undergone partial hydrolysis in solution to form products with PF₂O₂ and BF₂OH ligands, respectively. A number of transition metals have been shown to form these types of complexes such as those with rhodium (Rh)⁴², manganese (Mn)⁴³, rhenium (Re)⁴⁴, ruthenium (Ru)^{39-41,45} and the subject of this research, palladium (Pd)^{37,46,47}. Fernandez-Galan *et al.*³⁷ reported the first example of a palladium complex supported by the difluorophosphate ion, [Pd(η³-2-Me-C₃H₄)(PF₂O₂)(PCy₃)]. The complex was characterised by ¹⁹F and ³¹P NMR spectroscopy as well as elemental analysis, mass spectrometry and X-ray crystallography. The authors were able to provide valuable information about how the hydrolysis of PF₆ might have occurred by detecting some of the intermediates to this process. They concluded that the

silver cation (Ag^+) has a significant role in activating residual water molecules to react with PF_6^- , as shown in equations **3.1** and **3.2**.



Initially, it seemed that this is similar to that observed in our reactions; however, our experimental studies showed that this was not the case as the hydrolysis was found to occur in the absence of Ag^+ (see **Scheme 3.21** as an example). This was further confirmed by adding hexafluorophosphoric acid, HPF_6 , into a CDCl_3 solution of **3.29** or **3.31** to form the hydrolysed product **3.50** in very high purity (**Scheme 3.25**)



Scheme 3.25: Synthesis of **3.50** from **3.29** or **3.31** using HPF_6

To determine if the hydroxy proton was involved in the hydrolysis, the reactions of the methoxy complex **2.23** with AgPF_6 , AgBF_4 and AgOTf in acetonitrile were performed

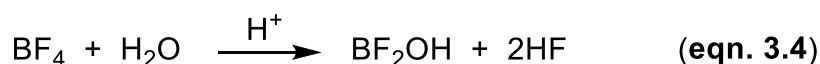
(see **Scheme 2.15**). The results showed non-hydrolysable counterions in solution over the time, demonstrating the significant role of the OH group in the hydrolysis process.

It should be noted that the presence of water is also necessary to initiate the hydrolysis. The authors found that complete elimination of water from AgPF₆ was not possible even after using P₂O₅ under reduced pressure for 5 days. Interestingly, they confirmed that water molecules can be also produced *in situ* by the reaction of HF (generated during the reaction) with glass (**eqn. 3.3**), as the presence of SiF₄ species was detected by ¹⁹F NMR spectroscopy and mass spectrometry.³⁷



More interestingly, Fernandez-Galan *et al.*³⁷ carried out their reactions in non-coordinating solvents (CH₂Cl₂, CHCl₃ or benzene). When acetone, acetonitrile and tetrahydrofuran were used as solvents, no hydrolysis was observed (even on addition of water) and the counterion remained unchanged over several days. The authors also showed that further hydrolysis of PO₂F₂ to phosphates did not occur as well during the reactions. This could be attributed to the coordination of the PO₂F₂ ligand to the Pd^{II} centre.³⁷

Partial hydrolysis of BF₄⁻ to BF₂OH was also observed by Pregosin *et al.* in the reactions between Ru^{II} acetate complexes and HBF₄.³⁹⁻⁴¹ The presence of the BF₂OH moiety was confirmed by ¹⁹F NMR spectroscopy, elemental analysis and single crystal X-ray crystallography. Although the authors did not provide any mechanistic information about how this hydrolysis may occur, they concluded that the hydrolysis cannot occur in the absence of water. This implies that the activation of a water molecule is a key mechanistic step, as seen in the case of PF₆ hydrolysis. Therefore, the mechanism, in general, might proceed by reacting BF₄⁻ with water with the help of the hydroxy proton (**eqn. 3.4**).



Unfortunately, none of these groups mentioned above provided insight into the actual hydrolysis process of PF₆ or BF₄. In our system, however, it may be concluded that the partial hydrolysis of the counterions (PF₆ and BF₄) has a direct dependence on the

presence of the OH proton. The catalytic effect of the hydroxy group, in particular that at 2-position of the pyridyl ring, could be confirmed by either comparison to those analogous methoxy complexes described for **Chapter 2** or by the loss of the OH proton and subsequent B-O bond formation in the BF₄ products.

Due to the two substituents, CF₃ and Me, at *para*-position of the phenyl ring, have almost similar steric hindrance, electronic effects in acceleration of PF₆ and BF₄ hydrolysis can be easily distinguished and compared with the unsubstituted ligand (**3.1**). It is clear that the ligand with the electron-withdrawing character of the CF₃ substituent had the most effect on accelerating the hydrolysis processes. This observation was expected and as the CF₃ group has a strong effect on the electronic structure of metal complexes and thus causing changes to their structural stabilisation and coordination ability. In consideration of the involvement of the appended OH proton in the hydrolysis process, the CF₃ group promotes the proton interactions with the counterion in order to undergo a transformation reaction. The superiority of the electron-withdrawing substituent here is consistent with those CF₃-containing catalysts used in a variety of catalytic systems.⁴⁸⁻⁵⁰ However, the Me group showed an unexpected influence when compared with the unsubstituted ligand, as the partial hydrolysis with the Me group was found to proceed faster. This suggested that the hydrolysis process may be affected by a combination of more than one electronic factor. Therefore, no obvious conclusions could be drawn about the effect of different substituents on the phenyl ring of the cyclopalladated ligands.

3.4 Conclusions and Future Work

The objective of this chapter was to synthesise and characterise a series of novel palladium(II) complexes containing bidentate pyridinol/pyridonate ligands (N[^]C-OH/N[^]C-O) and to determine whether they have similar structural and steric relationships to previously prepared analogous complexes (in **Chapter 2**) incorporating bidentate pyridine ligands (N[^]C-OMe). Therefore, in comparison to those results observed in the **Chapter 2**, an important conclusion of this work is that the role of the *ortho*-hydroxy group in the stability and reactivity was demonstrated, as remarkable differences have been shown between the two types (OMe- and OH-bidentate ligands). Examples include the relative stability of the acetate-bridged dimers in solution, the reactivity of these dimers with two equivalents of their associated free ligands, percentage conversion of the cleavage reaction of the dimers with 3,5-lutidine and PPh₃ and their ability to undergo

hydrolysis, subsequent ligand exchange reactions of terminal-acetate complexes with aqueous solution of NaCl and finally halide abstraction reactions with different silver salts.

In more detail, cyclopalladation of the 6-aryl-2-pyridones (aryl = Ph **3.1**, 4-MePh **3.2**, 4-CF₃Ph **3.3**, 4-FPh **3.4**, 2-MePh **3.5**) with Pd(OAc)₂ proceeded smoothly, forming the acetate-bridged complexes with the general formula [Pd(κ²-N[^]C)(μ-OAc)]₂ (**3.6-3.10**). However, on standing in solution at room temperature, **3.6**, **3.7**, **3.8** and **3.9** underwent slow pyridinol-pyridonate conversion to the tetrameric species [Pd(μ:κ²-N[^]C)]₄ (**3.11**, **3.12**, **3.13** and **3.14**, respectively) with loss of acetic acid; the related transformation with CF₃-containing **3.8** to give **3.13** required more forcing conditions. Substitution of the acetate groups in **3.6**, **3.7**, **3.8** and **3.9** for the corresponding aryl-pyridonate occurred readily, affording dimeric Pd(μ-N[^]C)(κ²-N[^]C)]₂ (**3.15**, **3.16**, **3.17** and **3.18**, respectively), in which monoanionic N[^]C tended to adopt either an N[^]O-bridging mode or acted as an N[^]C-chelate. By contrast, cleavage of the acetate bridge in **3.6**, **3.7**, **3.8** and **3.9** with 3,5-lutidine formed initially monometallic [Pd(κ²-N[^]C)(κ¹-OAc)(3,5-lutidine)] (**3.19**, **3.20**, **3.21** and **3.22**, respectively) and then, on crystallisation from bench solvents, hydrolysis of the acetate occurred to give the unusual aqua-bridged complexes [Pd(κ²-N[^]C)(3,5-lutidine)]₂(μ-OH₂) (**3.23**, **3.24**, **3.25** and **3.26**, respectively). A similar approach could be used to make the PPh₃ species [Pd(κ²-N[^]C)(κ¹-OAc)(PPh₃)] (**3.27**, **3.28**, **3.29** and **3.30**); notably, only the CF₃-containing **3.29** proved amenable to hydrolysis, forming the terminal aqua complex [Pd(κ²-N[^]C)(κ¹-OH₂)(PPh₃)] (**3.31**).

Subsequent ligand exchange reactions of **3.19**, **3.20** and **3.21** with NaCl gave a mixture of monomeric [Pd(κ²-N[^]C)(3,5-lutidine)Cl] (**3.32a**, **3.33a** and **3.34a**) and the unusual dimeric [Pd(μ:κ²-N[^]C)(3,5-lutidine)][Pd(κ²-N[^]C)](μ-Cl) (**3.32b**, **3.33b** and **3.34b**) complexes, respectively. Under similar conditions, PPh₃-containing complexes [Pd(κ²-N[^]C)(PPh₃)Cl] (**3.35**, **3.36** and **3.37**) were obtained in excellent yields.

Chloride abstraction reactions with AgPF₆, AgBF₄ and AgOTf were carried out in acetonitrile in order to form cation-anion pairs. The reaction of **3.32a** with AgOTf proceeded rapidly and afforded stable [Pd(κ²-N[^]C)(3,5-lutidine)(MeCN)][OTf] (**3.39**) in a quantitative yield, while the reactions with AgPF₆ and AgBF₄ gave complex mixtures of products from which only monomeric [Pd(κ²-N[^]C)(3,5-lutidine)(PO₂F₂)] (**3.38**) could be obtained as a result of partial hydrolysis after standing in solution for 5 days. The

reactions of **3.35**, **3.36** and **3.37** with one equivalent of AgPF₆, AgBF₄ and AgOTf in acetonitrile under nitrogen were also examined. These reactions gave the corresponding MeCN-containing complexes with the general formula [Pd(κ^2 -N[^]C)(PPh₃)(MeCN)][X], where X = PF₆ (**3.40** H, **3.44** Me, **3.49** CF₃), BF₄ (**3.42** H, **3.46** Me, **3.51** CF₃), OTf (**3.43** H, **3.48** Me, **3.35** CF₃). All OTf species showed their ability to remain intact in solution over time. However, all other complexes with PF₆ and BF₄ (except **3.42**) underwent partial hydrolysis and gave [Pd(κ^2 -N[^]C)(PPh₃)(PO₂F₂)] (**3.41** H, **3.45** Me, **3.50** CF₃) and [Pd(κ^2 -N[^]C)(PPh₃)(BF₂OH)] (**3.47** Me, **3.52** CF₃), respectively with different conversion time rates. The order of the hydrolysis time required was found as follows: CF₃/PF₆ (**3.50**) > CF₃/BF₄ (**3.52**) > Me/PF₆ (**3.45**) > Me/BF₄ (**3.47**) = H/PF₆ (**3.41**). In general, hydrolysis of PF₆ and BF₄ complexes with 3,5-lutidine were slower than those containing PPh₃.

Considering the above conclusions of this chapter, it would be interesting to design and synthesise corresponding bidentate ligands containing the hydroxyl substituent at the 4-position (*para*) instead of 2-position (*ortho*) (**Fig. 3.34**). This will provide further insight into the role of *ortho*-hydroxy group in the stability and reactivity.

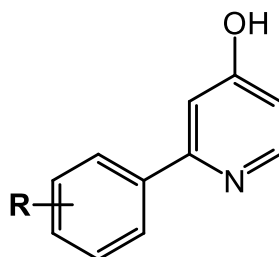


Figure 3.34: Potential ligands for applications in the coordination chemistry of transition metals

References

1. Z. Li, Z. Liu, D. W. Cho, J. Zou, M. Gong, R. M. Breece, A. Galkin, L. Li, H. Zhao and G. D. Maestas, *J. Inorg. Biochem.*, 2011, **105**, 509.
2. M. Ando, N. Sato, T. Nagase, K. Nagai, S. Ishikawa, H. Takahashi, N. Ohtake, J. Ito, M. Hirayama and Y. Mitobe, *Bioorg. Med. Chem.*, 2009, **17**, 6106.
3. A. H. Abadi, T. M. Ibrahim, K. M. Abouzid, J. Lehmann, H. N. Tinsley, B. D. Gary and G. A. Piazza, *Bioorg. Med. Chem.*, 2009, **17**, 5974.
4. H. J. Jessen, A. Schumacher, T. Shaw, A. Pfaltz and K. Gademann, *Angew. Chem. Int. Ed.*, 2011, **50**, 4222.
5. A. S. Alimmari, A. D. Marinković, D. Ž Mijin, N. V. Valentić, N. Todorović and G. S. Ušćumlić, *J. Serb. Chem. Soc.*, 2010, **75**, 1019.
6. M. Sellstedt, A. Nyberg, E. Rosenbaum, P. Engström, M. Wickström, J. Gullbo, S. Bergström, L. B. Johansson and F. Almqvist, *Eur. J. Org. Chem.*, 2010, **2010**, 6171.
7. J. M. Rawson and R. E. Winpenny, *Coord. Chem. Rev.*, 1995, **139**, 313.
8. B. Zhao, Z. Han and K. Ding, *Angew. Chem. Int. Ed.*, 2013, **52**, 4744.
9. Y. Himeda, *Eur. J. Inorg. Chem.*, 2007, **2007**, 3927.
10. T. Tomon, T. Koizumi and K. Tanaka, *Eur. J. Inorg. Chem.*, 2005, **2005**, 285.
11. F. Yu, C. Shen, T. Zheng, W. Chu, J. Xiang, Y. Luo, C. Ko, Z. Guo and T. Lau, *Eur. J. Inorg. Chem.*, 2016, **2016**, 3641.
12. R. Kawahara, K. Fujita and R. Yamaguchi, *J. Am. Chem. Soc.*, 2012, **134**, 3643.
13. X. Zhang, M. Tong and X. Chen, *Angew. Chem.*, 2002, **114**, 1071.
14. X. Zhang, M. Tong, M. Gong, H. Lee, L. Luo, K. Li, Y. Tong and X. Chen, *Chem. A Eur. J.*, 2002, **8**, 3187.
15. S. Zheng, J. Zhang, W. Wong and X. Chen, *J. Am. Chem. Soc.*, 2003, **125**, 6882.
16. Y. Han and G. Jin, *Chem. Soc. Rev.*, 2014, **43**, 2799.
17. K. Fujita, T. Yoshida, Y. Imori and R. Yamaguchi, *Org. Lett.*, 2011, **13**, 2278.
18. L. Munjanja, H. Yuan, W. W. Brennessel and W. D. Jones, *J. Organomet. Chem.*, 2017, **847**, 28.
19. K. Fujita, N. Tanino and R. Yamaguchi, *Org. Lett.*, 2007, **9**, 109.

20. S. Chakraborty, P. E. Piszal, W. W. Brennessel and W. D. Jones, *Organometallics*, 2015, **34**, 5203.
21. A. Singh, *Synthesis and Reactivity of Novel ONN- and ONO-Palladium(II) Pincer Complexes; Applications in CH-Halogenation of Aryl-Pyridones*, The University of Leicester, 2017.
22. K. Nakamoto, *Infrared and Raman spectra of inorganic and coordination compounds*, Wiley Interscience, New York, 1986.
23. D. J. Cárdenas, A. M. Echavarren and M. C. Ramírez de Arellano, *Organometallics*, 1999, **18**, 3337.
24. Y. B. Dudkina, D. Y. Mikhaylov, T. V. Gryaznova, A. I. Tufatullin, O. N. Kataeva, D. A. Vicic and Y. H. Budnikova, *Organometallics*, 2013, **32**, 4785.
25. R. F. Carina, A. F. Williams and G. Bernardinelli, *J. Organomet. Chem.*, 1997, **548**, 45.
26. R. Modak, Y. Sikdar, S. Mandal, S. Chatterjee, A. Bieńko, J. Mroziński and S. Goswami, *Inorg. Chim. Acta*, 2014, **416**, 122.
27. B. Lassalle-Kaiser, T. T. Boron III, V. Krewald, J. Kern, M. A. Beckwith, M. U. Delgado-Jaime, H. Schroeder, R. Alonso-Mori, D. Nordlund and T. Weng, *Inorg. Chem.*, 2013, **52**, 12915.
28. A. Karmakar, R. J. Sarma and J. B. Baruah, *Eur. J. Inorg. Chem.*, 2007, **2007**, 643.
29. C. Maxim, L. Sorace, P. Khuntia, A. M. Madalan, V. Kravtsov, A. Lascialfari, A. Caneschi, Y. Journaux and M. Andruh, *Dalton Trans.*, 2010, **39**, 4838.
30. L. Piche, J. Daigle, R. Poli and J. P. Claverie, *Eur. J. Inorg. Chem.*, 2010, **2010**, 4595.
31. D. Niedzielska, T. Pawlak, A. Wojtczak, L. Pazderski and E. Szlyk, *Polyhedron*, 2015, **92**, 41.
32. N. D. Ball, J. W. Kampf and M. S. Sanford, *Dalton Trans.*, 2010, **39**, 632.
33. M. D. Santana, R. García-Bueno, G. García, G. Sánchez, J. García, A. R. Kapdi, M. Naik, S. Pednekar, J. Pérez and L. García, *Dalton Trans.*, 2012, **41**, 3832.
34. Y. B. Dudkina, D. Y. Mikhaylov, T. V. Gryaznova, A. I. Tufatullin, O. N. Kataeva, D. A. Vicic and Y. H. Budnikova, *Organometallics*, 2013, **32**, 4785.
35. J. W. Suggs and K. S. Lee, *J. Organomet. Chem.*, 1986, **299**, 297.
36. S. B. Atla, A. A. Kelkar, V. G. Puranik, W. Bensch and R. V. Chaudhari, *J. Organomet. Chem.*, 2009, **694**, 683.

37. R. Fernandez-Galan, B. R. Manzano, A. Otero, M. Lanfranchi and M. A. Pellinghelli, *Inorg. Chem.*, 1994, **33**, 2309.
38. G. Deacon and J. Green, *Spectrochim. Acta, Pt. A: Mol. Spectrosc.*, 1968, **24**, 845.
39. C. J. den Reijer, H. Rüegger and P. S. Pregosin, *Organometallics*, 1998, **17**, 5213.
40. C. J. den Reijer, M. Würle and P. S. Pregosin, *Organometallics*, 2000, **19**, 309.
41. T. J. Geldbach, P. S. Pregosin, S. Rizzato and A. Albinati, *Inorg. Chim. Acta*, 2006, **359**, 962.
42. S. J. Thompson, P. M. Bailey, C. White and P. M. Maitlis, *Angew. Chem. Int. Ed.*, 1976, **15**, 490.
43. F. Wimmer and M. R. Snow, *Aust. J. Chem.*, 1978, **31**, 267.
44. E. Horn and M. R. Snow, *Aust. J. Chem.*, 1980, **33**, 2369.
45. G. Smith, D. J. Cole-Hamilton, A. C. Gregory and N. G. Gooden, *Polyhedron*, 1982, **1**, 97.
46. S. Kannan, A. J. James and P. R. Sharp, *Inorg. Chim. Acta*, 2003, **345**, 8.
47. M. Bröring, C. D. Brandt and S. Link, *Inorg. Chim. Acta*, 2005, **358**, 3122.
48. S. Paavola, K. Zetterberg, T. Privalov, I. Csöregy and C. Moberg, *Adv. Synth. Catal.*, 2004, **346**, 237.
49. J. M. Racowski, A. R. Dick and M. S. Sanford, *J. Am. Chem. Soc.*, 2009, **131**, 10974.
50. L. Maidich, G. Dettori, S. Stoccoro, M. A. Cinellu, J. P. Rourke and A. Zucca, *Organometallics*, 2015, **34**, 817.

Chapter 4

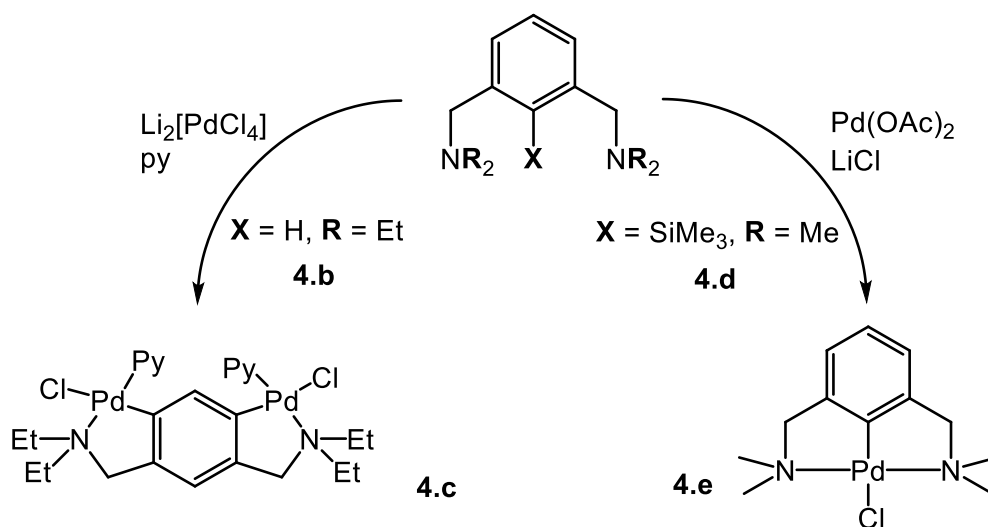
*Symmetrical, Monoanionic N[^]C[^]N Pincer
Ligands for Palladium, Platinum and Gold*

4.1 Introduction

Extensive studies have been conducted in the synthesis of organometallic complexes supported by monoanionic pincer ligands, especially those based on palladium and platinum metals.¹ There are two types of coordinating structures with carbon-based pincer ligands; these include E[∧]C[∧]E and C[∧]E[∧]E where E is a coordinating donor atom such as P or N (see **Section 1.3.3**). The Hope and Solan research group has recently investigated the reactivity of the pyridine-based N[∧]N[∧]C-type pincer ligands towards both Pd^{II} and Pt^{II} salts forming complexes through *sp*² and *sp*³ C-H activations.^{2,3} In this short introduction, however, only the N[∧]C[∧]N derivatives will be discussed. It is not possible to provide a complete overview of this type here. Instead, the reactivity of both amine- and pyridine-based pincer ligands centred with a phenyl ring will be briefly summarised.

4.1.1 Amine-based Pincer Ligands

Cyclopalladation with 1,3-bis[(dimethylamino)alkyl]benzene (alkyl = methyl **4.a** and ethyl **4.b**) has been achieved. Trofimenko⁴ examined the metallation of **4.b** with palladium(II) in the presence of pyridine and found that the system unexpectedly underwent an *ortho*-dipalladation reaction, forming the dipalladated complex (**4.c**) with C₄-H and C₆-H activation (**Scheme 4.1**). This organometallic compound was considered the first example of a cyclometallated complex containing more than one metal coordination site at the same phenyl ring. Later, van Koten *et al.*⁵ used the analogous ligand (**4.d**) which was already activated by SiMe₃ at the C₂ position with Pd(OAc)₂ in the presence of LiCl. The transmetalation reaction gave a monometallic, bicyclic complex (**4.e**) which was isolated in an excellent yield of 95%.



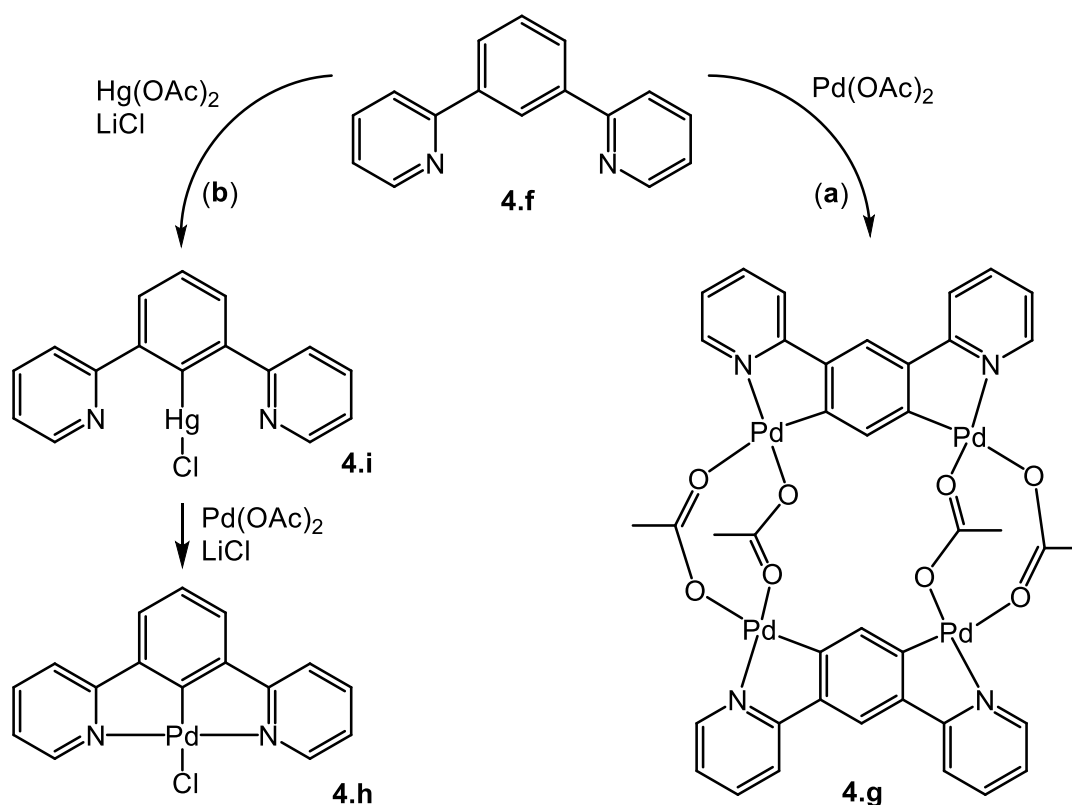
Scheme 4.1: Reactions of 1,3-bis[(dimethylamino)alkyl]benzene with Pd^{II} salts

Lithium⁶⁻¹⁰ and mercury¹¹ have been also used to activate the C₂ position of **4.a** in order to access different transition metal pincer complexes through transmetallation reactions. In the case of lithium, the organolithium complexes are usually prepared as a precursor by reacting *n*-butyl lithium with the ligand in hexane at very low temperature, followed by a transmetallation process in which transition metals, such as titanium, vanadium, niobium,⁶ rhenium,⁷ rhodium,⁸ palladium, platinum,⁹ iron and gold,¹⁰ react with an organolithium compound [N[^]C[^]N-Li] to replace the lithium. The same transmetallation could be achieved using highly toxic mercury salts such as Hg(OAc)₂.¹¹ With mercurated **4.a**, only gold salts have been used to obtain the cyclometallated Au^{III} complex, [Au(**4.a**)Cl]₂[Hg₂Cl₆].¹¹ This method is useful for studies on the reactivities of N[^]C[^]N ligands that cannot undergo a direct cyclometallation reaction.

4.1.2 Pyridine- and Pyridone-based Pincer Ligands

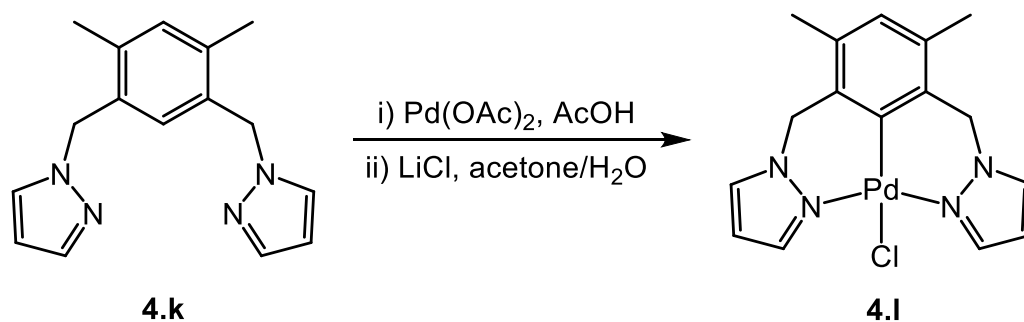
Pyridine-based pincer ligands containing a central aromatic ring with two pyridine arms have also been reported in the literature but not to the same extent as their analogous diamino species.¹² Unlike palladium(II), which has only recently been obtained by direct synthesis, a number of transition metals such as ruthenium, osmium and platinum have been used with 1,3-di(2-pyridyl)benzene (**4.f**) to synthesise N[^]C[^]N pincer-aryl complexes through direct C_{aryl}-H activation.^{1,13} In coordination chemistry, the unexpected behaviour of these types of ligands could be observed; therefore, the choice of an appropriate synthetic method has been the main challenge in this field.¹²

In 1999, the cyclometallation of 1,3-di(2-pyridyl)benzene (**4.f**) using Pd(OAc)₂ was investigated by Cárdenas *et al.*¹ The authors found that the reaction unexpectedly underwent a double palladation to form tetrameric **4.g** instead of the formation of an N[^]C[^]N-tridentate Pd^{II} complex (**a** in **Scheme 4.2**). The structure of the tetrameric complex (**4.g**) was confirmed and characterised, *inter alia*, by single crystal X-ray diffraction studies. Their attempts to cyclometallate **4.f** with other palladium(II) salts such as [Pd(MeCN)₄][BF₄]₂ and Li₂[PdCl₄], were unsuccessful. However, in 2005 Soro *et al.*¹² were able to report the synthesis of the desired monopalladated pincer N[^]C[^]N complex (**4.h**) as supported by **4.f** using transmetallation from the related organomercury compound (**4.i**) (**b** in **Scheme 4.2**). Only one year later, the same group successfully reported the synthesis of the palladium pincer complex of **4.f** by direct C_{aryl}-H activation using Na₂[PdCl₄] as a source of Pd^{II}. Notably, a high temperature (118 °C) was required for this reaction to proceed and give the desired complex (**4.g**) in a reasonable yield.



Scheme 4.2: Reactions of 1,3-di(2-pyridyl)benzene (**4.f**) with $\text{Pd}(\text{OAc})_2$

1,3-Bis(pyrazolylmethyl)benzene (**4.j**), which is structurally similar to **4.f** and features a combination of a central benzene ring and two pyrazole groups, was found to have a similar reactivity towards $\text{Pd}(\text{OAc})_2$ where a doubly cyclopalladated product was formed instead of an $\text{N}^{\wedge}\text{C}^{\wedge}\text{N}$ pincer complex.¹⁴ This observation encouraged Hartshorn and Steel¹⁵ to design a ligand in which the active *meta*-coordination sites on the benzene ring are blocked by a relatively inactive substituent, such as a methyl group, in the hope that this would lead to the formation of a cyclopalladated pincer complex. Therefore, the authors prepared 1,3-bis(pyrazolylmethyl)*m*-xylene (**4.k**), which was then reacted with one equivalent of $\text{Pd}(\text{OAc})_2$ in acetic acid followed by addition of LiCl in a mixture of acetone and water. As expected, the reaction gave the desired product (**4.l**) in which the ligand (**4.k**) coordinated to the Pd^{II} centre in a pincer mode through its three donor atoms (N, C and N) (**Scheme 4.3**). In this case, the presence of the methyl groups prevented the alternative $\text{C}_2\text{-H}$ activation pathway with $\text{Pd}(\text{OAc})_2$ from occurring, and led instead to a selective C-H activation at the C_2 position with two stable six-membered rings. This was the first direct synthesis of a cyclopalladated pincer complex reported in the literature that was derived directly from $\text{Pd}(\text{OAc})_2$.



Scheme 4.3: Direct synthesis of the Pd^{II} pincer complex (**4.1**) using Pd(OAc)₂

Functionalised ligands have been the subject of study over recent years due to their ability to influence the properties and take part in the catalytic reactivity of pincer complexes.¹⁶ The hydroxy group is one of the most widely studied functional groups that can be introduced into a ligand framework. As mentioned earlier in **Section 1.4.2**, ligands containing an amide group usually show keto-enol tautomerism which plays a significant role in metal-ligand reactivity. One of these is 2-pyridone and its derivatives which are the common ligands in the field of coordination chemistry. As tridentate ligands, applications to induce reactivity at a metal centre using an appended OH functional group have not, to the best of my knowledge, been extensively investigated. Only a few pincer complexes with a pendant OH group have been reported in the literature (**Fig. 4.1**).¹⁷⁻²²

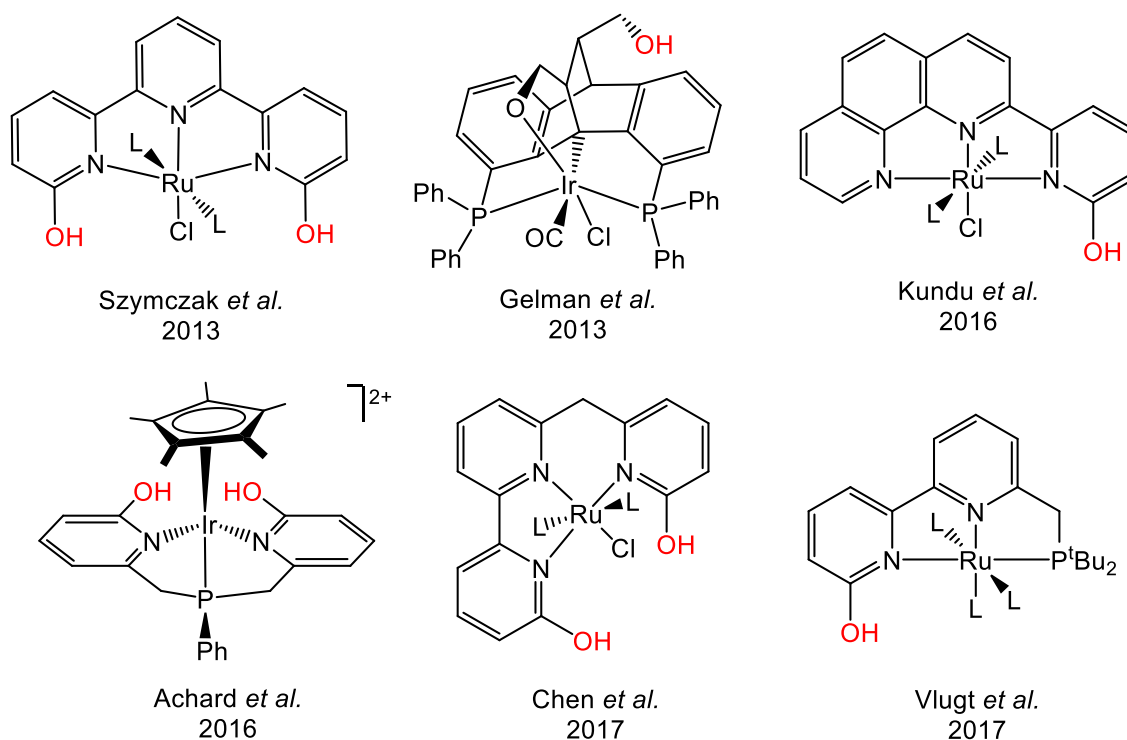
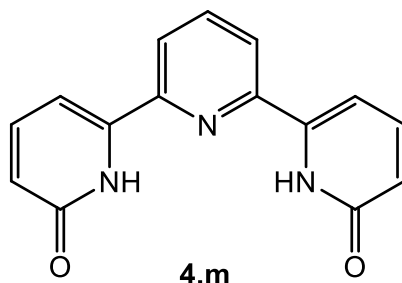
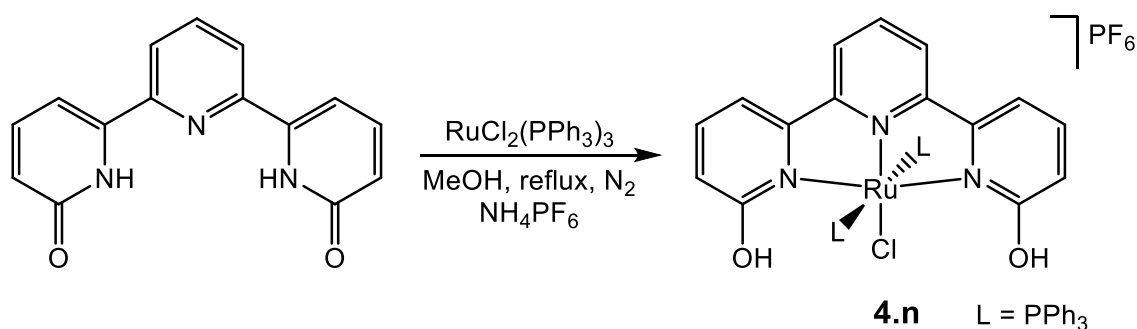


Figure 4.1: Selected examples of tridentate metal complexes bearing a pendant OH

Surprisingly, a comparative example of a 2-pyridone-based N[^]C[^]N pincer complex could not be found in the literature. Due to this, 6,6'-dihydroxy terpyridine (**4.m**), which is the most closely related to our system (see **Scheme 4.6**), will be discussed here instead.



Donohoe *et al.* first reported the synthesis of **4.m** in 2008 by a multistep route which involved ring-closing metathesis.²³ In 2013, the ligand (**4.m**) was also re-prepared by Szymczak and Moore¹⁷ but in a two-step reaction that started from commercially available 6,6'-dibromoterpyridine. The authors showed that the reaction of **4.m** with RuCl₂(PPh₃)₃ in methanol under reflux conditions and under an atmosphere of dry nitrogen gave *trans*-[RuCl(**4.m**)(PPh₃)₂][PF₆] (**4.n**) after adding a large excess of [NH₄][PF₆] at the end of the reaction (**Scheme 4.4**).



Scheme 4.4: Synthesis of *trans*-[RuCl(**4.m**)(PPh₃)₂][PF₆] (**4.n**)

The X-ray structure of **4.n** revealed a slightly distorted octahedral complex in which a ruthenium(II) chloride core is supported by an N[^]N[^]N pincer ligand with a mutually *trans* arrangement between the two PPh₃ ligands. The coordinated pincer ligand was found to exist in the pyridinol form with two pendent hydroxy groups whose protons were involved with intramolecular hydrogen-bonding interactions with the Ru-bound chloride (**Fig. 4.2**). However, it would also be possible for this complex to display keto-enol tautomerism due to the presence of the 2-pyridone unit.

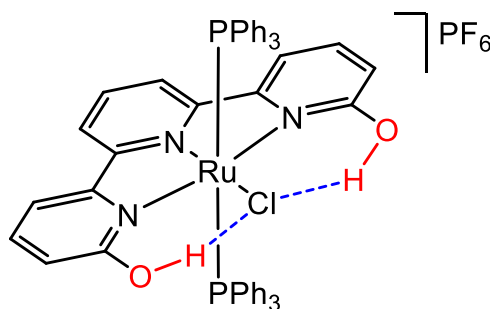


Figure 4.2: Intramolecular hydrogen-bonding interactions in **4.n**

Due to these geometric features, complex **4.n** was used as an efficient metal-ligand cooperative catalyst for the transfer hydrogenation of a variety of ketones.¹⁷ In comparison to the analogous Ru^{II} complexes containing 4,4'-dihydroxyterpyridine (**4.o**) or terpyridine (**4.p**) as pincer ligands, complex **4.n** showed a significantly higher activity and carbonyl hydrogenation selectivity (**Fig. 4.3**).²⁴ Therefore, the authors concluded that the hydroxy position was important to the catalytic activity of the complex. In the case of bulky ketones, however, complex **4.n** showed a remarkably lower activity (no product with benzophenone).²⁴

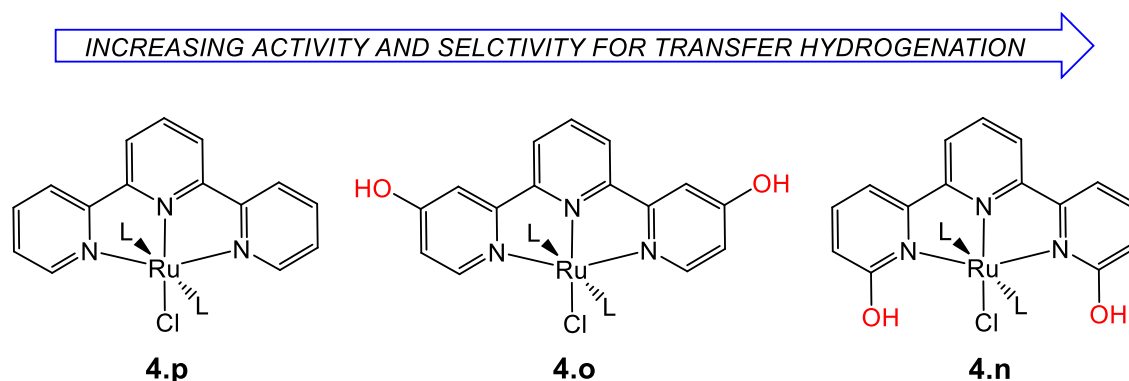
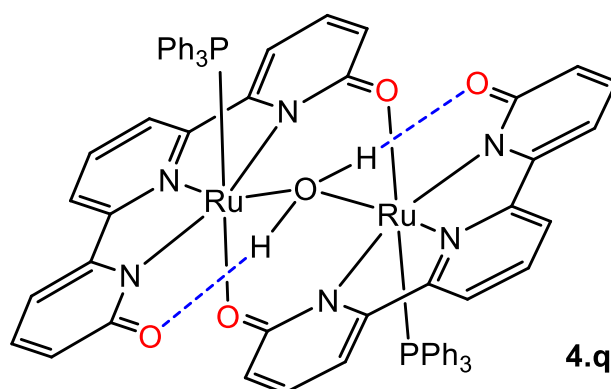


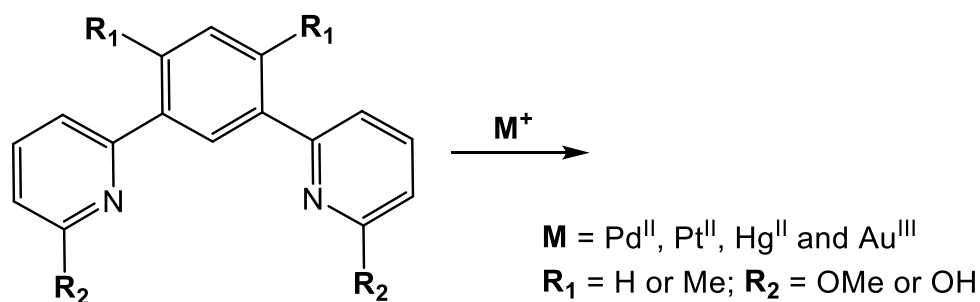
Figure 4.3: The relative reactivity of the N[^]N[^]N pincer complexes²⁴

Notably, the efficiency of **4.n** was completely lost during the catalytic transfer hydrogenation reactions. This was attributed to the deactivation of the catalyst and thus formation of the unusual aqua-bridged diruthenium complex [Ru(κ^3 -(6,6'-(pyridine-2,6-diyl)dipyridonate))(PPh₃)₂(μ -OH₂) (**4.q**). The dimer was obtained as a dark yellow precipitate at the end of the catalytic reaction. Fortunately, the authors were able to isolate the product and grow single crystals suitable for analysis by X-ray diffraction studies. The solid-state structure of **4.q** showed a neutral dimeric unit bridged by one water molecule through the oxygen atom and stabilised by hydrogen-bonding interactions.²⁴



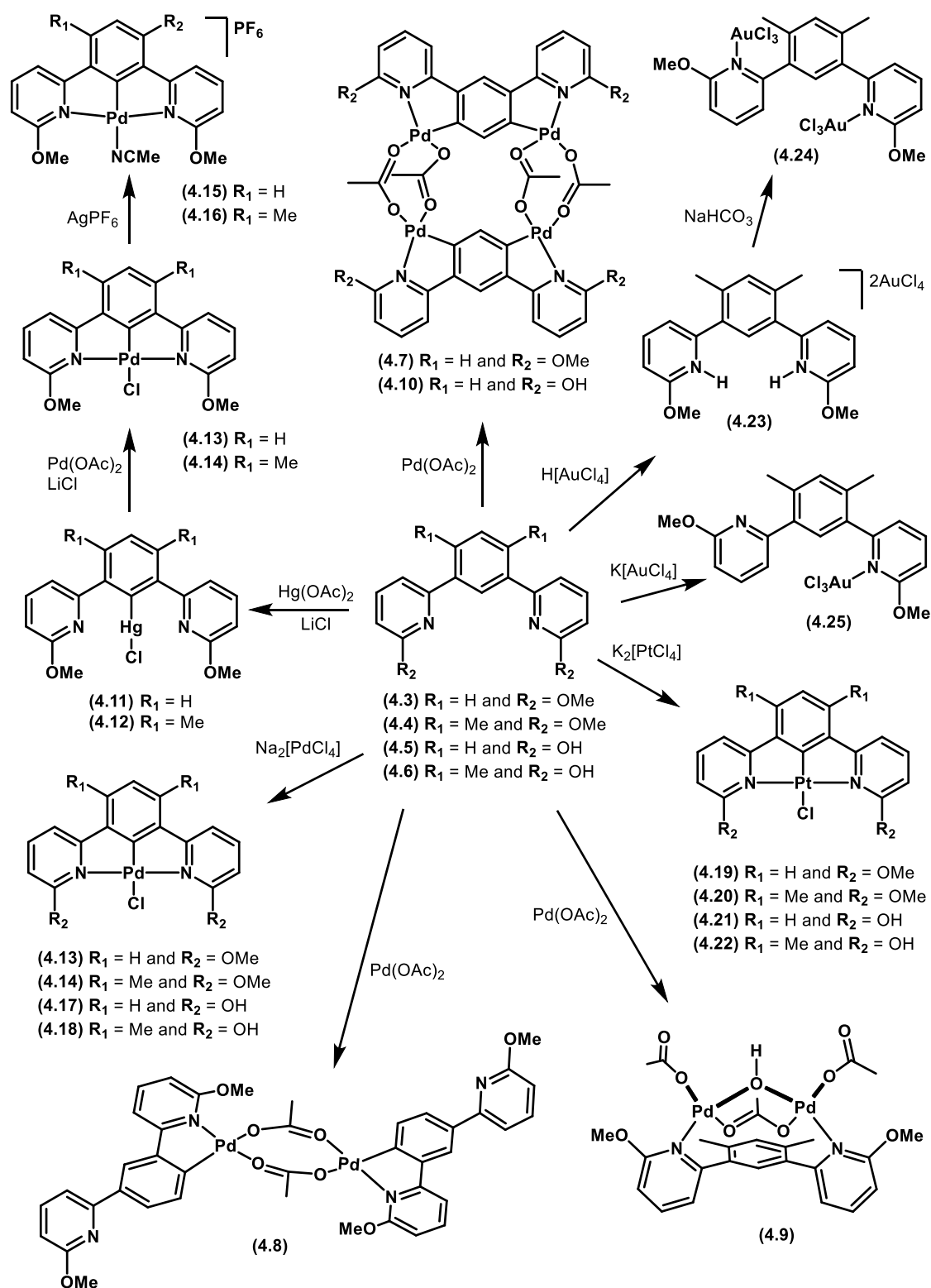
4.2 Aims and Objectives of Chapter 4

Since the numbers of pyridone-based pincer metal complexes are limited and there is a complete absence of those complexes containing pyridone-based N^CN pincer ligands, the aim of this chapter is to first synthesise two different pyridine-based N^CN pincer ligands (**4.3** and **4.4**) and investigate their reactivities towards a number of transition metals (such as Pd^{II}, Pt^{II}, Hg^{II} and Au^{III}) to allow a comparison between them and their corresponding pyridone-based N^CN pincer ligands (**4.5** and **4.6**) for applications in coordination chemistry (**Scheme 4.5**). The difference in reactivity and selectivity between the two different Pd sources, palladium acetate and palladium chloride, will be explored. Chloride-containing complexes will undergo a halide abstraction reaction with AgPF₆. Finally, attempts to cyclometallate **4.4** at a gold(III) centre “through C-H activation” will be shown and discussed.



Scheme 4.5: General synthesis of metal complexes using pincer ligands

All the resultant ligands and complexes shown in **Scheme 4.6** will be fully characterised using various techniques, including spectroscopic (¹H, ¹³C{¹H}, ³¹P and ¹⁹F NMR and IR) and spectrometric (ESMS, HRMS) techniques in addition to single crystal X-ray diffraction.

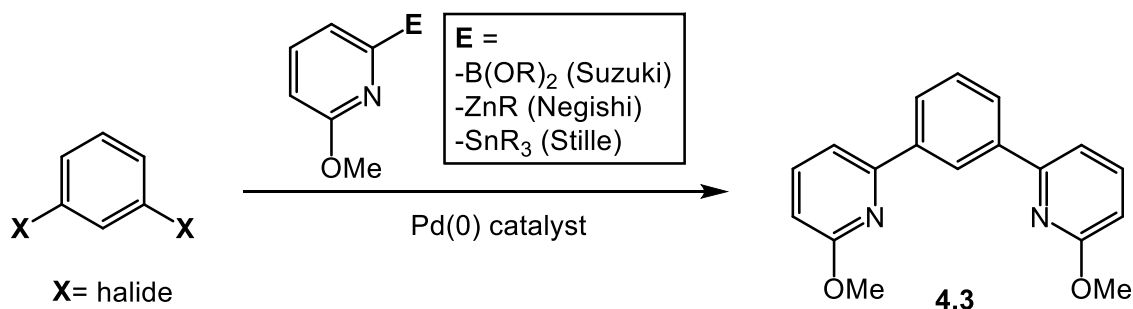


Scheme 4.6: Ligands and complexes described in Chapter 4

4.3 Results and Discussion

4.3.1 Synthesis of N[^]C[^]N Pyridine Ligands

There are three possible pathways to synthesise the target N[^]C[^]N ligand, namely through Suzuki, Negishi and Stille cross-coupling reactions (**Scheme 4.7**).²⁵



Scheme 4.7: Synthetic pathways to form N[^]C[^]N ligands. Adapted from ref. 25

The Suzuki cross-coupling reaction is an environmentally friendly procedure in comparison to the other reactions; therefore, it was considered the best choice to start with. Since boronation of 2-bromo-6-methoxypyridine (**2.1**) will give a reportedly unstable 2-(6-methoxypyridine)boronic acid,²⁵ an alternative way, in which 1,3-dibromobenzene undergoes the bromination reactions, was attempted. Three synthetic attempts were made to obtain 1,3-phenylenediboronic acid. These included: (i) the same synthetic approach used for Ar-B(OH)₂ synthesis (**2.2-2.4**), (ii) replacement of the reaction solvent (THF to Et₂O) and (iii) changing the reaction equivalent ratio between the 1,3-dibromobenzene and the *n*-BuLi solution. However, all these three attempts to obtain the desired product were unsuccessful and instead gave 3-(bromobenzene)boronic acid (**Fig. 4.4**) as the main product (formation of other products is possible). This was confirmed by the data obtained from ¹H NMR spectroscopy and mass spectrometry.

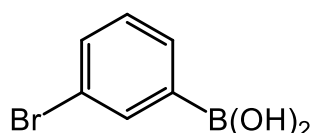
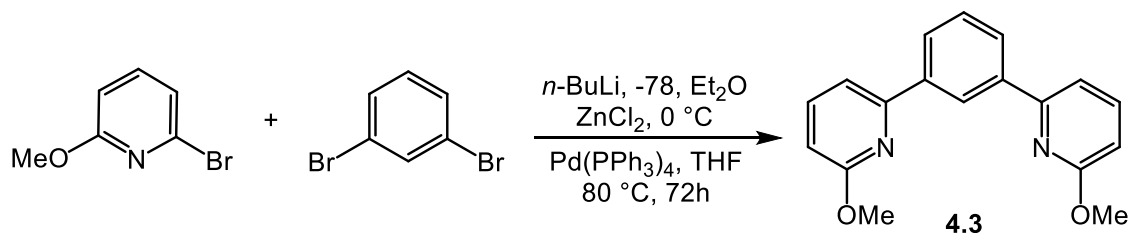


Figure 4.4: 3-(Bromobenzene)boronic acid

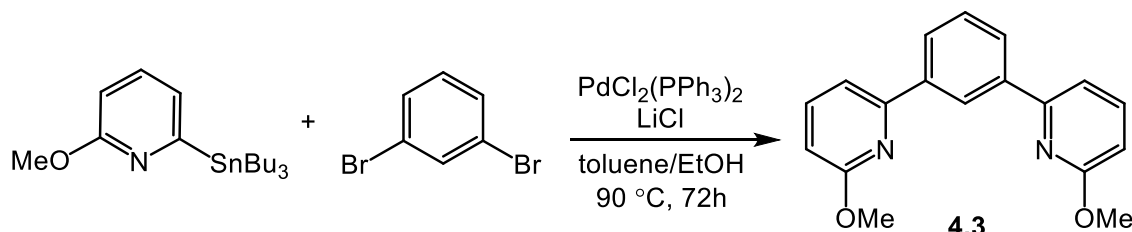
Alternatively, the py-ZnCl precursor was prepared for reaction with the 1,3-dibromobenzene under Negishi coupling conditions. After heating at reflux for three

days, the title ligand (**4.3**) was obtained in a very low yield (31%) as a white solid. The reaction conditions are described in **Scheme 4.8**.



Scheme 4.8: Synthesis of **4.3** using Negishi coupling conditions

Stille cross-coupling conditions could be also used to produce the target ligand (**4.3**) when 2-methoxy-6-(tributylstannyl)-pyridine (**4.1**) was used as a tin reagent. Although Stille's method involved highly toxic compounds, a good yield of 79% was obtained for the synthesis of **4.3**. In this reaction, 2-methoxy-6-(tributylstannyl)-pyridine (**4.1**), prepared according to the method of Honda *et al.*,²⁶ was reacted with 1,3-dibromobenzene in the presence of a palladium(II) catalyst and lithium chloride, and heated under reflux in a mixture of dry toluene and EtOH for 72 hours (**Scheme 4.9**). Silica gel chromatography was then employed to separate the pure product from the catalyst as well as the tin-starting material and the 2-methoxy-6-phenylpyridine by-product which was formed during the reaction.



Scheme 4.9: Synthesis of **4.3** using Stille cross-coupling conditions

This ligand (**4.3**) has recently been synthesised and then characterised using elemental analysis and ^1H and ^{13}C NMR spectroscopy.²⁷ The authors obtained the ligand as evidence to support their “new method” for making an organic N[^]C[^]N system. In their reaction, Pd(dppf)Cl₂ (where dppf = 1,1'-bis(diphenylphosphino)ferrocene) was used as a catalyst to couple 1,3-dibromobenzene with 2-chloro-6-methoxypyridine (1:2) in the presence of bis(pinacolato)diboron and a base. However, their method would be only useful if only a small amount of the ligand is required. The ^1H and $^{13}\text{C}\{^1\text{H}\}$ NMR data obtained for our ligand agreed with the data reported in their work.²⁷

It was possible to grow single crystals suitable for X-ray diffraction studies by slow evaporation of a solution of **4.3** in methanol. The solid-state data for the ligand revealed the proposed structure to have an almost perfectly planar geometry in one pyridyl ring with respect to the central phenyl ring ($C(9)$ - $C(10)$ - $C(12)$ - $C(13) = -0.2(4)^\circ$), as shown in **Figure 4.5**.

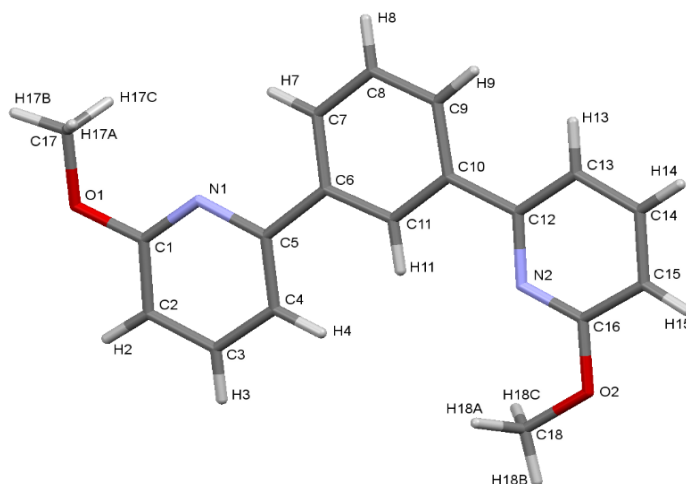
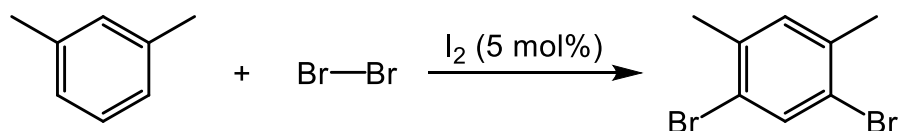


Figure 4.5: Molecular structure of **4.3** with full atom numbering

4,6-Bis(2-(6-methoxypyridonyl)-*m*-xylene (**4.4**) was also synthesised in order to investigate whether C-H activation would occur at the C_2 position with $\text{Pd}(\text{OAc})_2$ after blocking the other *ortho* C-H activation sites on the phenyl ring. The ligand **4.4** started with the preparation of 1,5-dibromo-2,4-dimethylbenzene (**4.2**) using a synthetic method established by Bonifacio *et al.*²⁸ The reaction of *m*-xylene with bromine was carried out in the absence of light using iodine as a catalyst (**Scheme 4.10**). After recrystallisation, white crystals were obtained in a slightly low yield (41%). ^1H and $^{13}\text{C}\{^1\text{H}\}$ NMR data were fully consistent with the proposed structure and with those previously reported.²⁸



Scheme 4.10: Synthesis of 1,5-dibromo-2,4-dimethylbenzene (**4.2**)

As mentioned earlier, the best reaction to try first, in order to obtain a pincer ligand, is Suzuki cross-coupling. In order to perform this reaction, *m*-xylene-diboronic acid needs to be synthesised and then reacted with two equivalents of 2-bromo-6-methoxypyridine (**2.1**). The same synthetic route as that used for the $\text{Ar-B}(\text{OH})_2$ synthesis was carried out

to produce *m*-xylene-diboronic acid; however, the reaction clearly resulted in a mixture containing 2,4-dimethylbenzeneboronic acid (**Fig. 4.6**) as the major product (>82%). The formation of this product was confirmed by ¹H NMR spectroscopy, as the spectrum illustrated a singlet and two doublets in the aromatic region.

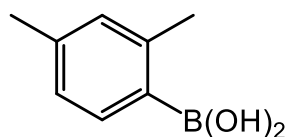
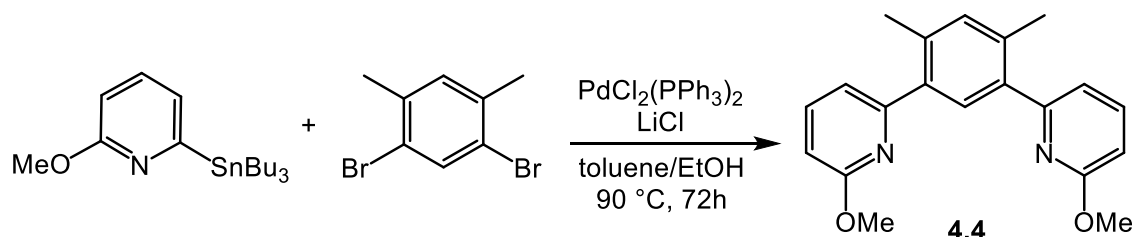


Figure 4.6: 2,4-dimethylbenzeneboronic acid

A palladium-catalysed cross-coupling reaction performed under Negishi conditions to synthesise the desired N[^]C[^]N ligand was also unsuccessful. The ¹H NMR spectrum of the crude product showed that the starting material (**4.2**) had not reacted at all. Therefore, the Stille cross-coupling reaction was the last possibility for synthesising the ligand *via* the undesirable toxic compound (**4.1**). 4,6-bis(2-(6-methoxypyridonyl)-*m*-xylene (**4.4**) could be obtained as a colourless solid (54%) using the same synthetic method employed for **4.3** (**Scheme 4.11**). The ¹H NMR spectrum of the crude reaction mixture showed that the mono pyridyl-substituted benzene was also formed during the reaction. This by-product, along with other impurities, was removed using silica gel chromatography.



Scheme 4.11: Synthesis of 4,6-bis(2-(6-methoxypyridonyl)*m*-xylene (**4.4**)

The ¹H NMR spectrum of the pure ligand (**4.4**) showed two singlets at 2.39 and 3.87 ppm corresponding to the methyl and methoxy protons, respectively. Two singlets also were observed in the aromatic region at 7.12 and 7.46 ppm representing the protons attached to the central ring. The ¹³C{¹H} NMR spectrum (CDCl₃) of **4.4** displayed eleven signals with the four quaternary aromatic carbon environments, indicating that the two pyridine rings are equivalent and exist in the same environments. ASAP mass spectrometry gave a very strong peak at 321 which is representative of the molecular ion [M+H]⁺. Further confirmation of the structure of the ligand (**4.4**) was given by X-ray

crystallography (**Fig. 4.7**). Single crystals of **4.4** suitable for X-ray analysis were grown by slow evaporation of a methanol solution containing the ligand.

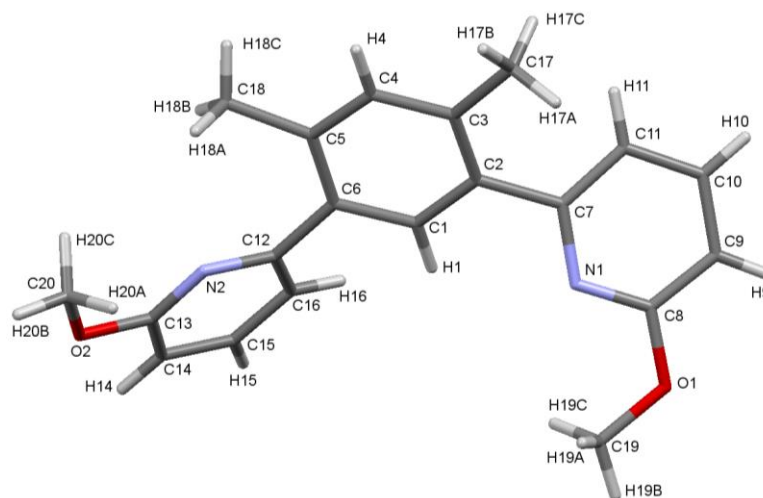
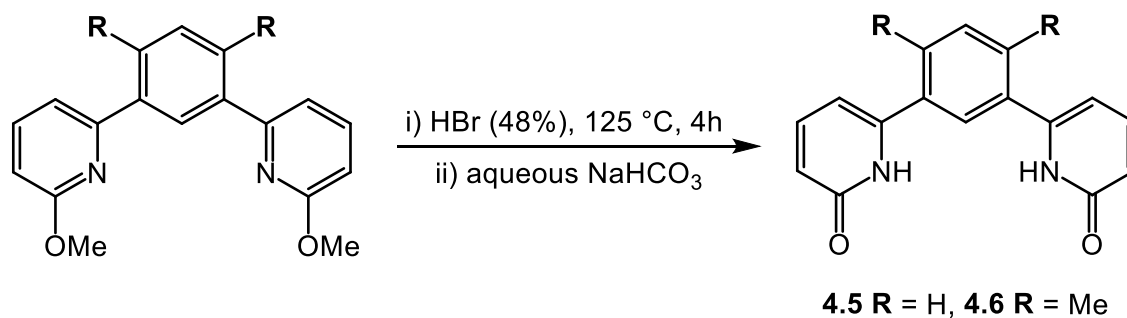


Figure 4.7: Molecular structure of **4.4** with full atom numbering

The solid-state data for **4.4** revealed the proposed structure with a central *m*-xylene directly coupled with two pyridine units at the 4 and 6 positions. It is clear that the two methyl groups of the central ring forced the two pyridyl rings into a non-planar orientation, quite unlike those in **4.3**. This was confirmed by torsion angles of the pyridines with respect to the *m*-xylene moiety, where C(3)-C(2)-C(7)-C(11) = -36.9(5)° and C(5)-C(6)-C(12)-N(2) = -39.9(4)°.

4.3.2 Synthesis of N[^]C[^]N Pyridone Ligands

The deprotection of the methoxy protecting groups in both ligands **4.3** and **4.4** resulted in the formation of 1,3-bis(2-pyridon-6-yl)benzene (**4.5**) and 4,6-bis(2-pyridon-6-yl)-*m*-xylene (**4.6**), respectively. **Scheme 4.12** shows the experimental conditions used for these syntheses.



Scheme 4.12: Synthesis of **4.5** and **4.6**

For **4.5**, the methoxy ligand (**4.3**) and an aqueous HBr solution (48%) were combined in a small flask and heated under reflux for four hours. On cooling to room temperature, a white precipitate was observed which was subsequently found to be insoluble in an organic phase; therefore, the resultant mixture was filtered, washed with water, collected and finally dried under reduced pressure to give a yield of 88%. **4.5** was also found to be stable up to 300 °C and was not soluble in the solvents that are commonly used to characterise products. However, the electrospray (ES) mass spectrum of **4.5** in MeOH illustrated a peak at m/z 265.0981 corresponding to the protonated molecular ion ($[M+H]^+$). In the solid-state IR spectrum of the product a C=O stretching peak at 1643 cm^{-1} was observed as additional evidence for the formation of this ligand. Attempts to obtain X-ray quality crystals were unsuccessful.

Under similar conditions as those used for the synthesis of **4.5**, a deprotection reaction of **4.4** afforded **4.6** as a white solid with a slightly low yield (40%). Unlike **4.5**, the ligand (**4.6**) was found to be highly soluble in organic solvents; therefore, a full characterisation using different spectroscopic techniques was successfully performed. In the ^1H NMR spectrum, the signal appearing as a 6H singlet, corresponding to the protons of the two methyl groups, was observed at 2.37 ppm. In comparison to the starting methoxypyridine ligand (**4.4**), the two singlets observed at 7.17 and 7.60 ppm in the aromatic region were found to be shifted downfield by 0.05 and 0.13 ppm, respectively. Furthermore, the methyl signals of the methoxy moiety disappeared and a downfield broad singlet peak at 12.20 ppm, representing the NH proton, appeared instead. This significant downfield shift of the NH proton could be attributed to the hydrogen-bonding interactions between the NH hydrogen and a hydrogen bond acceptor from other molecules. As expected, ten signals were seen in the $^{13}\text{C}\{^1\text{H}\}$ NMR spectrum, indicating that the ligand existed in a symmetrical arrangement. The IR spectrum of **4.6** displayed a very strong peak at 1637 cm^{-1} which corresponded to the $(\text{C}=\text{O})_{\text{ketone}}$ stretching vibration; this suggested that the dominant form of this ligand in its solid state should be the pyridinol tautomer. Further evidence for the formation of **4.6** was obtained due to the presence of a strong protonated molecular ion peak (at m/z 293.1301 $[M+H]^+$) upon analysis by ASAP mass spectrometry.

The structure of **4.6** has been further confirmed by X-ray diffraction studies on a suitable single crystal grown by slow evaporation of a solution of the ligand in methanol (**Fig. 4.8**). Selected bond lengths and angles are given in **Table 4.1**.

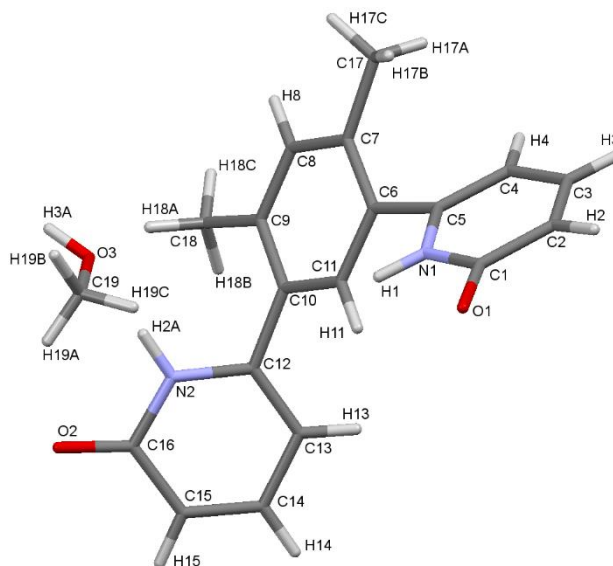


Figure 4.8: Full X-ray structure of **4.6** with a solvent MeOH molecule

Table 4.1: Selected bond lengths and angles of complex **4.6**

Ligand	Bond lengths (Å)		Bond angles (°)	Torsion angles (°)
	C1-O1	C16-O2	N1-C1-O1	N(1)-C(5)-C(6)-C(11)
4.6	1.252(2)	1.245(2)	120.13(14)	-45.88(19)

The X-ray crystal structure of **4.6** showed that the ligand exists in the lactam (pyridone) form where the hydrogen atom bonds with the nitrogen atom rather than the oxygen atom. This observation was supported by the carbon-oxygen bond lengths of 1.252(2) and 1.245(2) Å, which are both in agreement with double-bond character. The solid-state showed that the ligand was protonated at each pyridyl nitrogen. Each two neighbouring molecules in the crystal structure are found to be linked either by direct hydrogen-bonding interactions or with the help of two methanol molecules of solvation (**Fig. 4.9**).

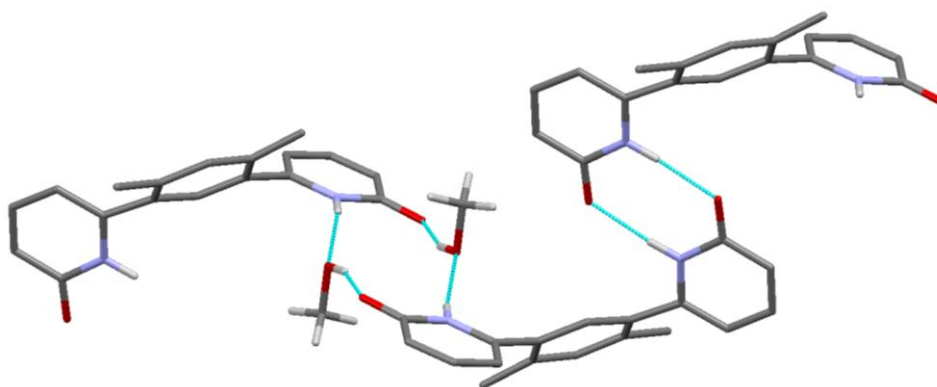
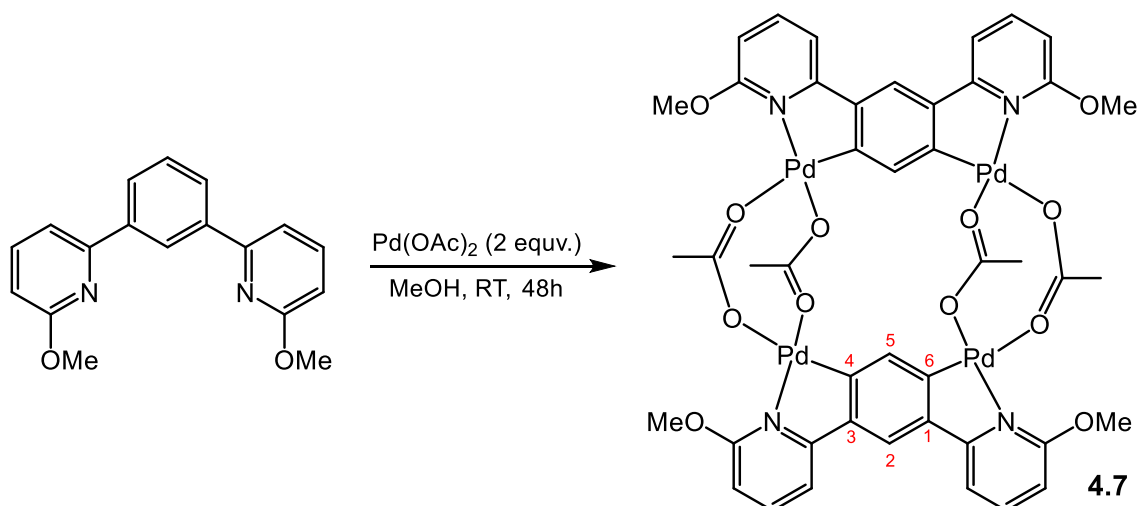


Figure 4.9: Intra- and intermolecular hydrogen bonding in **4.6**

4.3.3 Complexation of Tridentate N[^]C[^]N Ligands to Palladium (Pd^{II})

Coordination of the pre-ligand **4.3** with a Pd^{II} centre was achieved using Pd(OAc)₂. Initially, the reaction was attempted on a 1:1 (Pd^{II}/ligand) scale to try to obtain a monopalladated pincer complex with both nitrogen atoms coordinated to one metal centre. The reaction was carried out by stirring in MeOH at room temperature for 48 hours which resulted in a yellow solution with a precipitate. After stopping the reaction, the yellow solid was separated by filtration, washed with Et₂O, and collected and dried under reduced pressure to give a 41% yield of a tetrameric complex (**4.7**) in which four acetate bridges bind two doubly metallated ligands (**Scheme 4.13**). As will be discussed separately, the filtrate from this reaction was concentrated and dried in a rotary evaporator to surprisingly afford a dimeric complex (**4.8**) in a very low yield (29%) (see **Scheme 4.14**).



Scheme 4.13: Synthesis of [Pd₂(**4.3**)(μ-OAc)₂]₂ (**4.7**)

Unfortunately, the tetrameric **4.7** was only slightly soluble in DMSO and completely insoluble at room temperature in other organic solvents such as CDCl₃, DCM, MeCN and benzene. This insolubility meant that using **4.7** in any subsequent reactions, such as disassembly and catalytic reactions, would be difficult.

The ¹H NMR spectrum of **4.7** (DMSO-*d*₆) showed two singlets at 6.18 and 7.09 ppm indicating that the C₍₂₎-H bond between the two pyridine rings had not been activated (**Scheme 4.13**). Therefore, the complex was proposed to contain a doubly palladated ligand in which each palladium coordinates to the ligand by two atoms, the pyridyl nitrogen and *o*-carbon (C_{4/6}). Two different 6H singlets were also observed at 1.9 and 2.14

ppm which were assigned to the methyl groups of the acetate ligands. This indicated that the bridging acetates are found in two different environments; the X-ray structure of this complex later confirmed this point. The ^{13}C NMR signals for **4.7** were assigned using HSQC and HMBC NMR experiments and also based on experimental data for a structurally similar complex (**4.g**).¹ The 2D HMBC NMR spectrum showed five aromatic CH carbon environments, which was consistent with the proposed structure. The IR spectrum displayed two strong bands at 1567 and 1406 cm^{-1} which are representative of asymmetric and symmetric carboxylate vibrations, respectively. According to the results obtained by Nakamoto,²⁹ the acetates must be in a bridging fashion when $\Delta\nu > 40 \text{ cm}^{-1}$. The electrospray mass spectrum of the tetrameric complex (**4.7**) showed molecular ion and fragmentation peaks at m/z 1241 $[\text{M}]^+$ and 1182 $[\text{M-OAc}]^+$, respectively.

Once the structure of this complex had been determined to be that of a tetrameric complex, the stoichiometric amount in the second attempt was addressed through the use of a two-fold ratio of the Pd salt to the ligand **4.3** (2:1). As expected, this increased the yield of **4.7** to 83%.

A single crystal suitable for X-ray diffraction analysis was obtained from a diffusion process using a DMSO solution of **4.7** and EtOH as a precipitant. The X-ray structure of the complex **4.7** was found to be essentially identical to that previously obtained by Cárdenas *et al.*¹ with the exception of the presence of methoxy groups in our complex (**Fig. 4.10**).

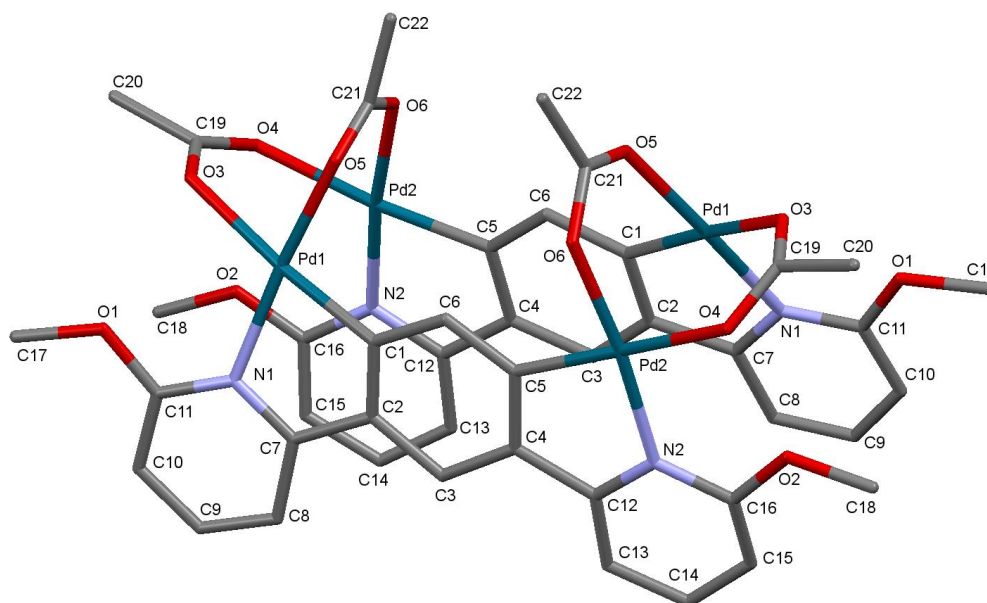


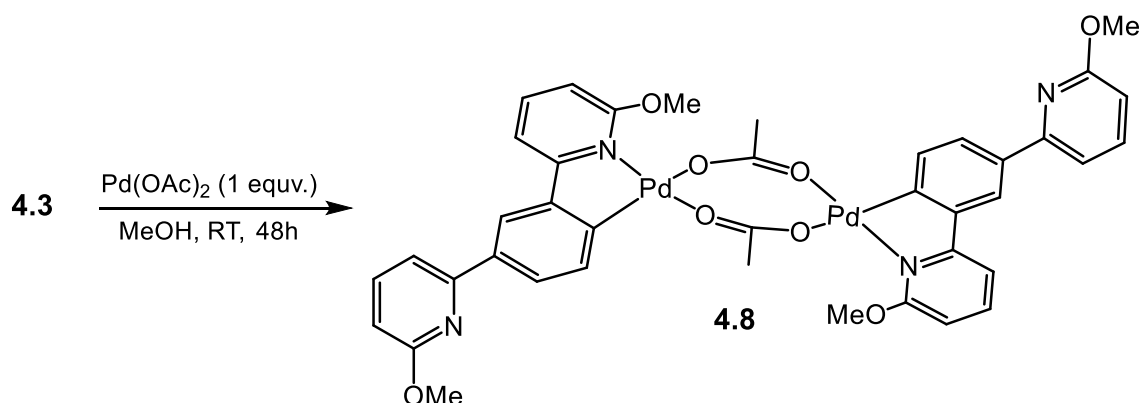
Figure 4.10: Structure of **4.7** with hydrogen atoms omitted for clarity

The complex tends to adopt an “open-book” structure supported by two ligands bridged by four acetate ligands. The X-ray structure revealed that the two acetate ligands are located *trans* to nitrogen atoms while the other two are *trans* to carbon atoms. This observation clearly explains why two different 6H singlets appeared in the ^1H NMR spectrum. **Table 4.2** shows that there are two different types of Pd-O bonds in complex **4.7**; one is *trans* to a carbon atom whilst the other Pd-O bond is *trans* to a pyridyl nitrogen atom. The Pd-O bonds *trans* to C are found to be longer than those *trans* to N, exactly as observed in the dimeric N \wedge C complexes described in Chapter 2 (**2.10-2.14**). This is again due to the stronger *trans* influence of the phenyl carbon atom. The complex has a bite angle (N-Pd-C) of approximately 81.1° , which is almost identical to the corresponding angle (81.2°) in the complex previously synthesised by Cárdenas *et al.*¹ (**Fig. 4.g**). Typical Pd-N and Pd-C bond lengths were observed in this complex, which are similar to those reported for **4.g**.¹

Table 4.2: Selected bond lengths and bite angles of complex **4.7**

Complex	Bond lengths (Å)					Bond angles (°)
	Pd...Pd	Pd-O (<i>trans</i> to C)	Pd-O (<i>trans</i> to N)	Pd-N	Pd-C	N-Pd-C
4.7	2.847(1)	2.127(7)	2.045(6)	2.090(7)	1.956(8)	80.1(5)

As mentioned earlier, another dimeric complex (**4.8**) was formed as a minor product during the course of the reaction of **4.3** with Pd(OAc)₂ (**Scheme 4.14**). The concentration of the filtrate *via* rotary evaporation gave a complex mixture of products from which **4.8** was obtained upon recrystallisation as very thin yellow needles in a 29% yield.



Scheme 4.14: Formation of **4.8** as a minor product from the reaction with Pd(OAc)₂

It should be noted that the dimeric **4.8** is not a precursor to the tetrameric **4.7**, as each bridged acetate ligand here is *trans* to different atoms (unlike those in **4.7**) and the non-coordinated pyridines were distal from each other, indicating that formation of the tetramer (**4.7**) is not possible from **4.8**.

The dimeric **4.8** was found to be highly soluble in different organic solvents; therefore, a full characterisation of this product was possible. The ^1H NMR spectrum showed the formation of a 1:1 (L/OAc)-Pd complex. Two 3H singlets representing the methoxy (OMe) protons were observed at 3.64 and 4.06 ppm in the ^1H NMR spectrum of **4.8**. This indicated that the two methoxy groups are not in equivalent environments; this was further confirmed by the presence of two peaks at 53.2 and 55.7 ppm in the $^{13}\text{C}\{^1\text{H}\}$ NMR spectra of **4.8**. A 3H singlet at 2.23 ppm confirmed the presence of the bridged acetate ligand. In addition, nine unique aromatic proton and carbon environments were observed in the ^1H and $^{13}\text{C}\{^1\text{H}\}$ NMR spectra of **4.8**, respectively. These observations were found to be in agreement with the proposed structure. The infrared spectrum of this complex showed two strong bands at 1559 and 1405 cm^{-1} which were assigned to the asymmetric and symmetric carboxylate bridges, respectively. The $\Delta\nu$ value was greater than 40 cm^{-1} and hence it can be concluded that the carboxylate group is not in a chelating mode.²⁹ Analysis of the dimeric complex (**4.8**) by electrospray mass spectrometry revealed a fragmentation peak at m/z 855 corresponding to the loss of an acetate from the molecular ion $[\text{M-OAc}]^+$.

It was possible to grow a single crystal of **4.8** suitable for X-ray diffraction studies by slow diffusion of hexanes into a concentrated CH_2Cl_2 solution of the crude product. The X-ray structure of the complex is shown in **Figure 4.11**. The solid-state data showed a dimeric acetate-bridged complex in which the tridentate ligand (**4.3**) acted as an N[^]C-chelating ligand to the Pd^{II} centre with the second pyridine left “dangling”. The X-ray data clearly confirmed that this bidentate complex cannot be considered as an intermediate for **4.7** due to the anti-position of the two available pyridines. From **Table 4.3**, all bond lengths, including Pd \cdots Pd interactions, and angles were found to be within the normal range for related dimeric acetate-bridged complexes previously described in this work. Additional conclusions on structure **4.8** should not be drawn since the structure refinement was very weak due to crystal quality with an R1 value for all data of 0.2948 and $wR2 = 0.2857$ (see **Table A8** in the **Appendix**), as this would lead to significantly

larger errors in bond lengths and angles. Values in **Table 4.3** should be viewed with caution.

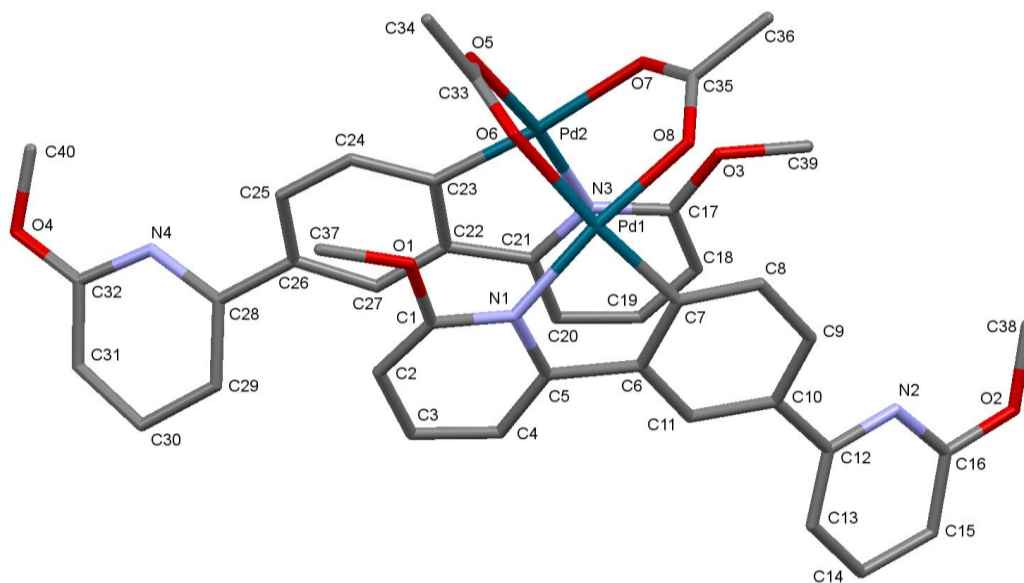
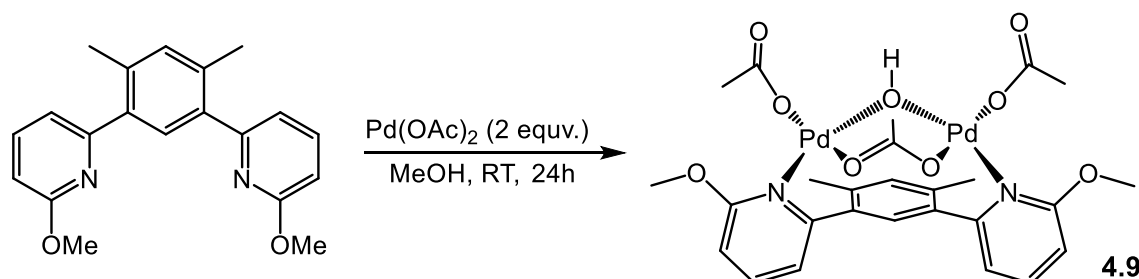


Figure 4.11: Structure of **4.8** with hydrogen atoms omitted for clarity

Table 4.3: Selected bond lengths and bite angles of complex **4.8**

Complex	Bond lengths (Å)					Bond angles (°)
	Pd···Pd	Pd-O (<i>trans</i> to C)	Pd-O (<i>trans</i> to N)	Pd-N	Pd-C	N-Pd-C
4.8	2.836(2)	2.175(12)	1.997(14)	2.102(15)	1.954(18)	~81.5(8)

Upon reaction of the ligand **4.4** with two equivalents of Pd(OAc)₂ in MeOH at room temperature, the dimeric **4.9** was obtained very cleanly in an 84% yield (**Scheme 4.15**).



Scheme 4.15: Synthesis of **4.9**

The reaction with one equivalent of Pd(OAc)₂ was attempted under the same conditions and gave the same product (**4.9**). Treatment of the ligand with one equivalent of Pd(OAc)₂ in dry MeOH under an inert atmosphere did not help to obtain a monopalladated complex

and thus the complex remained unchanged. The coordination reaction formed a dimeric complex in which the C₂ was not metallated and both pyridine rings coordinated to different Pd^{II} centres, which are bridged by both OH and acetate ligands.

In the ¹H NMR spectrum of **4.9**, 6H and 3H singlets corresponding to the acetate methyl protons were observed at 1.61 and 1.7 ppm, respectively. These peaks, as well as two signals at 22.4 and 22.7 ppm in the ¹³C{¹H} NMR spectrum, indicated the presence of inequivalent acetate groups where one acted as a bridge between the two Pd^{II} centres and the other two acted as monodentate ligands. A singlet was also observed at 5.64 ppm in the ¹H NMR spectrum which represents the bridging hydroxy-ligand. The unsuccessful attempt at CH activation was confirmed by the presence of five unique aromatic proton and CH environments in the ¹H and ¹³C{¹H} NMR spectra, respectively. The two peaks at 1574 and 1380 cm⁻¹ in the IR spectrum may indicate the asymmetric and symmetric ν(COO) vibrations of the acetate ligand, respectively. The electrospray mass spectrum of the dimeric complex showed a variety of fragmentation peaks at 669, 650, 590 and 425 which represent [M-OAc]⁺, [M-OAc-OH]⁺, [M-2OAc-OH]⁺ and [L+Pd]⁺, respectively.

Suitable X-ray crystals of complex **4.9** were grown by slow diffusion of hexanes into a dichloromethane solution of the product. The X-ray structure is shown in **Figure 4.12** and selected bond lengths and angles are reported in **Table 4.4**.

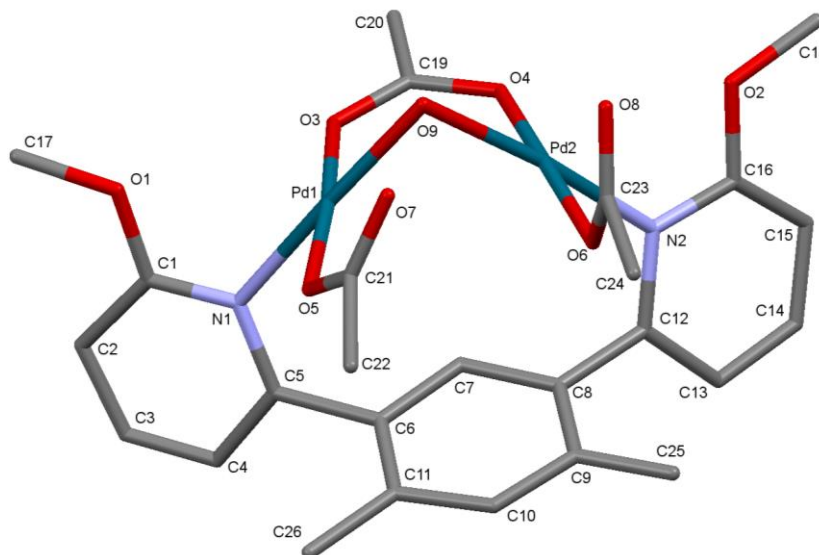


Figure 4.12: Structure of **4.9** with hydrogen atoms omitted for clarity

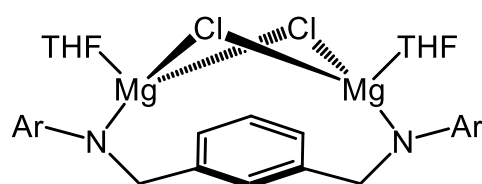
The solid-state structure showed a doubly palladated ligand in which each Pd^{II} centre tends to adopt a square planar geometry with three different types of Pd-O bonds and one Pd-N bond. The lengths of all three Pd-O bonds are found to be almost identical to each

other, within experimental error, although the Pd-OH bonds are exposed to different *trans* influences. The Pd-N bond lengths of $\sim 2.055(10)$ Å were also found to be similar to those previously reported.¹

Table 4.4: Selected bond lengths and angles of complex **4.9**

Complex	Bond lengths (Å)					Bond angles (°)
	Pd···Pd	Pd-O _{bridge}	Pd-O _{mono}	Pd-OH	Pd-N	Pd-O-Pd
4.9	2.940(2)	2.018(9)	2.001(9)	1.999(8)	2.055(10)	93.9(3)

Comparable structures of this complex could not be found in the literature; however, there is an example that showed similar reaction behaviour. The one which most closely resembles **4.9** is $[(N^{\wedge}CH^{\wedge}N)(\mu\text{-MgCl}\cdot\text{THF})_2]$ (**4.r**), where $N^{\wedge}CH^{\wedge}N = N,N'$ -[1,3-phenylenebis(methylene)]bis-(2,6-diisopropyl aniline). The dimeric magnesium complex was obtained as a result of the reaction of 2 equivalents of MeMgCl with the $N^{\wedge}CH^{\wedge}N$ ligand. The authors confirmed the structure, *inter alia*, by single crystal X-ray diffraction studies and attributed this observation to the bridging chlorides, which were thought to help stabilise the dimeric formulation.³⁰

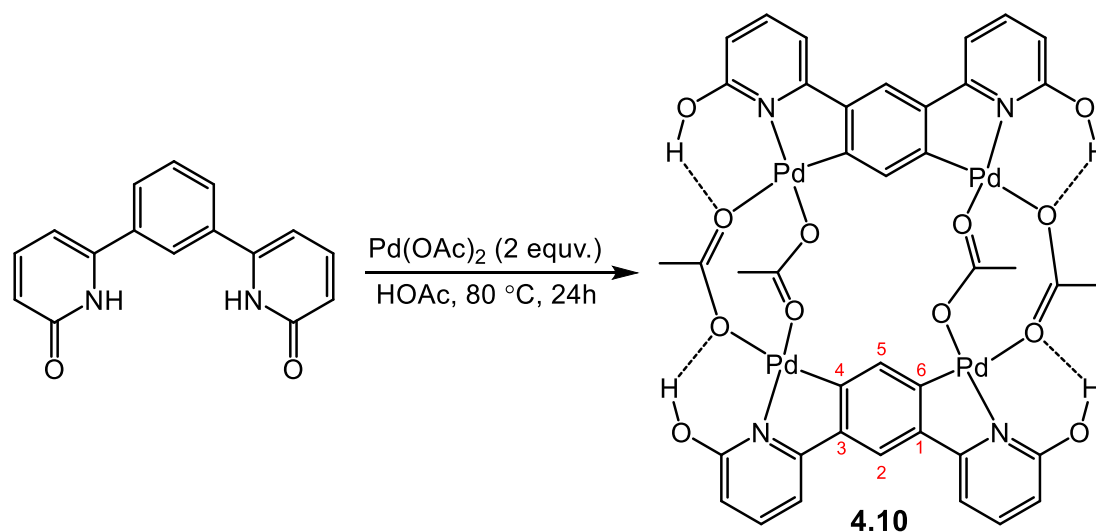


4.r

Ar = 1,3-diisopropylbenzene

Since the ligand **4.5** is not soluble at room temperature in any organic solvents, more forcing conditions were required to carry out reactions. Acetic acid was the best choice among a variety of solvents for complexation of **4.5** with Pd(OAc)₂. To increase the solubility – and therefore the reactivity – of the ligand, the reaction mixture was heated at 80 °C for 24 hours with a solution demonstrating a colour change from dark red to light orange. After approximately three to four hours, the solution stopped changing colour, suggesting that the reaction was mostly complete at this point; however, the reflux was continued to maximise the yield. After cooling to room temperature, the orange

precipitate was filtered and washed with HOAc to give **4.10** as an orange solid in high purity but with a low yield of 44% (**Scheme 4.16**).



Scheme 4.16: Synthesis of $[\text{Pd}_2(\mathbf{4.4})(\mu\text{-OAc})_2]_2$ (**4.10**)

The tetrameric **4.10** was found to be slightly soluble in only CDCl_3 and completely insoluble at room temperature in other organic solvents, including DMSO. This meant that full characterisation of **4.10** would be difficult.

Upon analysis of **4.10** by ^1H NMR spectroscopy, two aromatic singlets were observed at 6.42 and 6.54 ppm indicating that the $\text{C}_{(2)}\text{-H}$ bond between the two pyridine rings had not been activated (**Scheme 4.16**). In this case, the proposed structure of **4.10** would be similar to **4.7** in which two ligands were dipalladated and bridged by four acetates. Two different 6H singlets corresponding to the acetate methyl protons were also observed at 2.10 and 2.23 ppm indicating that each of the two acetate groups was in a different environment, as confirmed by X-ray crystallography. The downfield-shifted OH peak was represented by a singlet at 9.20 ppm, confirming that the ligands coordinated to the metal centre in the pyridinol form. This significant downfield shift of the OH proton was attributed to the hydrogen-bonding interactions between the OH hydrogen and the adjacent oxygen of the bridging acetate. The 2D HSQC spectrum of **4.10** showed five unique aromatic CH carbon resonances, which was in agreement with the proposed structure. Two strong bands representing asymmetric and symmetric carboxylates were observed at 1558 and 1407 cm^{-1} upon analysis by IR spectroscopy. The electrospray mass spectrum of the tetrameric complex (**4.10**) displayed a molecular ion peak at m/z 1186 $[\text{M}]^+$ which was in good accordance with the calculated mass.

Further confirmation of the tetrameric structure of **4.10** was obtained by X-ray diffraction analysis on single crystals, grown by slow evaporation of a chloroform solution of the complex. The structural diagram of **4.10** is provided in **Figure 4.13** with selected bond lengths and angles for the structure reported in **Table 4.5**.

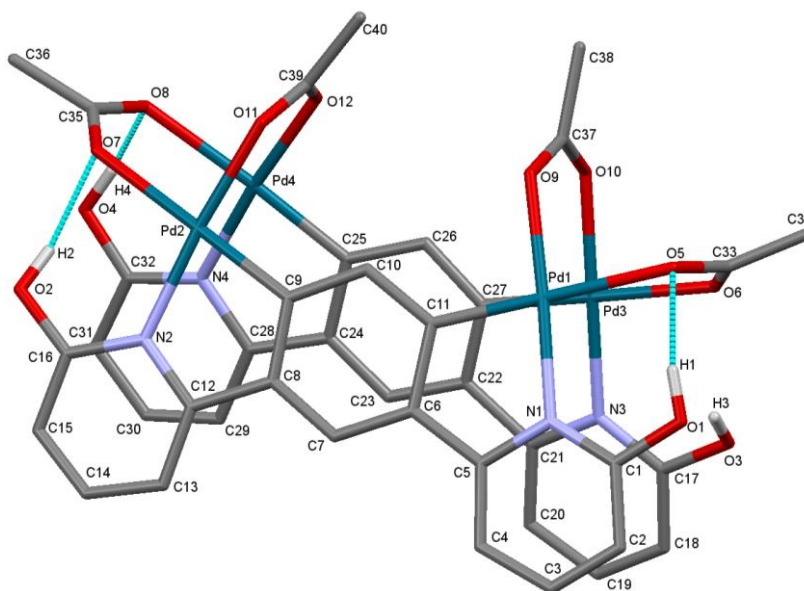


Figure 4.13: Structure of **4.10** with hydrogen atoms omitted for clarity

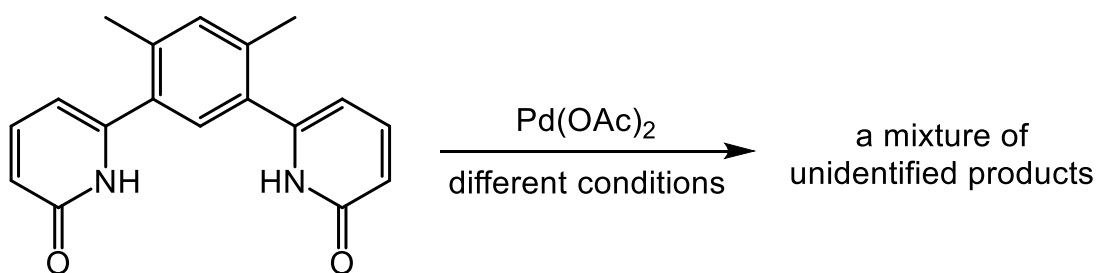
Table 4.5: Selected bond lengths and bite angles of complex **4.10**

Complex	Bond lengths (Å)					Bond angles (°)
	Pd···Pd	Pd-O (<i>trans</i> to C)	Pd-O (<i>trans</i> to N)	Pd-N	Pd-C	N-Pd-C
4.10	2.890(1)	2.173(8)	2.063(7)	2.049(8)	1.881(11)	82.6(4)

The X-ray structure of the tetrameric complex (**4.10**) showed two doubly palladated ligands bridged by four acetates. Each Pd^{II} centre has a distorted square planar geometry with, for example, a N(1)-Pd(1)-O(5) angle of 98.5(3)°. In common to most acetate-bridged complexes, the tetramer (**4.10**) was forced to adopt an “open-book” geometry¹ by the four acetate ligands, with Pd···Pd bond lengths of about 2.890(1) Å (shorter than the sum of their van der Waals radii of 3.26 Å).³¹ The C-OH bond lengths of approximately 1.325(12) Å indicated that the coordinated ligands were in the pyridinol form. Furthermore, each pyridinol OH hydrogen atom was found to be able to form a hydrogen bond with a neighbouring acetate oxygen atom (OH···H). The electronic nature of the pyridinol ligand (in comparison with those for the tetrameric **4.7**) does not seem to

have a significant effect on the overall structure of the product, and therefore all Pd-X (X = N, C and O) bond lengths and angles are in agreement with those observed in complex **4.7** and reported in the literature.³² As mentioned for previous acetate-bridged complexes, a significant *trans* influence in complex **4.10** was inferred from the differences in the Pd-O bond lengths (where those *trans* to carbon atoms were longer than those *trans* to nitrogen atoms by approximately 0.11 Å). This was due to the stronger *trans* influence of the aryl group versus the N-donor ligand.³³ It is worth mentioning that the tetramer (**4.10**) proved to have a stable structure in NMR solution over time (3 weeks).

Treatment of 4,6-bis(2-pyridon-6-yl)*m*-xylene (**4.6**) with Pd(OAc)₂ in different conditions resulted in the formation of complex mixtures of products for which purification was attempted but ultimately failed (**Scheme 4.17**). Despite several modifications to the procedure, ¹H NMR spectra of the attempted reactions showed the same complex mixtures with the absence of the downfield NH peak of the ligand.

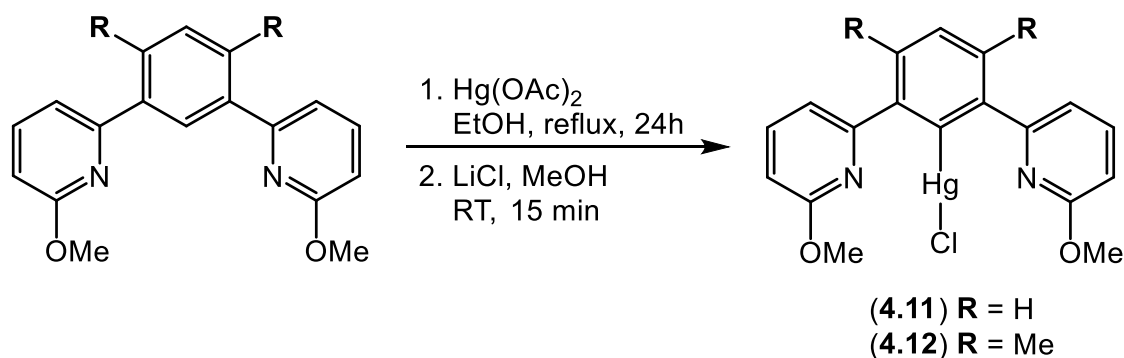


Scheme 4.17: Reaction of **4.6** with Pd(OAc)₂

4.3.4 Transmetallation Reactions

Since the direct syntheses of pincer complexes using Pd(OAc)₂ had been unsuccessful, transmetallation reactions of appropriate C₂-H-activated precursors became an alternative choice by which to achieve the C₂ cyclopalladation. Despite transmetallation of appropriate aryl-lithiated precursors with several transition metals being widely used in the literature, the regioselectivity of these C-H activation processes was found to be very difficult to control if there were more than one possible position available for C-H activation. Therefore, it was necessary to synthesise mercurated complexes for use as precursors for the metal-exchange reaction.

Reactions of **4.3** and **4.4** with Hg(OAc)₂ in absolute ethanol, after being treated with a solution of LiCl in methanol, gave the corresponding mercury complexes (**4.11** and **4.12**) with yields of 27% and 40%, respectively (**Scheme 4.18**).



Scheme 4.18: Synthesis of $[\text{Hg}(\mathbf{4.3})\text{Cl}]$ (**4.11**) and $[\text{Hg}(\mathbf{4.4})\text{Cl}]$ (**4.12**)

Analysis of **4.11** and **4.12** by ^1H NMR spectroscopy revealed the symmetry in these complexes, as the two pyridine rings appeared in equivalent environments. In addition to the absence of the $\text{C}_2\text{-H}$ proton, a doublet with satellites ($^4J_{\text{H-Hg}} = 68$ Hz) at 7.82 ppm in the ^1H NMR spectrum of **4.11** indicated that the covalent C-Hg bond had formed. This was further confirmed by ^{13}C DEPT 135 NMR spectroscopy wherein four unique quaternary aromatic carbon environments were found. In the case of complex **4.12**, similar observations were found upon ^1H and ^{13}C NMR spectroscopies, confirming the formation of the covalent C-Hg bond; this was further demonstrated by the X-ray structure of **4.12** (*vide infra*). In addition, the three peaks of the pyridine rings in both complexes were almost identical to those observed for the starting materials, suggesting uncoordinated pyridyl rings. Moreover, it was possible to view strong fragmentation peaks at m/z 493 and 521 corresponding to $[\text{M-Cl}]^+$ as well as molecular protonated ion peaks at m/z 529 and 557 by ASAP mass spectrometry of **4.11** and **4.12**, respectively.

It was only possible to grow single crystals of **4.12** suitable for an X-ray diffraction study through slow diffusion of isopropyl ether into a solution of the complex in dichloromethane. The structural diagram of **4.12** is given in **Figure 4.14** with selected bond lengths and angles reported in **Table 4.6**.

The solid-state structural data for **4.12** revealed a linear mercury(II) coordination complex with a C1-Hg1-Cl1 bond angle of $177.9(3)^\circ$. It was clear that the two pyridine rings were orientated away from the central metal with a C1-C2-C7-N1 torsion angle of $54.8(15)^\circ$, and thus remained nonbonding. These observations are normal for R-Hg-Cl species.¹² The Hg-C and Hg-Cl bond lengths were found to be within the normal range for related complexes previously reported in the literature.¹² On the whole, the X-ray data is very similar to that previously reported by Soro *et al.*¹²

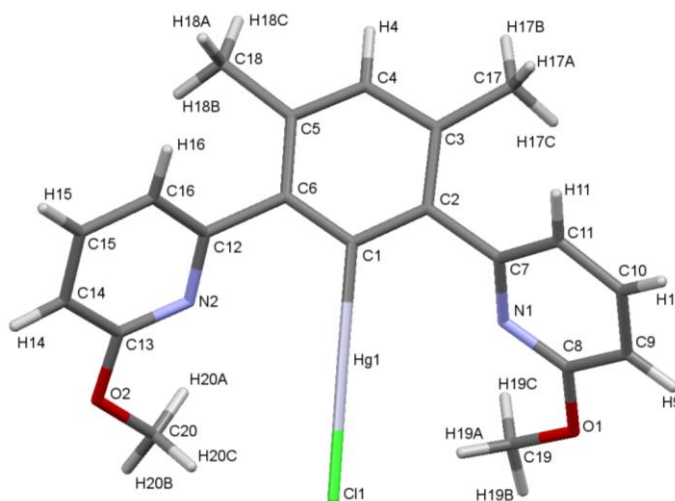
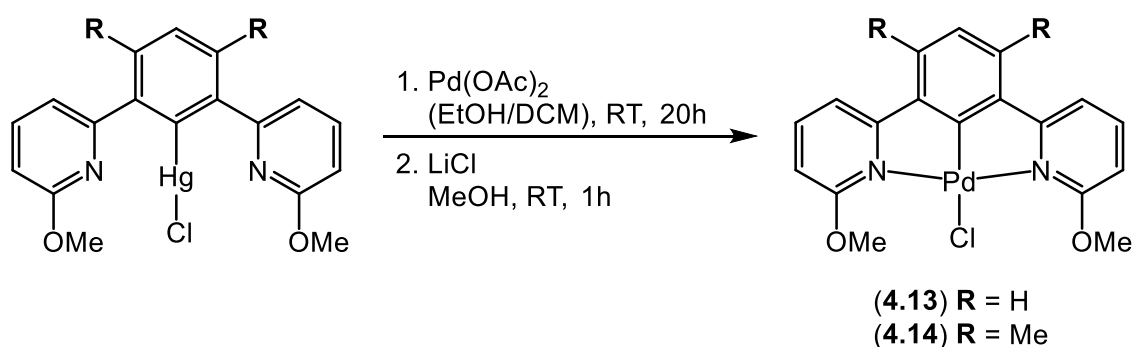


Figure 4.14: Structure of **4.12** with full atom numbering

Table 4.6: Selected bond lengths and angles of complex **4.12**

Complex	Bond lengths (Å)		Bond angles (°)	Torsion angles (°)	
	Hg1-C1	Hg1-Cl1	C1-Hg1-Cl1	C1-C2-C7-N1	Hg1-C1-C2-C3
4.12	2.055(12)	2.326(3)	177.9(3)	54.8(15)	174.6(9)

Following these mercuration reactions, transmetalation of **4.11** and **4.12** to Pd^{II} complexes was carried out in a mixture of ethanol and dichloromethane using Pd(OAc)₂, followed by addition of LiCl to cleanly give the corresponding pincer complexes (**4.13** and **4.14**) in 27 and 26% yields, respectively (**Scheme 4.19**). It should be noted that attempts to isolate the acetate intermediates were unsuccessful.



Scheme 4.19: Synthesis of **4.13** and **4.14** via transmetalation reactions

Both cyclometallated complexes (**4.13** and **4.14**) were found to have poor solubility in organic solvents, such as CHCl₃ and MeCN; however, for NMR characterisation,

DMSO demonstrated a slightly better ability to dissolve both complexes at room temperature. Analysis of **4.13** and **4.14** by ^1H NMR spectroscopy revealed five and four aromatic proton environments, respectively, consistent with their proposed structures. The 6H singlets at 3.96 and 3.79 ppm were assigned to the methoxy protons in **4.13** and **4.14**, respectively. The two methyl protons in the complex **4.14** were also observed as a singlet at 2.34 ppm. The 2D HSQC spectrum of **4.13** and $^{13}\text{C}\{^1\text{H}\}$ NMR spectrum of **4.14** showed the expected carbon resonances, confirming that the ligands had been successfully bound to a metal centre by their anionic aryl carbon atoms (C_2). In the mass spectra of **4.13** and **4.14**, a strong fragmentation peak corresponding to the loss of chloride was observed in each at m/z 397.0176 (requires m/z 397.0168) and 425.0498 (requires m/z 425.0481), respectively. The Pd-chloride species were further proven from the reactions of both ligands (**4.3** and **4.4**) with $\text{Na}_2[\text{PdCl}_4]$ (*vide infra*). Although these data cannot confirm that the ligands in both complexes behaved as pincer, coordination around the palladium ion in similar complexes is normally considered to take a square planar geometry with two nitrogen atoms bound to a Pd^{II} centre in a *trans* arrangement.¹

Unfortunately, attempts to obtain crystals of **4.13** and **4.14** suitable for X-ray diffraction studies were unsuccessful. Instead, orange blocks grown in a residual amount of the reaction mixture of **4.14**, left to undergo slow evaporation, were submitted for X-ray analysis. Unexpectedly, the molecular structure revealed a cationic palladium pincer complex supported by a water molecule and Hg_2Cl_6 as a counterion (**Figure 4.15**).

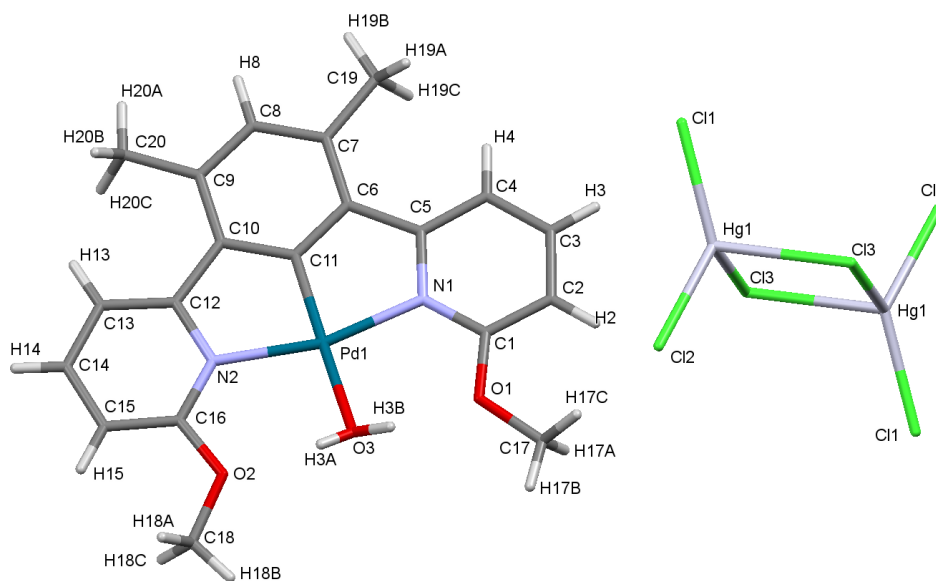
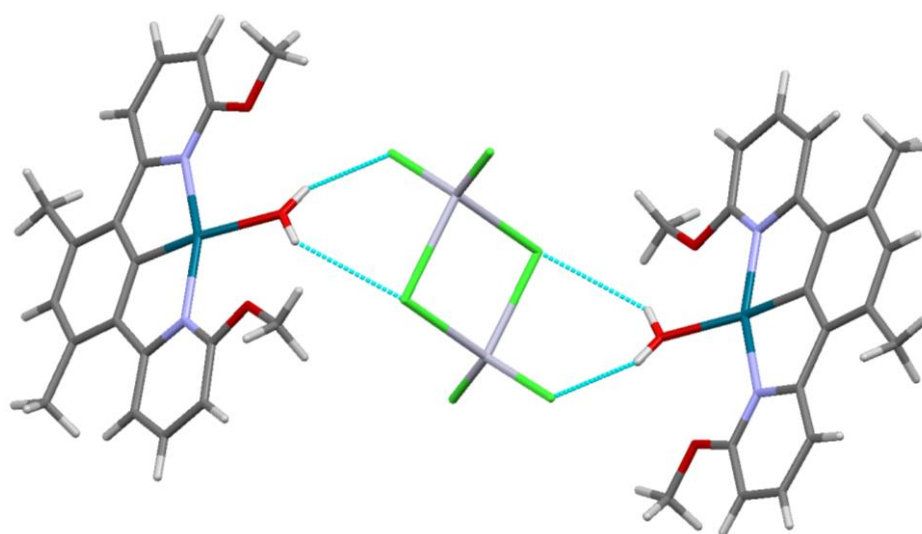


Figure 4.15: X-ray structure of $[\text{Pd}(\mathbf{4.4})(\text{H}_2\text{O})]_2[\text{Hg}_2\text{Cl}_6]$ (**4.14'**) with another Pd^{II} species omitted

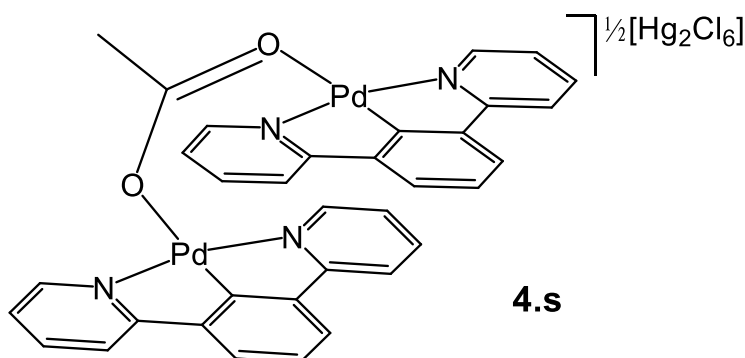
Table 4.7: Selected bond lengths and angles of [Pd(**4.4**)(H₂O)][Hg₂Cl₆] (**4.14'**)

Complex	Bond lengths (Å)					Bond angles (°)
	Pd-C	Pd-N	Pd-O	Hg-Cl1	Hg-Cl3	C11-Pd-N1
4.14'	1.909(7)	2.075(10)	2.197(5)	2.358(2)	2.633(2)	80.3(3)
						N1-Pd-O3
						100.0(2)

The solid-state data of **4.14'** showed a distorted square planar geometry about the Pd^{II} centre with the almost identical C-Pd-N bite angles of 80.3(3)°, which are normal for those forming a five-membered ring. The tridentate monoanionic pincer ligand was found to be close to planar with respect to the chelating rings. The two Pd–N bond lengths were almost identical to within experimental error, and found to be longer than the Pd–C bond length of 1.909(7) Å and significantly shorter than the Pd–O bond length of 2.197(5) Å, as reported in **Table 4.7**. For the [Hg₂Cl₆]²⁻, the X-ray structure revealed a distorted tetrahedral geometry around each Hg atom that was supported by two terminal and two double-bridged chloride ligands. The Hg–Cl bond lengths were almost identical to those previously reported in the literature.¹² Each two neighbouring cations in the crystal structure of **4.14'** were found to be united by one anionic Hg₂Cl₆ through OH···Cl hydrogen bonds (**Figure 4.16**).

**Figure 4.16:** Intermolecular hydrogen bonding interactions in **4.14'**

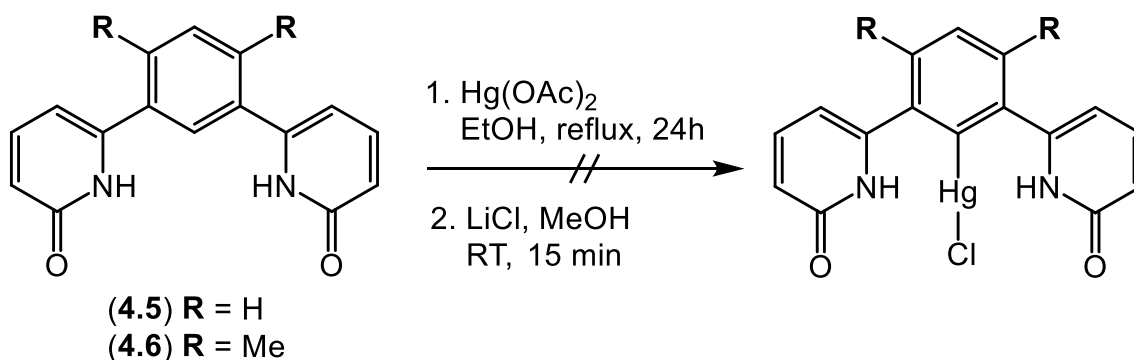
The aqua complex (**4.14'**) is likely to be formed as a by-product during the reaction or generated from **4.14** as a result of substitution of a chloride ligand by a water molecule. The water molecule, coordinated to the Pd^{II} centre, possibly came from the bench solvents used for the reaction. The presence of the anionic [Hg₂Cl₆]²⁻ in the unit cell of **4.14'** has raised the question of where this counterion came from; in other words, any mercury derivatives generated after adding Pd(OAc)₂ should have been removed upon filtration through Celite to leave a solution containing only palladium acetate complexes. Soro *et al.*¹² answered this question when they described all possible palladium intermediates that may have been formed from the reaction of their mercurated complexes with Pd(OAc)₂ (after the first step and before being treated with LiCl). They suggested that their transmetallation reactions may have resulted in a mixture of [Pd(N[^]C[^]N)(OAc)] and other dinuclear acetate-bridged species, such as [Pd₂(N[^]C[^]N)₂(μ-OAc)][OAc] and [Pd₂(N[^]C[^]N)₂(μ-OAc)][Hg₂Cl₆] (**4.s**). The latter dimer (**4.s**) was confirmed by X-ray crystallography and it is likely that it was similarly present in our system. The ESI negative mass spectrum of **4.14** showed a small peak at *m/z* 543 which may represent [Hg₂Cl₄] species. If this was the case, formation of **4.14'** with Hg₂Cl₆ as a counterion upon recrystallisation would clearly be expected.



Since the NMR data previously provided did not give enough information to determine the exact structure of **4.13** and **4.14**, the observation of the unexpected complex (**4.14'**) may now result in a degree of confusion and disagreement in terms of the synthesis of these palladium chloride complexes. There is no doubt, however, from the mass spectra of both complexes that transmetallation to palladium(II) had been successfully achieved in each instance. In order to eliminate this confusion, further evidence confirming the synthesis of **4.13** and **4.14** will be provided in the following section (**4.3.5**).

It should be noted that reactions of pyridone ligands (**4.5** and **4.6**) with Hg(OAc)₂ have been tried under various conditions (**Scheme 4.20**). Unfortunately, however, all

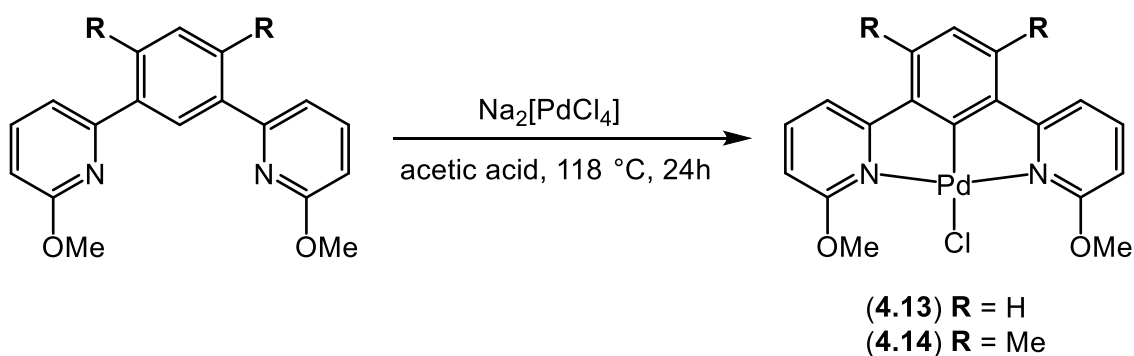
attempts to obtain mercurated complexes derived from **4.5** and **4.6** were unsuccessful, as their reactions always resulted in the formation of complex mixtures of products with no sign of the starting materials upon analysis by ^1H NMR spectroscopy.



Scheme 4.20: Attempted mercuration of **4.5** and **4.6** using $\text{Hg}(\text{OAc})_2$

4.3.5 Direct Synthesis of Palladium Pyridine and Pyridone complexes (**4.13-4.16**)

Given the regioselective C-H activation with $\text{Pd}(\text{OAc})_2$, the reactivity of **4.3** and **4.4** towards other palladium(II) salts, such as $\text{Na}_2[\text{PdCl}_4]$, was explored. Due to the insolubility of $\text{Na}_2[\text{PdCl}_4]$ in organic solvents at room temperature, the reactions with **4.3** and **4.4** were performed in glacial acetic acid under reflux ($118\text{ }^\circ\text{C}$) for 24 hours. Rather surprisingly, these did not result in the formation of tetrameric and/or dimeric complexes, but rather the direct complexation of **4.3** and **4.4** to palladium chloride gave palladium pincer complexes (**4.13** and **4.14**) in 69 and 71% yields, respectively (**Scheme 4.21**).

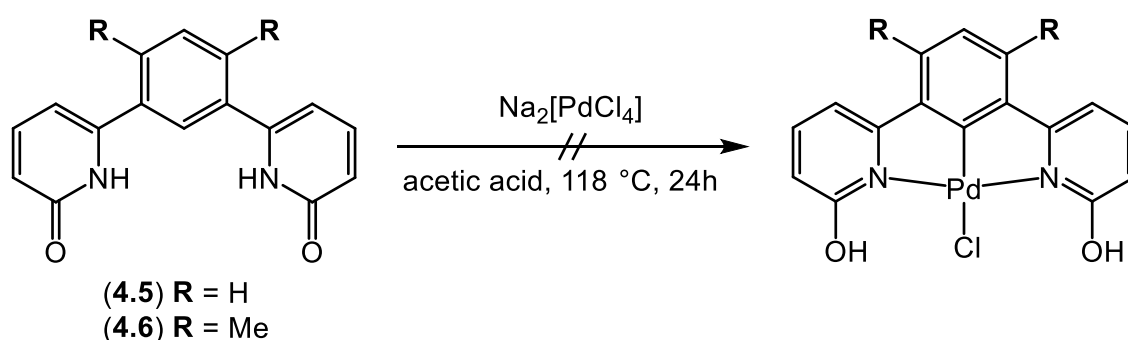


Scheme 4.21: Direct synthesis of **4.13** and **4.14** using $\text{Na}_2[\text{PdCl}_4]$

Analysis of both complexes (**4.13** and **4.14**) by ^1H and ^{13}C NMR spectroscopy and mass spectrometry revealed almost identical data to previous complexes obtained from the transmetalation reactions. This observation provided further evidence for the successful synthesis of **4.13** and **4.14** using $\text{Pd}(\text{OAc})_2$ with mercurated complexes.

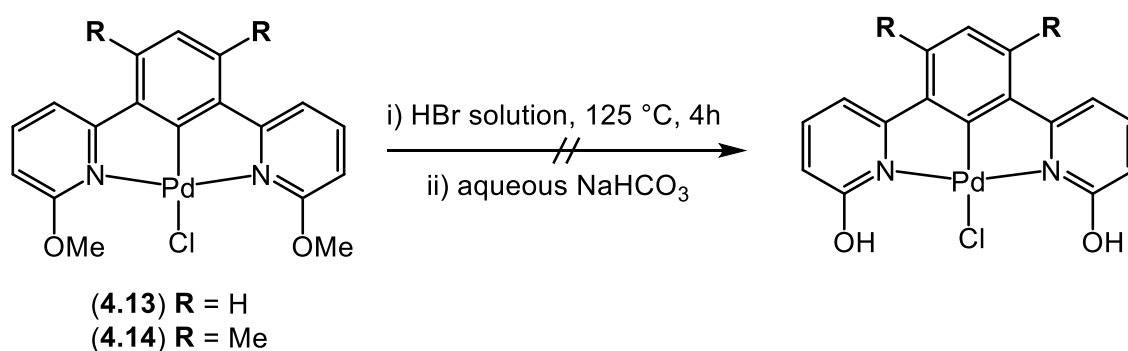
Compared to the previously described transmetallation route for the synthesis of these complexes (**4.13** and **4.14**), the direct synthesis using $\text{Na}_2[\text{PdCl}_4]$ provided both a safe alternative approach and significantly higher yields.

The procedure used for the synthesis of **4.13** and **4.14** was applied to the pyridone ligands (**4.5** and **4.6**) with $\text{Na}_2[\text{PdCl}_4]$. Unfortunately, despite various modifications to the procedure, the reactions were unsuccessful and resulted in the formation of complex mixtures of products with no sign of the starting materials upon analysis by ^1H NMR spectroscopy (**Scheme 4.22**). These failed reactions could be attributed to the presence of the hydroxy protons which might have been involved in coordination during the reactions.



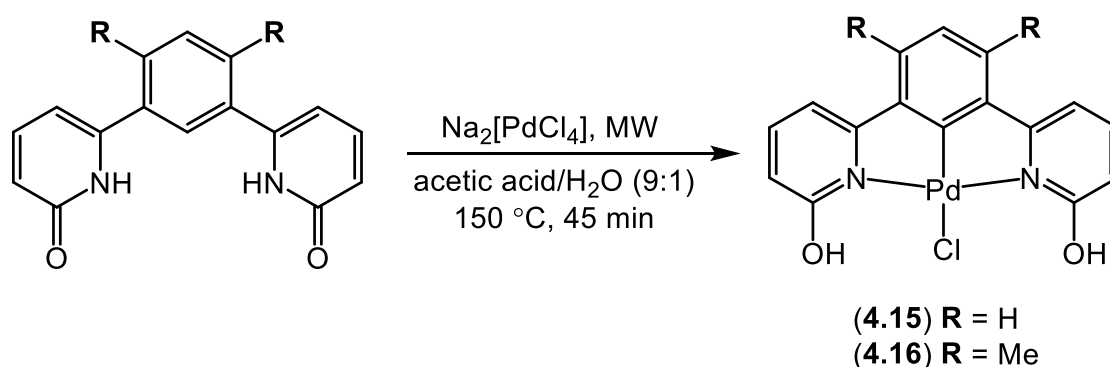
Scheme 4.22: Attempted direct synthesis of **4.5** and **4.6** using $\text{Na}_2[\text{PdCl}_4]$

In order to determine if the pyridone complexes could be obtained from the pyridine ones, demethylation reactions of the palladium pincer complexes (**4.13** and **4.14**) were attempted under reflux with a hydrobromic acid (HBr) solution in water or acetic acid (48 or 45%, respectively) for 4 hours (**Scheme 4.23**). Unfortunately, these reactions were unsuccessful and the starting methoxy complexes were recovered unreacted, as confirmed by ^1H NMR spectroscopy.



Scheme 4.23: Attempted deprotection reactions of **4.13** and **4.14**

These several unsuccessful attempts encouraged us to try to find a new method for the synthesis of pyridone pincer complexes. Therefore, the reactions of **4.5** and **4.6** with $\text{Na}_2[\text{PdCl}_4]$ were successfully developed through the use of microwave irradiation as a means of heating the reactions. In this case, $150\text{ }^\circ\text{C}$, with a maximum pressure of 150 psi, were sufficient to afford the desired complexes (**4.15** and **4.16**) as grey solids in good yields (83 and 78%, respectively), as shown in **Scheme 4.24**. These products were found to have extremely low solubility in organic solvents, and were only sparingly soluble in CDCl_3 .



Scheme 4.24: Synthesis of **4.15** and **4.16** using microwave heating

Analysis of **4.15** and **4.16** by ^1H NMR spectroscopy revealed the absence of the $\text{C}_2\text{-H}$ proton resonance (7.91 and 7.17 ppm in the starting materials, **4.5** and **4.6**, respectively), indicating that ligands had successfully undergone C-H activation to form symmetric palladium pincer complexes. A singlet assigned to the hydroxy protons was observed at 10.82 and 11.04 ppm in the ^1H NMR spectra of **4.15** and **4.16**, respectively. This significant downfield shift of the OH proton was attributed to the hydrogen-bonding interactions between the OH hydrogen and the adjacent chloride atom, and also confirmed that the ligands coordinated to the metal centre (Pd^{II}) in the pyridinol form. The 2D HSQC NMR spectra of **4.15** and **4.16** showed five and four unique aromatic CH carbon environments, respectively, which are in agreement with the expected structures. The IR spectra of both complexes showed a broad peak between 2900 and 3100 cm^{-1} which was assigned to the $\nu(\text{OH})$ absorption band. Upon analysis by ASAP mass spectrometry, **4.15** and **4.16** displayed a peak representing the loss of the chloride ligand at m/z 368.9868 and 397.0187, respectively.

It was possible to grow single crystals of **4.15** suitable for analysis by X-ray diffraction by slow evaporation of a solution of the complex in chloroform. The X-ray

structure of **4.15** is shown in **Figure 4.17**; selected bond lengths and angles are reported in **Table 4.8**.

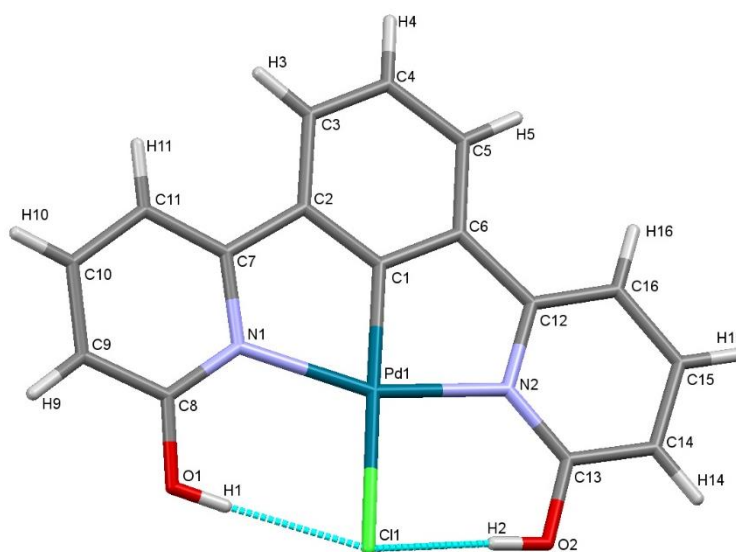


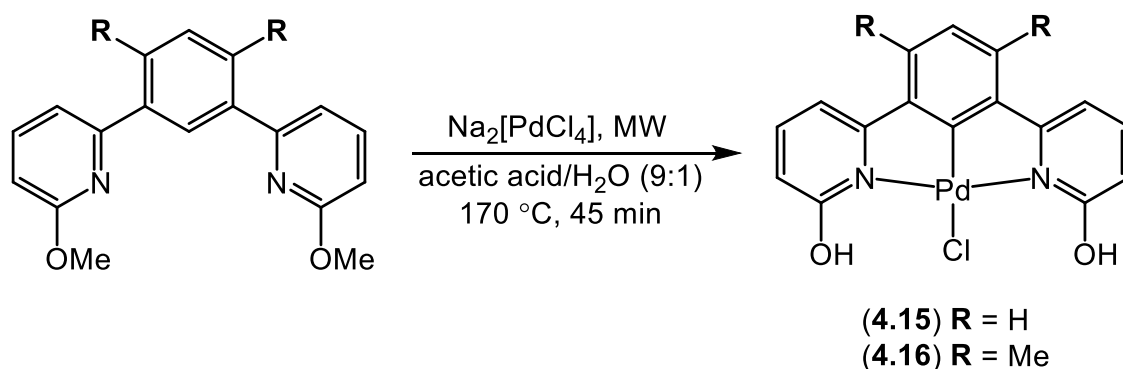
Figure 4.17: X-ray structure of **4.15** with full atom numbering

Table 4.8: Selected bond lengths and angles of complex **4.15**

Complex	Bond lengths (Å)				Bond angles (°)	
	Pd-N1	Pd-N2	Pd-C1(1)	Pd-C(1)	N1-Pd-C(1)	C1-Pd-Cl(1)
4.15	2.112(5)	2.110(5)	2.471(2)	1.921(5)	80.2(2)	174.13(17)

The molecular structure of **4.15** revealed a palladium(II) chloride complex supported by an almost perfectly planar monoanionic N⁺C⁻N tridentate ligand adopting a distorted square planar geometry. The two Pd–N bond lengths are almost identical, within experimental error, and found to be longer than the Pd–C bond length of 1.921(5) Å and significantly shorter than the Pd–Cl bond length of 2.471(2) Å, as reported in **Table 4.8**. These observations are consistent with those observed for [Pd(1,3-bis(2-pyridyl)benzene)Cl] (see **Scheme 4.2**). The C–O bond length is approximately 1.324(10) Å, which is consistent with having single bond character, confirming the presence of the coordinated ligand in a pyridinol form. Thus, intramolecular hydrogen-bonding interactions involving both pendant OH protons and the Pd-bound chloride were observed, as expected.

Interestingly, the previous pyridone complexes (**4.15** and **4.16**) were found to be alternatively synthesised from the pyridine ligands (**4.3** and **4.4**) by using the same microwave reaction conditions but at a higher temperature than 150 °C (namely, 170 °C) (**Scheme 4.25**). Compared to the previously described procedure for the synthesis of **4.15** and **4.16** from their pyridone ligands (**4.5** and **4.6**), the present reactions provided slightly lower yields (74 and 66%, respectively).



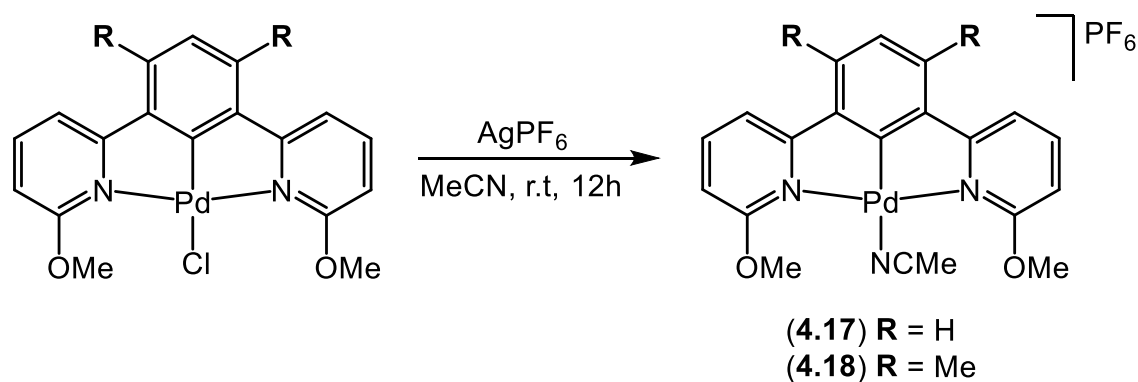
Scheme 4.25: Alternative method for synthesising **4.15** and **4.16** using pyridine ligands

In these reactions, it was clear that the pyridine ligands had undergone demethylation; however, it was unclear whether the demethylation process occurred while the ligands are still free in the solution or after they have been bound to the Pd^{II} centre. In order to investigate this further, similar conditions were applied to the palladium pyridine complexes (**4.13** and **4.14**) in a mixture of acetic acid and water. These reactions showed that both complexes were particularly stable and were left unchanged during the reactions. However, employing the same conditions for the free pyridine ligands (**4.3** and **4.4**) successfully resulted in the formation of the corresponding demethylated ligands (**4.5** and **4.6**) in very high purity. Thus, these observations suggest the demethylation of the pyridine ligands to occur first, followed by the coordination with the Pd^{II} centre.

4.3.6 Stoichiometric Reactions with AgPF₆

Since all palladium pincer complexes previously described showed very low solubility in common organic solvents, any subsequent reactions would obviously be difficult. However, the ability of both these pyridine complexes (**4.13** and **4.14**) to undergo chloride substitution reactions with a neutral two-electron donor ligand such as acetonitrile was tested in the presence of AgPF₆ (**Scheme 4.26**). The substitution reactions were carried out under an inert atmosphere (nitrogen) at room temperature. Over time, the solubility of the reaction mixtures increased to eventually give light brown

suspensions with the precipitation of silver chloride. After filtration *via* cannula, the solvent was removed by reduced pressure to afford **4.17** and **4.18** in good yields (72 and 86%, respectively).

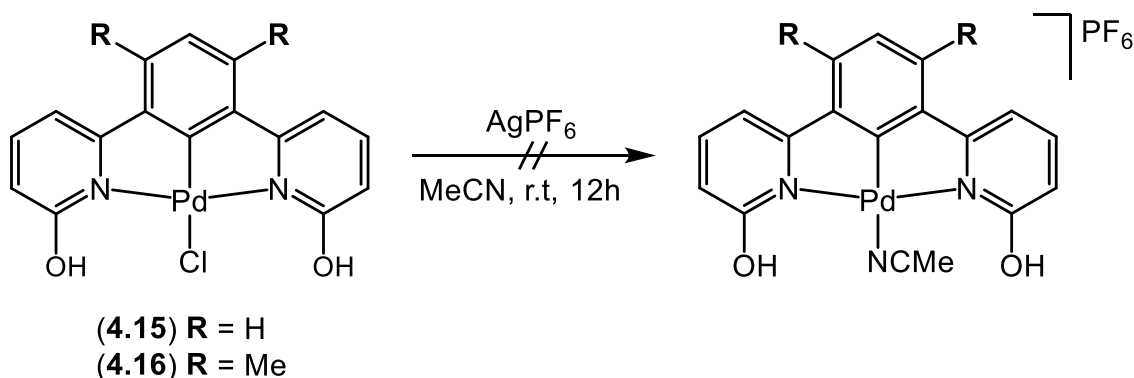


Scheme 4.26: Synthesis of **4.17** and **4.18** using chloride abstraction reactions

Again, the solubility of these complexes (**4.17** and **4.18**) was extremely poor in common organic solvents and thus DMSO was chosen as the best solvent to perform characterisation by NMR spectroscopy. Analysis of **4.17** and **4.18** revealed 3H singlet peaks at 1.98 and 2.08 ppm, respectively. These peaks are representative of the coordinated MeCN protons and indicated the successful replacement of the chloride with acetonitrile ligands. Further confirmation for this was found upon analysis by 2D HMQC NMR spectroscopy wherein a characteristic acetonitrile-methyl carbon peak was observed in each of their spectra. In the ^1H NMR spectra of **4.17** and **4.18**, methoxy protons were represented by a singlet, confirming the symmetry in these complexes. Compared to their starting materials, proton peaks in the aromatic region of both complexes were found to be shifted slightly upfield as a result of exchange reactions. In their ^{31}P NMR spectra, as is common to both complexes, was the presence of a septet peak at approximately -144 ppm, representing the counterion (PF_6^-). Additionally, the ^{19}F NMR spectra showed a doublet at about -73 ppm with a coupling constant of 711 Hz representing the fluorine counterion. Both complexes showed P-F stretching peaks in the range of 829-833 cm^{-1} . This stretching mode is representative of the PF_6^- counterion used throughout. Upon analysis of **4.17** and **4.18** by electrospray mass spectrometry, strong fragmentation peaks ascribed to $[\text{M-MeCN}]^+$ were observed at m/z 397.0181 and 425.0490, respectively.

Unfortunately, all attempts to grow single crystals of **4.17** and **4.18** suitable for analysis by X-ray diffraction studies were unsuccessful.

Chloride abstraction reactions of **4.15** and **4.16** in MeCN were attempted under the same conditions as previously used for **4.17** and **4.18** (Scheme 4.27). However, these reactions did not work, which was likely to be due to the insolubility of the starting materials in the reaction solvent (acetonitrile).

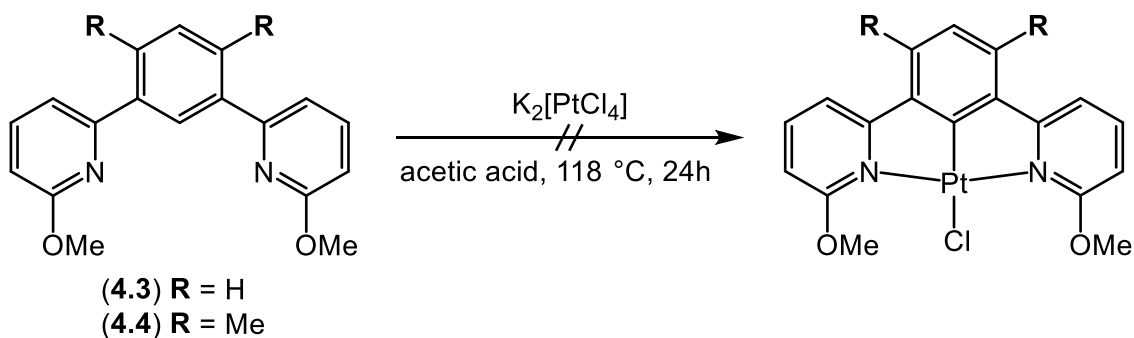


Scheme 4.27: Attempted synthesis of MeCN-containing pyridone complexes

4.3.7 Complexation of Tridentate N[^]C[^]N Ligands to Platinum (Pt^{II})

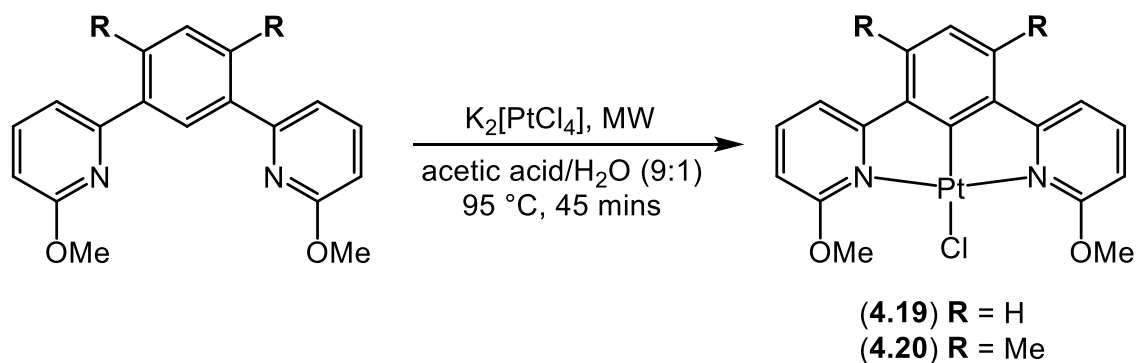
Following a thorough investigation of the reactivity of the tridentate N[^]C[^]N pyridine and pyridone ligands (**4.3-4.6**) with two different sources of palladium(II), platinum(II), as represented by K₂[PtCl₄], was chosen for reaction with these ligands. Platinum(II) derivatives with monoanionic N[^]C[^]N ligands are well-known and usually compared with the corresponding palladium(II) complexes,¹ as their derivatives, in most cases, show similar chemistry.

Under traditional heating, reactions of the pyridine pre-ligands (**4.3** and **4.4**) with K₂[PtCl₄] in glacial acetic acid have been tried (Scheme 4.28). Unfortunately, despite several modifications to the procedure, the ¹H NMR and mass spectra showed that these reactions resulted in the formation of a complex mixture of products.



Scheme 4.28: Attempted synthesis of **4.19** and **4.20** under traditional heating

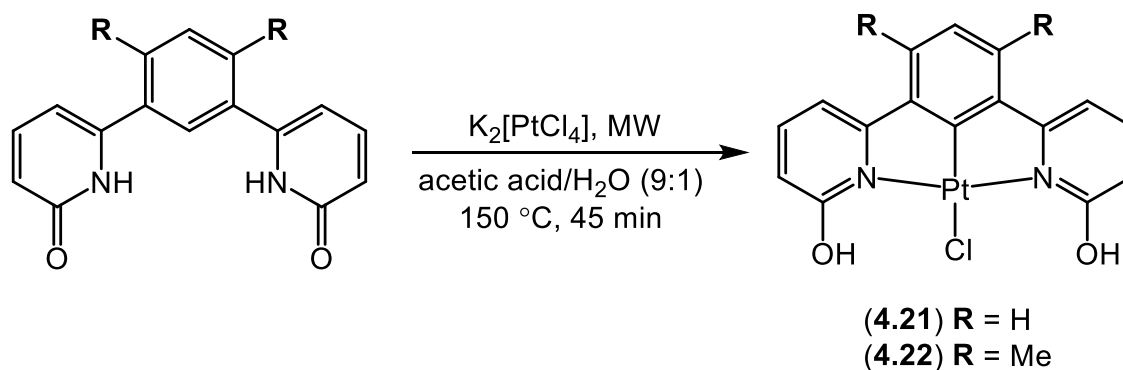
These failed attempts encouraged us to look for another procedure that may help to produce our desired products. The best method found to carry out these reactions was the use of microwave irradiation as a means of heating the reaction mixtures. The use of microwave reaction conditions between $K_2[PtCl_4]$ and the tridentate N[^]C[^]N pyridine ligands (**4.3** and **4.4**) at 90 °C in a mixture of acetic acid and H₂O (9:1) afforded the target platinum pincer complexes (**4.19** and **4.20**, respectively) in low yields (26 and 19%, respectively) within only 45 minutes (**Scheme 4.29**).



Scheme 4.29: Synthesis of **4.19** and **4.20** using microwave conditions

The identity of each complex was confirmed by the usual spectroscopic techniques. In the ¹H NMR spectra of **4.19** and **4.20**, the absence of the singlet peak representing C₂-H proton indicated C-H activation had been achieved by the metal centre (Pt^{II}). This was further confirmed through the analysis of both complexes by 2D HSQC NMR spectroscopy, wherein five and four proton-carbon correlations were observed for **4.19** and **4.20**, respectively. 6H singlets at 4.00 and 4.09 ppm, corresponding to the methoxy protons, were observed in the ¹H NMR spectra of **4.19** and **4.20**, respectively. This observation indicated the symmetry in these complexes, where both pendant methoxy groups are in the same environment. Upon analysis by electrospray mass spectrometry, complexes **4.19** and **4.20** each displayed a fragmentation peak assigned to the loss of chloride at *m/z* 486.0783 and 514.1086, respectively. Unfortunately, attempts to obtain single crystals suitable for analysis by X-ray crystallography were unsuccessful.

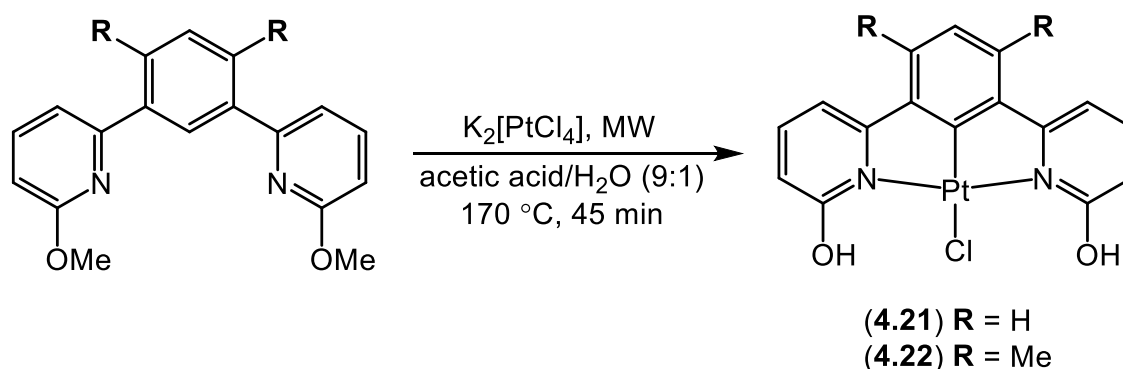
Under similar microwave conditions to those used for the reactions of palladium chloride (Na₂[PdCl₄]) with pyridone ligands, platinum pincer complexes **4.21** and **4.22** were obtained from the reactions of $K_2[PtCl_4]$ with the pyridone ligands (**4.5** and **4.6**, respectively). In these reactions, N[^]C[^]N ligand coordination to the Pt^{II} centre occurred to produce the poorly soluble species **4.21** (71%) and **4.22** (62%) (**Scheme 4.30**).



Scheme 4.30: Synthesis of **4.21** and **4.22** using microwave heating

Upon analysis by ^1H NMR spectroscopy, **4.21** and **4.22** revealed the absence of the $\text{C}_2\text{-H}$ proton, indicating the achievement of C-H activation on the phenyl ring. In general, the ^1H NMR pattern of the peaks in the aromatic region were consistent with the proposed structures and found to be different from those with the methoxy substituents (**4.19** and **4.20**). This was further confirmed by displaying five and four unique proton-carbon correlations in the 2D HSQC NMR spectra of **4.21** and **4.22**, respectively. Due to the hydrogen-bonding interaction with the chloride ligand, a downfield singlet assigned to the OH protons was observed at 11.29 and 11.34 ppm in the respective ^1H NMR spectra of **4.21** and **4.22**. A broad peak assigned to the $\nu(\text{OH})$ absorption band was observed between 2900 and 3100 cm^{-1} in the IR spectra of both complexes. Common to the chloride complexes, a fragmentation peak representing the loss of the chloride ligand at m/z 458.0468 and 486.0783 was observed upon analysis of **4.21** and **4.22** by ASAP mass spectrometry, respectively.

Alternatively, **4.21** and **4.22** could be also prepared, but in slightly lower yields, using the pyridine ligands (**4.3** and **4.4**) under microwave heating at 170 °C (**Scheme 4.31**).



Scheme 4.31: Alternative synthesis of **4.21** and **4.22** using pyridine ligands

These reactions are similar to those shown in **Scheme 4.25** and thought to be started by demethylation of the pyridine ligands followed by pyridone ligand coordination to the Pt^{II} centre, as previously confirmed for the analogous Pd^{II} complexes. It should be noted that the previous microwave reactions involving methoxy pre-ligands required a carefully controlled temperature. Therefore, it was important not to leave the microwave reaction mixtures at temperatures higher than 170 °C since this resulted in decomposition of the pincer complexes formed during the reactions. In contrast, using a lower temperature than 170 °C, such as 135 °C, led to the formation of a complex mixture of products in which the pyridine (**4.19** and **4.20**) and pyridone (**4.21** and **4.22**) complexes previously described could be identified. In addition, demethylation of only one methoxy group of the pyridine ligands was also possible, eventually forming a complex with two different pendant groups, OMe and OH (**Figure 4.18**).

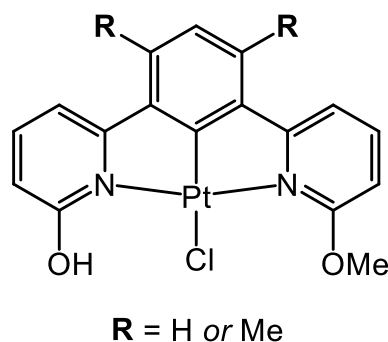


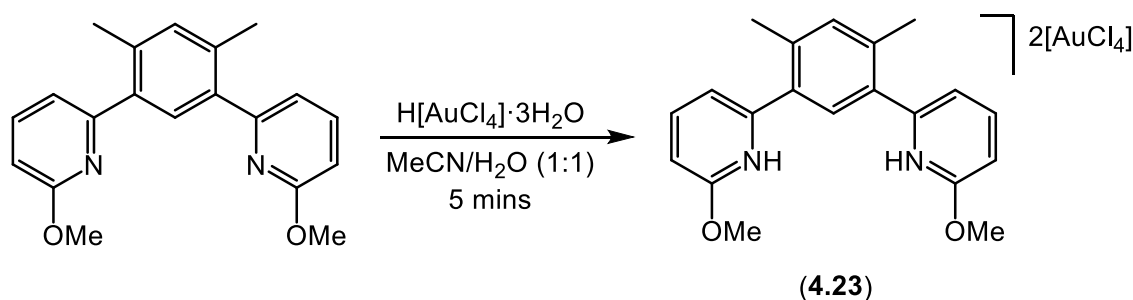
Figure 4.18: Possible product formation at 135 °C using microwave heating

4.3.8 Complexation of Tridentate N[^]C[^]N Ligands to Gold (Au^{III})

Following these previous reactions with Pd^{II} and Pt^{II}, the reactivity of 4,6-bis(2-(6-methoxypyridonyl)*m*-xylene (**4.4**) towards Au^{III} was investigated. Before starting to study the reactivity, it was realised that the reaction of gold(III) species with N[^]CH[^]N ligands is complicated, and different species might be expected to form during the reaction. Since **4.4** is able to act as a pincer, the main aim of this section was to prepare pure cycloaurated pincer complexes containing pyridine or pyridone ligands. Unfortunately, however, all attempts to cyclometallate **4.4** at an Au^{III} centre *through* C-H activation were ultimately unsuccessful, as the achievement of C-H activation *via* Au^{III} salts is considered as a difficult task and usually only obtained under harsh experimental conditions.³⁴

Tetrachloroauric acid, H[AuCl₄], was first chosen as a source of gold(III) for reaction with **4.4** in a mixture of acetonitrile and water (1:1) at room temperature for only five minutes. This reaction gave a yellow precipitate, which was identified as a di-

protonated salt, [(**4.4**)(κ^1 -H)₂][AuCl₄]₂ (**4.23**), in an 88% yield (**Scheme 4.32**). Although the ligand was reacted with one equivalent of H[AuCl₄], the reaction resulted in a cationic ligand countered by two tetrachloroaurate anions. It is possible to obtain a mono-protonated salt from this type of reaction;³⁴ however, this was not observed in the present study. The salt of the di-protonated ligand was characterised, *inter alia*, by single crystal X-ray diffraction studies.



Scheme 4.32: Synthesis of [(**4.4**)(κ^1 -H)₂][AuCl₄]₂ (**4.23**)

In the ¹H NMR spectrum of **4.23**, the singlets corresponding to the methyl and methoxy protons had shifted downfield compared to those for the free ligand by approximately 0.03 and 0.36 ppm, respectively. The presence of five downfield aromatic proton signals between 7.46 and 8.50 ppm indicated that *sp*² CH activation has not been achieved. The downfield position of these signals could be attributed to removal of electron density caused by a coordinated hydrogen. A resonance representing the newly introduced proton on the pyridyl ring (NH) was observed at 12.89 ppm as a broad singlet in the ¹H NMR spectrum when recorded in CD₃CN. The downfield position of the NH proton could be attributed to the hydrogen-bonding interaction with neighbouring species (which could be MeOH or AuCl₄). ¹³C{¹H} NMR spectroscopy also confirmed the inability of the Au^{III} salt to activate a C-H bond due to the presence of five unique aromatic CH carbon environments, which is in agreement with the expected structure. The N-H stretch was observed as a broad band at *ca.* 3200 cm⁻¹ in the IR spectrum of the di-protonated ligand. Upon analysis of **4.23** by ASAP-MS spectrometry, a di-protonated molecular ion peak at *m/z* 321.1602 (Calculated: *m/z* 321.1681) was observed.

Further confirmation of the structure of **4.23** was obtained *via* X-ray diffraction analysis (**Figure 4.19**). Single crystals suitable for analysis were grown by slow evaporation of a methanol solution of **4.23**. Selected bond lengths and angles are reported in **Table 4.9**.

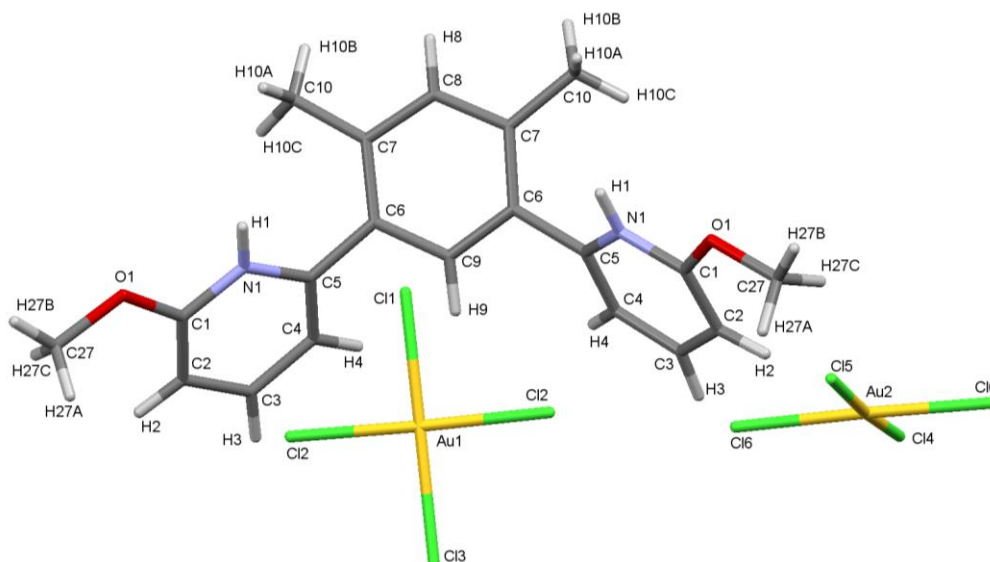


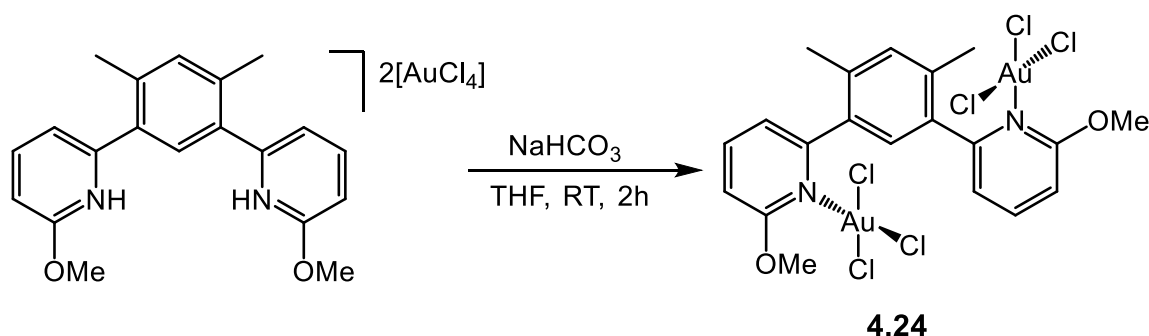
Figure 4.19: X-ray structure of **4.23** with full atom numbering

Table 4.9: Selected bond lengths and angles of complex **4.23**

Complex	Bond lengths (Å)			Bond angles (°)	
	N1-H1	C1-O1	Au-Cl	Cl1-Au-Cl2	C1-N1-C5
4.23	0.8600	1.328(18)	2.277(7)	89.32(12)	121.9(14)

The solid-state structure of **4.23** revealed a packing of the [HN⁺CH⁺NH] cation and two anionic [AuCl₄]⁻ with two methanol molecules of solvation, the latter being involved in hydrogen-bonding interactions with the NH protons. All bond lengths and angles in the di-protonated ligand and the tetrachloroaurate(III) counterion were as normal and consistent with those previously observed in the literature.³⁴ The two pyridyl rings are sterically forced by the two methyl groups into a perpendicular direction with respect to the plane of the central ring, with the N(1)-C(5)-C(6)-C(7) torsion angle of 55(2)°. It is clear that the organic cation was di-protonated at the pyridyl nitrogen atoms. The X-ray structure of the complex showed a slightly distorted square planar geometry about Au^{III} supported by four chloride ions with Au-Cl bond lengths of 2.277 ± 0.005 Å.

When **4.23** was treated with a stoichiometric amount of NaHCO₃ in THF at room temperature, deprotonation of the di-protonated ligand occurred to subsequently afford the doubly *N*-bonded gold Au^{III} complex, [κ^1 -*N,N*-(**4.4**)(AuCl₃)₂] (**4.24**) in a 72% yield (Scheme 4.33).



Scheme 4.33: Synthesis of $[\kappa^1\text{-}N,N\text{-(4.4)(AuCl}_3\text{)}_2]$ (**4.24**)

The ^1H NMR spectrum of **4.24** revealed five proton environments with two singlets at 7.52 and 8.10 ppm in the aromatic region, indicating that the ligand did not undergo C-H activation with the gold salt; instead, each pyridyl nitrogen atom was monodentately coordinated to the AuCl_3 . Due to the addition of electron density into the ligand system, the 6H singlet representing the methyl protons was shifted to slightly lower frequency (*ca.* 0.10 ppm) with respect to that for the protonated ligand (**4.23**), while the methoxy proton peak was found to not vary between the two spectra. Upon analysis of **4.24** by $^{13}\text{C}\{^1\text{H}\}$ NMR spectroscopy, eleven carbon peaks with five aromatic CH carbons and four quaternary carbon environments were observed. The N-H stretch was not observed in the IR spectrum of **4.24**, confirming successful deprotonation. Complex **4.24** also displayed a molecular ion peak at m/z 925.8959 by electrospray mass spectrometry.

The structure of **4.24** has been further confirmed by X-ray diffraction studies (**Figure 4.20**). Selected bond lengths and angles are reported in **Table 4.10**.

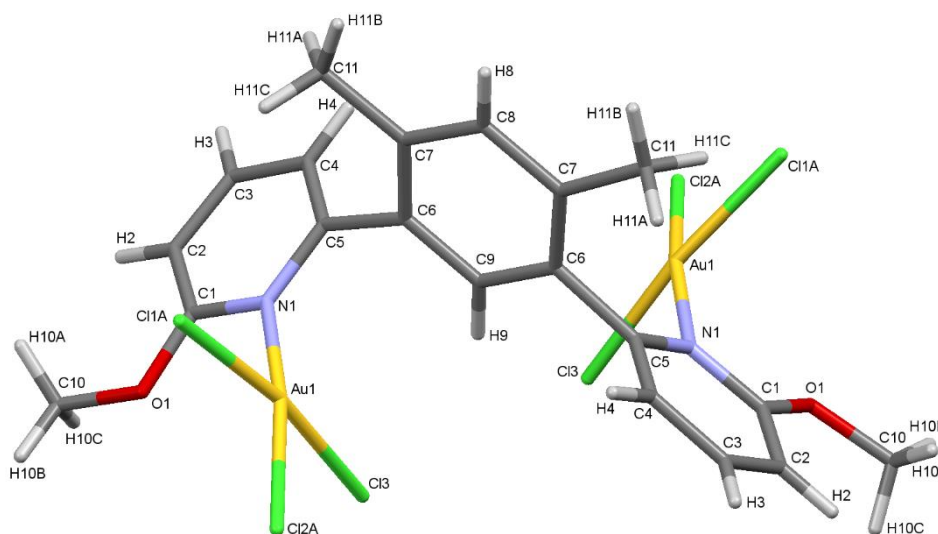


Figure 4.20: X-ray structure of **4.24** with full atom numbering

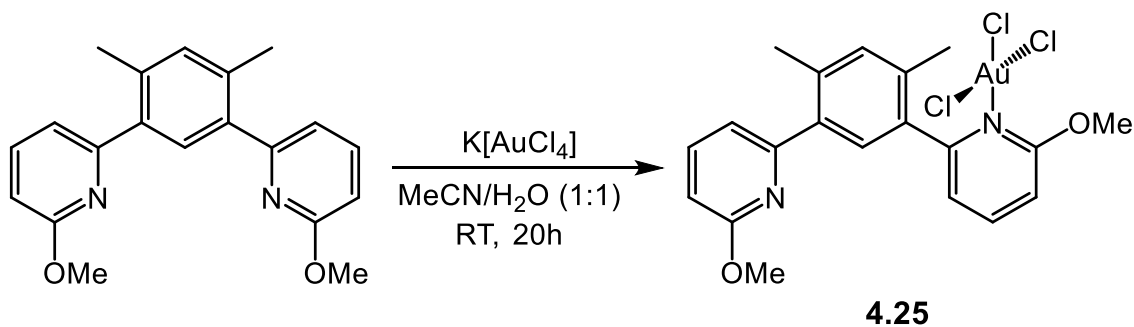
Table 4.10: Selected bond lengths and angles of complex **4.24**

Complex	Bond lengths (Å)				Bond angles (°)	
	Au-N1	Au-Cl2A	Au-Cl1A	Au-Cl3	N1-Au-Cl3	N1-Au-Cl2A
4.24	2.047(13)	2.392(11)	2.263(15)	2.293(4)	89.3(3)	169.8(5)

The single crystals of **4.24** were grown by slow diffusion of hexanes into a solution of the complex in dichloromethane. The X-ray data revealed a diaurated complex in which each pyridyl nitrogen was coordinated by AuCl₃, adopting a square planar geometry. The AuCl₃ unit was found to coordinate to the pyridyl ring in an almost perfectly perpendicular manner, as evidenced by the Cl(1A)-Au(1)-N(1)-C(5) torsion angle of 90.5(12)°. In addition, two chloride atoms were disordered with two possible locations and thus a total of five chloride positions are possible instead of three in each AuCl₃ unit. The data reported in **Table 4.10** shows that the Au-N(1) bond length of 2.047(13) Å was similar to those previously reported for Au^{III} complexes containing a pyridine ligand.³⁵⁻³⁸ The distance between the central metal and Cl2A was 2.392(11) Å and was significantly longer than those of 2.263(15) and 2.293(4) Å for Au-Cl1A and Au-Cl3, respectively. The difference could be attributed to the mutual *trans* effect of chloride atoms that are opposite to each other.³⁹

It should be noted that this diaurated complex (**4.24**) was found to be unstable in solution and decomposed to the free ligand, in particular after heating. Therefore, attempts to make this complex undergo cyclometallation were unsuccessful.

The decision to use K[AuCl₄] as the gold(III) source with **4.4**, rather than H[AuCl₄]·3H₂O, was made to give a different activity (**Scheme 4.34**).

**Scheme 4.34:** Synthesis of [κ^1 -N-(**4.4**)(AuCl₃)] (**4.25**)

In detail, the reaction illustrated in **Scheme 4.34** was carried out in a mixture of acetonitrile and water (1:1) at room temperature and resulted in the formation of the *N*-bonded gold Au^{III} complex (**4.25**) with excellent purity in an 89% yield. The identity of **4.25** was confirmed by ¹H and ¹³C{¹H} NMR and IR spectroscopies as well as by electrospray mass spectrometry and single crystal X-ray diffraction studies.

In addition to the two methoxy and two methyl proton peaks, the ¹H NMR spectrum of **4.25** revealed eight resonances in the aromatic region, indicating an unsymmetrical complex with non-activated C-H bonds. In this case, ligand coordination to the AuCl₃ occurred at only one pyridyl nitrogen atom, with another ring left “dangling”. The methoxy proton peaks observed at 3.95 ppm corresponded to those on the free ring while the other experienced a significant downfield shift (4.26 ppm) as a result of the pyridyl ring coordination. Moreover, analysis of **4.25** by ¹³C{¹H} NMR spectroscopy revealed twenty carbon peaks with eight aromatic CH carbons and eight quaternary carbon environments. The electrospray mass spectrum of **4.25** exhibited a protonated molecular ion peak at *m/z* 623.0334.

Further confirmation of the structure of **4.25** was provided by X-ray crystallography (**Figure 4.21**). Crystals suitable for analysis were grown from a dichloromethane solution of the complex layered with hexane. Selected bond distances and angles are reported in **Table 4.11**.

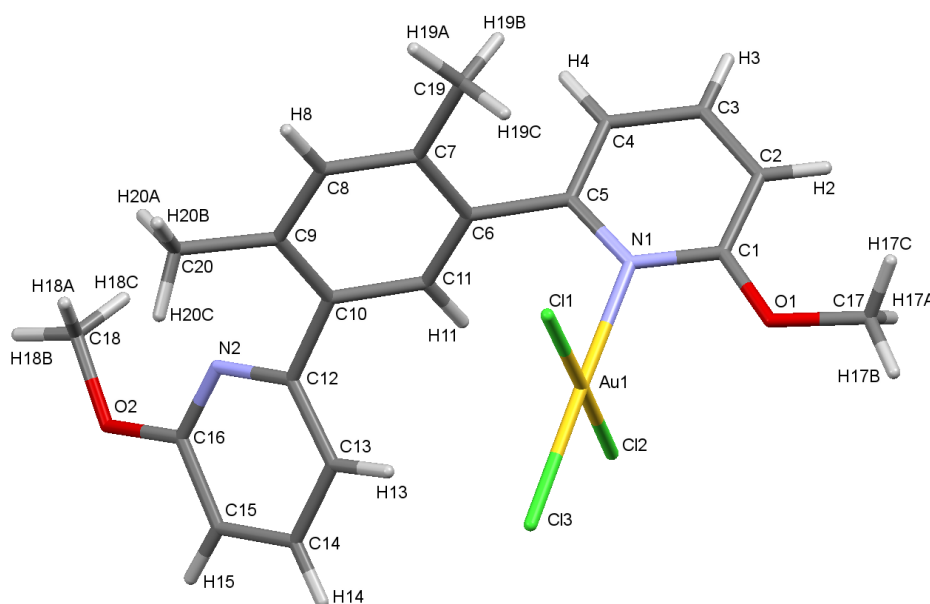


Figure 4.21: X-ray structure of **4.25** with full atom numbering

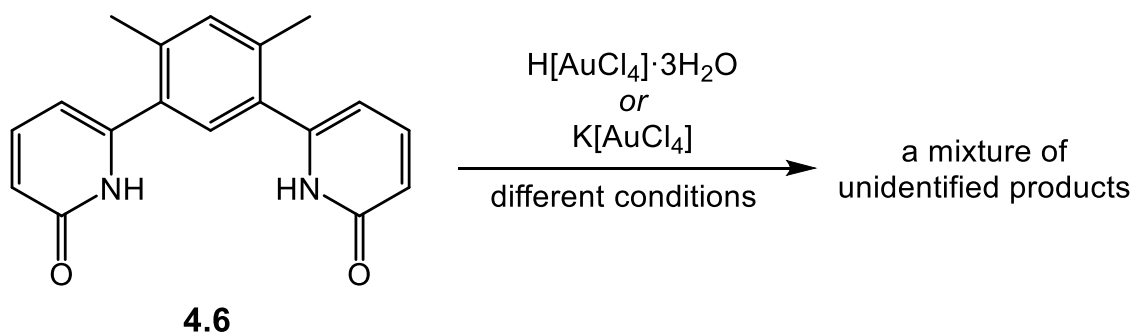
Table 4.11: Selected bond lengths and angles of complex **4.25**

Complex	Bond lengths (Å)				Bond angles (°)	
	Au-N1	Au-Cl3	Au-Cl1	Au-Cl2	N1-Au-Cl1	N1-Au-Cl3
4.25	2.079(10)	2.274(4)	2.254(4)	2.273(4)	91.3(3)	177.5(3)

The solid-state structure of **4.25** showed a gold(III) chloride (AuCl₃) core supported by an *N*-monodentate ligand with an almost perfectly square-planar geometry, as confirmed by the N1-Au-Cl1 and N1-Au-Cl3 bond angles (**Table 4.11**). The AuCl₃ unit was found to be nearly perpendicular to the plane of the pyridyl ring, as evidenced by the Cl(1)-Au(1)-N(1)-C(1) torsion angle of 100.9(10)°. All Au-X (X = N and Cls) bond lengths are within the typical range of values and in agreement with those reported in the literature.⁴⁰ The torsion angle between the pyridine and phenyl ring is distorted from 180°, which is likely to be due to the presence of the two methyl groups.

Again, all attempts under different conditions, including changes to the reaction solvent, temperature and time, to make this complex (**4.25**) to undergo cyclometallation were unsuccessful. This could be due to the instability and subsequent decomposition of the complex in various solutions.

When the tridentate pyridone ligand (**4.6**) was reacted under different conditions with either H[AuCl₄] \cdot 3H₂O or K[AuCl₄]. The reactions did not work particularly efficiently and instead resulted in complex mixtures of different products from which no overall product could be identified (**Scheme 4.35**). This was attributed to the presence of OH groups in the ligand.

**Scheme 4.35:** Attempted reactions to react **4.6** with different Au^{III} salts

4.4 Conclusions and Future Work

The objective of this chapter was to explore the reactivity of pyridine and pyridone pincer ligands towards different metal centres, such as Pd^{II}, Pt^{II} and Au^{III}. The reactions of pyridine and pyridone pincer ligands with these metals gave an important conclusion of this work, which is that the differences in the solubility and reactivity. Cyclometallation of the pyridine pincer ligands usually proceeds smoothly forming new products while the related pyridone pincer ligands require more forcing conditions due to solubility issues. Different reactivity patterns for these pincer ligands with different palladium sources were investigated. Under traditional heating, these ligands with K₂[PtCl₄] gave a mixture of products; however, pincer complexes were successfully obtained when their reactions exposed to microwave irradiation as a means of heating. Interesting reactivities were also explored on attempts to cyclometallate **4.4** with H[AuCl₄]·3H₂O and K[AuCl₄]. All complexes described in this chapter proved to have stable structures in solution over time.

In more detail, the reactions of **4.3** and **4.5** with Pd(OAc)₂ resulted in the formation of doubly cyclopalladated complexes (**4.7** and **4.10**, respectively), while ligand **4.4** gave an unusual dimeric structure (**4.9**) where C-H activation was not achieved. Interestingly, another dimeric complex (**4.8**) was formed as a minor product when **4.3** was reacted with Pd(OAc)₂. Treatment of **4.6** with Pd(OAc)₂ under different conditions was unsuccessful. It was desirable to obtain palladium pincer complexes from the previous reactions; therefore, undesirable mercurated complexes (**4.11** and **4.12**) were synthesised to undergo transmetallation reactions with Pd(OAc)₂. Unfortunately, the palladium acetate complexes could not be isolated, and instead treatment of the resultant products with LiCl was carried out to afford palladium chloride complexes (**4.13** and **4.14**), which were also obtained by direct synthesis with Na₂[PdCl₄] in high purity. After several unsuccessful attempts, a new method for the synthesis of pyridone pincer complexes with a Pd^{II} centre was explored through the use of microwave technology. In this case, 150 °C with a maximum pressure of 150 psi were sufficient to afford **4.15** and **4.16** from **4.5** and **4.6**, respectively. Alternatively, these products (**4.15** and **4.16**) could be also obtained, with lower yields, from the related methoxy ligands but at a higher temperature (170 °C). The potential of the Pd-Cl complexes (**4.13** and **4.14**) to act as precursors to cation-anion pairs was explored using a halide abstraction reaction in acetonitrile with AgPF₆ to yield **4.17** and **4.18**, respectively. All palladium complexes described in this chapter were found to be stable in solution over time.

Despite several modifications to the traditional heating procedure, reactions of the pyridine (**4.3** and **4.4**) and pyridone (**4.5** and **4.6**) ligands with $K_2[PtCl_4]$ usually resulted in a complex mixture of unidentifiable products. However, employment of the microwave reaction conditions with the tridentate N[^]C[^]N pyridine ligand (**4.3** and **4.4**) at 90 °C afforded **4.19** and **4.20**, respectively; increasing the temperature of the reactions to 170 °C resulted in formation of **4.21** and **4.22**, respectively. Complexes **4.21** and **4.22** could be also obtained in an alternative manner whereby 150 °C with a maximum pressure of 150 psi were used for the reactions starting with **4.5** and **4.6**, respectively. It was concluded that the reactions of **4.3** and **4.4** with $K_2[PtCl_4]$ to obtain **4.21** and **4.22** were initiated by the demethylation of the pyridine ligands followed by pyridone ligand coordination to the Pt^{II} centre. In addition, microwave reactions involving methoxy ligands required carefully controlled temperatures to avoid decomposition or excessive formation of by-products.

All attempts, including traditional and direct heating, as well as transmetallation, and cyclometallation of 4,6-bis(2-(6-methoxypyridonyl)*m*-xylene (**4.4**) at a gold(III) centre “*through* C-H activation” were unsuccessful. Instead, reactions of **4.4** with $H[AuCl_4] \cdot 3H_2O$ and $K[AuCl_4]$ gave **4.23** and **4.25**, respectively. In addition, treatment of the di-protonated **4.23** with a stoichiometric amount of $NaHCO_3$ in THF at room temperature afforded the doubly *N*-bonded gold Au^{III} complex (**4.24**) in a good yield

Since all the pincer ligands used in this chapter were symmetrical, it would be of interest to design and synthesis new pyridine-based, unsymmetrical, monoanionic N[^]C[^]N pincer ligands (**Fig. 4.22**) and investigate their reactivity and selectivity towards various transition metals.

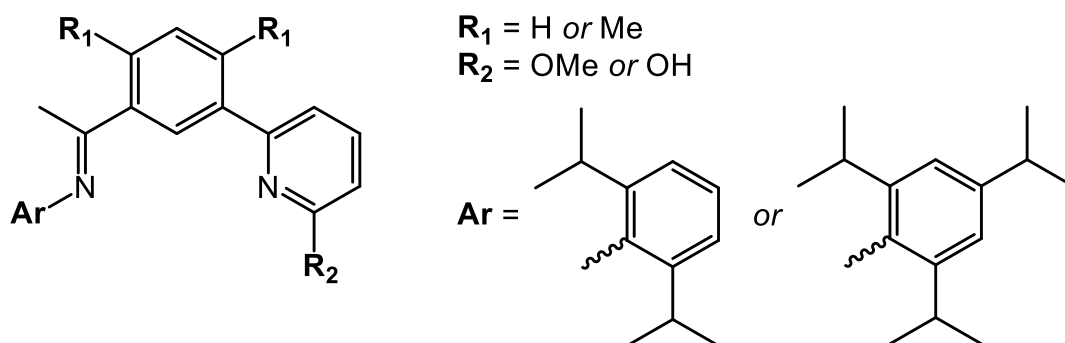


Figure 4.22: Unsymmetrical N[^]C[^]N pincer ligands

References

1. D. J. Cárdenas, A. M. Echavarren and M. C. Ramírez de Arellano, *Organometallics*, 1999, **18**, 3337.
2. R. Simayi, *Synthesis and Reaction Chemistry of Various N,N,C- and O,N,C-Palladium Pincer Complexes*, The University of Leicester, 2017.
3. W. B. Cross, E. G. Hope, Y. Lin, S. A. Macgregor, K. Singh, G. A. Solan and N. Yahya, *Chem. Commun.*, 2013, **49**, 1918.
4. S. Trofimenko, *J. Am. Chem. Soc.*, 1971, **93**, 1808.
5. G. v. Koten, P. Steenwinkel, R. Gossage, T. Maunula and D. Grove, *Chem. Eur. J.*, 1998, **4**, 763.
6. A. V. Chuchuryukin, R. Huang, E. E. van Faassen, G. P. van Klink, M. Lutz, J. C. Chadwick, A. L. Spek and G. van Koten, *Dalton Trans.*, 2011, **40**, 8887.
7. M. H. Rietveld, L. Nagelholt, D. M. Grove, N. Veldman, A. L. Spek, M. U. Rauch, W. A. Herrmann and G. van Koten, *J. Organomet. Chem.*, 1997, **530**, 159.
8. Van der Zeijden, Adolphus AH, G. Van Koten, R. Luijk, K. Vrieze, C. Slob, H. Krabbendam and A. L. Spek, *Inorg. Chem.*, 1988, **27**, 1014.
9. M. Q. Slagt, G. Rodríguez, M. M. Grutters, R. J. Klein Gebbink, W. Klopper, L. W. Jenneskens, M. Lutz, A. L. Spek and G. van Koten, *Chem. Eur. J.*, 2004, **10**, 1331.
10. M. Contel, M. Stol, M. A. Casado, G. P. van Klink, D. D. Ellis, A. L. Spek and G. van Koten, *Organometallics*, 2002, **21**, 4556.
11. P. A. Bonnardel, R. Parish and R. G. Pritchard, *J. Chem. Soc. Dalton Trans.*, 1996, 3185.
12. B. Soro, S. Stoccoro, G. Minghetti, A. Zucca, M. A. Cinellu, S. Gladiali, M. Manassero and M. Sansoni, *Organometallics*, 2005, **24**, 53.
13. M. Beley, J. P. Collin and J. P. Sauvage, *Inorg. Chem.*, 1993, **32**, 4539.
14. C. M. Hartshorn and P. J. Steel, *Aust. J. Chem.*, 1995, **48**, 1587.
15. C. M. Hartshorn and P. J. Steel, *Organometallics*, 1998, **17**, 3487.
16. R. H. Crabtree, *New J. Chem.*, 2011, **35**, 18.
17. C. M. Moore and N. K. Szymczak, *Chem. Commun.*, 2013, **49**, 400.
18. S. Musa, S. Fronton, L. Vaccaro and D. Gelman, *Organometallics*, 2013, **32**, 3069.
19. B. Paul, K. Chakrabarti and S. Kundu, *Dalton Trans.*, 2016, **45**, 11162.

20. A. R. Sahoo, F. Jiang, C. Bruneau, G. Sharma, S. Suresh and M. Achard, *RSC Advances*, 2016, **6**, 100554.
21. J. Shi, B. Hu, X. Chen, S. Shang, D. Deng, Y. Sun, W. Shi, X. Yang and D. Chen, *ACS Omega*, 2017, **2**, 3406.
22. S. Y. de Boer, T. J. Korstanje, S. R. La Rooij, R. Kox, J. N. Reek and van der Vlugt, Jarl Ivar, *Organometallics*, 2017, **36**, 1541.
23. T. J. Donohoe, L. P. Fishlock and P. A. Procopiou, *Org. Lett.*, 2008, **10**, 285.
24. C. M. Moore, B. Bark and N. K. Szymczak, *ACS Catalysis*, 2016, **6**, 1981.
25. J. G. Williams, *Chem. Soc. Rev.*, 2009, **38**, 1783.
26. T. Honda, R. Takahashi and H. Namiki, *J. Org. Chem.*, 2005, **70**, 499.
27. B. Avitia, E. MacIntosh, S. Muhia and E. Kelson, *Tetrahedron Lett.*, 2011, **52**, 1631.
28. M. C. Bonifacio, C. R. Robertson, J. Jung and B. T. King, *J. Org. Chem.*, 2005, **70**, 8522.
29. K. Nakamoto, *Infrared and Raman spectra of inorganic and coordination compounds*, Wiley Interscience, New York, 1986.
30. S. Sarkar, K. P. McGowan, J. A. Culver, A. R. Carlson, J. Koller, A. J. Peloquin, M. K. Veige, K. A. Abboud and A. S. Veige, *Inorg. Chem.*, 2010, **49**, 5143.
31. J. E. Bercaw, A. C. Durrell, H. B. Gray, J. C. Green, N. Hazari, J. A. Labinger and J. R. Winkler, *Inorg. Chem.*, 2010, **49**, 1801.
32. L. Piche, J. Daigle, R. Poli and J. P. Claverie, *Eur. J. Inorg. Chem.*, 2010, **2010**, 4595.
33. R. F. Carina, A. F. Williams and G. Bernardinelli, *J. Organomet. Chem.*, 1997, **548**, 45.
34. S. Stoccoro, G. Alesso, M. A. Cinellu, G. Minghetti, A. Zucca, M. Manassero and C. Manassero, *Dalton Trans.*, 2009, 3467.
35. V. Ferretti, P. Gilli, V. Bertolasi, G. Marangoni, B. Pitteri and G. Chessa, *Acta Crystallogr. Sect. C: Cryst. Struct. Commun.*, 1992, **48**, 814.
36. K. Ortner and U. Abram, *Inorg. Chem. Comm.*, 1998, **1**, 251.
37. V. Bertolasi, G. Annibale, G. Marangoni, G. Paolucci and B. Pitteri, *J. Coord. Chem.*, 2003, **56**, 397.
38. T. V. Segapelo, I. A. Guzei, L. C. Spencer, W. E. Van Zyl and J. Darkwa, *Inorg. Chim. Acta*, 2009, **362**, 3314.

39. A. G. Orpen and M. J. Quayle, *J. Chem. Soc. Dalton Trans.*, 2001, 1601.
40. H. von Wachenfeldt, A. V. Polukeev, N. Loganathan, F. Paulsen, P. Röse, M. Garreau, O. F. Wendt and D. Strand, *Dalton Trans.*, 2015, **44**, 5347.

Chapter 5

Experimental

5.1 General Experimental

All experiments, unless otherwise stated, were carried out under an inert atmosphere of dry nitrogen using standard Schlenk techniques or/and a nitrogen-containing glove box. Microwave reactions were performed using a *CEM-Discover Explorer Hybrid* instrument.

5.1.1 Reagents

2,6-Dibromopyridine (Aldrich, 98%), sodium sticks, in mineral oil (Alfa Aesar, 99%), potassium carbonate (Fisher Scientific Co.), iodine (Fisher Scientific Co.), potassium hydroxide (Fisher Scientific Co.), hydrogen peroxide (VWR International, 30%), magnesium sulfate (Fisher Scientific Co.), phenylboronic acid (Aldrich, 97%), 4-fluorophenylboronic acid (Aldrich), 2-bromotoluene (Aldrich, 99%), 4-bromobenzotrifluoride (Aldrich, 99%), 4-bromotoluene (Aldrich, 98%), palladium(II) acetate, palladium (II) chloride (Fluorochem, 99%), hydrogen tetrachloroaurate(III) trihydrate (Alfa Aesar, 99.99%), potassium gold(III) chloride (Aldrich, 98%), (*n*-butyllithium solution (1.6 M in hexane) (Aldrich), triisopropyl borate (Aldrich, $\geq 98\%$), *m*-xylene (Hopkin & Williams Ltd, 99%), bromine (Aldrich, reagent grade), 1,3-dibromobenzene (Aldrich, 97%), zinc chloride solution (1.0 M in diethyl ether), ethylenediaminetetraacetic acid disodium salt dihydrate (EDTA) (Aldrich, 99%), hydrobromic acid (HBr) (Lancaster Synthesis, aqueous 48%), tributyltin chloride (Aldrich, 96%) and lithium chloride (Aldrich, 99.9%) were all used as received.

5.1.2 Solvents

Methanol, toluene, tetrahydrofuran (THF), acetonitrile and diethyl ether were distilled before being used as main solvents in the synthesis reactions while dichloromethane, hexane (fraction from petroleum ether), diethyl ether (used for work up), acetonitrile, methanol (used for Pd(OAc)₂ reactions), ethanol and glacial acetic acid were not subjected to any further purification and used as received from the Fisher Scientific Co. Chloroform-D (CDCl₃) (Apollo Scientific Ltd, 99.8%, 0.03% TMS) was used as a solvent in some NMR scale reactions.

5.1.3 Physical Measurements

5.1.3.1 Elemental Analysis

Elemental analysis (combustion analysis) of carbon, hydrogen, and nitrogen was performed on dry, clean and microcrystalline products at the Science Technical Support Unit, London Metropolitan University.

5.1.3.2 Infrared Spectroscopy

Infrared spectra for all novel ligands and complexes were obtained using solid state Perkin Elmer Spectrum One FTIR instrument. Air background scans were performed for all samples and the range of the scans was 600-4000 cm^{-1} .

5.1.3.3 Mass Spectrometry

The electrospray (ES) mass spectra were recorded on a micromass Quattro LC mass spectrometer in either acetonitrile or methanol as solvents. Fast atom bombardment (FAB) mass spectra were obtained using a Kratos Concept mass spectrometer with NBA as matrix. For samples analysed using ASAP (atmospheric solids analysis probe), a Waters Xevo QToF mass spectrometer was used.

5.1.3.4 Nuclear Magnetic Resonance (NMR) Spectroscopy

NMR spectroscopic data were collected using a Bruker DRX 400 spectrometer at 400.13 (^1H), 161.98 (^{31}P), 376.46 (^{19}F) and 100.61 MHz (^{13}C) or using a Bruker Avance III 500 spectrometer at 500.13 (^1H) and 125.77 MHz (^{13}C). Samples were prepared as solutions using deuterated solvents and run at ambient temperature unless otherwise stated. All spectra were recorded in ppm; ^1H and ^{13}C NMR spectra were referred to an internal reference (TMS) while ^{19}F and ^{31}P NMR spectra were referred externally to CFCl_3 and H_3PO_4 , respectively.

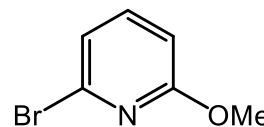
5.1.3.5 X-ray Crystallography

X-ray diffraction of single crystals was performed by Mr. Kuldip Singh at the University of Leicester using a Bruker APEX 2000 CCD diffractometer. The data were corrected for Lorentz and polarisation effects and empirical absorption corrections applied. Structure solution by direct methods and structure refinement based on full-matrix least-squares on F^2 employed SHELXTL version 6.10.¹ H atoms were included in calculated positions (C-H = 0.96 – 1.00 Å) riding on the bonded atom with isotropic displacement parameters set to 1.5 $U_{\text{eq}}(\text{C})$ for methyl H atoms and 1.2 $U_{\text{eq}}(\text{C})$ for all other H atoms. All non-H atoms were refined with anisotropic displacement parameters.

5.2 Experimental Procedures for Chapter 2

5.2.1 Synthesis of 6-bromo-2-methoxypyridine (2.1)

Procedure was based on that described by Snieckus *et al.*² A three necked round bottom flask, equipped with a magnetic stir bar and reflux condenser was evacuated and backfilled with nitrogen. The flask was loaded with freshly distilled methanol (14 mL) and small pieces of sodium metal (1.35 g, 58.5 mmol, 1.7 eq.: weighed on the balance in a beaker of hexane) added. Once addition was completed, the mixture was stirred to react. The flask was heated (with a heat gun) to react the majority of the sodium. 2,6-Dibromopyridine (8.167 g, 34.5 mmol) was added through a solids funnel followed by more methanol (26 mL). The mixture was heated at reflux for 23 h (set oil bath temperature to 120 °C). After cooling to room temperature, 5% NaHCO₃ (100 mL) was added and the mixture was extracted with diethyl ether (3 x 100 mL). The combined organic layers were washed with brine (2 x 20 mL), dried over MgSO₄ and concentrated under reduced pressure affording the product (2.1) as a light brown oil (5.126 g, 79%). ¹H NMR (400 MHz, CDCl₃, 298 K): δ 3.92 (s, OMe, 3H), 6.67 (dd, *J*_{H-H} 8.1, 0.5, 1H), 7.04 (dd, *J*_{H-H} 7.4, 0.5, 1H), 7.39 (t, *J*_{H-H} 8.1, 1H). ¹³C{¹H} NMR (100 MHz, CDCl₃, 298 K): δ 54.0 (OMe), 109.3 (CH), 120.1 (CH), 138.6 (CH), 140.3 (C), 163.7 (C). Data are consistent with those reported in the literature.²



Synthesis of Boronic Acids

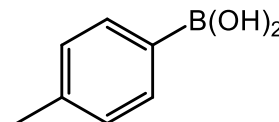
General Procedure for Synthesis of Aryl-B(OH)₂

A medium-sized oven-dried Schlenk flask equipped with a magnetic stir bar was evacuated and backfilled with nitrogen. The flask was charged with the appropriate Ar-Br (0.0096 mol) in dry THF (45 mL), cooled to -78 °C (dry-ice acetone) and *n*-BuLi (6.3 mL, 0.0099 mol, 1.1 eq.) added dropwise over 30 min. The mixture was allowed to stir at -78 °C for 30 min and then triisopropylborate (5.7 mL, 4.63 g, 0.0246 mol, 2.5 eq.) was added dropwise. The mixture was allowed to stir at -78 °C for a further 30 min and then warmed to room temperature and stirred overnight to produce a white precipitate. Aqueous 2M HCl (10 mL) was then added and the solution was stirred for 10 min until all the precipitate had dissolved. The organic phase was separated and the aqueous phase extracted with diethyl ether (3 x 30 mL). The combined organic extracts were dried over anhydrous MgSO₄ and following filtration, the volatiles were removed under reduced

pressure (firstly on a rotary evaporator and then on a vacuum line) to give the appropriate Ar-B(OH)₂ as white solids.

5.2.2 Synthesis of 4-methylphenylboronic acid (2.2)

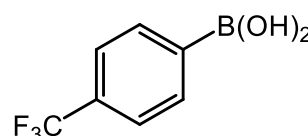
This was prepared from 4-bromotoluene (1.65 g, 0.0096 mol) and after work up gave **2.2** (1.29 g, 98%). ¹H NMR (400 MHz, CDCl₃, 298 K): δ 2.36 (s, Me, 3H), 7.23 (d, *J*_{H-H} 7.8, 2H),



8.05 (d, *J*_{H-H} 7.8, 2H). ¹³C{¹H} NMR (100 MHz, CDCl₃, 298 K): δ 21.0 (Me), 127.9 (CH), 132.6 (C), 134.8 (CH), 142.0 (C). MS (ES): *m/z* 135 [M]⁺, 253 [2M-H₂O]⁺. Data are consistent with those reported in the literature.³

5.2.3 Synthesis of (4-trifluoromethyl)-phenylboronic acid (2.3)

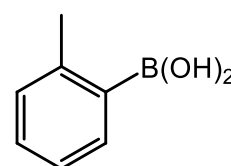
This was prepared from 4-(trifluoromethyl)phenyl bromide (2.16 g, 0.0096 mol) and after work up gave **2.3** (1.70 g, 93%). ¹H NMR (400 MHz, MeOD, 298 K): δ 7.51 (d, *J*_{H-H}



7.8, 2H), 7.78 (d, *J*_{H-H} 7.8, 2H). ¹³C{¹H} NMR (100 MHz, MeOD, 298 K): δ 117.7 (C), 124.6 (q, ³*J*_{C-F} 3.1, CH), 125.3 (q, ¹*J*_{C-F} 270.3, CF₃), 132.3 (q, ²*J*_{C-F} 31.7, C), 134.8 (CH). ¹⁹F NMR (376 MHz, MeOD, 298 K): δ -64.1 (s, CF₃). MS (ES): *m/z* 189 [M]⁺, 361 [2M-H₂O]⁺. Data are consistent with those reported in the literature.³

5.2.4 Synthesis of 2-methylphenylboronic acid (2.4)

This was prepared from 2-bromotoluene (1.65 g, 0.0096 mol) and after work up gave **2.4** (1.25 g, 95%). ¹H NMR (400 MHz, CDCl₃, 298 K): δ 2.81 (s, 3H, CH₃), 7.25-7.32 (m, 2H), 7.45 (td, *J*_{H-H}



*J*_{H-H} 7.4, 1.5, 1H), 8.21 (dd, *J*_{H-H} 7.4, 1.3, 1H). ¹³C{¹H} NMR (100 MHz, CDCl₃, 298 K): δ 23.1 (Me), 125.2 (CH), 130.4 (C), 130.6 (CH), 132.2 (CH), 137.2 (CH), 146.2 (C). MS (ES): *m/z* 135 [M]⁺, 253 [2M-H₂O]⁺. Data are consistent with those reported in the literature.⁴

General Procedure for Synthesis of 6-aryl-2-methoxypyridine Ligands

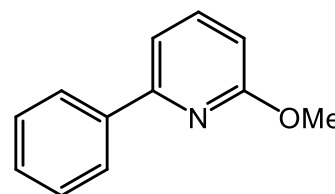
A medium-sized Schlenk flask equipped with a magnetic stir bar was evacuated and backfilled with nitrogen. The flask was loaded with 6-bromo-2-methoxypyridine (1 eq.), 2M K₂CO₃ (2 eq.), Pd(PPh₃)₄ (0.02 eq.) and toluene (57 mL). The contents were stirred for 15 min to give a yellow solution. Aryl-boronic acid (1.1 eq.) was added as a slurry in ethanol (24 mL) and the mixture was then heated at 90 °C (oil-bath temperature)

for about 72 h. On cooling to room temperature, 30% hydrogen peroxide (1.4 mL) was introduced and the contents were stirred at room temperature for 30 min. the reaction mixture was then extracted with diethyl ether (3 x 80 mL) and the combined organic layers were washed with water (2 x 70 mL) and then with brine (1 x 50 mL) before being dried over MgSO₄. Following filtration, the volatiles were removed under reduced pressure.

The catalyst residues were removed *via* a short (10 cm) silica column employing dichloromethane: petroleum ether: diethyl ether (80: 20: 1) as the eluting solvent; the catalyst residues stayed on the base of the column. After removing the solvent under reduced pressure (rotary evaporator and Schlenk line), the product was obtained.

5.2.5 Synthesis of 6-phenyl-2-methoxypyridine (2.5)

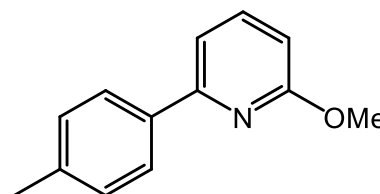
This was prepared from 6-bromo-2-methoxy pyridine (2.1) (1.5 g, 7.98 mmol) and phenylboronic acid (1.07 g, 8.77 mmol) and after work up and column chromatography gave 2.5 as a colourless oil (1.022 g, 69%).



¹H NMR (400 MHz, CDCl₃, 298 K): δ 4.01 (s, OMe, 3H), 6.60 (d, *J*_{H-H} 8.2, 1H), 7.29 (d, *J*_{H-H} 7.4, 1H), 7.35 (m, 1H), 7.40 (m, 2H), 7.50 (t, *J*_{H-H} 8.1, 1H), 8.02 (m, 2H). ¹³C{¹H} NMR (100 MHz, CDCl₃, 298 K): δ 53.3 (OMe), 109.4 (CH), 112.9 (CH), 126.8 (CH), 128.7 (CH), 129 (CH), 139.2 (C), 139.3 (CH), 154.7 (C) and 163.9 (C). MS (ES): *m/z* 186 [M]⁺. Data are consistent with those reported in the literature.⁵

5.2.6 Synthesis of 6-(4-methylphenyl)-2-methoxypyridine (2.6)

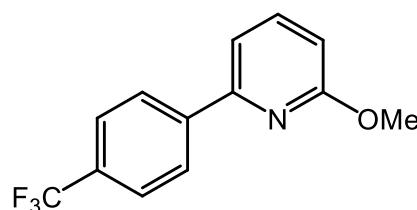
This was prepared from 6-bromo-2-methoxy pyridine (2.1) (1.5 g, 7.98 mmol) and 4-methylphenylboronic acid (2.2) (1.62 g, 11.9 mmol) and after work up and column chromatography gave 2.6 as a colourless oil



(1.52 g, 97%). ¹H NMR (400 MHz, CDCl₃, 298 K): δ 2.31 (s, Me, 3H), 3.95 (s, OMe, 3H), 6.50 (d, *J*_{H-H} 8.2, 1H), 7.14 (d, *J*_{H-H} 8.0, 2H), 7.17 (d, *J*_{H-H} 7.4, 1H), 7.40 (t, *J*_{H-H} 8.0, 1H), 7.80 (d, *J*_{H-H} 8.2, 2H). ¹³C{¹H} NMR (100 MHz, CDCl₃): δ 21.3 (Me), 53.1 (OMe), 108.8 (CH), 112.4 (CH), 126.6 (CH), 129.3 (CH), 136.4 (C), 138.8 (C), 139.1 (CH), 154.7 (C), 163.7 (C). MS (ES): *m/z* 200 [M]⁺. Data are consistent with those reported in the literature.⁶

5.2.7 Synthesis of 6-(4-trifluoromethylphenyl)-2-methoxypyridine (2.7)

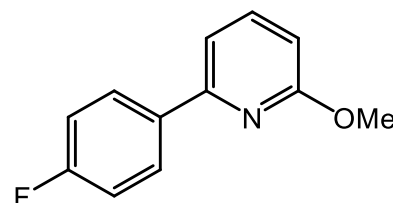
This was prepared from 6-bromo-2-methoxy pyridine (**2.1**) (1.5 g, 7.98 mmol) and (4-trifluoromethyl)phenylboronic acid (**2.3**) (1.66 g, 8.77 mmol) and after work up and column chromatography



gave **2.7** as a dark green oil (1.47 g, 72%). ^1H NMR (400 MHz, CDCl_3 , 298 K): δ 4.03 (s, OMe, 3H), 6.74 (d, $J_{\text{H-H}}$ 8.2, 1H), 7.36 (d, $J_{\text{H-H}}$ 7.4, 1H), 7.64 (t, $J_{\text{H-H}}$ 7.4, 1H), 7.69 (d, $J_{\text{H-H}}$ 8.1, 2H), 8.13 (d, $J_{\text{H-H}}$ 8.7, 2H). $^{13}\text{C}\{^1\text{H}\}$ NMR (100 MHz, CDCl_3 , 298 K): δ 53.2 (OMe), 110.4 (CH), 113.2 (CH), 124.4 (q, $^1J_{\text{C-F}}$ 271.7, CF_3), 125.5 (q, $^3J_{\text{C-F}}$ 3.1, CH), 126.9 (CH), 130.5 (q, $^2J_{\text{C-F}}$ 32.1, C), 139.2 (CH), 142.4 (C), 153.0 (C), 163.9 (C). ^{19}F NMR (376 MHz, CDCl_3 , 298 K): δ -62.5 (s, CF_3). MS (ES): m/z 254 $[\text{M}]^+$. Data are consistent with those reported in the literature.⁷

5.2.8 Synthesis of 6-(4-fluorophenyl)-2-methoxypyridine (2.8)

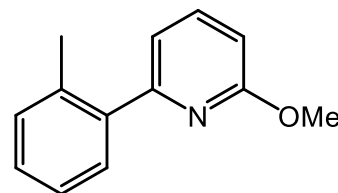
This was prepared from 6-bromo-2-methoxy pyridine (**2.1**) (1.5 g, 7.98 mmol) and 4-fluorophenylboronic acid (1.22 g, 8.77 mmol) and after work up and column chromatography



gave **2.8** as a light brown oil (1.37 g, 85%). $^1\text{H}\{^{19}\text{F}\}$ NMR (400 MHz, CDCl_3 , 298 K): δ 4.02 (s, OMe, 3H), 6.68 (d, $J_{\text{H-H}}$ 8.2, 1H), 7.12 (d, $J_{\text{H-H}}$ 8.8, 2H), 7.2 (d, $J_{\text{H-H}}$ 7.4, 1H), 7.61 (t, $J_{\text{H-H}}$ 8.1, 1H), 8.02 (d, $J_{\text{H-H}}$ 9.0, 2H). $^{13}\text{C}\{^1\text{H}\}$ NMR (100 MHz, CDCl_3 , 298 K): δ 53.2 (OMe), 109.1 (CH), 112.4 (CH), 115.4 (d, $^2J_{\text{C-F}}$ 22.1, CH), 128.4 (d, $^3J_{\text{C-F}}$ 8.0, CH), 135.2 (C), 139.2 (CH), 153.6 (C), 163.4 (d, $^1J_{\text{C-F}}$ 248.4, C), 163.8 (C). ^{19}F NMR (376 MHz, CDCl_3 , 298 K): δ -113.3 (s, F). MS (ES): m/z 204 $[\text{M}]^+$. Data are consistent with those reported in the literature.⁷

5.2.9 Synthesis of 6-(2-methylphenyl)-2-methoxypyridine (2.9)

This was prepared from 6-bromo-2-methoxy pyridine (**2.1**) (1.5 g, 7.98 mmol) and 2-methylphenylboronic acid (**2.4**) (1.19 g, 8.77 mmol) and after work up and column chromatography



gave **2.9** as a yellow oil (1.10 g, 69%). ^1H NMR (400 MHz, CDCl_3 , 298 K): δ 2.44 (s, Me, 3H), 3.95 (s, OMe, 3H), 6.60 (dd, $J_{\text{H-H}}$ 8.2, 0.5, 1H), 6.90 (dd, $J_{\text{H-H}}$ 7.5, 0.5, 1H), 7.22-7.3 (m, 3H), 7.40 (d, $J_{\text{H-H}}$ 6.2, 1H), 7.60 (t, $J_{\text{H-H}}$ 7.3, 1H). $^{13}\text{C}\{^1\text{H}\}$ NMR (100 MHz, CDCl_3 , 298 K): δ 20.7 (Me), 53.3 (OMe), 108.7 (CH), 116.7 (CH), 125.8 (CH), 128.1 (CH), 129.6 (CH), 130.9 (CH), 136.2 (C),

138.6 (CH), 140.1 (C), 157.6 (C), 163.2 (C). MS (ES): m/z 200 [M]⁺. Data are consistent with those reported in the literature.⁸

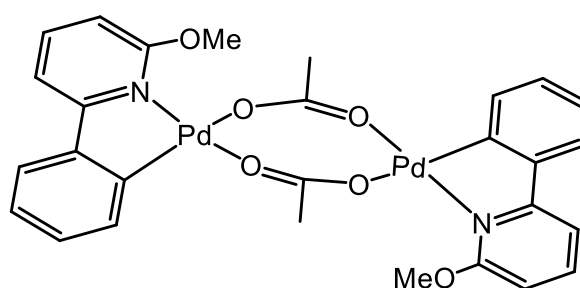
Synthesis of Novel Complexes Containing an N[^]C Ligand

General Procedure for Synthesis of [Pd(κ^2 -BL)(μ -OAc)]₂

The 6-aryl-2-methoxypyridine (1.4 eq.) and Pd(OAc)₂ (1 eq.) were combined in MeOH in a 5-mL flask equipped with a magnetic stir bar and stirred at room temperature for 18 h. The precipitate was then filtered, washed with diethyl ether or hexane (5 mL), collected and dried. The products were obtained as yellow solids (14-87% yield).

5.2.10 Synthesis of [Pd(κ^2 -6-phenyl-2-methoxypyridine)(μ -OAc)]₂ (**2.10**)

This was synthesised by combining 6-phenyl-2-methoxypyridine (**2.5**) (0.017 g, 0.0935 mmol, 1.4 eq.) and Pd(OAc)₂ (0.015 g, 0.0668 mmol, 1 eq.) in MeOH (1 mL) and after filtration and washing gave **2.10** (0.0103 g, 45%).

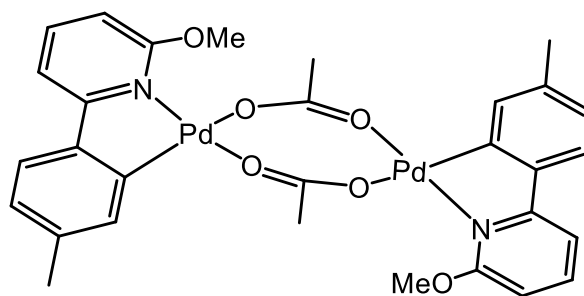


Crystals suitable for single crystal X-ray diffraction were grown by slow evaporation of a methanol solution of the complex. Mp: 212-213 °C. ¹H NMR (400 MHz, CDCl₃, 298 K): δ 2.19 (s, O₂CMe, 6H), 3.56 (s, OMe, 6H), 5.80 (d, J_{H-H} 7.9, 2H), 6.78 (app t, J_{H-H} 8.4, 4H), 6.80 (m, 4H), 7.06 (d, J_{H-H} 7.3, 2H), 7.30 (t, J_{H-H} 7.9, 2H). ¹³C{¹H} NMR (100 MHz, CDCl₃, 298 K): δ 24.3 (O₂CMe), 55.5 (OMe), 102.8 (CH), 110 (CH), 122.5 (CH), 123.5 (CH), 127.1 (CH), 130.8 (C), 131.7 (CH), 140.1 (CH), 144.8 (C), 163.1 (C), 165.7 (C), 178.7 (O₂CMe). IR (selected bands, cm⁻¹): 1594, 1571, 1485, 1399, 1281, 1054, 753. TOFMS (ES): m/z 698.9662 [M]⁺ (C₂₈H₂₆N₂O₆¹⁰⁶Pd₂ requires 698.9881), 640.9784 [M-OAc]⁺ (C₂₆H₂₃N₂O₄¹⁰⁶Pd₂ requires 640.9732).

5.2.11 Synthesis of [Pd(κ^2 -6-(4-methylphenyl)-2-methoxypyridine)(μ -OAc)]₂ (**2.11**)

This was synthesised by combining 6-(4-methylphenyl)-2-methoxypyridine (**2.6**) (0.022 g, 0.11 mmol, 1.4 eq.) and Pd(OAc)₂ (0.018 g, 0.0788 mmol, 1 eq.) in MeOH (1.5 mL) and after filtration and washing gave **2.11** (0.025 g, 87%). Crystals suitable for single crystal X-ray diffraction were grown by slow evaporation of a methanol solution of the

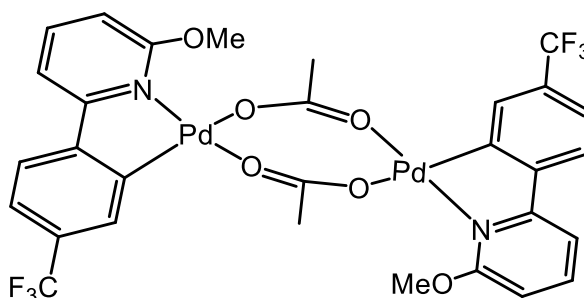
complex. Mp: 216-217 °C. ^1H NMR (400 MHz, CDCl_3 , 298 K): δ 2.20 (s, O_2CMe , 6H), 2.23 (s, Me, 6H), 3.56 (s, OMe, 6H), 5.80 (d, $J_{\text{H-H}}$ 7.5, 2H), 6.59 (d, $J_{\text{H-H}}$ 7.4, 2H), 6.71 (d, $J_{\text{H-H}}$ 7.8, 2H), 6.73 (d, $J_{\text{H-H}}$ 7.9, 2H), 6.84 (s, 2H), 7.29



(t, $J_{\text{H-H}}$ 7.7, 2H). $^{13}\text{C}\{^1\text{H}\}$ NMR (100 MHz, CDCl_3 , 298 K): δ 21.8 (Me), 24.3 (O_2CMe), 55.4 (OMe), 101.9 (CH), 109.8 (CH), 122.4 (CH), 124.5 (CH), 132.1 (CH), 136.9 (C), 140.1 (CH), 142.1 (C), 149.3 (C), 163.3 (C), 165.6 (C), 178.8 (O_2CMe). IR (selected bands, cm^{-1}): 1570, 1486, 1404, 1279, 1110, 1053, 788. MS (ES): m/z 669 $[\text{M-OAc}]^+$. TOFMS (ASAP): m/z 669.0058 $[\text{M-OAc}]^+$ ($\text{C}_{28}\text{H}_{27}\text{N}_2\text{O}_4^{106}\text{Pd}_2$ requires 669.0045).

5.2.12 Synthesis of $[\text{Pd}(\kappa^2\text{-6-(4-trifluoromethylphenyl)-2-methoxypyridine})(\mu\text{-OAc})_2]$ (**2.12**)

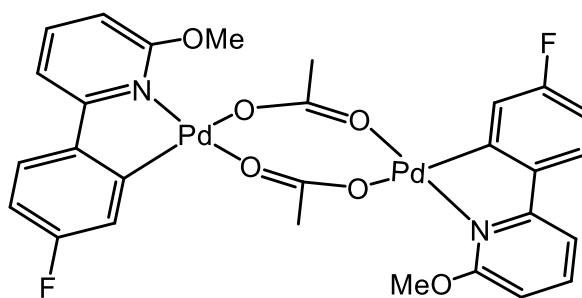
This was synthesised by combining 6-(4-trifluoromethylphenyl)-2-methoxypyridine (**2.7**) (0.07 g, 0.28 mmol, 1.4 eq.) and $\text{Pd}(\text{OAc})_2$ (0.045 g, 0.2 mmol, 1 eq.) in MeOH (3 mL) and after the stirring was stopped, the



solvent was removed *in vacuo* leaving behind a solid which was dissolved in DCM (7 mL) and passed through Celite. The filtrate was reduced in volume and hexane was added slowly to induce precipitation. The precipitate was isolated, washed with hexane and dried *in vacuo* to give **2.12** (0.018 g, 22%). Crystals suitable for single crystal X-ray diffraction were grown by slow evaporation of a chloroform solution of the complex. Mp: 217-218 °C. ^1H NMR (400 MHz, CDCl_3 , 298 K): δ 2.22 (s, O_2CMe , 6H), 3.69 (s, OMe, 6H), 6.04 (d, $J_{\text{H-H}}$ 8.3, 2H), 6.83 (d, $J_{\text{H-H}}$ 7.6, 2H), 6.96 (d, $J_{\text{H-H}}$ 8.1, 2H), 7.02 (d, $J_{\text{H-H}}$ 8.0, 2H), 7.30 (s, 2H), 7.38 (t, $J_{\text{H-H}}$ 8.0, 2H). $^{13}\text{C}\{^1\text{H}\}$ NMR (125 MHz, CDCl_3 , 298 K): δ 24.1 (O_2CMe), 55.7 (OMe), 104.2 (CH), 110.7 (CH), 120.5 (q, $^3J_{\text{C-F}}$ 3.7, CH), 122.1 (CH), 125.5 (q, $^1J_{\text{C-F}}$ 270.1, CF_3), 127.8 (q, $^3J_{\text{C-F}}$ 3.7, CH), 128.1 (q, $^2J_{\text{C-F}}$ 30.0, C), 140.8 (CH), 148.0 (C), 149.3 (C), 161.8 (C), 165.8 (C), 179.7 (O_2CMe). ^{19}F NMR (376 MHz, CDCl_3 , 298 K): δ -62.1 (s, CF_3). IR (selected bands, cm^{-1}): 1575, 1490, 1404, 1282, 1316, 1107, 1071, 787, 679. TOFMS (ES): 777.9493 $[\text{M-OAc}]^+$ ($\text{C}_{28}\text{H}_{21}\text{F}_6\text{N}_2\text{O}_4^{106}\text{Pd}_2$ requires 777.9508), 357.9688 $[\text{M}/2\text{-OAc}]^+$ ($\text{C}_{13}\text{H}_9\text{F}_3\text{NO}^{106}\text{Pd}$ requires 357.9671).

5.2.13 Synthesis of [Pd(κ^2 -6-(4-fluorophenyl)-2-methoxypyridine)(μ -OAc)]₂ (**2.13**)

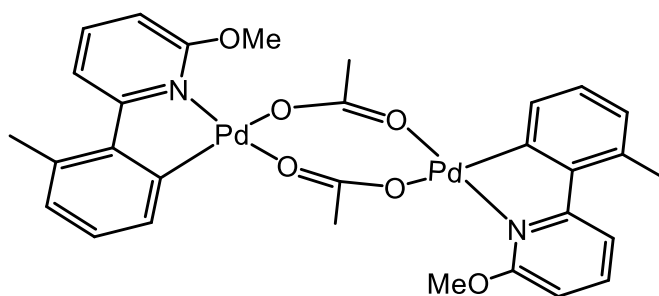
This was synthesised by combining 6-(4-fluorophenyl)-2-methoxypyridine (**2.8**) (0.019 g, 0.0935 mmol, 1.4 eq.) and Pd(OAc)₂ (0.015 g, 0.0668 mmol, 1 eq.) in MeOH (1 mL) and after filtration and washing gave



2.13 (0.0084 g, 35%). Crystals suitable for single crystal X-ray diffraction were grown by slow evaporation of a methanol solution of the complex. Mp: 215-216 °C. ¹H{¹⁹F} NMR (400 MHz, CDCl₃, 298 K): δ 2.21 (s, O₂CMe, 6H), 3.69 (s, OMe, 6H), 5.90 (d, *J*_{H-H} 7.4, 2H), 6.40 (t, *J*_{H-H} 8.5, 2H), 6.70 (d, *J*_{H-H} 8.6, 2H), 6.71 (s, 2H), 6.80 (d, *J*_{H-H} 8.3, 2H), 7.30 (t, *J*_{H-H} 7.9, 2H). ¹³C{¹H} NMR (100 MHz, CDCl₃, 298 K): δ 24.3 (O₂CMe), 55.7 (OMe), 102.6 (CH), 109.9 (CH), 110.8 (d, ²*J*_{C-F} 23.0, CH), 117.9 (d, ²*J*_{C-F} 19.5, CH), 123.6 (d, ³*J*_{C-F} 7.5, CH), 140.5 (CH), 140.9 (C), 151.7 (C), 160.1 (d, ¹*J*_{C-F} 248.3, C), 162.4 (C), 165.7 (C), 179.3 (O₂CMe). ¹⁹F NMR (376 MHz, CDCl₃, 298 K): δ -110.7 (s, F). IR (selected bands, cm⁻¹): 1597, 1563, 1489, 1396, 1282, 1172, 1046, 794, 781, 685. TOFMS (ES): *m/z* 734.9364 [M]⁺ (C₂₈H₂₄F₂N₂O₆¹⁰⁶Pd₂ requires 734.9692), 676.9556 [M-OAc]⁺ (C₂₆H₂₁F₂N₂O₄¹⁰⁶Pd₂ requires 676.9543).

5.2.14 Synthesis of [Pd(κ^2 -6-(2-methylphenyl)-2-methoxypyridine)(μ -OAc)]₂ (**2.14**)

This was synthesised by combining 6-(2-methylphenyl)-2-methoxypyridine (**2.9**) (0.018 g, 0.093 mmol, 1.4 eq.) and Pd(OAc)₂ (0.015 g, 0.066 mmol, 1 eq.) in MeOH (1 mL) and after the



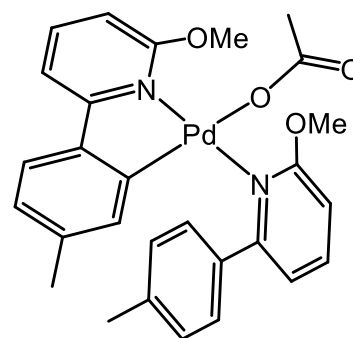
stirring was stopped, the solvent was removed *in vacuo* leaving behind a solid which was dissolved in DCM (5 mL) and passed through Celite. The filtrate was reduced in volume and hexane was added slowly to induce precipitation. The precipitate was isolated, washed with hexane and dried *in vacuo* to give **2.14** (0.007 g, 14%). Crystals suitable for single crystal X-ray diffraction were grown by slow evaporation of a methanol solution of the complex. Mp: 214-215 °C. ¹H NMR (400 MHz, CDCl₃, 298 K): δ 2.17 (s, O₂CMe, 6H), 2.34 (s, Me, 6H), 3.54 (br s, OMe, 6H), 5.82 (m, 2H), 6.65 (m, 2H), 6.73 (t, *J*_{H-H} 7.4, 2H), 7.02 (m, 4H), 7.32 (m, 2H). ¹³C{¹H} NMR (125 MHz, CDCl₃, 298 K): δ 23.7 (Me),

24.3 (O₂CMe), 55.5 (OMe), 102.6 (CH), 113.7 (CH), 126.1 (CH), 128.2 (CH), 129.5 (CH), 133.8 (C), 139.6 (CH), 142.7 (C), 151 (C), 163.4 (C), 165.7 (C), 178.2 (O₂CMe). IR (selected bands, cm⁻¹): 1591, 1570, 1480, 1392, 1320, 1275, 1122, 774, 738, 682. TOFMS (ES): *m/z* 669.0058 [M-OAc]⁺ (C₂₈H₂₇N₂O₄¹⁰⁶Pd₂ requires 669.0045).

Synthesis of Mononuclear Pd(II) Complexes

5.2.15 Synthesis of [Pd(κ²-6-(4-methylphenyl)-2-methoxypyridine)(OAc)(κ¹-6-(4-methylphenyl)-2-methoxypyridine)] (2.15)

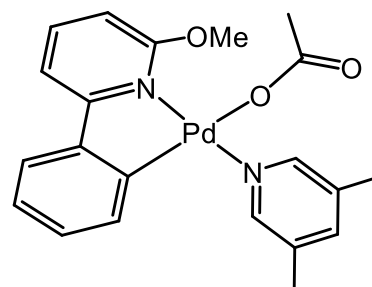
To a round bottom flask equipped with a magnetic stir bar was added [Pd(κ²-6-(4-methylphenyl)-2-methoxypyridine)(μ-OAc)]₂ (**2.11**) (30 mg, 0.041 mmol), 6-(4-methylphenyl)-2-methoxypyridine (**2.6**) (16.5 mg, 0.082 mmol) and CDCl₃ (3 mL). After stirring at room temperature overnight, the product was obtained in > 99% conversion. ¹H NMR (400 MHz, CDCl₃, 298 K): δ 2.20 (s,



O₂CMe, 3H), 2.23 (s, N[∧]C-Me, 3H), 2.40 (s, N-Me, 3H), 3.57 (s, N[∧]C-OMe, 3H), 4.03 (s, N-OMe, 3H), 5.82 (app br s, 1H), 6.60 (d, *J*_{H-H} 7.5, 1H), 6.65 (dd, *J*_{H-H} 8.2, 0.6, 1H), 6.73 (m, 2H), 6.84 (s, 1H), 7.25 (m, 3H), 7.31 (dd, *J*_{H-H} 7.4, 0.6, 1H), 7.60 (t, *J*_{H-H} 7.6, 1H), 7.94 (d, *J*_{H-H} 8.2, 2H). ¹³C{¹H} NMR (100 MHz, CDCl₃, 298 K): δ 21.3 (O₂CMe), 21.9 (N[∧]C-Me), 24.4 (N-Me), 53.2 (N-OMe), 55.5 (N[∧]C-OMe), 102.0 (CH), 108.8 (CH), 109.9 (CH), 112.4 (CH), 120.2 (C), 122.5 (CH), 124.5 (CH), 126.6 (CH), 129.3 (CH), 132.2 (CH), 136.4 (C), 138.8 (C), 139.1 (CH), 140.2 (CH), 140.4 (C), 142.2 (C), 154.8 (C), 163.4 (C), 163.7 (C), 165.7 (C), 178.9 (O₂CMe). MS (ES): *m/z* 503 [M-OAc].

5.2.16 Synthesis of [Pd(κ²-6-phenyl-2-methoxypyridine)(OAc)(3,5-lutidine)] (2.16)

This was obtained by combining [Pd(κ²-6-phenyl-2-methoxypyridine)(μ-OAc)]₂ (**2.10**) (30.3 mg, 0.043 mmol, 1 eq.), 3,5-lutidine (13.8 mg, 0.129 mmol, 3 eq.) and CDCl₃ in a round bottom flask equipped with a magnetic stir bar, and after 24 h **2.16** was obtained in 96.3% conversion. ¹H NMR (400 MHz, CDCl₃, 298 K):

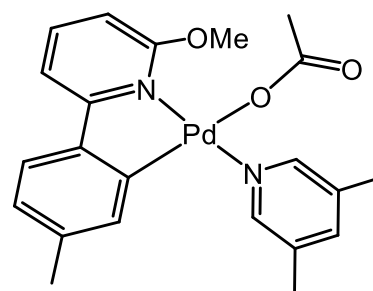


δ 1.93 (s, O₂CMe, 3H), 2.34 (s, py-Me, 6H), 3.93 (s, OMe, 3H), 6.02 (d, *J*_{H-H} 7.6, 1H), 6.55 (d, *J*_{H-H} 8.3, 1H), 6.82 (t, *J*_{H-H} 7.4, 1H), 7.01 (t, *J*_{H-H} 7.4, 1H), 7.29 (m, 1H), 7.39 (d, *J*_{H-H} 7.3, 1H), 7.44 (s, 1H), 7.76 (t, *J*_{H-H} 7.8, 1H), 8.71 (s, 2H). ¹³C{¹H} NMR (100 MHz,

CDCl₃, 298 K): δ 18.3 (py-Me), 24.8 (O₂CMe), 56.3 (OMe), 104 (CH), 110.8 (CH), 123.5 (CH), 124.2 (CH), 128.8 (CH), 133.5 (CH), 134.6 (C), 139.2 (CH), 141.3 (CH), 146.1 (C), 150.4 (CH), 151.5 (C), 164.4 (C), 166.8 (C), 176.8 (O₂CMe). MS (ES): m/z 397 [M-OAc]⁺.

5.2.17 Synthesis of [Pd(κ^2 -6-(4-methylphenyl)-2-methoxypyridine)(OAc)(3,5-lutidine)] (2.17)

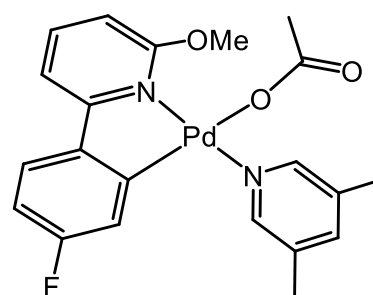
This was obtained by combining [Pd(κ^2 -6-(4-methylphenyl)-2-methoxypyridine)(μ -OAc)]₂ (2.11) (32 mg, 0.044 mmol, 1 eq.), 3,5-lutidine (13.8 mg, 0.129 mmol, 3 eq.) and CDCl₃ in a round bottom flask equipped with a magnetic stir bar, and after 24 h 2.17 was obtained in 98% conversion. ¹H NMR (400 MHz, CDCl₃, 298 K):



δ 1.92 (s, O₂CMe, 3H), 2.09 (s, *p*-Me, 3H), 2.34 (s, py-Me, 6H), 3.91 (s, OMe, 3H), 5.83 (s, 1H), 6.5 (d, J_{H-H} 8.3, 1H), 6.83 (d, J_{H-H} 7.8, 1H), 7.23 (d, J_{H-H} 7.7, 1H), 7.27 (m, 1H), 7.44 (s, 1H), 7.75 (t, J_{H-H} 8.1, 1H), 8.71 (s, 2H). ¹³C{¹H} NMR (100 MHz, CDCl₃, 298 K): δ 18.2 (py-Me), 21.7 (*p*-Me), 24.8 (O₂CMe), 56.3 (OMe), 103.4 (CH), 110.5 (CH), 123.3 (CH), 125.1 (CH), 134.2 (CH), 134.5 (C), 138.8 (C), 139.2 (CH), 141.2 (CH), 143.4 (C), 150.4 (CH), 151.3 (C), 164.5 (C), 166.8 (C), 176.8 (O₂CMe). MS (ES): m/z 411 [M-OAc]⁺.

5.2.18 Synthesis of [Pd(κ^2 -6-(4-fluorophenyl)-2-methoxypyridine)(OAc)(3,5-lutidine)] (2.18)

This was obtained by combining [Pd(κ^2 -6-(4-fluorophenyl)-2-methoxypyridine)(μ -OAc)]₂ (2.13) (35 mg, 0.047 mmol, 1 eq.), 3,5-lutidine (13.8 mg, 0.129 mmol, 3 eq.) and CDCl₃ in a round bottom flask equipped with a magnetic stir bar, and after 24 h 2.18 was obtained in 94% conversion. ¹H{¹⁹F} NMR (400 MHz, CDCl₃,



298 K): δ 1.92 (s, O₂CMe, 3H), 2.35 (s, py-Me, 6H), 3.92 (s, OMe, 3H), 5.68 (s, 1H), 6.54 (d, J_{H-H} 8.3, 1H), 6.70 (dd, J_{H-H} 8.5, 2.1, 1H), 7.19 (d, J_{H-H} 7.7, 1H), 7.37 (d, J_{H-H} 8.6, 1H), 7.46 (s, 1H), 7.75 (t, J_{H-H} 8.0, 1H), 8.68 (s, 2H). ¹³C{¹H} NMR (100 MHz, CDCl₃, 298 K): δ 18.3 (py-Me), 24.6 (O₂CMe), 56.3 (OMe), 103.8 (CH), 110.8 (CH), 111.3 (d, ² J_{C-F} 23.1, CH), 119.8 (d, ² J_{C-F} 19.9, CH), 124.7 (d, ³ J_{C-F} 7.9, CH), 134.9 (C), 139.5 (CH), 141.5 (CH), 142.2 (C), 150.2 (CH), 153.8 (C), 161.3 (d, ¹ J_{C-F} 254.5, C), 163.6

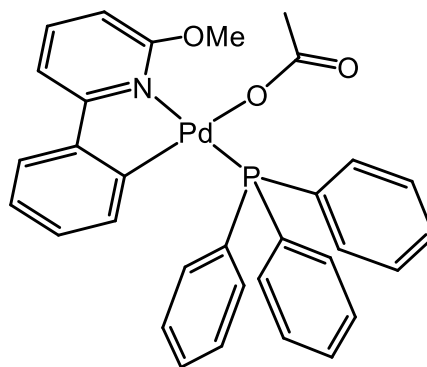
(C), 166.8 (C), 176.9 (O₂CMe). ¹⁹F NMR (376 MHz, CDCl₃, 298 K): δ -109.9 (s, F). MS (ES): *m/z* 415 [M-OAc]⁺.

General procedure for synthesis of [Pd(κ²-6-aryl-2-methoxypyridine)(OAc)(PPh₃)]

A small-sized oven-dried Schlenk flask equipped with a magnetic stir bar was evacuated and backfilled with nitrogen. The flask was charged with the [Pd(κ²-6-aryl-2-methoxypyridine)(μ-OAc)]₂ (1 eq.), PPh₃ (2.1 eq.) and CDCl₃ (N₂ was bubbled through the solvent for 2 h before being used). The reaction mixture was left to stir under N₂ at room temperature for 24 h. After this time the solvent was removed *in vacuo* leaving behind a solid which was dissolved in DCM and hexane was added slowly to induce precipitation. The precipitate was isolated, washed with Et₂O and dried *in vacuo*. The products were obtained as light yellow solid (51-74% yield).

5.2.19 Synthesis of [Pd(κ²-6-phenyl-2-methoxypyridine)(OAc)(PPh₃)] (2.19)

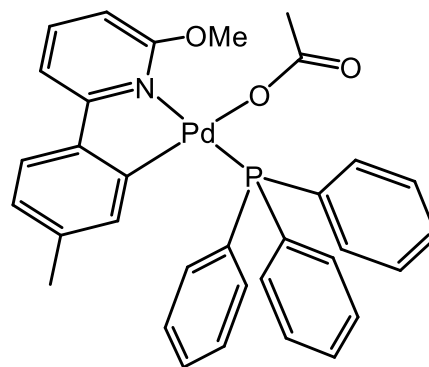
The title complex was synthesised by combining [Pd(κ²-6-phenyl-2-methoxypyridine)(μ-OAc)]₂ (**2.10**) (48.6 mg, 0.069 mmol, 1 eq.) and PPh₃ (38 mg, 0.144 mmol, 2.1 eq.) in CHCl₃ (4 mL). The mixture was left to stir at room temperature under N₂ for 24 h and after work up afforded **2.19** as a grey solid (63 mg, 71% yield). Mp: 128-129 °C. ¹H{³¹P} NMR (400 MHz, CDCl₃, 298 K): δ 1.38 (s, O₂CMe,



3H), 3.86 (s, OMe, 3H), 6.41 (td, *J*_{H-H} 7.2, 1.4, 1H), 6.52 (dd, *J*_{H-H} 7.8, 0.9, 1H), 6.60 (d, *J*_{H-H} 8.0, 1H), 6.86 (td, *J*_{H-H} 7.4, 1.1, 1H), 7.34 (app tt, *J*_{H-H} 7.2, 1.5, 6H), 7.41 (m, 4H), 7.45 (dd, *J*_{H-H} 7.8, 1.4, 1H), 7.79 (t, *J*_{H-H} 8.0, 1H), 7.85 (app d, *J*_{H-H} 7.0, 6H). ¹³C{¹H} NMR (125 MHz, CDCl₃, 298 K): δ 23.3 (O₂CMe), 56.2 (OMe), 104.1 (CH), 111.0 (CH), 123.9 (CH), 124.3 (CH), 128.0 (d, ³*J*_{C-P} 10.1, CH), 128.5 (CH), 130.4 (d, ⁴*J*_{C-P} 2.3, CH), 130.7 (d, ¹*J*_{C-P} 51.4, C), 135.7 (d, ²*J*_{C-P} 11.3, CH), 139.5 (CH), 141.6 (CH), 147.3 (C), 150.8 (C), 163.7 (C), 166.4 (C), 176.5 (O₂CMe). ³¹P NMR (162 MHz, CDCl₃, 298 K): δ 45.7 (s, PPh₃). IR (selected bands, cm⁻¹): 1572, 1484, 1433, 1279, 1096, 752, 689. MS (ES): *m/z* 552 [M-OAc]⁺. TOFMS (ASAP): *m/z* 552.0792 [M-OAc]⁺ (C₃₀H₂₅NOP¹⁰⁶Pd requires 552.0709).

5.2.20 Synthesis of [Pd(κ^2 -6-(4-methylphenyl)-2-methoxypyridine)(OAc)(PPh₃)] (2.20)

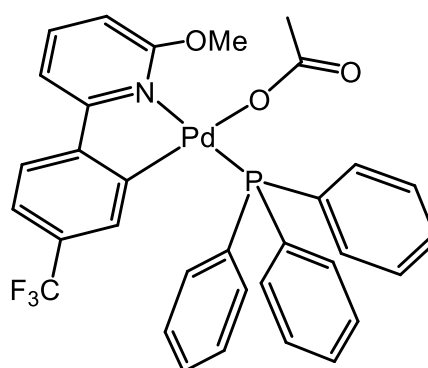
The title complex was synthesised by combining [Pd(κ^2 -6-(4-methylphenyl)-2-methoxypyridine)(μ -OAc)]₂ (**2.11**) (34.2 mg, 0.047 mmol, 1 eq.) and PPh₃ (26 mg, 0.099 mmol, 2.1 eq.) in CHCl₃ (3 mL). The mixture was left to stir at room temperature under N₂ for 24 h and after work up afforded **2.20** as a grey solid (41 mg, 69% yield). Mp:



175-176 °C. ¹H{³¹P} NMR (400 MHz, CDCl₃, 298 K): δ 1.29 (s, O₂CMe, 3H), 1.62 (s, Me, 3H), 3.84 (s, 3H, OMe), 6.33 (s, 1H), 6.54 (d, $J_{\text{H-H}}$ 7.9, 1H), 6.65 (dd, $J_{\text{H-H}}$ 7.9, 0.7, 1H), 7.33 (m, 8H), 7.40 (tt, $J_{\text{H-H}}$ 7.3, 1.4, 3H), 7.74 (t, $J_{\text{H-H}}$ 8.0, 1H), 7.85 (dd, $J_{\text{H-H}}$ 8.4, 1.5, 6H). ¹³C{¹H} NMR (100 MHz, CDCl₃, 298 K): δ 20.9 (Me), 23.4 (O₂CMe), 56.1 (OMe), 103.5 (CH), 110.7 (CH), 123.9 (CH), 124.3 (CH), 127.9 (d, ³J_{C-P} 11.3, CH), 130.4 (d, ⁴J_{C-P} 3.1, CH), 130.7 (d, ¹J_{C-P} 52.4, C), 135.7 (d, ²J_{C-P} 12.5, CH), 137.8 (C), 140.6 (CH), 141.5 (CH), 144.6 (C), 150.6 (C), 163.8 (C), 166.4 (C), 176.3 (O₂CMe). ³¹P NMR (162 MHz, CDCl₃, 298 K): δ 45.2 (s, PPh₃). IR (selected bands, cm⁻¹): 1572, 1485, 1433, 1382, 1336, 1285, 1181, 1093, 1053, 790, 688. MS (ES): m/z 566 [M-OAc]⁺. TOFMS (ASAP): m/z 566.0877 [M-OAc]⁺ (C₃₁H₂₇NOP¹⁰⁶Pd requires 566.0865).

5.2.21 Synthesis of [Pd(κ^2 -6-(4-trifluoromethylphenyl)-2-methoxypyridine)(OAc)(PPh₃)] (2.21)

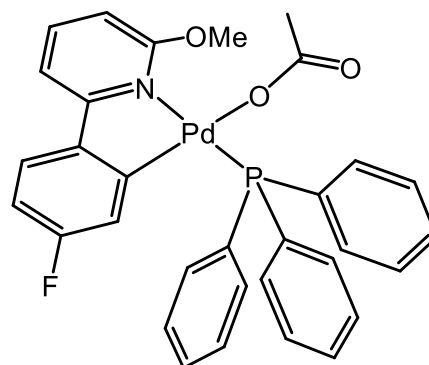
The title complex was synthesised by combining [Pd(κ^2 -6-(4-trifluoromethylphenyl)-2-methoxypyridine)(μ -OAc)]₂ (**2.12**) (15 mg, 0.018 mmol, 1 eq.) and PPh₃ (9.38 mg, 0.037 mmol, 2.1 eq.) in CHCl₃ (2 mL). The mixture was left to stir at room temperature under N₂ for 24 h and after work up afforded **2.21** as a pale yellow solid (19 mg, 75% yield). Mp: 185-187 °C. ¹H{³¹P} NMR (400 MHz, CDCl₃, 298 K): δ 1.36 (s, O₂CMe, 3H), 3.91 (s, OMe, 3H), 6.71 (d, $J_{\text{H-H}}$ 8.5, 1H), 6.82 (s, 1H), 7.11 (d, $J_{\text{H-H}}$ 8.1, 1H), 7.37 (t, $J_{\text{H-H}}$ 7.7, 6H), 7.46 (m, 4H), 7.53 (d, $J_{\text{H-H}}$ 8.1, 1H), 7.85 (m, 7H). Sample was insufficiently soluble for ¹³C{¹H}; therefore, selective ¹³C data was acquired by a DEPT 135 experiment. DEPT 135 NMR (125 MHz, CDCl₃, 298 K): δ 23.2 (O₂CMe), 56.4



(OMe), 105.4 (CH), 111.7 (CH), 120.6 (CH), 123.6 (CH), 128.1 (d, $^3J_{C-P}$ 11.0, CH), 130.7 (CH), 135.0 (d, $^2J_{C-P}$ 11.8, CH), 135.5 (CH), 142.0 (CH). ^{31}P NMR (162 MHz, CDCl_3 , 298 K): δ 44.6 (s, PPh_3). ^{19}F NMR (376 MHz, CDCl_3 , 298 K): δ -63.3 (s, CF_3). IR (selected bands, cm^{-1}): 1563, 1485, 1433, 1318, 1117, 1072, 1021, 800, 688. MS (ES): m/z 620 $[\text{M-OAc}]^+$. TOFMS (ASAP): m/z 620.0579 $[\text{M-OAc}]^+$ ($\text{C}_{31}\text{H}_{24}\text{F}_3\text{NOP}^{106}\text{Pd}$ requires 620.0582).

5.2.22 Synthesis of $[\text{Pd}(\kappa^2\text{-6-(4-fluorophenyl)-2-methoxypyridine})(\text{OAc})(\text{PPh}_3)]$ (2.22)

The title complex was synthesised by combining $[\text{Pd}(\kappa^2\text{-6-(4-fluorophenyl)-2-methoxy pyridine})(\mu\text{-OAc})_2]$ (**2.13**) (35.2 mg, 0.047 mmol, 1 eq.) and PPh_3 (25 mg, 0.095 mmol, 2.1 eq.) in CHCl_3 (4 mL). The mixture was left to stir at room temperature under N_2 for 24 h and after work up afforded **2.22** as a pale yellow solid (44 mg, 74% yield).

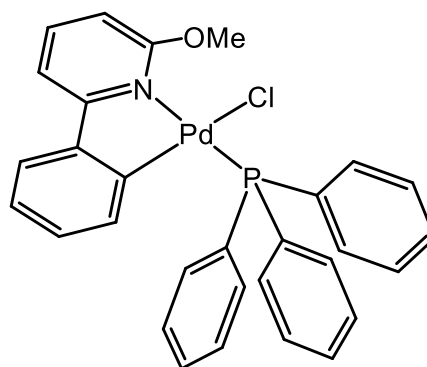


Crystals suitable for a single crystal X-ray diffraction study were grown from a dichloromethane solution of the complex layered with hexane. Mp: 176-177 °C. $^1\text{H}\{^{19}\text{F}\}$ NMR (400 MHz, CDCl_3 , 298 K): δ 1.27 (s, O_2CMe , 3H), 3.85 (s, OMe, 3H), 6.20 (dd, $J_{\text{H-P}}$ 7.3, 2.5, 1H), 6.55 (dd, $J_{\text{H-H}}$ 8.61, 2.5, 1H), 6.58 (d, $J_{\text{H-H}}$ 8.8, 1H), 7.30 (d, $J_{\text{H-H}}$ 7.9, 1H), 7.36 (m, 6H), 7.43 (m, 4H), 7.77 (t, $J_{\text{H-H}}$ 8.1, 1H), 7.84 (m, 6H). $^{13}\text{C}\{^1\text{H}\}$ NMR (125 MHz, CDCl_3 , 298 K): δ 23.3 (O_2CMe), 56.2 (OMe), 103.9 (CH), 110.9 (CH), 111.0 (CH), 125.3 (CH), 125.4 (CH), 128.1 (d, $^3J_{C-P}$ 11.2, CH), 130.1 (d, $^1J_{C-P}$ 51.3, C), 130.6 (d, $^4J_{C-P}$ 2.8, CH), 135.6 (d, $^2J_{C-P}$ 12.4, CH), 141.8 (CH), 143.6 (C), 153.6 (C), 161.0 (d, $^1J_{C-F}$ 252.6, C), 162.8 (C), 166.4 (C), 176.5 (O_2CMe). ^{31}P NMR (162 MHz, CDCl_3 , 298 K): δ 45.2 (s, PPh_3). ^{19}F NMR (376 MHz, CDCl_3 , 298 K): δ -111.5 (s, F). IR (selected bands, cm^{-1}): 1742, 1566, 1431, 1380, 1199, 1179, 1096, 1024, 786, 703. MS (ES): m/z 570 $[\text{M-OAc}]^+$. TOFMS (ASAP): m/z 570.0626 $[\text{M-OAc}]^+$ ($\text{C}_{30}\text{H}_{24}\text{FNOP}^{106}\text{Pd}$ requires 570.0614).

5.2.23 Synthesis of $[\text{Pd}(\kappa^2\text{-6-phenyl-2-methoxypyridine})(\text{PPh}_3)\text{Cl}]$ (2.23)

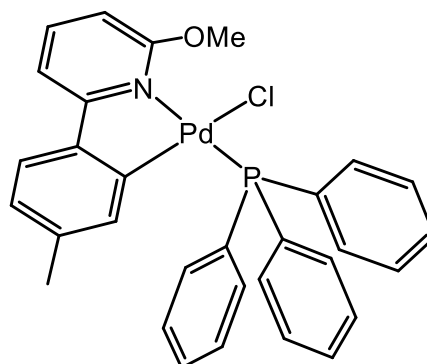
A round bottom flask equipped with stirrer bar and open to the air was loaded with $[\text{Pd}(\kappa^2\text{-6-phenyl-2-methoxypyridine})(\text{OAc})(\text{PPh}_3)]$ (**2.18**) (50 mg, 0.082 mmol), chloroform (5 mL) and brine (6 mL). After stirring vigorously at room temperature for 12 h the yellow phase was separated and washed with water (2 x 10 ml). The solvent was

reduced in volume and hexane added slowly to induce precipitation. The product was then filtered and washed with hexane to afford **2.23** as a yellow solid (46.5 mg, 96%). Mp: 170 °C (decomp.). $^1\text{H}\{^{31}\text{P}\}$ NMR (400 MHz, CDCl_3 , 298 K): δ 4.00 (s, OMe, 3H), 6.38 (t, $J_{\text{H-H}}$ 7.0, 1H), 6.51 (d, $J_{\text{H-H}}$ 7.8, 1H), 6.67 (d, $J_{\text{H-H}}$ 8.2, 1H), 6.86 (t, $J_{\text{H-H}}$ 7.4, 1H), 7.33 (app t, $J_{\text{H-H}}$ 7.6, 6H), 7.41 (m, 4H), 7.70 (dd, $J_{\text{H-H}}$ 8.0, 1.1, 1H), 7.80 (d, $J_{\text{H-H}}$ 7.4, 6H), 7.83 (t, $J_{\text{H-H}}$ 8.1, 1H). Sample was insufficiently soluble for $^{13}\text{C}\{^1\text{H}\}$. ^{31}P NMR (162 MHz, CDCl_3 , 298 K): δ 45.1 (s, PPh_3). IR (selected bands, cm^{-1}): 1607, 1574, 1483, 1433, 1288, 1134, 1094, 1023, 752, 691. MS (ES): m/z 552 [M-Cl]. TOFMS (ES): m/z 552.0719 [M-Cl] $^+$ ($\text{C}_{30}\text{H}_{25}\text{NOP}^{106}\text{Pd}$ requires 552.0709).



5.2.24 Synthesis of [Pd(κ^2 -6-(4-methylphenyl)-2-methoxypyridine)(PPh₃)Cl] (**2.24**)

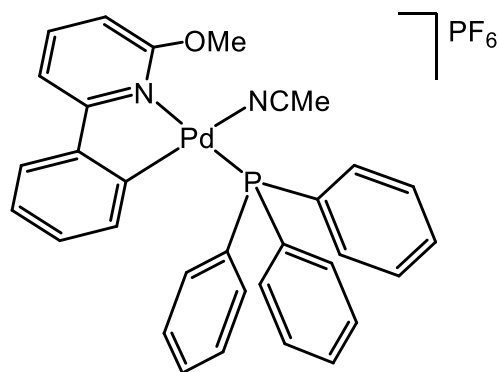
Based on the procedure described for **2.23**, using **2.19** (49 mg, 0.078 mmol) gave **2.24** as a light yellow solid (44 mg, 94%). Crystals suitable for a single crystal X-ray diffraction study were grown from a solution of the complex **2.24** in dichloromethane/MeCN (95/5 v/v) layered with hexane. Mp: > 270 °C. $^1\text{H}\{^{31}\text{P}\}$ NMR (400 MHz, CDCl_3 , 298 K): δ 1.62 (s, Me, 3H), 4.00 (s, OMe, 3H), 6.28 (s, 1H), 6.62 (d, $J_{\text{H-H}}$ 8.3, 1H), 6.67 (d, $J_{\text{H-H}}$ 7.4, 1H), 7.33 (m, 7H), 7.39 (m, 4H), 7.76 (t, $J_{\text{H-H}}$ 8.0, 1H), 7.79 (d, $J_{\text{H-H}}$ 7.2, 6H). Sample was insufficiently soluble for $^{13}\text{C}\{^1\text{H}\}$. ^{31}P NMR (162 MHz, CDCl_3 , 298 K): δ 44.1 (s, PPh_3). IR (selected bands, cm^{-1}): 1690, 1572, 1482, 1433, 1283, 1176, 1093, 1055, 781, 743, 690. MS (ES): m/z 566 [M-Cl]. TOFMS (ES): m/z 566.0880 [M-Cl] $^+$ ($\text{C}_{31}\text{H}_{27}\text{NOP}^{106}\text{Pd}$ requires 566.0865).



5.2.25 Synthesis of [Pd(κ^2 -6-phenyl-2-methoxypyridine)(PPh₃)(MeCN)]PF₆ (**2.25**)

A Schlenk flask equipped with a magnetic stir bar was evacuated and backfilled with nitrogen and loaded with [Pd(κ^2 -6-phenyl-2-methoxypyridine)(PPh₃)Cl] (**2.23**) (47 mg, 0.08 mmol), AgPF₆ (20.2 mg, 0.08 mmol) and MeCN (10 mL). The reaction mixture was stirred at room temperature for 12 h, at which point the suspension was allowed to settle and the solution was transferred by cannula filtration into a round bottom flask. All volatiles were removed under reduced pressure to afford **2.25** (55 mg, 93%) as a yellow

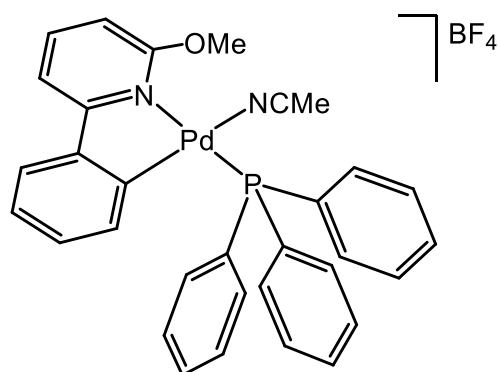
solid. Crystals suitable for a single crystal X-ray diffraction study were grown from a solution of the complex **2.25** in dichloromethane/MeCN (95/5 v/v) layered with hexane. Mp: 184 °C (decomp.). $^1\text{H}\{^{31}\text{P}\}$ NMR (400 MHz, CDCl_3 , 298 K): δ 1.90 (s, MeCN , 3H), 3.98 (s, OMe, 3H), 6.42 (t, $J_{\text{H-H}}$ 8.0, 1H), 6.48 (d, $J_{\text{H-H}}$ 7.7, 1H),



6.76 (d, $J_{\text{H-H}}$ 8.3, 1H), 6.93 (t, $J_{\text{H-H}}$ 7.7, 1H), 7.42 (t, $J_{\text{H-H}}$ 7.7, 6H), 7.50 (m, 4H), 7.67 (d, $J_{\text{H-H}}$ 8.3, 1H), 7.76 (d, $J_{\text{H-H}}$ 7.1, 6H), 7.90 (t, $J_{\text{H-H}}$ 8.1, 1H). Sample was insufficiently soluble for $^{13}\text{C}\{^1\text{H}\}$; therefore, selective ^{13}C data was acquired by an HMQC experiment. HMQC NMR (100 MHz, CDCl_3 , 298 K): δ 1.8 (MeCN), 56.7 (OMe), 105.2 (CH), 111.5 (CH), 125.2 (CH), 128.5 (CH), 128.8 (CH), 131.2 (CH), 132.3 (CH), 135.3 (CH), 139.7 (CH), 142.5 (CH). ^{31}P NMR (162 MHz, CDCl_3 , 298 K): δ 44.7 (s, PPh_3), -144.3 (sept, $^1J_{\text{P-F}}$ 705, PF_6). ^{19}F NMR (376 MHz, CDCl_3 , 298 K): δ -73.1 (d, $^1J_{\text{F-P}}$ 711, PF_6). IR (selected bands, cm^{-1}): 1576, 1484, 1433, 1280, 1112, 829, 795, 693. MS (ES): m/z 552 [M-MeCN] $^+$, 145 [PF_6] $^-$. TOFMS (ES): m/z 552.0723 [M-MeCN] $^+$ ($\text{C}_{30}\text{H}_{25}\text{NOPd}^{106}$ requires 552.0709).

5.2.26 Synthesis of $[\text{Pd}(\kappa^2\text{-6-phenyl-2-methoxypyridine})(\text{PPh}_3)(\text{MeCN})]\text{BF}_4$ (**2.26**)

Based on the procedure described for **2.25**, using **2.23** (52 mg, 0.088 mmol) and AgBF_4 (17.2 mg, 0.088 mmol) gave **2.26** as a yellow solid (47 mg, 78%). Crystals suitable for a single crystal X-ray diffraction study were grown from a solution of the complex **2.26** in dichloromethane/MeCN (95/5 v/v) layered with

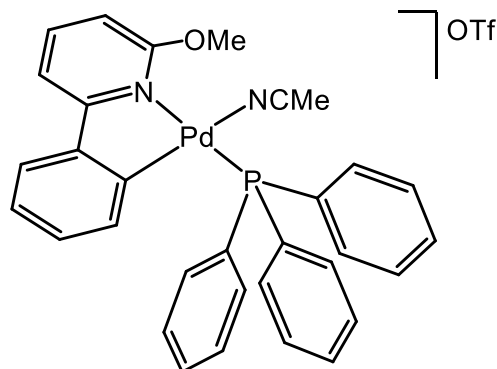


hexane. Mp: 109 °C (decomp.). $^1\text{H}\{^{31}\text{P}\}$ NMR (400 MHz, CDCl_3 , 298 K): δ 1.91 (s, MeCN , 3H), 3.98 (s, OMe, 3H), 6.40 (t, $J_{\text{H-H}}$ 7.3, 1H), 6.50 (d, $J_{\text{H-H}}$ 7.3, 1H), 6.71 (d, $J_{\text{H-H}}$ 8.3, 1H), 6.89 (t, $J_{\text{H-H}}$ 7.3, 1H), 7.38 (m, 7H), 7.44 (m, 4H), 7.77 (app d, $J_{\text{H-H}}$ 7.1, 6H), 7.84 (t, $J_{\text{H-H}}$ 7.8, 1H). Sample was insufficiently soluble for $^{13}\text{C}\{^1\text{H}\}$; therefore, selective ^{13}C data was acquired by an HMQC experiment. HMQC NMR (100 MHz, CDCl_3 , 298 K): δ 1.7 (MeCN), 56.7 (OMe), 105.7 (CH), 111.2 (CH), 124.3 (CH), 125.1 (CH), 128.2 (CH), 128.4 (CH), 131.1 (CH), 135.3 (CH), 139.0 (CH), 142.5 (CH). ^{31}P NMR (162 MHz, CDCl_3 , 298 K): δ 45.1 (s, PPh_3). ^{19}F NMR (376 MHz, CDCl_3 , 298 K): δ -153.4 (s, BF_4).

IR (selected bands, cm^{-1}): 1574, 1482, 1432, 1279, 1095, 1056, 1020, 995, 833, 751, 692. MS (ES): m/z 552 $[\text{M-MeCN}]^+$, 87 $[\text{BF}_4]^-$. TOFMS (ES): m/z 552.0726 $[\text{M-MeCN}]^+$ ($\text{C}_{30}\text{H}_{25}\text{NOP}^{106}\text{Pd}$ requires 552.0709).

5.2.27 Synthesis of $[\text{Pd}(\kappa^2\text{-phenyl-2-methoxypyridine})(\text{PPh}_3)(\text{MeCN})]\text{OTf}$ (**2.27**)

Based on the procedure described for **2.25**, using **2.23** (45 mg, 0.076 mmol) and $\text{AgOSO}_2\text{CF}_3$ (19.7 mg, 0.076 mmol) gave **2.27** as a yellow solid (55 mg, 97%). Crystals suitable for a single crystal X-ray diffraction study were grown from a solution of the complex **2.27** in dichloromethane/MeCN (95/5 v/v) layered with hexane. Mp: 115 °C (decomp.).

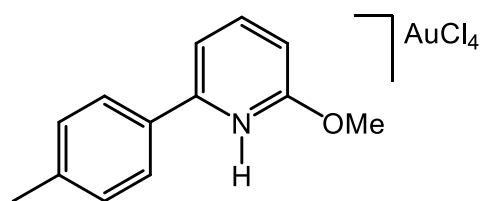


$^1\text{H}\{^3\text{P}\}$ NMR (400 MHz, CDCl_3 , 298 K): δ 1.88 (s, MeCN , 3H), 3.98 (s, OMe, 3H), 6.43 (t, $J_{\text{H-H}}$ 7.2, 1H), 6.49 (d, $J_{\text{H-H}}$ 7.9, 1H), 6.78 (d, $J_{\text{H-H}}$ 7.9, 1H), 6.94 (t, $J_{\text{H-H}}$ 7.2, 1H), 7.42 (m, 7H), 7.49 (m, 4H), 7.75 (d, $J_{\text{H-H}}$ 7.9, 6H), 7.91 (t, $J_{\text{H-H}}$ 7.9, 1H). Sample was insufficiently soluble for $^{13}\text{C}\{^1\text{H}\}$; therefore, selective ^{13}C data was acquired by a DEPT 135 experiment. DEPT 135 NMR (100 MHz, CDCl_3 , 298 K): δ -1.9 (MeCN), 54.9 (OMe), 103.6 (CH), 109.9 (CH), 123.2 (CH), 123.5 (CH), 126.2 (CH), 126.8 (d, $^3J_{\text{C-P}}$ 11.1, CH), 129.7 (CH), 133.3 (d, $^2J_{\text{C-P}}$ 12.7, CH), 137.4 (CH), 141.1 (CH). ^{31}P NMR (162 MHz, CDCl_3 , 298 K): δ 45.0 (s, PPh_3). ^{19}F NMR (376 MHz, CDCl_3 , 298 K): δ -78.1 (s, OTf). IR (selected bands, cm^{-1}): 1574, 1483, 1431, 1259, 1148, 1095, 1028, 800, 752, 691. MS (ES): m/z 552 $[\text{M-MeCN}]^+$, 149 $[\text{OTf}]^-$. TOFMS (ES): m/z 552.0723 $[\text{M-MeCN}]^+$ ($\text{C}_{30}\text{H}_{25}\text{NOP}^{106}\text{Pd}$ requires 552.0709).

Gold(III) Chemistry

5.2.28 Synthesis of $[\text{6-(4-methylphenyl)-2-methoxypyridine}(\kappa^1\text{-H})]\text{AuCl}_4$ (**2.28**)

The 6-(4-methylphenyl)-2-methoxy pyridine (**2.6**) (15.3 mg, 0.077 mmol, 1.1 eq.), dissolved in MeCN (1 mL), was added in one portion to $\text{H}[\text{AuCl}_4]$ (27.5 mg, 0.07 mmol) in H_2O

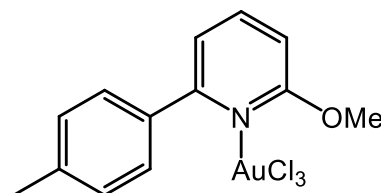


(1 mL). The reaction mixture was then stirred at room temperature for 2 h after which the solvent was removed leaving behind a yellow solid which was then washed by Et_2O and water and dried under reduced pressure to give 37 mg (98%) of the title product (**2.28**) as a yellow powder. Crystals suitable for a single crystal X-ray diffraction study were grown

from a dichloromethane solution of the complex layered with hexane. Mp: 108-109 °C. ^1H NMR (400 MHz, CDCl_3 , 298 K): δ 2.48 (s, Me, 3H), 4.36 (s, OMe, 3H), 7.20 (d, $J_{\text{H-H}}$ 8.7, 1H), 7.45 (d, $J_{\text{H-H}}$ 7.8, 2H), 7.59 (dd, $J_{\text{H-H}}$ 7.8, 0.7, 1H), 7.80 (dt, $J_{\text{H-H}}$ 8.2, 1.8, 2H), 8.38 (t, $J_{\text{H-H}}$ 7.8, 1H). ^1H NMR (400 MHz, CD_3CN , 298 K): δ 2.48 (s, Me, 3H), 4.24 (s, OMe, 3H), 7.40 (dd, $J_{\text{H-H}}$ 8.8, 0.8, 1H), 7.49 (dd, $J_{\text{H-H}}$ 8.5, 0.6, 2H), 7.70 (dd, $J_{\text{H-H}}$ 7.7, 0.7, 1H), 7.73 (dt, $J_{\text{H-H}}$ 8.5, 1.9, 2H), 8.48 (t, $J_{\text{H-H}}$ 8.3, 1H) 12.57 (br s, 1H, NH). $^{13}\text{C}\{^1\text{H}\}$ NMR (125 MHz, CDCl_3 , 298 K): δ 20.2 (Me), 58.5 (OMe), 107.7 (CH), 116.7 (CH), 127.2 (C), 127.9 (CH), 129.8 (CH), 143.1 (C), 149.2 (CH), 150.5 (C), 161.4 (C). IR (selected bands, cm^{-1}): 3180, 1623, 1434, 1379, 1274, 1177, 1080, 1027, 822, 793. MS (ES): m/z 200 $[\text{L}+\text{H}]^+$, 267 $[\text{AuCl}_2]^-$, 339 $[\text{AuCl}_4]^-$. TOFMS (ASAP): m/z 200.1080 $[\text{L}+\text{H}]^+$ ($\text{C}_{13}\text{H}_{14}\text{NO}$ requires 200.1075).

5.2.29 Synthesis of $[\text{Au}(\kappa^1\text{-6-(4-methylphenyl)-2-methoxypyridine})\text{Cl}_3]$ (**2.29**)

A: In a small bottom flask, 6.1 mg (0.072 mmol, 1.5 eq.) of NaHCO_3 were added under vigorous stirring to a solution of **2.28** of 26 mg (0.048 mmol) in 3 mL of THF and left 2 h to react at room temperature. The

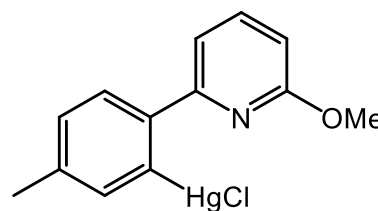


corresponding solution was evaporated and the crude solid was washed with Et_2O and water to give **2.29** as a yellow solid (12 mg, 50%).

B: The 6-(4-methylphenyl)-2-methoxypyridine (**2.6**) (8.7 mg, 0.044 mmol, 1.1 eq.), dissolved in MeCN (1 mL), was added in one portion to $\text{K}[\text{AuCl}_4]$ (15 mg, 0.04 mmol) in H_2O (1 mL). The reaction mixture was then stirred at room temperature for 24 h after which the yellow precipitate was filtered, washed with Et_2O and water and dried under reduced pressure to give 12 mg (60%) of **2.29** as a yellow powder. Crystals suitable for a single crystal X-ray diffraction study were grown from a dichloromethane solution of the complex layered with hexane. Mp: 176-178 °C. ^1H NMR (400 MHz, CDCl_3 , 298 K): δ 2.45 (s, Me, 3H), 4.25 (s, OMe, 3H), 7.10 (dd, $J_{\text{H-H}}$ 8.5, 1.1, 1H), 7.31 (dd, $J_{\text{H-H}}$ 7.6, 1.2, 1H), 7.39 (app d, $J_{\text{H-H}}$ 7.9, 2H), 7.73 (dt, $J_{\text{H-H}}$ 8.2, 1.7, 2H), 8.10 (t, $J_{\text{H-H}}$ 8.5, 1H). $^{13}\text{C}\{^1\text{H}\}$ NMR (100 MHz, CDCl_3 , 298 K): δ 21.6 (Me), 58.2 (OMe), 107.4 (CH), 121.1 (CH), 129.1 (CH), 130.0 (CH), 134.0 (C), 141.5 (C), 144.6 (CH), 159.1 (C), 161.7 (C). IR (selected bands, cm^{-1}): 1601, 1570, 1474, 1435, 1272, 1121, 1004, 822, 795. MS (ES): m/z 267 $[\text{AuCl}_2]^-$, 304 $[\text{AuCl}_3]^-$. TOFMS (ES): m/z 523.9623 $[\text{M}+\text{Na}]^+$ ($\text{C}_{13}\text{H}_{13}^{197}\text{AuCl}_3\text{NONa}$ requires 523.9626), 1026.9327 $[\text{2M}+\text{Na}]^+$ ($\text{C}_{26}\text{H}_{26}^{197}\text{Au}_2\text{Cl}_6\text{N}_2\text{O}_2\text{Na}$ requires 1026.9325).

5.2.30 Synthesis of [Hg(κ^1 -6-(4-methylphenyl)-2-methoxypyridine)Cl] (2.30)

The 6-(4-methylphenyl)-2-methoxypyridine (**2.6**) (150 mg, 0.75 mmol, 1 eq.) in EtOH (5 mL) was added slowly to a stirred solution of Hg(OAc)₂ (240 g, 0.75 mmol) in EtOH (5 mL). The mixture was heated at reflux



for 12 h and filtered (hot) into a solution of LiCl (32 mg, 0.75 mmol) in MeOH (5 mL). This mixture was heated at reflux for 1 h and allowed to cool overnight. The precipitate was filtered off, washed with H₂O (10 mL) and EtOH (10 mL, 0 °C) to give an organomercury intermediate (63 mg, 19%). Mp: 163-165 °C. ¹H NMR (400 MHz, CD₂Cl₂, 298 K): δ 2.30 (s, Me, 3H), 4.04 (s, OMe, 3H), 6.71 (dd, *J*_{H-H} 8.3, 0.7, 1H), 7.31 (app d, *J*_{H-H} 7.8, 1H), 7.25 (s and dd, ³*J*_{H-Hg} 202, 7.5, 1H), 7.27 (dd, *J*_{H-H} 8.7, 0.5, 1H), 7.62 (dd, *J*_{H-H} 8.2, 7.5, 1H), 7.66 (d, *J*_{H-H} 8.0, 1H). Sample was insufficiently soluble for ¹³C{¹H}; therefore, selective ¹³C data was acquired by an HMQC experiment. HMQC NMR (125 MHz, CD₂Cl₂, 298 K): δ 21.0 (Me), 55.0 (OMe), 109.6 (CH), 114.6 (CH), 128.5 (CH), 130.0 (CH), 137.8 (CH), 140.0 (CH). IR (selected bands, cm⁻¹): 1574, 1408, 1321, 1247, 1013, 789. MS (ES): *m/z* 439 [(M-Cl)+MeCN]. TOFMS (ASAP): *m/z* 436.0384 [M+H]⁺ (C₁₃H₁₃Cl²⁰¹HgNO requires 436.0347), 400.0627 [M-Cl]⁺ (C₁₃H₁₂²⁰¹HgNO requires 400.0625).

General Procedure for Alcohol Oxidation Using OMe-containing Complexes

Base (0.20 mmol), MS 3 Å (500 mg) and naphthalene were added to a mixture of palladium complex (5 mol% Pd, 0.025 mmol) and toluene (3 mL) in a dry 25-mL two-neck flask equipped with cooler and drying tube. The mixture was heated at 80 °C for 15 min and then a solution of benzyl alcohol (108.2 mg, 1 mmol) in toluene (4 mL) was added dropwise with a syringe. Additional toluene (2 mL) was added to rinse the syringe. The reaction mixture was stirred at 80 °C for the time indicated (see **Table 2.7**). A sample was taken, dissolved in CDCl₃ and analysed by ¹H NMR spectroscopy. The conversion was determined by ¹H NMR analysis of the reaction mixture based on the starting material, benzyl alcohol.

5.3 Experimental Procedures for Chapter 3

General Procedure for Synthesis of 6-aryl-2-pyridone Ligands

A 10-mL round bottom flask with a magnetic stir bar and reflux condenser, was loaded with 6-aryl-2-methoxypyridine (0.557 mmol) and aqueous 48% HBr (2.5 mL, 22 mmol, 40 eq.). This solution was heated at reflux for 4 hours (set oil bath to 125 °C). The solution was then allowed to cool to room temperature and neutralised with saturated NaHCO₃. The product was extracted with DCM (3 x 50 mL). The organic layers were combined, dried over MgSO₄ and the solvent was removed under reduced pressure to yield a solid. This was taken up in minimum amount of methanol and heated to dissolve all products. After cooling, crystals were afforded (64-90%).

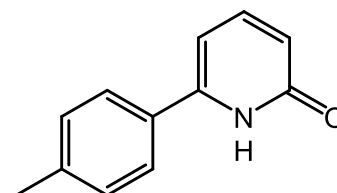
5.3.1 Synthesis of 6-phenyl-2-pyridone (3.1)

This was prepared from 6-phenyl-2-methoxypyridine (**2.5**) (103 mg) and aqueous 48% HBr and after work up and recrystallisation gave **3.1** as white crystals (61.9 mg, 65%). Mp: 196-198 °C. ¹H NMR (400 MHz, CDCl₃, 298 K): δ 6.47 (dd, *J*_{H-H} 7.0, 0.8, 1H), 6.53 (dd, *J*_{H-H} 9.1, 0.8, 1H), 7.48 (m, 4H), 7.71 (m, 2H), 12.15 (br s, NH, 1H). ¹³C{¹H} NMR (100 MHz, CDCl₃, 298 K): δ 104.7 (CH), 118.7 (CH), 126.5 (CH), 129.1 (CH), 130 (CH), 133.5 (C), 141.3 (CH), 146.8 (C), 165.0 (C). IR (selected bands, cm⁻¹): 2793, 1641, 1610, 1492, 1442, 1152, 992, 794, 759, 692. MS (ES): *m/z* 172 [M]⁺. TOFMS (ES): *m/z* 172.0762 [M+H]⁺ (C₁₁H₁₀NO requires 172.0718). Data are consistent with those reported in the literature.⁹



5.3.2 Synthesis of 6-(4-methylphenyl)-2-pyridone (3.2)

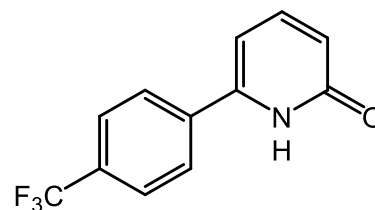
This was prepared from 6-(4-methylphenyl)-2-methoxypyridine (**2.6**) (110.9 mg) and aqueous 48% HBr and after work up and recrystallisation gave **3.2** as white crystals (93.5 mg, 91%). Mp: 202-204 °C. ¹H NMR (400 MHz, CDCl₃, 298 K): δ 2.31 (s, Me, 3H), 6.36 (d, *J*_{H-H} 6.8, 1H), 6.43 (d, *J*_{H-H} 9.0, 1H), 7.20 (d, *J*_{H-H} 7.8, 2H), 7.37 (dd, *J*_{H-H} 8.8, 7.1, 1H), 7.54 (d, *J*_{H-H} 8.2, 2H), 12.34 (br s, NH, 1H). ¹³C{¹H} NMR (100 MHz, CDCl₃, 298 K): δ 20.3 (Me), 103.4 (CH), 117.2 (CH), 125.5 (CH), 128.7 (CH), 129.6 (C), 139.2 (C), 140.3 (CH), 146.1 (C), 164.3 (C). IR (selected bands, cm⁻¹): 2970, 1638, 1602, 1510, 1157, 989, 933, 816, 787, 715. MS (ES):



m/z 186 $[M]^+$. TOFMS (ES): m/z 186.0905 $[M+H]^+$ ($C_{12}H_{12}NO$ requires 186.0874). Data are consistent with those reported in the literature.¹⁰

5.3.3 Synthesis of 6-(4-trifluoromethylphenyl)-2-pyridone (3.3)

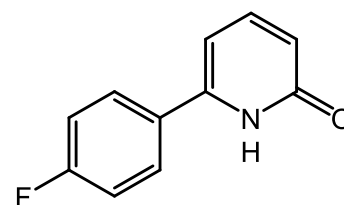
This was prepared from 6-(4-trifluoromethylphenyl)-2-methoxypyridine (**2.7**) (141 mg) and aqueous 48% HBr and after work up and recrystallisation gave **3.3** as white crystals (100 mg, 75%). Crystals suitable for single crystal X-ray



diffraction were grown by slow evaporation of a methanol solution of the ligand. Mp: 203-205 °C. 1H NMR (400 MHz, $CDCl_3$, 298 K): δ 6.4 (d, J_{H-H} 7.0, 1H), 6.52 (d, J_{H-H} 9.1, 1H), 7.44 (dd, J_{H-H} 9.1, 7.0, 1H), 7.66 (d, J_{H-H} 8.2, 2H), 7.80 (d, J_{H-H} 8.2, 2H), 13.13 (br s, NH, 1H). $^{13}C\{^1H\}$ NMR (100 MHz, $CDCl_3$, 298 K): δ 106.0 (CH), 119.6 (CH), 123.8 (q, $^1J_{C-F}$ 271.6, CF_3), 126.0 (q, $^3J_{C-F}$ 3.0, CH), 127.3 (CH), 131.7 (q, $^2J_{C-F}$ 33.1, C), 136.8 (C), 141.3 (CH), 145.6 (C), 165.6 (C). ^{19}F NMR (376 MHz, $CDCl_3$, 298 K): δ -62.8 (s, CF_3). IR (selected bands, cm^{-1}): 2912, 1642, 1604, 1574, 1334, 1158, 1110, 986, 828, 789. MS (ES): m/z 240 $[M]^+$. TOFMS (ES): m/z 240.0628 $[M+H]^+$ ($C_{12}H_9F_3NO$ requires 240.0592). Data are consistent with those reported in the literature.⁹

5.3.4 Synthesis of 6-(4-fluorophenyl)-2-pyridone (3.4)

This was prepared from 6-(4-fluorophenyl)-2-methoxypyridine (**2.8**) (113.1 mg) and aqueous 48% HBr and after work up and recrystallisation gave **3.4** as white crystals (93.4 mg, 88%). Mp: 193-195 °C. $^1H\{^{19}F\}$ NMR

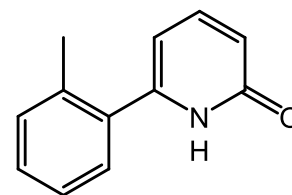


(400 MHz, $CDCl_3$, 298 K): δ 6.36 (d, J_{H-H} 6.9, 1H), 6.45 (d, J_{H-H} 9.0, 1H), 7.11 (d, J_{H-H} 8.7, 2H), 7.4 (t, J_{H-H} 8.5, 1H), 7.67 (d, J_{H-H} 8.8, 2H), 12.68 (br s, NH, 1H). $^{13}C\{^1H\}$ NMR (100 MHz, $CDCl_3$, 298 K): δ 104.9 (CH), 116.2 (d, $^2J_{C-F}$ 21.3, CH), 118.5 (CH), 128.8 (d, $^3J_{C-F}$ 9.1, CH), 129.7 (C), 141.4 (CH), 146.1 (C), 163.8 (d, $^1J_{C-F}$ 250.4, C), 165.4 (C). ^{19}F NMR (376 MHz, $CDCl_3$, 298 K): δ -110.6 (s, F). IR (selected bands, cm^{-1}): 2913, 1651, 1614, 1509, 1226, 1158, 986, 831, 788, 723. MS (ES): m/z 190 $[M]^+$. TOFMS (ES): m/z 190.0653 $[M+H]^+$ ($C_{11}H_9FNO$ requires 190.0623).

5.3.5 Synthesis of 6-(2-methylphenyl)-2-pyridone (3.5)

This was prepared from 6-(2-methylphenyl)-2-methoxypyridine (**2.9**) (110.9 mg) and aqueous 48% HBr and after work up and recrystallisation gave **3.5** as light brown

crystals (82.3 mg, 74%). Mp: 159-161 °C. ¹H NMR (400 MHz, CDCl₃, 298 K): δ 2.26 (s, Me, 3H), 6.06 (dd, *J*_{H-H} 6.7, 0.6, 1H), 6.33 (dd, *J*_{H-H} 9.0, 0.5, 1H), 7.21 (m, 4H), 7.33 (dd, *J*_{H-H} 9.1, 6.8, 1H), 12.17 (br s, NH, 1H). ¹³C{¹H} NMR (100 MHz, CDCl₃, 298 K): δ 20.0 (Me), 107.1 (CH), 118.5 (CH), 126.0 (CH), 129.2 (CH), 129.6 (CH), 130.9 (CH), 134.1.3 (C), 136 (C), 141.0 (CH), 147.3 (C), 164.9 (C). IR (selected bands, cm⁻¹): 2778, 1637, 1609, 1548, 1459, 1160, 984, 810, 765, 726. MS (ES): *m/z* 186 [M+H]⁺. TOFMS (ES): *m/z* 186.0870 [M+H]⁺ (C₁₂H₁₂NO requires 186.0874). Data are consistent with those reported in the literature.¹⁰



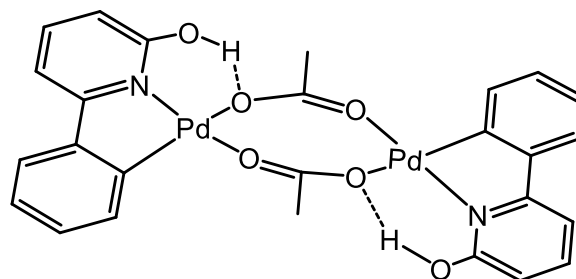
Synthesis of Novel Complexes Containing an OH-N⁺C Ligand

General Procedure for Synthesis of [Pd(κ²-6-aryl-2-pyridinol)(μ-OAc)]₂

The 6-aryl-2-pyridone (1 eq.) and Pd(OAc)₂ (1 eq.) were combined in glacial acetic acid in a 10-mL flask equipped with a magnetic stir bar and stirred at 90 °C for 12 h. The precipitate was then filtered, washed with diethyl ether or hexane (5 mL), collected and dried. The product was obtained as a solid (63-77% yield).

5.3.6 Synthesis of [Pd(κ²-6-phenyl-2-pyridinol)(μ-OAc)]₂ (3.6)

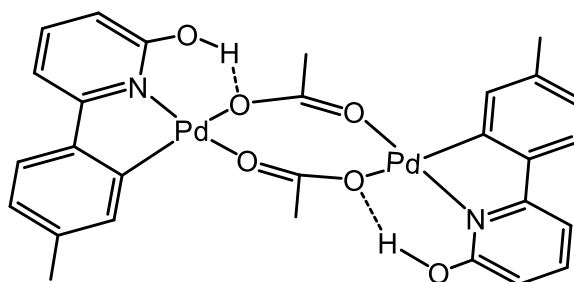
The flask was loaded with **3.1** (0.017 g, 0.104 mmol), Pd(OAc)₂ (0.023 g, 0.104 mmol) and glacial acetic acid (3 mL) and after work up gave **3.6** as a dark orange solid (0.026 g, 73%). Mp > 270 °C. ¹H NMR (400 MHz, CDCl₃, 298 K):



δ 2.27 (s, O₂CMe, 6H), 5.95 (d, *J*_{H-H} 8.3, 2H), 6.72 (m, 4H), 6.84 (m, 6H), 7.28 (t, *J*_{H-H} 7.3, 2H), 9.63 (s, OH, 2H). ¹³C{¹H} NMR (100 MHz, CDCl₃, 298 K): δ 25.01 (O₂CMe), 109.2 (CH), 109.3 (CH), 122.6 (CH), 124.6 (CH), 128.2 (CH), 129.0 (CH), 140.1 (CH), 145.1 (C), 147.3 (C), 161.4 (C), 164.9 (C), 184.4 (O₂CMe). IR (selected bands, cm⁻¹): 3057, 1620, 1548, 1408, 1341, 1222, 801, 677. MS (ES): *m/z* 317 [Pd(L_H)+MeCN]⁺, 358 [Pd(L_H)+2MeCN]⁺, 635 [Pd₂(HL_H)₂+2MeCN]⁺. TOFMS (ASAP): *m/z* 279.0935 [Pd(L_H)]⁺ (C₁₁H₈NO¹⁰⁶Pd requires 278.9678). Anal Calcd for C₂₆H₂₂N₂O₆Pd₂: C, 46.52; H, 3.30; N, 4.17; found: C, 46.61; H, 3.21; N, 4.23%.

5.3.7 Synthesis of [Pd(κ^2 -6-(4-methylphenyl)-2-pyridinol)(μ -OAc)]₂ (3.7)

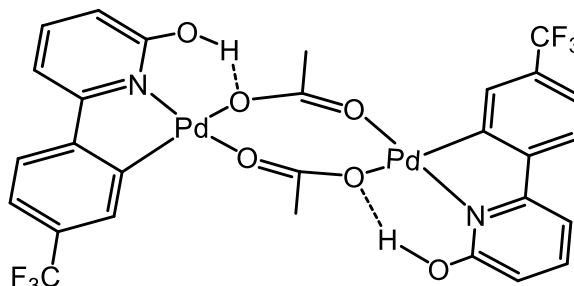
The flask was loaded with **3.2** (0.029 g, 0.158 mmol), Pd(OAc)₂ (0.036 g, 0.155 mmol) and glacial acetic acid (3 mL) and after work up gave **3.7** as a dark yellow solid (0.036 g, 65%). Mp > 270 °C. ¹H NMR (400 MHz, CDCl₃, 298 K):



δ 2.20 (s, Me, 6H), 2.26 (s, O₂CMe, 6H), 5.98 (dd, $J_{\text{H-H}}$ 8.3, 0.9, 2H), 6.48 (s, 2H), 6.56 (d, $J_{\text{H-H}}$ 8.0, 2H), 6.64 (dd, $J_{\text{H-H}}$ 7.7, 0.9, 2H), 6.71 (d, $J_{\text{H-H}}$ 7.9, 2H), 7.24 (t, $J_{\text{H-H}}$ 7.9, 2H), 9.62 (s, OH, 2H). ¹³C{¹H} NMR (125 MHz, CDCl₃, 298 K): δ 21.7 (Me), 25.2 (O₂CMe), 108.3 (CH), 108.8 (CH), 122.4 (CH), 125.5 (CH), 131.6 (CH), 138.3 (C), 140.1 (CH), 142.3 (C), 147.1 (C), 161.7 (C), 164.8 (C), 184.2 (O₂CMe). IR (selected bands, cm⁻¹): 1547, 1405, 1340, 1162, 787, 674. MS (ES): m/z 331 [Pd(L_{Me})+MeCN]⁺, 372 [Pd(L_{Me})+2MeCN]⁺, 663 [Pd₂(L_{Me})₂+2MeCN]⁺. TOFMS (ASAP): m/z 1159.9000 [Pd(L_{Me})₄]⁴⁺ (C₄₈H₄₀N₄O₄¹⁰⁶Pd₄ requires 1159.9189). Anal Calcd for C₂₈H₂₆N₂O₆Pd₂: C, 48.09; H, 3.75; N, 4.01; found: C, 47.93; H, 3.81; N, 4.11%.

5.3.8 Synthesis of [Pd(κ^2 -6-(4-trifluoromethylphenyl)-2-pyridinol)(μ -OAc)]₂ (3.8)

The flask was loaded with **3.3** (0.017 g, 0.071 mmol), Pd(OAc)₂ (0.016 g, 0.071 mmol) and glacial acetic acid (3 mL) and after work up gave **3.8** as a yellow solid (0.022 g, 77%). Crystals suitable for a single crystal X-ray

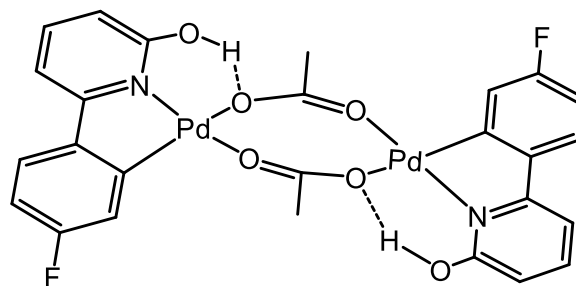


diffraction study were grown from a dichloromethane solution of the complex layered with hexane. Mp > 270 °C. ¹H NMR (400 MHz, CDCl₃, 298 K): δ 2.30 (s, O₂CMe, 6H), 6.09 (d, $J_{\text{H-H}}$ 8.4, 2H), 6.77 (dd, $J_{\text{H-H}}$ 7.6, 0.9, 2H), 6.93 (d, $J_{\text{H-H}}$ 8.0, 2H), 6.96 (s, 2H), 7.05 (dd, $J_{\text{H-H}}$ 8.1, 0.9, 2H), 7.33 (t, $J_{\text{H-H}}$ 7.9, 2H), 9.66 (s, OH, 2H). Sample was insufficiently soluble for ¹³C{¹H}; therefore, selective ¹³C data was acquired by an HSQC experiment. HSQC NMR (125 MHz, CDCl₃, 298 K): δ 25.2 (O₂CMe), 109.8 (CH), 110.9 (CH), 121.6 (CH), 122.1 (CH), 127.2 (CH), 140.9 (CH). ¹⁹F NMR (376 MHz, CDCl₃, 298 K): δ -63.2 (s, CF₃). IR (selected bands, cm⁻¹): 3050, 1545, 1412, 1317, 1240, 1118, 1073, 794, 722, 678. MS (ES): m/z 385 [Pd(L_{CF3})+MeCN]⁺, 426 [Pd(L_{CF3})+2MeCN]⁺, 771 [Pd₂(L_{CF3})₂+2MeCN]⁺. TOFMS (ASAP): m/z 807.9313 [M]⁺ (C₂₈H₂₀F₆N₂O₆¹⁰⁶Pd₂

requires 807.9299). Anal Calcd for C₂₈H₂₀F₆N₂O₆Pd₂: C, 41.66; H, 2.50; N, 3.47; found: C, 41.58; H, 2.43; N, 3.54%.

5.3.9 Synthesis of [Pd(κ^2 -6-(4-fluorophenyl)-2-pyridinol)(μ -OAc)]₂ (3.9)

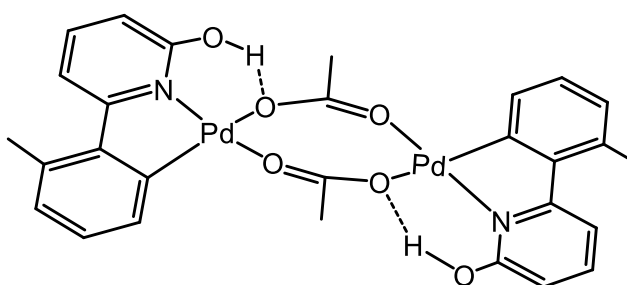
The flask was loaded with **3.4** (0.029 g, 0.155 mmol), Pd(OAc)₂ (0.035 g, 0.155 mmol) and glacial acetic acid (3 mL) and after work up gave **3.9** as a yellow solid (0.042 g, 77%). Mp: > 270 °C. ¹H{¹⁹F} NMR (400 MHz, CDCl₃,



298 K): δ 2.28 (s, O₂CMe, 6H), 6.06 (dd, J_{H-H} 8.3, 0.9, 2H), 6.38 (d, J_{H-H} 2.4, 2H), 6.53 (dd, J_{H-H} 8.5, 2.2, 2H), 6.62 (dd, J_{H-H} 7.6, 0.9, 2H), 6.83 (d, J_{H-H} 8.6, 2H), 7.3 (t, J_{H-H} 7.9, 2H), 9.53 (s, OH, 2H). ¹³C{¹H} NMR (125 MHz, CDCl₃, 298 K): δ 25.0 (O₂CMe), 109.1 (CH), 109.2 (CH), 111.9 (d, ²J_{C-F} 23.0, CH), 117.7 (d, ²J_{C-F} 20.5, CH), 123.7 (d, ³J_{C-F} 8.5, CH), 140.5 (CH), 141.2 (d, ³J_{C-F} 2.0, C), 148.9 (C), 160.2 (d, ¹J_{C-F} 255.6, C), 161.2 (C), 165.0 (C), 184.7 (O₂CMe). ¹⁹F NMR (376 MHz, CDCl₃, 298 K): δ -109.0 (s, F). IR (selected bands, cm⁻¹): 1544, 1412, 1248, 1188, 1159, 855, 788, 679. MS (ES): m/z 335 [Pd(L_F)+MeCN]⁺, 376 [Pd(L_F)+2MeCN]⁺, 671 [Pd₂(L_F)₂+2MeCN]⁺. TOFMS (ASAP): 1173.8048 [Pd(L_F)₄]⁺ (C₄₄H₂₈F₄N₄O₄¹⁰⁶Pd₄ requires 1173.8218).

5.3.10 Synthesis of [Pd(κ^2 -6-(2-methylphenyl)-2-pyridinol)(μ -OAc)]₂ (3.10)

The flask was loaded with **3.5** (0.029 g, 0.158 mmol), Pd(OAc)₂ (0.036 g, 0.155 mmol) and glacial acetic acid (3 mL) and after work up gave **3.10** as a dark yellow solid (0.045 g, 68%). Mp: > 270 °C. ¹H

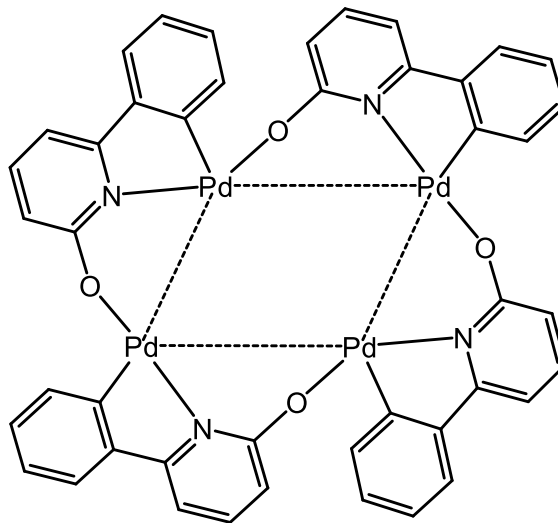


NMR (400 MHz, CDCl₃, 298 K): δ 2.24 (s, O₂CMe, 6H), 2.29 (s, Me, 6H), 5.96 (dd, J_{H-H} 8.3, 0.9, 2H), 6.67 (m, 4H), 6.74 (t, J_{H-H} 7.7, 2H), 6.92 (d, J_{H-H} 6.6, 2H), 7.30 (t, J_{H-H} 8.0, 2H), 9.77 (s, OH, 2H). ¹³C{¹H} NMR (125 MHz, CDCl₃, 298 K): δ 23.7 (Me), 25.0 (O₂CMe), 109.2 (CH), 113.1 (CH), 126.9 (CH), 129.0 (CH), 129.3 (CH), 134.0 (C), 139.5 (CH), 142.8 (C), 149.4 (C), 161.7 (C), 164.8 (C), 184.0 (O₂CMe). IR (selected bands, cm⁻¹): 1544, 1406, 1340, 1221, 1163, 1019, 798, 676. MS (ES): m/z 331 [Pd(L_{Me})+MeCN]⁺, 372 [Pd(L_{Me})+2MeCN]⁺, 663 [Pd₂(L_{Me})₂+2MeCN]⁺. TOFMS (ASAP): m/z 1159.9000 [Pd(L_{Me})₄]⁺ (C₄₈H₄₀N₄O₄¹⁰⁶Pd₄ requires 1159.9189).

Tetrameric Complexes with the General Formula $[\text{Pd}(\mu:\kappa^2\text{-6-aryl-2-pyridonate})]_4$

5.3.11 Synthesis of $[\text{Pd}(\mu:\kappa^2\text{-6-phenyl-2-pyridonate})]_4$ (**3.11**)

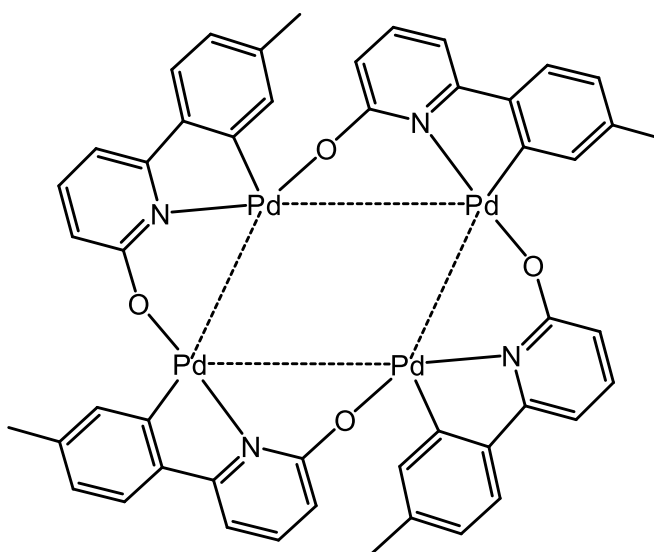
A 5-mL round bottom flask, open to the air, was loaded with **3.6** (9 mg, 0.013 mmol) and CDCl_3 (0.5 mL). A stopper was attached and the mixture left to stand at room temperature for 24 h. The reaction was monitored by ^1H NMR spectroscopy revealing a mixture of **3.11** and unreacted **3.6**. After 48 h, ^1H NMR spectrum showed no further change. All volatiles were removed under reduced pressure and the



remaining solid was re-dissolved in CDCl_3 (0.5 mL) and left for 24 h. The process of solvent removal and dissolving in CDCl_3 was repeated three more times to afford pure **3.11** as a yellow solid (7 mg, 95%). $\text{Mp} > 270\text{ }^\circ\text{C}$. ^1H NMR (400 MHz, CDCl_3 , 298 K): δ 5.92 (dd, $J_{\text{H-H}}$ 8.6, 0.9, 1H), 6.74 (dd, $J_{\text{H-H}}$ 7.4, 1.0, 1H), 6.93 (m, 2H), 7.01 (m, 1H), 7.17 (m, 1H), 7.37 (d, $J_{\text{H-H}}$ 7.7 Hz, 1H). $^{13}\text{C}\{^1\text{H}\}$ (125 MHz, CDCl_3 , 298 K): δ 105.6 (CH), 115.1 (CH), 123.4 (CH), 127.4 (CH), 128.6 (CH), 131.1, (CH), 138.3 (CH), 145.5 (C), 147.0 (C), 159.9 (C), 171.5 (C). IR (selected bands, cm^{-1}): 1609, 1543, 1479, 1435, 1028, 790. MS (ES): m/z 1130 $[\text{M}]^+$. Anal Calcd for $\text{C}_{46}\text{H}_{34}\text{N}_4\text{O}_4\text{Pd}_4$: C, 48.79; H, 3.03; N, 4.95; found: C, 48.01; H, 2.77; N, 4.98%.

5.3.12 Synthesis of $[\text{Pd}(\mu:\kappa^2\text{-6-(4-methylphenyl)-2-pyridonate})]_4$ (**3.12**)

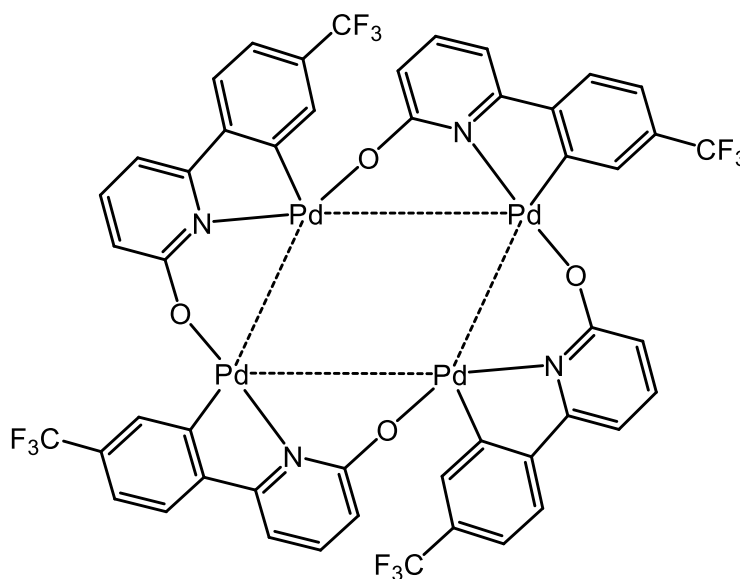
Based on the procedure described for **3.11**, using **3.7** (20 mg, 0.029 mmol) in CDCl_3 (4 mL), gave **3.12** as a yellow solid (15 mg, 87%). Crystals suitable for single crystal X-ray diffraction were grown by slow evaporation of a chloroform solution of the complex. $\text{Mp} > 270\text{ }^\circ\text{C}$. ^1H NMR (400 MHz, CDCl_3 , 298 K): δ 2.17 (s, Me, 3H), 5.88 (dd, $J_{\text{H-H}}$ 8.6, 1.0,



1H), 6.68 (dd, $J_{\text{H-H}}$ 7.3, 1.0, 1H), 6.71 (dd, $J_{\text{H-H}}$ 0.7, 1H), 6.96 (dd, $J_{\text{H-H}}$ 7.8, 0.7, 1H), 6.99 (dd, $J_{\text{H-H}}$ 7.3, 8.5, 1H), 7.24 (d, $J_{\text{H-H}}$ 7.8, 1H). $^{13}\text{C}\{^1\text{H}\}$ (125 MHz, CDCl_3 , 298 K): δ 21.8 (Me), 105.1 (CH), 114.5 (CH), 123.0 (CH), 128.2 (CH), 132.5 (CH), 138.3 (CH), 138.9 (C), 144.1 (C), 145.4 (C), 160.1 (C), 171.4 (C). IR (selected bands, cm^{-1}): 1609, 1542, 1481, 1455, 1031, 785. MS (ES): m/z 1159 $[\text{M}]^+$. TOFMS (ASAP): m/z 1185.8998 $[\text{M}]^+$ ($\text{C}_{50}\text{H}_{42}\text{N}_4\text{O}_4^{106}\text{Pd}_4$ requires 1185.9345). Anal Calcd for $\text{C}_{50}\text{H}_{42}\text{N}_4\text{O}_4\text{Pd}_4 \cdot 1.6\text{CHCl}_3$: C, 44.92; H, 3.19; N, 4.06; found: C, 44.86; H, 3.01; N, 4.92%.

5.3.13 Synthesis of $[\text{Pd}(\mu\text{:}\kappa^2\text{-6-(4-trifluoromethylphenyl)-2-pyridonate})_4]$ (**3.13**)

Based on the procedure described for **3.11**, using **3.8** (22 mg, 0.027 mmol) in CDCl_3 (4 mL), gave **3.13** as a yellow solid (13 mg, 69%). To allow full conversion of **3.8** to **3.13** the process of solvent removal and heating at 50 °C in CDCl_3 was repeated up to 15 times.

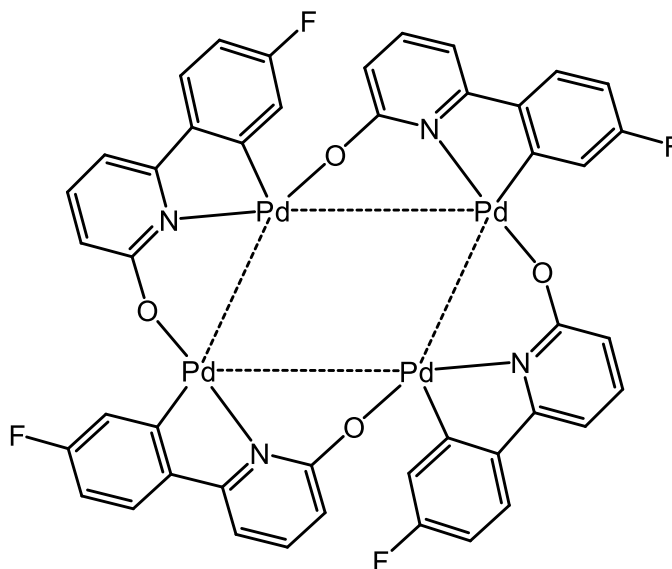


Crystals suitable for single crystal X-ray diffraction were grown by slow evaporation of a chloroform solution of the complex. Mp > 270 °C. ^1H NMR (400 MHz, CDCl_3 , 298 K): δ 6.03 (dd, $J_{\text{H-H}}$ 8.6, 0.9, 1H), 6.87 (dd, $J_{\text{H-H}}$ 7.3, 0.8, 1H), 7.12 (s, 1H), 7.13 (dd, $J_{\text{H-H}}$ 7.1, 8.6, 1H), 7.5 (m, 2H). Sample was insufficiently soluble for $^{13}\text{C}\{^1\text{H}\}$; therefore, selective ^{13}C data was acquired by a DEPT 135 experiment. DEPT 135 NMR (125 MHz, CDCl_3 , 298 K): δ 107.3 (CH), 116.3 (CH), 123.4 (CH), 124.8 (CH), 128.2 (CH), 139.1 (CH). ^{19}F NMR (376 MHz, CDCl_3 , 298 K): δ -62.6 (s, CF_3). IR (selected bands, cm^{-1}): 1613, 1544, 1484, 1461, 1314, 1121, 790. MS (ES): m/z 1374 $[\text{M}]^+$. TOFMS (ASAP): m/z 1374.7856 $[\text{M}]^+$ ($\text{C}_{48}\text{H}_{24}\text{F}_{12}\text{N}_4\text{O}_4^{106}\text{Pd}_4$ requires 1374.4048). Anal Calcd for $\text{C}_{48}\text{H}_{24}\text{F}_{12}\text{N}_4\text{O}_4\text{Pd}_4$: C, 41.95; H, 1.76; N, 4.08; found: C, 41.94; H, 1.73; N, 4.16%.

5.3.14 Synthesis of $[\text{Pd}(\mu\text{:}\kappa^2\text{-6-(4-fluorophenyl)-2-pyridonate})_4]$ (**3.14**)

Based on the procedure described for **3.11**, using **3.9** (28 mg, 0.04 mmol) in CDCl_3 (4 mL), gave **3.14** as a yellow solid (13 mg, 56%). To allow full conversion of **3.9** to **3.14** the process of solvent removal and heating at 50 °C in CDCl_3 was repeated up to 5 times.

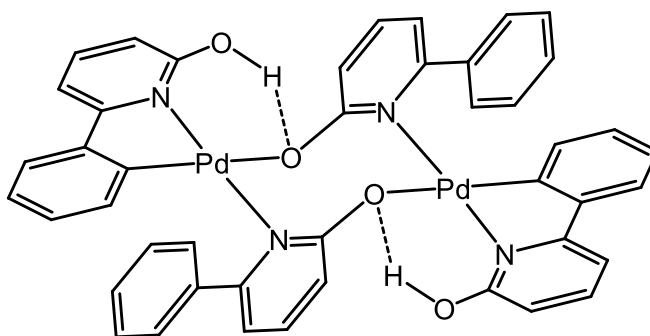
Mp > 270 °C. $^1\text{H}\{^{19}\text{F}\}$ NMR (400 MHz, CDCl_3 , 298 K): δ 5.84 (dd, $J_{\text{H-H}}$ 8.6, 0.9, 1H), 6.55 (d, $J_{\text{H-H}}$ 2.5, 1H), 6.61 (dd, $J_{\text{H-H}}$ 7.3, 0.9, 1H), 6.86 (dd, $J_{\text{H-H}}$ 8.5, 2.5, 1H), 6.98 (t, $J_{\text{H-H}}$ 7.3, 1H), 7.30 (d, $J_{\text{H-H}}$ 8.6, 1H). Sample was insufficiently soluble for $^{13}\text{C}\{^1\text{H}\}$; therefore, selective ^{13}C data was acquired by an HSQC experiment. HSQC NMR (125 MHz, CDCl_3 , 298 K): δ 105.3 (CH), 114.5 (CH), 124.7 (CH), 118.7 (CH), 124.0 (CH), 138.6 (CH). ^{19}F NMR (376 MHz, CDCl_3 , 298 K): δ -108.5 (s, F). IR (selected bands, cm^{-1}): 1609, 1568, 1543, 1481, 1451, 1187, 1027, 854, 783, 720. TOFMS (ASAP): m/z 1174.8033 $[\text{M}]^+$ ($\text{C}_{44}\text{H}_{24}\text{F}_4\text{N}_4\text{O}_4^{106}\text{Pd}_4$ requires 1174.7897).



Dimeric Complexes with the General Formula $[\text{Pd}(\mu\text{-6-aryl-2-pyridonate})(\kappa^2\text{-6-aryl-2-pyridinol})_2]$

5.3.15 Synthesis of $[\text{Pd}(\mu\text{-6-phenyl-2-pyridonate})(\kappa^2\text{-6-phenyl-2-pyridinol})_2]$ (**3.15**)

A small-sized Schlenk flask, equipped with a magnetic stir bar, was evacuated and backfilled with nitrogen. The flask was loaded with **3.1** (16 mg, 0.09 mmol), **3.6** (30.2 mg, 0.045 mmol) and CDCl_3 (3 mL). The mixture was stirred at

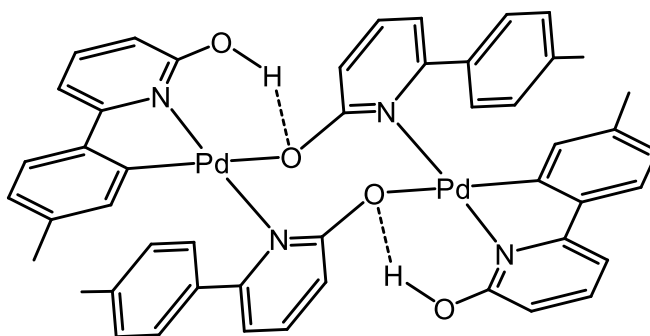


room temperature for 20 h. The solvent was then removed under reduced pressure. The resulting residue was dissolved in dichloromethane (2 mL) and hexane added slowly to induce precipitation. The precipitate was then collected, washed with hexane and dried under reduced pressure to give **3.15** as a yellow solid (33 mg, 82%). Mp > 270 °C. ^1H NMR (400 MHz, CDCl_3 , 298 K): δ 5.67 (d, $J_{\text{H-H}}$ 8.3, 2H), 5.85 (d, $J_{\text{H-H}}$ 7.7, 2H), 6.46 (d, $J_{\text{H-H}}$ 7.4, 2H), 6.66 (m, 10H), 7.08 (t, $J_{\text{H-H}}$ 7.8, 2H), 7.37 (t, $J_{\text{H-H}}$ 7.1, 4H), 7.44 (t, $J_{\text{H-H}}$ 7.2, 2H), 7.49 (t, $J_{\text{H-H}}$ 7.7, 2H), 7.97 (d, $J_{\text{H-H}}$ 7.2, 4H), 12.35 (s, OH, 2H). $^{13}\text{C}\{^1\text{H}\}$ NMR (125 MHz, CDCl_3 , 298 K): δ 108.2 (CH), 109.7 (CH), 113.8 (CH), 115.8 (CH), 122.6 (CH),

123.3 (CH), 127.9 (CH), 128.0 (CH), 128.4 (CH), 129.3 (CH), 133.2 (CH), 139.0 (CH), 139.1 (CH), 141.8 (C), 145.6 (C), 149.1 (C), 158.9 (C), 161.0 (C), 166.5 (C), 169.8 (C). IR (selected bands, cm^{-1}): 3051, 1682, 1593, 1568. TOFMS (ASAP): m/z 893.0577 $[\text{M}+\text{H}]^+$ ($\text{C}_{44}\text{H}_{32}\text{N}_4\text{O}_4^{106}\text{Pd}_2$ requires 893.0513). Anal Calcd for $\text{C}_{44}\text{H}_{32}\text{N}_4\text{O}_4\text{Pd}_4$: C, 59.14; H, 3.61; N, 6.27; found: C, 58.84; H, 3.50; N, 6.18%.

5.3.16 Synthesis of $[\text{Pd}(\mu\text{-}6\text{-}(4\text{-methylphenyl})\text{-}2\text{-pyridonate})(\kappa^2\text{-}6\text{-}(4\text{-methylphenyl})\text{-}2\text{-pyridinol})]_2$ (**3.16**)

Based on the procedure described for **3.15** using **3.2** (8 mg, 0.04 mmol) and **3.7** (15 mg, 0.02 mmol) gave **3.16** as a yellow solid (11 mg, 58%). Crystals suitable for single crystal X-ray diffraction were grown by slow evaporation of



a chloroform solution of the complex. $\text{Mp} > 270\text{ }^\circ\text{C}$. ^1H NMR (400 MHz, CDCl_3 , 298 K): δ 2.05 (s, $\text{N}^{\wedge}\text{C}\text{-Me}$, 6H), 2.32 (s, $\text{N}^{\wedge}\text{O}\text{-Me}$, 6H), 5.70 (s, 2H), 5.72 (d, $J_{\text{H-H}}$ 8.4, 2H), 6.47 (d, $J_{\text{H-H}}$ 7.6, 2H), 6.55 (d, $J_{\text{H-H}}$ 7.3, 2H), 6.63 (d, $J_{\text{H-H}}$ 8.5, 2H), 6.67 (m, 4H), 7.12 (t, $J_{\text{H-H}}$ 7.9, 2H), 7.19 (d, $J_{\text{H-H}}$ 7.6, 4H), 7.42 (t, $J_{\text{H-H}}$ 7.6, 2H), 7.95 (d, $J_{\text{H-H}}$ 7.7, 4H), 12.27 (s, OH, 2H). $^{13}\text{C}\{^1\text{H}\}$ (125 MHz, CDCl_3 , 298 K): δ 21.4 ($\text{N}^{\wedge}\text{O}\text{-Me}$), 21.8 ($\text{N}^{\wedge}\text{C}\text{-Me}$), 107.7 (CH), 109.1 (CH), 113.6 (CH), 115.5 (CH), 122.3 (CH), 124.1 (CH), 128.6 (CH), 129.1 (CH), 133.9 (CH), 137.8 (C), 138.0 (C), 138.8 (CH), 138.9 (CH), 139.1 (C), 142.8 (C), 149.0 (C), 158.9 (C), 161.1 (C), 166.5 (C), 169.9 (C). IR (selected bands, cm^{-1}): 1596, 1571, 1435, 1313, 786. MS (ES): m/z 949 $[\text{M}]^+$. TOFMS (ASAP): m/z 951.1226 $[\text{M}]^+$ ($\text{C}_{48}\text{H}_{40}\text{N}_4\text{O}_4^{106}\text{Pd}_2$ requires 951.1157). Anal Calcd for $\text{C}_{48}\text{H}_{40}\text{N}_4\text{O}_4\text{Pd}_2 \cdot 1.1\text{CHCl}_3$: C 54.55; H, 3.83; N, 5.18; found: C, 54.48; H, 3.75; N, 5.80%.

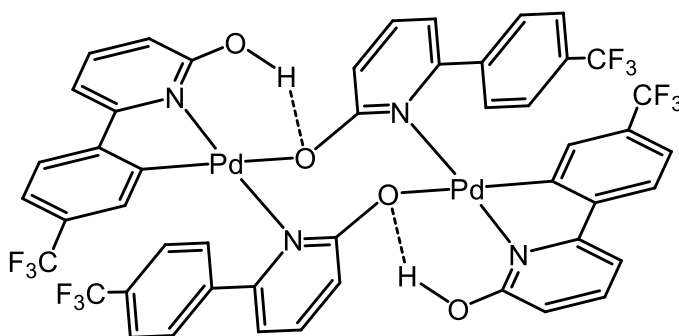
5.3.17 Synthesis of $[\text{Pd}(\mu\text{-}6\text{-}(4\text{-trifluoromethylphenyl})\text{-}2\text{-pyridonate})(\kappa^2\text{-}6\text{-}(4\text{-trifluoromethylphenyl})\text{-}2\text{-pyridinol})]_2$ (**3.17**)

Based on the procedure described for **3.15** using **3.3** (9 mg, 0.038 mmol) and **3.8** (15 mg, 0.019 mmol) gave **3.17** as a yellow solid (18 mg, 81%). Crystals suitable for single crystal X-ray diffraction were grown by slow evaporation of a chloroform solution of the complex. $\text{Mp} > 270\text{ }^\circ\text{C}$. ^1H NMR (400 MHz, CDCl_3 , 298 K): δ 5.83 (dd, $J_{\text{H-H}}$ 8.4, 1.0, 2H), 6.03 (s, 2H), 6.60 (dd, $J_{\text{H-H}}$ 7.7, 1.0, 2H), 6.80 (m, 6H), 7.00 (dd, $J_{\text{H-H}}$ 7.8, 1.0, 2H), 7.20 (t, $J_{\text{H-H}}$ 7.9, 2H), 7.6 (dd, $J_{\text{H-H}}$ 7.1, 8.4, 2H), 7.67 (d, $J_{\text{H-H}}$ 8.2, 4H), 8.10 (d, $J_{\text{H-H}}$

δ 8.0, 4H), 12.12 (s, OH, 2H).

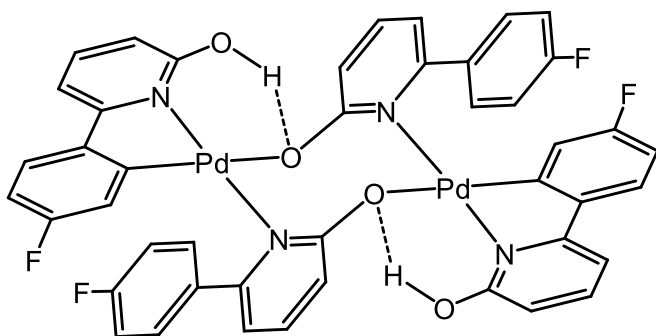
Sample was insufficiently soluble for $^{13}\text{C}\{^1\text{H}\}$; therefore, selective ^{13}C data was acquired by a DEPT 135 experiment. DEPT 135 (125 MHz, CDCl_3 , 298 K): δ 109.2 (CH), 111.2

(CH), 114.3 (CH), 116.7 (CH), 120.3 (CH), 122.3 (CH), 124.9 (CH), 128.9 (CH), 129.5 (CH), 139.7 (CH), 139.9 (CH). ^{19}F NMR (376 MHz, CDCl_3 , 298 K): δ -62.5 (s, CF_3), -63.2 (s, CF_3). IR (selected bands, cm^{-1}): 1601, 1570, 1437, 1314, 1115, 791. MS (ES): m/z 1166 $[\text{M}]^+$. TOFMS (ASAP): m/z 1167.0142 $[\text{M}]^+$ ($\text{C}_{48}\text{H}_{28}\text{F}_{12}\text{N}_4\text{O}_4^{106}\text{Pd}_2$ requires 1167.0026). Anal Calcd for $\text{C}_{48}\text{H}_{28}\text{F}_{12}\text{N}_4\text{O}_4\text{Pd}_2$: C, 49.46; H, 2.42; N, 4.81; found: C, 49.28; H, 2.29; N, 4.94%.



5.3.18 Synthesis of $[\text{Pd}(\mu\text{-}6\text{-}(4\text{-fluorophenyl})\text{-}2\text{-pyridonate})(\kappa^2\text{-}6\text{-}(4\text{-fluorophenyl})\text{-}2\text{-pyridinol})_2$ (**3.18**)

Based on the procedure described for **3.15** using **3.4** (11 mg, 0.056 mmol) and **3.9** (20 mg, 0.028 mmol) gave **3.18** as a dark yellow solid (27 mg, 97%). Crystals suitable for single crystal X-ray diffraction were grown by



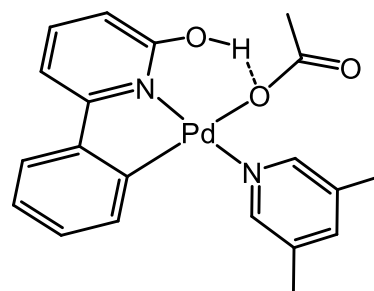
slow evaporation of a chloroform solution of the complex. Mp > 270 °C. $^1\text{H}\{^{19}\text{F}\}$ NMR (400 MHz, CDCl_3 , 298 K): δ 5.52 (d, $J_{\text{H-H}}$ 2.6, 2H), 5.82 (dd, $J_{\text{H-H}}$ 8.3, 1.0, 2H), 6.46 (dd, $J_{\text{H-H}}$ 7.8, 0.9, 2H), 6.48 (dd, $J_{\text{H-H}}$ 8.6, 2.5, 2H), 6.71 (dd, $J_{\text{H-H}}$ 8.4, 1.2, 2H), 6.73 (dd, $J_{\text{H-H}}$ 7.2, 1.3, 2H), 6.77 (d, $J_{\text{H-H}}$ 8.6, 2H), 7.10 (td, $J_{\text{H-H}}$ 8.8, 2.1, 4H), 7.17 (t, $J_{\text{H-H}}$ 7.9, 2H), 7.49 (dd, $J_{\text{H-H}}$ 8.4, 7.2, 2H), 8.00 (td, $J_{\text{H-H}}$ 8.9, 2.1, 4H), 12.11 (s, OH, 2H). Sample was insufficiently soluble for $^{13}\text{C}\{^1\text{H}\}$; therefore, selective ^{13}C data was acquired by HMQC and HMBC experiments. HMQC (100 MHz, CDCl_3 , 298 K): δ 108.2 (CH), 109.7 (CH), 110.4 (CH), 114.0 (CH), 114.8 (CH), 116.1 (CH), 119.2 (CH), 123.4 (CH), 131.0 (CH), 139.3 (CH), 139.4 (CH). HMBC (125 MHz, CDCl_3): δ 137.4 (C), 141.7 (C), 150.4 (C), 157.8 (C), 160.1 (C), 161.4 (C), 164.1 (C), 166.5 (C), 169.5 (C). ^{19}F NMR (376 MHz, CDCl_3 , 298 K): δ -110.4 (s, F), -113.1 (s, 1F). IR (selected bands, cm^{-1}): 1566, 1508,

1434, 1352, 1223, 1159, 1014, 914, 782, 727. MS (ES): m/z 965 $[M]^+$. TOFMS (ASAP): m/z 967.0218 $[M]^+$ ($C_{44}H_{28}F_4N_4O_4^{106}Pd_2$ requires 967.0154).

Monomeric Complexes with the General Formula $[Pd(\kappa^2-HL_R)(\kappa^1-OAc)(3,5-lutidine)]$

5.3.19 Synthesis of $[Pd(\kappa^2-6-phenyl-2-pyridinol)(\kappa^1-OAc)(3,5-lutidine)]$ (**3.19**)

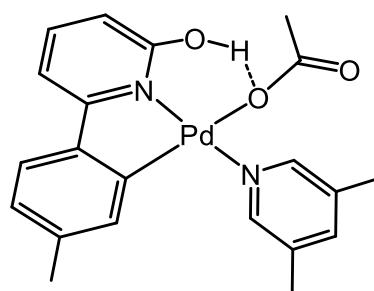
A 5-mL round bottom flask, equipped with a magnetic stir bar and open to the air, was loaded with **3.6** (35 mg, 0.052 mmol), 3,5-lutidine (11 mg, 0.105 mmol) and $CDCl_3$ (4 mL). A stopper was attached and the mixture was left to stir at room temperature for 3 min. The reaction was monitored by 1H NMR spectroscopy



revealing complete conversion. All volatiles were removed under reduced pressure affording **3.19** as a dark brown solid (44 mg, 95%). Mp 98 °C (dec.). 1H NMR (400 MHz, $CDCl_3$, 298 K): δ 1.94 (s, O_2CMe , 3H), 2.33 (s, py-Me, 6H), 5.98 (d, J_{H-H} 6.5, 1H), 6.46 (d, J_{H-H} 6.6, 1H), 6.82 (t, J_{H-H} 7.3, 1H), 7.03 (app t, 2H), 7.35 (d, J_{H-H} 7.5, 1H), 7.44 (s, 1H), 7.56 (t, J_{H-H} 7.5, 1H), 8.72 (s, 2H), OH is not observable. $^{13}C\{^1H\}$ (125 MHz, $CDCl_3$, 298 K): δ 18.3 (py-Me), 23.6 (O_2CMe), 108.3 (CH), 111.6 (CH), 123.2 (CH), 124.8 (CH), 128.5 (CH), 132.9 (CH), 134.7 (C), 139.8 (CH), 140.5 (CH), 146.8 (C), 148.8 (C), 149.0 (C), 150.5 (CH), 161.7 (C), 176.3 (O_2CMe). IR (selected bands, cm^{-1}): 2921, 1600, 1574, 1542, 1472, 1435, 1355, 1277, 1155, 755, 698. MS (ES): m/z 381 $[M-OAc]$, 424 $[(M-OAc)+MeCN]^+$. TOFMS (ES): m/z 443.0595 $[M]^+$ ($C_{20}H_{20}N_2O_3^{106}Pd$ requires 443.0592). FABMS: m/z 383 $[M-OAc]^+$. Anal Calcd for $C_{20}H_{20}N_2O_3Pd \cdot 0.36CHCl_3$: C, 50.34; H, 4.22; N, 5.78; found: C, 50.23; H, 4.31; N, 6.18%.

5.3.20 Synthesis of $[Pd(\kappa^2-6-(4-methylphenyl)-2-pyridinol)(\kappa^1-OAc)(3,5-lutidine)]$ (**3.20**)

Based on the procedure described for **3.19**, using **3.7** (35 mg, 0.05 mmol) and 3,5-lutidine (11 mg, 0.10 mmol), gave **3.20** as a dark brown solid (44 mg, 94%). Mp 103-104 °C. 1H NMR (400 MHz, $CDCl_3$, 298 K): δ 1.92 (s, O_2CMe , 3H), 2.09 (s, *p*-Me, 3H), 2.35 (s, py-Me, 6H), 5.79 (s, 1H), 6.43 (d, J_{H-H} 7.4, 1H), 6.85 (d, J_{H-H} 7.40, 1H), 7.00 (d, J_{H-H} 6.7, 1H), 7.25 (d, J_{H-H} 8.9, 1H), 7.46 (s, 1H), 7.54 (t, J_{H-H} 8.2,

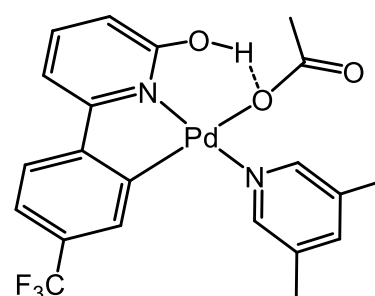


1H), 8.72 (s, 2H), OH is not observable. $^{13}\text{C}\{^1\text{H}\}$ NMR (125 MHz, CDCl_3 , 298 K): δ 18.3 (py-Me), 21.8 (*p*-Me), 23.7 (O_2CMe), 107.8 (CH), 111.1 (CH), 122.9 (CH), 125.7 (CH), 133.5 (CH), 134.7 (C), 138.5 (C), 139.8 (CH), 140.4 (C), 144.1 (C), 148.9 (C), 150.5 (CH), 161.9 (C), 168.7 (C), 176.3 (O_2CMe). IR (selected bands, cm^{-1}): 2918, 1584, 1542, 1435, 1318, 1250, 1154, 795, 696. MS (ES): m/z 397 $[\text{M-OAc}]^+$, 438 $[(\text{M-OAc})+\text{MeCN}]^+$. FABMS: m/z 396 $[\text{M-OAc}]$. Anal Calcd for $\text{C}_{21}\text{H}_{22}\text{N}_2\text{O}_3\text{Pd}$: C, 55.21; H, 4.85; N, 6.13; found: C, 54.97; H, 4.76; N, 6.15%.

5.3.21 Synthesis of $[\text{Pd}(\kappa^2\text{-6-(4-trifluoromethylphenyl)-2-pyridinol})(\kappa^1\text{-OAc})(3,5\text{-lutidine})]$ (**3.21**)

Based on the procedure described for **3.19**, using **3.8** (15 mg, 0.019 mmol) and 3,5-lutidine (4.2 mg, 0.038 mmol), gave **3.21** as a dark yellow solid (17 mg, 90%).

Mp 108-109 °C. ^1H NMR (400 MHz, CDCl_3 , 298 K): δ 1.96 (s, O_2CMe , 3H), 2.34 (s, py-Me, 6H), 6.22 (s, 1H), 6.51 (br s, 1H), 7.06 (br s, 1H), 7.27 (d, $J_{\text{H-H}}$ 8.5, 1H),

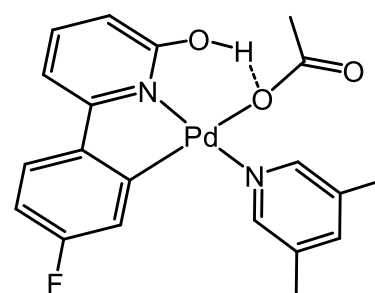


7.43 (d, $J_{\text{H-H}}$ 8.2, 1H), 7.47 (s, 1H), 7.59 (br s, 1H), 8.71 (s, 2H), OH is not observable. Sample was insufficiently soluble for $^{13}\text{C}\{^1\text{H}\}$; therefore, selective ^{13}C data was acquired by an HMQC experiment. HMQC NMR (100 MHz, CDCl_3 , 298 K, 298 K): δ 18.1 (py-Me), 23.5 (O_2CMe), 109.1 (CH), 112.7 (CH), 121.6 (CH), 122.5 (CH), 128.9 (CH), 140.0 (CH), 140.3 (CH), 150.3 (CH). ^{19}F NMR (376 MHz, CDCl_3 , 298 K): δ -62.9 (s, CF_3). IR (selected bands, cm^{-1}): 2926, 1599, 1544, 1455, 1365, 1315, 1253, 1158, 1109, 1070, 795, 698. MS (ES): m/z 451 $[\text{M-OAc}]^+$, 492 $[(\text{M-OAc})+\text{MeCN}]^+$. TOFMS (ES): m/z 451.0257 $[\text{M-OAc}]^+$ ($\text{C}_{19}\text{H}_{16}\text{F}_3\text{N}_2\text{O}^{106}\text{Pd}$ requires 451.0250). FABMS: m/z 450 $[\text{M-OAc}]$. Anal Calcd for $\text{C}_{21}\text{H}_{19}\text{F}_3\text{N}_2\text{O}_3\text{Pd}\cdot 0.41\text{CHCl}_3$: C, 45.94; H, 3.50; N, 5.00; found: C, 45.93; H, 3.36; N, 5.31%.

5.3.22 Synthesis of $[\text{Pd}(\kappa^2\text{-6-(4-fluorophenyl)-2-pyridinol})(\kappa^1\text{-OAc})(3,5\text{-lutidine})]$ (**3.22**)

Based on the procedure described for **3.19**, using **3.9** (22 mg, 0.031 mmol) and 3,5-lutidine (6.65 mg, 0.062 mmol), gave **3.22** as a dark yellow solid (27 mg, 93%).

Mp 76 °C (dec.). $^1\text{H}\{^{19}\text{F}\}$ NMR (400 MHz, CDCl_3 , 298 K): δ 1.93 (s, O_2CMe , 3H), 2.32 (s, py-Me, 6H), 5.67 (d, $J_{\text{H-H}}$ 2.1, 1H), 6.41 (d, $J_{\text{H-H}}$ 7.4, 1H), 6.73 (dd, $J_{\text{H-H}}$ 8.6,

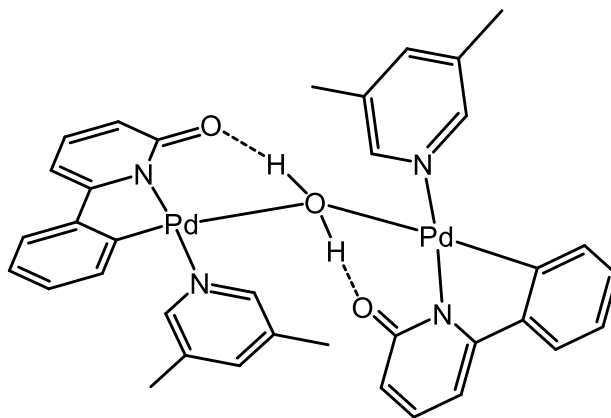


2.6, 1H), 6.90 (d, $J_{\text{H-H}}$ 6.4, 1H), 7.32 (d, $J_{\text{H-H}}$ 8.5, 1H), 7.44 (s, 1H), 7.52 (t, $J_{\text{H-H}}$ 7.7, 1H), 8.72 (s, 2H), OH is not observable. $^{13}\text{C}\{^1\text{H}\}$ NMR (100 MHz, CDCl_3 , 298 K): δ 18.3 (py-Me), 23.5 (O_2CMe), 107.7 (CH), 111.7 (CH), 111.7 (d, $^2J_{\text{C-F}}$ 22.8, CH), 119.3 (d, $^2J_{\text{C-F}}$ 19.5, CH), 124.2 (d, $^3J_{\text{C-F}}$ 8.4, CH), 135.0 (C), 140.0 (CH), 140.4 (CH), 143.0 (C), 150.4 (CH), 151.1 (C), 160.9 (C), 161.1 (d, $^1J_{\text{C-F}}$ 253.2, C), 168.9 (C), 176.3 (O_2CMe). ^{19}F NMR (376 MHz, CDCl_3 , 298 K): δ -110.3 (s, F). IR (selected bands, cm^{-1}): 2920, 1714, 1601, 1583, 1567, 1451, 1251, 1191, 792, 698. MS (ES): m/z 401 $[\text{M-OAc}]^+$. FABMS: m/z 400 $[\text{M-OAc}]^+$.

Dimeric Complexes with the General Formula $[\text{Pd}(\kappa^2\text{-L}_R)(3,5\text{-lutidine})]_2(\mu\text{-OH}_2)$

5.3.23 Synthesis of $[\text{Pd}(\kappa^2\text{-6-phenyl-2-pyridone})(3,5\text{-lutidine})]_2(\mu\text{-OH}_2)$ (3.23)

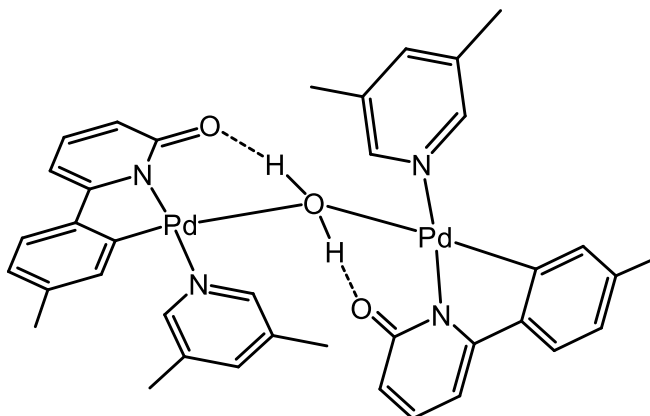
A small vial open to the air was loaded with **3.19** (10 mg, 0.023 mmol), dissolved in dichloromethane (0.7 mL) and layered with hexane (3 mL). A cap was attached and the mixture left to stand at room temperature for one day. The cap was then pierced and the solvent mixture



allowed to slowly evaporate over several days. The resulting solid was placed under reduced pressure to give **3.23** as light brown crystals (8 mg, 81%). $\text{Mp} > 270\text{ }^\circ\text{C}$. ^1H NMR (400 MHz, CDCl_3 , 298 K): δ 2.12 (s, py-Me, 12H), 6.04 (br s, 2H), 6.18 (d, $J_{\text{H-H}}$ 7.5, 2H), 6.61 (br s, 2H), 6.78 (dt, $J_{\text{H-H}}$ 7.7, 0.1, 2H), 6.99 (t, $J_{\text{H-H}}$ 7.4, 2H), 7.19 (s, 2H), 7.24 (m, 2H), 7.28 (d, $J_{\text{H-H}}$ 7.6, 2H), 8.95 (s, 4H), 13.39 (br s, H_2O , 2H). Sample was insufficiently soluble for $^{13}\text{C}\{^1\text{H}\}$; therefore, selective ^{13}C data was acquired by an HMQC experiment. HMQC NMR (100 MHz, CDCl_3 , 298 K): δ 17.97 (py-Me), 103.2 (CH), 114.3 (CH), 122.3 (CH), 124.2 (CH), 127.5 (CH), 132.6 (CH), 137.8 (CH), 139.5 (CH), 150.3 (CH). IR (selected bands, cm^{-1}): 2983, 1569, 1480, 1271, 791. MS (ES): m/z 319 $[\text{Pd}(\text{L}_\text{H})+\text{MeCN}]^+$, 424 $[\text{Pd}(\text{L}_\text{H})(3,5\text{-lutidine})+\text{MeCN}]^+$, 869 $[\text{Pd}_3(\text{L}_\text{H})_3+\text{MeCN}]^+$, 935 $[\text{Pd}_3(\text{L}_\text{H})_3(3,5\text{-lutidine})]^+$. FABMS: m/z 382 $[\text{Pd}(\text{L}_\text{H})(3,5\text{-lutidine})]^+$, 767 $[\text{M-OH}_2]^+$. Anal Calcd for $\text{C}_{36}\text{H}_{34}\text{N}_4\text{O}_3\text{Pd}_2 \cdot 0.3\text{CH}_2\text{Cl}_2$: C, 53.89; H, 4.32; N, 6.92; found: C, 53.79; H, 4.67; N, 6.79%.

5.3.24 Synthesis of $[\text{Pd}(\kappa^2\text{-6-(4-methylphenyl)-2-pyridone})(3,5\text{-lutidine})]_2(\mu\text{-OH}_2)$ (3.24)

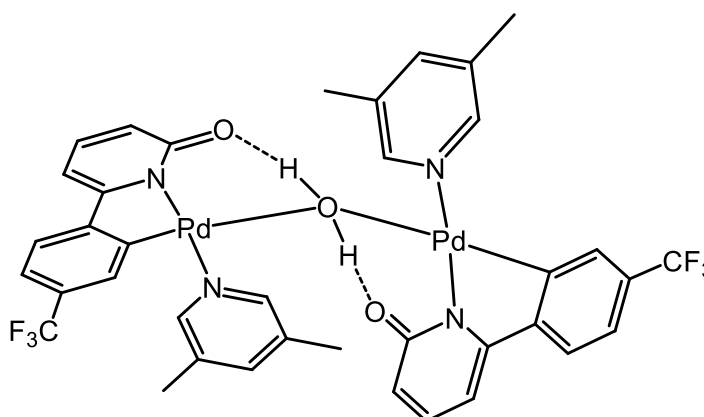
Based on the procedure described for **3.23**, using **3.20** (10 mg, 0.022 mmol) gave **3.24** as yellow crystals (7 mg, 72%). Mp > 270 °C. ^1H NMR (400 MHz, CDCl_3 , 298 K): δ 2.08 (s, *p*-Me, 6H), 2.11 (s, py-Me, 12H), 5.95 (br s, 2H), 5.99 (s, 2H), 6.52 (br s, 2H),



6.80 (d, $J_{\text{H-H}}$ 7.6, 2H), 7.17 (m, 6H), 8.98 (s, 4H) 13.36 (br s, H_2O , 2H). Sample was insufficiently soluble for $^{13}\text{C}\{^1\text{H}\}$; therefore, selective ^{13}C data was acquired by a DEPT 135 experiment. DEPT 135 NMR (100 MHz, CDCl_3 , 298 K): δ 21.6 (*p*-Me), 18.2 (py-Me), 102.5 (CH), 113.9 (CH), 122.0 (CH), 125.0 (CH), 133.3 (CH), 137.7 (CH), 139.6 (CH), 150.5 (CH). IR (selected bands, cm^{-1}): 2917, 1586, 1482, 1448, 795. MS (ES): m/z 397 $[\text{Pd}(\text{L}_{\text{Me}})(3,5\text{-lutidine})]^+$, 795 $[\text{M-OH}_2]^+$, 1085 $[\text{Pd}_3(\text{L}_{\text{Me}})_3(3,5\text{-lutidine})_2]^+$. FABMS: m/z 795 $[\text{M-OH}_2]^+$. Anal Calcd for $\text{C}_{38}\text{H}_{38}\text{N}_4\text{O}_3\text{Pd}_2 \cdot 0.5\text{CH}_2\text{Cl}_2$: C, 54.14; H, 4.60; N, 6.56; found: C, 54.04; H, 5.11; N, 6.47%.

5.3.25 Synthesis of $[\text{Pd}(\kappa^2\text{-6-(4-trifluoromethylphenyl)-2-pyridone})(3,5\text{-lutidine})]_2(\mu\text{-OH}_2)$ (3.25)

Based on the procedure described for **3.23**, using **3.21** (15 mg, 0.029 mmol) gave **3.25** as yellow crystals (8 mg, 67%). Mp > 270 °C. ^1H NMR (400 MHz, CDCl_3 , 298 K): δ 2.16 (s, py-Me, 12H), 6.13 (br s, 2H), 6.38 (br s, 2H), 6.69 (br

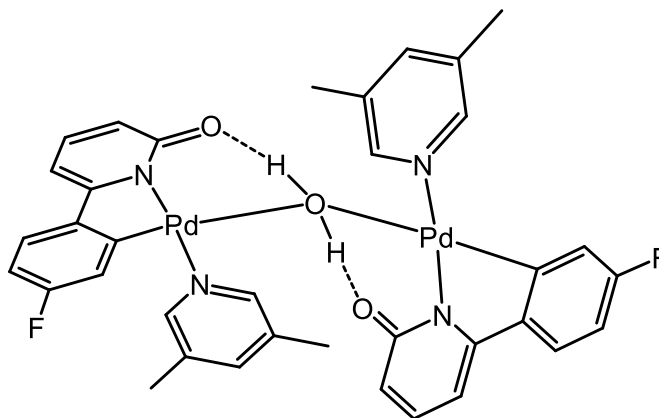


s, 2H), 7.36 (m, 8H), 8.92 (s, 4H), 14.28 (br s, H_2O , 2H). $^{13}\text{C}\{^1\text{H}\}$ NMR (100 MHz, CDCl_3 , 298 K): δ 18.12 (py-Me), 104.8 (CH), 115.8 (CH), 121.3 (q, $^3J_{\text{C-F}}$ 3.2, CH), 122.1 (CH), 123.9 (q, $^1J_{\text{C-F}}$ 274.5, CF_3), 128.5 (q, $^2J_{\text{C-F}}$ 34.2, C), 128.9 (q, $^3J_{\text{C-F}}$ 3.2, CH), 134.9 (C), 138.5 (CH), 139.9 (CH), 147.3 (C), 149.3 (C), 150.3 (CH), 151.4 (C), 159.7 (C). ^{19}F NMR (376 MHz, CDCl_3 , 298 K): δ -62.6 (s, CF_3). IR (selected bands, cm^{-1}): 2925, 1592,

1455, 1315, 1122, 1069, 783. MS (ES): m/z 451 $[\text{Pd}(\text{L}_{\text{CF}_3})(3,5\text{-lutidine})]^+$, 492 $[\text{Pd}(\text{L}_{\text{CF}_3})(3,5\text{-lutidine})+\text{MeCN}]^+$, 903 $[\text{M}-\text{H}_2\text{O}]^+$, 1246 $[\text{Pd}_3(\text{L}_{\text{CF}_3})_3(3,5\text{-lutidine})_2]^+$. TOFMS (ES): m/z 903.0804 $[\text{M}-\text{OH}_2]^+$ ($\text{C}_{38}\text{H}_{30}\text{F}_6\text{N}_4\text{O}_2^{106}\text{Pd}_2$ requires 903.0347). Anal Calcd for $\text{C}_{38}\text{H}_{32}\text{F}_6\text{N}_4\text{O}_3\text{Pd}_2$: C, 49.64; H, 3.51; N, 6.09; found: C, 49.59; H, 3.63; N, 6.07%.

5.3.26 Synthesis of $[\text{Pd}(\kappa^2\text{-6-(4-fluorophenyl)-2-pyridone})(3,5\text{-lutidine})]_2(\mu\text{-OH}_2)$ (3.26)

Based on the procedure described for **3.23**, using **3.22** (13 mg, 0.028 mmol) gave **3.26** as yellow crystals (9 mg, 78%). Mp > 270 °C. $^1\text{H}\{^{19}\text{F}\}$ NMR (400 MHz, CDCl_3 , 298 K): δ 2.11 (s, py-Me, 12H), 5.88 (d, $J_{\text{H-H}}$ 1.8, 2H), 6.00 (d, $J_{\text{H-H}}$ 8.2, 2H), 6.46



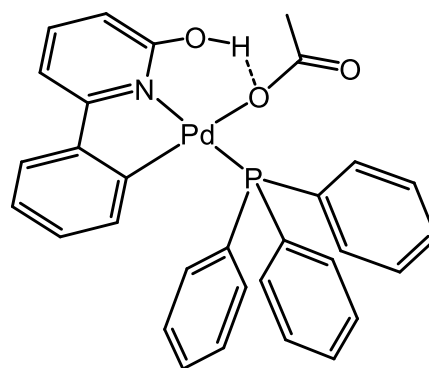
(d, $J_{\text{H-H}}$ 6.7, 2H), 6.70 (dd, $J_{\text{H-H}}$ 8.6, 2.5, 2H), 7.20 (m, 4H), 7.25 (s, 4H), 8.95 (br s, 4H), 14.18 (br s, H_2O , 2H). Sample was insufficiently soluble for $^{13}\text{C}\{^1\text{H}\}$; therefore, selective ^{13}C data was acquired by a DEPT 135 experiment. DEPT 135 NMR (100 MHz, CDCl_3 , 298 K): δ 18.15 (py-Me), 102.7 (CH), 111.3 (d, $^2J_{\text{C-F}}$ 22.0, CH), 114.6 (CH), 119.1 (d, $^2J_{\text{C-F}}$ 18.9, CH), 123.5 (CH), 138.3 (CH), 139.8 (CH), 150.3 (CH). ^{19}F NMR (376 MHz, CDCl_3 , 298 K): δ -112.2 (s, F). IR (selected bands, cm^{-1}): 2923, 1568, 1543, 1442, 1249, 1189, 1008, 854, 792, 696. MS (ES): m/z 442 $[\text{Pd}(\text{L}_{\text{F}})(3,5\text{-lutidine})+\text{MeCN}]^+$, 737 $[\text{Pd}_2(\text{L}_{\text{F}})_2(3,5\text{-lutidine})]^+$, 803 $[\text{M}-\text{OH}_2]^+$, 1096 $[\text{Pd}_3(\text{L}_{\text{F}})_3(3,5\text{-lutidine})_2]^+$. FABMS: m/z 400 $[\text{Pd}(\text{L}_{\text{F}})(3,5\text{-lutidine})]^+$, 801 $[\text{M}-\text{OH}_2]^+$.

Monomeric Complexes with the General Formula $[\text{Pd}(\kappa^2\text{-HL}_R)(\kappa^1\text{-X})(\text{PPh}_3)]$ (X = OAc or H_2O)

5.3.27 Synthesis of $[\text{Pd}(\kappa^2\text{-6-phenyl-2-pyridinol})(\kappa^1\text{-OAc})(\text{PPh}_3)]$ (3.27)

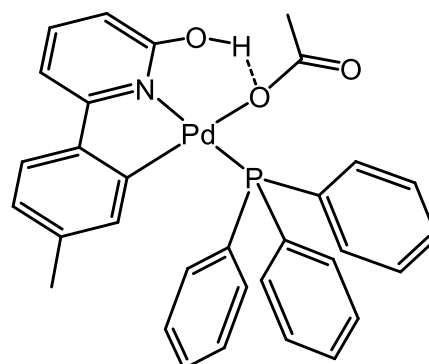
Complex **3.6** (23.6 mg, 0.035 mmol, 1 eq.) and PPh_3 (18.9 mg, 0.072 mmol, 2.1 eq.) were combined in CDCl_3 (2 mL) in a 5-mL flask equipped with a magnetic stir bar and stirred at room temperature for 3 min. The reaction was monitored by ^1H NMR spectroscopy revealing complete conversion. The solvent was then removed under reduced pressure to give the acetate-containing complex (**3.27**) as a brown solid (40 mg,

96% yield). Mp 105 (dec.) °C. $^1\text{H}\{^{31}\text{P}\}$ NMR (400 MHz, CDCl_3 , 298 K): δ 1.29 (s, O_2CMe , 3H), 6.36 (dt, $J_{\text{H-H}}$ 8.1, 7.0, 1H), 6.41 (dd, $J_{\text{H-H}}$ 7.9, 0.9, 1H), 6.47 (d, $J_{\text{H-H}}$ 8.2, 1H), 6.81 (t, $J_{\text{H-H}}$ 7.1, 1H), 7.12 (d, $J_{\text{H-H}}$ 7.1, 1H), 7.29 (t, $J_{\text{H-H}}$ 7.7, 6H), 7.36 (app t, 1H, 3H), 7.55 (t, $J_{\text{H-H}}$ 8.0, 3H), 7.73 (d, $J_{\text{H-H}}$ 7.7, 6H), 13.19 (br s, OH, 1H). $^{13}\text{C}\{^1\text{H}\}$ NMR (100 MHz, CDCl_3 , 298 K): δ 22.9 (O_2CMe), 109.1 (CH), 111.2 (CH), 123.9 (CH), 124.5 (CH), 128.2 (CH), 128.3 (d, $^3J_{\text{P-C}}$ 10.2, CH), 130.6 (CH), 130.7 (d, $^1J_{\text{P-C}}$ 50.4, C), 135.6 (d, $^2J_{\text{P-C}}$ 11.7, CH), 139.4 (CH), 141.1 (CH), 148.0 (C), 148.5 (C), 161.1 (C), 167.6 (C), 176.9 (O_2CMe). ^{31}P NMR (162 MHz, CDCl_3 , 298 K): δ 43.1 (s, PPh_3). IR (selected bands, cm^{-1}): 1610, 1567, 1480, 1433, 1354, 1269, 1235, 1094, 800, 689. MS (ES): m/z 538 $[\text{M-OAc}]^+$, 1076 $[\text{Pd}(\text{L}_\text{H})(\text{PPh}_3)]_2^+$. FABMS: m/z 537 $[\text{M-OAc}]^+$. Anal Calcd for $\text{C}_{31}\text{H}_{26}\text{NO}_3\text{PPd}\cdot 0.9\text{CH}_2\text{Cl}_2$: C, 56.82; H, 4.16; N, 2.08; found: C, 56.91; H, 4.18; N, 2.14%.



5.3.28 Synthesis of $[\text{Pd}(\kappa^2\text{-6-(4-methylphenyl)-2-pyridinol})(\kappa^1\text{-OAc})(\text{PPh}_3)]$ (**3.28**)

Based on the procedure described for **3.27**, using **3.7** (53.2 mg, 0.076 mmol, 1 eq.) and PPh_3 (42 mg, 0.160 mmol, 2.1 eq.), gave **3.28** as a pale yellow solid (42 mg, 91%). Mp 116-117 °C. $^1\text{H}\{^{31}\text{P}\}$ NMR (400 MHz, CDCl_3 , 298 K): δ 1.35 (s, O_2CMe , 3H), 1.64 (s, $p\text{-Me}$, 3H), 6.28 (s, 1H), 6.50 (dd, $J_{\text{H-H}}$ 8.25, 0.7, 1H), 6.68 (dd, $J_{\text{H-H}}$ 7.9, 0.6, 1H), 7.13 (d, $J_{\text{H-H}}$ 7.6, 1H), 7.30 (d, $J_{\text{H-H}}$ 7.9, 1H), 7.36 (tt, $J_{\text{H-H}}$ 7.6, 1.4, 6H), 7.42 (tt, $J_{\text{H-H}}$ 7.2, 2.2, 3H), 7.59 (t, $J_{\text{H-H}}$ 8.1, 1H), 7.79 (d, $J_{\text{H-H}}$ 6.6, 6H), 13.10 (br s, OH, 1H). $^{13}\text{C}\{^1\text{H}\}$ NMR (100 MHz, CDCl_3 , 298 K): δ 20.9 ($p\text{-Me}$), 22.9 (O_2CMe), 108.7 (CH), 110.7 (CH), 123.5 (CH), 125.2 (CH), 128.2 (d, $^3J_{\text{P-C}}$ 11.1, CH), 130.5 (d, $^1J_{\text{P-C}}$ 49.5, C), 130.6 (CH), 135.6 (d, $^2J_{\text{P-C}}$ 12.3, CH), 138.0 (C), 140.2 (CH), 141.0 (CH), 145.2 (C), 148.2 (C), 161.1 (C), 167.4 (C), 176.8 (O_2CMe). ^{31}P NMR (162 MHz, CDCl_3 , 298 K): δ 42.7 (s, PPh_3). IR (selected bands, cm^{-1}): 1567, 1481, 1434, 1352, 1282, 1234, 1096, 794, 692. MS (ES): m/z 552 $[\text{M-OAc}]^+$, 1105 $[\text{Pd}(\text{L}_\text{Me})(\text{PPh}_3)]_2^+$, 1349 $[\text{Pd}_3(\text{L}_\text{Me})_3(\text{PPh}_3)_2]^+$. MS (ASAP): m/z 553.0755 $[\text{M-OAc}]^+$ ($\text{C}_{30}\text{H}_{25}\text{NOP}^{106}\text{Pd}$ requires 553.0742). Anal Calcd for

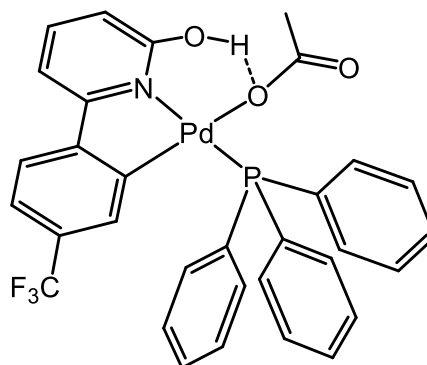


$C_{32}H_{28}NO_3PPd \cdot 0.35CH_2Cl_2$: C, 60.55; H, 4.51; N, 2.20; found: C, 60.52; H, 3.94; N, 2.48%.

5.3.29 Synthesis of $[Pd(\kappa^2\text{-6-(4-trifluoromethylphenyl)-2-pyridinol})(\kappa^1\text{-OAc})(PPh_3)]$ (**3.29**)

Based on the procedure described for **3.27**, using **3.8** (15 mg, 0.019 mmol, 1 eq.) and PPh_3 (10.2 mg, 0.04 mmol, 2.1 eq.), gave **3.29** as a pale yellow solid (19 mg, 73%). Crystals suitable for single crystal X-ray diffraction were grown by slow evaporation of a chloroform solution of the complex.

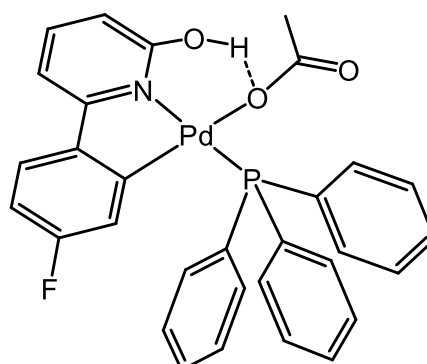
MP 128-129 °C. $^1H\{^{31}P\}$ NMR (400 MHz, $CDCl_3$, 298 K): δ 1.40 (s, O_2CMe , 3H), 6.61 (d, J_{H-H} 8.3, 1H), 6.74 (s, 1H), 7.10 (d, J_{H-H} 8.1, 1H), 7.24 (d, J_{H-H} 7.5, 1H), 7.38 (app t, 6H), 7.45 (tt, J_{H-H} 7.4, 2.4, 3H), 7.48 (d, J_{H-H} 8.1, 1H), 7.67 (t, J_{H-H} 7.9, 1H), 7.80 (d, J_{H-H} 7.2, 6H), 13.16 (s, OH, 1H). $^{13}C\{^1H\}$ NMR (100 MHz, $CDCl_3$, 298 K): δ 22.8 (O_2CMe), 109.9 (CH), 112.6 (CH), 121.1 (CH), 123.3 (CH), 123.5 (d, $^1J_{C-F}$ 274.0, CF_3), 128.3 (d, $^3J_{C-P}$ 4.2, CH), 128.7 (d, $^2J_{C-F}$ 32.3, C), 129.5 (d, $^1J_{C-P}$ 51.2, C), 130.9 (CH), 135.4 (CH), 135.5 (d, $^2J_{C-P}$ 11.1, CH), 141.3 (CH), 148.2 (C), 151.3 (C), 159.5 (C), 167.8 (C), 179.9 (O_2CMe). ^{31}P NMR (162 MHz, $CDCl_3$, 298 K): δ 41.7 (s, PPh_3). ^{19}F NMR (376 MHz, $CDCl_3$, 298 K): δ -63.2 (s, CF_3). IR (selected bands, cm^{-1}): 1610, 1571, 1480, 1453, 1434, 1364, 1316, 1163, 1117, 1096, 1070, 796, 721, 688. MS (ES): m/z 606 $[M-OAc]^+$, 647 $[(M-OAc)+MeCN]^+$, 1213 $[2M-2OAc]^+$. FABMS: m/z 605 $[M-OAc]^+$. Anal Calcd for $C_{32}H_{25}F_3NO_3PPd \cdot 0.46CHCl_3$: C, 54.09; H, 3.56; N, 1.94; found: C, 54.07; H, 3.39; N, 2.15%.



5.3.30 Synthesis of $[Pd(\kappa^2\text{-6-(4-fluorophenyl)-2-pyridinol})(\kappa^1\text{-OAc})(PPh_3)]$ (**3.30**)

Based on the procedure described for **3.27**, using **3.9** (20.2 mg, 0.029 mmol, 1 eq.) and PPh_3 (15 mg, 0.058 mmol, 2 eq.), gave **3.30** as a pale yellow solid (42 mg, 91%). Crystals suitable for single crystal X-ray diffraction were grown by slow evaporation of a chloroform solution of the complex.

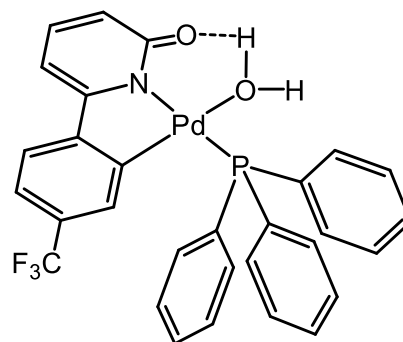
MP 120-121 °C. $^1H\{^{31}P\}$ NMR (400 MHz, $CDCl_3$, 298 K): δ 1.39 (s, O_2CMe , 3H), 6.15 (dd, J_{H-F} 10.5, 2.6, 1H), 6.54 (d, J_{H-H} 8.23, 1H), 6.60 (dt, J_{H-H} 8.3, J_{H-F} 2.5, 1H), 7.09 (d, J_{H-H} 7.4, 1H), 7.39 (m, 7H), 7.46 (tt, J_{H-H} 7.22, 1.2,



3H), 7.62 (t, $J_{\text{H-H}}$ 7.9, 1H), 7.79 (d, $J_{\text{H-H}}$ 7.2, 6H), 13.03 (s, OH, 1H). $^{13}\text{C}\{^1\text{H}\}$ NMR (100 MHz, CDCl_3 , 298 K): δ 22.8 (O_2CMe), 109.0 (CH), 111.1 (CH), 111.5 (d, $^2J_{\text{C-F}}$ 22.4, CH), 124.8 (d, $^3J_{\text{C-F}}$ 8.1, CH), 125.1 (d, $^2J_{\text{C-F}}$ 20.3, CH), 128.4 (d, $^3J_{\text{C-P}}$ 11.2, CH), 130.1 (d, $^1J_{\text{C-P}}$ 49.5, C), 130.8 (CH), 135.5 (d, $^2J_{\text{C-P}}$ 12.7, CH), 141.2 (CH), 144.2(C), 150.5(C), 160.2(C), 160.8 (d, $^1J_{\text{C-F}}$ 252.4, C), 167.5(C), 176.9 (O_2CMe). ^{31}P NMR (162 MHz, CDCl_3 , 298 K): δ 41.0 (s, PPh_3). ^{19}F NMR (376 MHz, CDCl_3 , 298 K): δ -111.2 (s, F). IR (selected bands, cm^{-1}): 1613, 1563, 1481, 1450, 1435, 1285, 1094, 906, 793, 691. MS (ES): m/z 558 [M-OAc] $^+$, 1113 [2M-2OAc] $^+$, 1407 [$\text{Pd}_3(\text{L})_3(\text{PPh}_3)_2$] $^+$. TOFMS (ES): m/z 556.0469 [M-OAc] $^+$ ($\text{C}_{29}\text{H}_{22}\text{FNOP}^{106}\text{Pd}$ requires 556.0458).

5.3.31 Synthesis of [$\text{Pd}(\kappa^2\text{-6-(4-trifluoromethylphenyl)-2-pyridone})(\kappa^1\text{-OH}_2)(\text{PPh}_3)$] (3.31)

A small vial open to the air was loaded with **3.29** (20 mg, 0.03 mmol), dissolved in wet dichloromethane (1 mL) and layered with hexane (3 mL). A cap was attached and the mixture left to stand at room temperature for two days forming a yellow powder on the base of the vial. The remaining solution was decanted and yellow microcrystalline was dried under



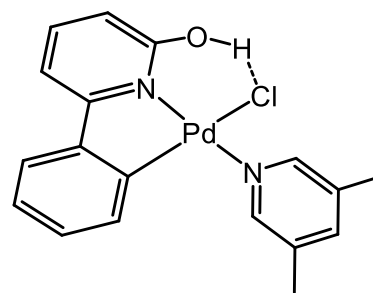
reduced pressure. The process of solvent removal and dissolving in wet DCM/hexane was repeated three more times to afford **3.31** as a yellow solid (9 mg, 48%; 92% conversion). Crystals suitable for single crystal X-ray diffraction were grown from a dichloromethane solution of the complex layered with hexane. Mp: 198-200 °C. $^1\text{H}\{^{31}\text{P}\}$ NMR (400 MHz, CDCl_3 , 298 K): δ 5.45 (d, $J_{\text{H-H}}$ 8.4, 1H), 6.53 (d, $J_{\text{H-H}}$ 6.6, 1H), 6.66 (dd, $J_{\text{H-H}}$ 7.0, 8.5, 1H), 6.75 (s, 1H), 6.95 (t, $J_{\text{H-H}}$ 7.6, 6H), 7.20 (m, 4H), 7.41 (d, $J_{\text{H-H}}$ 7.1, 6H), 7.74 (d, $J_{\text{H-H}}$ 7.2, 1H), H_2O protons are not observable. Sample was insufficiently soluble for $^{13}\text{C}\{^1\text{H}\}$; therefore, selective ^{13}C data was acquired by HMQC and DEPT 135 experiments. HMQC and DEPT 135 NMR (100 MHz, CDCl_3 , 298 K): δ 102.3 (CH), 115.7 (CH), 122.4 (CH), 127.9 (CH), 130.2 (CH), 133.6 (CH), 134.7(CH), 134.8 (CH), 138.0 (CH). ^{31}P NMR (162 MHz, CDCl_3 , 298 K): δ 40.1 (PPh_3). ^{19}F NMR (376 MHz, CDCl_3 , 298 K): δ -62.9 (s, CF_3). IR (selected bands, cm^{-1}): 1640, 1439, 1322, 1276, 1163, 1121, 1101, 1070, 1012, 807, 741, 694. MS (ES): m/z 606 [M-OH] $^+$, 1213 [$2\text{M-2(OH}_2)$] $^+$. TOFMS (ES): m/z 606.0438 [M-OH] $^+$ ($\text{C}_{30}\text{H}_{22}\text{F}_3\text{NOP}^{106}\text{Pd}$ requires 606.0381), 1213.0853 [2M-2OH] $^+$ ($\text{C}_{60}\text{H}_{44}\text{F}_6\text{N}_2\text{O}_2\text{P}_2^{106}\text{Pd}_2$ requires 1213.8019).

Mono- and Dimeric Complexes Derived from Saturated Aqueous NaCl Solution

5.3.32 Synthesis of [Pd(κ^2 -6-phenyl-2-pyridinol)(3,5-lutidine)Cl] (3.32a) and [Pd(μ : κ^2 -6-phenyl-2-pyridonate)(3,5-lutidine)(κ^2 -6-phenyl-2-pyridinol)(μ -Cl)] (3.32b)

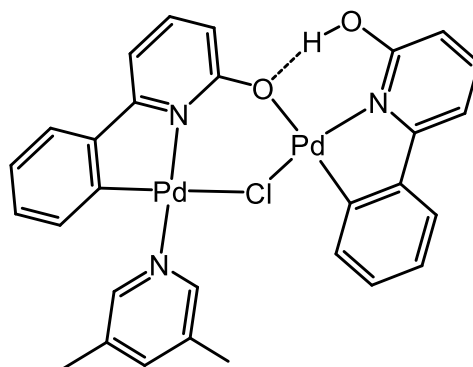
A round bottom flask equipped with stirrer bar and open to the air was loaded with complex **3.19** (30 mg, 0.068 mmol), chloroform (3 mL) and brine (4 mL). After stirring vigorously at room temperature for 12 h the yellow phase was separated, washed with water (2 x 10 ml) and filtered through a Celite plug and washed with chloroform. Hexane (20 mL) was added to precipitate the product which was then filtered and washed with hexane to afford a mixture of **3.32a** (95%) and **3.32b** (5%) as a brown solid (0.022 g, 87%). Crystals suitable for a single crystal X-ray diffraction study were grown from a dichloromethane solution of the complex **3.32b** layered with hexane.

3.32a: ^1H NMR (400 MHz, CDCl_3 , 298 K): δ 2.37 (s, py-Me, 6H), 5.91 (dd, $J_{\text{H-H}}$ 7.8, 1.0, 1H), 6.60 (dd, $J_{\text{H-H}}$ 8.3, 1.1, 1H), 6.84 (td, $J_{\text{H-H}}$ 7.8, 1.5, 1H), 7.06 (td, $J_{\text{H-H}}$ 7.5, 1.5, 1H), 7.17 (dd, $J_{\text{H-H}}$ 7.6, 1.0, 1H), 7.39 (dd, 7.8, 1.4, 1H), 7.49 (s, 1H), 7.64 (t, $J_{\text{H-H}}$ 7.9, 1H), 8.59 (s, 2H), 11.98 (s, OH, 1H). $^{13}\text{C}\{^1\text{H}\}$ NMR (100 MHz, CDCl_3 , 298



K): δ 18.37 (py-Me), 109.7 (CH), 111.0 (CH), 123.5 (CH), 125.1 (CH), 129.0 (CH), 132.4 (CH), 135.3 (C), 139.8 (CH), 141.1 (CH), 146.5 (C), 150.2 (CH), 151.0 (C), 162.2 (C), 166.9 (C). MS (ES): m/z 424 [(M-Cl)+MeCN] $^+$. TOFMS (ASAP): m/z 383.0426 [M-Cl] $^+$ ($\text{C}_{18}\text{H}_{17}\text{N}_2\text{O}^{106}\text{Pd}$ requires 383.0376).

3.32b: ^1H NMR (400 MHz, CDCl_3 , 298 K): δ 2.21 (s, py-Me, 6H), 5.88 (dd, $J_{\text{H-H}}$ 7.9, 1.1, 1H), 6.49 (dd, $J_{\text{H-H}}$ 8.3, 1.1, 1H), 6.51 (dd, $J_{\text{H-H}}$ 9.4, 1.1, 1H), 6.64 (dd, $J_{\text{H-H}}$ 7.9, 1.6, 1H), 6.73 (dt, $J_{\text{H-H}}$ 7.8, 1.4, 1H), 6.90 (dd, $J_{\text{H-H}}$ 7.5, 1.2, 1H), 6.93 (dd, $J_{\text{H-H}}$ 8.1, 1.2, 1H), 7.00 (m, 2H), 7.09 (dd, $J_{\text{H-H}}$ 7.7, 0.9, 1H), 7.32 (dd, $J_{\text{H-H}}$ 7.7, 1.5,



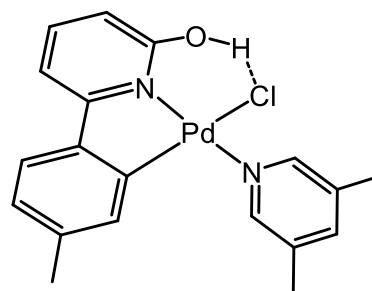
1H), 7.34 (dd, $J_{\text{H-H}}$ 7.7, 1.4, 1H), 7.44 (s, 1H), 7.47 (dd, $J_{\text{H-H}}$ 8.5, 1.2, 1H), 7.60 (t, $J_{\text{H-H}}$ 8.2, 1H), 8.45 (s, 2H), 13.44 (s, OH, 1H). Sample was insufficiently soluble for $^{13}\text{C}\{^1\text{H}\}$; therefore, selective ^{13}C data was acquired by a DEPT 135 experiment. DEPT 135 NMR

(100 MHz, CDCl₃, 298 K): δ 18.28 (py-Me), 106.6 (CH), 108.9 (CH), 110.8 (CH), 115.6 (CH), 123.0 (CH), 123.1 (CH), 124.5 (CH), 124.9 (CH), 127.7 (CH), 127.9 (CH), 131.9 (CH), 135.0 (CH), 135.4 (CH), 139.5 (CH), 140.5 (CH), 150.6 (CH). MS (ES): m/z 699 [(M-Cl)+MeCN]⁺. TOFMS (ES): m/z 552.9218 [Pd(L_H)+H]₂⁺ (C₂₂H₁₄N₂O₂¹⁰⁶Pd₂ requires 552.9129), 593.9490 [(Pd(L_H))₂+MeCN]⁺ (C₂₄H₁₈N₃O₂¹⁰⁶Pd₂ requires 593.9473).

5.3.33 Synthesis of [Pd(κ^2 -6-(4-methylphenyl)-2-pyridinol)(3,5-lutidine)Cl] (3.33a) and [Pd(μ : κ^2 -6-(4-methylphenyl)-2-pyridonate)(3,5-lutidine)(κ^2 -6-(4-methylphenyl)-2-pyridinol)(μ -Cl)] (3.33b)

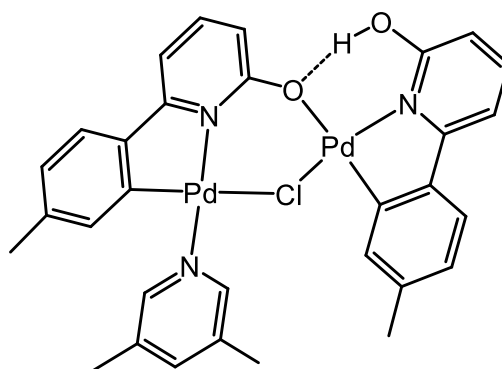
Based on the procedure described for **3.32**, using **3.20** (25 mg, 0.054 mmol) gave a mixture of **3.33a** (80%) and **3.33b** (20%) as a yellow solid (19 mg, 91%). Crystals suitable for a single crystal X-ray diffraction study were grown slow evaporation of a solution of **3.33a** and **3.33b** in MeOH.

3.33a: ¹H NMR (400 MHz, CDCl₃, 298 K): δ 2.10 (s, *p*-Me, 3H), 2.38 (s, py-Me, 6H), 5.72 (s, 1H), 6.57 (dd, *J*_{H-H} 8.1, 1.1, 1H), 6.88 (dd, *J*_{H-H} 7.9, 0.9, 1H), 7.12 (dd, *J*_{H-H} 7.6, 1.1, 1H), 7.28 (d, *J*_{H-H} 7.8, 1H), 7.50 (s, 1H), 7.62 (t, *J*_{H-H} 7.9, 1H), 8.60 (s, 2H), 11.94 (s, OH, 1H). ¹³C{¹H} NMR (100 MHz, CDCl₃, 298 K): δ 18.36 (py-



Me), 21.79 (*p*-Me), 109.3 (CH), 110.4 (CH), 123.3 (CH), 126.0 (CH), 133.0 (CH), 135.3 (C), 139.1 (C), 139.7 (CH), 141.0 (CH), 143.8 (C), 150.2 (CH), 150.8 (C), 162.3 (C), 166.9 (C). MS (ES): m/z 396 [M-Cl]⁺, 438 [(M-Cl)+MeCN]⁺. TOFMS (ES): m/z 397.0540 [M-Cl]⁺ (C₁₉H₁₉N₂O¹⁰⁶Pd requires 397.0532).

3.33b: ¹H NMR (400 MHz, CDCl₃, 298 K): δ 1.97 (s, *p*-Me, 3H), 2.05 (s, *p*-Me, 3H), 2.21 (s, py-Me, 6H), 5.66 (s, 1H), 6.45 (dd, *J*_{H-H} 8.0, 0.9, 1H), 6.47 (dd, *J*_{H-H} 8.1, 1.1, 1H), 6.65 (s, 1H), 6.82 (m, 3H), 7.04 (dd, *J*_{H-H} 7.5, 0.9, 1H), 7.19 (d, *J*_{H-H} 7.9, 1H), 7.22 (d, *J*_{H-H} 7.8, 1H), 7.43 (m, 2H), 7.57 (t, *J*_{H-H} 7.8, 1H), 8.50 (s, 2H), 13.36 (s, OH, 1H). Sample was



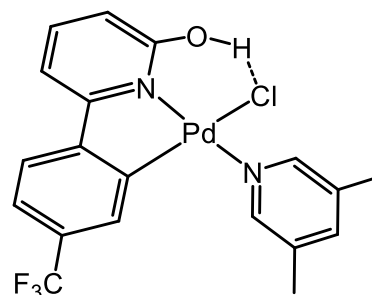
insufficiently soluble for ¹³C{¹H}; therefore, selective ¹³C data was acquired by a DEPT

135 experiment. DEPT 135 NMR (100 MHz, CDCl₃, 298 K): δ 18.2 (py-Me), 21.6 (*p*-Me), 21.7 (*p*-Me), 106.2 (CH), 108.5 (CH), 110.2 (CH), 115.0 (CH), 122.8 (CH), 122.9 (CH), 125.4 (CH), 125.8 (CH), 132.4 (CH), 132.5 (CH), 135.7 (CH), 139.2 (CH), 140.4 (CH), 150.8 (CH). MS (ES): m/z 729 [(M-Cl)+MeCN]⁺. TOFMS (ES): m/z 688.0269 [M-Cl]⁺ (C₃₁H₂₈N₃O₂¹⁰⁶Pd₂ requires 688.0255).

5.3.34 Synthesis of [Pd(κ^2 -6-(4-trifluoromethylphenyl)-2-pyridinol)(3,5-lutidine)Cl] (3.34a) and [Pd(μ : κ^2 -6-(4-trifluoromethylphenyl)-2-pyridonate)(3,5-lutidine)(κ^2 -6-(4-trifluoromethylphenyl)-2-pyridinol)(μ -Cl)] (3.34b)

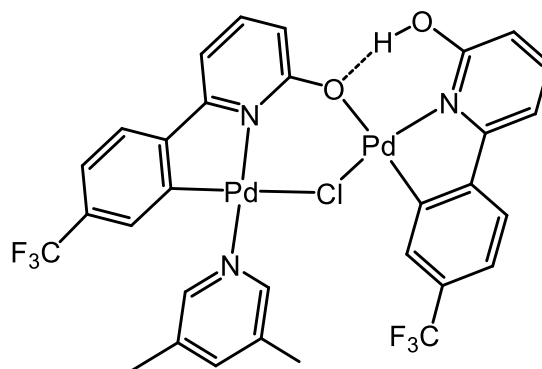
Based on the procedure described for **3.32**, using **3.21** (19 mg, 0.037 mmol) gave a mixture of **3.34a** (52%) and **3.34b** (48%) as a yellow solid (13 mg, 80%). Crystals suitable for a single crystal X-ray diffraction study were grown from a dichloromethane solution of the complexes **3.34a** and **3.34b** layered with hexane.

3.34a: ¹H NMR (400 MHz, CDCl₃, 298 K): δ 2.39 (s, py-Me, 6H), 6.12 (s, 1H), 6.70 (dd, J_{H-H} 8.4, 1.2, 1H), 7.24 (dd, J_{H-H} 8.6, 0.9, 1H), 7.32 (d, J_{H-H} 8.0, 1H), 7.48 (d, J_{H-H} 8.2, 1H), 7.54 (s, 1H), 7.71 (t, J_{H-H} 8.2, 1H), 8.56 (s, 2H), 12.09 (s, OH, 1H). Sample was insufficiently soluble for ¹³C{¹H}; therefore, selective ¹³C data was



acquired by an HMQC experiment. HMQC NMR (100 MHz, CDCl₃, 298 K): δ 18.3 (py-Me), 109.9 (CH), 112.2 (CH), 121.6 (CH), 123.0 (CH), 128.5 (CH), 140.1 (CH), 140.9 (CH), 149.6 (CH). ¹⁹F NMR (376 MHz, CDCl₃, 298 K): δ -63.01 (s, CF₃). MS (ES): m/z 451 [M-Cl]⁺, 492 [(M-Cl)+MeCN]⁺. TOFMS (ES): m/z 451.0257 [M-Cl]⁺ (C₁₉H₁₆F₃N₂O¹⁰⁶Pd requires 451.0250).

3.34b: ¹H NMR (400 MHz, CDCl₃, 298 K): δ 2.20 (s, py-Me, 6H), 6.06 (s, 1H), 6.59 (dd, J_{H-H} 8.4, 0.9, 1H), 6.60 (dd, J_{H-H} 8.4, 0.9, 1H), 6.97 (dd, J_{H-H} 7.4, 1.0, 1H), 7.16 (s, 1H), 7.25 (m, 3H), 7.48 (m, 4H), 7.67 (t, J_{H-H} 8.1, 1H), 8.47 (s, 2H), 13.35 (s, OH, 1H). Sample was insufficiently soluble

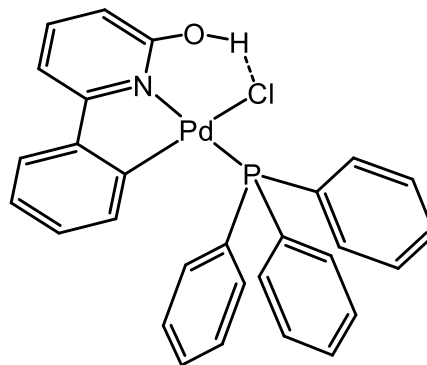


for ¹³C{¹H}; therefore, selective ¹³C data was acquired by an HMQC experiment. HMQC NMR (100 MHz, CDCl₃, 298 K): δ 18.1 (py-Me), 107.6 (CH), 110.3 (CH), 112.3 (CH),

116.6 (CH), 121.8 (CH), 121.9 (CH), 122.6 (CH), 122.7 (CH), 127.8 (CH), 131.0 (CH), 139.9 (CH), 140.2 (CH), 141.2 (CH), 149.7 (CH). ^{19}F NMR (376 MHz, CDCl_3 , 298 K): δ -62.5 (s, CF_3), -62.9 (s, CF_3). MS (ES): m/z 836 $[(\text{M}-\text{Cl})+\text{MeCN}]^+$. TOFMS (ES): m/z 795.9704 $[\text{M}-\text{Cl}]^+$ ($\text{C}_{31}\text{H}_{22}\text{F}_6\text{N}_3\text{O}_2^{106}\text{Pd}_2$ requires 795.9690).

5.3.35 Synthesis of $[\text{Pd}(\kappa^2\text{-6-phenyl-2-pyridinol})(\text{PPh}_3)\text{Cl}]$ (**3.35**)

A round bottom flask equipped with stirrer bar and open to the air was loaded with **3.27** (50 mg, 0.084 mmol), chloroform (3 mL) and brine (4 mL). After stirring vigorously at room temperature for 12 h the yellow phase was separated, washed with water (2 x 10 ml) and filtered through a Celite plug and washed with extra chloroform. Hexane (20 mL) was



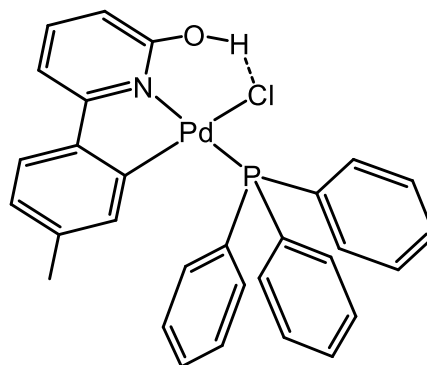
added to precipitate the product which was then filtered and washed with hexane to afford **3.35** (46 mg, 95%) as a dark brown solid. Crystals suitable for a single crystal X-ray diffraction study were grown from a dichloromethane solution of the complex layered with hexane. Mp: 190 °C. $^1\text{H}\{^{31}\text{P}\}$ NMR (400 MHz, CDCl_3 , 298 K): δ 6.42 (td, $J_{\text{H-H}}$ 7.2, 1.6, 1H), 6.51 (dd, $J_{\text{H-H}}$ 8.0, 1.1, 1H), 6.64 (dd, $J_{\text{H-H}}$ 8.2, 1.1, 1H), 6.90 (td, $J_{\text{H-H}}$ 7.3, 1.1, 1H), 7.27 (dd, $J_{\text{H-H}}$ 7.7, 0.9, 1H), 7.37 (app t, $J_{\text{H-H}}$ 7.8, 6H), 7.45 (app tt, $J_{\text{H-H}}$ 7.2, 1.8, 4H), 7.67 (t, $J_{\text{H-H}}$ 7.8, 1H), 7.79 (d, $J_{\text{H-H}}$ 7.7, 6H), 12.29 (s, OH, 1H). $^{13}\text{C}\{^1\text{H}\}$ NMR (100 MHz, CDCl_3 , 298 K): δ 109.7 (CH), 111.4 (CH), 124.2 (CH), 124.6 (CH), 128.1 (CH), 128.2 (d, $^3J_{\text{C-P}}$ 10.6, CH), 130.9 (d, $^4J_{\text{C-P}}$ 3.1, CH), 130.8 (d, $^1J_{\text{C-P}}$ 50.9, C), 135.5 (d, $^2J_{\text{C-P}}$ 11.3, CH), 139.0 (CH), 141.2 (CH), 148.0 (C), 151.6 (C), 161.5 (C), 167.0 (C). ^{31}P NMR (162 MHz, CDCl_3 , 298 K): δ 44.9 (s, PPh_3). IR (selected bands, cm^{-1}): 1567, 1432, 1219, 1157, 1092, 1023, 998, 806, 746, 690. MS (ES): m/z 579 $[(\text{M}-\text{Cl})+\text{MeCN}]^+$, 1077 $[2(\text{M}-\text{Cl})]^+$. TOFMS (ES): m/z 538.0569 $[\text{M}-\text{Cl}]^+$ ($\text{C}_{29}\text{H}_{23}\text{NOP}^{106}\text{Pd}$ requires 538.0552), 1077.1091 $[2(\text{M}-\text{Cl})+\text{H}]^+$ ($\text{C}_{58}\text{H}_{46}\text{N}_2\text{O}_2\text{P}_2^{106}\text{Pd}_2$ requires 1077.1124).

5.3.36 Synthesis of $[\text{Pd}(\kappa^2\text{-6-(4-methylphenyl)-2-pyridinol})(\text{PPh}_3)\text{Cl}]$ (**3.36**)

Based on the procedure described for **3.35**, using **3.28** (60 mg, 0.1 mmol) gave **3.36** as a yellow solid (54 mg, 92%). Crystals suitable for a single crystal X-ray diffraction study were grown from a dichloromethane solution of the complex layered with hexane. Mp: 194 °C. $^1\text{H}\{^{31}\text{P}\}$ NMR (400 MHz, CDCl_3 , 298 K): δ 1.63 (s, Me, 3H), 6.29 (s, 1H), 6.60 (dd, $J_{\text{H-H}}$ 8.2, 0.8, 1H), 6.70 (d, $J_{\text{H-H}}$ 7.8, 1H), 7.21 (dd, $J_{\text{H-H}}$ 7.7, 0.8, 1H), 7.32 (d, $J_{\text{H-H}}$ 7.9, 1H), 7.38 (app t, $J_{\text{H-H}}$ 7.7, 6H), 7.45 (tt, $J_{\text{H-H}}$ 7.3, 2.2, 3H), 7.65 (t, $J_{\text{H-H}}$ 7.7, 1H),

7.80 (app d, $J_{\text{H-H}}$ 7.1, 6H), 12.22 (s, OH, 1H).

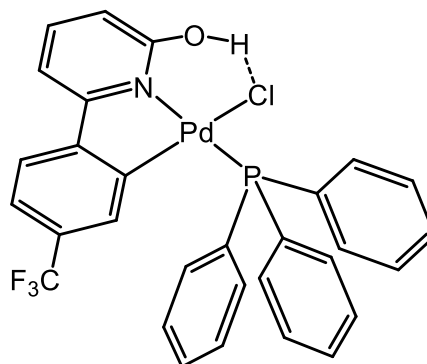
$^{13}\text{C}\{^1\text{H}\}$ NMR (100 MHz, CDCl_3 , 298 K): δ 21.0 (Me), 109.3 (CH), 110.8 (CH), 123.8 (CH), 125.3 (CH), 128.1 (d, $^3J_{\text{C-P}}$ 10.3, CH), 130.7 (d, $^4J_{\text{C-P}}$ 3.1, CH), 130.8 (d, $^1J_{\text{C-P}}$ 50.0, C), 135.5 (d, $^2J_{\text{C-P}}$ 11.0, CH), 138.1 (C), 139.9 (CH), 141.1 (CH), 145.2 (C), 151.4 (C), 161.6 (C), 166.9 (C). ^{31}P NMR (162 MHz,



CDCl_3 , 298 K): δ 44.8 (s, PPh_3). IR (selected bands, cm^{-1}): 1563, 1434, 1215, 1168, 1090, 1030, 792, 742, 701, 687. MS (ES): m/z 1103 $[\text{2(M-Cl)}]^+$. TOFMS (ES): m/z 552.0727 $[\text{M-Cl}]^+$ ($\text{C}_{30}\text{H}_{25}\text{NOP}^{106}\text{Pd}$ requires 552.0709), 1105.1411 $[\text{2(M-Cl)+H}]^+$ ($\text{C}_{60}\text{H}_{50}\text{N}_2\text{O}_2\text{P}_2^{106}\text{Pd}_2$ requires 1105.1437). Anal Calcd for $\text{C}_{30}\text{H}_{25}\text{ClINOPPd} \cdot 0.3\text{CH}_2\text{Cl}_2$: C, 59.29; H, 4.20; N, 2.28; found: C, 59.55; H, 4.02; N, 2.60%.

5.3.37 Synthesis of $[\text{Pd}(\kappa^2\text{-6-(4-trifluoromethylphenyl)-2-pyridinol})(\text{PPh}_3)\text{Cl}]$ (3.37)

Based on the procedure described for **3.35**, using **3.29** (43 mg, 0.065 mmol) gave **3.37** as a yellow solid (33 mg, 79%). Crystals suitable for a single crystal X-ray diffraction study were grown from a dichloromethane solution of the complex layered with hexane. Mp: 208 °C. $^1\text{H}\{^{31}\text{P}\}$ NMR (400 MHz, CDCl_3 , 298 K): δ 6.72 (dd, $J_{\text{H-H}}$ 8.3, 0.9,

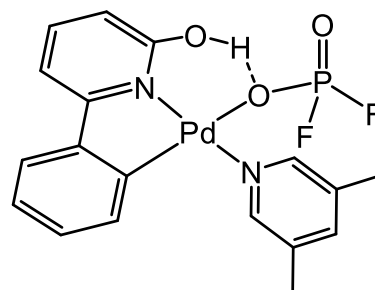


1H), 6.80 (s, 1H), 7.13 (dd, $J_{\text{H-H}}$ 8.1, 0.9, 1H), 7.32 (dd, $J_{\text{H-H}}$ 7.6, 0.8, 1H), 7.39 (app tt, $J_{\text{H-H}}$ 7.2, 1.3, 6H), 7.47 (tt, $J_{\text{H-H}}$ 7.3, 1.1, 3H), 7.52 (d, $J_{\text{H-H}}$ 8.2, 1H), 7.72 (t, $J_{\text{H-H}}$ 7.9, 1H), 7.78 (d, $J_{\text{H-H}}$ 7.3, 6H), 12.36 (s, OH, 1H). $^{13}\text{C}\{^1\text{H}\}$ NMR (100 MHz, CDCl_3 , 298 K): δ 110.6 (CH), 112.8 (CH), 121.2 (CH), 123.5 (q, $^1J_{\text{C-F}}$ 274.2, C), 123.6 (CH), 128.3 (d, $^3J_{\text{C-P}}$ 11.2, CH), 128.9 (q, $^2J_{\text{C-F}}$ 32, C), 130.0 (d, $^1J_{\text{C-P}}$ 52.0, C), 131.1 (CH), 135.2 (CH), 135.3 (d, $^2J_{\text{C-P}}$ 11.9, CH), 141.4 (CH), 151.2 (C), 151.3 (C), 160.1 (C), 167.2 (C). ^{31}P NMR (162 MHz, CDCl_3 , 298 K): δ 44.9 (s, PPh_3). ^{19}F NMR (376 MHz, CDCl_3 , 298 K): δ -63.3 (s, CF_3). IR (selected bands, cm^{-1}): 1435, 1314, 1290, 1157, 1114, 1092, 1069, 798, 688, 655. MS (ES): m/z 1211 $[\text{2(M-Cl)}]^+$. TOFMS (ES): m/z 606.0472 $[\text{M-Cl}]^+$ ($\text{C}_{30}\text{H}_{22}\text{F}_3\text{NOP}^{106}\text{Pd}$ requires 606.0426), 1213.0975 $[\text{2(M-Cl)+H}]^+$ ($\text{C}_{60}\text{H}_{44}\text{F}_6\text{N}_2\text{O}_2\text{P}_2^{106}\text{Pd}_2$ requires 1213.0872). Anal Calcd for $\text{C}_{30}\text{H}_{22}\text{ClF}_3\text{NOPPd}$: C, 56.10; H, 3.45; N, 2.18; found: C, 55.93; H, 3.45; N, 2.24%.

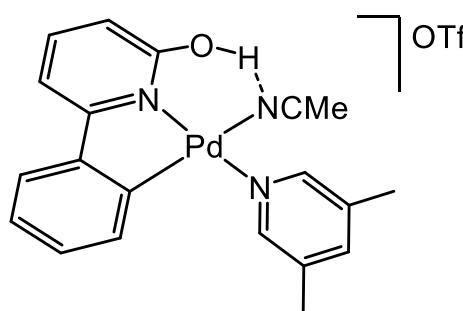
Silver Salts Reactions

5.3.38 Synthesis of $[\text{Pd}(\kappa^2\text{-6-phenyl-2-pyridinol})(3,5\text{-lutidine})(\text{PO}_2\text{F}_2)]$ (**3.38**)

A small-sized Schlenk flask equipped with a magnetic stir bar was evacuated and backfilled with nitrogen and loaded with **3.32a** (~95% pure) (0.039 g, 0.093 mmol), AgPF_6 (0.024 g, 0.093 mmol) and MeCN (10 mL). The reaction mixture was stirred at room temperature for 12 h, at which point the suspension was allowed to settle and the solution was transferred by cannula filtration into a round bottom flask. All volatiles were removed under reduced pressure to afford 40 mg as a crude product which was then dissolved in chloroform and left for 3 days to give a yellow solution with a black solid. The yellow solution was separated and the solvent was removed to afford **3.38** as a yellow solid (33 mg, 73%). Mp: 77 °C (decomp.). ^1H NMR (400 MHz, CDCl_3 , 298 K): δ 2.40 (s, py-Me, 6H), 5.94 (d, $J_{\text{H-H}}$ 7.9, 1H), 6.61 (d, $J_{\text{H-H}}$ 8.4, 1H), 6.83 (td, $J_{\text{H-H}}$ 7.4, 1.2, 1H), 7.15 (d, $J_{\text{H-H}}$ 7.5, 1H), 7.37 (dd, $J_{\text{H-H}}$ 7.8, 1.2, 1H), 7.57 (s, 1H), 7.67 (t, $J_{\text{H-H}}$ 8.0, 1H), 8.62 (s, 2H), 11.70 (br s, OH, 1H). $^{13}\text{C}\{^1\text{H}\}$ NMR (100 MHz, CDCl_3 , 298 K): δ 18.35 (py-Me), 109.6 (CH), 111.2 (CH), 123.6 (CH), 125.5 (CH), 129.1 (CH), 132.9 (CH), 135.8 (C), 140.6 (CH), 141.4 (CH), 146.2 (C), 148.3 (C), 150.0 (CH), 160.9 (C), 166.7 (C). ^{31}P NMR (162 MHz, CDCl_3 , 298 K): δ -15.3 (t, $J_{\text{P-F}}$ 973.2, PO_2F_2). ^{19}F NMR (376 MHz, CDCl_3 , 298 K): δ -80.0 (d, $J_{\text{F-P}}$ 976.2, PO_2F_2). IR (selected bands, cm^{-1}): 1623, 1570, 1427, 1292, 1231, 1102, 1034, 841, 756, 966. MS (ES): m/z 383 $[\text{M-PO}_2\text{F}_2]^+$, 767 $[2(\text{M-PO}_2\text{F}_2)]^+$, 101 $[\text{PO}_2\text{F}_2]^-$. TOFMS (ES): m/z 383.0445 $[\text{M-PO}_2\text{F}_2]^+$ ($\text{C}_{18}\text{H}_{17}\text{N}_2\text{O}_2^{106}\text{Pd}$ requires 383.0376).

5.3.39 Synthesis of $[\text{Pd}(\kappa^2\text{-6-phenyl-2-pyridinol})(3,5\text{-lutidine})(\text{MeCN})]\text{OTf}$ (**3.39**)

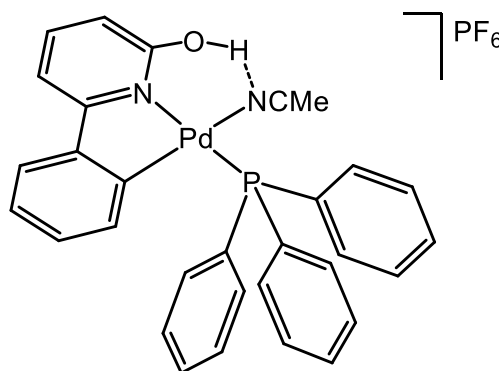
Based on the procedure described for **3.38**, using **3.32a** (~95% pure) (0.048 g, 0.11 mmol) and $\text{AgOSO}_2\text{CF}_3$ (30 mg, 0.11 mmol) gave **3.39** as a yellow solid (45 mg, 71%). Mp: 151 °C (decomp.). ^1H NMR (400 MHz, CDCl_3 , 298 K): δ 2.02 (s, MeCN, 3H), 2.37 (s, py-Me, 6H), 5.90 (d, $J_{\text{H-H}}$ 8.3, 1H), 6.67 (d, $J_{\text{H-H}}$ 8.2, 1H), 6.83 (t, $J_{\text{H-H}}$ 7.3, 1H), 7.07 (t, $J_{\text{H-H}}$ 7.2, 1H), 7.16 (d, $J_{\text{H-H}}$ 7.3, 1H), 7.35 (dd, $J_{\text{H-H}}$ 7.7, 1.1, 1H), 7.53 (s, 1H), 7.68 (t, $J_{\text{H-H}}$ 7.4, 1H), 8.57 (s, 2H), 10.39 (br s, OH, 1H). Sample was insufficiently soluble for $^{13}\text{C}\{^1\text{H}\}$; therefore, selective ^{13}C



data was acquired by an HMQC experiment. HMQC NMR (100 MHz, CDCl₃, 298 K): δ MeCN is not observable, 18.5 (py-Me), 110.1 (CH), 111.1 (CH), 123.9 (CH), 125.9 (CH), 129.1 (CH), 133.0 (CH), 140.7 (CH), 141.5 (CH), 150.0 (CH). ¹⁹F NMR (376 MHz, CDCl₃, 298 K): δ -78.1 (s, OTf). IR (selected bands, cm⁻¹): 2035, 1621, 1569, 1425, 1222, 1154, 1026, 802, 756, 699. MS (ES): m/z 383 [M-MeCN]⁺, 767 [2(M-MeCN)]⁺, 149 [OSO₂CF₃]⁻. TOFMS (ES): m/z 383.0461 [M-MeCN]⁺ (C₁₈H₁₇N₂O₂¹⁰⁶Pd requires 383.0376), 767.0651 [2(M-MeCN)]⁺ (C₃₆H₃₄N₄O₄¹⁰⁶Pd₂ requires 767.0772).

5.3.40 Synthesis of [Pd(κ^2 -6-phenyl-2-pyridinol)(PPh₃)(MeCN)]PF₆ (**3.40**)

A small-sized Schlenk flask equipped with a magnetic stir bar was evacuated and backfilled with nitrogen and loaded with **3.35** (59.5 mg, 0.1 mmol), AgPF₆ (26.2 mg, 0.1 mmol) and MeCN (10 mL). The reaction mixture was stirred at room temperature for 12 h, at which point the suspension was allowed to

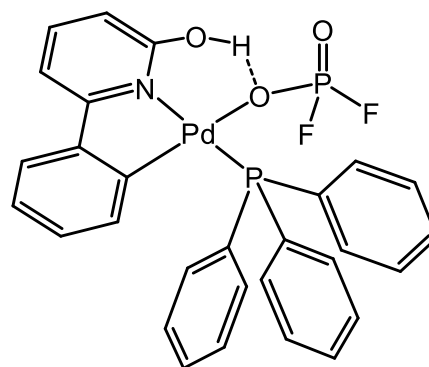


settle and the solution was transferred by cannula filtration into a round bottom flask. All volatiles were removed under reduced pressure to afford **3.40** (60 mg, 82%) as a dark yellow solid. Mp: 95 °C (decomp.). ¹H{³¹P} NMR (400 MHz, CDCl₃, 298 K): δ 1.88 (s, MeCN, 3H), 6.42 (d, J_{H-H} 7.8, 1H), 6.45 (t, J_{H-H} 7.9, 1H), 6.85 (d, J_{H-H} 7.9, 1H), 6.95 (t, J_{H-H} 7.6, 1H), 7.29 (d, J_{H-H} 7.6, 1H), 7.36 (d, J_{H-H} 7.3, 1H), 7.44 (t, J_{H-H} 7.6, 6H), 7.52 (t, J_{H-H} 7.3, 3H), 7.71 (t, J_{H-H} 8.1, 1H), 7.73 (d, J_{H-H} 7.5, 6H), 9.44 (br s, OH, 1H). ¹³C{¹H} NMR (100 MHz, CDCl₃, 298 K): δ 0.0 (MeCN), 108.7 (CH), 116.9 (MeCN), 123.0 (CH), 123.9 (CH), 126.7 (CH), 126.8 (CH), 127.1 (d, ³J_{C-P} 10.6, CH), 127.6 (d, ¹J_{C-P} 50.2, C), 130.0 (CH), 133.4 (d, ²J_{C-P} 12.8, CH), 137.5 (d, J_{C-P} 14.7, CH), 140.6 (CH), 145.9 (C), 146.2 (C), 159.5 (C), 163.5 (C). ³¹P NMR (162 MHz, CDCl₃, 298 K): δ 44.4 (s, PPh₃), -144.1 (sept, ¹J_{P-F} 711, PF₆). ¹⁹F NMR (376 MHz, CDCl₃, 298 K): δ -72.6 (d, ¹J_{F-P} 714, PF₆). IR (selected bands, cm⁻¹): 1608, 1572, 1480, 1435, 1275, 1095, 830, 745, 691. MS (ES): m/z 538 [M-MeCN]⁺, 1076 [2(M-MeCN)]⁺, 145 [PF₆]⁻. TOFMS (ES): m/z 538.0563 [M-MeCN]⁺ (C₂₉H₂₃NOP¹⁰⁶Pd requires 538.0552).

5.3.41 Synthesis of [Pd(κ^2 -6-phenyl-2-pyridinol)(PPh₃)(PO₂F₂)] (**3.41**)

The product **3.40** (40 mg, 0.055 mmol) was dissolved in chloroform and left for three days in an NMR tube. The solvent was then removed to afford **3.41** (34 mg, 97%)

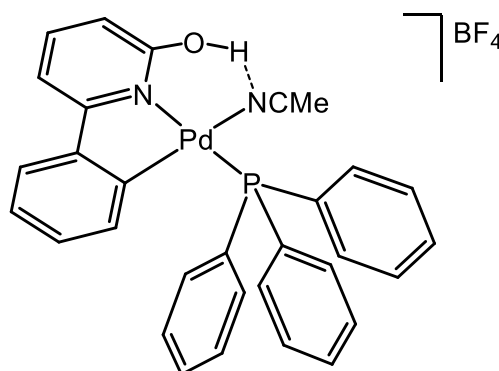
as a yellow solid. $^1\text{H}\{^{31}\text{P}\}$ NMR (400 MHz, CDCl_3 , 298 K): δ 6.44 (app d, $J_{\text{H-H}}$ 3.8, 1H, 1H), 6.68 (d, $J_{\text{H-H}}$ 8.3, 1H), 6.93 (sept, $J_{\text{H-H}}$ 3.7, 1H), 7.26 (d, $J_{\text{H-H}}$ 7.2, 1H), 7.40 (t, $J_{\text{H-H}}$ 7.6, 6H), 7.47 (app t, $J_{\text{H-H}}$ 6, 3H, 1H), 7.71 (t, $J_{\text{H-H}}$ 7.9, 1H), 7.78 (app d, $J_{\text{H-H}}$ 7.1, 6H), 11.54 (br s, OH, 1H). $^{13}\text{C}\{^1\text{H}\}$ NMR (100 MHz, CDCl_3 , 298 K): δ 110.0 (CH), 111.4 (CH), 124.5



(CH), 125.3 (CH), 128.4 (CH), 128.6 (d, $^3J_{\text{C-P}}$ 10.8, CH), 129.2 (d, $^1J_{\text{C-P}}$ 49.8, C), 131.3 (CH), 135.5 (d, $^2J_{\text{C-P}}$ 11.4, CH), 138.8 (d, $J_{\text{C-P}}$ 14.8, CH), 141.8 (CH), 144.5 (C), 147.4 (C), 159.9 (C), 156.8 (C). ^{31}P NMR (162 MHz, CDCl_3 , 298 K): δ 42.6 (s, PPh_3), -15.2 (t, $^1J_{\text{P-F}}$ 970, PO_2F_2). ^{19}F NMR (376 MHz, CDCl_3 , 298 K): δ -81.0 (d, $^1J_{\text{F-P}}$ 978, PO_2F_2). IR (selected bands, cm^{-1}): 1620, 1571, 1435, 1290, 1094, 844, 745, 691. MS (ES): m/z 538 $[\text{M-PO}_2\text{F}_2]^+$, 101 $[\text{PO}_2\text{F}_2]^-$. TOFMS (ES): m/z 538.0663 $[\text{M-PO}_2\text{F}_2]^+$ ($\text{C}_{29}\text{H}_{23}\text{NOP}^{106}\text{Pd}$ requires 538.0552).

5.3.42 Synthesis of $[\text{Pd}(\kappa^2\text{-6-phenyl-2-pyridinol})(\text{PPh}_3)(\text{MeCN})]\text{BF}_4$ (3.42)

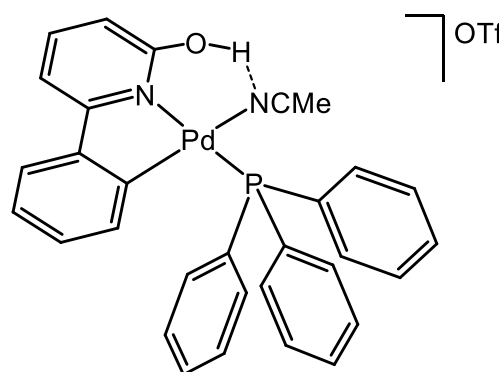
Based on the procedure described for **3.40**, using **3.35** (60 mg, 0.1 mmol) and AgBF_4 (20 mg, 0.1 mmol) gave **3.42** as a yellow solid (55 mg, 83%). Mp: 133 °C (decomp.). $^1\text{H}\{^{31}\text{P}\}$ NMR (400 MHz, CDCl_3 , 298 K): δ 1.82 (s, MeCN , 3H), 6.42 (t, $J_{\text{H-H}}$ 7.6, 1H), 6.47 (d, $J_{\text{H-H}}$ 7.8, 1H), 6.86 (br s, 1H), 6.93 (t, $J_{\text{H-H}}$ 7.2, 1H),



7.27 (d, $J_{\text{H-H}}$ 7.6, 1H), 7.43 (m, 6H), 7.49 (m, 4H), 7.69 (t, $J_{\text{H-H}}$ 7.6, 1H), 7.74 (d, $J_{\text{H-H}}$ 7.3, 6H), 12.31 (br s, OH, 1H). Sample was insufficiently soluble for $^{13}\text{C}\{^1\text{H}\}$; therefore, selective ^{13}C data was acquired by an HMQC experiment. HMQC NMR (100 MHz, CDCl_3 , 298 K): δ 110.0 (CH), 124.3 (CH), 125.3 (CH), 128.2 (CH), 128.9 (CH), 131.5 (CH), 134.5 (CH), 135.2 (CH), 139.3 (CH), 142.1 (CH). ^{31}P NMR (162 MHz, CDCl_3 , 298 K): δ 44.6 (s, PPh_3). ^{19}F NMR (376 MHz, CDCl_3 , 298 K): δ -151.6 (s, BF_4). IR (selected bands, cm^{-1}): 1607, 1570, 1480, 1434, 1289, 1090, 1025, 996, 804, 745, 690. MS (ES): m/z 538 $[\text{M-MeCN}]^+$, 87 $[\text{BF}_4]^-$. TOFMS (ES): m/z 538.0573 $[\text{M-MeCN}]^+$ ($\text{C}_{29}\text{H}_{23}\text{NOP}^{106}\text{Pd}$ requires 538.0552), 1077.0858 $[2(\text{M-MeCN})]^+$ ($\text{C}_{58}\text{H}_{46}\text{N}_2\text{O}_2\text{P}_2^{106}\text{Pd}_2$ requires 1077.0824).

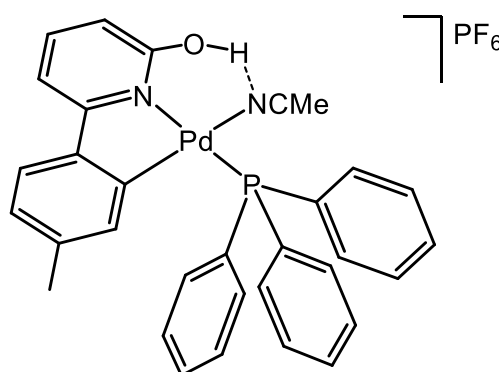
5.3.43 Synthesis of [Pd(κ^2 -6-phenyl-2-pyridinol)(PPh₃)(MeCN)]OTf (3.43)

Based on the procedure described for **3.40**, using **3.35** (60 mg, 0.1 mmol) and AgOSO₂CF₃ (26 mg, 0.1 mmol) gave **3.43** as a yellow solid (61 mg, 84%). Mp: 91 °C (decomp.). ¹H{³¹P} NMR (400 MHz, CDCl₃, 298 K): δ 1.81 (s, MeCN, 3H), 6.42 (t, $J_{\text{H-H}}$ 7.5, 1H), 6.46 (d, $J_{\text{H-H}}$ 7.1, 1H), 6.94 (t, $J_{\text{H-H}}$ 7.4, 1H), 6.97 (d, $J_{\text{H-H}}$ 8.3, 1H), 7.25 (d, $J_{\text{H-H}}$ 7.6, 1H), 7.44 (app t, $J_{\text{H-H}}$ 7.5, 6H, 1H), 7.52 (app t, $J_{\text{H-H}}$ 7.3, 3H), 7.68 (t, $J_{\text{H-H}}$ 7.9, 1H), 7.75 (d, $J_{\text{H-H}}$ 7.5, 6H), 11.03 (br s, OH, 1H). ¹³C{¹H} NMR (100 MHz, CDCl₃, 298 K): δ 0.0 (MeCN), 108.2 (CH), 109.5 (CH), 117.6 (MeCN), 122.7 (CH), 123.7 (CH), 126.5 (CH), 126.9 (d, ³ $J_{\text{C-P}}$ 11.3, CH), 127.7 (d, ¹ $J_{\text{C-P}}$ 50.4, C), 129.9 (CH), 133.3 (d, ² $J_{\text{C-P}}$ 13.7, CH), 137.5 (d, $J_{\text{C-P}}$ 15.2, CH), 140.2 (CH), 146.3 (C), 146.4 (C), 159.4 (C), 163.5 (C). ³¹P NMR (162 MHz, CDCl₃, 298 K): δ 44.5 (s, PPh₃). ¹⁹F NMR (376 MHz, CDCl₃, 298 K): δ -78.2 (s, OTf) IR (selected bands, cm⁻¹): 1604, 1570, 1434, 1024, 1092, 994, 802, 743, 691. MS (ES): m/z 538 [M-MeCN]⁺, 149 [OTf]⁻. TOFMS (ES): m/z 538.0577 [M-MeCN]⁺ (C₂₉H₂₃NOP¹⁰⁶Pd requires 538.0552), 1077.0862 [2(M-MeCN)]⁺ (C₅₈H₄₆N₂O₂P₂¹⁰⁶Pd₂ requires 1077.0824).



5.3.44 Synthesis of [Pd(κ^2 -6-(4-methylphenyl)-2-pyridinol)(PPh₃)(MeCN)]PF₆ (3.44)

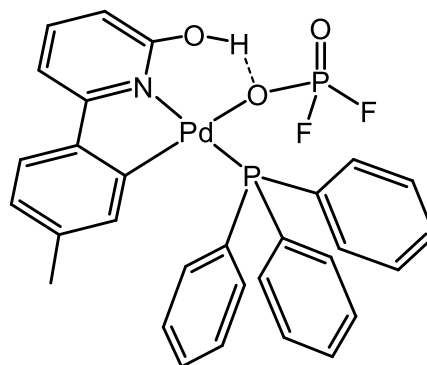
Based on the procedure described for **3.40**, using **3.36** (45 mg, 0.08 mmol) and AgPF₆ (13.3 mg, 0.08 mmol) gave **3.44** as a yellow solid (55 mg, 93%). Mp: 129 °C (decomp.). ¹H{³¹P} NMR (400 MHz, CDCl₃, 298 K): δ 1.62 (s, *p*-Me, 3H), 1.83 (s, MeCN, 3H), 6.23 (s, 1H), 6.75 (d, $J_{\text{H-H}}$ 7.3, 1H), 6.82 (d, $J_{\text{H-H}}$ 8.3, 1H), 7.24 (d, $J_{\text{H-H}}$ 7.6, 1H), 7.33 (d, $J_{\text{H-H}}$ 8.1, 1H), 7.44 (t, $J_{\text{H-H}}$ 7.3, 6H), 7.52 (app t, $J_{\text{H-H}}$ 7.5, 3H), 7.69 (t, $J_{\text{H-H}}$ 8.1, 1H), 7.73 (d, $J_{\text{H-H}}$ 8.3, 6H), 9.11 (br s, OH, 1H). Sample was insufficiently soluble for ¹³C{¹H}; therefore, selective ¹³C data was acquired by a DEPT 135 experiment. DEPT 135 NMR (100 MHz, CDCl₃, 298 K): δ 0.0 (MeCN), 19.2 (*p*-Me), 108.4 (CH), 108.6 (CH), 122.6 (CH), 124.5 (CH), 127.0 (d, ³ $J_{\text{C-P}}$ 11.2, CH), 129.9 (CH), 133.5 (d, ² $J_{\text{C-P}}$ 12.6, CH), 138.5 (d, $J_{\text{C-P}}$ 14.7, CH), 140.5 (CH). ³¹P NMR (162



MHz, CDCl₃, 298 K): δ 43.9 (s, PPh₃), -144.1 (sept, $^1J_{P-F}$ 711, PF₆). ^{19}F NMR (376 MHz, CDCl₃, 298 K): δ -72.5 (d, $^1J_{F-P}$ 714, PF₆). IR (selected bands, cm⁻¹): 1606, 1570, 1482, 1435, 1290, 1095, 831, 794, 744, 691. MS (ES): m/z 552 [M-MeCN]⁺, 145 [PF₆]⁻. TOFMS (ES): m/z 552.0720 [M-MeCN]⁺ (C₃₀H₂₅NOP¹⁰⁶Pd requires 552.0709), 1105.1368 [2(M-MeCN)]⁺ (C₆₀H₅₀N₂O₂P₂¹⁰⁶Pd₂ requires 1105.1437).

5.3.45 Synthesis of [Pd(κ^2 -6-(4-methylphenyl)-2-pyridinol)(PPh₃)(PO₂F₂)] (3.45)

The product **3.44** (40 mg, 0.054 mmol) was dissolved in chloroform and left for one day in an NMR tube. The solvent was then removed to afford **3.45** (32 mg, 91%) as a yellow solid. Crystals suitable for a single crystal X-ray diffraction study were grown from a solution of the complex **3.45** in dichloromethane/MeCN (95/5 v/v) layered with hexane. Mp: 160 °C (decomp.).

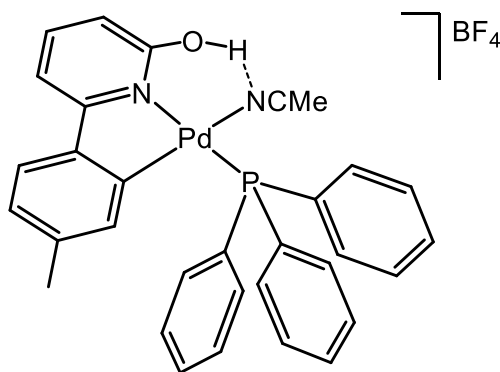


$^1H\{^{31}P\}$ NMR (400 MHz, CDCl₃, 298 K): δ 1.65 (s, Me, 3H), 6.23 (s, 1H), 6.64 (d, J_{H-H} 8.7, 1H), 6.74 (d, J_{H-H} 7.8, 1H), 7.20 (d, J_{H-H} 7.6, 1H), 7.31 (d, J_{H-H} 7.9, 1H), 7.40 (app t, J_{H-H} 7.6, 6H), 7.48 (tt, J_{H-H} 7.4, 1.2, 3H), 7.68 (t, J_{H-H} 7.9, 1H), 7.77 (d, J_{H-H} 7.1, 6H), 11.51 (br s, OH, 1H). Sample was insufficiently soluble for $^{13}C\{^1H\}$; therefore, selective ^{13}C data was acquired by a DEPT 135 experiment. DEPT 135 NMR (100 MHz, CDCl₃, 298 K): δ 20.9 (Me), 109.6 (CH), 110.8 (CH), 124.1 (CH), 126.0 (CH), 128.5 (d, $^3J_{C-P}$ 11.1, CH), 131.2 (CH), 135.5 (d, $^2J_{C-P}$ 11.8, CH), 139.6 (d, J_{C-P} 14.7, CH), 141.6 (CH). ^{31}P NMR (162 MHz, CDCl₃, 298 K): δ 42.2 (s, PPh₃), -15.0 (t, $^1J_{P-F}$ 975, PO₂F₂). ^{19}F NMR (376 MHz, CDCl₃, 298 K): δ -81.1 (d, $^1J_{F-P}$ 984, PO₂F₂). IR (selected bands, cm⁻¹): 1569, 1435, 1292, 1232, 1091, 1087, 842, 793, 748, 690. MS (ES): m/z 552 [M-PO₂F₂]⁺, 1105 [2(M-PO₂F₂)]⁺, 101 [PO₂F₂]⁻. TOFMS (ES): m/z 552.0720 [M-PO₂F₂]⁺ (C₃₀H₂₅NOP¹⁰⁶Pd requires 552.0709), 1105.1415 [2(M-PO₂F₂)]⁺ (C₆₀H₅₀N₂O₂P₂¹⁰⁶Pd₂ requires 1105.1437).

5.3.46 Synthesis of [Pd(κ^2 -6-(4-methylphenyl)-2-pyridinol)(PPh₃)(MeCN)]BF₄ (3.46)

Based on the procedure described for **3.40**, using **3.36** (36 mg, 0.065 mmol) and AgBF₄ (12.6 mg, 0.065 mmol) gave **3.46** as a yellow solid (41 mg, 93%). Mp: 91 °C (decomp.). $^1H\{^{31}P\}$ NMR (400 MHz, CDCl₃, 298 K): δ 1.62 (s, *p*-Me, 3H), 2.00 (s, MeCN, 3H), 6.24 (s, 1H), 6.75 (d, J_{H-H} 7.9, 1H), 6.87 (br s, 1H), 7.22 (d, J_{H-H} 7.8, 1H), 7.33 (d, J_{H-H} 7.8, 1H), 7.45 (app t, J_{H-H} 7.9, 6H), 7.50 (m, 3H), 7.70 (t, J_{H-H} 8.1, 1H), 7.75

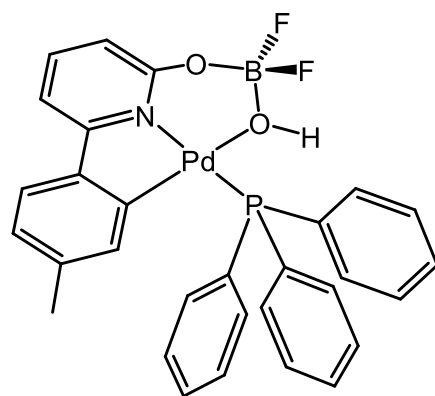
(app d, $J_{\text{H-H}}$ 7.7, 6H), 9.78 (br s, OH, 1H). Sample was insufficiently soluble for $^{13}\text{C}\{^1\text{H}\}$; therefore, selective ^{13}C data was acquired by an HMQC experiment. HMQC NMR (100 MHz, CDCl_3 , 298 K): δ 1.0 (MeCN), 20.8 (*p*-Me), 109.7 (CH), 110.3 (CH), 126.2 (CH), 128.8 (CH), 131.5 (CH), 133.9 (CH), 135.1 (CH),



140.2 (CH), 141.6 (CH). ^{31}P NMR (162 MHz, CDCl_3 , 298 K): δ 44.1 (s, PPh_3). ^{19}F NMR (376 MHz, CDCl_3 , 298 K): δ -151.6 (s, BF_4). IR (selected bands, cm^{-1}): 1608, 1572, 1482, 1436, 1293, 1095, 1054, 995, 798, 764, 692. MS (ES): m/z 552 $[\text{M-MeCN}]^+$, 1104 $[2(\text{M-MeCN})]^+$, 87 $[\text{BF}_4]^-$. TOFMS (ES): m/z 552.0731 $[\text{M-MeCN}]^+$ ($\text{C}_{30}\text{H}_{25}\text{NOP}^{106}\text{Pd}$ requires 552.0709), 1105.1407 $[2(\text{M-MeCN})]^+$ ($\text{C}_{60}\text{H}_{50}\text{N}_2\text{O}_2\text{P}_2^{106}\text{Pd}_2$ requires 1105.1437).

5.3.47 Synthesis of $[\text{Pd}(\kappa^2\text{-6-(4-methylphenyl)-2-pyridonate})(\text{PPh}_3)(\text{BF}_2\text{OH})]$ (**3.47**)

The product **3.46** (30 mg, 0.044 mmol) was dissolved in chloroform and left for one day in an NMR tube. The solvent was then removed to afford **3.47** (26 mg, 96%) as a yellow solid. Crystals suitable for a single crystal X-ray diffraction study were grown from a solution of the complex in dichloromethane/MeCN (95/5 v/v) layered with hexane. $^1\text{H}\{^{31}\text{P}\}$ NMR (400 MHz, CDCl_3 , 298 K): δ

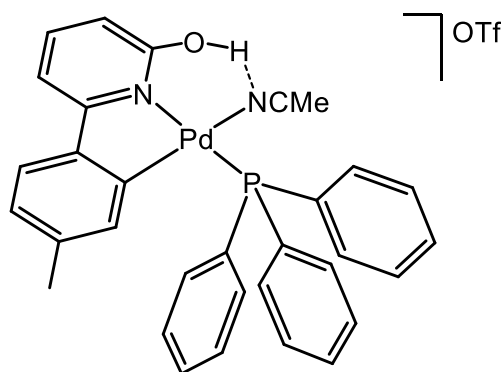


1.67 (s, Me, 3H), 3.48 (br s, OH, 1H), 6.23 (s, 1H), 6.70 (dd, $J_{\text{H-H}}$ 8.2, 0.9, 1H), 6.75 (d, $J_{\text{H-H}}$ 7.9, 1H), 7.17 (d, $J_{\text{H-H}}$ 7.6, 1H), 7.34 (d, $J_{\text{H-H}}$ 7.8, 1H), 7.46 (app tt, $J_{\text{H-H}}$ 7.2, 1.2, 6H), 7.54 (tt, $J_{\text{H-H}}$ 7.6, 1.4, 3H), 7.64 (t, $J_{\text{H-H}}$ 7.9, 1H), 7.77 (app d, $J_{\text{H-H}}$ 7.2, 6H). Sample was insufficiently soluble for $^{13}\text{C}\{^1\text{H}\}$; therefore, selective ^{13}C data was acquired by a DEPT 135 experiment. DEPT 135 NMR (100 MHz, CDCl_3 , 298 K): δ 20.0 (Me), 108.2 (CH), 113.8 (CH), 122.8 (CH), 124.7 (CH), 128.1 (d, $^3J_{\text{C-P}}$ 9.9, CH), 130.3 (CH), 133.9 (d, $^2J_{\text{C-P}}$ 12.7, CH), 139.1 (d, $J_{\text{C-P}}$ 14.2, CH), 140.2 (CH). ^{31}P NMR (162 MHz, CDCl_3 , 298 K): δ 42.6 (s, PPh_3). ^{19}F NMR (376 MHz, CDCl_3 , 298 K): δ -149.4 (d, $^2J_{\text{F-F}}$ 13.7, BF_2OH), -149.5 (d, $^2J_{\text{F-F}}$ 13.7, BF_2OH). IR (selected bands, cm^{-1}): 1563, 1481, 1454, 1435, 1260, 1094, 1017, 997, 799, 744, 691. MS (ES): m/z 552 $[\text{M-BF}_2\text{OH}]^+$, 1104 $[2(\text{M-BF}_2\text{OH})]^+$, 65 $[\text{BF}_2\text{OH}]^-$. TOFMS (ES): m/z 552.0768 $[\text{M-BF}_2\text{OH}]^+$ ($\text{C}_{30}\text{H}_{25}\text{NOP}^{106}\text{Pd}$ requires 552.0709).

5.3.48 Synthesis of $[\text{Pd}(\kappa^2\text{-6-(4-methylphenyl)-2-pyridinol})(\text{PPh}_3)(\text{MeCN})]\text{OTf}$ (3.48)

Based on the procedure described for **3.40**, using **3.36** (37 mg, 0.067 mmol) and $\text{AgOSO}_2\text{CF}_3$ (17.2 mg, 0.067 mmol) gave **3.48** as a yellow solid (45 mg, 90%). Crystals suitable for a single crystal X-ray diffraction study were grown from a solution of the complex in DCM/MeCN (95/5 v/v) layered with hexane. Mp: 110 °C (decomp.).

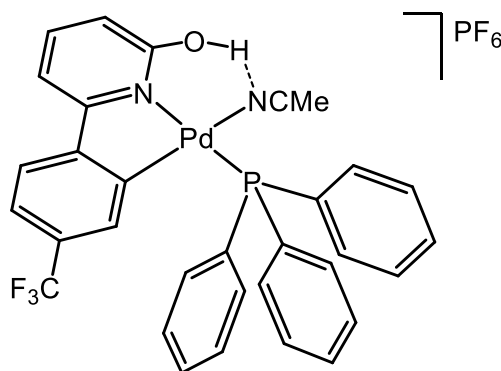
$^1\text{H}\{^{31}\text{P}\}$ NMR (400 MHz, CDCl_3 , 298 K): δ 1.62 (s, *p*-Me, 3H), 1.80 (s, MeCN, 3H), 6.23 (s, 1H), 6.75 (d, $J_{\text{H-H}}$ 8.6, 1H), 6.92 (d, $J_{\text{H-H}}$ 7.5, 1H), 7.21 (d, $J_{\text{H-H}}$ 7.7, 1H), 7.32 (d, $J_{\text{H-H}}$ 7.9, 1H), 7.45 (t, $J_{\text{H-H}}$ 7.4, 6H), 7.52 (t, $J_{\text{H-H}}$ 7.4, 3H), 7.67 (t, $J_{\text{H-H}}$ 7.8, 1H), 7.74 (d, $J_{\text{H-H}}$ 7.4, 6H), 10.61 (br s, OH, 1H). Sample was insufficiently soluble for $^{13}\text{C}\{^1\text{H}\}$; therefore, selective ^{13}C data was acquired by a DEPT 135 experiment. DEPT 135 NMR (100 MHz, CDCl_3 , 298 K): δ -1.9 (MeCN), 19.1 (*p*-Me), 108.1 (CH), 109.0 (CH), 122.4 (CH), 124.3 (CH), 126.9 (d, $^3J_{\text{C-P}}$ 11.2, CH), 129.8 (CH), 133.3 (d, $^2J_{\text{C-P}}$ 12.5, CH), 138.5 (d, $J_{\text{C-P}}$ 14.8, CH), 140.2 (CH). ^{31}P NMR (162 MHz, CDCl_3 , 298 K): δ 44.0 (s, PPh_3). ^{19}F NMR (376 MHz, CDCl_3 , 298 K): δ -78.2 (s, OTf). IR (selected bands, cm^{-1}): 1607, 1572, 1481, 1435, 1287, 1221, 1158, 1095, 1025, 795, 744, 691. MS (ES): m/z 552 $[\text{M-MeCN}]^+$, 1104 $[2(\text{M-MeCN})]^+$, 149 $[\text{OTf}]^-$. TOFMS (ES): m/z 552.0691 $[\text{M-MeCN}]^+$ ($\text{C}_{30}\text{H}_{25}\text{NOP}^{106}\text{Pd}$ requires 552.0709), 1105.1326 $[2(\text{M-MeCN})]^+$ ($\text{C}_{60}\text{H}_{50}\text{N}_2\text{O}_2\text{P}_2^{106}\text{Pd}_2$ requires 1105.1437).



5.3.49 Synthesis of $[\text{Pd}(\kappa^2\text{-6-(4-trifluoromethylphenyl)-2-pyridinol})(\text{PPh}_3)(\text{MeCN})]\text{PF}_6$ (3.49)

Based on the procedure described for **3.40**, using **3.37** (40 mg, 0.062 mmol) and AgPF_6 (15.7 mg, 0.062 mmol) gave **3.49** as a yellow solid (48 mg, 98%). Mp: 125 °C (decomp.).

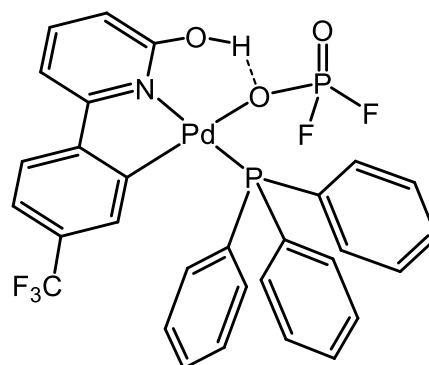
$^1\text{H}\{^{31}\text{P}\}$ NMR (400 MHz, CDCl_3 , 298 K): δ 1.77 (s, MeCN, 3H), 6.72 (s, 1H), 6.92 (d, $J_{\text{H-H}}$ 7.2, 1H), 7.19 (d, $J_{\text{H-H}}$ 8.0, 1H), 7.37 (d, $J_{\text{H-H}}$ 7.5, 1H), 7.46 (t, $J_{\text{H-H}}$ 7.2, 6H), 7.53 (d, $J_{\text{H-H}}$ 8.1, 1H), 7.54 (t, $J_{\text{H-H}}$ 7.5, 3H), 7.74 (d, $J_{\text{H-H}}$ 7.7, 6H), 7.79 (t, $J_{\text{H-H}}$ 8.4, 1H), 9.74 (br s, OH, 1H). Sample was



insufficiently soluble for $^{13}\text{C}\{^1\text{H}\}$; therefore, selective ^{13}C data was acquired by a DEPT 135 experiment. DEPT 135 NMR (100 MHz, CDCl_3 , 298 K): δ 0.0 (MeCN), 109.2 (CH), 110.8 (CH), 120.3 (CH), 122.2 (CH), 127.1 (d, $^3J_{\text{C-P}}$ 11.1, CH), 130.0 (CH), 133.4 (CH), 133.5 (d, $^2J_{\text{C-P}}$ 12.4, CH), 140.4 (CH). ^{31}P NMR (162 MHz, CDCl_3 , 298 K): δ 43.4 (s, PPh_3), -144.1 (sept, $^1J_{\text{P-F}}$ 712, PF_6). ^{19}F NMR (376 MHz, CDCl_3 , 298 K): δ -63.4 (s, CF_3), -72.3 (d, $^1J_{\text{F-P}}$ 714, PF_6). IR (selected bands, cm^{-1}): 1436, 1319, 1164, 1119, 1095, 1072, 834, 740, 691. MS (ES): m/z 606 $[\text{M-MeCN}]^+$, 1213 $[2(\text{M-MeCN})]^+$, 145 $[\text{PF}_6]^-$. TOFMS (ES): m/z 606.0444 $[\text{M-MeCN}]^+$ ($\text{C}_{30}\text{H}_{22}\text{F}_3\text{NOP}^{106}\text{Pd}$ requires 606.0426), 1213.0739 $[2(\text{M-MeCN})]^+$ ($\text{C}_{60}\text{H}_{44}\text{F}_6\text{N}_2\text{O}_2\text{P}_2^{106}\text{Pd}_2$ requires 1213.0872).

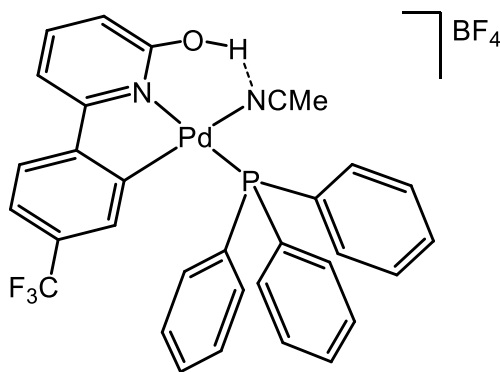
5.3.50 Synthesis of $[\text{Pd}(\kappa^2\text{-6-(4-trifluoromethylphenyl)-2-pyridinol})(\text{PPh}_3)(\text{PO}_2\text{F}_2)]$ (3.50)

The product **3.49** (40 mg, 0.05 mmol) was dissolved in chloroform and left for three hours in an NMR tube. The solvent was then removed to afford **3.50** (33 mg, 93%) as a yellow solid. Crystals suitable for a single crystal X-ray diffraction study were grown from a solution of the complex **3.50** in dichloromethane/MeCN (95/5 v/v) layered with hexane. Mp: 115 °C (decomp.). $^1\text{H}\{^{31}\text{P}\}$ NMR (400 MHz, CDCl_3 , 298 K): δ 6.72 (s, 1H), 6.77 (d, $J_{\text{H-H}}$ 8.3, 1H), 7.18 (d, $J_{\text{H-H}}$ 8.1, 1H), 7.32 (d, $J_{\text{H-H}}$ 7.3, 1H), 7.42 (t, $J_{\text{H-H}}$ 8.1, 6H), 7.50 (m, 4H), 7.76 (m, 7H), 11.63 (br s, OH, 1H). Sample was insufficiently soluble for $^{13}\text{C}\{^1\text{H}\}$; therefore, selective ^{13}C data was acquired by an HMQC experiment. HMQC NMR (100 MHz, CDCl_3 , 298 K): δ 110.6 (CH), 112.9 (CH), 122.1 (CH), 123.3 (CH), 128.8 (CH), 131.5 (CH), 135.0 (CH), 135.1 (CH), 142.1 (CH). ^{31}P NMR (162 MHz, CDCl_3 , 298 K): δ 42.0 (s, PPh_3), -15.3 (t, $^1J_{\text{P-F}}$ 974, PO_2F_2). ^{19}F NMR (376 MHz, CDCl_3 , 298 K): δ -63.3 (s, CF_3), -80.8 (d, $^1J_{\text{F-P}}$ 984, PO_2F_2). IR (selected bands, cm^{-1}): 1625, 1578, 1439, 1306, 1116, 1090, 1069, 1030, 740, 688. MS (ES): m/z 606 $[\text{M-PO}_2\text{F}_2]^+$, 1212 $[2(\text{M-PO}_2\text{F}_2)]^+$, 101 $[\text{PO}_2\text{F}_2]^-$, 444 $[\text{M-(PPh}_3)]^-$. TOFMS (ES): m/z 606.0453 $[\text{M-PO}_2\text{F}_2]^+$ ($\text{C}_{30}\text{H}_{22}\text{F}_3\text{NOP}^{106}\text{Pd}$ requires 606.0426), 1213.0837 $[2(\text{M-PO}_2\text{F}_2)+\text{H}]^+$ ($\text{C}_{60}\text{H}_{44}\text{F}_6\text{N}_2\text{O}_2\text{P}_2^{106}\text{Pd}_2$ requires 1213.0872), 443.9045 $[\text{M-(PPh}_3)]^-$ (requires 443.9135).



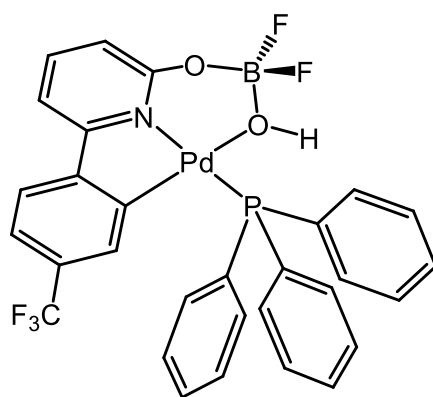
5.3.51 Synthesis of [Pd(κ^2 -6-(4-trifluoromethylphenyl)-2-pyridinol)(PPh₃)(MeCN)] BF₄ (3.51)

Based on the procedure described for **3.40**, using **3.37** (40 mg, 0.062 mmol) and AgBF₄ (12.1 mg, 0.062 mmol) gave **3.51** as a yellow solid (44 mg, 97%). Mp: 139 °C (decomp.). ¹H{³¹P} NMR (400 MHz, CDCl₃, 298 K): δ 1.81 (s, MeCN, 3H), 6.71 (s, 1H), 6.98 (d, $J_{\text{H-H}}$ 7.3, 1H), 7.17 (d, $J_{\text{H-H}}$ 8.0, 1H), 7.32 (d, $J_{\text{H-H}}$ 7.3, 1H), 7.45 (t, $J_{\text{H-H}}$ 8.2, 6H), 7.53 (m, 4H), 7.73 (m, 7H), 15.30 (br s, OH, 1H). Sample was insufficiently soluble for ¹³C{¹H}; therefore, selective ¹³C data was acquired by an HMQC experiment. HMQC NMR (100 MHz, CDCl₃, 298 K): δ 110.6 (CH), 112.5 (CH), 121.9 (CH), 123.6 (CH), 129.0 (CH), 131.7 (CH), 134.8 (CH), 135.5 (CH), 142.7 (CH). ³¹P NMR (162 MHz, CDCl₃, 298 K): δ 43.5 (s, PPh₃). ¹⁹F NMR (376 MHz, CDCl₃, 298 K): δ -63.4 (s, CF₃), -151.3 (s, BF₄). IR (selected bands, cm⁻¹): 1608, 1436, 1318, 1116, 1094, 1070, 997, 801, 742, 691. MS (ES): m/z 606 [M-MeCN]⁺, 1213 [2(M-MeCN)]⁺, 87 [BF₄]⁻. TOFMS (ES): m/z 606.0444 [M-MeCN]⁺ (C₃₀H₂₂F₃NOP¹⁰⁶Pd requires 606.0426), 1213.0803 [2(M-MeCN)]⁺ (C₆₀H₄₄F₆N₂O₂P₂¹⁰⁶Pd₂ requires 1213.0872).



5.3.52 Synthesis of [Pd(κ^2 -6-(4-trifluoromethylphenyl)-pyridonate)(PPh₃)(BF₂OH)] (3.52)

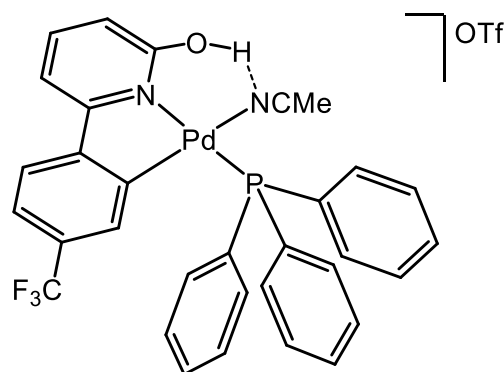
The product **3.51** (35 mg, 0.048 mmol) was dissolved in chloroform and left for eight hours in an NMR tube. The solvent was then removed to afford **3.52** (29 mg, 89%) as a yellow solid. Crystals suitable for a single crystal X-ray diffraction study were grown from a solution of the complex **3.52** in dichloromethane/MeCN (95/5 v/v) layered with hexane. Mp: 211 °C (decomp.). ¹H{³¹P} NMR (400 MHz, CDCl₃, 298 K): δ 3.54 (br s, OH, 1H), 6.68 (s, 1H), 6.82 (dd, $J_{\text{H-H}}$ 8.3, 0.9, 1H), 7.18 (dd, $J_{\text{H-H}}$ 8.1, 0.8, 1H), 7.28 (dd, $J_{\text{H-H}}$ 7.6, 0.9, 1H), 7.47 (app t, $J_{\text{H-H}}$ 8.1, 6H), 7.54 (m, 4H), 7.72 (t, $J_{\text{H-H}}$ 8.3, 1H), 7.74 (d, $J_{\text{H-H}}$ 7.1, 6H). Sample was insufficiently soluble for ¹³C{¹H}; therefore, selective ¹³C data was acquired by an HMQC experiment. HMQC



NMR (100 MHz, CDCl₃, 298 K): δ 110.3 (CH), 116.8 (CH), 121.9 (CH), 123.4 (CH), 129.1 (CH), 132.0 (CH), 134.5 (CH), 135.6 (CH), 141.9 (CH). ³¹P NMR (162 MHz, CDCl₃, 298 K): δ 41.9 (s, PPh₃). ¹⁹F NMR (376 MHz, CDCl₃, 298 K): δ -62.9 (s, CF₃), -149.5 (d, ²J_{F-F} 13.7, BF₂OH), -149.6 (d, ²J_{F-F} 13.7, BF₂OH). IR (selected bands, cm⁻¹): 1567, 1481, 1435, 1318, 1156, 1118, 1096, 1070, 1040, 882, 800, 741, 690. MS (ES): m/z 605 [M-BF₂OH]⁺, 1213 [2(M-BF₂OH)]⁺, 65 [BF₂OH]⁻. TOFMS (ASAP): m/z 606.0445 [M-BF₂OH]⁺ (C₃₀H₂₂F₃NOP¹⁰⁶Pd requires 606.0426). TOFMS (ES): m/z 1213.1398 [2(M-BF₂OH)]⁺ (C₆₀H₄₄F₆N₂O₂P₂¹⁰⁶Pd₂ requires 1213.0872). Anal Calcd for C₃₀H₂₂BF₃NO₂PPd: C, 53.64; H, 3.30; N, 2.09; found: C, 53.72; H, 3.31; N, 2.11%.

5.3.53 Synthesis of [Pd(κ^2 -6-(4-trifluoromethylphenyl)-2-pyridinol)(PPh₃)(MeCN)] OTf (3.53)

Based on the procedure described for **3.40**, using **3.37** (40 mg, 0.062 mmol) and AgOSO₂CF₃ (15.9 mg, 0.062 mmol) gave **3.53** as a yellow solid (49 mg, 99%). Crystals suitable for a single crystal X-ray diffraction study were grown from a solution of the complex **3.53** in dichloromethane/MeCN (95/5

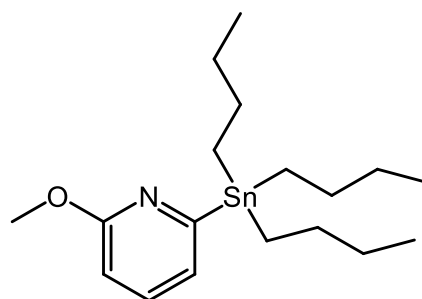


v/v) layered with hexane. Mp: 96 °C (decomp.). ¹H{³¹P} NMR (400 MHz, CDCl₃, 298 K): δ 1.88 (s, MeCN, 3H), 6.71 (s, 1H), 7.06 (d, J_{H-H} 8.4, 1H), 7.19 (dd, J_{H-H} 8.1, 0.9, 1H), 7.33 (d, J_{H-H} 7.5, 1H), 7.41 (app d, J_{H-H} 8.1, 1H), 7.46 (t, J_{H-H} 7.8, 6H), 7.54 (app tt, J_{H-H} 7.7, 1.2, 3H), 7.74 (d, J_{H-H} 8.1, 6H), 7.78 (t, J_{H-H} 7.8, 6H), 11.19 (br s, OH, 1H). Sample was insufficiently soluble for ¹³C{¹H}; therefore, selective ¹³C data was acquired by a DEPT 135 experiment. DEPT 135 NMR (100 MHz, CDCl₃, 298 K): δ 0.0 (MeCN), 109.0 (CH), 110.7 (CH), 120.2 (CH), 122.0 (CH), 127.0 (d, ³J_{C-P} 11.1, CH), 130.0 (CH), 133.1 (d, ²J_{C-P} 11.7, CH), 133.7 (d, J_{C-P} 14.6, CH), 140.4 (CH). ³¹P NMR (162 MHz, CDCl₃, 298 K): δ 43.4 (s, PPh₃). ¹⁹F NMR (376 MHz, CDCl₃, 298 K): δ -63.5 (s, CF₃), -77.9 (s, OTf). IR (selected bands, cm⁻¹): 1607, 1572, 1481, 1436, 1319, 1224, 1160, 1096, 1025, 799, 742, 691. MS (ES): m/z 605 [M-MeCN]⁺, 1212 [2(M-MeCN)]⁺, 149 [OTf]⁻. TOFMS (ES): m/z 606.0453 [M-MeCN]⁺ (C₃₀H₂₂F₃NOP¹⁰⁶Pd requires 606.0426), 1213.0800 [2(M-MeCN)]⁺ (C₆₀H₄₄F₆N₂O₂P₂¹⁰⁶Pd₂ requires 1213.0872). Anal Calcd for C₃₃H₂₅F₆N₂O₄PSPd.1.2CH₂Cl₂: C, 45.70; H, 3.07; N, 3.12; found: C, 45.56; H, 3.38; N, 2.65%.

5.4 Experimental Procedures for Chapter 4

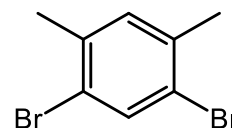
5.4.1 Synthesis of 2-methoxy-6-(tributylstannyl)pyridine (4.1)

A solution containing 6-bromo-2-methoxypyridine (**2.1**) (1.22 mL, 1.88 g, 10 mmol) in diethyl ether (25 mL) at -78 °C was treated with *n*-butyllithium (11.86 mmol, 7.55 mL, 1.6 M in hexanes) dropwise, stirred for 0.5 h, warmed to 0 °C for 10 minutes, re-cooled to -78 °C, treated with tributyltin chloride (4.22 mL, 15.6 mmol), stirred at -78 °C for 0.5 h, and then at 0 °C for 0.5 h. The mixture was allowed to stir at room temperature for 3 h and then treated with brine and extracted with ethyl acetate. The organic layer was dried over MgSO₄. Evaporation of the solvent gave a residue, which was subjected to column chromatography on silica gel. Elution with hexane: AcOEt (100:1, v/v) gave 2-methoxy-6-(tributylstannyl)pyridine (**4.1**) (3.2 g, 81%) as a colourless oil. ¹H NMR (400 MHz, CDCl₃, 298 K): δ 0.88 (t, *J*_{H-H} 7.2, 9H), 1.08, (t, *J*_{H-H} 8.2, 6H), 1.33 (sext, *J*_{H-H} 7.3, 6H), 1.58 (m, 6H), 3.92 (s, OMe, 3H), 6.55 (dd, *J*_{H-H} 8.3, 0.96, 1H), 6.97 (dd, *J*_{H-H} 6.8, 0.92, 1H), 7.38 (dd, *J*_{H-H} 8.4, 6.8, 1H). ¹³C{¹H} NMR (100 MHz, CDCl₃, 298 K): δ 9.9 (CH₂), 13.7 (CH₃), 27.3 (CH₂), 29.0 (CH₂), 53.0 (OMe), 108.9 (CH), 125.9 (CH), 135.9 (CH), 163.1 (C), 170.6 (C). Data are consistent with those reported in the literature.¹¹



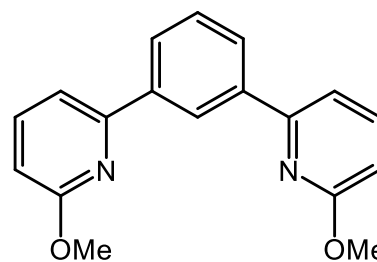
5.4.2 Synthesis of 1,5-dibromo-2,4-dimethylbenzene (4.2)

A 250-mL round bottom flask wrapped in aluminium foil was charged with *m*-xylene (19.6 mL, 160 mmol) and iodine (0.2 g, 0.79 mmol). The mixture was stirred for about an hour while cooling in an ice bath. Bromine (17.4 mL, 340 mmol) was added *via* a dropping funnel over a period of one hour. After overnight reaction, potassium hydroxide (KOH) (20 percent aq., 100 mL) was added and the resulting mixture was heated gently using an oil bath. The solid was melted and the biphasic mixture was stirred for about one hour as the yellow colour slowly faded. After cooling, the liquid was decanted and the white solid was collected by filtration and washed with water (4 x 50 mL), then recrystallised from absolute ethanol (80 mL) to give **4.2** as white crystals (17.13 g, 41%). ¹H NMR (400 MHz, CDCl₃, 298 K): δ 2.28 (s, Me, 6H), 7.06 (s, 1H), 7.65 (s, 1H). ¹³C{¹H} NMR (100 MHz, CDCl₃, 298 K): δ 22.3 (Me), 122.0 (C), 132.6 (CH), 134.8 (CH), 136.8 (C). Data are consistent with those reported in the literature.¹²



5.4.3 Synthesis of 1,3-bis(2-(6-methoxypyridyl)benzene) (4.3)

A 250 mL, 3-necked, dry, nitrogen flushed flask was charged with n-BuLi (1.6 M in hexanes, 8.5 mL, 13.5 mmol) and the solution was cooled to $-78\text{ }^{\circ}\text{C}$. To the flask, a solution of 6-bromo-2-methoxypyridine (**2.1**) (1.69 g, 1.1 mL, 9 mmol) in dry diethyl ether (10 mL) was added dropwise. After stirring for 30 min, the reaction mixture was warmed to $0\text{ }^{\circ}\text{C}$, and zinc chloride solution (1.0 M in diethyl ether, 13.5 mL, 13.5 mmol) was added dropwise. The mixture was then warmed to room temperature. 1,3-Dibromobenzene (0.707 g, 0.354 mL, 3 mmol), Pd(PPh₃)₄ (350 mg, 0.3 mmol, 10%) and 45 mL of THF (tetrahydrofuran) were added and the reaction mixture was heated to reflux for 72 h. After cooling, the reaction mixture was quenched with a saturated aqueous solution of sodium hydrogen carbonate (50 mL), washed with a saturated aqueous solution of EDTA (50 mL) and extracted with ethyl acetate (3 × 75 mL). The combined organic phases were washed with water (100 mL), brine (100 mL), dried over MgSO₄, filtered and evaporated. The crude product was purified by column chromatography with hexane and ethyl acetate (9:1) as eluting solvents. The product (**4.3**) was obtained as a white solid (270 mg, 31%). Crystals suitable for single crystal X-ray diffraction were grown by slow evaporation of a methanol solution of the ligand. Mp: $82\text{--}83\text{ }^{\circ}\text{C}$. ¹H NMR (400 MHz, CDCl₃, 298 K): δ 4.06 (s, OMe, 6H), 6.71 (dd, $J_{\text{H-H}}$ 8.2, 0.5, 2H), 7.42 (dd, $J_{\text{H-H}}$ 7.4, 0.6, 2H), 7.54 (t, $J_{\text{H-H}}$ 7.8, 1H), 7.65 (t, $J_{\text{H-H}}$ 8.1, 2H), 8.07 (dd, $J_{\text{H-H}}$ 7.8, 1.8, 2H), 8.75 (app t, $J_{\text{H-H}}$ 1.6, 1H). ¹³C{¹H} NMR (100 MHz, CDCl₃, 298 K): δ 53.2 (OMe), 109.4 (CH), 112.9 (CH), 125.1 (CH), 127.1 (CH), 128.9 (CH), 139.2 (CH), 139.4 (C), 154.5 (C), 163.7 (C). IR (selected bands, cm⁻¹): 1575, 1463, 1419, 1303, 1255, 1237, 1019, 778, 684. MS (ES): m/z 293 [M]⁺. TOFMS (ES): m/z 293.1262 [M]⁺ (C₁₈H₁₆N₂O₂ requires 293.1245). Data are consistent with those reported in the literature.¹³

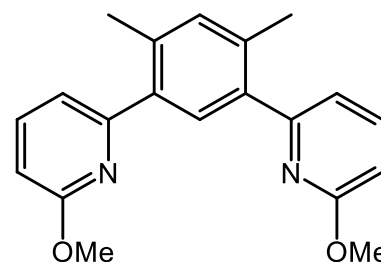


It should be noted that this ligand was also obtained by the following procedure (Stille Coupling Reaction) and gave the product in 79% yield.

5.4.4 Synthesis of 4,6-bis(2-(6-methoxypyridonyl)*m*-xylene) (4.4)

A mixture of 2-methoxy-6-(tributylstannyl)-pyridine (**4.1**) (2.00 g, 4.79 mmol, 2.3 eq.), 1,5-dibromo-2,4-dimethylbenzene (**4.2**) (0.55 g, 2.08 mmol), bis(triphenylphosphine)-palladium(II) chloride (54.8 mg, 0.076 mmol) and lithium chloride (0.659 g, 15.18 mmol, 7.3 eq.) were combined in a mixture of EtOH (5 mL) and

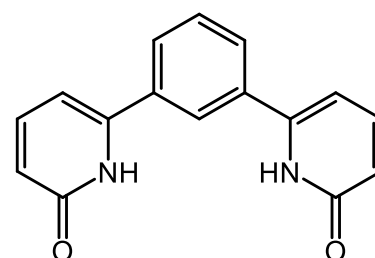
dry toluene (20 mL) (N_2 was also bubbled through the mixture for 2 h) and the mixture was then heated at 90 °C under a nitrogen atmosphere for 48 h. After the reaction mixture had cooled to room temperature, saturated KF solution (10 mL) was added and the solution stirred for



30 min. The precipitated solid was removed by filtration and washed with water (25 mL). $NaHCO_3$ solution (10%, 50 mL) was then added to the combined filtrates, which were extracted with dichloromethane (2 x 100 mL), separated and dried over $MgSO_4$. Removal of solvent under reduced pressure and purification of the residue by column chromatography (silica, DCM/petroleum ether, 90:10) gave the desired product (**4.4**) as a white solid (360 g, 54%). Crystals suitable for single crystal X-ray diffraction were grown by slow evaporation of a methanol solution of the ligand. Mp: 55-56 °C. 1H NMR (400 MHz, $CDCl_3$, 298 K): δ 2.39 (s, Me, 6H), 3.87 (s, OMe, 6H), 6.59 (dd, J_{H-H} 8.2, 0.6, 2H), 6.94 (dd, J_{H-H} 7.2, 0.6, 2H), 7.12 (s, 1H), 7.46 (s, 1H), 7.52 (dd, J_{H-H} 8.2, 7.5, 2H). $^{13}C\{^1H\}$ NMR (100 MHz, $CDCl_3$, 298 K): δ 19.4 (Me), 52.3 (OMe), 107.5 (CH), 115.5 (CH), 130 (CH), 132.6 (CH), 135.1 (C), 136.6 (C), 137.6 (CH), 156.3 (C), 162.1 (C). IR (selected bands, cm^{-1}): 2945, 1576, 1458, 1429, 1406, 1305, 1252, 1153, 1026, 861, 793, 740. MS (ES): m/z 321 $[M]^+$. TOFMS (ASAP): 321.1603 $[M]^+$ ($C_{20}H_{20}N_2O_2$ requires 321.1525).

5.4.5 Synthesis of 1,3-bis(2-pyridon-6-yl)benzene (4.5)

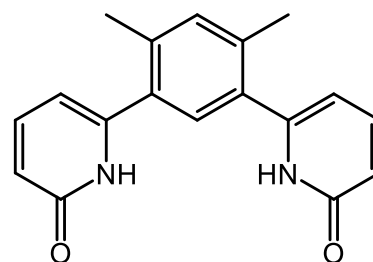
A 10-mL round bottom flask with a magnetic stir bar and reflux condenser, was loaded with 1,3-bis(2-(6-methoxypyridyl)benzene (**4.3**) (100 mg, 0.342 mmol) and aqueous 48% HBr (3.1 mL, 27.4 mmol, 80 eq). The mixture was heated at reflux for 4 hours (set oil bath to



125 °C). The solution was then allowed to cool to room temperature and neutralised with saturated $NaHCO_3$ solution. The resultant mixture was then filtered, and the precipitate was washed with water (10 mL), collected and dried. The product **4.5** was obtained as a light brown solid (79.4 mg, 88% yield). Mp: > 300 °C. 1H NMR (400 MHz, MeOD, 298 K): δ 6.46 (d, J_{H-H} 9.0, 2H), 6.68 (d, J_{H-H} 6.6, 2H), 7.50 (m, 3H), 7.72 (dd, 7.7, 1.6, 1H), 7.91 (s, 1H), NH is not observable. Sample was insufficiently soluble for $^{13}C\{^1H\}$. IR (selected bands, cm^{-1}): 1643, 1554, 1159, 988, 775, 697. MS (ES): m/z 265 $[M]^+$. TOFMS (ASAP): 265.0981 $[M]^+$ ($C_{16}H_{12}N_2O_2$ requires 265.0932).

5.4.6 Synthesis of 4,6-bis(2-pyridon-6-yl)*m*-xylene (4.6)

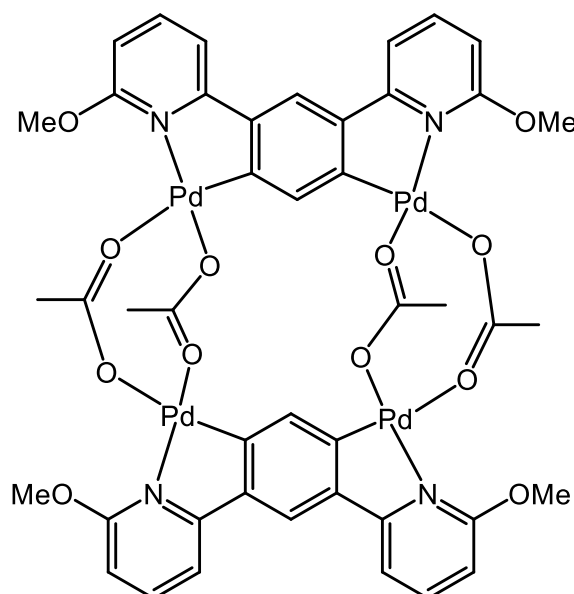
A 10-mL round bottom flask with a magnetic stir bar and reflux condenser, was loaded with 1,3-bis(2-(6-pyridonyl)*m*-xylene (4.4) (153 mg, 0.476 mmol) and aqueous 48% HBr (4.33 mL, 38.1 mmol, 80 eq). This solution was heated at reflux for 4 hours (set oil bath to



125 °C). The solution was then allowed to cool to room temperature and neutralised with saturated NaHCO₃ solution. The product was extracted with DCM (3 x 50 mL). Drying with MgSO₄ and placed under pressure to remove any volatiles, a white solid (4.6) was afforded. This was taken up in the minimum amount of methanol and heated to dissolve all products. After cooling, crystals suitable for single crystal X-ray diffraction were obtained (55 mg, 40 %). Mp: > 270 °C. ¹H NMR (400 MHz, CDCl₃, 298 K): δ 2.37 (s, Me, 6H), 6.26 (dd, *J*_{H-H} 6.8, 0.8, 2H), 6.70 (dd, *J*_{H-H} 9.1, 0.6, 2H), 7.17 (s, 1H), 7.42 (dd, *J*_{H-H} 11.2, 8.9, 2H) 7.60 (s, 1H), 12.20 (br s, 2H). ¹³C{¹H} NMR (100 MHz, CDCl₃, 298 K): δ 20.3 (Me), 107.7 (CH), 119.5 (CH), 130.7 (CH), 131.3 (C), 134.3 (CH), 136.9 (C), 140.3 (CH), 145 (C), 165.4 (C). IR (selected bands, cm⁻¹): 3063, 1637, 1594, 1543, 1286, 1154, 974, 801, 720. MS (ES): *m/z* 293 [M]⁺. TOFMS (ASAP): 293.1301 [M]⁺ (C₁₈H₁₆N₂O₂ requires 293.1245).

5.4.7 Synthesis of [Pd₂(κ²-1,3-bis(2-(6-methoxypyridyl)benzene)₂(μ-OAc)₂]₂ (4.7)

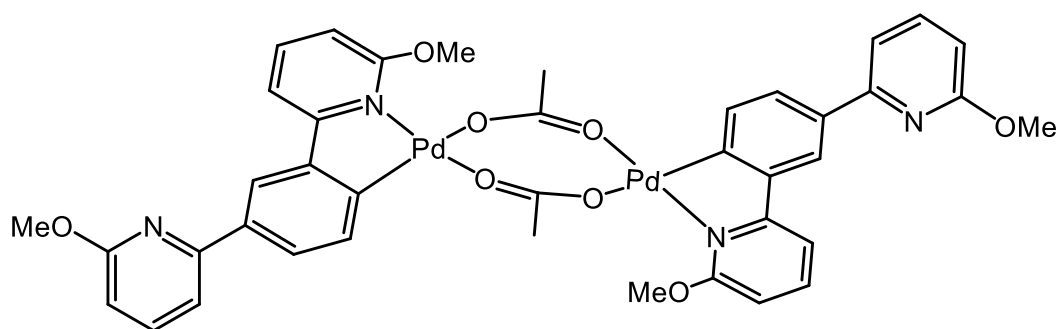
A mixture of 1,3-bis(2-(6-methoxypyridyl)benzene (4.3) (6.4 mg, 0.022 mmol), Pd(OAc)₂ (10 mg, 0.044 mmol) and MeOH (1.7 mL) was stirred at room temperature for 48 h. The reaction mixture was then filtered, and the precipitate was washed with diethyl ether (4 mL), collected and dried. The product 4.7 was obtained as a yellow solid (13 mg, 95% yield). A single crystal suitable for X-ray diffraction analysis was obtained



from a diffusion process using a DMSO solution of 4.7 and EtOH as a precipitant. Mp: 229-231 °C (dec.). ¹H NMR (400 MHz, DMSO-*d*₆, 298 K): δ 1.9 (s, O₂CMe, 6H), 2.14 (s, O₂CMe, 6H), 3.76 (s, OMe, 12H), 6.18 (s, 2H), 6.51 (d, *J*_{H-H} 8.04, 4H), 7.09 (s, 2H),

7.24 (d, $J_{\text{H-H}}$ 7.5, 4H), 7.70 (t, $J_{\text{H-H}}$ 8.0, 4H). Sample was insufficiently soluble for $^{13}\text{C}\{^1\text{H}\}$; therefore, selective ^{13}C data was acquired by HSQC and HMBC experiments. HSQC NMR (125 MHz, $\text{DMSO-}d_6$, 298 K): δ 24.6 (O_2CMe), 24.9 (O_2CMe), 56.4 (OMe), 103.0 (CH), 110.2 (CH), 118.1 (CH), 137.6 (CH), 141.3 (CH). HMBC NMR (125 MHz, $\text{DMSO-}d_6$, 298 K): 140.1 (C), 152.8 (C), 163.0 (C), 165.1 (C), 174.6 (O_2CMe), 179.3 (O_2CMe). IR (selected bands, cm^{-1}): 1567, 1483, 1406, 1269, 1056, 787, 685. TOFMS (ES): m/z 1241.8824 $[\text{M}]^+$ ($\text{C}_{44}\text{H}_{40}\text{N}_4\text{O}_{12}^{106}\text{Pd}_4$ requires 1241.8796), 1182.8633 $[\text{M-OAc}]^+$ ($\text{C}_{42}\text{H}_{37}\text{N}_4\text{O}_{10}^{106}\text{Pd}_4$ requires 1182.8663).

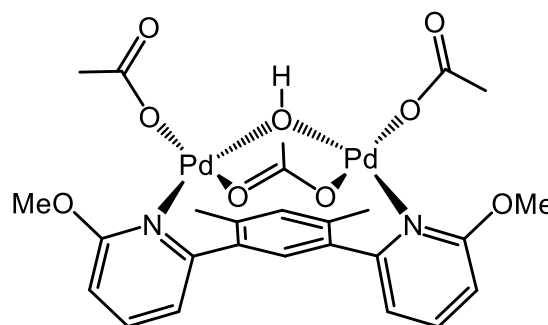
5.4.8 Synthesis of $[\text{Pd}(\kappa^2\text{-1,3-bis(2-(6-methoxypyridyl)benzene))}(\mu\text{-OAc})_2]$ (**4.8**)



A mixture of 1,3-bis(2-(6-methoxypyridyl)benzene) (**4.3**) (29.2 mg, 0.1 mmol), $\text{Pd}(\text{OAc})_2$ (22.5 mg, 0.1 mmol) and MeOH (4 mL) was stirred at room temperature for 24 h. After this time the solvent was removed *in vacuo* leaving behind a solid which was dissolved in DCM and then hexane was slowly added to induce precipitation. The precipitate was isolated, washed with Et_2O and dried *in vacuo* to give **4.8** as a yellow solid (13 mg, 29% yield). Crystals suitable for a single crystal X-ray diffraction study were grown from a dichloromethane solution of the complex layered with hexane. Mp > 270 °C. ^1H NMR (400 MHz, CDCl_3 , 298 K): δ 2.23 (s, O_2CMe , 6H), 3.64 (s, OMe, 6H), 4.06 (s, OMe, 6H), 5.78 (d, $J_{\text{H-H}}$ 8.0, 2H), 6.69 (d, $J_{\text{H-H}}$ 8.0, 2H), 6.91 (d, $J_{\text{H-H}}$ 7.5, 2H), 7.16 (d, $J_{\text{H-H}}$ 8.1, 2H), 7.21 (d, $J_{\text{H-H}}$ 7.4, 2H), 7.25 (t, $J_{\text{H-H}}$ 7.6, 2H), 7.49 (d, $J_{\text{H-H}}$ 8.1, 2H), 7.52 (s, 2H), 7.62 (t, $J_{\text{H-H}}$ 7.5, 2H). $^{13}\text{C}\{^1\text{H}\}$ NMR (125 MHz, CDCl_3 , 298 K): δ 24.4 (O_2CMe), 53.2 (OMe), 55.7 (OMe), 103.3 (CH), 108.4 (CH), 110.3 (CH), 112.0 (CH), 120.9 (CH), 125.4 (CH), 131.8 (CH), 134.8 (C), 139.2 (CH), 140.1 (CH), 145.0 (C), 151.3 (C), 155.4 (C), 162.9 (C), 163.8 (C), 165.8 (O_2CMe). IR (selected bands, cm^{-1}): 1593, 1559, 1484, 1405, 1267, 1055, 784, 686. MS (ES): m/z 855 $[\text{M-OAc}]^+$. FABMS: m/z 397 $[\text{L}+\text{Pd}]^+$. TOFMS (ES): m/z 397.0457 $[\text{L}+\text{Pd}]^+$ ($\text{C}_{18}\text{H}_{15}\text{N}_2\text{O}_2^{106}\text{Pd}$ requires 397.0168).

5.4.9 Synthesis of $[\text{Pd}_2(4,6\text{-bis}(2\text{-(6-methoxypyridonyl)}m\text{-xylene)})(\mu\text{-OAc})(\kappa^1\text{-OAc})_2(\mu\text{-OH})]$ (**4.9**)

A small-sized oven-dried Schlenk flask equipped with a magnetic stir bar was evacuated and backfilled with nitrogen. The flask was charged with the 4,6-bis(2-(6-methoxypyridonyl)*m*-xylene (**4.4**) (14.3 mg, 0.044 mmol, 1 eq.), $\text{Pd}(\text{OAc})_2$ (20 mg, 0.089 mmol, 2 eq.) and freshly distilled

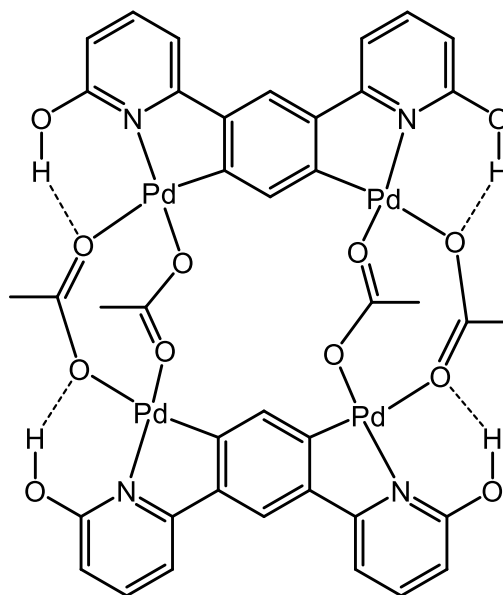


MeOH (5 mL) (N_2 was also bubbled through the solvent for 2 h). The reaction mixture was left to stir under N_2 at room temperature for 24 h. After this time the solvent was removed *in vacuo* leaving behind a solid which was dissolved in DCM (7 mL) and passed through Celite. The filtrate was reduced in volume and hexane was added slowly to induce precipitation. The precipitate was isolated, washed with hexane and dried *in vacuo*. The title product (**4.9**) was obtained as a light orange solid (27 mg, 84% yield). Crystals suitable for a single crystal X-ray diffraction study were grown from a dichloromethane solution of the complex layered with hexane. Mp: 245-247 °C. ^1H NMR (400 MHz, CDCl_3 , 298 K): δ 1.61 (s, O_2CMe , 6H), 1.70 (s, O_2CMe , 3H), 2.25 (s, Me, 6H), 4.27 (s, OMe, 6H), 5.64 (s, OH, 1H), 6.82 (dd, $J_{\text{H-H}}$ 8.5, 0.9, 2H), 7.15 (dd, $J_{\text{H-H}}$ 7.4, 0.9, 2H), 7.35 (s, 1H), 7.86 (dd, $J_{\text{H-H}}$ 8.4, 7.4, 2H), 9.30 (s, 1H). $^{13}\text{C}\{^1\text{H}\}$ NMR (100 MHz, CDCl_3 , 298 K): δ 20.3 (Ar-Me), 22.4 (O_2CMe), 22.7 (O_2CMe), 57.3 (OMe), 105.7 (CH), 119.3 (CH), 131.8 (CH), 132.3 (CH), 135.7 (C), 138.2 (C), 140.9 (CH), 160.4 (C), 165.7 (C), 179.4 (O_2CMe), 183.1 (O_2CMe). IR (selected bands, cm^{-1}): 1574, 1543, 1474, 1380, 1322, 1075, 1013, 798, 690. TOFMS (ES): m/z 669.0067 [M-OAc] $^+$ ($\text{C}_{24}\text{H}_{27}\text{N}_2\text{O}_7^{106}\text{Pd}_2$ requires 668.9892), 650.9943 [$(\text{M-OAc})\text{-OH}$] $^+$ ($\text{C}_{24}\text{H}_{26}\text{N}_2\text{O}_6^{106}\text{Pd}_2$ requires 650.9881), 425.0552 [$\text{L}+\text{Pd}$] $^+$ ($\text{C}_{20}\text{H}_{20}\text{N}_2\text{O}_2^{106}\text{Pd}$ requires 425.0576).

5.4.10 Synthesis of $[\text{Pd}_4(1,3\text{-bis}(2\text{-pyridon-6-yl})\text{benzene})_2(\text{OAc})_4]$ (**4.10**)

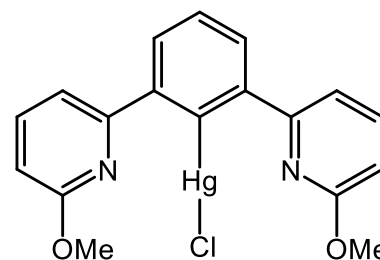
A mixture of 1,3-bis(2-pyridon-6-yl)benzene (**4.5**) (6.5 mg, 0.025 mmol), $\text{Pd}(\text{OAc})_2$ (11.2 mg, 0.05 mmol) and acetic acid (1.5 mL) was stirred and heated at 80 °C for 24 h. After being cooled to room temperature the orange precipitate was filtered and washed with HOAc and Et_2O to give the complex **4.10** as an orange solid (6.5 mg, 44%). Crystals suitable for single crystal X-ray diffraction were grown by slow evaporation of a chloroform solution of the complex. Mp: > 270 °C. ^1H NMR (400 MHz, CDCl_3 , 298

K): δ 2.10 (s, O₂CMe, 6H), 2.23 (s, O₂CMe, 6H), 6.18 (dd, $J_{\text{H-H}}$ 8.2, 0.8, 4H), 6.42 (s, 2H), 6.54 (s, 2H), 6.64 (dd, $J_{\text{H-H}}$ 7.6, 0.7, 4H), 7.31 (t, $J_{\text{H-H}}$ 7.6, 4H), 9.20 (s, OH, 4H). Sample was insufficiently soluble for $^{13}\text{C}\{^1\text{H}\}$; therefore, selective ^{13}C data was acquired by an HSQC experiment. HSQC NMR (125 MHz, CDCl₃, 298 K): δ 24.6 (O₂CMe), 24.9 (O₂CMe), 108.1 (CH), 108.6 (CH), 115.9 (CH), 136.8 (CH), 140.6 (CH). IR (selected bands, cm⁻¹): 1723, 1622, 1558, 1490, 1407, 1256, 1221, 1016, 790, 725. TOFMS (ES): m/z 1186.8275 [M]⁺ (C₄₀H₃₂N₄O₁₂¹⁰⁶Pd requires 1186.8180).



5.4.11 Synthesis of [Hg(1,3-bis(2-(6-methoxypyridyl)benzene))Cl] (4.11)

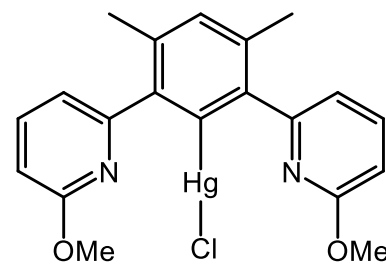
A mixture of 1,3-bis(2-(6-methoxypyridyl)benzene) (**4.3**) (63 mg, 0.215 mmol) and mercury(II) acetate (66.6 mg, 0.209 mmol) in absolute ethanol (4.2 mL) was heated under reflux for 24 h. Afterward a solution of lithium chloride (19.7 mg) in methanol (3.1 mL) was added and the mixture was heated for 15 min. The solution was poured into distilled water (20 mL): the white precipitate formed was filtered off, washed with water and ice-cold methanol, and dried to give the product **4.11** as a white solid (30.1 mg, 27%). Mp: 217-219 °C. ^1H NMR (400 MHz, CDCl₃, 298 K): δ 4.18 (s, OMe, 6H), 6.82 (dd, $J_{\text{H-H}}$ 8.2, 0.65, 2H), 7.30 (dd, $J_{\text{H-H}}$ 7.4, 0.64, 2H), 7.50 (t, $J_{\text{H-H}}$ 7.7, 1H), 7.68 (t, $J_{\text{H-H}}$ 7.4, 2H), 7.82 (d, $J_{\text{H-H}}$ 7.6 and dd, $^4J_{\text{H-Hg}}$ 68, 7.4, 2H). $^{13}\text{C}\{^1\text{H}\}$ NMR (125 MHz, CDCl₃, 298 K): δ 54.3 (OMe), 110.5 (CH), 115.6 (CH), 129.1 (CH), 129.3 (CH), 139.7 (CH), 145.3 (C), 148.3 (C), 157.7 (C), 164.7 (C). IR (selected bands, cm⁻¹): 2955, 1574, 1456, 1318, 1247, 1019, 775, 725. TOFMS (ASAP): m/z 529.0629 [M]⁺ (C₁₈H₁₅Cl²⁰¹HgN₂O₂ requires 529.0528), 493.0843 [M-Cl]⁺ (C₁₈H₁₅²⁰¹HgN₂O₂ requires 493.0840).



5.4.12 Synthesis of [Hg(4,6-bis(2-(6-methoxypyridonyl)*m*-xylene))Cl] (4.12)

A mixture of 4,6-bis(2-(6-methoxypyridonyl)*m*-xylene) (**4.4**) (120 mg, 0.374 mmol) and mercury(II) acetate (119.4 mg, 0.374 mmol) in absolute ethanol (7.5 mL) was heated under reflux for 24 h. Afterward a solution of lithium chloride (34 mg) in methanol (5.5 mL) was added and the mixture was heated for 15 min. The solution was then poured

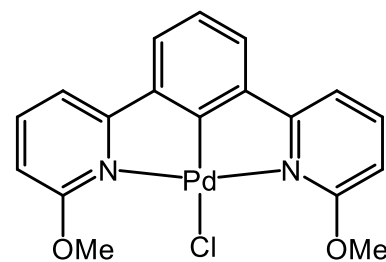
into distilled water (40 mL): the white and grey precipitate formed was filtered off, washed with water and Et₂O, and dried to give the product **4.12** as a grey solid (84 mg, 40%). Crystals suitable for single crystal X-ray diffraction were grown by slow diffusion of isopropyl



ether into a solution of the complex in dichloromethane. Mp: 215-217 °C. ¹H NMR (500 MHz, CDCl₃, 298 K): δ 2.39 (s, Me, 6H), 4.07 (s, OMe, 6H), 6.76 (d, *J*_{H-H} 8.3, 2H), 7.03 (d, *J*_{H-H} 7.2, 2H), 7.19 (s, 1H), 7.63 (t, *J*_{H-H} 7.8, 2H). ¹³C{¹H} NMR (125 MHz, CDCl₃, 298 K): δ 21.5 (Me), 53.8 (OMe), 110.0 (CH), 118.2 (CH), 134.4 (CH), 136.1 (C), 138.7 (CH), 142.8 (C), 155.3 (C), 158.0 (C), 164.6 (C). IR (selected bands, cm⁻¹): 2955, 1573, 1463, 1389, 1268, 1252, 1012, 984, 801, 781, 724. TOFMS (ASAP): *m/z* 557.0953 [M]⁺ (C₂₀H₁₉Cl²⁰¹HgN₂O₂ requires 557.0841), 521.1274 [M-Cl]⁺ (C₂₀H₁₉²⁰¹HgN₂O₂ requires 521.1153).

5.4.13 Synthesis of [Pd(1,3-bis(2-(6-methoxypyridyl)benzene))Cl] (4.13)

By Transmetalation: A suspension of compound [Hg(1,3-bis(2-(6-methoxypyridyl)benzene))Cl] (**4.11**) (50 mg, 0.095 mmol) in ethanol (10 mL) was added to a solution of palladium(II) acetate (21.3 mg, 0.095 mmol) in dry dichloromethane (5 mL), and the mixture was left



to stir at room temperature for 20 h under nitrogen. The black solution was filtered through Celite, and the resulting solution was evaporated to dryness. The solid residue was washed with diethyl ether (2 x 7 mL) and dried *in vacuo* to yield a yellow solid (56 mg).

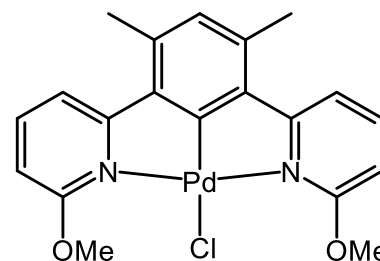
Typically, to a suspension of the yellow solid in methanol (21 mL) was added, with stirring, an excess of lithium chloride (8.2 mg). The mixture was stirred for 1 h at room temperature. The solvent was removed and the product was washed with methanol and diethyl ether, and finally dried *in vacuo* to give **4.13** (11 mg, 27%) as a greenish yellow solid. Mp: > 270 °C. ¹H NMR (500 MHz, DMSO-*d*, 298 K): δ 3.96 (s, OMe, 6H), 7.07 (d, *J*_{H-H} 9.5, 2H), 7.23 (t, *J*_{H-H} 8.2, 1H), 7.62 (app d, 2H, 2H), 8.11 (t, *J*_{H-H} 8.2, 2H). Sample was insufficiently soluble for ¹³C{¹H}; therefore, selective ¹³C data was acquired by an HSQC experiment. HSQC NMR (125 MHz, DMSO-*d*, 298 K): δ 56.1 (OMe), 106.4 (CH), 111.7 (CH), 124.5 (CH), 124.7 (CH), 142.9 (CH). IR (selected bands, cm⁻¹): 1601,

1568, 1480, 1271, 1105, 1026, 791, 746. MS (ES): m/z 397 [M-Cl]⁺. TOFMS (ASAP): m/z 397.0176 [M-Cl]⁺ (C₁₈H₁₅N₂O₂¹⁰⁶Pd requires 397.0168).

By Direct Synthesis with Na₂[PdCl₄]: To a solution of 1,3-bis(2-(6-methoxy-pyridyl)benzene) (**4.3**) (32 mg, 0.11 mmol) in acetic acid (4 mL) was added Na₂[PdCl₄] (32 mg, 0.11 mmol), and a white precipitate immediately appeared. The mixture was heated at 118 °C (reflux) for 24 h. After being cooled to room temperature, the brown precipitate was filtered and washed with MeOH, H₂O, EtOH, and Et₂O to yield 30.2 mg (69%) of **4.13**. The ¹H and ¹³C{¹H} NMR spectra showed identical peaks to those for the complex previously obtained by the transmetalation reaction.

5.4.14 Synthesis of [Pd(4,6-bis(2-(6-methoxy-pyridonyl)*m*-xylene))Cl] (**4.14**)

By Transmetalation: A suspension of compound [Hg(1,3-bis(2-(6-methoxy-pyridyl)benzene))Cl] (**4.12**) (70 mg, 0.126 mmol) in ethanol (13 mL) was added to a solution of palladium(II) acetate (28.3 mg, 0.126 mmol) in dry dichloromethane (7 mL), and the mixture was left

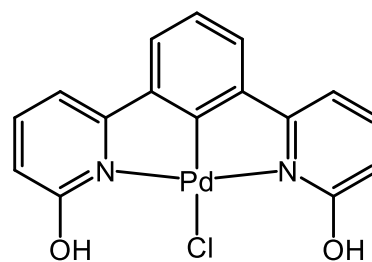


to stir at room temperature for 20 hours under nitrogen. The black solution was filtered through Celite, and the resulting solution was evaporated to dryness. The solid residue was washed with diethyl ether (2 x 10 mL) and dried *in vacuo* to yield **4.14** as a yellow solid (15 mg, 26%). Mp: 245-247 °C. ¹H NMR (400 MHz, DMSO-*d*, 298 K): δ 2.34 (s, Me, 6H), 3.79 (s, OMe, 6H), 6.55 (s, 1H), 6.65 (d, *J*_{H-H} 8.4, 2H), 7.08 (d, *J*_{H-H} 7.9, 2H), 7.74 (t, *J*_{H-H} 8.2, 2H). ¹³C{¹H} NMR (125 MHz, DMSO-*d*, 298 K): δ 22.6 (Me), 56.1 (OMe), 104.6 (CH), 114.6 (CH), 132.7 (CH), 134.8 (C), 138.8 (C), 141.9 (CH), 162.6 (C), 165.7 (C), 169.0 (C). IR (selected bands, cm⁻¹): 3394, 1600, 1570, 1480, 1313, 1271, 1105, 1027, 792, 747. MS (ES): m/z 425 [M-Cl]⁺. TOFMS (ES): m/z 425.0498 [M-Cl]⁺ (C₂₀H₁₉N₂O₂¹⁰⁶Pd requires 425.0481).

By Direct Synthesis with Na₂[PdCl₄]: To a solution of 4,6-bis(2-(6-methoxy-pyridonyl)*m*-xylene) (**4.4**) (23 mg, 0.072 mmol) in acetic acid (4 mL) was added Na₂[PdCl₄] (21 mg, 0.072 mmol), and a white precipitate immediately appeared. The mixture was heated at 118 °C (reflux) for 24 h. After being cooled to room temperature, the brown precipitate was filtered and washed with MeOH, H₂O, EtOH, and Et₂O to yield 12.8 mg (72%) of **4.14**. ¹H NMR spectrum showed identical peaks to those for the complex previously obtained by the transmetalation reaction.

5.4.15 Synthesis of [Pd(1,3-bis(2-pyridon-6-yl)benzene)Cl] (**4.15**)

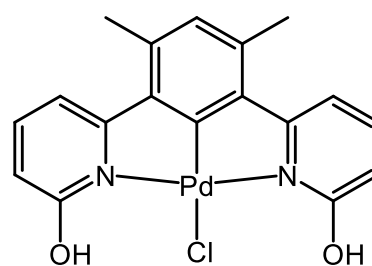
1,3-bis(2-(6-methoxypyridyl)benzene) (**4.3**) (29.23 mg, 0.1 mmol) *or* 1,3-bis(2-pyridon-6-yl)benzene (**4.5**) (30 mg, 0.113 mmol) and Na₂[PdCl₄] (1 eq.) were placed in a microwave vial along with a mixture of AcOH/H₂O (9:1; 3 mL). Nitrogen was bubbled through the solution



for 2 min and the vial was then sealed with a septum cap. The vial was placed in the microwave reactor and heated under microwave irradiation at 170 °C (for **4.3**) *or* 150 °C (for **4.5**) for 45 min, at a maximum pressure of 150 psi. After cooling to room temperature, the reaction mixture was filtered. The grey precipitate was washed with methanol, water, ethanol, and diethyl ether to give **4.15** as a grey solid (30 mg, 74%) and (38 mg, 83%), respectively. Crystals suitable for a single crystal X-ray diffraction study were grown from a chloroform solution of the complex. Mp > 270 °C. ¹H NMR (500 MHz, CDCl₃, 323K): δ 6.69 (dd, *J*_{H-H} 8.2, 1.1, 2H), 7.14 (d, *J*_{H-H} 8.3, 2H), 7.15 (t, *J*_{H-H} 6.8, 1H), 7.26 (d, *J*_{H-H} 7.8, 2H), 7.7 (t, *J*_{H-H} 7.5, 2H), 10.82 (s, OH, 2H). Sample was insufficiently soluble for ¹³C{¹H}; therefore, selective ¹³C data was acquired by an HSQC experiment. HSQC (125 MHz, CDCl₃, 298 K): δ 110.5 (CH), 112.9 (CH), 123.7 (CH), 124.7 (CH), 1401.3 (CH). IR (selected bands, cm⁻¹): 3024, 1616, 1572, 1484, 1426, 1272, 1205, 1163, 1003, 795, 743. TOFMS (ASAP): *m/z* 368.9868 [M-Cl]⁺ (C₁₆H₁₁N₂O₂¹⁰⁶Pd requires 368.9855).

5.4.16 Synthesis of [Pd(4,6-bis(2-pyridon-6-yl)*m*-xylene)Cl] (**4.16**)

4,6-bis(2-(6-methoxypyridonyl)*m*-xylene) (**4.4**) (30 mg, 0.093 mmol) *or* 4,6-bis(2-pyridon-6-yl)*m*-xylene (**4.6**) (29.23 mg, 0.1 mmol) and Na₂[PdCl₄] (1 eq.) were placed in a microwave vial along with a mixture of AcOH/H₂O (9:1; 3 mL). Nitrogen was bubbled through

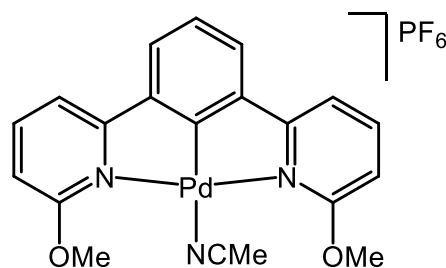


the solution for 2 min and the vial was then sealed with a septum cap. The vial was placed in the microwave reactor and heated under microwave irradiation at 170 °C (for **4.4**) *or* 150 °C (for **4.6**) for 45 min, at a maximum pressure of 150 psi. After cooling to room temperature, the reaction mixture was filtered. The grey precipitate was washed with methanol, water, ethanol, and diethyl ether to give **4.16** as a grey solid (27 mg, 66%) and (34 mg, 78%), respectively. Mp > 270 °C. ¹H NMR (500 MHz, CDCl₃, 298 K): δ 2.55 (s, Me, 6H), 6.66 (d, *J*_{H-H} 8.8, 2H), 6.79 (s, 1H), 7.29 (d, *J*_{H-H} 7.9, 2H), 7.68 (t, *J*_{H-H} 8.2, 2H),

11.04 (s, OH, 2H). Sample was insufficiently soluble for $^{13}\text{C}\{^1\text{H}\}$; therefore, selective ^{13}C data was acquired by an HSQC experiment. HSQC (125 MHz, CDCl_3 , 298 K): δ 22.8 (Me), 110.9 (CH), 113.4 (CH), 133.7 (CH), 140.7 (CH). IR (selected bands, cm^{-1}): 3013, 1619, 1571, 1488, 1407, 1216, 1157, 770. TOFMS (ASAP): m/z 397.0187 $[\text{M}-\text{Cl}]^+$ ($\text{C}_{18}\text{H}_{15}\text{N}_2\text{O}_2^{106}\text{Pd}$ requires 397.0168).

5.4.17 Synthesis of [Pd(1,3-bis(2-(6-methoxypyridyl)benzene))Cl] (4.17)

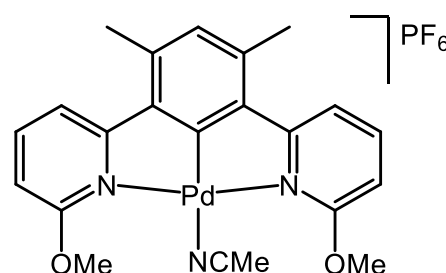
A small-sized Schlenk flask equipped with a magnetic stir bar was evacuated and backfilled with nitrogen and loaded with $[\text{Pd}(1,3\text{-bis}(2\text{-(6-methoxypyridyl)benzene))Cl}]$ (**4.13**) (30 mg, 0.1 mmol), AgPF_6 (25.3 mg, 0.1 mmol) and MeCN (10 mL). The reaction mixture was stirred at room



temperature for 12 h, at which point the suspension was allowed to settle and the solution was transferred by cannula filtration into a round bottom flask. All volatiles were removed under reduced pressure to afford **4.17** (42 mg, 72%) as a dark brown solid. Mp: 135 °C (decomp.). ^1H NMR (400 MHz, $\text{DMSO}-d_6$, 298 K): δ 1.98, (s, $\underline{\text{MeCN}}$, 3H), 3.92 (s, OMe, 3H), 7.05 (d, $J_{\text{H-H}}$ 8.5, 2H), 7.19 (t, $J_{\text{H-H}}$ 7.6, 1H), 7.57 (d, $J_{\text{H-H}}$ 7.7, 2H), 7.62 (d, $J_{\text{H-H}}$ 7.6, 2H), 8.07 (t, $J_{\text{H-H}}$ 7.9, 2H). Sample was insufficiently soluble for $^{13}\text{C}\{^1\text{H}\}$; therefore, selective ^{13}C data was acquired by an HMQC experiment. HMQC NMR (100 MHz, $\text{DMSO}-d_6$, 298 K): δ -0.3 ($\underline{\text{MeCN}}$), 57.0 (OMe), 107.9 (CH), 112.8 (CH), 125.3 (CH), 126.2 (CH), 144.0 (CH). ^{31}P NMR (162 MHz, $\text{DMSO}-d_6$, 298 K): δ -144.1 (sept, $^1J_{\text{P-F}}$ 712, PF_6). ^{19}F NMR (376 MHz, $\text{DMSO}-d_6$, 298 K): δ -70.14 (d, $^1J_{\text{F-P}}$ 710, PF_6). IR (selected bands, cm^{-1}): 1610, 1571, 1485, 1471, 1282, 1179, 1094, 1050, 998, 833, 775, 722. MS (ES): m/z 397 $[\text{M}-\text{MeCN}]^+$, 145 $[\text{PF}_6]^-$. TOFMS (ES): m/z 397.0181 $[\text{M}-\text{MeCN}]^+$ ($\text{C}_{18}\text{H}_{15}\text{N}_2\text{O}_2^{106}\text{Pd}$ requires 397.0168).

5.4.18 Synthesis of [Pd(4,6-bis(2-(6-methoxypyridonyl)*m*-xylene))Cl] (4.18)

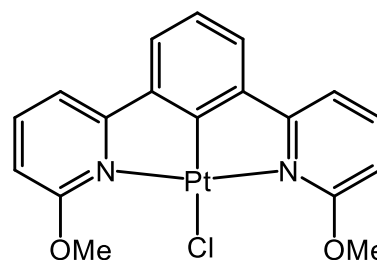
Based on the procedure described for **4.17**, using $[\text{Pd}(4,6\text{-bis}(2\text{-(6-methoxypyridonyl)}m\text{-xylene))Cl}]$ (**4.14**) (45 mg, 0.065 mmol) and AgPF_6 (16.5 mg, 0.065 mmol) gave **4.18** as a brown solid (34 mg, 86%). Mp: 223-225 °C. ^1H NMR (400 MHz, $\text{DMSO}-d_6$, 298 K): δ 2.08, (s, $\underline{\text{MeCN}}$, 3H), 2.60 (Me, 3H), 4.01 (s, OMe, 3H), 6.99 (s, 1H), 7.16 (d, $J_{\text{H-H}}$ 9.1, 2H), 7.60 (d, $J_{\text{H-H}}$ 7.9, 2H), 8.14



(t, $J_{\text{H-H}}$ 8.5, 2H). Sample was insufficiently soluble for $^{13}\text{C}\{^1\text{H}\}$; therefore, selective ^{13}C data was acquired by an HMQC experiment. HMQC NMR (100 MHz, DMSO-*d*, 298 K): δ -0.6 (MeCN), 22.5 (Me), 57.3 (OMe), 107.0 (CH), 116.3 (CH), 133.8 (CH), 143.7 (CH). ^{31}P NMR (162 MHz, DMSO-*d*, 298 K): δ -144.1 (sept, $^1J_{\text{P-F}}$ 713, PF₆). ^{19}F NMR (376 MHz, DMSO-*d*, 298 K): δ -70.12 (d, $^1J_{\text{F-P}}$ 714, PF₆). IR (selected bands, cm⁻¹): 1481, 1460, 1274, 1106, 1029, 997, 829, 792, 721. MS (ES): m/z 425 [M-MeCN]⁺, 145 [PF₆]⁻. TOFMS (ES): m/z 425.0490 [M-MeCN]⁺ (C₂₀H₁₉N₂O₂¹⁰⁶Pd requires 425.0481).

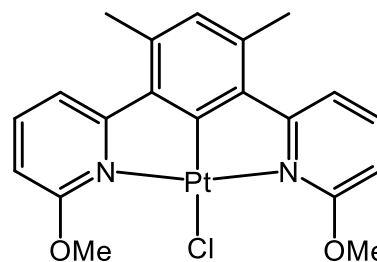
5.4.19 Synthesis of [Pt(1,3-bis(2-(6-methoxypyridyl)benzene))Cl] (4.19)

1,3-bis(2-(6-methoxypyridyl)benzene) (**4.3**) (25 mg, 0.085 mmol) and K₂[PtCl₄] (35.5 mg, 0.085, 1 eq.) were placed in a microwave vial along with a mixture of AcOH/H₂O (9:1; 3 mL). Nitrogen was bubbled through the solution for 2 min and the vial was then sealed with a septum cap. The vial was placed in the microwave reactor and heated under microwave irradiation at 95 °C for 45 min, at a maximum pressure of 150 psi. After cooling to room temperature, the reaction mixture was filtered. The brown precipitate was washed with methanol, water, ethanol, and diethyl ether to give **4.19** as a dark brown solid (11.5 mg, 26%). Mp: > 270 °C. ^1H NMR (400 MHz, DMSO-*d*, 298 K): δ 4.00 (s, OMe, 6H), 7.12 (d, $J_{\text{H-H}}$ 8.4, 2H), 7.25 (t, $J_{\text{H-H}}$ 7.8, 1H), 7.64 (d, $J_{\text{H-H}}$ 7.7, 2H), 7.70 (d, $J_{\text{H-H}}$ 7.1, 2H), 8.14 (t, $J_{\text{H-H}}$ 8.0, 2H). Sample was insufficiently soluble for $^{13}\text{C}\{^1\text{H}\}$; therefore, selective ^{13}C data was acquired by HSQC and HMBC experiments. HSQC (125 MHz, DMSO-*d*, 298 K): δ 57.1 (OMe), 107.2 (CH), 112.2 (CH), 123.4 (CH), 125.1 (CH), 143.1 (CH). HMBC (125 MHz, DMSO-*d*, 298 K): δ 141.6 (C), 155.4 (C), 165.2 (C), 167.3 (C). IR (selected bands, cm⁻¹): 1612, 1654, 1483, 1430, 1281, 1098, 1030, 772. MS (ES): m/z 486 [M-Cl]⁺, 528 [(M-Cl)+MeCN]. TOFMS (ES): m/z 486.0783 [M-Cl]⁺ (C₁₈H₁₅N₂O₂¹⁹⁵Pt requires 486.0781).



5.4.20 Synthesis of [Pt(4,6-bis(2-(6-methoxypyridonyl)*m*-xylene))Cl] (4.20)

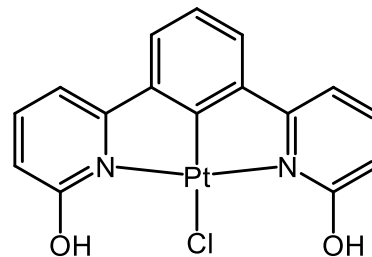
Based on the procedure described for **4.19** using 4,6-bis(2-(6-methoxypyridonyl)*m*-xylene) (**4.4**) (32 mg, 0.1 mmol) and K₂[PtCl₄] (41.5 mg, 0.1 mmol, 1 eq.) gave **4.20** as a greenish yellow solid (10.3 mg, 19%). Mp: > 270 °C. ^1H NMR (400 MHz, DMSO-*d*, 298 K): δ 2.60 (s, Me, 6H), 4.09 (s, OMe, 6H), 6.96 (s, 1H), 7.23 (d, $J_{\text{H-H}}$ 8.5, 2H), 7.60 (d, $J_{\text{H-H}}$ 7.9, 2H),



8.17 (d, $J_{\text{H-H}}$ 8.2, 2H). Sample was insufficiently soluble for $^{13}\text{C}\{^1\text{H}\}$; therefore, selective ^{13}C data was acquired by an HSQC experiment. HSQC (125 MHz, DMSO-*d*, 298 K): δ 22.1 (Me), 57.3 (OMe), 106.7 (CH), 116.2 (CH), 132.5 (CH), 144.0 (CH). IR (selected bands, cm^{-1}): 1601, 1566, 1482, 1437, 1317, 1272, 1033, 796, 755. MS (ES): m/z 514 [M-Cl] $^+$, 554 [(M-Cl)+MeCN]. TOFMS (ES): m/z 514.1086 [M-Cl] $^+$ ($\text{C}_{20}\text{H}_{19}\text{N}_2\text{O}_2^{195}\text{Pt}$ requires 514.1094).

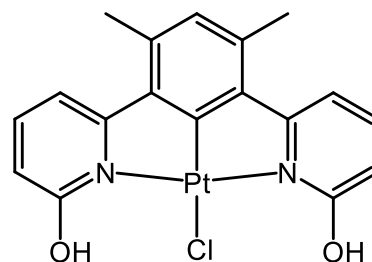
5.4.21 Synthesis of [Pt(1,3-bis(2-pyridon-6-yl)benzene)Cl] (4.21)

1,3-bis(2-(6-methoxypyridyl)benzene) (4.3) (29.23 mg, 0.1 mmol) *or* 1,3-bis(2-pyridon-6-yl)benzene (4.5) (26.5 mg, 0.1 mmol) and K_2PtCl_4 (0.1 mmol, 1 eq.) were placed in a microwave vial along with a mixture of AcOH/ H_2O (9:1; 3 mL). Nitrogen was bubbled through the solution for 2 min and the vial was then sealed with a septum cap. The vial was placed in the microwave reactor and heated under microwave irradiation at 170 °C (for 4.3) *or* 150 °C (for 4.5) for 45 min, at a maximum pressure of 150 psi. After cooling to room temperature, the reaction mixture was filtered. The yellow precipitate was washed with methanol, water, ethanol, and diethyl ether to give 4.21 as a yellow solid (23 mg, 46%) and (35 mg, 71%), respectively. Mp: > 270 °C. ^1H NMR (500 MHz, DMSO-*d*, 298 K): δ 6.87 (d, $J_{\text{H-H}}$ 8.7, 2H), 7.26 (t, $J_{\text{H-H}}$ 7.6, 1H), 7.60 (m, 4H), 8.00 (t, $J_{\text{H-H}}$ 7.8, 2H), 11.29 (s, OH, 2H). Sample was insufficiently soluble for $^{13}\text{C}\{^1\text{H}\}$; therefore, selective ^{13}C data was acquired by an HSQC experiment. HSQC (125 MHz, DMSO-*d*, 298 K): δ 111.6 (CH), 111.8 (CH), 123.9 (CH), 124.2 (CH), 143.1 (CH). IR (selected bands, cm^{-1}): 2977, 1621, 1570, 1491, 1406, 1206, 1156, 791, 769. TOFMS (ASAP): m/z 458.0468 [M-Cl] $^+$ ($\text{C}_{16}\text{H}_{11}\text{N}_2\text{O}_2^{195}\text{Pt}$ requires 458.0468).



5.4.22 Synthesis of [Pt(4,6-bis(2-pyridon-6-yl)*m*-xylene)Cl] (4.22)

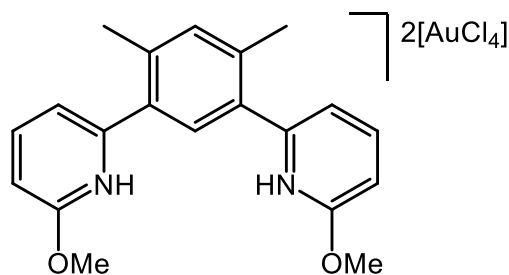
4,6-bis(2-(6-methoxypyridonyl)*m*-xylene) (4.4) (40 mg, 0.125 mmol) *or* 4,6-bis(2-pyridon-6-yl)*m*-xylene (4.6) (25 mg, 0.086 mmol) and K_2PtCl_4 (1 eq.) were placed in a microwave vial along with a mixture of AcOH/ H_2O (9:1; 3 mL). Nitrogen was bubbled through the solution for 2 min and the vial was then sealed with a septum cap. The vial was placed in the microwave reactor and heated under microwave irradiation at 170 °C (for 4.4) *or* 150 °C (for 4.6) for 45 min, at a maximum pressure of 150 psi. After cooling to room



temperature, the reaction mixture was filtered. The yellow precipitate was washed with methanol, water, ethanol, and diethyl ether to give **4.22** as a yellow solid (27 mg, 41%) and (28 mg, 62%), respectively. Mp: > 270 °C. ^1H NMR (400 MHz, DMSO-*d*, 298 K): δ 2.55 (s, Me, 6H), 6.80 (d, $J_{\text{H-H}}$ 8.2, 2H), 6.90 (s, 1H), 7.43 (d, $J_{\text{H-H}}$ 7.7, 2H), 7.94 (t, $J_{\text{H-H}}$ 8.2, 2H), 11.34 (s, OH, 2H). Sample was insufficiently soluble for $^{13}\text{C}\{^1\text{H}\}$; therefore, selective ^{13}C data was acquired by HSQC and HMBC experiments. HSQC NMR (125 MHz, DMSO-*d*, 298 K): δ 22.2 (Me), 110.8 (CH), 114.5 (CH), 132.6 (CH), 142.4 (CH). HMBC NMR (125 MHz, DMSO-*d*, 298 K): δ 136.4 (C), 137.2 (C), 162.9 (C), 164.0 (C), 166.7 (C). IR (selected bands, cm^{-1}): 3054, 1620, 1573, 1488, 1201, 1164, 795, 745. TOFMS (ASAP): m/z 486.0783 $[\text{M-Cl}]^+$ ($\text{C}_{18}\text{H}_{15}\text{N}_2\text{O}_2^{195}\text{Pt}$ requires 486.0781).

5.4.23 Synthesis of [4,6-bis(2-(6-methoxyppyridonyl)*m*-xylene)($\kappa^1\text{-H}$) $_2$][AuCl $_4$] $_2$ (**4.23**)

H[AuCl $_4$] (43 mg, 0.11 mmol, 2 eq.), dissolved in AcOH (1 mL), was added to 4,6-bis(2-(6-methoxyppyridonyl)*m*-xylene **4.4** (17.5 mg, 0.055 mmol) in AcOH (1 mL). The reaction mixture was then stirred at room temperature for 5 min after which the solvent

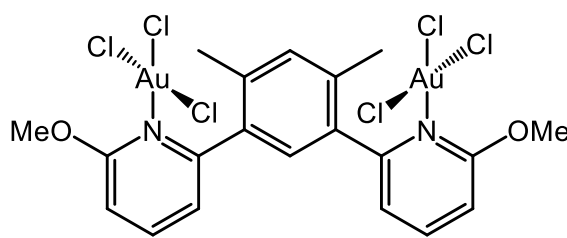


was removed leaving behind a yellow solid which was then washed with Et $_2$ O and water and dried under reduced pressure to give **4.23** as a yellow powder (45 mg, 88%). Crystals suitable for a single crystal X-ray diffraction study were grown from a MeOH solution of the complex. Mp: 214-216 °C. ^1H NMR (400 MHz, CD $_3$ CN, 298 K): δ 2.42 (s, Me, 3H), 4.23 (s, OMe, 3H), 7.46 (d, $J_{\text{H-H}}$ 8.1, 1H), 7.48 (s, 1H), 7.50 (d, $J_{\text{H-H}}$ 7.7, 1H), 7.52 (s, 1H), 8.50 (t, $J_{\text{H-H}}$ 8.0, 1H), 12.89 (br s, 1H, NH). $^{13}\text{C}\{^1\text{H}\}$ NMR (100 MHz, CD $_3$ CN, 298 K): δ 18.7 (Me), 58.6 (OMe), 109.4 (CH), 119.6 (CH), 128.6 (C), 131.3 (CH), 133.7 (CH), 140.1 (C), 148.8 (C), 149.3 (CH), 161.4 (C). IR (selected bands, cm^{-1}): 3100, 1617, 1540, 1333, 1288, 1280, 1186, 1018, 809. MS (ES): m/z 321 $[\text{M}]^+$, 267 $[\text{AuCl}_2]^-$. TOFMS (ASAP): m/z 321.1602 $[\text{M}]^+$ ($\text{C}_{20}\text{H}_{22}\text{N}_2\text{O}_2$ requires 321.1681).

5.4.24 Synthesis of [$\kappa^1\text{-N,N}$ -(4,6-bis(2-(6-methoxyppyridonyl)*m*-xylene))](AuCl $_3$) $_2$] (**4.24**)

2.3 mg (0.027 mmol, 3 eq.) of NaHCO $_3$ were added under vigorous stirring to a solution of **4.23** (9 mg, 0.009 mmol) in THF (2 mL) and left 2 hours to stir at room

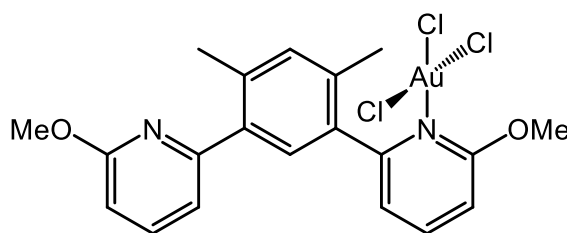
temperature. The corresponding solution was evaporated and the crude solid was washed with Et₂O and water to give **4.24** as a yellow solid (6 mg, 72%). Crystals



suitable for a single crystal X-ray diffraction study were grown from a dichloromethane solution of the complex layered with hexane. Mp: 203-205 °C. ¹H NMR (400 MHz, CD₃CN, 298 K): δ 2.32 (s, Me, 3H), 4.26 (s, OMe, 3H), 7.42 (dd, *J*_{H-H} 8.6, 1.0, 1H), 7.48 (dd, *J*_{H-H} 7.2, 1.1, 1H), 7.52 (s, 1H), 8.10 (s, 1H), 8.31 (dd, *J*_{H-H} 8.6, 7.5, 1H). Sample was insufficiently soluble for ¹³C{¹H}; therefore, selective ¹³C data was acquired by an HMQC experiment. HMQC NMR (100 MHz, CD₃CN, 298 K): δ 19.7 (Me), 58.6 (OMe), 109.9 (CH), 121.9 (CH), 133.2 (CH), 133.3 (CH), 145.8 (CH). IR (selected bands, cm⁻¹): 1571, 1478, 1433, 1323, 1264, 1246, 1075, 798. MS (ES): *m/z* 321 [L]⁺, 515 [L+Au]⁺, 267 [AuCl₂]⁻, 339 [AuCl₄]⁻, 609 [Au₂Cl₆]. TOFMS (ES): *m/z* 925.8959 [M]⁺ (C₂₀H₂₀¹⁹⁷Au₂Cl₆N₂O₂ requires 925.8957).

5.4.25 Synthesis of [κ^1 -*N*-(4,6-bis(2-(6-methoxypyridonyl)*m*-xylene))](AuCl₃)] (**4.25**)

K[AuCl₄] (23.5 mg, 0.062 mmol, 2 eq.), dissolved in water (1 mL), was added to 4,6-bis(2-(6-methoxypyridonyl) *m*-xylene (**4.4**) (10 mg, 0.031 mmol) in MeCN (1 mL). The reaction mixture was



then left to stir at room temperature for 20 h to give a yellow precipitate which was filtered, washed with Et₂O and water and dried under reduced pressure to yield 16.5 mg (89%) of **4.25** as a yellow powder. Crystals suitable for a single crystal X-ray diffraction study were grown from a dichloromethane solution of the complex layered with hexane. Mp: 183-185 °C. ¹H NMR (400 MHz, CDCl₃, 298 K): δ 2.24 (s, Me, 3H), 2.52 (s, Me, 3H), 3.95 (s, OMe, 3H), 4.26 (s, OMe, 3H), 6.68 (d, *J*_{H-H} 8.2, 1H), 7.11 (d, *J*_{H-H} 8.4, 1H), 7.24 (d, *J*_{H-H} 7.4, 1H), 7.27 (s, 1H), 7.30 (d, *J*_{H-H} 7.3, 1H) 7.66 (t, *J*_{H-H} 8.0, 1H), 7.81 (s, 1H), 8.07 (t, *J*_{H-H} 8.0, 1H). ¹³C{¹H} NMR (100 MHz, CDCl₃, 298 K, 298 K): δ 20.2 (Me), 20.9 (Me), 53.5 (OMe), 58.2 (OMe), 107.7 (CH), 109.1 (CH), 117.4 (CH), 122.0 (CH), 131.3 (CH), 133.5 (C), 134.0 (CH), 136.1 (C), 138.0 (C), 139.4 (CH), 139.8 (C), 144.1 (CH), 156.4 (C), 158.3 (C), 161.9 (C), 163.0 (C). IR (selected bands, cm⁻¹): 1574, 1485, 1462, 1434, 1313, 1250, 1051, 978, 803. MS (ES): *m/z* 321 [L]⁺, 623 [M]⁺, 267 [AuCl₂]⁻

, 339 [AuCl₄]⁻. TOFMS (ES): m/z 623.0334 [M]⁺ (C₂₀H₂₀¹⁹⁷AuCl₃N₂O₂ requires 623.0256), 645.0162 [M+Na]⁺ (C₂₀H₂₀¹⁹⁷AuCl₃N₂O₂Na requires 645.0154).

References

1. G. Sheldrick, *Bruker AXS Inc., Madison, Wisconsin, USA*, 2000.
2. T. Nguyen, M. A. Wicki and V. Snieckus, *J. Org. Chem.*, 2004, **69**, 7816.
3. C. Zhao, D. Xue, Z. Jia, C. Wang and J. Xiao, *Synlett*, 2014, **25**, 1577.
4. S. Bruns, V. Sinnwell and J. Voss, *Magn. Reson. Chem.*, 2003, **41**, 269.
5. G. Kerric, E. Le Grogneec, F. Zammattio, M. Paris and J. Quintard, *J. Organomet. Chem.*, 2010, **695**, 103.
6. N. Liu and Z. Wang, *J. Org. Chem.*, 2011, **76**, 10031.
7. L. Ackermann, H. K. Potukuchi, A. R. Kapdi and C. Schulzke, *Chem. A Eur. J.*, 2010, **16**, 3300.
8. D. X. Yang, S. L. Colletti, K. Wu, M. Song, G. Y. Li and H. C. Shen, *Org. Lett.*, 2008, **11**, 381.
9. C. L. Smith, C. Hirschhäuser, G. K. Malcolm, D. J. Nasrallah and T. Gallagher, *Synlett*, 2014, **25**, 1904.
10. R. Bodalski and A. Katritzky, *J. Chem. Soc. B: Phys. Org.*, 1968, 831.
11. T. Honda, R. Takahashi and H. Namiki, *J. Org. Chem.*, 2005, **70**, 499.
12. M. C. Bonifacio, C. R. Robertson, J. Jung and B. T. King, *J. Org. Chem.*, 2005, **70**, 8522.
13. B. Avitia, E. MacIntosh, S. Muhia and E. Kelson, *Tetrahedron Lett.*, 2011, **52**, 1631.

Appendix

Crystal Data and Structure Refinements

Table A1: Crystal Data and Structure Refinement for **2.10**, **2.11**, **2.12**, **2.13** and **2.14**

	2.10	2.11	2.12	2.13	2.14
Identification code	15047	15085	15089	15041	15100
Empirical formula	C168 H158 N12 O37 Pd12	C30 H30 N2 O6 Pd2	C184 H154 Cl12 F36 N12 O39 Pd12	C28 H24 F2 N2 O6 Pd2	C30 H32 N2 O7 Pd2
Formula weight	4213.86	727.36	5543.39	735.29	745.38
Temperature	150(2) K	150(2) K	150(2) K	150(2) K	150(2) K
Wavelength	0.71073 Å	0.71073 Å	0.71073 Å	0.71073 Å	0.71073 Å
Crystal system	Orthorhombic	Orthorhombic	Orthorhombic	Orthorhombic	Tetragonal
Space group	Pbcn	Pbcn	Pbcn	Pbcn	I4(1)/a
Unit cell dimensions	a = 24.139(8) Å b = 15.258(5) Å c = 21.504(7) Å $\alpha = 90^\circ$ $\beta = 90^\circ$ $\gamma = 90^\circ$	a = 23.615(3) Å b = 14.849(2) Å c = 23.814(3) Å $\alpha = 90^\circ$ $\beta = 90^\circ$ $\gamma = 90^\circ$	a = 23.71(11) Å b = 14.625(7) Å c = 29.206(14) Å $\alpha = 90^\circ$ $\beta = 90^\circ$ $\gamma = 90^\circ$	a = 23.648(3) Å b = 15.128(2) Å c = 22.311(3) Å $\alpha = 90^\circ$ $\beta = 90^\circ$ $\gamma = 90^\circ$	a = 13.625(2) Å b = 13.625(2) Å c = 29.964(5) Å $\alpha = 90^\circ$ $\beta = 90^\circ$ $\gamma = 90^\circ$
Volume	7920(5) Å ³	8351(2) Å ³	10129(8) Å ³	7981.9(19) Å ³	5562.8(16) Å ³
Z	2	12	2	12	8
Density (calculated)	1.767 Mg/m ³	1.736 Mg/m ³	1.818 Mg/m ³	1.836 Mg/m ³	1.780 Mg/m ³
Absorption coefficient	1.409 mm ⁻¹	1.339 mm ⁻¹	1.304 mm ⁻¹	1.412 mm ⁻¹	1.345 mm ⁻¹
F(000)	4196	4368	5468	4368	2992
Crystal size	0.34 x 0.08 x 0.03 mm ³	0.19 x 0.12 x 0.03 mm ³	0.43 x 0.14 x 0.04 mm ³	0.20 x 0.05 x 0.03 mm ³	0.21 x 0.15 x 0.10 mm ³
Theta range for data collection	1.58 to 26.00°	1.62 to 26.00°	1.39 to 26.00°	1.60 to 26.00°	1.64 to 25.99°
Index ranges	-29<=h<=29, -18<=k<=18, -26<=l<=26	-29<=h<=29, -18<=k<=18, -29<=l<=29	-29<=h<=29, -18<=k<=18, -36<=l<=36	-28<=h<=29, -18<=k<=18, -27<=l<=27	-16<=h<=16, -16<=k<=16, -36<=l<=36
Reflections collected	59363	62520	73592	60060	21582
Independent reflections	7783 [R(int) = 0.3130]	8214 [R(int) = 0.1851]	9959 [R(int) = 0.1219]	7853 [R(int) = 0.2616]	2739 [R(int) = 0.0658]
Completeness to theta = 26.00°	100.0 %	100.0 %	100.0 %	99.9 %	100.0 %
Absorption correction	Empirical	Empirical	Empirical	Empirical	Empirical
Max. and min. transmission	0.831 and 0.519	0.831 and 0.702	0.831 and 0.561	0.831 and 0.664	0.831 and 0.626
Refinement method	Full-matrix least-squares on F ²	Full-matrix least-squares on F ²	Full-matrix least-squares on F ²	Full-matrix least-squares on F ²	Full-matrix least-squares on F ²
Data / restraints / parameters	7783 / 3 / 529	8214 / 0 / 550	9959 / 32 / 700	7853 / 0 / 547	2739 / 0 / 184
Goodness-of-fit on F²	0.870	0.886	0.988	0.781	0.989
Final R indices [I>2sigma(I)]	R1 = 0.0790, wR2 = 0.1259	R1 = 0.0552, wR2 = 0.0777	R1 = 0.0523, wR2 = 0.1072	R1 = 0.0604, wR2 = 0.0783	R1 = 0.0267, wR2 = 0.0648
R indices (all data)	R1 = 0.2088, wR2 = 0.1627	R1 = 0.1207, wR2 = 0.0908	R1 = 0.0903, wR2 = 0.1185	R1 = 0.1733, wR2 = 0.1035	R1 = 0.0337, wR2 = 0.0668
Largest diff. peak and hole	1.047 and -1.533 e.Å ⁻³	0.735 and -0.743 e.Å ⁻³	0.888 and -0.589 e.Å ⁻³	0.544 and -0.708 e.Å ⁻³	0.596 and -0.373 e.Å ⁻³

Table A2: Crystal Data and Structure Refinement for **2.22**, **2.25**, **2.27**, **2.28** and **2.29**

	2.22	2.25	2.27	2.28	2.29
Identification code	15125	18001	18010	17014	17023
Empirical formula	C ₃₂ H ₂₇ F _N O ₃ P Pd	C ₃₂ H ₂₈ F ₆ N ₂ O P ₂ Pd	C ₃₃ H ₂₈ F ₃ N ₂ O ₄ P Pd S	C ₂₆ H ₃₀ Au ₂ Cl ₈ N ₂ O ₃	C ₁₃ H ₁₃ AuCl ₃ N O
Formula weight	629.92	738.90	743.00	1096.05	502.56
Temperature	150(2) K	150(2) K	150(2) K	150(2) K	150(2) K
Wavelength	0.71073 Å	0.71073 Å	0.71073 Å	0.71073 Å	0.71073 Å
Crystal system	Triclinic	Triclinic	Triclinic	Monoclinic	Monoclinic
Space group	P-1	P-1	P-1	P2/n	P2(1)/c
Unit cell dimensions	a = 9.601(3) Å b = 9.790(3) Å c = 14.907(5) Å α = 89.679(6)° β = 85.669(5)° γ = 77.343(5)°	a = 9.274(3) Å b = 10.735(4) Å c = 15.366(5) Å α = 85.100(6)° β = 88.465(6)° γ = 88.155(6)°	a = 9.152(2) Å b = 10.978(3) Å c = 15.539(4) Å α = 90.010(4)° β = 91.382(4)° γ = 90.829(4)°	a = 13.521(3) Å b = 7.0086(18) Å c = 18.362(5) Å α = 90° β = 107.467(4)° γ = 90°	a = 12.187(6) Å b = 7.903(4) Å c = 16.162(8) Å α = 90° β = 103.143(10)° γ = 90°
Volume	1363.2(8) Å ³	1523.0(9) Å ³	1560.6(7) Å ³	1659.8(7) Å ³	1515.9(12) Å ³
Z	2	2	2	2	4
Density (calculated)	1.535 Mg/m ³	1.611 Mg/m ³	1.581 Mg/m ³	2.193 Mg/m ³	2.202 Mg/m ³
Absorption coefficient	0.781 mm ⁻¹	0.781 mm ⁻¹	0.772 mm ⁻¹	9.505 mm ⁻¹	10.223 mm ⁻¹
F(000)	640	744	752	1036	944
Crystal size	0.24 x 0.10 x 0.04 mm ³	0.33 x 0.23 x 0.15 mm ³	0.48 x 0.30 x 0.12 mm ³	0.40 x 0.12 x 0.06 mm ³	0.12 x 0.08 x 0.03 mm ³
Theta range for data collection	2.13 to 26.00°	1.33 to 26.00°	1.86 to 26.00°	1.66 to 27.00°	1.72 to 26.00°
Index ranges	-11<=h<=11, -12<=k<=12, -18<=l<=18	-11<=h<=11, -13<=k<=13, -18<=l<=18	-11<=h<=11, -13<=k<=13, -19<=l<=18	-16<=h<=17, -8<=k<=8, -23<=l<=23	-14<=h<=15, -9<=k<=9, -19<=l<=19
Reflections collected	10637	11907	12095	13365	11398
Independent reflections	5281 [R(int) = 0.0436]	5897 [R(int) = 0.0616]	6055 [R(int) = 0.0296]	3624 [R(int) = 0.0690]	2969 [R(int) = 0.1764]
Completeness to theta = 26.00°	98.9 %	98.6 %	98.6 %	99.9 %	100.0 %
Absorption correction	Empirical	Empirical	Empirical	Empirical	Empirical
Max. and min. transmission	0.831 and 0.683	0.831 and 0.547	0.831 and 0.648	0.831 and 0.309	0.831 and 0.419
Refinement method	Full-matrix least-squares on F ²	Full-matrix least-squares on F ²	Full-matrix least-squares on F ²	Full-matrix least-squares on F ²	Full-matrix least-squares on F ²
Data / restraints / parameters	5281 / 0 / 354	5897 / 6 / 399	6055 / 0 / 408	3624 / 0 / 188	2969 / 145 / 174
Goodness-of-fit on F²	0.969	1.001	1.030	0.979	0.866
Final R indices [I>2σ(I)]	R1 = 0.0360, wR2 = 0.0746	R1 = 0.0536, wR2 = 0.1193	R1 = 0.0346, wR2 = 0.0851	R1 = 0.0360, wR2 = 0.0707	R1 = 0.0626, wR2 = 0.1029
R indices (all data)	R1 = 0.0433, wR2 = 0.0771	R1 = 0.0673, wR2 = 0.1250	R1 = 0.0396, wR2 = 0.0874	R1 = 0.0475, wR2 = 0.0736	R1 = 0.1196, wR2 = 0.1173
Largest diff. peak and hole	0.727 and -0.589 e.Å ⁻³	1.611 and -1.128 e.Å ⁻³	0.788 and -0.419 e.Å ⁻³	2.884 and -0.878 e.Å ⁻³	2.009 and -1.763 e.Å ⁻³

Table A3: Crystal Data and Structure Refinement for **3.3**, **3.8**, **3.12**, **3.13** and **3.16**

	3.3	3.8	3.12	3.13	3.16
Identification code	16041	15117	15149	16082	16022
Empirical formula	C12 H8 F3 N O	C28 H20 F6 N2 O6 Pd2	C48 H36 N4 O4 Pd4	C52 H28 Cl12 F12 N4 O4 Pd4	C48 H40 N4 O4 Pd2
Formula weight	239.19	807.26	1158.41	1851.78	949.64
Temperature	150(2) K	150(2) K	150(2) K	150(2) K	150(2) K
Wavelength	0.71073 Å	0.71073 Å	0.71073 Å	0.71073 Å	0.71073 Å
Crystal system	Orthorhombic	Triclinic	Monoclinic	Tetragonal	Monoclinic
Space group	Pbca	P-1	Cc	I4(1)/a	C2/c
Unit cell dimensions	a = 14.160(2) Å b = 6.5322(11) Å c = 21.825(3) Å $\alpha = 90^\circ$ $\beta = 90^\circ$ $\gamma = 90^\circ$	a = 9.880(3) Å b = 12.466(4) Å c = 12.942(4) Å $\alpha = 97.620(6)^\circ$ $\beta = 109.714(6)^\circ$ $\gamma = 109.828(6)^\circ$	a = 15.121(6) Å b = 15.114(6) Å c = 17.441(6) Å $\alpha = 90^\circ$ $\beta = 103.392(6)^\circ$ $\gamma = 90^\circ$	a = 21.544(3) Å b = 21.544(3) Å c = 12.697(3) Å $\alpha = 90^\circ$ $\beta = 90^\circ$ $\gamma = 90^\circ$	a = 17.344(13) Å b = 14.670(10) Å c = 16.650(12) Å $\alpha = 90^\circ$ $\beta = 105.830(15)^\circ$ $\gamma = 90^\circ$
Volume	2018.7(5) Å ³	1355.5(8) Å ³	3878(2) Å ³	5893.4(17) Å ³	4076(5) Å ³
Z	8	2	4	4	4
Density (calculated)	1.574 Mg/m ³	1.978 Mg/m ³	1.984 Mg/m ³	2.087 Mg/m ³	1.548 Mg/m ³
Absorption coefficient	0.139 mm ⁻¹	1.416 mm ⁻¹	1.880 mm ⁻¹	1.834 mm ⁻¹	0.933 mm ⁻¹
F(000)	976	792	2272	3584	1920
Crystal size	0.38 x 0.11 x 0.10 mm ³	0.16 x 0.11 x 0.03 mm ³	0.21 x 0.11 x 0.05 mm ³	0.24 x 0.17 x 0.14 mm ³	0.09 x 0.07 x 0.06 mm ³
Theta range for data collection	1.87 to 26.00°	1.74 to 26.00°	1.93 to 27.00°	1.86 to 27.00°	1.85 to 26.00°
Index ranges	-17<=h<=17, -8<=k<=8, -25<=l<=26	-12<=h<=12, -15<=k<=15, -15<=l<=15	-19<=h<=19, -19<=k<=19, -22<=l<=22	-27<=h<=27, -27<=k<=27, -16<=l<=16	-20<=h<=21, -18<=k<=18, -20<=l<=20
Reflections collected	14492	10676	15762	24015	15768
Independent reflections	1970 [R(int) = 0.0904]	5266 [R(int) = 0.0757]	8243 [R(int) = 0.0669]	3218 [R(int) = 0.0631]	3999 [R(int) = 0.2895]
Completeness to theta = 26.00°	99.7 %	98.8 %	99.6 %	100.0 %	99.9 %
Absorption correction	Empirical	Empirical	Empirical	Empirical	Empirical
Max. and min. transmission	0.962 and 0.547	0.831 and 0.636	0.831 and 0.515	0.831 and 0.623	0.831 and 0.516
Refinement method	Full-matrix least-squares on F ²	Full-matrix least-squares on F ²	Full-matrix least-squares on F ²	Full-matrix least-squares on F ²	Full-matrix least-squares on F ²
Data / restraints / parameters	1970 / 0 / 154	5266 / 0 / 399	8243 / 2 / 544	3218 / 1 / 217	3999 / 54 / 264
Goodness-of-fit on F²	0.924	0.965	0.952	0.996	0.708
Final R indices [I>2sigma(I)]	R1 = 0.0514, wR2 = 0.1150	R1 = 0.0620, wR2 = 0.1352	R1 = 0.0463, wR2 = 0.0936	R1 = 0.0372, wR2 = 0.0914	R1 = 0.0734, wR2 = 0.1272
R indices (all data)	R1 = 0.0843, wR2 = 0.1257	R1 = 0.0974, wR2 = 0.1477	R1 = 0.0570, wR2 = 0.0966	R1 = 0.0521, wR2 = 0.0962	R1 = 0.2318, wR2 = 0.1622
Largest diff. peak and hole	0.332 and -0.272 e.Å ⁻³	3.221 and -0.820 e.Å ⁻³	1.336 and -1.137 e.Å ⁻³	1.025 and -0.779 e.Å ⁻³	1.965 and -0.629 e.Å ⁻³

Table A4: Crystal Data and Structure Refinement for **3.17**, **3.23**, **3.24**, **3.25** and **3.26**

	3.17	3.23	3.24	3.25	3.26
Identification code	16042	16116	15144	16074	16119
Empirical formula	C ₄₈ H ₂₈ F ₁₂ N ₄ O ₄ Pd ₂	C ₂₁₆ H ₂₁₄ N ₂₄ O ₂₃ Pd ₁₂	C ₇₉ H ₈₂ Cl ₆ N ₈ O ₆ Pd ₄	C ₄₀ H ₃₆ Cl ₄ F ₆ N ₄ O ₃ Pd ₂	C ₁₅₁ H ₁₄₆ Cl ₆ F ₈ N ₁₆ O ₁₈ Pd ₈
Formula weight	1165.54	4790.91	1877.83	1089.33	3688.74
Temperature	150(2) K	150(2) K	150(2) K	150(2) K	150(2) K
Wavelength	0.71073 Å	0.71073 Å	0.71073 Å	0.71073 Å	0.71073 Å
Crystal system	Monoclinic	Monoclinic	Tetragonal	Tetragonal	Monoclinic
Space group	C2/c	P2(1)/n	P4(1)2(1)2	P4(1)2(1)2	P2(1)/n
Unit cell dimensions	a = 27.861(12) Å b = 16.017(7) Å c = 20.790(9) Å α = 90° β = 108.340(9)° γ = 90°	a = 12.811(3) Å b = 12.737(3) Å c = 29.904(8) Å α = 90° β = 97.407(5)° γ = 90°	a = 15.9341(19) Å b = 15.9341(19) Å c = 16.624(3) Å α = 90° β = 90° γ = 90°	a = 15.8758(12) Å b = 15.8758(12) Å c = 17.606(2) Å α = 90° β = 90° γ = 90°	a = 27.758(6) Å b = 8.3178(19) Å c = 32.580(8) Å α = 90° β = 94.497(5)° γ = 90°
Volume	8806(7) Å ³	4839(2) Å ³	4220.7(10) Å ³	4437.4(7) Å ³	7499(3) Å ³
Z	8	1	2	4	2
Density (calculated)	1.758 Mg/m ³	1.644 Mg/m ³	1.478 Mg/m ³	1.631 Mg/m ³	1.634 Mg/m ³
Absorption coefficient	0.919 mm ⁻¹	1.161 mm ⁻¹	1.081 mm ⁻¹	1.118 mm ⁻¹	1.122 mm ⁻¹
F(000)	4608	2414	1892	2168	3700
Crystal size	0.11 x 0.09 x 0.05 mm ³	0.13 x 0.12 x 0.06 mm ³	0.36 x 0.28 x 0.24 mm ³	0.17 x 0.13 x 0.08 mm ³	0.37 x 0.10 x 0.02 mm ³
Theta range for data collection	1.49 to 26.00°	1.37 to 26.00°	1.77 to 26.99°	1.73 to 25.99°	1.47 to 26.00°
Index ranges	-34 ≤ h ≤ 34, -19 ≤ k ≤ 19, -25 ≤ l ≤ 25	-15 ≤ h ≤ 15, -15 ≤ k ≤ 15, -36 ≤ l ≤ 36	-20 ≤ h ≤ 20, -20 ≤ k ≤ 20, -21 ≤ l ≤ 21	-19 ≤ h ≤ 19, -19 ≤ k ≤ 19, -21 ≤ l ≤ 21	-33 ≤ h ≤ 34, -10 ≤ k ≤ 10, -39 ≤ l ≤ 40
Reflections collected	34022	36984	35330	35117	57004
Independent reflections	8654 [R(int) = 0.3761]	9494 [R(int) = 0.1740]	4611 [R(int) = 0.0453]	4370 [R(int) = 0.1343]	14738 [R(int) = 0.2321]
Completeness to theta = 26.00°	100.0 %	99.9 %	99.9 %	100.0 %	99.9 %
Absorption correction	Empirical	Empirical	Empirical	Empirical	Empirical
Max. and min. transmission	0.831 and 0.341	0.831 and 0.671	0.831 and 0.698	0.831 and 0.624	0.831 and 0.611
Refinement method	Full-matrix least-squares on F ²	Full-matrix least-squares on F ²	Full-matrix least-squares on F ²	Full-matrix least-squares on F ²	Full-matrix least-squares on F ²
Data / restraints / parameters	8654 / 642 / 633	9494 / 9 / 466	4611 / 1 / 243	4370 / 2 / 242	14738 / 16 / 955
Goodness-of-fit on F²	0.709	0.841	1.048	0.819	0.754
Final R indices [I > 2σ(I)]	R1 = 0.0755, wR2 = 0.1009	R1 = 0.0630, wR2 = 0.0908	R1 = 0.0299, wR2 = 0.0808	R1 = 0.0422, wR2 = 0.0813	R1 = 0.0677, wR2 = 0.1042
R indices (all data)	R1 = 0.3041, wR2 = 0.1416	R1 = 0.1586, wR2 = 0.1090	R1 = 0.0343, wR2 = 0.0823	R1 = 0.0720, wR2 = 0.0867	R1 = 0.1734, wR2 = 0.1315
Largest diff. peak and hole	0.787 and -0.757 e.Å ⁻³	1.019 and -0.727 e.Å ⁻³	0.658 and -0.266 e.Å ⁻³	0.399 and -0.371 e.Å ⁻³	0.990 and -1.459 e.Å ⁻³

Table A5: Crystal Data and Structure Refinement for **3.29**, **3.30**, **3.31**, **3.32b** and **3.33a**

	3.29	3.30	3.31	3.32b	3.33a
Identification code	16112	16122	16125	17116	17105
Empirical formula	C ₃₂ H ₂₅ F ₃ N ₃ O ₃ P Pd	C ₃₃ H ₂₉ Cl ₄ F ₃ N ₃ O ₃ P Pd	C ₃₀ H ₂₃ F ₃ N ₃ O ₂ P Pd	C ₂₉ H ₂₄ Cl ₃ N ₃ O ₂ Pd ₂	C ₁₉ H ₁₉ Cl ₂ N ₂ O Pd
Formula weight	665.90	785.74	623.86	694.76	433.21
Temperature	150(2) K	150(2) K	150(2) K	150(2) K	150(2) K
Wavelength	0.71073 Å	0.71073 Å	0.71073 Å	0.71073 Å	0.71073 Å
Crystal system	Monoclinic	Triclinic	Monoclinic	Monoclinic	Monoclinic
Space group	P2(1)/c	P-1	P2(1)/n	P2(1)/c	P2(1)/n
Unit cell dimensions	a = 9.832(3) Å b = 25.206(7) Å c = 11.789(3) Å α = 90° β = 104.428(5)° γ = 90°	a = 9.827(2) Å b = 12.534(3) Å c = 14.051(3) Å α = 95.448(4)° β = 99.091(4)° γ = 110.698(3)°	a = 10.655(8) Å b = 18.540(13) Å c = 13.793(10) Å α = 90° β = 112.721(9)° γ = 90°	a = 10.892(2) Å b = 21.388(4) Å c = 11.221(2) Å α = 90° β = 102.861(4)° γ = 90°	a = 9.7957(15) Å b = 18.712(3) Å c = 19.203(3) Å α = 90° β = 92.671(3)° γ = 90°
Volume	2829.5(13) Å ³	1577.1(6) Å ³	2513(3) Å ³	2548.6(9) Å ³	3516.0(9) Å ³
Z	4	2	4	4	8
Density (calculated)	1.563 Mg/m ³	1.655 Mg/m ³	1.649 Mg/m ³	1.811 Mg/m ³	1.637 Mg/m ³
Absorption coefficient	0.767 mm ⁻¹	1.021 mm ⁻¹	0.854 mm ⁻¹	1.549 mm ⁻¹	1.215 mm ⁻¹
F(000)	1344	792	1256	1376	1744
Crystal size	0.34 x 0.11 x 0.04 mm ³	0.22 x 0.18 x 0.07 mm ³	0.22 x 0.16 x 0.06 mm ³	0.46 x 0.07 x 0.05 mm ³	0.14 x 0.13 x 0.06 mm ³
Theta range for data collection	1.62 to 27.00°	1.49 to 27.00°	1.94 to 25.99°	1.90 to 26.00°	1.52 to 26.00°
Index ranges	-12 ≤ h ≤ 12, -32 ≤ k ≤ 32, -15 ≤ l ≤ 14	-12 ≤ h ≤ 12, -16 ≤ k ≤ 16, -17 ≤ l ≤ 17	-13 ≤ h ≤ 13, -22 ≤ k ≤ 22, -17 ≤ l ≤ 16	-13 ≤ h ≤ 13, -25 ≤ k ≤ 26, -13 ≤ l ≤ 13	-12 ≤ h ≤ 12, -23 ≤ k ≤ 23, -23 ≤ l ≤ 23
Reflections collected	23631	13281	19253	19852	27136
Independent reflections	6158 [R(int) = 0.0982]	6742 [R(int) = 0.0430]	4918 [R(int) = 0.1082]	5003 [R(int) = 0.1238]	6887 [R(int) = 0.1282]
Completeness to theta = 26.00°	99.8 %	98.0 %	99.9 %	99.8 %	99.9 %
Absorption correction	Empirical	Empirical	Empirical	Empirical	Empirical
Max. and min. transmission	0.831 and 0.638	0.831 and 0.718	0.831 and 0.595	0.837 and 0.595	0.837 and 0.630
Refinement method	Full-matrix least-squares on F ²	Full-matrix least-squares on F ²	Full-matrix least-squares on F ²	Full-matrix least-squares on F ²	Full-matrix least-squares on F ²
Data / restraints / parameters	6158 / 0 / 372	6742 / 0 / 398	4918 / 2 / 343	5003 / 0 / 336	6887 / 0 / 438
Goodness-of-fit on F²	0.834	0.989	0.956	1.013	0.843
Final R indices [I > 2σ(I)]	R1 = 0.0451, wR2 = 0.0769	R1 = 0.0487, wR2 = 0.1188	R1 = 0.0461, wR2 = 0.0939	R1 = 0.0685, wR2 = 0.1473	R1 = 0.0527, wR2 = 0.0823
R indices (all data)	R1 = 0.0742, wR2 = 0.0826	R1 = 0.0663, wR2 = 0.1250	R1 = 0.0685, wR2 = 0.1000	R1 = 0.1174, wR2 = 0.1656	R1 = 0.1017, wR2 = 0.0942
Largest diff. peak and hole	0.926 and -0.647 e.Å ⁻³	1.196 and -0.955 e.Å ⁻³	1.004 and -1.069 e.Å ⁻³	1.427 and -1.466 e.Å ⁻³	0.629 and -0.803 e.Å ⁻³

Table A6: Crystal Data and Structure Refinement for **3.33b**, **3.34a/b**, **3.35**, **3.36** and **3.37**

	3.33b	3.34a/b	3.35	3.36	3.37
Identification code	17109	17066	17093	17084	17079
Empirical formula	C ₃₂ H ₃₂ Cl ₁ N ₃ O ₃ Pd ₂	C ₆₅ H ₆₈ Cl ₂ F ₉ N ₅ O ₃ Pd ₃	C ₂₉ H ₂₃ Cl ₁ N ₁ O ₁ P	C ₃₀ H ₂₅ Cl ₁ N ₁ O ₁ P	C ₃₀ H ₂₂ Cl ₁ F ₃ N O ₁ P Pd
Formula weight	754.86	1528.34	574.30	588.33	642.31
Temperature	150(2) K	150(2) K	150(2) K	150(2) K	150(2) K
Wavelength	0.71073 Å	0.71073 Å	0.71073 Å	0.71073 Å	0.71073 Å
Crystal system	Orthorhombic	Monoclinic	Monoclinic	Triclinic	Triclinic
Space group	Pbca	P2(1)/c	P2(1)/c	P-1	P-1
Unit cell dimensions	a = 22.577(4) Å b = 8.9363(15) Å c = 29.098(5) Å α = 90° β = 90° γ = 90°	a = 23.165(8) Å b = 16.647(6) Å c = 14.859(6) Å α = 90° β = 104.969(9)° γ = 90°	a = 9.300(6) Å b = 26.328(16) Å c = 19.889(12) Å α = 90° β = 90.736(11)° γ = 90°	a = 9.919(2) Å b = 11.441(2) Å c = 13.058(3) Å α = 75.381(3)° β = 68.558(3)° γ = 66.261(3)°	a = 10.092(3) Å b = 11.420(3) Å c = 13.353(4) Å α = 73.876(5)° β = 68.814(4)° γ = 64.955(4)°
Volume	5870.7(17) Å ³	5536(3) Å ³	4869(5) Å ³	1252.9(5) Å ³	1285.8(7) Å ³
Z	8	4	8	2	2
Density (calculated)	1.708 Mg/m ³	1.834 Mg/m ³	1.567 Mg/m ³	1.559 Mg/m ³	1.659 Mg/m ³
Absorption coefficient	1.355 mm ⁻¹	1.148 mm ⁻¹	0.961 mm ⁻¹	0.936 mm ⁻¹	0.935 mm ⁻¹
F(000)	3024	3080	2320	596	644
Crystal size	0.46 x 0.09 x 0.06 mm ³	0.43 x 0.18 x 0.03 mm ³	0.24 x 0.19 x 0.10 mm ³	0.41 x 0.27 x 0.20 mm ³	0.47 x 0.13 x 0.07 mm ³
Theta range for data collection	1.40 to 26.00°	1.52 to 26.00°	1.28 to 26.00°	1.69 to 26.00°	1.65 to 26.00°
Index ranges	-27<=h<=27, -10<=k<=10, -35<=l<=34	-28<=h<=28, -20<=k<=20, -18<=l<=18	-11<=h<=11, -32<=k<=32, -24<=l<=24	-12<=h<=12, -14<=k<=14, -16<=l<=16	-12<=h<=12, -14<=k<=14, -16<=l<=16
Reflections collected	43502	42633	37058	9666	9980
Independent reflections	5763 [R(int) = 0.1313]	10872 [R(int) = 0.3346]	9575 [R(int) = 0.2032]	4854 [R(int) = 0.0238]	4987 [R(int) = 0.0380]
Completeness to theta = 26.00°	100.0 %	99.9 %	99.9 %	98.6 %	98.5 %
Absorption correction	Empirical	Empirical	Empirical	Empirical	Empirical
Max. and min. transmission	0.831 and 0.652	0.831 and 0.260	0.831 and 0.262	0.831 and 0.614	0.831 and 0.522
Refinement method	Full-matrix least-squares on F ²	Full-matrix least-squares on F ²	Full-matrix least-squares on F ²	Full-matrix least-squares on F ²	Full-matrix least-squares on F ²
Data / restraints / parameters	5763 / 0 / 375	10872 / 643 / 654	9575 / 0 / 613	4854 / 0 / 317	4987 / 0 / 343
Goodness-of-fit on F²	0.930	0.819	0.986	1.058	1.014
Final R indices [I>2sigma(I)]	R1 = 0.0513, wR2 = 0.0899	R1 = 0.0996, wR2 = 0.2048	R1 = 0.0862, wR2 = 0.1502	R1 = 0.0288, wR2 = 0.0734	R1 = 0.0363, wR2 = 0.0851
R indices (all data)	R1 = 0.0904, wR2 = 0.1002	R1 = 0.2291, wR2 = 0.2540	R1 = 0.1849, wR2 = 0.1813	R1 = 0.0317, wR2 = 0.0747	R1 = 0.0421, wR2 = 0.0874
Largest diff. peak and hole	0.845 and -1.039 e.Å ⁻³	1.071 and -1.116 e.Å ⁻³	1.334 and -1.032 e.Å ⁻³	0.712 and -0.327 e.Å ⁻³	1.016 and -0.654 e.Å ⁻³

Table A7: Crystal Data and Structure Refinement for **3.45**, **3.47**, **3.50**, **3.52** and **3.53**

	3.45	3.47	3.50	3.52	3.53
Identification code	17131	17142	17103	17120	17133
Empirical formula	C ₃₀ H ₂₅ F ₂ N ₃ O ₃ P ₂ Pd	C ₉₁ H ₇₇ B ₃ Cl ₂ F ₆ N ₃ O ₆ P ₃ Pd ₃	C ₃₀ H ₂₂ F ₅ N ₃ O ₃ P ₂ Pd	C ₃₀ H ₂₂ B ₅ F ₅ N ₃ O ₂ P ₂ Pd	C ₃₃ H ₂₇ F ₆ N ₂ O ₅ P ₂ Pd ₂ S
Formula weight	653.85	1938.00	707.83	671.67	815.00
Temperature	150(2) K	150(2) K	150(2) K	150(2) K	150(2) K
Wavelength	0.71073 Å	0.71073 Å	0.71073 Å	0.71073 Å	0.71073 Å
Crystal system	Triclinic	Triclinic	Triclinic	Triclinic	Triclinic
Space group	P-1	P-1	P-1	P-1	P-1
Unit cell dimensions	a = 10.879(3) Å b = 11.322(3) Å c = 12.885(4) Å α = 75.313(4)° β = 87.316(4)° γ = 64.787(4)°	a = 12.116(3) Å b = 16.791(4) Å c = 20.905(5) Å α = 85.631(5)° β = 87.314(5)° γ = 79.731(4)°	a = 9.4012(17) Å b = 9.9015(18) Å c = 14.713(3) Å α = 95.212(3)° β = 91.273(3)° γ = 92.115(3)°	a = 10.5477(18) Å b = 10.9795(19) Å c = 12.522(2) Å α = 68.704(3)° β = 84.004(3)° γ = 80.389(3)°	a = 10.527(7) Å b = 12.594(8) Å c = 13.207(9) Å α = 72.755(12)° β = 80.016(12)° γ = 83.365(12)°
Volume	1385.6(7) Å ³	4170.2(18) Å ³	1362.5(4) Å ³	1330.7(4) Å ³	1643.1(19) Å ³
Z	2	2	2	2	2
Density (calculated)	1.567 Mg/m ³	1.543 Mg/m ³	1.725 Mg/m ³	1.676 Mg/m ³	1.647 Mg/m ³
Absorption coefficient	0.832 mm ⁻¹	0.832 mm ⁻¹	0.868 mm ⁻¹	0.823 mm ⁻¹	0.756 mm ⁻¹
F(000)	660	1956	708	672	820
Crystal size	0.38 x 0.27 x 0.18 mm ³	0.28 x 0.22 x 0.10 mm ³	0.31 x 0.20 x 0.08 mm ³	0.20 x 0.18 x 0.10 mm ³	0.47 x 0.35 x 0.05 mm ³
Theta range for data collection	1.64 to 26.00°	1.52 to 26.00°	2.07 to 27.00°	1.75 to 26.00°	1.63 to 26.00°
Index ranges	-13<=h<=13, -13<=k<=13, -15<=l<=15	-14<=h<=14, -20<=k<=20, -25<=l<=25	-11<=h<=11, -12<=k<=12, -18<=l<=18	-12<=h<=13, -13<=k<=13, -15<=l<=15	-12<=h<=12, -15<=k<=15, -16<=l<=16
Reflections collected	10742	32319	11401	10499	12825
Independent reflections	5353 [R(int) = 0.0455]	16132 [R(int) = 0.0816]	5826 [R(int) = 0.0376]	5171 [R(int) = 0.0426]	6355 [R(int) = 0.0853]
Completeness to theta = 26.00°	98.3 %	98.4 %	98.0 %	98.7 %	98.4 %
Absorption correction	Empirical	Empirical	Empirical	Empirical	Empirical
Max. and min. transmission	0.831 and 0.663	0.825 and 0.476	0.831 and 0.603	0.837 and 0.704	0.831 and 0.443
Refinement method	Full-matrix least-squares on F ²	Full-matrix least-squares on F ²	Full-matrix least-squares on F ²	Full-matrix least-squares on F ²	Full-matrix least-squares on F ²
Data / restraints / parameters	5353 / 0 / 353	16132 / 2 / 1057	5826 / 0 / 379	5171 / 1 / 370	6355 / 3 / 443
Goodness-of-fit on F²	1.015	0.909	1.009	0.973	1.001
Final R indices [I>2σ(I)]	R1 = 0.0430, wR2 = 0.0972	R1 = 0.0604, wR2 = 0.0976	R1 = 0.0347, wR2 = 0.0771	R1 = 0.0411, wR2 = 0.0846	R1 = 0.0734, wR2 = 0.1682
R indices (all data)	R1 = 0.0529, wR2 = 0.1008	R1 = 0.1055, wR2 = 0.1095	R1 = 0.0407, wR2 = 0.0797	R1 = 0.0513, wR2 = 0.0877	R1 = 0.1064, wR2 = 0.1812
Largest diff. peak and hole	1.456 and -0.826 e.Å ⁻³	1.263 and -0.847 e.Å ⁻³	0.649 and -0.574 e.Å ⁻³	0.739 and -0.551 e.Å ⁻³	2.362 and -1.808 e.Å ⁻³

Table A8: Crystal Data and Structure Refinement for **4.3, 4.4, 4.6, 4.7** and **4.8**

	4.3	4.4	4.6	4.7	4.8
Identification code	15070	16064	15145	15059	16158
Empirical formula	C18 H16 N2 O2	C20 H20 N2 O2	C19 H20 N2 O3	C60 H88 N4 O20 Pd4 S8	C40 H36 N4 O8 Pd2
Formula weight	292.33	320.38	324.37	1867.42	913.53
Temperature	150(2) K	150(2) K	150(2) K	150(2) K	150(2) K
Wavelength	0.71073 Å	0.71073 Å	0.71073 Å	0.71073 Å	0.71073 Å
Crystal system	Monoclinic	Monoclinic	Monoclinic	Tetragonal	Tetragonal
Space group	P2(1)/c	P2(1)/c	P2(1)/c	P43212	I4(1)/a
Unit cell dimensions	a = 14.975(2) Å b = 5.2759(8) Å c = 19.728(3) Å $\alpha = 90^\circ$ $\beta = 111.775(3)^\circ$ $\gamma = 90^\circ$	a = 11.905(4) Å b = 3.9067(13) Å c = 35.585(11) Å $\alpha = 90^\circ$ $\beta = 105.942(11)^\circ$ $\gamma = 90^\circ$	a = 15.174(2) Å b = 8.2104(13) Å c = 14.280(2) Å $\alpha = 90^\circ$ $\beta = 112.349(3)^\circ$ $\gamma = 90^\circ$	a = 14.236(3) Å b = 14.236(3) Å c = 32.572(8) Å $\alpha = 90^\circ$ $\beta = 90^\circ$ $\gamma = 90^\circ$	a = 29.555(4) Å b = 29.555(4) Å c = 19.150(4) Å $\alpha = 90^\circ$ $\beta = 90^\circ$ $\gamma = 90^\circ$
Volume	1447.4(4) Å ³	1591.4(9) Å ³	1645.4(5) Å ³	6601(3) Å ³	16727(5) Å ³
Z	4	4	4	4	16
Density (calculated)	1.341 Mg/m ³	1.337 Mg/m ³	1.309 Mg/m ³	1.879 Mg/m ³	1.451 Mg/m ³
Absorption coefficient	0.089 mm ⁻¹	0.087 mm ⁻¹	0.089 mm ⁻¹	1.404 mm ⁻¹	0.913 mm ⁻¹
F(000)	616	680	688	3792	7360
Crystal size	0.21 x 0.13 x 0.04 mm ³	0.29 x 0.07 x 0.04 mm ³	0.29 x 0.10 x 0.06 mm ³	0.12 x 0.08 x 0.07 mm ³	0.45 x 0.06 x 0.05 mm ³
Theta range for data collection	1.46 to 26.00°	1.78 to 25.00°	1.45 to 26.00°	1.56 to 25.99°	1.27 to 24.64°
Index ranges	-18<=h<=18, -6<=k<=6, -24<=l<=24	-14<=h<=14, -4<=k<=4, -41<=l<=42	-18<=h<=18, -10<=k<=10, -17<=l<=17	-17<=h<=17, -17<=k<=17, -40<=l<=40	-23<=h<=24, 0<=k<=34, 0<=l<=22
Reflections collected	10700	10599	12410	51742	7060
Independent reflections	2858 [R(int) = 0.0898]	2806 [R(int) = 0.1597]	3228 [R(int) = 0.0483]	6493 [R(int) = 0.1939]	7060 [R(int) = 0.0000]
Completeness to theta = 26.00°	100.0 %	100.0 %	99.9 %	100.0 %	99.8 %
Absorption correction	Empirical	Empirical	Empirical	Empirical	Empirical
Max. and min. transmission	0.981 and 0.609	0.981 and 0.426	0.981 and 0.718	0.831 and 0.642	0.831 and 0.439
Refinement method	Full-matrix least-squares on F ²	Full-matrix least-squares on F ²	Full-matrix least-squares on F ²	Full-matrix least-squares on F ²	Full-matrix least-squares on F ²
Data / restraints / parameters	2858 / 0 / 201	2806 / 0 / 221	3228 / 0 / 221	6493 / 271 / 294	7060 / 480 / 493
Goodness-of-fit on F²	0.970	0.773	0.961	0.914	0.773
Final R indices [I>2sigma(I)]	R1 = 0.0606, wR2 = 0.1258	R1 = 0.0595, wR2 = 0.1029	R1 = 0.0434, wR2 = 0.1034	R1 = 0.0591, wR2 = 0.1134	R1 = 0.0936, wR2 = 0.2278
R indices (all data)	R1 = 0.1047, wR2 = 0.1500	R1 = 0.1210, wR2 = 0.1171	R1 = 0.0600, wR2 = 0.1090	R1 = 0.1002, wR2 = 0.1229	R1 = 0.2948, wR2 = 0.2857
Largest diff. peak and hole	0.275 and -0.235 e.Å ⁻³	0.239 and -0.272 e.Å ⁻³	0.290 and -0.255 e.Å ⁻³	0.592 and -0.596 e.Å ⁻³	1.512 and -0.826 e.Å ⁻³

Table A9: Crystal Data and Structure Refinement for **4.9**, **4.10**, **4.12**, **4.14'** and **4.15**

	4.9	4.10	4.12	4.14'	4.15
Identification code	15113	15060	16059	17082	16114
Empirical formula	C ₂₉ H ₄₆ N ₂ O ₁₄ Pd ₂	C _{41.50} H _{33.50} Cl _{4.50} N ₄ O ₁₂ Pd ₄	C ₂₀ H ₁₉ Cl Hg N ₂ O ₂	C ₂₀ H ₂₁ Cl ₃ Hg N ₂ O ₃ Pd	C ₁₆ H ₁₁ Cl N ₂ O ₂ Pd
Formula weight	859.48	1365.35	555.41	750.73	405.12
Temperature	150(2) K	150(2) K	150(2) K	150(2) K	150(2) K
Wavelength	0.71073 Å	0.71073 Å	0.71073 Å	0.71073 Å	0.71073 Å
Crystal system	Monoclinic	Triclinic	Monoclinic	Triclinic	Monoclinic
Space group	P2(1)/n	P-1	P2(1)	P-1	P2(1)/c
Unit cell dimensions	a = 9.270(5) Å b = 18.657(10) Å c = 18.088(10) Å α = 90° β = 99.622(12)° γ = 90°	a = 12.1399(14) Å b = 12.2887(15) Å c = 14.6842(18) Å α = 101.191(2)° β = 92.400(3)° γ = 100.440(3)°	a = 11.284(3) Å b = 7.541(2) Å c = 12.231(4) Å α = 90° β = 115.394(5)° γ = 90°	a = 8.3632(18) Å b = 10.702(2) Å c = 13.359(3) Å α = 77.173(4)° β = 76.489(4)° γ = 73.056(4)°	a = 21.440(3) Å b = 7.1241(11) Å c = 21.233(3) Å α = 90° β = 119.494(2)° γ = 90°
Volume	3084(3) Å ³	2106.7(4) Å ³	940.2(5) Å ³	1096.8(4) Å ³	2822.9(7) Å ³
Z	4	2	2	2	8
Density (calculated)	1.851 Mg/m ³	2.152 Mg/m ³	1.962 Mg/m ³	2.273 Mg/m ³	1.906 Mg/m ³
Absorption coefficient	1.242 mm ⁻¹	2.037 mm ⁻¹	8.344 mm ⁻¹	8.201 mm ⁻¹	1.511 mm ⁻¹
F(000)	1752	1334	532	712	1600
Crystal size	0.13 x 0.11 x 0.03 mm ³	0.07 x 0.05 x 0.04 mm ³	0.29 x 0.23 x 0.02 mm ³	0.33 x 0.19 x 0.05 mm ³	0.17 x 0.07 x 0.06 mm ³
Theta range for data collection	2.18 to 26.00°	1.71 to 26.00°	1.84 to 26.00°	1.59 to 26.00°	1.09 to 26.00°
Index ranges	-11<=h<=11, -22<=k<=22, -22<=l<=22	-14<=h<=14, -15<=k<=15, -18<=l<=18	-13<=h<=13, -9<=k<=9, -15<=l<=15	-10<=h<=10, -12<=k<=13, -16<=l<=16	-25<=h<=26, -8<=k<=8, -26<=l<=26
Reflections collected	24096	16638	7375	8566	21247
Independent reflections	6070 [R(int) = 0.3311]	8167 [R(int) = 0.1149]	3631 [R(int) = 0.0984]	4264 [R(int) = 0.0580]	5533 [R(int) = 0.0967]
Completeness to theta = 26.00°	99.9 %	98.8 %	99.9 %	98.9 %	100.0 %
Absorption correction	Empirical	Empirical	Empirical	Empirical	Empirical
Max. and min. transmission	0.831 and 0.452	0.831 and 0.661	0.894 and 0.409	0.831 and 0.314	0.831 and 0.638
Refinement method	Full-matrix least-squares on F ²	Full-matrix least-squares on F ²	Full-matrix least-squares on F ²	Full-matrix least-squares on F ²	Full-matrix least-squares on F ²
Data / restraints / parameters	6070 / 319 / 360	8167 / 0 / 549	3631 / 98 / 240	4264 / 0 / 275	5533 / 0 / 397
Goodness-of-fit on F²	0.867	0.786	0.966	0.990	0.860
Final R indices [I>2σ(I)]	R1 = 0.0966, wR2 = 0.2015	R1 = 0.0641, wR2 = 0.1147	R1 = 0.0515, wR2 = 0.1043	R1 = 0.0433, wR2 = 0.0955	R1 = 0.0489, wR2 = 0.0751
R indices (all data)	R1 = 0.1952, wR2 = 0.2329	R1 = 0.1341, wR2 = 0.1284	R1 = 0.0629, wR2 = 0.1110	R1 = 0.0510, wR2 = 0.0987	R1 = 0.0946, wR2 = 0.0843
Largest diff. peak and hole	1.787 and -2.147 e.Å ⁻³	0.988 and -0.764 e.Å ⁻³	1.646 and -1.650 e.Å ⁻³	1.708 and -1.318 e.Å ⁻³	0.746 and -0.605 e.Å ⁻³

Table A10: Crystal Data and Structure Refinement for **4.23**, **4.24** and **4.25**

	4.23	4.24	4.25
Identification code	17044	17050	17057
Empirical formula	C ₂₂ H ₃₀ Au ₂ Cl ₈ N ₂ O ₄	C ₂₇ H _{37.50} Au ₂ Cl ₆ N ₂ O _{3.75}	C ₂₀ H ₂₀ AuCl ₃ N ₂ O ₂
Formula weight	1064.01	1056.72	623.70
Temperature	150(2) K	150(2) K	150(2) K
Wavelength	0.71073 Å	0.71073 Å	0.71073 Å
Crystal system	Monoclinic	Monoclinic	Monoclinic
Space group	P2(1)/m	C2/c	P2(1)/n
Unit cell dimensions	a = 8.056(6) Å b = 16.727(13) Å c = 12.022(9) Å α = 90° β = 99.450(16)° γ = 90°	a = 17.935(5) Å b = 13.073(4) Å c = 15.835(5) Å α = 90° β = 121.953(6)° γ = 90°	a = 7.220(2) Å b = 20.881(6) Å c = 14.454(4) Å α = 90° β = 99.118(6)° γ = 90°
Volume	1598(2) Å ³	3150.3(16) Å ³	2151.7(10) Å ³
Z	2	4	4
Density (calculated)	2.211 Mg/m ³	2.228 Mg/m ³	1.925 Mg/m ³
Absorption coefficient	9.870 mm ⁻¹	9.848 mm ⁻¹	7.228 mm ⁻¹
F(000)	1004	2014	1200
Crystal size	0.23 x 0.14 x 0.04 mm ³	0.24 x 0.06 x 0.04 mm ³	0.40 x 0.12 x 0.10 mm ³
Theta range for data collection	1.72 to 26.00°	2.05 to 26.00°	1.73 to 26.00°
Index ranges	-9<=h<=9, -20<=k<=20, -14<=l<=14	-22<=h<=22, -16<=k<=16, -19<=l<=19	-8<=h<=8, -25<=k<=25, -17<=l<=17
Reflections collected	12621	12170	16778
Independent reflections	3252 [R(int) = 0.2412]	3107 [R(int) = 0.1458]	4230 [R(int) = 0.2431]
Completeness to theta = 26.00°	99.9 %	99.9 %	100.0 %
Absorption correction	Empirical	Empirical	Empirical
Max. and min. transmission	0.831 and 0.182	0.850 and 0.465	0.831 and 0.388
Refinement method	Full-matrix least-squares on F ²	Full-matrix least-squares on F ²	Full-matrix least-squares on F ²
Data / restraints / parameters	3252 / 6 / 188	3107 / 146 / 166	4230 / 13 / 257
Goodness-of-fit on F²	0.992	0.922	0.909
Final R indices [I>2σ(I)]	R1 = 0.0901, wR2 = 0.2047	R1 = 0.0784, wR2 = 0.1760	R1 = 0.0777, wR2 = 0.1508
R indices (all data)	R1 = 0.1289, wR2 = 0.2235	R1 = 0.1372, wR2 = 0.1967	R1 = 0.1424, wR2 = 0.1712
Largest diff. peak and hole	7.413 and -2.720 e.Å ⁻³	1.925 and -2.587 e.Å ⁻³	3.149 and -2.047 e.Å ⁻³

Conferences and Symposia Attended

Internal Symposia

- University of Leicester Department of Chemistry: One day Symposium on Catalytic C-H Functionalization 23/01/2015: attended.
- University of Leicester Department of Chemistry Postgraduate Research day 06/2015: attended.
- RSC Organic Division Midlands Meeting 2017, University of Leicester 5/04/2017: attended.
- University of Leicester Department of Chemistry Postgraduate Research day 04/07/2017: Poster presentation.

External Symposia/Conferences

- Dalton Division Southern Regional Meeting 2017 in London 28/06/2017: Poster presentation with the title “Cyclopalladated 6-aryl-2-pyridones: Synthesis, Intra-/Inter-molecular Reactivity and their role in Catalytic C-H Halogenation”.
- Coordination and Organometallic Chemistry Discussion Group Meeting 2017 at Lancaster University 14-15/09/2017: Poster presentation with the title “Cyclopalladated 6-aryl-2-pyridones: Synthesis, Intra-/Inter-molecular Reactivity and their role in Catalytic C-H Halogenation”.